# Pregnancy in the Stroke-Prone Spontaneously Hypertensive Rat: Investigating Impaired Vascular Remodelling and Establishing a Novel Model of Superimposed Pre-Eclampsia

**Hannah Louise Morgan**
BSc (Hons), MRes

Thesis submitted in fulfilment of the requirements for the degree of Doctor of Philosophy (PhD)


Institute of Cardiovascular and Medical Sciences
College of Medical, Veterinary and Life Sciences
University of Glasgow

June 2018

# Author's Declaration

"I declare that this thesis has been written by myself and is the result of my own work; with exception of urine collection and recording by Ms Shona Ritchie, urine biochemistry assays performed by Ms Elaine Butler, ELISA of AngII in neonatal plasma performed by Ms Laura Downie. The RNA Sequencing and the bioinformatics associated with differential expression analysis was conducted by Glasgow Polyomics. This work was supervised by Dr Delyth Graham and Dr Martin W. McBride, and has not been submitted for any other degree at the University of Glasgow or any other institution."

Signature: _____

Hannah L Morgan

*June 2018*

# Acknowledgements

Foremost, I would like to thank my supervisors, Dr Delyth Graham and Dr Martin W. McBride, without them this research would not have been possible. Del always provided help and guidance with anything and everything (both professional and personal). I am so grateful for her continued mentorship and support. Martin deserves special mention for his patience in explaining bioinformatics basics to me, in often excessively long meetings. They were an incredible supervisory team, and made Thursday morning lab meetings fun. I would also like to extend thanks to Dr Tamara Martin and Dr Lesley Graham, for helping me along the way and giving me all sorts of advice and being there for chats. Also, thanks to Elisabeth Beattie and Laura Haddow, for providing me with excellent technical help and keeping me entertained in myography. They all went above and beyond helping me these past 3 and a half years. Importantly, thanks also need extending to the Medical Research Council for awarding the funding for my PhD studentship and making this research to be possible.

Special thanks to Dr Jo Glazier and her group at the University of Manchester for teaching me techniques to assess placental function and for being so accommodating and helpful. And thanks to Dr Ian Salt for his radioisotope guidance, support and lab space.

Almost everyone in the BHF GCRC has helped me along the way during this PhD. Thank you to all the BSU staff who helped with the rats, especially Charlie who was always there to help and knew which radio station the rats enjoyed the most for their special activities. Everyone on level 4 has helped me out in some way, shape or form and all made me feel like part of an amazing community. Special thanks need to be extended to the original PhD friends, Mags, Nina, Lisa, Emma, Laura and little Hannah. My PhD experience would have not been the same without you guys, you have shared all the laughter, tears and frustrations with me and really lived up to the group-chat name of ‘Science Besties’. Further thanks to Aisling, Tuuli, Sonya, Julian and Sammy, the other office buddies that really made my time in Glasgow so great, always being there to share success and failure and ready for a drink at either occasion. Also, thank you to Lauren, I’m glad you snuck into the office and stayed there. We had so much fun

demonstrating and it wouldn’t have been the same without you. You all made my time in Glasgow unforgettable for the right reasons.

Finally, I cannot put into words how truly grateful I am for the continued support of my loving parents. They have helped me every step of the way in my research career and have continually believed in me, and that has been invaluable. I am also thankful my sisters, Liz and Sophie, they both provided fantastic support and wildly different guidance. Also thanks to my friends outside of the PhD bubble, for keeping me in the real world and giving perspective and encouragement. Lastly, I would not have made it through without my partner, Adam. You were always there for me and let me rant at you, listened to everything good, bad and in between, and most importantly kept me fed! I couldn’t have done this without your love and support.

# Summary

Hypertensive disorders of pregnancy are an increasingly common disorder in modern society. The increasing prevalence of women with pre-eclampsia superimposed on a background of chronic hypertension is a significant burden in modern society and is profoundly detrimental to both mother and child; during pregnancy and beyond. Little is understood about the development of these multifactorial hypertensive disorders, however there is increasing evidence that the manifestation of hypertensive disorders during pregnancy is not solely due to placental-derived dysfunctions and has important maternally-driven components. The stroke-prone spontaneously hypertensive (SHRSP) rat is a well-established model of human essential hypertension. SHRSP dams remain hypertensive throughout pregnancy and demonstrate an abnormal uterine artery structure and function at term.

This project aimed to more fully characterise pregnancy in the SHRSP rat. The objectives were to assess maternal responses and determine how maternal hypertension impacts maternal and fetal well-being as well as placental development; to investigate the underlying genetic mechanisms behind the eventual abnormal pregnancy-dependent uterine artery remodelling; and, finally, to increase the maternal cardiovascular load in SHRSP pregnancy to establish a model of superimposed pre-eclampsia. *In vivo* and *ex vivo* techniques were used to characterise cardiovascular function in the hypertensive SHRSP and normotensive WKY rats during gestation, as well as assess pregnancy outcomes. The SHRSP dams were found to have similar cardiac function compared to WKY, yet there was evidence of impaired systemic vascular structure and function in late gestation and placental abnormalities. Nevertheless, the SHRSP maintained similar litter sizes to WKY and did not demonstrate any major impact on fetal growth. Further similarities between SHRSP and WKY pregnancy were revealed with the assessment of uterine artery function in early gestation. However, using RNA sequencing to elucidate the transcriptomic profiles of the uterine arteries, SHRSP were found to have strikingly different responses to pregnancy at the transcript expression level, compared to WKY. Finally, a model of superimposed pre-eclampsia was established by increasing the cardiovascular stress in the dam using angiotensin II infusion during pregnancy in SHRSP. This model had a

significantly higher systolic and diastolic blood pressure than the already hypertensive SHRSP. The pregnancy-dependent increase in cardiac output, observed in SHRSP, was negated by AngII infusion and was reduced in the highest treatment group. These major cardiovascular impairments were observed alongside increased proteinuria and reduced fetal growth; all phenotypes found in severely pre-eclamptic women.

This work has provided information on systemic and uterine specific vascular responses to pregnancy in SHRSP and WKY rats alongside detail of underlying transcriptional differences. This study was the first to examine uterine artery gene expression changes during pregnancy. The different transcriptomic profiles of early pregnancy changes in the two strains make this an intriguing model to study maternal-driven vascular remodelling in hypertensive pregnancy. Furthermore, this work demonstrated that increasing the cardiovascular load during pregnancy in SHRSP successfully mimics superimposed pre-eclamptic phenotypes and could be used in the assessment of novel therapeutic strategies. To conclude, the SHRSP has the potential to aid our understanding of human pre-eclamptic conditions, especially when endeavouring to determine the impact of maternally-driven components of hypertensive disorders of pregnancy.

# Table of Contents

# List of Tables

# List of Figures

# List of Abbreviations

| | |
|---|---|
| °C | Degrees Celsius |
| µg | Micrograms |
| µl | Microliter |
| µM | Micromolar |
| µm | Micrometer |
| ΔCT | Delta cycle threshold |
| ACE | Angiotensin converting enzyme |
| ACR | Albumin:creatinine ratio |
| ADH | Anti-diuretic hormone |
| AngII | Angiotensin II |
| AT1-AA | Angiotensin II type I receptor agonistic autoantibody |
| $AT_1R$ | Angiotensin receptor type 1 |
| $AT_2R$ | Angiotensin receptor type 2 |
| ATP | Adenosine triphosphate |
| AWT(s/d) | Anterior wall thickness (systole/diastole) |
| BP | Blood pressure |
| bp | Base pairs |
| $Ca^{2+}$ | Calcium ion |
| Calm1 | Calmodulin 1 |
| Camk2 | $Ca^{2+}$ /calmodulin-dependent protein kinase II |
| CCT | Column cytotrophoblast cells |
| cDNA | Complimentary DNA |
| cm | centimetre |
| CO | Cardiac output |
| COMT | Catechol-O-methyltransferase |
| CP | Chorionic plate |
| CT | Cycle threshold |
| DAB | Diaminobenzene |
| DBP | Diastolic blood pressure |
| DE | Differentially expressed |
| dH2O | Distilled water |
| $D_i$ | Internal diameter |
| $D_e$ | External diamter |
| DMEM | Dulbecco's Modified Eagle's medium |
| DMSO | Dimethyl sulfoxide |
| DMT | Danish Myo Technologies |
| DNA | Deoxyribonucleic acid |
| dNTP | Deoxyribonucleotide triphosphate |
| DPM | Disintegrations per minute |
| EDD | End diastolic dimension |
| EDTA | Ethylenediaminetetraacetic acid |
| EDV | End diastolic velocity |
| EDVol | End diastolic volume |
| EF | Ejection Fraction |
| ENVT | Endovascular trophoblast cells |
| ESD | End systolic dimensions |
| ESV | End systolic volume |
| EVB | Extracellular vesicle buffers |
| EVT | Extravillous trophoblasts |
| FBM | Fetal facing basal membrane |

| | |
|---|---|
| FBS | Fetal bovine serum |
| FC | Fetal cell |
| FPKM | Fragments per kilobase of transcript per million mapped reads |
| FS | Fractional shortening |
| FSH | Follicular stimulating hormone |
| g | Grams |
| GD | Gestational day |
| GFR | Glomerular filtration rate |
| GT | Giant trophoblast |
| IPA | Ingenuity® Pathway Analysis |
| $H_2O$ | Water |
| hCG | Human chorionic gonadotropin |
| HDP | Hypertensive disorders of pregnancy |
| HEPES | 4-(2-hydroxyethyl)-1-piperazineethanesulfonic acid |
| Hif1α | Hypoxia-inducible factor 1-α |
| HR | Heart rate |
| ICM | Inner cell mass |
| IHC | Immunohistochemistry |
| Ip3r | Inositol-trisphosphate receptor |
| Itpr1 | Inositol trisphosphate receptor type 1 |
| IVB | Intravesicular buffer |
| Jx | Junctional zone |
| $K^+$ | Potassium ion |
| kDa | Kilodaltons |
| kg | Kilogram |
| KPa | Kilopascals |
| KPSS | High potassium physiological salt solution |
| L/min | Litres per minute |
| Lab | Labyrinth zone |
| LH | Luteinising hormone |
| L-NAME | NG-nitro-L-arginine methyl ester |
| lncRNA | Long non-coding RNA |
| LV | Left ventricle |
| LVM | Left ventricular mass |
| M | Molar |
| MAP | Mean arterial pressure |
| MB | Maternal blood |
| Mes | Mesometrial traingle |
| mg/ml | Milligrams per millilitre |
| min | Minutes |
| miRNA | Micro RNA |
| ml | Millilitre |
| mM | Millimolar |
| mmHg | Millimetres of mercury |
| MMP | Matrix metalloproteinase |
| mN | Millinewtons |
| mRNA | Messenger RNA |
| MVM | Microvillus plasma membrane |
| Mylk | Myosin light chain kinase |
| $Na^+$ | Sodium ion |
| NaCl | Sodium chloride |
| NADPH | Nicotinamide adenine dinucleotide phosphate-oxidase |

| | |
|---|---|
| ng | Nanograms |
| ng/kg/min | Nanograms per kilogram per minute |
| NICE | National Institute for Health and Care Excellence |
| NIH | National Institute of Health |
| NO | Nitric oxide |
| Nox2 | NADPH oxidase 2 |
| NP | Non-pregnant |
| P | Pregnant |
| padj | Adjusted p-value for false discovery rate |
| PAS | Periodic acid Schiff |
| PBS | Phosphate buffered saline |
| PCR | Polymerase chain reaction |
| Pla2g2a | Phospholipase A2 |
| Plc | Phospholipase C |
| PlGF | Placental growth factor |
| PSS | Physiological salt solution |
| PSV | Peak systolic velocity |
| PWT (s/d) | Posterior wall thickness (systole/diastole) |
| qRT-PCR | Quantitative real-time PCR |
| RAS | Renin angiotensin system |
| RI | Resistance index |
| RNA | Ribonucleic acid |
| RNA-Seq | RNA Sequencing |
| ROS | Reactive oxygen species |
| Rpm | Revolutions per minute |
| RQ | Relative quantity |
| RT-PCR | Reverse transcription PCR |
| RUPP | Reduced uterine perfusion pressure |
| S/D | Systolic: diastolic ration |
| SBP | Systolic blood pressure |
| sec | Second |
| SEM | Standard error of the mean |
| s-Flt1 | Soluble fms-like tyrosine kinase-1 |
| SHRSP | Stroke-prone spontaneously hypertensive rat |
| snRNA | Small nuclear RNA |
| SpA | Spiral arteries |
| SpT | Spongiotrophoblast |
| ST | Syncytium |
| SV | Stroke volume |
| TBS | Tris-buffered saline |
| TGF-ß | Transforming growth factor beta |
| TPR | Total peripheral resistance |
| U/µl | Units per microlitre |
| uNK | Uterine natural killer cell |
| Ut | Uterine lumen |
| v/v | Volume to volume |
| VEGF | Vascular endothelial growth factor |
| VSMC | Vascular smooth muscle cell |
| w/v | Weight to volume |
| WHO | World Health Organisation |
| WKY | Wistar Kyoto rat |
| xg | G-force |

# List of Published Work and Awards

**Journal Articles**

**Morgan HL**, Ritchie S, Butler E, Beattie E, Herse F, Dechend R, McBride M, Graham D. *Modelling Superimposed Preeclampsia Using Angiotensin II Infusion in Pregnant Stroke-Prone Spontaneously Hypertensive Rats*. **Hypertension**; 2018 Jul 72(1):208-218

Small HY, Nosalski R, **Morgan H**, Beattie E, Guzik TJ, Graham D, Delles C. *Role of Tumor Necrosis Factor-a and Natural Killer Cells in Uterine Artery Function and Pregnancy Outcome in the Stroke-Prone Spontaneously Hypertensive Rat* **Hypertension**; 2016 68(5):1298-1307

Small HY, **Morgan H**, Beattie E, Griffin S, Indahl M, Delles C, Graham D. *Abnormal Uterine Artery Remodelling in the Stroke-Prone Spontaneously Hypertensive Rat*. Placenta; 2016 Jan 37:34-44

**Abstracts**

**Morgan HL**, Beattie E, MW McBride and D Graham 'Pregnancy Dependent Transcriptomic Changes in Uterine Arteries from Hypertensive and Normotensive Rat Models' American Hypertension Association Joint Scientific Sessions, September 2017 (Oral communication)

**Morgan HL**, Beattie E, Butler E, McBride MW, Graham D 'Modelling superimposed pre-eclampsia in the pregnant SHRSP rat using angiotensin II' International Federation of Placenta Associations August 2017, (Oral communication)

**Morgan HL**, Beattie E, McBride MW, Graham D 'Transcriptomic Changes in Early Pregnancy-Associated Uterine Artery Remodelling in Stroke-Prone Spontaneously Hypertensive Rat' European Meeting on Hypertension and Cardiovascular Protection, June 2016, (Oral communication)

**Morgan HL**, Beattie E, Butler E, McBride MW, Graham D 'Investigating Angiotensin II Infusion as a Model of Superimposed Preeclampsia in Pregnant SHRSP Rats' American Hypertension Association Joint Scientific Sessions, September 2017 (Poster communication)

**Morgan HL**, Beattie E, McBride MW, Graham D 'Characterisation of early pregnancy dependent gene expression changes in the uterine artery of hypertensive and normotensive rats' International Federation of Placenta Associations August 2017, (Poster communication)

**Morgan HL**, Beattie E, McBride MW, Graham D 'The Impact of Increasing Cardiovascular Stress in the Pregnant Stroke-Prone Spontaneously Hypertensive Rat by Angiotensin II Infusion' Scottish Cardiovascular Forum Meeting, February 2017, (Poster presentation)

**Morgan HL**, Small HY, Beattie E, McBride MW, Graham D 'Transcriptomic Changes in Early Pregnancy-Associated Uterine Artery Remodelling in Stroke-Prone Spontaneously Hypertensive Rat' Scottish Cardiovascular Forum Meeting, February 2016 (Poster communication)

**Morgan HL**, Small HY, McBride MW, Graham D 'Characterisation of Pregnancy in Stroke-Prone Spontaneously Hypertensive (SHRSP) Rats with Focus on Placental Abnormalities' Centre for Trophoblast Research Annual Meeting; July 2015, (Poster presentation)

**Awards**

**Onsite Poster Presentation Award: Graduate Student AHA (2017)** – $400 awarded for poster presented at the AHA Joint Scientific Sessions, San Francisco, USA.
**The Harold Fox New Investigator Award (2017) -** £490 awarded at IFPA 2017 meeting, Manchester, UK.
**MCR2017 Travel Award (2017)** - $500 towards travel support to attend the IFPA meeting, Manchester, UK.
**European Society of Hypertension Accommodation Grant (2016)** - Funding for accommodation and registration for the European Meeting on Hypertension and Cardiovascular Protection, Paris, France.
**Graham Wilson Travel Award (2016) -** £800 awarded to visit Max Delbrück Centre to develop an *in vivo* rat model of hypertensive pregnancy and learn to assess trophoblast invasion histologically.
**Lister/Bellahouston Travelling Fellowship (2015) –** £780 awarded to visit the Maternal and Fetal Health Research Centre at the University of Manchester.

# Chapter 1 Introduction

## 1.1 Physiological changes during pregnancy

Healthy human pregnancy typically lasts for 40 weeks from the last known menstrual period of the mother. During this relatively short time major physiological adaptations need to occur to support the growth of the developing fetus whilst maintaining the health of the mother. These physiological changes occur in almost all organ systems of the mother and it is important that there is understanding of these changes so that when complications of pregnancy arise they can be correctly diagnosed, managed and treated.

### 1.1.1 Cardiovascular Adaptations

Maternal cardiovascular adaptions to pregnancy have been recognised for over one hundred years; with maternal dilation, compensatory cardiac hypertrophy and changes to heart rate and rhythm all originally observed (Marshall, 1910). In order to establish and sustain appropriate nutrient and oxygen delivery to the fetus a re-direction of blood flow to the placenta is required. Successful maternal cardiovascular and haemodynamic adaptations are crucial for this to be achieved. The major changes are summarised in Table 1-1. The mechanisms controlling these changes are still much debated. The majority of maternal cardiovascular adaptations occur in the first trimester, starting as early as 5 weeks gestation, preceding placentation (Robson et al., 1989). One of the earliest findings was that of increased cardiac output (CO) (Lindhard, 1915). This rapid increase occurs due to the pregnancy-associated increase in stroke volume and heart rate (Hunter and Robson, 1992). For singleton pregnancies, CO increases can reach as much as 50% by 16-20 weeks gestation (Hunter and Robson, 1992). There has been some discrepancy on the trend of CO after this gestational time point (possibly due to differing measurement techniques and positioning), however most conclude that CO reaches a plateau or has a continued but slowed increase until onset of labour (Robson et al., 1989, Poppas et al., 1997, Clapp and Capeless, 1997, Simmons et al., 2002). Blood and plasma volume also increase progressively over gestation and a peak, approximately 25-50% greater than pre-pregnancy, is reached at term (Pritchard, 1965). Contrary to this change in blood volume and CO, the maternal systolic and diastolic blood pressures have been found to decease during gestation in healthy normotensive pregnancies (Christianson, 1976, Duvekot et al., 1993). Mean blood pressure,

measured using ambulatory 24-hour blood pressure monitoring, has been observed to be at its lowest between 16-20 weeks of gestation (approximately 100/60 mmHg) and gradually rises to pre-pregnancy levels during the third trimester (Hermida and Ayala, 2002). There is evidence of hormonal control of these changes as they have been found to occur in the luteal phase (receptive period) of the menstrual cycle and post-conception (Christianson, 1976). These coordinated adaptations are tailored to increase the blood flow to all major organ systems (Chapman et al., 1998), with the placenta receiving the largest proportion of re-directed blood flow (~25%) (Hunter and Robson, 1992, Kliman, 2000). This ensures the increased metabolic demands of the mother are met whilst supporting the developing fetus.

The reduced vascular resistance during pregnancy, first reported as increased dilation in 1910 (Marshall, 1910), has been an area of frequent study (Duvekot et al., 1993, Poppas et al., 1997, Corsini et al., 2017, Ferrazzi et al., 2018). There is a reduced vascular resistance in the uteroplacental vasculature as well as systemically (Robson et al., 1989, Clapp and Capeless, 1997, Mandala and Osol, 2012). This leads to a systemic decrease in vascular resistance and vasodilation; a driving force behind many of the observed haemodynamic changes and a solution to the paradox of the increased blood volume and heart rate not elevating maternal blood pressure. Poppas *et al* found that healthy pregnant women demonstrated increased arterial compliance, resulting in a substantial reduction in total peripheral resistance (TPR) (reduced by ~40% in the first trimester) (Poppas et al., 1997). The systemic vascular systems in pregnant women have also been shown to be refractory to the vasoactive peptide angiotensin II (AngII). AngII plays a crucial role in maintaining vascular tone (detailed further in section1.1.2.1). Gant *et al* found lower infusions of AngII elicited a greater vasoconstrictive response in non-pregnant women than in pregnant women (Gant et al., 1973). The systemic vasculature, i.e. aorta and mesentery, has also been shown to have decreased contractile and increased dilatory responses to vasoactive substances during pregnancy in animal models (Giardina et al., 2002, Gerber et al., 1998, Cooke and Davidge, 2003, Davidge and McLaughlin, 1992, Paller, 1984).

**Table 1-1: Summary of maternal cardiovascular adaptations to healthy pregnancy**

| *Cardiovascular Parameter* | *Trimester* | | |
|---|---|---|---|
| | *First* | *Second* | *Third* |
| Cardiac Output | ↑↑ | ↑ | - or ↑ |
| Stroke Volume | ↑↑ | ↑ | - |
| Heart Rate | ↑ | ↑ | ↑ |
| TPR | ↓ | ↓ | ↓ |
| Systolic BP | - or ↓ | - or ↓ | ↑ |
| Diastolic BP | - or ↓ | - or ↓ | ↑ |
| MAP | - | - | - |
| Blood volume | - or ↑ | ↑ | - |
| LVM | ↑ | ↑ | ↑ |

The trends of different measured parameters of cardiovascular function during various stages of pregnancy, compared to the previous trimester (first trimester compared to pre-pregnancy levels). All parameters have been found to return to pre-pregnancy levels post-partum. TPR= total peripheral resistance, BP= blood pressure, MAP = mean arterial pressure and LVM = left ventricular mass (↓ decrease, ↑ increase, - plateau). (Clapp and Capeless, 1997, Hibbard et al., 2015, Poppas et al., 1997, Thornburg et al., 2000, Thornburg et al., 2015, Sanghavi and Rutherford, 2014, Rovinsky and Jaffin, 1965, Simmons et al., 2002)

### 1.1.2 Renal changes

The kidneys are central to orchestrating the haemodynamic changes and reduced systemic vascular resistance associated with pregnancy, whilst also maintaining renal function in the pregnant woman. The cardiovascular and renal systems are so interlinked that changes to one will impact the other and during pregnancy is no exception. The main changes are increased renal vasodilation, increased plasma flow and increased glomerular filtration (summarised in Figure 1-1), which all occur in tandem to the changes observed in the cardiovascular system. Renal haemodynamics are influenced by a vasodilation of the renal vasculature; akin to the changes in systemic vasculature (Conrad, 1984, Odutayo and Hladunewich, 2012). There is evidence that organ-specific vasodilation occurs early in pregnancy due to maternal hormonal changes (Chapman et al., 1998). Studies examining pseudopregnancy in rodents that have induced ovulation, found that renal vascular vasodilation occurs in the absence of any fetoplacental material (Atherton et al., 1982). This suggests that there are hormonal influences on kidney function in early pregnancy. Of the main sex steroids that have been reported to increase during pregnancy (progesterone and oestrogen), only progesterone has been found to influence the kidney (Chesley and Tepper, 1967). An increased renal plasma flow (RPF), by 40-50%, and glomerular filtration rate (GFR), of 30-40% compared to the pre-pregnancy, have been observed in the first trimester of human pregnancy (Davison and Dunlop, 1980,

Dunlop, 1981, Odutayo and Hladunewich, 2012). The increased GFR, usually measured in 24-hour urine samples by the clearance of creatinine, is maintained throughout pregnancy, whereas the increased RPF peaks and then returns towards pre-pregnancy levels in the third trimester (Odutayo and Hladunewich, 2012, Dunlop, 1981). However, the GFR and RPF are consistently underestimated in the pregnant woman as the methods used to assess non-pregnant kidney function do not account for the greater 'dead space' volume associated with the increase in renal vasodilation during pregnancy (Conrad, 1984, Conrad et al., 2015). Hydronephrosis, a swelling of the kidney, can also occur in around 90% of pregnancies, however, this has been associated with the increased interstitial and vascular volume. This process is often termed renal dilation as it is a physiological response to pregnancy and not pathological in this context (Wadasinghe et al., 2016). Ultimately the kidneys of pregnant women have been found increase in length and size (Odutayo and Hladunewich, 2012). Tubular function is also influenced by pregnancy, with regards to the altered reabsorption and excretion of various metabolites, summarised in Figure 1-1, with the aim of increasing the blood volume of pregnant women via retention of fluid.

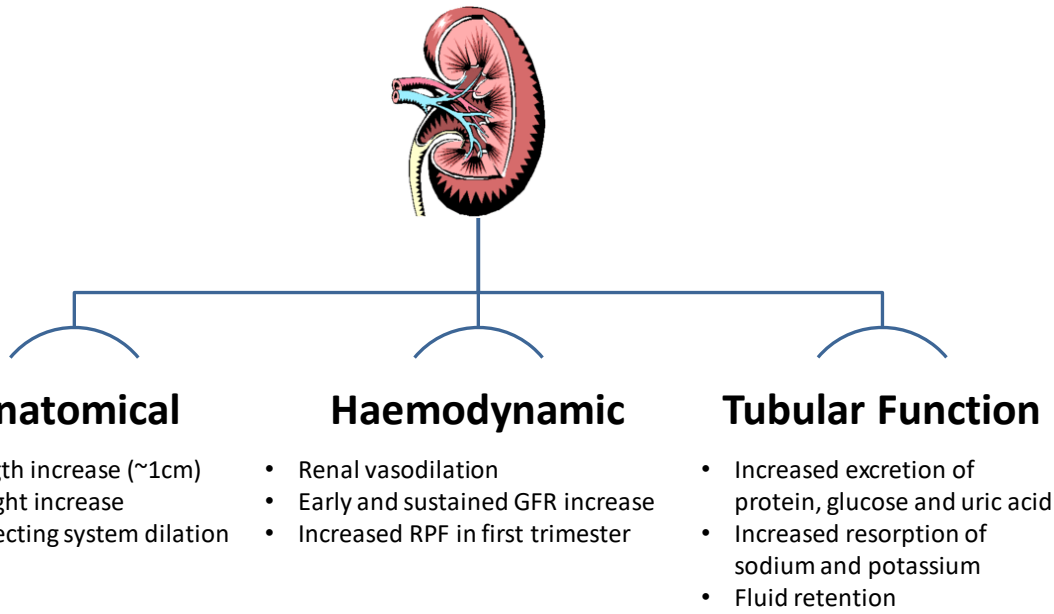


**Figure 1-1: The pregnancy induced physiological changes of the kidney**
Summary of main anatomical, haemodynamic and functional kidney adaptations to pregnancy (Odutayo and Hladunewich, 2012).

#### 1.1.2.1 The Classical Renin-Angiotensin System

A major factor in controlling blood pressure and fluid balance in all physiological states is the renin angiotensin system (RAS). This system is crucial to cardiovascular and renal physiology during pregnancy. The RAS consists of the co-ordinated cascade of enzymes and peptides that ultimately produce the vasoactive peptide angiotensin II (AngII) that acts on receptors within the vasculature to modulate vascular tone (Figure 1-2) (Irani and Xia, 2011). The classical RAS cascade occurs in the systemic circulation, yet it is centred on the kidney for regulation (Sparks et al., 2014). Renin is the rate limiting enzyme of the RAS and is produced and released from juxtaglomerular cells in the kidney (Tobian et al., 1959). The release and expression of renin are controlled by the renal baroreceptors that sense hypotension and initiate production or inhibit release of renin in hypertensive states (Tobian et al., 1959). There is also a degree of sympathetic regulation; $ß_1$-adrenergic stimulation can initiate renin release, and local control; low levels of NaCl detected by the macula densa within the kidney can initiate renin release (Sparks et al., 2014). Circulating renin cleaves the peptide angiotensinogen to angiotensin I (Skeggs et al., 1956). Angiotensinogen is produced by many tissues, but it's main site of synthesis is the liver (Matsusaka et al., 2012). The final stages of the enzyme cascade rely on the cleavage of angiotensin I to AngII. This is typically modulated by angiotensin converting enzyme (ACE) in the lungs. AngII has a main role in systemic vasoconstriction of the vasculature, via the AngII receptor type-1, and stimulates release of the anti-diuretic hormone (ADH) from the brain, to encourage a thirst response as well as increasing $Na^+$ resorption, both mechanisms increase extracellular fluid and plasma volume. All these effects are in place to ultimately increase the blood pressure (Sparks et al., 2014).

In normal pregnancy all components of the RAS have been found to increase and the system is activated (Langer et al., 1998). The production of angiotensinogen has been found to be induced by oestrogen (Immonen et al., 1983). The levels of this sex steroid hormone are increased during pregnancy, especially in the first trimester, therefore angiotensinogen gene transcription in the liver is induced during this period; increasing angiotensinogen in the circulation. Increased ovarian production of pro-renin increases plasma renin levels early in pregnancy (Itskovitz et al., 1987). Since the descriptions of the classical RAS, tissue specific

RAS have been reported, in a wide range of tissues. This allows for independent local regulation of organ circulations. An important extra-renal source of components of the RAS during pregnancy is the placenta (Herse et al., 2007). The placenta and decidua have been found to independently produce and release into circulation all major components of the RAS (Ihara et al., 1987, Morgan et al., 1998, Li et al., 2000). This increased production and activation encourages the increased blood and plasma volume observed in pregnancy, in order to maintain the blood pressure and organ perfusion that would fall in response to the systemic vasodilation and reduced vascular resistance.

A paradox of pregnancy is that whilst the increase in RAS activity ultimately leads to an increase in AngII (Massani et al., 1967), there is a reduced vascular resistance and propagated systemic vasodilation. This is due to pregnancy being associated with a refractoriness to AngII, where, even though more abundant, it does not elicit as great a contractile response in pregnant women as in non-pregnant women (Gant et al., 1973). AngII acts mainly through the two major angiotensin receptors subtypes, type-1 and type-2 ($AT_1R$ and $AT_2R$). These have contradictory actions, with $AT_1R$ responsible for vasoconstriction and $AT_2R$ mediating vasodilation (Sparks et al., 2014). The identification of the two receptor subtypes occurred in the late 1980s, and it was originally suggested that the maintenance of cardiovascular homeostasis was predominantly controlled by the more abundant $AT_1R$, with $AT_2R$ located only in fetal tissue (Chiu et al., 1989, Speth and Kim, 1990, Whitebread et al., 1989). However, there is more evidence now that the $AT_2R$ is more widely distributed throughout the adult vasculature and located in the ovary, adrenals and skin (Horiuchi et al., 1999). Specifically important for pregnancy, was the discovery of $AT_2R$ in the uteroplacental vasculature (Nielsen et al., 2000). With the $AT_1R$ mediating vasoconstriction and the $AT_2R$ promoting vasodilation, it is possible that the ratio of receptors is more important than their absolute presence/absence.

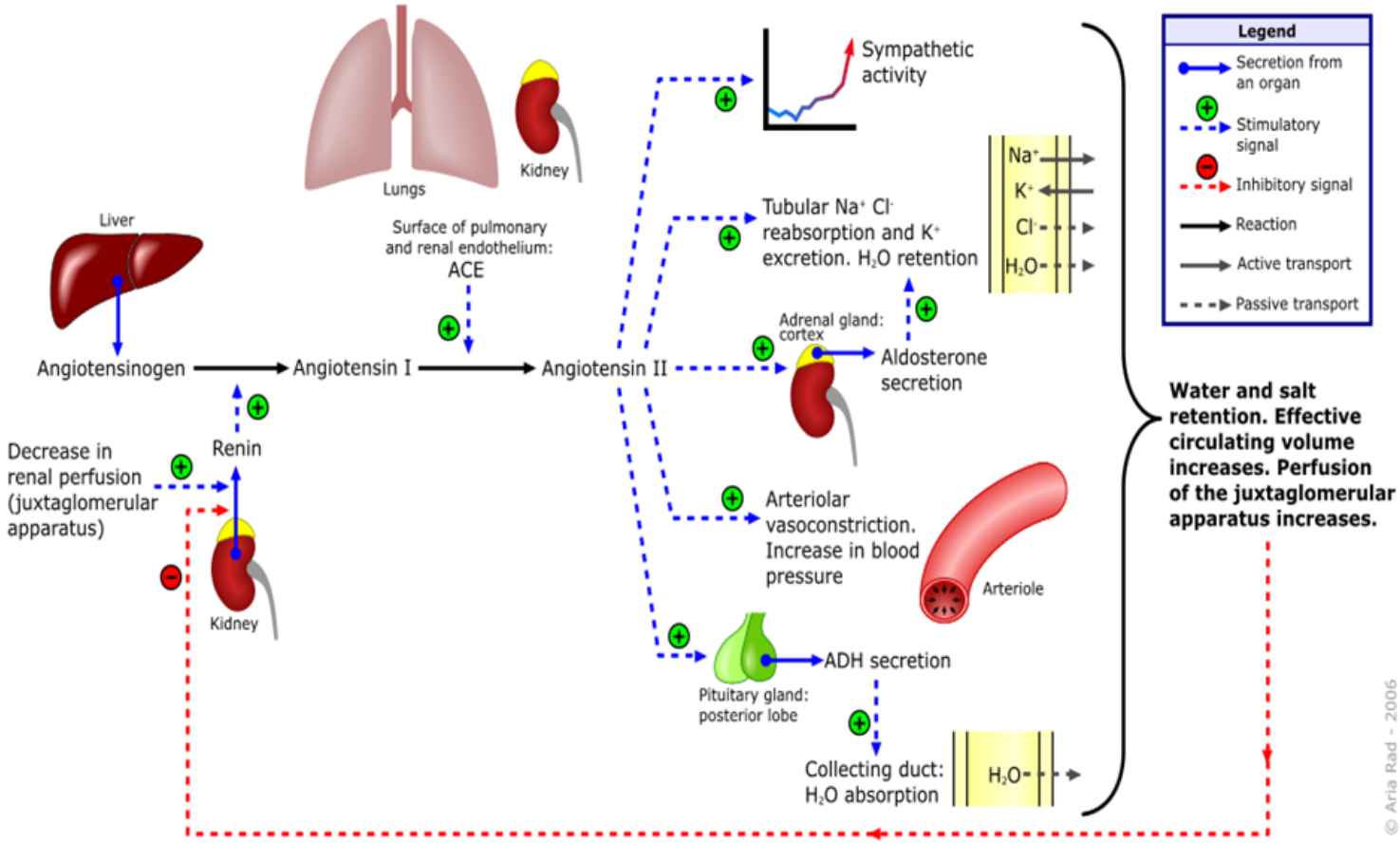


**Figure 1-2: The classical renin-angiotensin system**
The diagram illustrates the classical cascade of enzymes in the production of angiotensin II. Components for the classical system are found in the liver, kidney and lungs with the vasculature acting as the main target organ of AngII. ACE: Angiotensin converting enzyme, ADH: Anti-diuretic hormone. Diagram designed by Aria Rad and made available for public reproduction under the terms of the GNU Free Documentation License.

### 1.1.3 Human placental development

Human placentation is a complex process that occurs during pregnancy to create and maintain an organ that exists only for the period of gestation; the placenta. This organ's main role is to allow the exchange of nutrients and gases between the fetus and the mother without the two circulations coming into direct contact. The placenta develops from the outer cells of the blastocyst, the trophoblast cells (Figure 1-3). These cells eventually make the epithelial parts of the placenta (with the mesenchyme stemming from the inner cell mass). The placenta is composed of two main trophoblast cell types: the cytotrophoblasts and the syncytiotrophoblasts (Huppertz, 2008). It is the multinucleated syncytiotrophoblasts that begin invading the maternal uterine decidua on implantation, approximately 7 days post-conception. By post-conception day 15 the cytotrophoblasts invade through the maternal decidua. The presence of these placental derived cells was first noted in 1870 (Friedlaender, 1870), however at this time they were not attributed as placental in origin. A review in 1927 by Grosser, summarised the trophoblastic origin of these cells (Grosser, 1927, Pijnenborg et al., 2006). This also highlighted the trophoblast-associated remodelling that occurs in the early stages of placentation. This remodelling changes the maternal spiral arteries from highly coiled, muscular high resistance arteries to wide vessels with low resistance in order to increase blood flow to the placenta (further detail in section 1.1.3.2). This 'hijacking' of the maternal blood flow is unique to the placenta and tumours (Holtan et al., 2009). The early placental development (prior to 12 weeks post-conception) occurs in low oxygen tensions, as the invading trophoblasts form trophoblastic plugs in the spiral arteries. This is an essential mechanism to protect placental development from damaging reactive oxygen species produced in oxygen rich environments (Pijnenborg et al., 2006). During this period the developing placenta is supported by uterine glands providing essential nutrition (Burton et al., 2002).

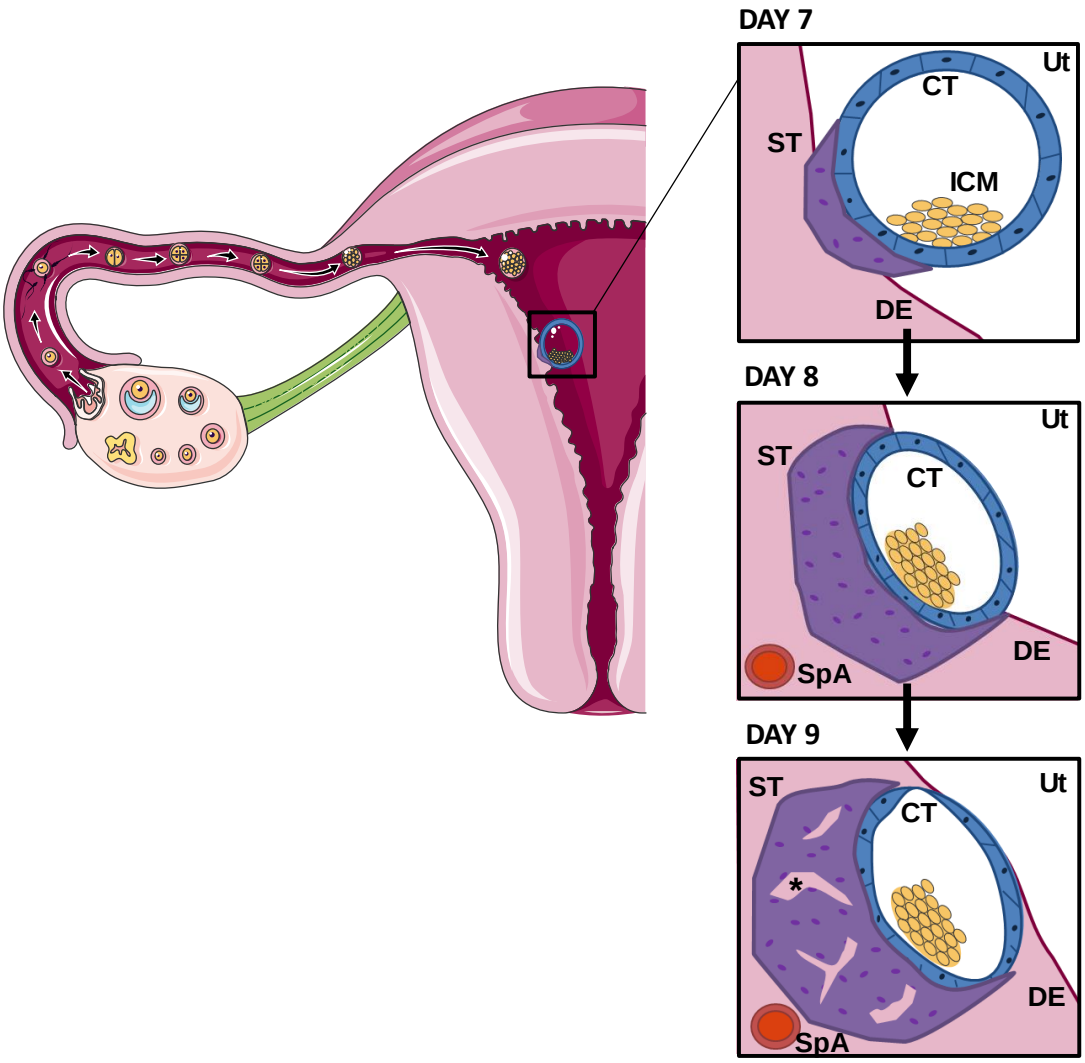


**Figure 1-3: The first stages of implantation in the human**
(A) The human ovulation process occurs at approximately day 14 of the menstrual cycle. Fertilisation and then the first divisions occur in the fallopian tube before a blastocyst enters the uterus lumen and embeds in the decidualized endometrium approximately 6-7 days after fertilisation. (B) The panels show the implantation process and the beginning of the trophoblast invasion into the decidua and formation of lacunar (*marked with asterix), which will go on to form the placental villous tree. Ut: Uterine lumen, CT: Cytotrophoblast, ST: Syncytiotrophoblast, ICM: Inner cell mass, DE: Decidualized endometrium, SpA: Spiral artery. Ovulation cycle and uterus image from Servier Medical ART, adapted from (Frank, 2017).

#### 1.1.3.1 Early Placental-Maternal Interactions

The uterine lining, the endometrium, is a dynamic tissue that undergoes cyclical changes in post-pubescent women, known as the menstrual cycle. This key reproductive process prepares the uterus for reception of an embryo. The 'implantation window' in humans is approximately 4 days after the release of the egg from the ovary. This cycle is controlled by co-ordinated fluctuations in hormones; progesterone, oestrogen, luteinising hormone (LH) and follicular stimulating hormone (FSH) (Figure 1-4). Ovulation coincides with LH, FSH and oestrogen peaks, at the end of the follicular phase. At this point in the cycle the endometrium lining the uterus decidualizes. This is a proliferative state that involves the enlargement and accumulation of glycogen and lipids in endometrial cells and the angiogenesis of the maternal spiral arteries (Kaiserman-Abramof and Padykula, 1989, Kliman, 2000). This decidualization prepares the uterus for implantation of a fertilised embryo and it is maintained throughout the luteal phase by the corpus luteum secreting progesterone (Kliman, 2000). In the event no implantation occurs, the decidualized lining is shed and the corpus luteum regresses, however if an embryo successfully implants the corpus luteum is 'rescued' due to trophoblastic production of the hormone human chorionic gonadotropin (hCG) and decidualization of the uterine lining is maintained (Kliman, 2000).

Implantation in humans, primates and rodents is interstitial, this is where the embryo fully embeds in the decidualized endometrium (Figure 1-3). By approximately day 8-9 post-conception lacunae appear in the syncytiotrophoblast, this is the formation of primary stem villus (Frank, 2017). Secondary villi have formed by day 16, these consist of an outer layer of syncytiotrophoblasts, inner cytotrophoblasts and a core of extraembryonic mesoderm. Tertiary stem villi are the final stage of development for the placenta (occurring after approximately 21 days post-conception/gestational week 5) and consist of a core of fetal capillaries with one layer of syncytiotrophoblasts between fetal and maternal blood. This creates the environment for exchange between mother and fetus, without the mixing of the two circulatory systems.

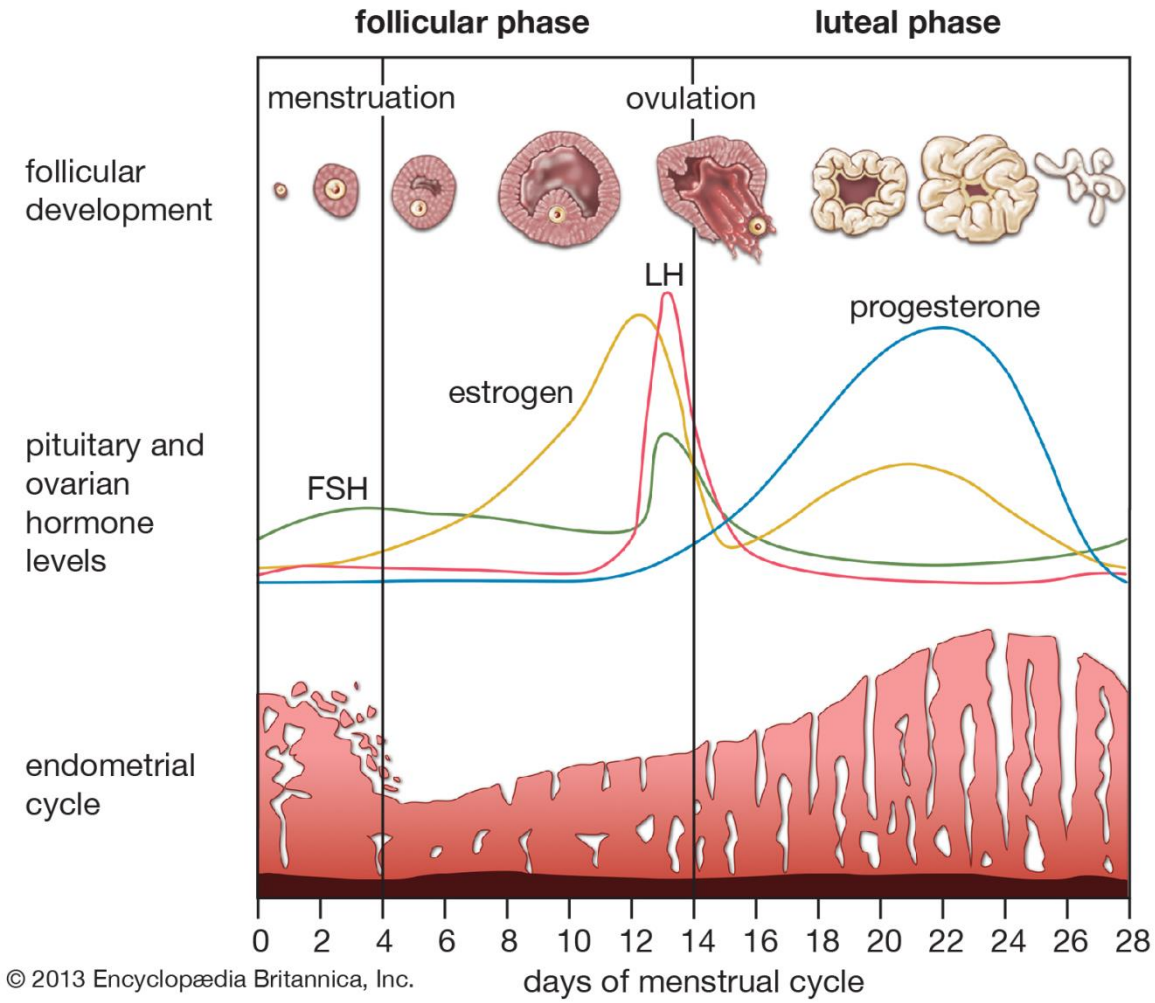


**Figure 1-4: The human menstrual cycle**
Figure obtained from Encyclopaedia Britannica (Menstruation: human menstrual cycle [Image]. Encyclopaedia Britannica. Retrieved 7 April 2018, from https://academic-eb-com.ezproxy.lib.gla.ac.uk/levels/collegiate/assembly/view/112920)

#### 1.1.3.2 Uteroplacental vascular remodelling

The human uterine circulation consists of main uterine arteries parallel to the left and right sides of the uterus. These arteries supply blood to the arcuate arteries which then branch to radial arteries which in turn flow into spiral arteries. These spiral arteries (SpA) are terminal vessels extending from the outer muscular region of the uterus, the myometrium, into the endometrium. This vascular system undergoes physiological remodelling during pregnancy which is reversed without intervention after delivery. The SpA also undergo minor monthly remodelling during the menstrual cycle. This angiogenesis is vital for the proliferation and decidualization of the endometrium (Maas et al., 2001). However, the major remodelling has been found to occur during pregnancy. This remodelling can be split into two phases, the trophoblast independent and trophoblast dependent remodelling (Pijnenborg et al., 2006). The aim of remodelling is to establish an enhanced blood supply to the placenta and the SpA transform from narrow, muscular, and vasoactive arteries to more flaccid, open vessels that are less responsive to vasoconstrictive and dilatory agents (Figure 1-5). Maternal blood is then able to freely flow into the intervillous space thus allowing adequate exchange of nutrients, gases, and waste products between mother and fetus and vice versa, via the placenta.

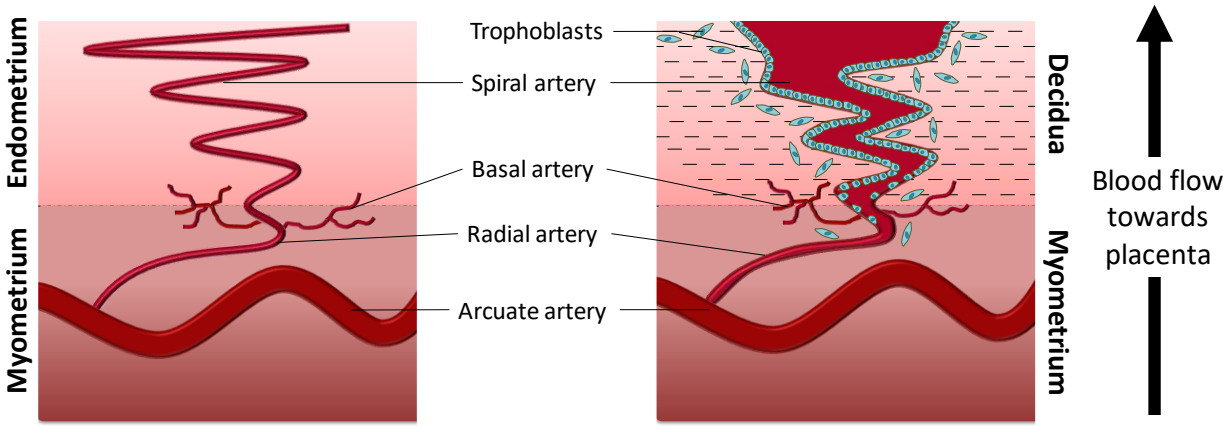


**Figure 1-5: Spiral artery structure before and during pregnancy**
Uterine arteries extend into the myometrium as radial arteries, with some branches of basal arteries, before becoming tightly coiled and extending into the endometrium (in the non-pregnant state). In pregnancy (right image) the endometrium decidualizes and spiral arteries remodel to allow increased blood flow to the placenta. This process is heavily influenced by the invasive placental trophoblasts. Diagram adapted from (Moffett-King, 2002)

The stages of remodelling have been elegantly reviewed by Pijnenborg *et al* and the stages are illustrated in Figure 1-6. The first trophoblast-independent stage is decidual-associated early vascular remodelling. This involves the vacuolation of endothelial cells and some swelling of the vascular muscle cells. Uterine natural killer (uNK) cells and other immune cells in the maternal uterus have been implicated in initiating these early remodelling changes and also in priming the uterine tissue for the second trophoblast-associated stage of remodelling (Chakraborty et al., 2011, Lash et al., 2010b). uNK cells account for 70% of the immune cell population in the uterine tissue (Robson et al., 2012). They are distinct from the peripheral blood populations and secret many angiogenic factors such as vascular endothelial growth factor (VEGF), placental growth factors (PlGF), angiopoietin (1 and 2) and TGF-ß (Lash et al., 2010b). Secretions of some of these angiogenic factors from uNK cells, specifically angiopoietin 2 and VEGF, have been found to be highest in maternal decidua from 8-10 weeks of pregnancy compared to later gestations (Lash et al., 2010a). This suggests that these factors could be initiating spiral artery remodelling prior to trophoblast invasion. Studying very early (pre-trophoblast invasion) remodelling in human decidua is a difficult concept, due to these early stages often taking place before the mother knows of the pregnancy. However, there is evidence that trophoblast independent remodelling events take place in the absence of placentally derived cells, as remodelling has been observed in the decidualized lining of the uterus when the embryo has implanted ectopically and further characterised in pseudopregnancies in animal models (King and Loke, 1997, Norambuena et al., 1984).

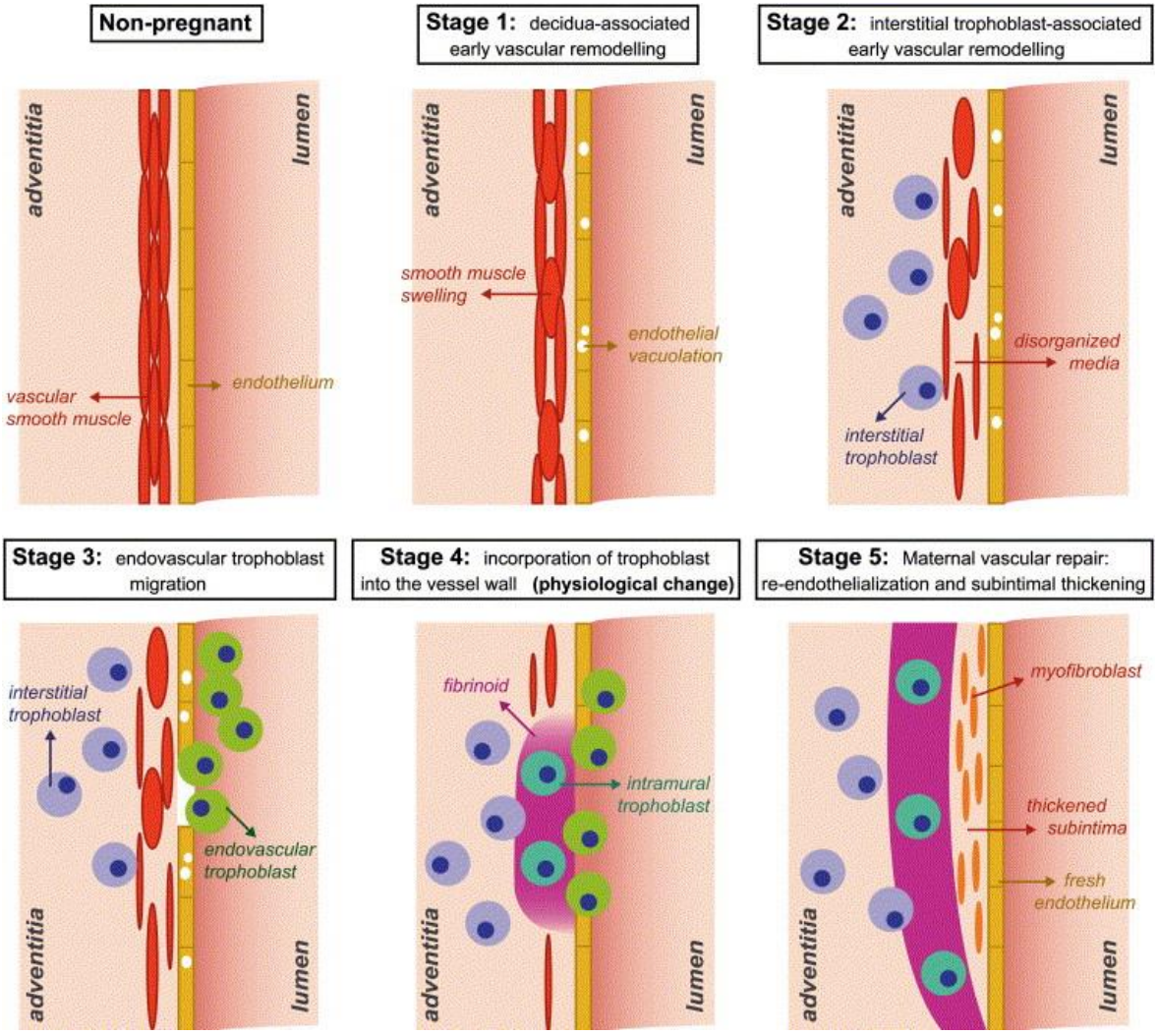


**Figure 1-6: Pijnenborg's stages of trophoblast independent and dependent spiral artery remodelling**

The stages of spiral artery remodelling in pregnancy. Stage 1 and 2 occur independently of any placentally derived trophoblast involvement. Stage 3 is the first associated with invading extravillous trophoblasts, these quickly propagate the remodelling process and stage 5 shows the final spiral artery state that will remain for the duration of pregnancy. Image reproduced with permission from (Pijnenborg et al., 2006)

The trophoblast associated remodelling has been associated with the greatest 'physiological change' of the SpA (Craven 1998). This remodelling occurs in tandem to placental villous development, and cytotrophoblast cells, that do not form the syncytium layer, differentiate to become extravillous trophoblasts (EVTs). The SpA are first influenced by the presence of interstitial EVTs that have invaded the decidual tissue surrounding the SpA. These cells eventually invade into the lower part of the myometrium in humans and rats, encouraging remodelling along the full length of the SpAs. EVTs produce pro-invasion factors such as matrix-metalloproteases (MMPs) (Bischof et al., 1995). The decidua and uNK cells mediate EVT invasion, balancing pro and anti-invasive factors secreted by the uNK cells and resistance against invasion by the thickened decidual layer (Lash et al., 2010a, Cohen et al., 2010). This ensures appropriate invasion for placental attachment and utilisation of the maternal blood supply. Excess and insufficient invasion are both associated with various placental pathologies (Pijnenborg et al., 2006). In healthy pregnancies, the EVTs cause a disorganisation of the vascular smooth muscle cells (VSMC) and media of the SpAs. This has been found to be, in part, due to EVTs secreting extracellular matrix degradation factors, specifically MMPs (Harris et al., 2010, Staun-Ram et al., 2004). The presence of endovascular EVTs are observed in the later stages of remodelling, and their origin is still under investigation (Pijnenborg et al., 2006). There is evidence that they are derived from EVTs at the terminal villi of the placenta and they travel through the artery lumen, or that they are derived from interstitial EVTs that migrate into the SpA from the surrounding decidua (Pijnenborg et al., 2006). Regardless, of origin these EVTs have been found to embed intramurally within the SpA wall. This stage of remodelling is associated with a complete loss of VSMCs and a replacement with a fibrinoid layer that interlocks the EVTs (Whitley and Cartwright, 2010). This semi-permanent physiological remodelling is then maintained for the duration of pregnancy in order to allow a constant yet steady flow of maternal blood into the intervillous space. This is necessary to prevent a pulsatile flow that would expose the fully developed placenta to periods of ischemia. It is of importance that, after delivery of the placenta, these remodelled arteries constrict and the remodelling is reversed. The vessels become narrower more structured arteries as in pre-pregnancy, however they never fully return to their exact pre-pregnancy state (Khong et al., 2003). It is therefore possible that spiral arteries

retain some remodelling ‘memory’ and may have an improved, more immediate respond to remodelling signals in subsequent pregnancies.

#### 1.1.3.3 Maternofetal Transport

Once the placenta is established it is the sole source of nutrient and oxygen provision for the fetus. The tertiary villous structure of the placenta is complete at approximately gestational week 5 yet there is continued branching of the stem villi which allows for a maximal surface area for exchange (reaching $13m^2$ by term). In the last trimester, the only barrier between maternal blood and fetal capillaries is the single layer of syncytiotrophoblasts and the single endothelium of the fetal capillaries (Figure 1-7), for this reason human placentation is known as haemomonochorial. The syncytiotrophoblast layer (syncytium) is the most important barrier for nutrient/waste transport to and from the fetus (Sideri et al., 1984). Many molecules, such as water, oxygen and carbon dioxide, move to and from the placental barrier via diffusion. However, larger substances, such as glucose, amino acids and some ions, can only cross the placenta via specific transporters on the maternal facing microvillus plasma membrane (MVM) and the fetal facing basal membrane (FBM) (Sideri et al., 1984). A number of different transporters exist on both membranes to control this movement (Desforges and Sibley, 2010). Of specific importance are the $Na^+/K^+$ ATPase, found on both the MVM and FBM, which sets up a concentration gradient of low $Na^+$ in the syncytium and drives amino acid transport systems (Johansson et al., 2000). There is evidence of at least 15 amino acid transporters in the placenta responsible for the transport of a range of basic, neutral and acidic amino acids (Jansson, 2001). One of the well characterised amino acid transporters is the system A transporter. This transporter relies on the electrochemical gradient of $Na^+$ to transport small, neutral amino acids across the MVM and FBM. There is evidence that as gestation progresses this transport rate increases, ensuring the increased demand from the growing fetus is met, however the mechanisms of this increased activity are still unknown (Desforges et al., 2009).

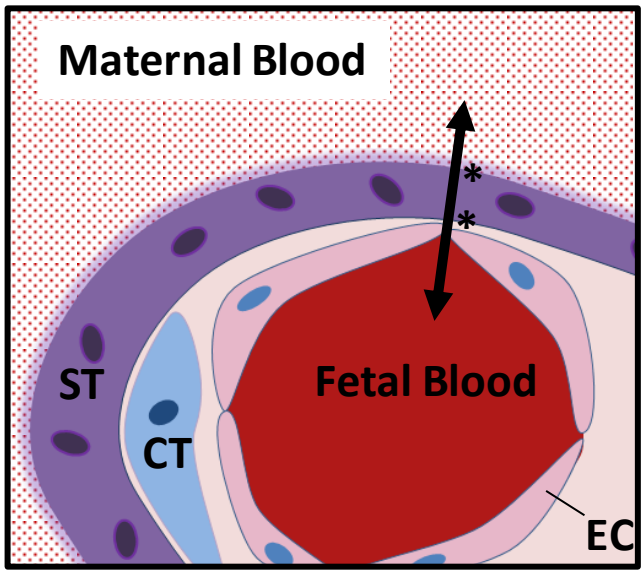


**Figure 1-7: Human maternofetal barrier for placental exchange**
A cross-sectional representation of the villous structure of the human placenta composing of a core fetal capillary surrounded by trophoblasts. The fully formed multinucleated syncytium (ST) is the main barrier to movement of substances between maternal and fetal blood (arrow). Substances must cross the microvillus membrane and basal membrane indicated by *. CT: cytotrophoblast, EC: endothelial cell. Schematic created using information from (Jones and Fox, 1991).

## 1.2 Hypertension during pregnancy

Failure to correctly adapt to the physiological challenges posed by pregnancy can result in serious complications. Pregnancy has been compared to a stress test for the cardiovascular system, as it can reveal previously unknown cardiovascular pathology (Sattar and Greer, 2002). Some of the most common pathologies of pregnancy are hypertensive disorders. Like classical hypertension these disorders are multi-factorial, relatively little is understood about the underlying causes and they can have a detrimental effect on nearly all organs in the body as well as influencing placental function. Hypertensive disorders of pregnancy can have serious detrimental effects on maternal mortality and morbidity as well as the wellbeing of the developing child. Hypertension that occurs spontaneously during pregnancy is only evident in humans, and in some old-world monkeys (symptoms have been described in the gorilla and chimpanzee), and was first described by Hippocrates in the 5$^{th}$ century BC. (Stout and Lemmon, 1969, Baird, 1981, Thornton and Onwude, 1992). However, these disorders can occur under many guises, and for disorders that have been known for millennia the treatment options are poor (the only 'cure' being the delivery of the placenta) and its causes are not fully understood.

### 1.2.1 Classification of Hypertensive Disorders in Pregnancy

Hypertensive disorders of pregnancy (HDP) can be classed into four major groups; gestational hypertension, pre-eclampsia, chronic hypertension and superimposed pre-eclampsia. All these conditions are classified by the elevation of blood pressure greater than 140mmHg systolic and 90mmHg diastolic (ACOG, 2013). Gestational hypertension and pre-eclampsia are pregnancy specific, presenting ≥20 weeks gestation and resolving postpartum (Steegers et al., 2010). The arguably most severe of these conditions is pre-eclampsia, therefore this condition tends to be more frequently studied. A basic definition of pre-eclampsia is the spontaneous pregnancy specific appearance of hypertension after 20 weeks gestation with the presence of proteinuria (>300mg/24 hours). Diagnosis has remained mostly unchanged for 50 years. Pre-eclampsia can range from mild to severe depending on the elevation of blood pressure (mild: ≥140/90mmHg, moderate: ≥150/100mmHg and severe ≥160/110mmHg) (NICE Guidelines, 2010). A more severe prognosis is associated with the presentation of

a combination of following features: platelet count <100,000/µl; impaired liver function; new development of renal insufficiency; pulmonary oedema; headaches and/or new-onset cerebral or visual disturbances (Tranquilli et al., 2014). Gestational hypertension presents in a similar fashion to pre-eclampsia without the more severe phenotypes, such as proteinuria and others outlined above. Hypertensive disorders of pregnancy are commonly described as resolving after delivery, however this is not the case. In instances of superimposed pre-eclampsia, which is classed strictly as a hypertensive disorder of pregnancy (NICE Guidelines, 2010), the mother remains hypertensive post-pregnancy. There is also mounting evidence that some 'pregnancy specific' hypertensive disorders are diagnosed when there is a previously undetected cardiovascular impairment that only presents during pregnancy due to the increased cardiovascular stress. This can then manifest as hypertension in later life (Sattar and Greer, 2002). This hypothesis would highlight a women's future risk of hypertension and/or cardiovascular disease development if they suffered from HDP, illustrated in Figure 1-8.

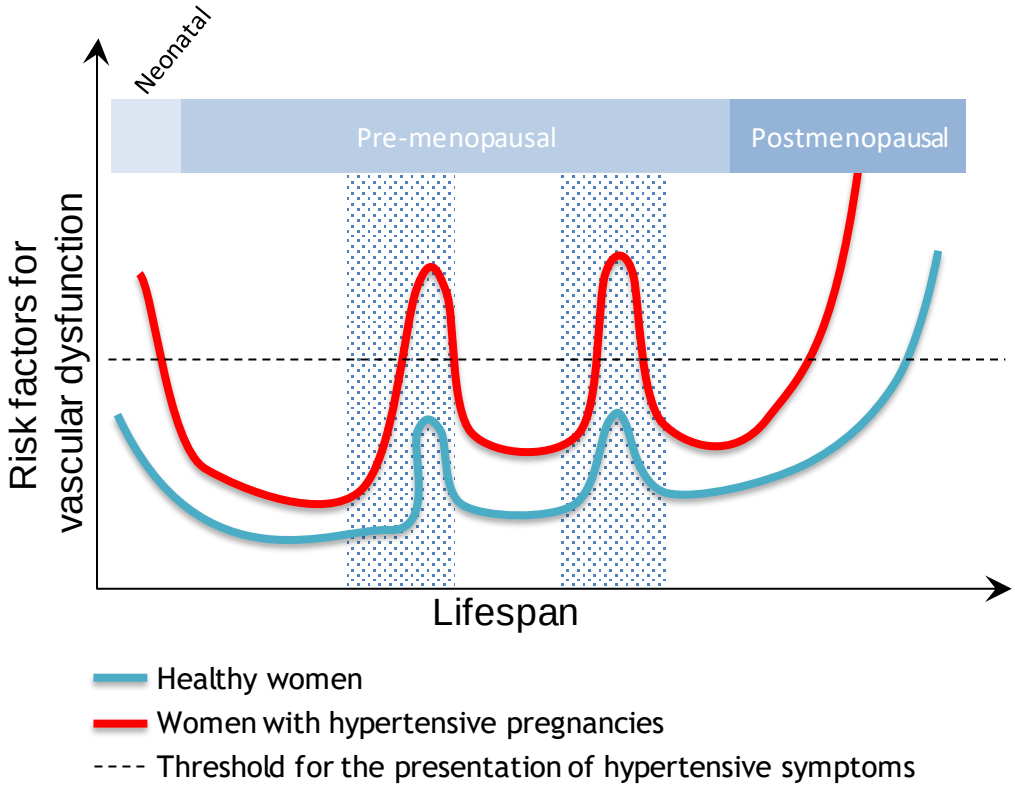


**Figure 1-8: Pregnancy as a cardiovascular 'stress-test'**
The healthy female population (blue line) have a lower risk of vascular dysfunction than those that develop hypertensive disorders in pregnancy (red line). Pregnancy (shaded peaks) presents a significant cardiovascular stress in pre-menopausal women and those women with higher underlying vascular risk factors develop a dysfunction during these periods, and also present earlier in the postmenopausal portion of life. Adapted from (Sattar and Greer, 2002).

#### 1.2.1.1 Pre-eclampsia

Pre-eclampsia is the one of the most studied HDP due having the greatest severity, and therefore able to be delineated from gestational hypertension by stringent criteria. Changes in the maternal population such as an increased prominence of advanced age, obesity and diabetes (which are all risk factors for the development of hypertension) increase the likelihood of pre-eclampsia development (Lawler et al., 2007). Cases of pre-eclampsia complicate between 2-8% of pregnancies globally (Duley, 2009). However, it is hard to distinguish pre-eclampsia from superimposed pre-eclampsia if no information on pre-pregnancy blood pressure is available, thus the two are often merged and studied together. Pre-eclampsia has been mainly thought of as a placental disorder, due to the large placental involvement in disease progression and the removal of the placenta being the only 'cure' for this multifactorial disorder. However, more evidence is emerging to suggest the maternal cardiovascular system dysfunction plays an important role in the disease development (Ferrazzi et al., 2018). Pre-eclampsia may have many subtypes and can be most easily classified as early or late onset (Kalafat and Thilaganathan, 2017). These subtypes can only be assigned at delivery, with early onset classified as delivery occurring prior to 34 weeks gestation and late pre-eclampsia diagnosed with delivery on or after 34 weeks (Valensise et al., 2008). It is early pre-eclampsia that is mainly attributed to placental dysfunction and is often more severe and associated with fetal growth restriction (FGR). Whereas late pre-eclampsia is believed to be more of a maternal disorder resulting in failure of the cardiovascular system adaptations, which may cause secondary placental dysfunction (Kalafat and Thilaganathan, 2017).

#### 1.2.1.2 Chronic Hypertension and Superimposed Pre-eclampsia

Essential hypertension, which is hypertension without secondary causes, accounts for at least 90% of hypertensive cases and is strongly correlated to the development of cardiovascular disease (Messerli et al., 2007). Whilst premenopausal women have a lower incidence of hypertension than men of the same age, their risk of development increases exponentially after menopause with hypertension being more likely in women than men aged over 65 (Roger et al., 2012). The reasons for this are not fully understood but have been linked to

the cardiovascular protective roles of oestrogen and its beneficial effects on the RAS. These crucial hormones and systems need precise coordination during pregnancy to establish the appropriate cardiovascular response (section 1.1.1).

The NICE definition of hypertension is a clinically measured blood pressure higher than 140/90mmHg, with an average daytime blood pressure (measured using several ambulatory blood pressure measurements or at home monitoring) of ≥135/85mmHg. This is classed as stage 1 hypertension, with the stages increasing with severity. Guidelines produced by the American College of Cardiology and American Heart Association Task Force have suggested lowering the blood pressure threshold to 130/80mmHg for the diagnosis of hypertension (Whelton et al., 2017). It is of note that the lowest threshold for blood pressure elevation used to diagnose many HDP is still a clinical measure of ≥140/90mmHg (NICE Guidelines, 2010). This limit may be too high to detect 'pre-hypertensive' women. It is likely that an abnormal blood pressure response to pregnancy occurs in these borderline hypertensive women due to the increased cardiovascular stress imposed (Sattar and Greer, 2002). Separating this group of women from those that suffer from other HDP would greatly benefit the study of the effect of chronic hypertension on pregnancy.

At present chronic hypertension affects between 1-5% of pregnancies (Sibai, 2002, Lawler et al., 2007, ACOG, 2013). Women with chronic hypertension during pregnancy are 8 times more likely to develop superimposed pre-eclampsia than the general population of pregnant women (Bramham et al., 2014, Lawler et al., 2007). This increases the risk pregnancy places upon these women, as well as increasing the likelihood of adverse neonatal outcomes (Bramham et al., 2014). The prevalence of chronic hypertension in a population of US pregnancies was found to increase from 1.01% in 1995 to 1.76% by 2008 (Bateman et al., 2012). This rise is likely partly attributed to the rise in age and obesity amongst childbearing women; as these factors are also attributed to the likelihood of developing hypertension (Lean et al., 2017, Guedes and Canavarro, 2014, Kanagalingam et al., 2005, Heslehurst et al., 2007).

HDP are easily diagnosed if chronic hypertension has been well documented pre-pregnancy or is present before 20 weeks gestation. However, most women of childbearing age are not regularly screened for hypertension and, as discussed

above, women who are borderline hypertensive may not be identified pre-pregnancy. Also confounding this is that maternal blood pressure has typically been found to reduce during pregnancy, beginning relatively early in gestation (section 1.1.1). This can lead to borderline hypertensive women appearing to have blood pressure within the normal range when first screened during pregnancy, yet they could later go on to present as hypertensive and could be misdiagnosed with gestational hypertension or pre-eclampsia depending on severity.

The pre-eclampsia foundation defines superimposed pre-eclampsia as the development of pre-eclampsia during a pregnancy already compromised by pre-existing hypertension of another cause (Preeclampsia-Foundation, 2010). As the likelihood of pre-eclampsia development is significantly increased in hypertensive women, the incidences of superimposed pre-eclampsia are high (Lecarpentier et al., 2013, Sibai, 2002). Whilst age has been associated with increases in incidence of pre-eclampsia it is more difficult to dissect the relationship it has with superimposed pre-eclampsia. This is due to women identified as hypertensive pre-pregnancy (or at first antenatal appointment) are on average more mature (>35 years old), but it is unclear whether this is due to the fact an older mother is more likely to become hypertensive, thus more likely to develop superimposed pre-eclampsia, or that within the chronic hypertensive population of pregnant women age increases the risk of superimposed pre-eclampsia (Bramham et al., 2014). Lecarpentier *et al* found that in a group of 211 women with treated chronic hypertension prior to conception there was no age association, similar findings were previously observed by Sibai *et al* in a population (n=763) of chronically hypertensive women with and without treatment (Lecarpentier et al., 2013, Sibai et al., 1998). In both studies there were a larger proportion of older women with chronic hypertension, yet this did not positively correlate with development of superimposed pre-eclampsia.

### 1.2.2 Prevalence worldwide and impact

Hypertensive disorders during pregnancy were found to be responsible for the second largest proportion of maternal deaths worldwide between 2003 and 2012 (Say et al., 2014). Maternal mortality reduction was one of the Millennium Development Goals; to reduce maternal deaths by 75% (from the period of 1990 to 2015). Maternal mortality has reduced globally since 1990, however only by 45%. This was most likely achieved by better antenatal care in rural, developing countries as there was a documented increase in skilled health personnel assisting in births and an increase in antenatal visits and accessibility (The Millennium Development Goals Report, 2015). However, the reduction of maternal mortality is limited by the knowledge surrounding the conditions responsible for these deaths.

Hypertension accounted for 343,000 maternal deaths worldwide in 2013 (Say et al., 2014). This was 14% of the pregnant population and the second largest cause of deaths, after haemorrhage. Interestingly, whereas haemorrhage related deaths were more prominent in the developing regions, hypertension related death prevalence was similar in both the developing and developed areas (14% and 12.9% respectively) (Say et al., 2014). Furthermore, it is important to note that in this systemic analysis of global deaths, it is not clearly explained which hypertensive disorders were included in this direct cause group. It is not clear whether this group only examined pregnancy induced hypertension (gestational hypertension and PE) or included chronically hypertensive disorders. It does state that women with co-morbidities were grouped with indirect causes of maternal death. This makes it difficult to dissect the true impact of hypertensive pregnancies.

There are several risk factors for the development of hypertension during pregnancy (outlined in Table 1-2) (Tranquilli et al., 2014). Many of these risk factors are common to the risk factors associated with the development of essential hypertension, such as age, obesity, race etc. These make both essential and pregnancy specific hypertension difficult diseases to easily classify due to their multifactorial influences and presentations. A further cause for concern is that risk factors, such as advanced age and obesity, are becoming increasingly more common in women of childbearing age (Heslehurst et al.,

2007, Roberts et al., 2011); which places these women at greater risk of developing pregnancy induced hypertension or developing hypertension prior to conceiving.

The primary cause of deaths (both maternal and fetal/neonatal) is driven by the time of diagnosis and delay in initiating any of the few treatment options that exist. The prediction of these disorders and establishing appropriate treatments is key to reducing the mortality

**Table 1-2: Risk factors for the development of hypertensive pregnancy disorders**

| Common Maternal Risk Factors |
| --- |
| ▪ Nulliparity<br>▪ Multiparity<br>▪ Advance maternal age (older than 40 years)<br>▪ Race (Caribbean and Latin heritages at highest risk)<br>▪ Family history<br>▪ Previous affected pregnancy<br>▪ Chronic hypertension<br>▪ Chronic renal disease<br>▪ Obesity and high body mass index<br>▪ Diabetes mellitus<br>▪ Antiphospholipid syndrome |

### 1.2.3 Maternal Cardiovascular Pathophysiology

Maternal cardiovascular adaptations are crucial to successful pregnancy, as outlined in section 1.1.1. Any failure of these adaptations can have serious impact on the wellbeing of mother, pregnancy and the fetus. Hypertension during pregnancy is understandably linked with cardiovascular system dysfunction.

HDP, pre-eclampsia especially, are referred to as endothelial disorders. This is evident in the increased vascular resistance of pregnant women with these conditions (Melchiorre et al., 2013, Valensise et al., 2008, Vasapollo et al., 2008, Ferrazzi et al., 2018, Stott et al., 2017). It is probable that this dysfunction drives the increase in blood pressure, due to the maternal cardiovascular system failing to adapt to the increased blood/plasma volume. This can also impact the cardiac output of these women. Many studies have agreed upon the increased total vascular resistance associated with HDP, yet there are discrepancies regarding the impact on CO. Several groups have found pre-term pre-eclampsia (i.e. diagnosis prior to 34 weeks gestation) is associated with a reduction in CO (Melchiorre et al., 2013, Stott et al., 2017, Valensise et al., 2008). These findings suggest that there is a failure of CO to increase in more severely affected pre-eclamptic patients. What is unclear is whether there is simply no increase and women retain their pre-pregnancy cardiac function or that it rises early but fails in later gestation. Farrazzi *et al* and Stott *et al* identified that CO decreases are more likely in pregnancies with poorer fetal outcomes, such as lower birthweights (Stott et al., 2017, Ferrazzi et al., 2018). Discrepancies in classification of HDP used in these studies could confound measurements and is an area of where a consensus would greatly benefit research.

There is evidence that some cardiac dysfunction persists even after delivery. Most HDP stated as pregnancy specific resolve after the removal of the placenta, yet studies have found evidence that women who have suffered from pre-eclampsia have a higher (although not hypertensive) blood pressure and increased vascular resistance postpartum (Valensise et al., 2008, Soma-Pillay et al., 2017). Some suggest these cardiovascular abnormalities still exists decades after the affected pregnancy (Bokslag et al., 2017). Whether the hypertensive pregnancy is a cause or consequence remains to be identified, yet it does add to

the theory of pregnancy being a cardiovascular stress test and the possibility that HDP could be used to indicate which women will be more at risk in later life.

### 1.2.4 Hypertensive Pregnancies and Vascular Remodelling

An abnormal systemic vasculature response to pregnancy is associated with HDP, this includes vasoconstriction and endothelial dysfunction which contribute to the increased TPR and hypertension (Crews et al., 2000). Insufficient spiral artery remodelling and improper placentation have been found to reduce uteroplacental blood flow. Of specific importance to the wellbeing of the mother and pregnancy is the uteroplacental blood flow, which is the main delivery route of maternal blood to the placenta. In HDP the uteroplacental blood flow is often reduced, indicated by an increased pulsatility index of the uterine artery and resistance to flow resulting in the appearance of notching on Doppler waveforms (Poon et al., 2010, Ferrazzi et al., 2018, Fleischer et al., 1986). Detection of diastolic notching has proved useful as it can be found prior to the hypertensive phenotypes in pre-eclampsia, and thus can be used as a predictor of HDP, particularly early-onset pre-eclampsia (Tayyar et al., 2015, Poon et al., 2010). Reduced placental blood flow is thought to stem from an impairment in the spiral artery remodelling (Pijnenborg et al., 1991). Spiral arteries from pre-eclamptic patients have been found to have shallower remodelling (i.e. limited to decidual, not extending into the myometrium) and retain a contractile phenotype and do not show a pregnancy dependent increase in flow mediated vasodilation (Lyall et al., 2013, Brosens et al., 1972, Kublickiene et al., 1998, Kublickiene et al., 2000). This impairment has been associated with poorer trophoblast invasion in women with pre-eclampsia, however the mechanisms for this are still unknown (Figure 1-9). Ultimately the impaired remodelling creates a hypoxic uterine environment leading to placental damage and an increase of antiangiogenic and pro-inflammatory factors, which are released into the circulation leading to systemic vascular dysfunction. The increase in blood pressure and peripheral resistance that occur in HDP further propagates the restricted placental blood flow leading to worsening of the disorder (Brennan et al., 2014).

The balance of pro and antiangiogenic factors is disturbed in HDP with the increased release of soluble VEGF receptor-1 (s-Flt-1) which sequesters VEGF and PlGF and prevents their proangiogenic influences. Levels of vasodilatory oestrogen metabolites and the activity of the enzymes that produce them have also been found to be lower in pre-eclamptic women, such as catechol-O-methyltransferase (COMT) and its product 2-methoxyoestradiol (Kanasaki et al., 2008). Oxidative stress increases substantially in HDP due to an imbalance in reactive oxygen species (ROS) and anti-oxidant productions (Myatt and Cui, 2004, Madazli et al., 2002). These are thought to be produced by the struggling placenta due to the increased pulsatility of the uterine artery blood flow (Hung et al., 2001). This subjects the placenta to periods of hypoxia followed by reperfusion with stimulates ROS production and also transports them systemically.

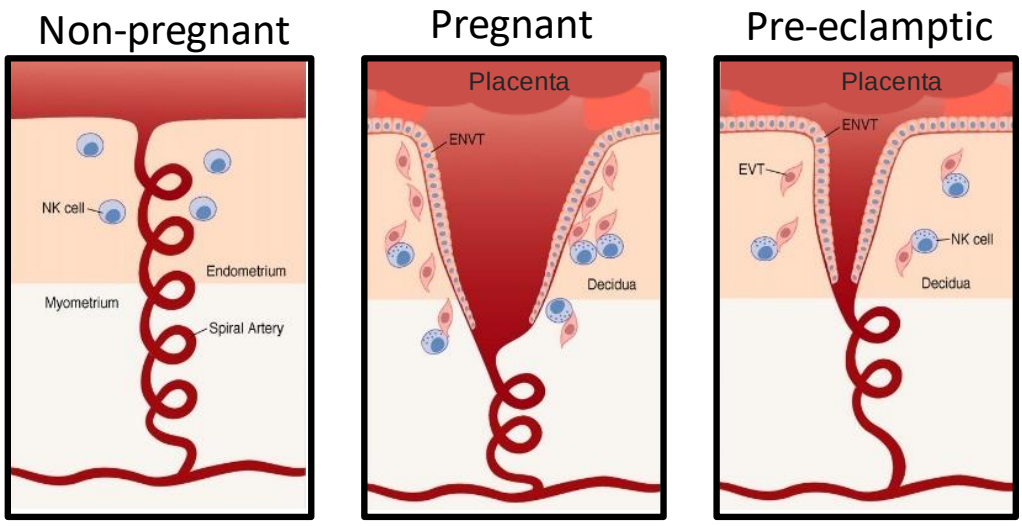


**Figure 1-9: Pregnancy induced remodelling of the spiral arteries are lessened in pre-eclampsia**
The extent of spiral artery remodelling is less in pre-eclamptic pregnancies compared to normal pregnancies. The deficient remodelling results in a shallower, narrower vessel lumen. ENVT: endovascular trophoblast cells, EVT: extravillous trophoblasts, NK cells: natural killer cells Adapted from Parham 2004 (Parham, 2004)

### 1.2.5 Dysregulation of the RAS in Hypertensive Pregnancy

Pre-eclampsia is associated with a reduction of RAS components despite an increased sensitivity to the main vasoactive peptide (AngII) (Herse et al., 2007, Shah, 2005). Historic experiments show that pregnancy increases women's resistance to AngII's pressor effects, with pregnant women requiring twice as much AngII as non-pregnant women to increase blood pressure (Gant et al., 1973). However, pre-eclamptic women do not demonstrate this refractoriness and have increased sensitivity to AngII, which remains after parturition (Saxena et al., 2010). This increased response to AngII occurs even though AngII production has been found to be reduced in pre-eclampsia (Langer et al., 1998). The main AngII receptor responsible for the contractile effects of AngII ($AT^1R$) has been found to have an upregulated expression in the placenta of pre-eclamptic women (Leung et al., 2001). This could increase the pressor responses of AngII in the placental vasculature, regardless of reduced AngII levels, due to a higher abundance of $AT^1R$. However, Knock *et al* found that whilst $AT^1R$ expression increases, the binding capacity for AngII is reduced in pre-eclampsia (Knock et al., 1994). Pre-eclampsia has been associated with an increase in the circulating autoantibody to AngII receptor 1 (AT1-AA) (Herse and LaMarca, 2013). AT1-AA has been found to stimulate $AT^1R$, binding to this receptor with a higher affinity than AngII, thus propagating pressor responses in pre-eclampsia (Wallukat et al., 1999). AT1-AA are also proposed to stimulate NADPH oxidases and induce the generation of ROS in both maternal vasculature and placental trophoblasts, thereby enhancing the endothelial dysfunction and inflammatory responses associated with pre-eclampsia (Dechend et al., 2003). The dysregulation of the RAS in pre-eclampsia is complex and it is not clear whether it is a direct contributor to the pathophysiology or is altered in response to the dramatic increase in blood pressure.

### 1.2.6 Impact on Offspring's Health

The *in-utero* environment of the developing fetus is crucial not only to the success of pregnancy but also to the offspring's health in adult life (Gluckman et al., 2008). Offspring from compromised pregnancies, such as those in hypertensive mothers, are more likely to have poor cardiovascular, metabolic, and developmental outcomes in later life (Staley et al., 2015, Gaillard et al., 2014, Himmelmann et al., 1994). It was first realised that children of Dutch women exposed to a period of famine in the Netherlands in the winter of 1944-1945 had lower birthweights than women with a normal diet (Roseboom et al., 2006). These babies born small for gestational age or growth restricted have an increased risk of developing cardiovascular disease and hypertension in adulthood (Barker, 1991, Barker et al., 1993, Sinclair et al., 2007). The Barker hypothesis has highlighted the importance of these developmental origins of health and disease, in which it is presented that the fetal environment plays a key role in the development of health problems later life (Barker, 1991). It is now widely recognised that, alongside the adverse effects of poor maternal diet, maternal hypertension during pregnancy can negatively impact early-life development and influence fetal growth. FGR is a common occurrence alongside severe HDP, mainly due to a poor placental perfusion which reduces maternofetal transfer of nutrients and oxygen (Steel et al., 1988, Verlohren et al., 2010, Himmelmann et al., 1994). FGR is associated with a vast number of health problems for the offspring in childhood and into adult life (Crispi et al., 2018, Hack et al., 2002). This stems from fetal programming, which takes cues from the *in utero* environment and influences from maternal and paternal genetics to adapt the development to suit the outside world it will be born into. This is a useful evolutionary trait that ensures survival if the child is born into the same environment it was exposed to during development. This is problematic, however when the poor uterine environment does not reflect the outside environment. Both human and animal studies have shown that offspring born to hypertensive mothers have a raised blood pressure in childhood, adolescent and into adulthood, placing them at greater risk of developing hypertension (Himmelmann et al., 1994, Staley et al., 2015). A dysregulation of RAS during pregnancy has been found to increase AngII sensitivity and hypertensive responses in adult offspring (Xue et al., 2017)

### 1.2.7 Current interventions

Treatment for HDP is supportive, with the symptoms monitored and managed, but due to the paucity of information on the exact causes, clinical treatment options are lacking. The only way to stop the disorders progressing is to deliver the baby, which requires a balance between the risk to the mother and gestational age of the fetus. Premature delivery is associated with lower survival rates and an increased risk of many disorders of the child's health (Iacovidou et al., 2010). A review of treatment options for pregnancy disorders, conducted by Fisk and Atun, noted that whilst there were 660 drugs under development for cardiovascular disease, only 17 drugs were being developed for maternal pregnancy disorders, the majority focusing on manipulations of labour (Fisk and Atun, 2008). Only 2 were specifically investigated for treatment of pre-eclampsia and these were in early clinical trial stages (phase II) and are re-purposed drugs, previously licensed for other conditions, thus were not specifically designed to treat pre-eclampsia. The current strategy of hypertension management reduces maternal blood pressure in severely hypertensive mothers, yet these women do not always reach normotension (NICE Guidelines, 2010). The target blood pressure for these interventions is 140/90mmHg, which is the borderline for hypertension diagnosis and, as discussed previously, blood pressures between 129-139mmHg systolic and 79-89mmHg diastolic are classed as pre-hypertensive and would not sufficiently remove the pregnant women from risk of HDP development.

The main barriers to designing new interventions/treatments is that there is still difficulty in prediction, diagnosis, and treatment of HDP. All these disorders require much more in-depth study to elucidate causes, abnormalities and mechanisms of dysfunction. Yet, prediction of HDP is advancing with the utilisation of the uterine artery Doppler blood flow and the identification of potential biomarkers, such as sFlt-1/PlGF ratios, to detect impaired placental perfusion before the onset of hypertensive symptoms (Steel et al., 1988, Liu et al., 2013). Many of the circulating factors appear in maternal plasma prior to onset of any symptoms and a number of biomarkers have been identified (Liu et al., 2013, Kenny et al., 2014, Navaratnam et al., 2013, Myers et al., 2013). These studies help detect pregnancy pathologies and diagnose the conditions but do not tell us key information about why they are occurring. The need for more

reliable biomarkers of pre-eclampsia, FGR and other pregnancy complications have been identified by many studies and reviews previously published (Liu et al., 2013).

## 1.3 Maternal Genetics

There is evidence of a large genetic influence in the development of HDP. Women with a maternal family history of pre-eclampsia are 35% more likely to develop pre-eclampsia themselves (Cnattingius et al., 2004). This is not a new concept as there are also many genetic influences for essential hypertension (Redman et al., 1999).

The majority of genetic studies in human pregnancy have focused on the placenta. Successful placentation requires a coordinated function between the placental trophoblasts and the maternal immune system. Therefore, the placental genome, which obtains 50% of its genetic information from the father, is an important consideration and is crucial in understanding genetic influences of pregnancy disorder. Whilst the placenta plays a pivotal role in these conditions, the maternal genomic contribution should not be overlooked. It is the maternal response to pregnancy that ultimately controls placentation and the ability of the maternal cardiovascular system to adapt appropriately.

### 1.3.1 Transcriptomics

Prediction of pre-eclampsia has been a driving force in the use of 'omic' technologies in pregnancy research. 'Omic' technologies comprise of genomics; examining the genome, transcriptomics; the study of transcribed genes (mRNA), proteomics; large scale study of proteins, and metabolomics; study of metabolite production. Proteomics and metabolomics are leading the way for 'omics' in pregnancy research and they are instrumental in detecting potential biomarkers, which can be used in the prediction of HDP (Kenny et al., 2014, Navaratnam et al., 2013). This type of information is essential; however, in order to fully understand the molecular mechanisms that underlie specific conditions, it is important to look prior to translation and protein metabolism, to the dynamic gene expression changes that are occurring in response to placentation and pregnancy. The transcriptomic profiling of various tissues is a valid method for determining the control of protein production, as well as control of gene expression.

Transcriptomics is the study of the RNA transcripts produced by the genome. This method of examination allows the identification of differentially expressed

genes in different tissues and cell types, under specific conditions and/or at various time points. Thus providing comparisons that can help delineate differences in the genetic regulations and responses to pregnancy adaptations. Transcriptome profiling can provide dynamic information on the uterine environment, such as inflammation, oxidative stress and the maternal immune regulation (Cox et al., 2015)

### 1.3.2 Microarray and RNA-Sequencing Technologies

The methods utilised to provide a transcriptome profile of tissue/cells are high-throughput sequencing technologies, such as microarrays and RNA-sequencing. The majority of transcriptome studies focusing on pregnancy and its disorders have utilised microarray technology (Enquobahrie et al., 2008, Akehurst et al., 2015, De Felice et al., 2015, Sitras et al., 2015, Zhao et al., 2014, Lian et al., 2010, Cox et al., 2015). These studies allow for a vast number of gene expressions to be assessed at the same time and have revealed large numbers of gene changes; however, they do not cover the entire genome (Cox et al., 2015, Chandran et al., 2016). Microarray studies have revealed many genes that are differentially expressed in the placenta of normal and hypertensive pregnancies (Kleinrouweler et al., 2013). However, the systematic review by Kleinrouweler *et al* found inconsistencies with the differential expression of reported genes (Kleinrouweler et al., 2013). Microarrays produce information about expression of specific genes due to defined probes on the arrays themselves, meaning different study designs will lead to investigations examining different sets of specified genes and thus not reaching consensus easily. Alternatively, studies using similar arrays of gene probes may artificially inflate the significance of certain gene changes. The more recent next generation sequencing technique of high-throughput RNA sequencing (RNA-Seq) allows for the profiling of all transcribed RNAs across an entire genome, and may be more appropriate in examining gene changes in pregnancy (Wang et al., 2009). This technology provides information on gene expression that is not limited to the known genomic sequence (Wang et al., 2009). RNA-Seq also highlights all RNA populations in a cellular/molecular system (Table 1-3); including long non-coding RNAs (lncRNA), which are becoming known to have a more prominent role in many cellular functions and diseases, having been found to be associated with the regulation of gene expression (He et al., 2013, Wang and Chang, 2011). RNA-

Seq is being utilised in pregnancy research, mainly in examination of the placental transcriptome (Shankar et al., 2012, Kaartokallio et al., 2015). The first of the large-scale studies identified 53 differentially expressed genes between 'normal' and pre-eclamptic placenta (Kaartokallio et al., 2015). RNA-Seq has also been utilised to examine the different transcriptome signatures of single cell types in the human placenta (Nelson et al., 2016, Tan et al., 2016). A study specifically focused on examining the transcriptome profile of the maternofetal interface using single cell RNA-seq provided information on the transcriptome signatures of individual cell populations that stem from the placenta and influence maternal decidua (Nelson et al., 2016). However, the nature of this analysis meant that maternal responses were only assessed in relation to shallow trophoblast invasion and no vasculature was examined. Whilst this does provide in-depth detail of gene regulation of specific functional biological pathways of the placental and decidual cell types alone, it does not detail how one influences the other.

**Table 1-3: Most common transcript biotypes detected in RNA-Seq studies and the known number annotated in human, rat and mouse**

| Transcript Biotype | Human | Mouse | Rat |
|---|---|---|---|
| **Protein coding** | 20,376 | 22,630 | 22,250 |
| **Non-coding** | 22,305 | 15,537 | 8,934 |
| ***Small non-coding*** | *5,363* | *5,531* | *5,122* |
| ***Long non-coding*** | *14,720* | *9,443* | *3,288* |
| ***Misc. non-coding*** | *2,222* | *536* | *524* |
| **Pseudogenes** | 14,692 | 12,522 | 1,668 |
| **All transcripts** | **203,903** | **135,276** | **41,078** |

Only a small number of studies have examined gene expression in maternal tissue and the majority have isolated the transcript signatures of term pregnancies when a myometrial biopsy is taken during caesarean sections. Kim *et al* examined the transcriptome landscape of the placenta which included identifying the gene signature of the maternal tissue (the decidua) using RNA sequencing (Kim et al., 2012). This revealed that there is a vast difference in the transcriptome profile between the maternal decidua and the placenta as well as

between different tissues in the body. However, genes involved in vascular remodelling and development were identified (from Gene Ontology terms) in the chorion of the placenta (where placental angiogenesis occurs), yet were not identified in the decidua suggesting the presence of the spiral arteries in the decidua were not reflected in the gene data. (Kim et al., 2012). This may be due to decidual samples being macroscopically dissected from term placentas, and therefore would only be very superficial placental bed samples. This could suggest that the method of maternal decidua tissue collection is not appropriate for sampling the changes in the maternal uteroplacental vasculature. A flaw in these human studies is that they only isolate tissue and cells at term. This is understandable due to the inaccessibility of early gestation tissue; however, the gestational time point will most likely heavily influence the transcriptome profile of both the placenta, decidua and spiral arteries due to the relatively short timescale of placental development compared to other organs. Furthermore, studies in term placental tissue have highlighted that the placenta has diversity in gene expression profiles that differ from other tissues. Therefore in this short-lived organ the gene expression and RNA processing changes may have a profound impact on function relatively quickly (Kim et al., 2012). The sampling of tissues from different gestational ages is difficult in humans due to ethical considerations of collecting early pregnancy tissue. Non-pregnant maternal tissue can only be collected from hysterectomies, yet this presents challenges with age matching samples and introduces increased variability as the hysterectomy may have been required due to another condition, such as cancer, which would impact the RNA profile of the tissue significantly. There has been some investigation into early pregnancy gene expression differences using human trophoblast cell lines (Highet et al., 2016). Highet *et al* attempted to investigate placental angiogenesis using the HTR8/SVneo trophoblast cell line which mimics blood vessel development. This focused on trophoblast invasion gene expression, and used a directed microarray so was comparatively limited. The microarray method is also more biased than RNA-Seq as the expression of genes are examined are targeted and planned, instead of examining the entire transcriptome. Furthermore, the approach using an *in vitro* mimic of blood vessel formation cannot detail the maternal uterine and spiral artery response to placentation. The transcription level knowledge in this area is lacking as no

studies have specifically examined maternal uteroplacental vasculature or the transcription-controlled responses of the spiral arteries to placentation.

## 1.4 Animal models of pregnancy

Animal models are crucial in fully understanding pregnancy and pregnancy disorders. Utilising appropriate animal models avoids placing human mothers and fetuses at risk. Most information of placental physiology in humans has been obtained at delivery; which only provides information on the fully formed placenta, or from elective abortions; which are infrequently used due to the ethical considerations and at this stage it cannot be determined whether the pregnancy was to go on to develop problems (Guttmacher et al., 2014). Furthermore, most pregnancy focused studies cannot accurately measure changes to the cardiovascular and renal systems in humans due to the most reliable measurements needing invasive procedures. The hazards associated with invasive measures of uterine blood flow and placental function *in vivo* also highlight the need to study these systems in animal models to gain better insight into the human condition.

Pregnancy and placental research have developed exponentially with the utilisation of experimental animal models and without these models a full understanding the physiological changes *in vivo* would be near impossible. However, care must be taken when choosing to study human pregnancy conditions in an animal model as placentation differs hugely across species and with a wide variety of placental structures making comparisons difficult. One group of mammals, however, are most appropriate for human research; those with haemochorial placentas. Haemochorial placentation occurs in humans and in higher order primates, guinea-pigs, rats and mice. This type of placentation allows maternal blood to come into direct contact with fetal cells (the chorion) allowing rapid transfer of gases, solutes and nutrients.

Animal models are a good substitute when investigating these maternal responses to placentation and pregnancy, especially at the early time points. Rodent placentation and humans have striking similarities and findings from these animals can guide knowledge on human pregnancies. Both humans and rodents have similar placentation with rats mimicking the deep trophoblast invasion that has been observed in humans (Wooding and Burton, 2008). These similarities allow us to carefully extrapolate the basic mechanisms of early pregnancy. The transcriptome of the rat placenta at term has been investigated

and compared with human pregnancy pathologies such as maternal obesity, gestational hypertension and placental ischemia and has also proven invaluable in understanding the normal physiological mechanisms of placentation and pregnancy induced gene expression changes (Shankar et al., 2012, Vaswani et al., 2015, George et al., 2014). Yet, no animal model is perfect in recapitulating human HDP. This is due to pregnancy-induced hypertension being specific to humans and some old-world monkeys (Thornton and Onwude, 1992). However, there is a wealth of possibility to study various phenotypes and impacts of HDP with the best course being the utilisation of a wide range of animal models.

### 1.4.1 Pregnancy in Rodents

The animals used in the study of pregnancy and placentation vary from routine laboratory animals, such as rabbits, rats and mice, to the more exotic, such as guinea pigs, chinchillas and baboons (Mikkelsen et al., 2017, Grigsby, 2016). Whilst all the afore mentioned animals have similar placentation to humans; rats and mice have proved the most appropriate animals to use due to their ease of use and maintenance (McCarthy et al., 2011, Dilworth and Sibley, 2013). Rat gestation differs greatly from human in that it occurs over 21-22 days, compared to the human 40 week gestation period. Implantation of multiple offspring in rodents occurs between 4 and 5 days postcoitous and decidualization differs from humans as it is stimulated by the implanting blastocyst and is not a cyclical process. However, there are major similarities between human and rat placentation, including the invasion of trophoblast cells into the maternal decidua and into the proximal region of the myometrium. The maternal uteroplacental vasculature of women and rats has a similar structure regardless of the uterine structural differences (Figure 1-10), as both have main uterine arteries that branches into arcuate, radial and finally spiral arteries. The spiral artery remodelling and changes observed to maternal uteroplacental circulation are also similar between rat and humans (Osol and Moore, 2014). Table 1-4 shows the similarities and differences between these animals and human placentation.

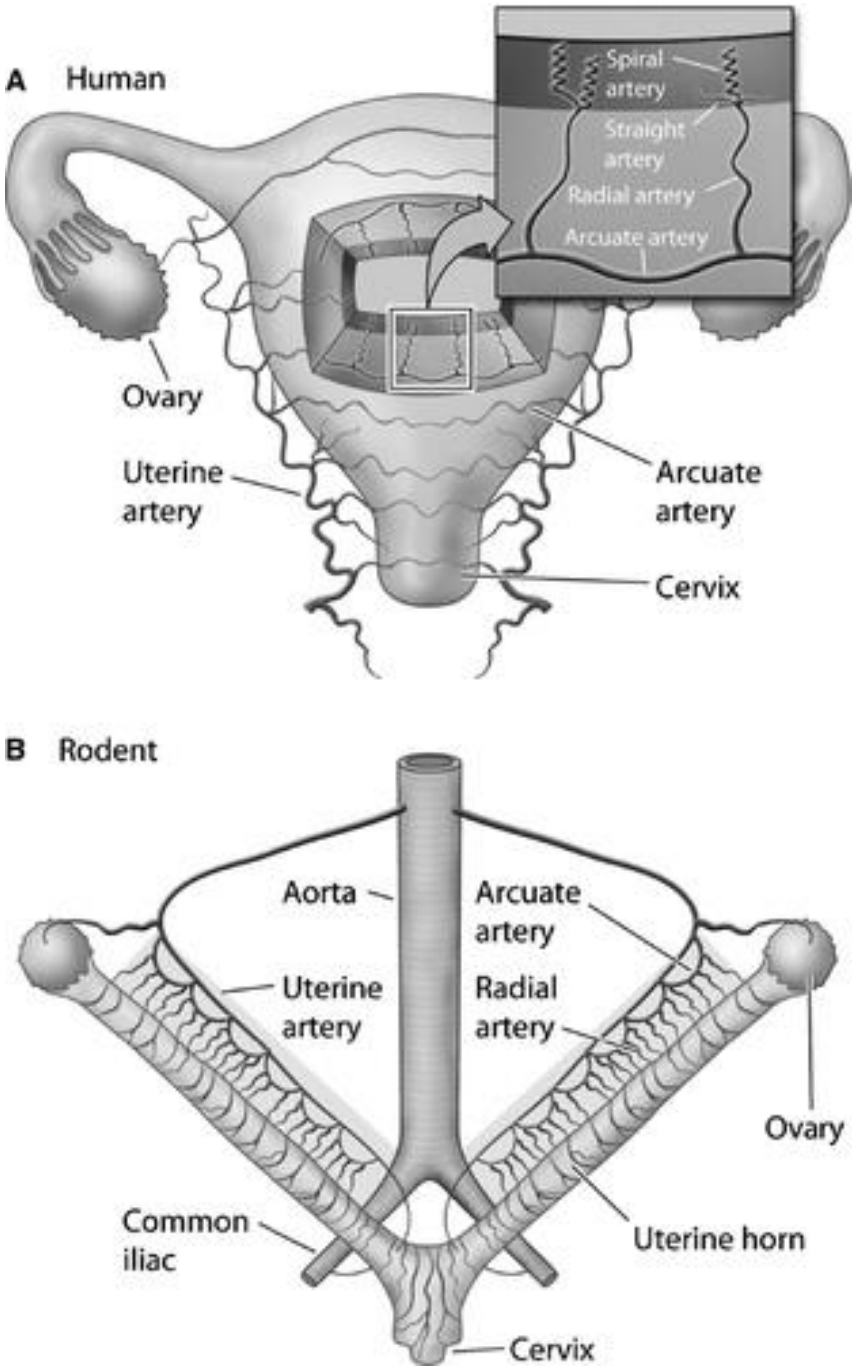


**Figure 1-10: Comparison of the human and rodent uterine vasculature**
The human (A) and rodent (B) uterus with blood supplied from main uterine arteries branching into uterine tissue culminating in spiral arteries. This image was reproduced with permission from (Osol and Moore, 2014)

**Table 1-4: Comparison between key placentation events in the human, rat and mouse**

| Human | Rat | Mouse |
|---|---|---|
| – Discoid and haemomonochorial placental structure<br>– Villous structure<br>– Remodelling of spiral arteries linked to trophoblast invasion<br>– Deep trophoblast invasion through decidua and proximal part of myometrium | – Discoid and haemotrichorial placental structure<br>– Labyrinthine structure<br>– Remodelling of spiral arteries linked to trophoblast invasion<br>– Deep trophoblast invasion through decidua and proximal part of myometrium | – Discoid and haemotrichorial placental structure<br>– Labyrinthine structure<br>– Remodelling of spiral arteries linked to trophoblast invasion<br>– Shallow trophoblast invasion |

#### 1.4.1.1 Rodent Placentation

Many reviews of *in vivo* pregnancy and placental research group rats and mice together under rodents or use evidence from one animal to establish a conclusion about the other (Soares et al., 2012). There are notable differences in mouse vs. rat vs. human gestation. Rats have a much shorter gestation time and a greater number of offspring compared to humans. Yet the placenta, even though it develops at a much more rapid pace in rats than in humans, has many similarities between the two. Analogous trophoblast cell types have been found with the human extra-villous trophoblasts showing similarities to invasive trophoblasts in rats. These invasive trophoblasts have been proposed to arise from the junctional placental zone (most proximal to the maternal decidua) and have been found to invade deep into the decidualized endometrium and into the myometrial portions of spiral arteries (Ain et al., 2003). This process is most similar to the deep trophoblast invasion observed in human placentation than in mice where trophoblast invasion is shallower (Ain et al., 2003, Verlohren et al., 2008). Furthermore, rats have a similar maternal vascular response to placentation as the uterine arteries undergo a similar remodelling process as in humans (Osol and Cipolla, 1993).

Both human and rat placenta are haemochorial, which means that the trophoblast cells of the placenta are in direct contact with maternal blood (Figure 1-11). Transport across the placenta in rats and humans is also analogous with the same transporters for specific amino acids (e.g. taurine and system A) being utilised for placental transport in both species (Glazier et al., 1996). The two placenta types do differ in that rats have haemotrichorial placentas (three trophoblast layers) whilst humans have haemomonochorial placentas (one layer). Therefore rat placentas, like in mice, have three trophoblast cell-layers as a barrier between fetal blood and maternal blood (Figure 1-11C), whereas humans only have one full layer, the cytotrophoblasts fuse to form the syncytiotrophoblast layer (Figure 1-11D) (Huppertz, 2008, Dilworth and Sibley, 2013). Figure 1-11 illustrates that whilst the gross placental structures of the two species seem very different, the cytoarchitecture is similar. Rat trophoblast layer I consists of very sparse mononuclear trophoblasts that do not create a sufficient permeability barrier, this proposes that the syncytial layer II is the first barrier to nutrient exchange, suggesting that it has the most functional

similarity to the human syncytiotrophoblast layer. The maternal facing syncytiotrophoblast (microvillus membrane (MVM)) of the human placenta is analogous to the maternal facing membrane of trophoblast layer II in rats. The human MVM and the apical trophoblast layer II of rat have both been found to utilise the same calcium transporters of the transient receptor potential gene family and both have been found to have the enzyme alkaline phosphatase localised to this area (Dilworth et al., 2010). The human syncytiotrophoblast basal membrane and possibly also the cytotrophoblast layer have been suggested to be analogous to the fetal facing side of rat trophoblast layer III, however, due to their fetal facing location it is very difficult to obtain samples and perform reliable experiments that can conclude any similarities/differences (Dilworth and Sibley, 2013).

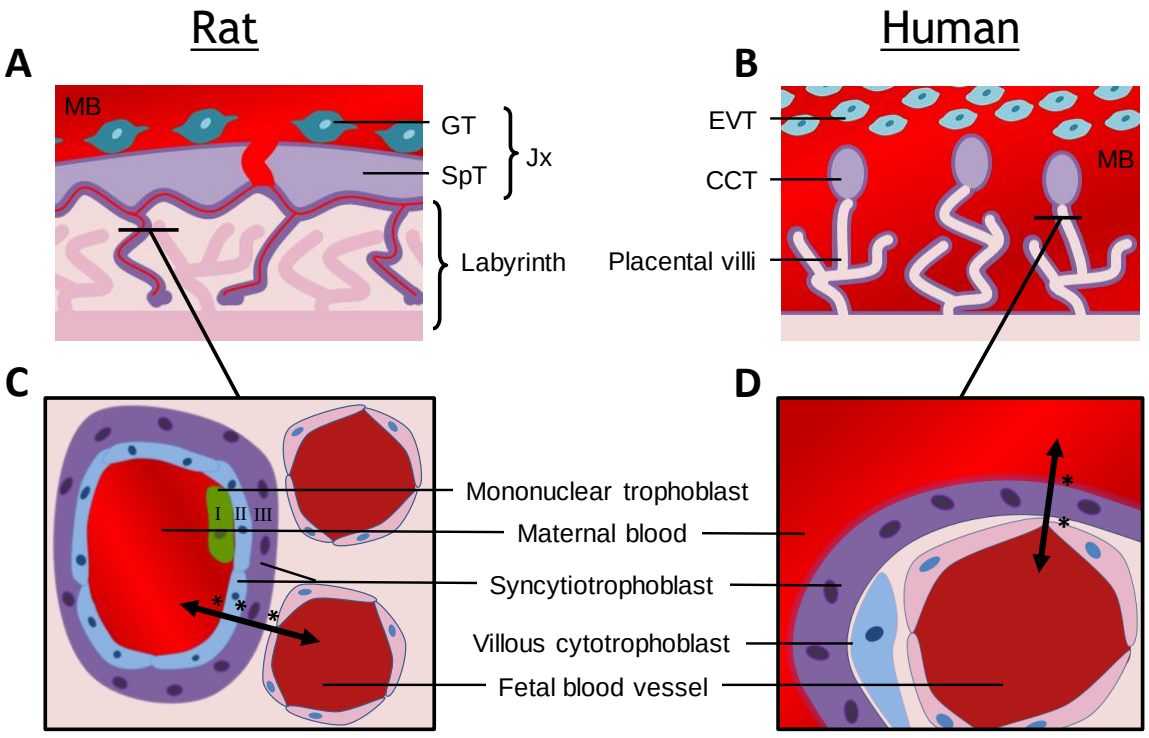


**Figure 1-11: Comparison of the rat and human placental cellular structure and villous compositions**
The structure of (A) the rat labyrinthine placenta and (B) the human villous placenta. Placental tissue is depicted in purple/green and fetal tissue is pink. Maternal blood (MB) is in red. (A) The rat placenta is composed of a junctional (Jx) zone near on the maternal side which consists of giant trophoblast cells (GT) and spongiotrophoblasts (SpT). (B) The human placenta consists of placental villi in direct contact with maternal blood in the intervillous space. The villi have clusters of column cytotrophoblast cells (CCT) which anchor the placenta to maternal decidua, also present are extravillous trophoblasts (EVT) which invade and remodel maternal spiral arteries (not shown). (C-D) Are cross-sectional diagrams of the maternofetal exchange area. * Barriers to maternofetal transport. Adapted from (Rossant and Cross, 2001).

#### 1.4.1.2 Rodent Models of Pre-eclampsia

Animal models are of paramount importance to pregnancy research as they can be used to investigate the underlying causes of abnormality and the fetal outcome. They are essential in understanding the molecular basis of pre-eclampsia which is crucial for developing the current understanding of this pregnancy disorder. A good animal model requires a multitude of factors to resemble the multi-phenotypic nature of the human condition, such as developing hypertension and proteinuria specific to pregnancy, but also having a disproportionate balance of angiogenic factors and displaying endothelial dysfunction as well as abnormal uterine artery remodelling (McCarthy et al., 2011). Despite pre-eclampsia being unique to humans and some higher order primates, there are a number of available animal models that can be used to study specific phenotypes of pregnancy induced hypertension and pre-eclamptic like symptoms with a varying degree of usefulness (McCarthy et al., 2011). The outline of some of the most used rodent models below is not exhaustive and many strategies of imposing HDP in rodents can be used in combination (Arguelles et al., 2017, Murphy et al., 2012, Shirasuna et al., 2015).

#### 1.4.1.3 The Reduced Uteroplacental Perfusion Model

A reduced uteroplacental blood flow has been implicated in the pathogenesis of some HDP, especially pre-eclampsia (Pijnenborg et al., 1991, Brosens et al., 1972). A model of studying early term pre-eclampsia is the reduced uterine perfusion pressure (RUPP) model. This model involves surgically restricting the aorta (above the iliac bifurcation) and ovarian arteries mid-way through gestation (GD14.5) to reduce blood flow to the uterus. This method induces hypertension during pregnancy and reduces uteroplacental blood flow by approximately 40% (Granger et al., 2006). The most common and well characterised of the RUPP models is the RUPP rat. Characterised by Granger *et al* this model of reduced uteroplacental perfusion mimics symptoms of early stage severe pre-eclampsia (Crews et al., 2000, Alexander et al., 2001, Granger et al., 2006). These include an increased blood pressure (around 30mmHg higher than normal pregnancy levels), an increased peripheral resistance, decreased cardiac output, decreased renal plasma flow and kidney function, proteinuria, systemic endothelial dysfunction and fetal growth restriction (Granger et al., 2006, Brennan et al., 2016, Walsh et al., 2009). Whilst not spontaneous, the

symptoms were found to be pregnancy specific as reducing perfusion to the uterus in non-pregnant rats did not elicit a blood pressure response (Alexander et al., 2001). Interestingly, the RUPP model does show a resolution of blood pressure back to normotensive levels after delivery yet retains some systemic vascular dysfunction, observed in mesenteric and thoracic arteries 3 months postpartum (Brennan et al., 2016). This is a useful caveat of this model due to the mounting evidence supporting the theory that women with a past pre-eclamptic pregnancy are more at risk to cardiovascular disease in later life (Sattar and Greer, 2002).

The advantages of this model as a model of pre-eclampsia are clear, in that it matches the major symptoms and stimulates placental ischemia. However, one major disadvantage of the RUPP rat model is the large number of animals required due to exclusion of dams with total loss of pregnancy. All previous studies using this method have stated that dams with no viable pups were excluded, and of those that reported the number of excluded animals, up to 37% removed from the studies (Brennan et al., 2016).

#### 1.4.1.4 Nutritional and Pharmacological Models

Both maternal and paternal nutrition prior to and during pregnancy can impact fetal development (Roseboom et al., 2006, Barker, 1991, Watkins et al., 2017). The majority of diet manipulation is used more to investigate the impact of obesity on pregnancy, or nutritional influence on the development and health quality of the offspring, with hypertension being studied in subsequent generations and not the mothers (Fraser et al., 2010, Gaillard et al., 2014, Richter et al., 2009).

HDP can be mimicked pharmacologically using infusions of substances known to cause systemic vascular dysfunction by promoting inflammation and endothelial damage, such as sFlt-1, TNF-α, interleukin-11, L-NAME and AngII. All these substances have the ability to ultimately increase uteroplacental vascular tone, thus mimicking the reduced placental perfusion (Murphy et al., 2012, Bobek et al., 2015, Zhou et al., 2007, Winship and Dimitriadis, 2018, Soobryan et al., 2017). All these models described can provide an insight into a variety of factors that arise as a consequence of pre-eclampsia (i.e. fetal growth restriction and

other conditions of fetal distress). However, they are simulating hypertension by means of applying the stressors that are caused by pre-eclampsia and other HDP, therefore may not be very useful in determining underlying predispositions or causal mechanisms of development.

#### 1.4.1.5 Renin-Angiotensin Manipulation Models

Healthy pregnancies in both humans and rodents have increased RAS activity and RAS component expression within the placenta (Vaswani et al., 2015). A dysregulation of the RAS has long been associated with development of HDP (Herse et al., 2007). Alterations of the RAS in rodents have been utilised to create hypertensive models for decades and have been used by several groups to mimic HDP (Xue et al., 2017, Hering et al., 2010, Brewer et al., 2013, Kawada et al., 2002). The chief focus has been on the assessment of hypertension development in adult offspring exposed to AngII *in utero,* with maternal maladaptation being presented only as evidence of HDP symptom development. For example, Xue *et al* utilised AngII infusion to mimic hypertensive pregnancy to investigate the impact on offspring brain development and pre-disposition to hypertension in adult life (Xue et al., 2017).

Pre-eclampsia has been associated with an increased AngII sensitivity proposed to be due to increased activation of the $AT^1R$ via the angiotensin II type I receptor. The $AT^1R$ receptor autoantibody ($AT^1$-AA) has been found to have higher affinity for this receptor than AngII and is increased in pre-eclampsia (Leung et al., 2001). Rat models have been developed that exploit this knowledge by infusing otherwise healthy rat pregnancies with $AT^1$-AA (Herse and LaMarca, 2013, Wallukat et al., 1999, Zhou et al., 2008). These models found that increasing $AT^1$AA in serum the pregnant rodents produced pre-eclamptic phenotypes such as elevated blood pressure, evidence of proteinuria, increased mediators of endothelial dysfunction (e.g. sFlt-1, soluble endoglin) and impaired renal function.

Another method of manipulation of the RAS comes from transgenic crosses which artificially elevate the concentrations of placental specific AngII. Female mice with the human angiotensinogen gene developed pregnancy specific hypertension when mated with males carrying the human renin gene (Takimoto

et al., 1996). This highlights the importance of AngII production in regulating maternal hypertension during pregnancy, and the important role the placenta plays in pregnancy specific hypertension. Many more studies have utilised this transgenic cross in both rats and mice (Hering et al., 2010, Bohlender et al., 2000, Denney et al., 2017). Due to the consensus that there is a sudden yet sustained increase in blood pressure from mid-gestation which returned to pre-pregnancy levels after delivery, this model is highly appropriate for studying outcomes of gestational hypertension, however its usefulness is limited in uncovering underlying mechanisms. The model mirrors symptoms of human pre-eclampsia with significantly increased blood pressure, increased proteinuria, evidence of kidney damage and a reduction in fetal weight. This model may be particularly useful for examining the offspring from these transgenic crosses, as these have been found to have vascular and cardiac dysfunctions later in life, however this may be confounded by the fact that the offspring themselves will possess both human renin and angiotensinogen (Bohlender et al., 2000).

#### 1.4.1.6 Genetic Models

The term HDP encompasses many conditions, each one multifactorial, which makes it impossible to perfectly reproduce a model of the entire disorder. Instead, one of the more successful approaches is to focus on a specific cause of a specific phenotype and create genetic manipulations that mimic this. Endothelial dysfunction is a common manifestation of many HDP (Crews et al., 2000). As such the genetic knockout of endothelial NO synthase (eNOS-/-) has shown promise in investigations of HDP due to its impaired uterine artery function (Kulandavelu et al., 2013, Kusinski et al., 2012, Hefler et al., 2001). However, not all studies have agreed on the profile of maternal blood pressure in the eNOS-/- model. Shesely *et al* found that whilst eNOS-/- mice had pre-pregnancy hypertension, these dams were not hypertensive during pregnancy; possibly due to the pregnancy associated BP reduction (Shesely et al., 2001). However, Hefler *et al* did not observe pregnancy dependent reduction in maternal BP in the eNOS-/- model and furthermore found a significant increase in maternal blood pressure in the 2$^{nd}$ and 3$^{rd}$ 'trimesters' compared to wild type animals. However this significant difference could be attributed to the pregnancy dependent decrease in BP of wild type animals (Hefler et al., 2001). The confusion surrounding the maternal BP profile of the eNOS-/- model may

place it as a more appropriate model to examine fetal growth restriction, caused by poor placental perfusion rather than HDP (Kusinski et al., 2012).

A deficiency in catechol-O-methyltransferase (COMT-/-) has also proved useful in replicating underlying causes of pre-eclampsia. COMT-/- mice are characterised by pregnancy hypertension and proteinuria (McCarthy et al., 2011, Kusinski et al., 2012, Kanasaki et al., 2008). The deficiency in COMT means that 2-methoxyestraadiol, a metabolite of oestrogen and prominent vasodilator, is not produced leading to antiangiogenic effects and increased Hif-1α and sFlt-1 levels (Kanasaki et al., 2008). These models also demonstrate abnormal uterine and umbilical Doppler waveforms with diastolic notching, indicative of impaired uteroplacental blood flow and placental hypoxia and commonly used as a diagnostic tool for pre-eclampsia (Stanley et al., 2012, Kanasaki et al., 2008, Fleischer et al., 1986). Indeed, the uterine arteries of these mice have been found to have a more propagated contractile response to vasoconstrictive agents (Stanley et al., 2012).

The borderline hypertensive mouse (BPH/5) is an inbred mouse strain that spontaneously develops hypertension and proteinuria during late gestation (Davisson et al., 2002). The BPH/5 mice are hypertensive prior to pregnancy with a blood pressure approximately 20mmHg higher than C57 reference strains, yet pregnancy worsens this hypertension, and by late gestation the blood pressure is approximately 1.5x times higher than the reference strain (Davisson et al., 2002). It has also been noted that this model has evidence of kidney damage, proteinuria, systemic endothelial dysfunction and increased decidual inflammation (Davisson et al., 2002, Heyward et al., 2017). This model is an interesting model as it is more likely than specific knockouts to have more relevance to the human multifactorial condition and can also be used to investigate the effects of pre-hypertension on pregnancy and effects on offspring development and health. However, the mouse placentation process is lacking in similarity to the human placenta when compared to the rat.

## 1.5 The Stroke-Prone Spontaneously Hypertensive Rat

The stroke-prone spontaneously hypertensive (SHRSP) rat is a genetically inbred hypertensive model, which has been used in the study of human essential hypertension and stroke for decades. Despite the breeding of this strain since the 1960s, very few studies have examined the SHRSP pregnancy and its use as a model of HDP has not been fully assessed.

### 1.5.1 SHRSP characteristics and history

SHRSP rat origins stem from the University of Kyoto where the selective breeding of Wistar Kyoto (WKY) rats with slightly elevated blood pressure produced the spontaneously hypertensive rat (SHR) in 1963 (Okamoto and Aoki, 1963). The SHR strain was subjected to further selective inbreeding to produce the SHRSP rat in 1974 (Yamori and Okamoto, 1974), which has been further inbred in many institutions (including the University of Glasgow) (Figure 1-12). The male SHRSP develops hypertension at approximately 8 weeks of age (Ueda et al., 1979). It has the highest blood pressure of these spontaneously hypertensive rat strains; >220mmHg (Yamori and Horie, 1977). In comparison the SHR blood pressure maximum is approximately 200mmHg. The SHRSP is also 70% more likely to suffer a stroke than the SHR strain, with incidence of stroke in SHRSP on high salt diets being 100%. This, therefore, is a model of a more extreme hypertensive condition associated with increased endothelial dysfunction and left ventricular hypertrophy as the animal ages (Harvey et al., 2017, Jesmin et al., 2005). It is these multiple pathologies that make it an incredibly relevant model for human cardiovascular disorders. The genome of both the SHRSP and normotensive WKY has been sequenced, for both the original strains and the colonies maintained at the University of Glasgow (Atanur et al., 2013), making this model even more suited to studying the genetic influences of hypertension (Delles et al., 2008).

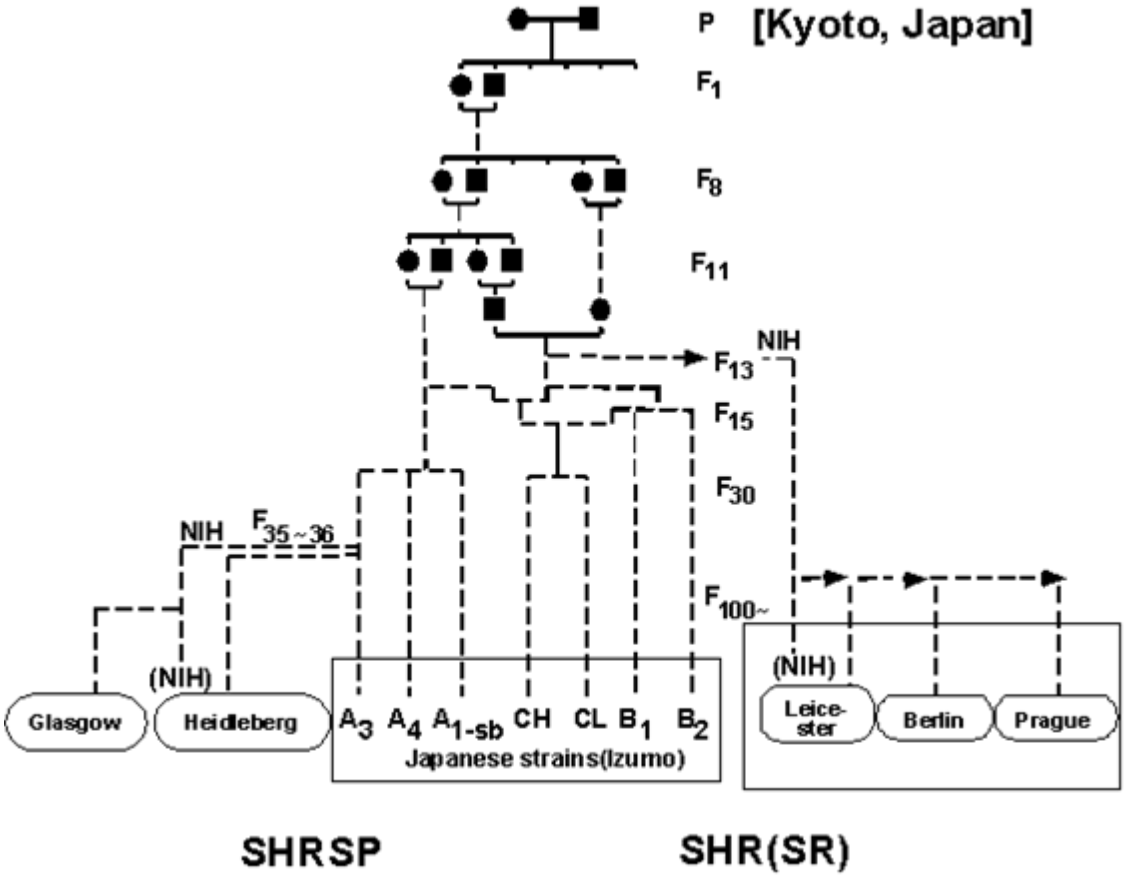


**Figure 1-12: Genealogy of the Stroke-Prone Spontaneously Hypertensive Rat**
Selective breeding of hypertensive WKY rats lead to the first generation of SHR rats in Kyoto, Japan (P). Subsequent generations (F) where in bred in many institutes and locations, eventually leading to the current strains available, detailed at the base of the diagram. NIH: National Institute of Health

### 1.5.2 Uses in Cardiovascular Disease and hypertension

The SHRSP rat has been key in the discoveries of the genetic basis of hypertension, specifically the revelation of specific quantitative trait loci involved in blood pressure regulation (Hilbert et al., 1991, Jacob et al., 1991). The hypertension in this model is multifactorial and, like the human condition, is worsened by elevated dietary salt and reduced potassium, which can lead to damage to the cardiovascular system; resulting in ischemic stroke, cardiac hypertrophy and renal disease (Di Castro et al., 2013, Takeda et al., 2001).

There is evidence of the SHRSP model having a dysregulated RAS. SHRSP have been found to have higher plasma renin activity and AngII levels as well as an increased renal sensitivity to AngII (Takemori et al., 2005, Berecek et al., 1980). With the RAS being intimately associated with blood pressure regulation, these dysregulations are important in the study of hypertensive disorders and treatment options. SHRSP rats have also been found to have high vascular oxidative stress, mediated by a dysregulation of the Nrf2-antioxidant system promoting a shift towards pro-oxidants and thus increasing endothelial dysfunction and vascular damage (Lopes et al., 2015). Evidence of vascular dysfunction is further supported by the findings of Kerr *et al* who found an increase in superoxide produced by NADPH oxidases in the vascular smooth muscle cells of SHRSP, and proposed this could account for the decreased nitric oxide availability observed in SHRSP rats (Kerr et al., 1999). However, this study also found a dissimilarity between male and female SHRSP, with female SHRSP having a lower aortic endothelial nitric oxide synthase (eNOS) expression than their male counterparts yet still generating increased superoxide levels than WKY females (Kerr et al., 1999).

The majority of studies examining cardiovascular disease, stroke and hypertension using the SHRSP rats have focused on the males. This is generally due to the males having higher blood pressure and associated end-organ damage, and it reduces experimental variability introduced by the hormone cycling specific to females. (Davidson et al., 1995, Clark et al., 1996). However, due to the preference of male use in pre-clinical research, knowledge of vascular disease in females is lacking (Anthony and Berg, 2002). This gender

disparity is important as it is only the female that must physiologically respond to pregnancy.

### 1.5.3 SHRSP Maternal Pregnancy Characterisation

The hypertensive pregnancy of the SHRSP rat was first examined and published in the late 1970s and early 1980s (Yamada et al., 1981, McCarty and Kopin, 1978). These early studies examined SHRSP blood pressure over gestation, finding dams remained hypertensive throughout pregnancy, yet were limited in their examinations of maternal and fetal impairments associated with HDP. More detailed pregnancy outcome characterisations of the SHR revealed that this model has hypertensive pregnancies, with blood pressure lowering towards delivery, associated with less maternal weight gain, an increased fetal loss and some histological evidence of placental haemorrhage (Lorenz et al., 1984, Scott et al., 1985, Lewis et al., 1997, Peracoli et al., 2001). There is some contradiction as to whether this hypertension impacts fetal weight with some finding a reduced weight compared to WKY and others no difference (Lewis et al., 1997, Scott, 1986, Peracoli et al., 2001). Fewer studies have been conducted specifically on the SHRSP than have been carried out on the SHR, with only 18 recorded publications found between 1979 and 2018 (search conducted May 2018). From the small numbers examining SHRSP pregnancy in comparison to normotensive WKYs, it was revealed that SHRSP pregnancies are hypertensive throughout, with a dip in blood pressure towards delivery (Gompf et al., 2002, Small et al., 2016, Barrientos et al., 2017). These studies further suggested that SHRSP fetal development may be impacted by this hypertension, due to reduced fetal weights, a smaller number of pups per litter and increased fetal loss (Fuchi et al., 1995a, Small et al., 2016, Barrientos et al., 2017). Placental abnormalities have been documented in SHRSP pregnancy. These include a reduced transport capacity (inferred from lower placental $Na^+/K^+$ ATPase activity), structural abnormalities (with a loss of glycogen cells in the placental junctional zone and reduced labyrinth vascularity) and a reduced endovascular trophoblast invasion into the spiral arteries (Fuchi et al., 1995a, Barrientos et al., 2017, Ferrazzi et al., 2018). Two studies have examined maternal vascular function in pregnant SHRSP (Gompf et al., 2002, Small et al., 2016). Gompf *et al*, focused on maternal aortic function and found increased vasodilatory responses in pregnant compared to non-pregnant vessels from both normotensive

WKY and hypertensive SHRSP (Gompf et al., 2002). SHRSP aortas from pregnant dams demonstrated a propagated relaxation response to stimulated NO release and increased eNOS expression compared to pregnant WKY (Gompf et al., 2002). A different vascular bed was examined by Small *et al*, this revealed that SHRSP uterine arteries have an impaired vasodilatory ability and enhanced contractile response (Small et al., 2016) (Figure 1-13). This was evident in virgin WKY and SHRSP comparisons, and whilst the pregnant SHRSP uterine arteries did become more responsive to vasodilatory agents it was still reduced compared to normotensive WKY dams. Also evident were structural variations in the pregnant arteries compared to normotensive WKY rats, with SHRSP arteries having smaller diameters both pre-pregnancy and at term. This study is suggestive that the SHRSP have an impairment in uterine artery remodelling during pregnancy and that the response is not due to a systemic hypertension, as antihypertensive treatment with Nifedipine failed to improve the structural and functional effects on the uterine artery. The impaired uteroplacental blood flow in the SHRSP could therefore be impacting the placental function and offspring outcome. Yet it is unclear why the SHRSP have these impairments and how the maternal cardiovascular impairment may play a role in their development.

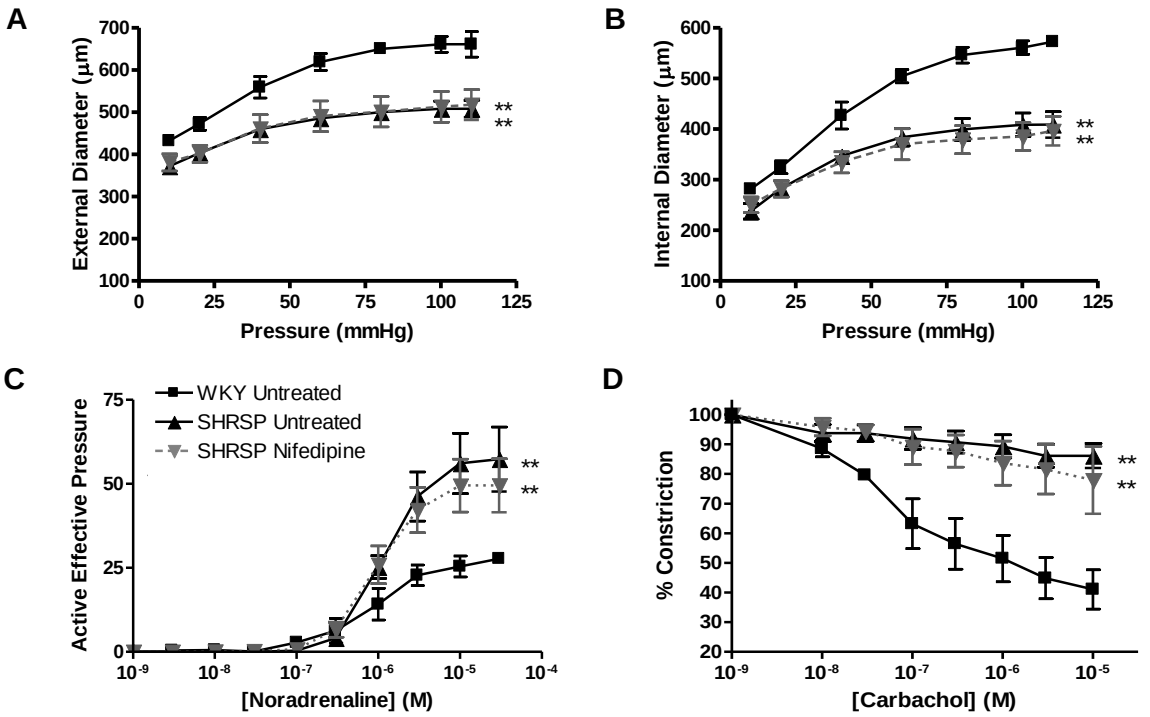


**Figure 1-13: Diameters and functional responses of uterine arteries from pregnant WKY and SHRSP dams**

The external and internal diameters (A-B) and functional responses to noradrenaline (C) and carbachol (D) of uterine arteries from pregnant (GD18.5) WKY, SHRSP and SHRSP treated with Nifedipine. SHRSP dams with and without Nifedipine treatment demonstrated reduced uterine artery diameter and impaired constriction and dilation; ** $p<0.01$ vs. WKY. Data analysed by comparing area under the curve values using one way ANOVA and Tukey's post-hoc test. Published in Small *et al.,* 2016

## 1.6 Hypothesis and Aims

The maternal SHRSP vasculature fails to adapt normally to the demands of pregnancy. In an exacerbated hypertensive pregnancy, SHRSP rats demonstrate pathophysiologies associated with human superimposed pre-eclampsia and the poorer pregnancy outcomes associated with hypertensive pregnancies.

- To fully assess maternal response to pregnancy in SHRSP dams by examining the cardiovascular and renal systems and haemodynamic changes through gestation.

- Examine placentation and fetal outcome in SHRSP pregnancies.

- Gain insight into underlying genetic differences between uterine arteries of SHRSP and WKY dams to examine how the uterine artery transcriptome changes in response to pregnancy.

- Create a model of hypertensive pregnancy with increased cardiovascular load to impose excess maternal stress and mimic superimposed pre-eclampsia.

# Chapter 2 General Materials and Methods

This section describes the standard laboratory practice and common methods. More specific methods are outlined in each chapter.

## 2.1 General Laboratory Practice

All procedures were carried out in a laboratory setting following general laboratory health and safety guidelines. A laboratory coat and non-latex powder free gloves were worn at all times during procedures. Hazardous reagents were handled as per manufactures safety datasheets and disposed of as described in the Control of Substances Hazardous to Health regulations.

Laboratory equipment was ensured to be in working order and cleaned prior to and after use. All glassware and re-usable plastic were cleaned by soaking in Decon 75 detergent (Decon Laboratories Ltd, Sussex, UK) and rinsed with distilled water and dried at 37°C. Other plastics used were sterile and disposable. These included microcentrifuge tubes of varying sizes (Greiner Bio-One, Gloucestershire, UK), 15ml and 50ml Corning® centrifuge tubes (VWR, Leicestershire, UK), 5ml and 20ml Sterilin™ containers (VWR, Leicestershire, UK) and Corning® cell culture flasks and plates (VWR, Leicestershire, UK).

Calibrated Gilson pipettes were used when necessary with sterile, appropriately sized pipette tips (Greiner Bio-One, Gloucestershire, UK), ranging from 0.1µl to 1000µl. For volumes of liquid between 1ml and 25ml Stripette® serological pipettes were used with an electronic pipette filler (ThermoFisher Scientific, Paisley, UK), for volumes larger than 25ml clean measuring cylinders were used. Regents were weighed on either a Mettler Toledo PB1501 balance (sensitive to 0.1g) or a Sartorius Extend balance (sensitive to 0.0001g). The measurement and adjustment of pH was conducted using a Jenway 3510 pH meter calibrated before each use following manufactures protocol.

Centrifugation of sample volumes less than 2ml was conducted using a desktop Eppendorf 5145 R microcentrifuge at 4-20°C. Larger volumes and 96 and 384 well plates were centrifuged using a Mega star 3.0R centrifuge (VWR, Leicestershire, UK).

All experiments involving ribonucleic acid (RNA) extraction required a ribonuclease (RNase) free environment, thus all micro centrifuge tubes and pipette tips used were RNase-free (Mettler-Toledo Rainin, California, USA) and sterile nuclease-free water (Qiagen, Manchester, UK) was used.

## 2.2 General Laboratory Techniques

### 2.2.1 Nucleic Acid Extraction

All RNA extraction was performed on animal tissue snap-frozen at time of sacrifice using Qiagen miRNeasy Mini Kit (Qiagen; Manchester, UK). RWT and RPE buffers were prepared prior to use by addition of 100% ethanol as per manufacturer's instructions.

Tissue was disrupted and homogenised in 700µl QIAzol Lysis Reagent using either Polytron™ PT 2100 homogenizer with 3mm rotor dispersion aggregate or bead-milling in TissueLyser at 25Hz for 30 seconds repeated twice, placing samples on ice between lysis periods. Bead-milling was performed for uterine tissue due to the small amounts; all other tissue was lysed using Polytron homogenization. Tissue lysates were either stored at -80°C or RNA extracted immediately. Homogenates were brought to room temperature for 5 minutes prior to starting extraction protocol.

Homogenates were shaken with 140µl chloroform and centrifuged at 12,000xg for 15 minutes at 4°C. The upper aqueous phase containing the RNA was transferred to separate tube and mixed with 1.5x volume of 100% ethanol (aqueous phase was approximately 400µl therefore 600µl ethanol was used). 700µl of the sample was placed onto RNeasy Mini spin column and centrifuged at 8000xg for 15 seconds at room temperature; this was repeated for the remaining 300µl of sample. DNA digest was performed at this stage for uterine artery samples only; samples were centrifuged with 350µl RWT buffer (8000xg for 15 seconds) and an on column DNA digest was performed using 80µl of DNase I stock solution diluted 1:7 with RDD buffer incubated for 15 minutes at room temperature. Samples were then centrifuged again with 350µl RWT buffer (8000xg for 15 seconds). All other samples did not require this step and 700µl RWT buffer was added and samples centrifuged at 8000xg for 15 seconds. Samples were then centrifuged with 500µl RPE buffer at 8000xg for 15 seconds, then again with 500µl RPE buffer at 8000xg for 2 minutes. Membranes were further dried by spinning columns at 13,000xg for 1 minute. RNA was eluted from membrane using 30µl RNase-free water and centrifuging at 8000xg for 1 minute.

RNA concentration and purity was determined using Nanodrop spectrophometer (ThermoFisher Scientific, Paisley, UK). Absorbance was read at 260nm ($A_{260}$) to detect nucleic acids, at 280nm ($A_{280}$) which identifies protein contaminants, and at 230nm to detect any organic or solvent contamination from the extraction process. $A_{260}/A_{280}$ ratios of between 1.9 and 2.1 signified appropriate sample purity and samples were stored at -80°C until needed.

#### 2.2.1.1 Agilent Bioanalysis

Total RNA was sent for Agilent Bioanalysis for concentration and quality measurements. Select samples of RNA were analysed using a eukaryote total RNA picochip assay (Agilent Technologies, Cheshire, UK) on the Agilent Bioanalyser 2100. This analysis was run by Glasgow Polyomics at the University of Glasgow. The analysis included separation of the samples using electrophoresis to establish the presence of the 18S and 28S ribosomal RNA (rRNA) species within the samples. Electrograms were produced using this information and enabled the quantification of 18S and 28S rRNA and thus the ratio between the two to be determined; this produces the RNA integrity number (RIN). All RNA with a RIN greater than 5 was accepted.

### 2.2.2 Reverse Transcriptase Polymerase Chain Reaction (PCR)

Complementary DNA (cDNA) was prepared using an input of between 400ng-1000ng RNA using the Multiscribe Reverse Transcription kit (ThermoFisher Scientific, Paisley, UK).

The RT-PCR was conducted in a 96-well plate where the final concentrations per well were: 1x reverse transcription buffer, 5.5mM $MgCl_2$, 0.5mM of each dNTP, 2.5µM random hexamers, 0.4U/µl RNase inhibitor and 1.25U/µl Multiscribe. A total volume of 20µl in each well was achieved using RNase free sterile water. Each plate contained a non-template control that had no RNA sample and instead had 7.7ul RNase free water. Plates were covered with adhesive PCR plate seal (ThermoFisher Scientific, Paisley, UK) and centrifuged at 8,000xg for 30 seconds to ensure appropriate mixing of reaction components. The PCR was run on a 96-well Dyad Disciple™ thermal cycler (MJ Research, Massachusetts, USA) with the following temperature cycles: Anneal primers at 25°C for 10

minutes, transcription and extension at 48°C for 30 minutes, heat denature enzyme at 95°C for 5 minutes. Samples were then cooled to 4°C and diluted to an approximate final concentration of 5ng/µl cDNA. Samples were stored at -20°C until use.

## 2.2.3 Quantitative Real Time PCR (qRT-PCR)

### 2.2.3.1 SYBR Green qRT-PCR

Custom PCR primers (Eurofins Genomics, Ebersberg, Germany) were utilised to determine mRNA expression of specific genes (Table 2-1) using SYBR® Green dye. This method relies on the fluorescent SYBR® green dye binding to all double stranded DNA, so as the target is amplified during PCR more dye is incorporated in the double stranded PCR product and fluorescence intensity increases proportional to the amount of product. All primers were designed to span exon-exon boundaries were possible and were reconstituted in RNase free water to make 10µM stock concentrations.

Samples were set up in a MicroAmp™ Optical 384-Well Reaction Plate (ThermoFisher Scientific, Paisley, UK) with 2.5µl cDNA (produced as in section 2.2.2, a final amount of 12.5ng cDNA per well) and 1x Power SYBR® Green Master Mix (ThermoFisher Scientific, Paisley, UK), 500nM forward primer, 500nM reverse primer made up to final volume of 12.5µl with RNase free water, all samples were performed in triplicate with separate samples run with Gapdh primers as a stable housekeeper for gene expression level comparison. Each plate also contained two triplicates of non-template controls in which the cDNA was replaced with the either the non-template control from section 2.2.2 or 2.5µl additional RNase free water. Plates were centrifuged at 8,000xg for 30 seconds to ensure appropriate mixing of reaction components and all volume is in the bottom of each well. Quantitative Real Time PCR (qRT-PCR) was run on 7900HT Fast Detection System (Applied Biosystems, California, USA). Samples were subject to a hold phase of 50°C for 2 minutes then 95°C for 10 minutes to activate the Taq polymerase enzyme before undergoing 40 cycles with the following conditions: 95°C for 15 seconds followed by 60°C for 60 seconds for denaturation, primer annealing and product extension. A final dissociation step

was performed to produce a melt curve analysis in order to assess that the product produced was singular and specific.

**Table 2-1: Primers for use in SYPR® Green qRT-PCR**

| Gene | Forward Primer | Reverse Primer |
|---|---|---|
| *Gapdh* | GACATGCCGCCTGGAGAAAC | AGCCCAGGATGCCCTTTAGT |
| *Desmin* | GGGACATCCGTGCTCAGTAT | AGAGCATCAATCTCGCAGGT |
| *Prl8a4 (Prolactin)* | GCATGTATGGTGGAAGAGGGT | GCAATCTTTTCCAGTTATGAGACA |
| *Vegfr2* | AAGCAAATGCTCAGCAGGAT | GAGGTAGGCAGGGAGAGTCC |
| *Nox2* | AACGTGGAGTGGTGTGTGAA | TTTGGTGGAGGATGTGATGA |
| *p22 phox* | TTGTTGCAGGAGTGCTCATC | CAGGGACAGCAGTAAGTGGA |

Primer sequences are in the 5’ to 3’ direction and were ordered from Eurofins Genomics (Ebersberg, Germany).

### 2.2.3.2 Taqman® Gene Expression Assay

The Taqman® assay used a fluorogenic probe, labelled with FAM™ or VIC™ dye, specific for the target gene and unlabelled target specific primers (detailed in Table 2-2). This assay allows for the probe to incorporate in the double strand DNA during the PCR. It is then cleaved in the next cycle and the dye is separated from a non-fluorescent quencher. The intensity of fluorescence increases proportional to the amount of PCR product produced.

Assays were prepared in a MicroAmp™ Optical 384-Well Reaction Plate (ThermoFisher Scientific, Paisley, UK) with 2µl cDNA (produced in section 2.2.2 with a final amount of 10ng cDNA per well). Assays utilised a duplex reaction, using a FAM™ labelled probe for the gene of interest and a VIC™ labelled housekeeper probe (0.25µl of each probe was added to the wells). The final volume was made up 1x Taqman® Universal Master Mix II to give a total volume of 5µl per well. Each assay plate also contained non-template controls in which the cDNA was replaced with the non-template control from section 2.2.2 or 2µl additional RNase free water. All samples and controls were run in triplicate. Plates were sealed with self-adhesive Advanced Polyolefin StarSeal (STARLAB, Milton Keynes, UK) and centrifuged at 8,000xg for 30 seconds to ensure reaction components were mixed and in the base each well. The qRT-PCR reactions were conducted using a QuantStudio 12K Flex Real-Time PCR System (ThermoFisher Scientific, Paisley, UK). The cycling conditions were the same as in section 2.2.3.1, however there was no requirement for producing a melt curve as the Taqman® assays use probes that are more specific in amplifying only the target product than standard primers.

**Table 2-2: Rat specific Taqman® probe details**

| Gene name | Gene Symbol | Assay ID | Fluorescent label |
|---|---|---|---|
| Angiotensin I converting enzyme 2 | *Ace2* | Rn01416293_m1 | FAM-MBG |
| α-adrenergic receptor 2C | *Adra2c* | Rn00593341_s1 | FAM-MBG |
| Angiotensin II receptor, type 1a | *Agtr1a* | Rn02758772_s1 | FAM-MBG |
| Angiotensin II Receptor , type 2 | *Agtr2* | Rn00560677_s1 | FAM-MBG |
| Corin | *Corin* | Rn00711040_m1 | FAM-MBG |
| P22phox | *Cyba* | Rn00577357_m1 | FAM-MBG |
| Gp91-phox | *Cybb* | Rn00576710_m1 | FAM-MBG |
| Ficolin B | *Fcnb* | Rn00586231_m1 | FAM-MBG |
| Hypoxia-inducible factor 1-α | *Hif1a* | Rn01472831_m1 | FAM-MBG |
| Inositol Trisphosphate Receptor Type 1 | *Itpr1* | Rn01425738_m1 | FAM-MBG |
| Matrix metalloproteinase-1 | *Mmp1* | Rn01486634_m1 | FAM-MBG |
| Matrix metalloproteinase-2 | *Mmp2* | Rn01538170_m1 | FAM-MBG |
| Matrix metalloproteinase-8 | *Mmp8* | Rn00573646_m1 | FAM-MBG |
| Matrix metalloproteinase-9 | *Mmp9* | Rn00579162_m1 | FAM-MBG |
| Phospholipase A2 | *Pla2g2a* | Rn00580999_m1 | FAM-MBG |
| Super oxide dismutase 1 | *Sod1* | Rn00566938_m1 | FAM-MBG |
| Tissue inhibitor of metalloproteinases | *Timp1* | Rn01430873_g1 | FAM-MBG |
| Vascular cell adhesion molecule 1 | *Vcam1* | Rn00563627_m1 | FAM-MBG |
| Vascular endothelial growth factor-α | *Vegfa* | Rn01511602_m1 | FAM-MBG |
| B actin | *B actin* | Rn00667869_m1 | VIC-MBG |
| ß-2-Microglobulin | *B2m* | Rn00560865_m1 | VIC-MBG |

Where suffix of assay ID is _m1 the probe spans exon junctions, therefore specific form mRNA. If suffix is _s1 (primers and probes are within single exon) or _g1 (primers and/or probe may span single exon) these probes can detect genomic DNA, however as a DNA digest was performed this should not have influenced the expression results.

### 2.2.4 Biochemical Urine Analysis

Urine was collected at different gestational time points (as described in section 2.3.5). Urine samples were thawed and prepared by briefly centrifuging at low speed (<500xg) for 1 minute at 4°C to remove any debris that remained from collection; 200µl of uncontaminated urine were used for biochemical analysis. The concentration of albumin and creatinine in each sample was determined using the Roche Cobas C311 Analyser. The assays used were the Albumin, Gen.2 Tina-Quant assay and the Creatinine Jaffe Gen.2 assay, both designed for the photometric detection of the respective protein in urine and used in with Total Protein Urine/CSF assay control kit (all from Roche, Mannheim, Germany). The concentrations were then expressed as a ratio of albumin to creatinine as creatinine is a constant and should not have been altered by gestation, strain or treatment.

### 2.2.5 Tissue Processing and Sectioning

Tissue was fixed in either 10% neutral buffered formalin or a formaldehyde free zinc-based fixative [100mM Tris, 3.16mM $Ca(CH_3OO)_2$, 27.25mM $Zn(CH_3COO)_2$, 36.68mM $ZnCl_2$; pH6.8] for 12-24 hours. Tissue was washed three times in PBS to remove all traces of fixative before being stored in 70% ethanol at 4°C. Tissues were dehydrated and placed into paraffin wax at 60°C in a Citadel 1000 processor (Thermo Scientific, Loughborough, UK) which exposed the tissues to a timed sequence of alcohol and xylene at different concentrations (outlined in Table 2-3). Tissues were then embedded in warmed paraffin wax (≤60°C) and cooled. Tissue blocks were kept at 4°C overnight before being sectioned using Leica RM2235 Microtome (Leica Biosystems, Milton Keynes, UK). 5µm sections were cut and placed on 40°C water to soften the wax before being transferred to a silane treated microscope slide and baked to dry the section in 50°C oven overnight. For placental tissue, fixed using zinc based fixative; sections were cut until the maternal channel was observed. This is indicative of the middle of the placenta and ensures all layers will be visible and all placentas sectioned in relatively the same areas. Between 8 and 10 serial 5µm sections were then cut and numbered before being placed on slides as stated above. Prior to staining all sections were dewaxed and rehydrated at room temperature by placing slides in Histo-Clear (Fisher Scientific, Loughborough, UK) (a safer substitute for xylene)

twice then a gradient of ethanol: 100%, 90%, 70% and placing the slides in deionised $H_2O$ for 5 minute periods each. All staining procedures were conducted at room temperature unless otherwise stated. After staining was complete sections were dehydrated by going up through the ethanol gradient; 70%, 90%, 100%, and cleared in Histo-Clear twice for 5 minute periods each. Coverslips were mounted over the sections using DPX mounting medium.

**Table 2-3: Conditions used to process formalin fixed tissues**

| Solution | Incubation time |
|---|---|
| 70% Ethanol | 15 minutes |
| 85% Ethanol | 15 minutes |
| 90% Ethanol | 25 minutes |
| 95% Ethanol | 25 minutes |
| 100% Ethanol | 15 minutes |
| 100% Ethanol | 15 minutes |
| 100% Ethanol | 15 minutes |
| Xylene | 30 minutes |
| Xylene | 30 minutes |
| Paraffin Wax | 30 minutes |
| Paraffin Wax | 30 minutes |

Details of different solutions and timings that formalin fixed tissue samples were exposed to during processing for embedding into paraffin wax to be used for histology and immunohistochemistry.

## 2.2.6 Histology

### 2.2.6.1 Haematoxylin and Eosin Staining

Haematoxylin and eosin staining was used as to assess basic tissue morphology. Tissue sections were placed in Harris haematoxylin for 2 minutes and then transferred to tepid running tap water to produce the blue nuclei stain. The sections were dipped in 70% ethanol then counterstained with Eosin Y for 1 minute to differentiate the cytoplasm (pink) and dipped several times into deionised $H_2O$ for 10 seconds. Sections were dehydrated, cleared and mounted as in section 2.2.5.

### 2.2.6.2 Periodic Acid Schiff Staining

Periodic Acid Schiff (PAS) staining was used to detected polysaccharides, thus determining glycogen containing cells. All reagents were brought to room temperature before use. Sections were incubated in 0.5% periodic acid (w/v in deionised (d)$H_2O$) for 5 minutes; excess stain was removed by washing 3 times in d$H_2O$ for a total of 10 minutes. Sections were then incubated in the dark with

Schiff reagent (Sigma, Dorset, UK) for 15 minutes at room temperature before being washed again in running tap $H_2O$. Sections were counterstained using Harris haematoxylin for 2 minutes. The excess stain was removed with running tap $H_2O$ for 5 minutes and sections were dehydrated, cleared and mounted as in section 2.2.5.

#### 2.2.6.3 Picrosirius Red Staining

After dewaxing and rehydrating sections slides were transferred to Weigert's haematoxylin; freshly made following manufacturer's instructions (Sigma, Dorset, UK) for 10 minutes. Excess stain was then washed in running tap $H_2O$ for 10 minutes. 0.1% picrosirius red solution was made using 0.1% w/v Sirius red F3B (Sigma, Dorset, UK) in $dH_2O$. Sections were incubated in 0.1% picrosirius red solution for 90 minutes protected from light. The excess picrosirius red stain was washed off the sections using acidified $dH_2O$ (0.01N HCl) for 5 minutes, repeated twice, and any excess moisture was removed before sections were dehydrated, cleared and mounted as stated in section 2.2.5.

### 2.2.7 Immunohistochemistry

Immunohistochemistry was used to assess placental sections for the presence of cytokeratin; a trophoblast cell marker, and α-actin; a vascular smooth muscle cell marker. Two serial sections cut from placentas fixed in the zinc-based fixative were used, one for trophoblast analysis and the other for α-actin. Sections were de-waxed and rehydrated as outlined in section 2.2.5. Sections were circled with an ImmEdge™ Hydrophobic Barrier PAP Pen (Vector Laboratories Ltd, Peterborough, UK) to provide a water repellent barrier to keep the sections covered with the antibody solutions and prevent sections drying out.

#### 2.2.7.1 Trophoblast Cell Stain

Alkaline phosphatase activity in the sections was quenched using incubation in 0.2M hydrochloric acid for 10 minutes. No antigen retrieval step was required due to the zinc-based fixative not masking the epitope of the antigen targeted by the cytokeratin antibody. Sections were then washed 3 times in 0.01M Tris-buffered saline (TBS) [20mM Tris, 150mM NaCl; pH7.6] for 5 minutes each time

with gentle agitation using a Rotatest plate shaker (LUCKHAM R100, at medium speed). Tissue sections were then incubated with a blocking solution of TBS with 2% bovine serum albumin (BSA), 1% non-fat dried milk and 0.1% Tween®-80 for 15 minutes at room temperature. This prevented non-specific immunoglobulin binding by blocking irrelevant binding sites and saturating these with irrelevant proteins in the BSA and milk. Tween®-80 is a non-ionic detergent that was added to reduce surface tension and allow the solution to spread over entire section. Tween®-80 was chosen over Tween®-20 as it is a stabilizing agent for proteins.

The primary mouse monoclonal antibody for cytokeratin clone MNF116 (M0821; DAKO, Glostrup, Denmark) was diluted 1:100 with TBS to give an approximate final immunoglobulin concentration of 0.6mg/L. The primary antibody was incubated on sections in a humidified chamber overnight at 4°C. All traces of the primary antibody were then removed by washing 3 times in TBS as previously described. The primary antibody was detected using with unconjugated goat anti-mouse immunoglobulins (Vector Laboratories Ltd, Peterborough, UK) diluted 1:50 in TBS and incubated on sections for 30 minutes at room temperature. The wash steps were repeated as previously stated. A tertiary step was needed to detect the unconjugated goat anti-mouse antibody; this allowed a greater signal amplification that would not have been achievable if a conjugated secondary antibody was used. A mouse monoclonal alkaline phosphatase anti-alkaline phosphatase (APAAP) complex (Bio-Rad, Oxford, UK) was diluted 1:100 in TBS and applied to the sections for 30 minutes. The sections were washed 3 times in TBS as previously. Sections were incubated in nitroblue tetrazolium / 5-bromo-4-chloro-3-indoyl phosphate (NBT/BCIP) (Roche, Mannheim, Germany) for 10 minutes to detect the alkaline phosphatase activity. The NBT/BCIP was prepared by dissolving one tablet in 10ml $dH_2O$ and used immediately whilst protecting from light. This chromogen develops a purple/black colour that was visualised as positive primary antibody conjugation to cytokeratin. Sections were then rinsed with $dH_2O$ for 5 minutes, 3 times, before being counterstained using a Periodic Acid Schiff stain (as detailed in section 2.2.6.2). Sections were not dehydrate and cleared using alcohol and Histo-Clear as NBT is soluble in solvents. For this reason, coverslips were mounted on the sections using a VectaMount aqueous-based mounting medium (Vector Laboratories Ltd, Peterborough, UK).

#### 2.2.7.2 Vascular Smooth Muscle Cell Stain

Endogenous peroxidase activity was blocked by incubating the sections in 3% hydrogen peroxide in methanol for 30 minutes. No antigen retrieval step is required as stated in section 2.2.7.1. Sections were then washed 3 times in TBS as previously stated. The placental sections were blocked as in section 2.2.7.1. The primary mouse monoclonal anti-α actin antibody (clone 1A4; DAKO, Glostrup, Denmark) was diluted 1:200 in TBS, giving an approximate immunoglobulin concentration of 0.5μg/ml. Primary antibody was incubated at 4°C overnight.

Peroxidase conjugated goat anti-mouse immunoglobulins (Vector Laboratories Ltd, Peterborough, UK) were used as the direct detection antibody. This was diluted 1:100 and incubated on the sections for 30 minutes at room temperature. Sections were then washed 3 times in TBS as previously stated. The secondary antibody was detected using hydrogen peroxide solution and colour was developed using diaminobenzene (DAB) (DAB Peroxidase (HRP) Substrate Kit; Vector Laboratories Ltd, Peterborough, UK). A stock solution containing DAB and hydrogen peroxide was made following the manufacturer's instructions; 2 drops of buffer stock solution, plus 4 drops of DAB and 2 drops of hydrogen peroxide were added to 5mls $dH_2O$. This solution as incubated on the sections for 2 minutes before being rinsed in $dH_2O$ for 5 minutes. The sections were then counterstained with Harris's Haematoxylin for 30 seconds and the blue counterstain colour developed in running, tepid tap $H_2O$. Sections were then dehydrated, cleared and mounted in DPX as stated in section 2.2.6.

### 2.2.8 Image Analysis

All slides were blinded before imaging. Sections were imaged on a Zeiss AX10 polarized light Microscope (Carl Zeiss Ltd, Cambridge, UK) and where necessary stitched together using Microsoft Image Composite editing software. Analysis was conducted using Image J software for stain intensity measurements using an observer blinded to section identity. The image type was converted into a red:blue:green stack image and viewed using the appropriate channel for each particular stain. Threshold was set to its maximum to get the number of all pixels within the image before the threshold was adjusted to identify only the

positively stained pixels. This would give area values for the positively stained pixels which could then be expressed as a percentage of the whole tissue.

## 2.3 *In Vivo* Procedures

The stroke-prone spontaneously hypertensive (SHRSP) and Wistar Kyoto (WKY) rats used were from inbred colonies that have been maintained in house at the University of Glasgow since 1991 by brother x sister mating. All rats were housed in controlled 12 hour light/dark conditions with a constant temperature (21±3°C) with ad libitum access to water and standard diet (rat and mouse No.1 maintenance diet, Special Diet Services). All animal procedures were approved by the Home Office according to the Animals (Scientific Procedures) Act 1986 (Project License 60/9021).

### 2.3.1 Time Mating

Virgin 12-week-old ± 4 days female rats were placed in time mating cages with males of the same strain for up to 4 days. Presence of a copulation plug on cage floor was evidence of successful mating and denoted as gestational day (GD) 0.5.

### 2.3.2 Anaesthetic Procedure

Rats were anaesthetised where necessary using an induction box filled with 5% isoflurane in 1.5L/min medical oxygen. Once anaesthetised, the rats where placed either in the supine or prone position with their nose and mouth fully inserted and secured in an anaesthetic mask. Isoflurane levels were adjusted depending on procedure. All rats were checked to be fully under anaesthesia before beginning any procedure.

### 2.3.3 Radiotelemetry

Radiotelemetry enables continuous live haemodynamic measurements using implantable transmitters and the Dataquest ART Telemetry System (Data Sciences International, Minneapolis, USA). Probes can measure systolic and diastolic blood pressure alongside heart rate and activity of a conscious animal. Probes were sterilised using 24 hour incubation in Actril® cold sterilant (VWR, Lutterworth, UK) at room temperature and the calibration was checked to be within ±3mmHg of factory calibration settings prior to use.

Surgery was conducted under sterile conditions with the operating table covered with sterile surgical cover and surgical gowns and gloves were worn at all times. All instruments were autoclaved prior to use. 10-week-old female rats were anaesthetised as in section 2.3.1 and maintained at 3% isoflurane in 1.5L/min medical oxygen in the supine position. Hair was removed from the abdomen and swabbed with povidone-iodine solution (Betadine®). A scalpel was used to perform a midline laparotomy through the abdominal wall. The peritoneal cavity was cleared to visualise the abdominal aorta and iliac bifurcation. Connective tissue and fat was cleared using cotton swabs and three MERSILK® Ethicon suture ties (NU-CARE, Bedfordshire, UK) were placed around the arteries (position indicated in Figure 2-1) to temporarily occlude blood flow. A 22-guage needle was bent to an approximate 45° angle and used to create an opening in the aorta. The catheter of a sterilised telemetry probe was inserted up towards the renal arteries and secured with tissue adhesive. The probe was secured in the abdominal wall using ETHILON® Ethicon nylon sutures (NU-CARE, Bedfordshire, UK) and the rat was sutured up using VICRYL® Ethicon sutures (NU-CARE, Bedfordshire, UK). Rats were given 5mg/kg Rymadil analgesic subcutaneously and recovered from surgery on surgical Vetbed bedding in 37°C incubator. After a one week recovery period, probes were switched on and data was collected using Dataquest ART system.

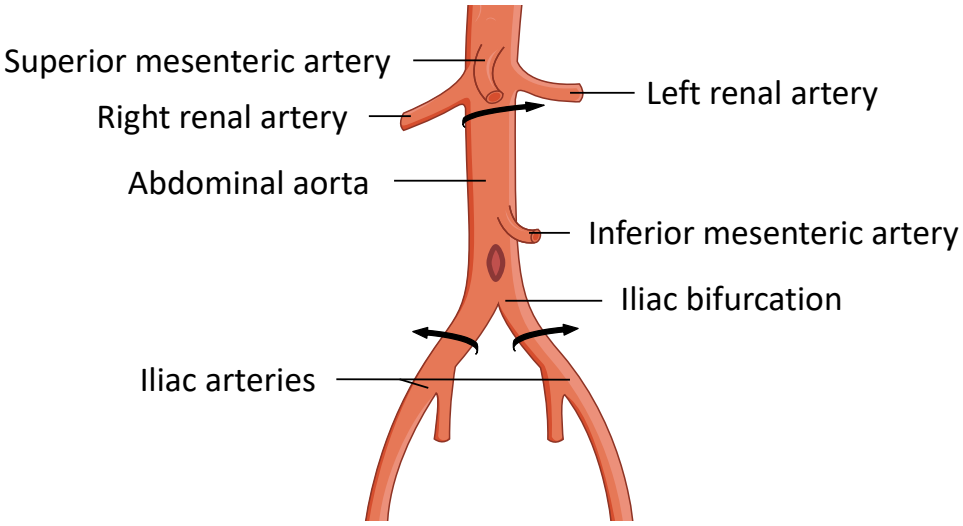


**Figure 2-1: Illustration of ligation points for radiotelemetry probe implantation.** Illustration shows the structure of arteries proximal to the abdominal aorta. Prior to probe implantation blood supply was restricted using suture ties (black arrows). An incision was made above the iliac bifurcation (red oval) and the catheter of the probe inserted along length of abdominal aorta. Probe was secured so that the open end of the catheter was just below the renal artery branches. Illustration creased using Servier Medical ART.

### 2.3.4 Tail Cuff Plethysmography

Blood pressure was measured on conscious rats at pre-pregnancy, GD6.5, GD14.5 and GD17.5 time points using tail cuff plethysmography. All measurements were made in the morning between 08:00 and 10:00 hours, to minimise diurnal variation. Rats were acclimatised to the procedure prior to pregnancy. Rats were placed in pre-warmed incubation boxes with heat lamps at 30-32°C for 5-10 minutes to allow dilation of the arteries in the tail so that measurements of blood pressure could be made. After warming, rats were gently restrained in a warm, dry towel and placed on a heated platform so that only the tail was exposed. A blood pressure occlusion cuff was placed at the base of the tail followed by a piezoceramic pressure transducer cuff. The pressure transducer relies on volume pressure recording (VPR) sensor technology which measures blood pressure based on volume changes. The occlusion cuff was inflated in controlled 1mmHg steps to 250mmHg and then deflated and the blood pressure was recorded using equipment designed and built in collaboration with the Electronics/Medical Devices Unit (NHS Greater Glasgow & Clyde) (Evans et al., 1994). The inflation/deflation cycle was repeated 5 consecutive times and an average was taken for each animal to obtain mean systolic blood pressure.

### 2.3.5 Metabolic Cage Urine Sampling

Rats were placed individually in metabolic cages pre-pregnancy for an acclimatization period of 2 hours before being placed in cages for 24 hours at a pre-pregnancy, GD6.5, GD14.5 and GD17.5 time points. Rats had access to 200ml water and standard rat chow ad libitum. Final water volume remaining and volume spilt was recorded at the end of the 24-hour period. Urine and faecal matter were separated and urine volume was recorded before being aliquoted in 2ml tubes and stored at -80°C.

### 2.3.6 Tail Vein Blood Sampling

Blood samples were collected pre-pregnancy and at GD6.5 and GD12.5 or GD14.5. Rats were anaesthetised as in section 2.3.1 and maintained at 2% isoflurane in 1.5L/min medical oxygen in a prone position. One of three veins (two lateral and one dorsal) in the tail were located and punctured using sterile scalpel. Gentle pressure was applied and approximately 1ml of blood was

collected in heparinised tubes. Plasma was isolated by centrifugation of the blood at 1200xg for 20 minutes at 4°C. Plasma was aliquoted and stored at -80°C.

### 2.3.7 Transthoracic Echocardiography

Echocardiography were performed at pre-pregnancy, GD6.5, GD12.5 or GD14.5 and GD18.5 time points using an Acuson Sequoia c512 ultrasound system with a linear array transducer at a frequency of 15MHz. Rats were anaesthetised as in section 2.3.1 and hair removed from chest and abdomen using electric shaver. Rats were placed in the supine position, with a slight rotation towards their right-hand side, and maintained at 1.5% isoflurane in 1.5L/min medical oxygen. Pre-warmed (room temperature) ultrasound gel was applied to the transducer and skin. The heart was imaged along the long-axis (Figure 2-2) and M-mode measurements recorded for 6-7 cardiac cycles. This was repeated 3 times.

Analysis of the echocardiograph images was conducted using Image J software. Distance between waveform peaks and troughs were measured as shown in Figure 2-2. These measures were inputted into formulae to calculate the stroke volume (SV) and cardiac output (CO), ejection fraction (EF), fractional shortening (FS) and left ventricular mass. The calculation formulae were:

Stroke volume (ml) = $EDV/ESV$

Cardiac output (ml/min) = $SV \times HR$

Ejection Fraction (%) = $(SV/EDVol) \times 100$

Fractional shortening (%) = $(EDD - ESD/EDD) \times 100$

Left ventricular mass (g) = $(0.8 \times ASEcube) + 0.6/1000$

*Where ASEcube* = $1.04 \times (IVSTd + LVIDd + PWTd)^3 - LVIDd^3$

*LVIDd = average EDD*10*

*IVSTd = average AWTd*10*

*APWTd = average PWTd*10*

EDVol = $1.047 \times LVIDd^3$

ESV = $1.047 \times (Average\ EDDs)^3$

HR = Taken from conscious animals on radiotelemetry (beats/min)

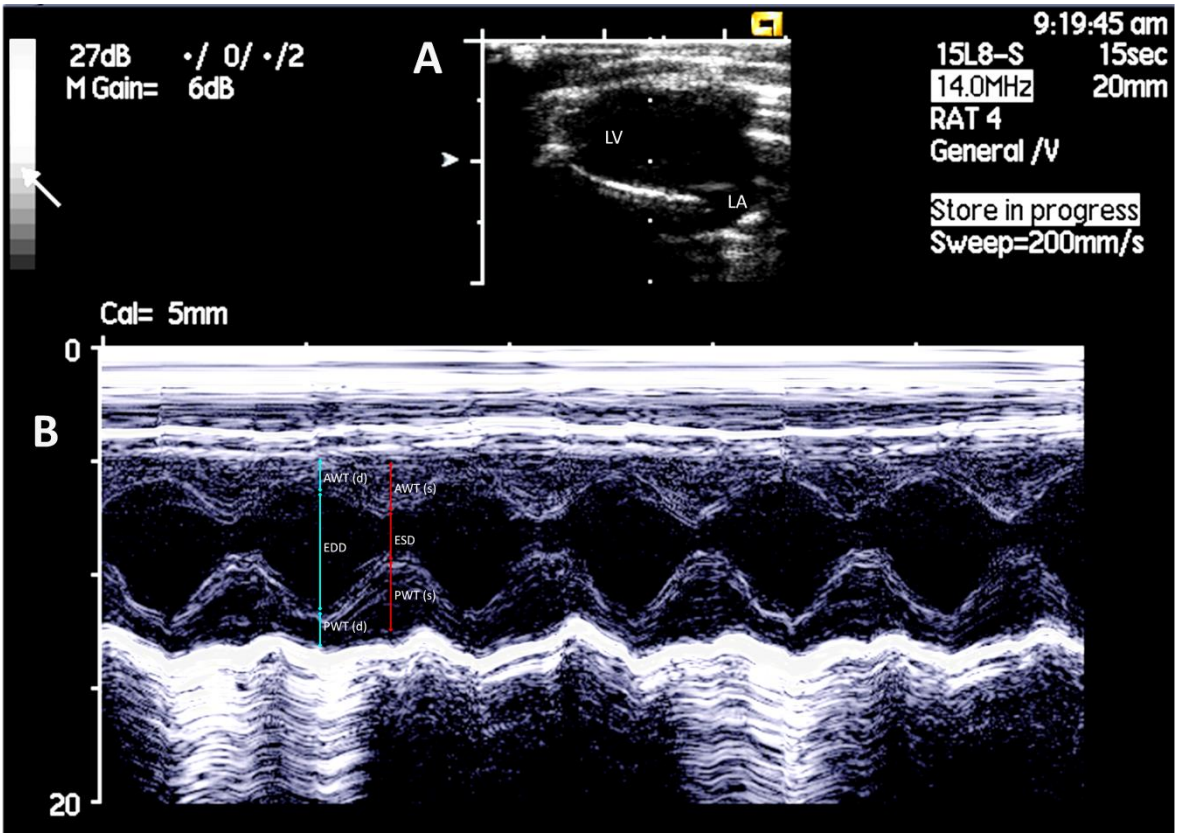


**Figure 2-2: Representative echocardiography image**
The heart echocardiography was performed on the long axis which can visualise the left atrium (LA) and left ventricle (LV) as C-shape shown in A, measurements are made along the dotted line. The waveforms in B visualise anterior wall thickness (AWT), posterior wall thickness (PWT); in systole (s) and diastole (d), end diastolic diameter (EDD) and end systolic diameter (ESD).

## 2.3.8 Uterine Artery Ultrasound Doppler

Uterine artery Dopplers were conducted at the same time as the echocardiography and the rats were prepared for the procedure as in section 2.3.7. The uterine artery was located lateral to the uterus using colour Doppler in P-mode. Once located the transducer was placed parallel to the uterine artery and pulse wave Doppler was recorded for at least 6 cardiac cycles. This was then repeated for the uterine artery on the opposite uterine horn. Peak systolic velocity (PSV) and end diastolic velocity (EDV) of the uterine arteries were measured from the 6 consecutive cardiac cycles and used to calculate resistance index (RI) (RI = [PSV-EDV]/PSV) and S/D ratio (PSV/EDV). As gestation progressed detect fetal heart beat was able to be detected. This was done by moving the transducer over the dam's abdomen until a fetus was visualised and the Doppler recording, as outlined above, was repeated for the fetal cardiac cycle. This measure was used to confirm the pregnancy was maintaining viable fetuses.

## 2.4 Sacrifice Procedure

Rats were anaesthetised as in section 2.3.1 and euthanized by exsanguination under sustained anaesthetic of 5% isoflurane in 1.5L/min medical oxygen at either GD6.5, GD14.5, GD18.5 or GD20.5 or non-pregnant age matched controls where appropriate. Exsanguination was performed by making a midline incision and opening the thoracic cavity by blunt dissection of the diaphragm and cutting along either side of the rib cage. Once the heart was exposed the aorta was severed and the heart removed. The rats were ensured to be dead before continuing with harvesting tissues.

### 2.4.1 Cardiac Puncture Blood Sampling

Blood sampling via cardiac puncture was performed just prior to exsanguination. Rats were maintained at 5% isoflurane in 1.5L/min medical oxygen. The heart was exposed as in section 2.4. A 21-gauge needle attached to a 5ml syringe was inserted into the left ventricle and 4-5mls of blood was slowly removed. This was collected in heparin and/or EDTA coated BD Vacutainer® tubes and kept on ice to allow plasma isolation; as detailed in section 2.3.6. Heparin tubes were used as standard; these tubes inhibit thrombin formation and allow for plasma separation. However, EDTA tubes prevent clotting by calcium chelation and allow the separation of plasma whilst conserving peptide structures; making this appropriate for measurement of angiotensin II levels.

### 2.4.2 Maternal Tissue Collection

Maternal heart, liver and kidneys were dissected and cleaned. The hearts were gently blotted on absorbent paper towel to remove any blood and renal fascia was removed from the kidneys. Whole organ weights were recorded (Appendix section 8.1). The atria and right ventricle were then removed from the whole heart and the left ventricle was weighed before being halved transversely. The lower apex was placed in 10% neutral buffered formalin; for histological assessment (section 2.2.5), and the upper portion snap frozen in liquid nitrogen for RNA extraction (section 2.2.1). The right kidney was cut in half perpendicular to the long axis; one half was fixed in 10% neutral buffered formalin for

histological assessment (section 2.2.5) and the other snap frozen in liquid nitrogen for RNA extraction (section 2.2.1)

The intestines were collected in their entirety and placed into chilled $Ca^{2+}$ free physiological salt solution (PSS) [120mM NaCl, 4.7mM KCl, 1.2mM $MgSO_4$, 25mM $NaHCO_3$, 1.2mM $KH_2PO_4$, 10mM glucose, 0.023mM EDTA] and kept on ice for preservation until the dissection of the mesenteric arteries (section 2.4.3). A hysterectomy was performed and the whole gravid uterus weighed and placed in chilled $Ca^{2+}$ free PSS to humanely euthanize the fetuses by cooling. The uterine artery and vein were dissected from the main uterine horn and placed on ice in chilled $Ca^{2+}$ free PSS as to be preserved for later dissection (section 2.4.3). The numbers of implantations were recorded as was the location of fetuses and resorptions.

### 2.4.3 Artery dissection

Uterine and mesenteric arteries were dissected for *ex vivo* analysis. The main uterine artery (illustrated in Figure 2-3) was microscopically dissected in $Ca^{2+}$ free PSS in a clean sylgard-coated plate. The surrounding adipose tissue was carefully removed to reveal the artery and vein before the vein was removed away. Small branches were kept on the dissected artery to be tied off if necessary when used for myography (section 2.5).

For mesenteric artery dissection, the intestines were pinned out on a clean sylgard plate in $Ca^{2+}$ free PSS so that the mesentery was gently spread out and the 1$^{st}$ order mesenteric artery was visualised. This was orientated so that the artery was on top of the vein. The arterial tree was followed down to the 3$^{rd}$ order mesenteric arteries, which were then microscopically dissected. The connective and adipose tissue was dissected and discarded before the vein was removed. Arteries for myography were placed in $Ca^{2+}$ free PSS overnight at 4°C before use, others were snap frozen in liquid nitrogen for extraction of RNA (section 2.5).

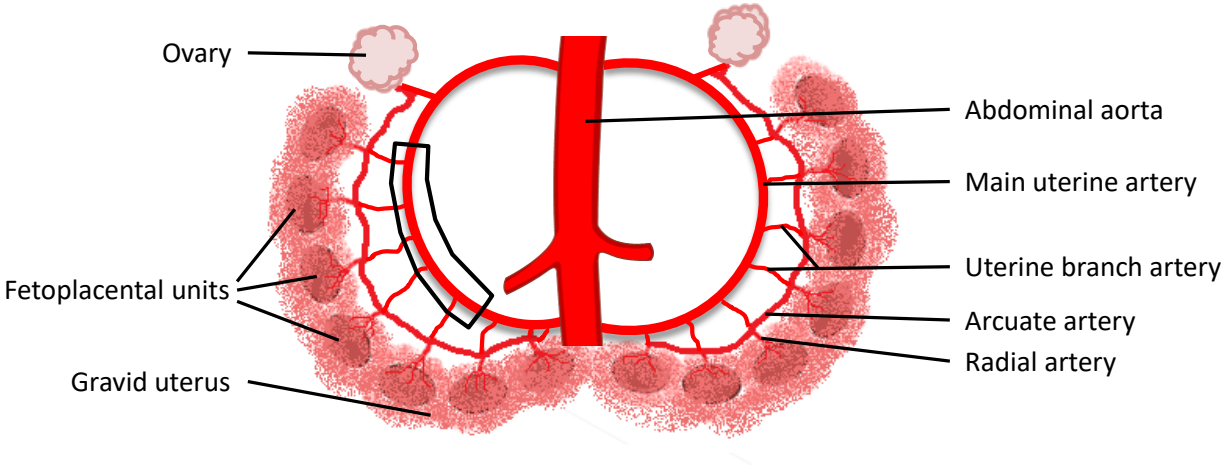


**Figure 2-3: Illustration of the pregnant rat uterus with vascular structure.**
The diagram highlights the bifurcation of a rodent uterine horn and the arrangement of major arteries that supply the fetoplacental units. The portion of the main uterine artery that was used for myography is indicated in the black box, the portion on the opposite horn was also taken. Image was created on Microsoft PowerPoint.

### 2.4.4 Fetoplacental tissue

At either GD14.5, GD18.5 or GD20.5 each fetoplacental unit was carefully dissected in phosphate buffered saline (PBS) [137mM NaCl, 2.7mM KCl, 4.3mM $Na_2HPO_4$, 1.47mM $KH_2PO_4$; pH7.4], separating the placenta and fetus and removing amniotic fluid and fetal membranes. Fetal and placental tissue was gently blotted on absorbent paper to remove excess fluid and weights were recorded. Two placentas (not weighed) were dissected so that they were still attached to the maternal mesometrial triangle and cut as shown in Figure 2-4, one placenta was placed into standard 10% neutral buffered formalin fixative and the other into a formaldehyde free zinc-based fixative (detailed in section 2.2.5) for 24 hours at room temperature. The zinc-based fixative was chosen due to better antigen presentation and increased sensitivity to specific antibodies. Three separate placentas were then dissected into the different tissue layers, mesometrial/decidua, junctional zone, labyrinth zone and chorionic plate (Figure 2-4) and snap frozen in liquid nitrogen. Fetal crown:rump length, head circumference and abdominal circumference were measured using a length of VICRYL® suture soaked in PBS (Figure 2-5) (Kusinski et al., 2012).

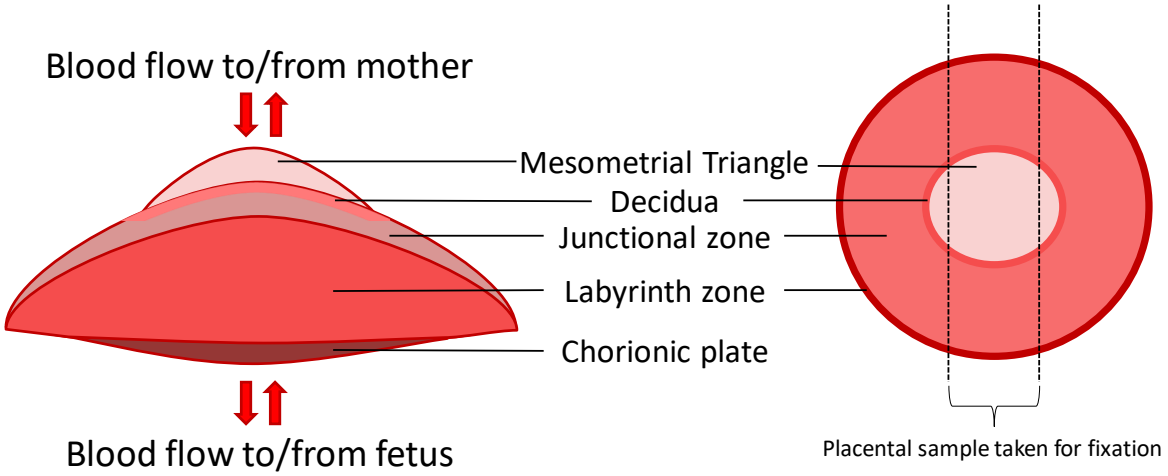


**Figure 2-4: Diagrammatic representation of the rat placenta**
The diagram shows a lateral and aerial view of the rodent placenta after dissection from the fetus. The left image shows the different layers; maternal = mesometrial triangle with decidua; placental = junctional and labyrinth zones; and fetal = chorionic plate. This is the view of the placenta that is achieved when sectioning for histology and also shows the bidirectional blood flow between mother and placenta and between fetus and placenta. The right-side image shows the aerial view of the placenta and the dashed lines indicating the cuts made to take the central placenta portion for fixation

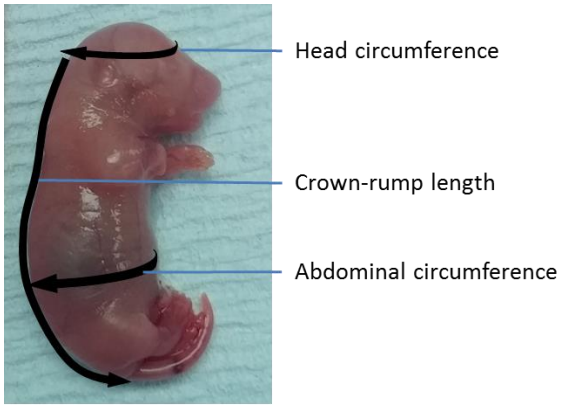


**Figure 2-5: Representation of measurements for fetal proportion**
Morphometry of the fetus was measured using a softened suture placed at different points on the fetus and measured in mm using a ruler. The head circumference was measured above the eyes and ears. Crown-rump length was measured from the top of the head (at the intersection with the head circumference) to the base of the tail, following the curvature of the spine. Abdominal circumference was taken around the abdomen of the fetus at the umbilical cord insertion site. Image depicts a GD20.5 WKY fetus.

### 2.4.5 Fetal Growth Trajectory and Weight Distribution

Fetal growth trajectories were determined by plotting the average fetal weight obtained at GD14.5, GD18.5 and GD20.5. The rate was determined by calculating the gradient of this line.

For fetal weight distributions, the individual fetal weights at GD18.5 were pooled for all fetuses of that strain and/or treatment group. These numbers were used to construct a histogram of the distribution of fetal weights using frequency distribution bin centres at 0.05g. Non-linear regressions were then performed using a Gaussian distribution. This presented the fetal weight distribution as a percentage of the total population. Clinically, fetal growth restriction can be determined by calculating the lowest $5^{th}$ percentile for predicted fetal weight; and if the fetus falls within this then is diagnosed with growth restriction. Using the fetal weight distributions, the lowest $5^{th}$ centile can be determined for WKY or vehicle control groups and the percentage of fetuses that fall below this in other strains/treatment groups can be calculated.

## 2.5 Uterine and Mesenteric Artery Myography

### 2.5.1 Wire Myography

Two vessel segments (approximately 2cm in length) from the central portion of each dissected artery (as described in section 2.4.3) were mounted on 40µm wire on a multi wire myograph system (620M, Danish Myo Technology, Aarhus, Denmark) in PSS containing $Ca^{+2}$ [120mM NaCl, 4.7mM KCl, 1.2mM $MgSO_4$, 25mM $NaHCO_3$, 1.2mM $KH_2PO_4$, 10mM glucose,2.5mM $CaCl_2$]. LabChart software (ADInstruments, Oxford, UK) was used to record and analyse vessel tension response. Vessels were then equilibrated to 37°C and gassed with 95% $O_2$ and 5% $CO_2$ for 20 minutes before normalisation using DMT normalisation procedure. This involves distending the vessel in a stepwise manner to determine the optimal tension at which the vessel segment has maximal active force production and sensitivity to agonists. The transmural pressure for mesenteric and uterine arteries was the internal circumference at 100mmHg = 13.3KPa multiplied by a factor of 0.9 ($IC_1$). Normalised vessels were left again to equilibrate for 60 minutes to reach a stable baseline tension before being subject to a 'wake-up' procedure with the addition of 5ml high potassium PSS (KPSS) [120mM KCl, 1.2mM $MgSO_4$, 25mM $NaHCO_3$, 1.2mM $KH_2PO_4$, 10mM glucose, 2.5mM $CaCl_2$] to the bath for 5 minutes. KPSS was removed and vessels were 'washed' with the addition of 5ml PSS, this was repeated 3 times and left for 8-10 minutes to return to baseline before beginning the experiment.

The vessels contractile response was assessed by adding noradrenaline to the bath in 2 minute increments to give final concentrations of $1x10^{-9}$M, $1x10^{-8}$M, $1x10^{-7}$M, $1x10^{-6}$M, $1x10^{-5}$M, and $3x10^{-5}$M. The previously described wash step and return to baseline was repeated before pre-constricting vessels with $2x10^{-5}$M noradrenaline. After 2-5 minutes (once the vessel reached a steady tension) vessels were subjected to varying doses of carbachol, the synthetic analogue of acetylcholine, in 2-minute increments at the following final concentrations: $1x10^{-8}$M, $1x10^{-7}$M, $1x10^{-6}$M, $1x10^{-5}$M, and $3x10^{-5}$M. Vessels were washed as before and a relaxation response was then repeated using sodium nitroprusside, a nitric oxide donator, at the following final concentrations: $1x10^{-9}$M, $1x10^{-8}$M, $1x10^{-7}$M, $1x10^{-6}$M, $1x10^{-5}$M, and $3x10^{-5}$M. Finally, vessels were washed again and 5ml KPSS

replaced the PSS in the bath to ensure vessels still exhibited a contractile response that signified they were alive.

Data analysis was conducted using LabChart Reader (ADInstruments, Oxford, UK). Mean baseline tension prior to each dose response curve, maximal contractile responses and mean relaxation responses were measured for each agonist concentration. The following equations were used to determine constriction response to noradrenaline:

$$\text{Normalised diameter (μm)} = \frac{Internal\ circumference\ (IC_1)}{\pi}$$

$$\text{Wall tension (mN/mm)} = \frac{Force\ change\ (mN)}{2\ x\ vessel\ length\ (mm)}$$

$$\text{Active Effective Pressure (KPa)} = \frac{Wall\ tension\ (mN/mm)}{(Normalised\ diameter \mu m/2) x\ 100}$$

Vasodilation response was expressed as a percentage of noradrenaline constriction, where 100% was fully constricted. Each dose response curve was also used to determine the half maximal effective concentration ($EC_{50}$). The active effective pressure curves for constriction response were normalised and the relaxation responses were inverted to produce a sigmoidal curve ranging from 0 (100% constriction) to 100 (0% constriction), all response curves were then transformed so that X=log(X) and a non-linear regression analysis conducted. The $EC_{50}$ values were then subject to further statistical analysis.

## 2.5.2 Pressure Myography

One vessel segment which had no or minimal branches was placed into a chamber containing $Ca^{2+}$ free PSS at 37°C aerated with 95% $O_2$, 5% $CO_2$ in the DMT pressure myograph system 110PXL (Danish Myo Technology, Aarhus, Denmark). The open ends of the vessel were mounted onto two glass cannulas and secured using nylon sutures, any branches were tied-off to ensure the flow system was closed. The chamber was mounted onto the pressure interface which contained a reservoir of $Ca^{2+}$ free PSS at 37°C. All bubbles were removed from the system before opening the valves to the glass cannulas and perfusing the vessel with $Ca^{2+}$ free PSS at 10mmHg. The vessel was checked for any holes or leaks in the system before being 'normalised' to 70mmHg for 1 hour. The vessel was exposed to incremental increases in a range of physiological pressures for 5

minute periods each, these pressures where 10mmHg, 20mmHg, 40mmHg, 60mmHg, 80mmHg, 100mmHg, 110mmHg and 120mmHg. The vessel was filmed and the external and internal diameter were continually recorded throughout the experiment using MyoView software (Danish Myo Technology, Aarhus, Denmark). At the end of the experiment pressure was maintained whilst the heating was turned off and $Ca^{2+}$ free PSS was replaced with 10% neutral buffered formalin. This was then left to fix the vessel at 120mmHg for 30 minutes at room temperature. Once complete the vessel was carefully removed and placed in fresh 10% neutral buffered formalin overnight before being processed for histology as in section 2.2.6. Measurements for internal ($D_i$) and external ($D_e$) diameter were derived from MyoView software using LabChart Reader (ADInstruments, Oxford, UK), these measures were then used to calculate the wall thickness ($D_e - D_i / 2$), cross-sectional area ( $\pi / 4(D_e^2 - D_i^2)$), circumferential wall strain ($D_i - D_{i@10mmHg} / D_{i@10mmHg}$) and the wall stress (*1332 x pressure x* $D_i$ */ 2 x wall thickness*), where 1mmHg = 1332 dynes/$cm^2$.

## 2.6 Vascular Smooth Muscle Cell Culture

### 2.6.1 Primary cell isolation

Uterine arteries were dissected as in section 2.4.3 from three non-pregnant rats or three pregnant dams between GD5.5 and GD8.5. These arteries were collected in chilled F-12 Ham media [1mM L-glutamine, 14mM sodium bicarbonate, 1mM sodium pyruvate] (N6658, Sigma, Dorset, UK) supplemented with 100IU/ml penicillin, 100µg/ml streptomycin, 2mM L-glutamine (all from Gibco™ ThermoFisher Scientific, Paisley, UK) and kept at 4°C for a maximum of 1 hour. The two uterine arteries (from both sides of the uterine horn) from the 3 rats were halved so that the isolation began with 12 artery segments. The segments were digested in the above F12 media supplemented with 2mg/ml bovine serum albumin (A7906, Sigma, Dorset, UK), 250 units/ml collagenase type-I (LS004196, Lorne Laboratories, Berkshire, UK) 0.5 units/ml elastase (E7885, Sigma, Dorset, UK) and 0.4mg/ml soybean trypsin inhibitor (T9003, Sigma, Dorset, UK); pre-heated to 37°C for 5 minutes prior to use, to ensure enzymes were active. Two artery segments were placed in 1ml of warmed digestion media and incubated with gentle agitation at 37°C using a Biometra OV2 mini hybridisation oven (Thistle Scientific, Glasgow, UK) for approximately 40 minutes. The incubation was stopped when the vessels were softened and had a 'fluffy' appearance. The vessels were then homogenised using needles of increasing gauges; 18G, 19G and 23G respectively. The vessels and digestion media were passed through each needles 5 times with the same syringe being used throughout. The homogenised vessels were then centrifuged at 1200xg for 3 minutes at room temperature before being resuspended in 500µl of complete F12 media [100IU/ml penicillin, 100µg/ml streptomycin, 2mM L-glutamine] with 10% fetal bovine serum. This results in a total of 3ml primary cell resuspension which was placed in a T25 flask and topped with 1ml complete F12 media. After cells had adhered to the plastic (after 48 hours) the media was changed to complete Dulbecco's Modified Eagle's medium (DMEM) with Glutamax™ supplement [4mM L-glutaime, 5.5mM D-glucose, 1mM sodium pyruvate, 44mM sodium bicarbonate] (Gibco™ ThermoFisher Scientific, Paisley, UK) supplemented with 100IU/ml penicillin, 100µg/ml streptomycin, 2mM L-glutamine and completed with 10% fetal bovine serum (FBS) (Gibco™ ThermoFisher Scientific, Paisley, UK).

### 2.6.2 Maintenance of primary cell line

Cells were checked daily and media was changed every 48-72 hours. Cells were passaged at 80% confluency. To passage the cells the complete media was removed and the flasks washed with sterile PBS. An amount of 1x trypsin-EDTA that sufficiently covered the entire base of the flask was added (approximately 1ml for T25, 3ml for T75). This was incubated for between 2-5 minutes and the flask was gently tapped against a solid surface every couple of minutes until the cells detached from the base and were floating freely in the trypsin solution. The trypsin was then inactivated by the addition of 3x volume of complete DMEM. The complete DMEM was able to stop the trypsinization as the FBS contains protease inhibitors. The media was pipetted against the base of the flask to ensure all cells were suspended in solution before being transferred to a sterile universal and centrifuged at 1500rpm for 5 minutes. The pellet was then resuspended in 1ml of complete DMEM. For the first passage (P1) the cells were seeded onto two T25 flasks by adding 500µl of cell suspension to 4ml complete DMEM in each flask. Once these two flasks reached confluency they were trypsinized and resuspended as previously described and then combined and seeded onto a T75 flask. From P2 onwards cells were split 1:2 when necessary. Cells were frozen between P2 and P4 during the exponential growth phase. Cells were trypsinized as previously described and resuspended in 1ml complete DMEM supplemented with 10% sterile dimethyl sulfoxide (DMSO); a cryoprotective agent that maintains the cellular osmotic balance. This suspension was placed in a cryovial (Alpha-laboratories, Hampshire, UK) which was in turn placed in a room temperature Mr. Frosty™ Freezing Container (ThermoFisher Scientific, Paisley, UK) filled with isopropanol which was then placed in a -80°C freezer. This ensured slow, uniform cooling of the cells (approximately 1°C per minute) and reduced intracellular ice crystal formation. After 24 hours the cells were removed from the Mr. Frosty™ Freezing Container and stored at -80°C.

Cells were thawed when required. This was done by removing cells from the freezer and placing them immediately into water at 37°C to warm the cells rapidly. The cryovial was removed from the water bath when only a small ice crystal was left in the cell suspension. 1ml of pre-warmed complete DMEM was gently added to the cryovial and then 1ml was removed and added to 10ml pre-warmed complete DMEM in a universal this was repeated 3-5 times and then the

entire contents of the cryovial was transferred to the universal. The cell suspension was centrifuged at room temperature 1500rpm for 5 minutes and the pellet resuspended and plated as above into a T25 flask.

### 2.6.3 Cell Viability

Cell viability was checked when cells were defrosted and at every passage thereafter. This was done using Trypan blue cell exclusion. Cells were revived and maintained once thawed as described in section 2.6.2. To determine the viability of the cells, 10µl of cell suspension was added to 10µl 0.4% solution of trypan blue (Sigma, Dorset, UK) to create a 1:1 dilution. The two were gently mixed and ~10µl was loaded onto a haemocytometer. All cells in the four outer grids were counted and an average was multiplied by $10^4$ and corrected for any dilution factor to give the total number of cells. The counting was then repeated only for cells that had a blue colour. This was the number of dead cells that had taken up Trypan Blue. Viability was calculated as a percentage by dividing the live count by the dead count. Viability in cells between P2 and P5 ranged from 90% to 50%. Cells with viability lower than 50% were not used.

## 2.7 Statistical Analysis

Coding was used to blind observers to different strain or treatment groups during data acquisition wherever possible. Blinding remained for any relevant assessments and decoded prior to statistical analysis. Animals were assigned to different treatment or gestational groups randomly and the ARRIVE (Animal Research: Reporting of *In Vivo* Experiments) guidelines were followed for all *in vivo* studies. Results are presented as a mean ± standard error of the mean (SEM) unless stated otherwise. The telemetry data obtained from the Dataquest system included hourly, daily and weekly averages. The best representation of the data was determined to be a presentation of the 12-hour averages of each measured parameter. These values were analysed using area under the curve (AUC) at specified pregnancy time points and compared using one-way ANOVA with Sidak post-hoc tests. Data that represented any rate of change were analysed using regression analysis; these gradients were then compared to a null hypothesis mean of 0 using a one-sample t-test to determine gestational dependent change. The cycle threshold values of gene expression data obtained from qPCR were normalised to the relevant housekeeper to obtain a delta cycle threshold (ΔCT; Ct value of the housekeeper gene subtracted from the Ct value of gene of interest). These ΔCT values were used for statistical analysis using the appropriate test for comparison. The mean ΔCT for each sample group where then expressed relative to the mean ΔCT of the control group (either WKY or the vehicle control) to give a ΔΔCT value. This was finally expressed as $2^{-\Delta\Delta CT}$, which accounted for primer efficiency and expressed the change in gene expression as a relative quantity in relation to 1. The error was calculated as a relative quantity minimum and maximum value for each group (minimum= $2^{-(\Delta\Delta CT+ SEM)} - 1$; maximum= $2^{-(\Delta\Delta CT- SEM)} - 1$). Statistical analysis and graphical representation was completed using Prism 6.0 GraphPad software. Statistical significance was accepted if a p-value was less than 0.05 and confidence intervals of 95% were used. Further information on the specific statistical tests used are detailed in the results chapters.

# Chapter 3 Characterisation of SHRSP Pregnancy

## 3.1 Introduction

Uncomplicated pregnancy requires major adaptations of the cardiovascular, renal and metabolic systems. It is associated with an increased cardiovascular burden that is intensified in hypertensive pregnancy complications such as pre-eclampsia. The WHO found that hypertensive complications during pregnancy account for 14% of direct maternal deaths worldwide (Say et al., 2014). This systematic review of global maternal deaths classed gestational hypertension as a direct cause of death; however it grouped pre-existing conditions, such as chronic hypertension and cardiovascular disease, separately as indirect causes (Say et al., 2014). This makes it unclear how many maternal deaths were due to hypertensive complication present during pregnancy, but it is probable that it is much greater than the stated 14%. In the developed world the proportion of maternal deaths directly attributed to gestational hypertension was 12.9% between 2003 and 2009 (Say et al., 2014). This is a complication that is becoming increasingly more prominent in the developed world, as mothers are having children later in life and are more likely to have pre-existing medical conditions; such as obesity, diabetes and pre-existing hypertension (ACOG, 2013, Antza et al., 2017, Sibai, 2002).

Modelling gestational hypertensive disorders has always been problematic due to the more severe pre-eclamptic conditions specifically occurring in humans and higher order primates (Steegers et al., 2010). Many pharmacological and surgical manipulations of animal models have been developed to explore the pathological consequences of gestational hypertension (Podjarny et al., 2004, McCarthy et al., 2011). The main drawback of these models is that they require an intervention or manipulation. Genetic modifications of mice and rats have been utilised in an attempt to replicate underlying molecular causes of gestational hypertensive disorders such as pre-eclampsia. The endothelial nitric oxide synthase knockout mouse ($eNOS^{-/-}$) has been found to mimic the abnormal uterine artery function associated with some cases of pre-eclampsia and the catechol-O-methyl transferase knockout ($COMT^{-/-}$) has demonstrated a pregnancy hypertensive phenotype and proteinuria; which are the major symptoms of pre-eclampsia (McCarthy et al., 2011, Kusinski et al., 2012, Kanasaki et al., 2008). Transgenic models have also been developed in order to mimic human pre-eclampsia more closely, as these models are often able to mimic the placental

dysfunction associated with pre-eclampsia (Takimoto et al., 1996). A transgenic rat model used by Bohlender *et al* imposed pre-eclamptic like symptoms in rats by increasing placental specific angiotensin II production (Bohlender et al., 2000). One caveat to these models is that they are not spontaneous, as in the human condition. A borderline hypertensive inbred mouse strain (BPH/5) has been identified as a spontaneous model of pre-eclamptic like phenotypes, with the borderline hypertensive blood pressure of these pregnant mice rising to hypertensive levels in the last week of pregnancy (Davisson et al., 2002). However, as this is a mouse model, it is limited when drawing comparisons between human uteroplacental vascular remodelling and placentation. The placenta plays a key role, alongside the maternal cardiovascular system, in the development of gestational hypertension and its impact on the fetus. Out of the commonly used laboratory rodents, rats are more akin to humans in their placentation and cardiovascular adaptations to pregnancy and thus may be more suitable than mice (McCarthy et al., 2011).

The spontaneously hypertensive rat (SHR) has been acknowledged as a potential model of hypertensive pregnancy and deficient maternal cardiovascular adaptations during pregnancy. The SHR was found to demonstrate fetal growth restriction, however only limited study was given to the underlying molecular mechanisms (Peracoli et al., 2001). Chu *et al* investigated the vascular reactivity in pregnancy but focused on systemic circulation and did not investigate uteroplacental circulation, which is of crucial importance in the detection of pre-eclampsia and the development of placental under perfusion which in turn can cause and/or aggravate gestational hypertensive disorders (Peracoli et al., 2001, Chu and Beilin, 1993). More recently, pregnancy in the stroke-prone SHR (SHRSP) has undergone preliminary investigations and could provide a more appropriate spontaneous hypertensive model (Barrientos et al., 2017, Small et al., 2016, Mary et al., 2017).

The uteroplacental blood flow and uterine artery vascular reactivity of the SHRSP rat has been found to be impaired during pregnancy (Small et al., 2016). This was found to be independent of the chronic hypertension exhibited by these rats pre-pregnancy, as defects were still observed when blood pressure was lowered using antihypertensive treatment from 7 weeks of age (Small et al.,

2016). This suggests that there is a major maternal influence in the development of impaired uteroplacental blood flow in the SHRSP. Yet pregnancy in these animals has not been fully characterised and understanding the physiological response to the hypertensive pregnancy exhibited by these rats will allow a more in depth understanding of the pathophysiological mechanisms of gestational hypertension.

## 3.2 Hypothesis and Aims

### 3.2.1 Hypothesis

SHRSP have an inappropriate maternal response to pregnancy, with impaired placentation and detrimental impact on the development of the fetus, when compared to pregnancy in the normotensive WKY.

### 3.2.2 Aims

- To profile the maternal response to pregnancy and examine cardiovascular and renal adaptations in SHRSP and WKY dams.

- To evaluate SHRSP and WKY fetal number and growth throughout gestation.

- To examine the structure, function and development of the SHRSP and WKY placenta.

## 3.3 Materials and Methods

Animals were housed and mated as described in general methods (Chapter 2). Urines were collected pre-pregnancy and during the first and second week of pregnancy using metabolic cages as outlined in section 2.3.5 and the albumin and creatinine ratio determined as in section 2.2.4. Maternal weights were recorded weekly to determine weight gain over gestation. At sacrifice the maternal weight was subtracted from that of the gravid uterus to obtain a measure of gravid-independent weight gain. Echocardiography was conducted as described in section 2.3.7. Maternal tissue and fetoplacental units were obtained at gestational ages GD12.5, GD14.5, GD18.5 and GD20.5, and the weights recorded, as described in general methods section 2.4. These time points allowed the full assessment of pregnancy in SHRSP and WKY rats. Litter number was recorded for each dam, furthermore the number of offspring born to WKY and SHRSP breeding females had been recorded for >10 years. These values were collected and analysed. In rodents the formation of the chorioallantoic placenta occurs between GD8.5 and 10.5 with placental cell lineage determined by GD12.5. At GD14.5 the chorioallantoic placenta is fully formed and the fetal and placental tissues can be accurately dissected. By GD18.5 the placental trophoblasts have reached maximal invasion and GD20.5 allows for an accurate measurement of fetal weight prior to birth. Placentas were dissected and fixed or frozen for histological, immunohistochemical or gene expression analysis, as outlined in section 2.4.4.

### 3.3.1 Vesicle Preparation

Transport across the placenta is adaptive and strives to meet the demands of the fetus. Obtaining an estimate of placental transport is a good measure of placental function, which can be detrimentally affected in hypertensive pregnancies. The main barrier to maternofetal transport is the maternal facing plasma membrane of the syncytiotrophoblast layer II of the placenta (Figure 3-1). This can be isolated from rodent placentas using $Mg^{2+}$ precipitation and ultracentrifugation. This layer can then be manipulated to form membrane vesicles that can be utilised to estimate maternofetal transport of particular amino acids across the placenta.

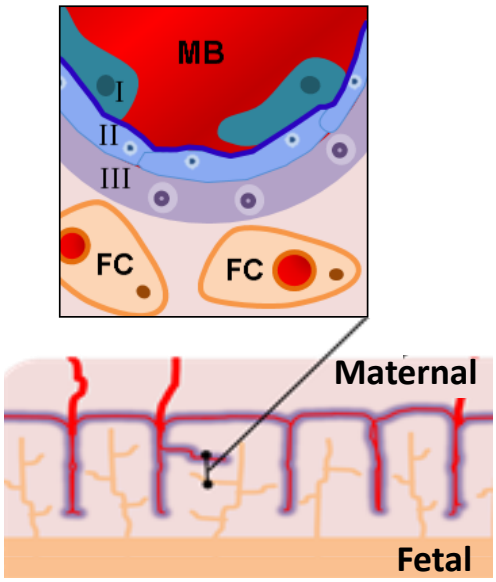


**Figure 3-1: Representation of the area of nutrient and gas exchange between mother and fetus in the rodent haemotrichorial placenta**
The rodent placenta has 3 syncytiotrophoblast layers (I, II and III). The 1st main barrier to maternofetal transport is the plasma membrane of syncytial layer II (highlighted in dark blue). This can be isolated and purified for *ex vivo* examination. MB = maternal blood; FC = fetal capillary.

GD18.5 placenta were dissected and weighed as described in general methods before being placed into a ~8ml of ice cold mannitol buffer solution [30mM mannitol, 1mM MgCl2, 10mM HEPES-Tris, pH 7.4] in a Sterilin® container on ice. All placentas were then weighed together and total placental weight was used to calculate the volume of ice cold mannitol buffer solution required for homogenisation. Homogenisation required a volume of mannitol buffer 4 times that of the placental weight (w/v). The placentas were homogenised using a Polytron™ PT 2100 homogenizer with 3mm rotor dispersion aggregate (blade attachment was cleaned with 3% hydrogen peroxide for 30 minutes and rinsed with 70% ethanol, $dH_2O$ then mannitol buffer prior to use). Homogenisation was conducted on ice in 30 second bursts and lasted between 2 and 4 minutes until a smooth homogenate was obtained. The homogenate containing all placental membranes was then placed into a glass beaker with magnetic stirrer and kept at approximately 4ºC by surrounding beaker with ice. Homogenates were stirred slowly and 10µl was removed for later purity analysis. 12mM $MgCl_2$ was added to the homogenate and stirring was continued for 10 minutes. $Mg^{2+}$ was used to precipitate unwanted membrane fractions as the apical plasma membrane of the syncytiotrophoblast layer has a net anionic charge therefore it cross-links with the $Mg^{2+}$ and other non-apical membranes aggregate in order to balance the

charge, thus precipitating from solution. Unwanted and unhomogenised tissue was removed by centrifugation at 2300xg for 15 minutes at 4°C. The supernatant was transferred to pre-weighed ultracentrifugation tubes (Beckman Coulter, High Wycombe, UK). Tubes were filled to the top with fresh mannitol buffer if required to prevent collapse during centrifugation. The tubes were then placed in a pre-cooled (4°C) Optima™ L-80 XP ultracentrifuge (Beckman Coulter, High Wycombe, UK) and spun at 23,500xg for 40 minutes, using a SW32-Ti rotor. This stage allowed the purified plasma membrane fraction of syncytiotrophoblast layer II to pellet. The supernatant was discarded and the tube re-weighed. The weight of the pellet was calculated and re-suspended in 2.8x intravesicular buffer (IVB) [290mM sucrose, 5mM Tris-base, 5mM HEPES: pH 7.4]. The suspension was then exposed to shear stress by passing through a 25 gauge needle 15 times in order to form the vesicles, due to the hydrophobic membrane segments joining to protect hydrophobic regions. 10µl of the vesicle suspension was placed on ice to later evaluate vesicle purity. Vesicles were finally placed into 500µl aliquots and snap-frozen in liquid nitrogen.

## 3.3.2 Vesicle Quality and Purity

### 3.3.2.1 BCA Protein Assay

The total protein concentration of the original placental homogenate and the prepared vesicles were determined using a Pierce™ BCA protein assay (ThermoFisher Scientific, Paisley, UK). The standards used were Pierce™ pre-diluted bovine serum albumin standards (ThermoFisher Scientific, Paisley, UK), the concentrations were 125µg/ml, 250µg/ml, 500µg/ml, 750µg/ml, 1000µg/ml, 1500µg/ml, 2000µg/ml. The working reagent was prepared immediately prior to use and consisted of 50 parts Reagent A and 1 part Reagent B. Placental homogenate samples were diluted 1:20 and vesicle suspensions were diluted 1:50 before use to place them in an optimal range for later calculations. The reactions were conducted in a 96-well flat-bottomed clear microplate. Each well had a sample/standard to working reagent ratio of 1:8; with 25µl of sample or standard and 200µl of working reagent. The solutions were mixed and the plate protected from light and incubated at 37°C for 30 minutes. Once the plate had cooled to room temperature the absorbance was measured on SpectraMax M2 microplate reader (Molecular Devices, Berkshire, UK) at 562nm. A standard curve

was constructed from the known standard concentrations and the concentrations of homogenate and vesicle were extrapolated.

#### 3.3.2.2 Alkaline Phosphatase Activity Assay

Alkaline phosphatase activity was measured to ensure the maternal facing plasma membrane of syncytiotrophoblast layer II was isolated and correctly orientated with the maternal facing alkaline phosphatase on the external surface of the vesicle (Kusinski et al., 2010). Samples of the homogenate were diluted 1:20 and vesicles were diluted 1:100. The assay relied on alkaline phosphatase converting p-nitrophenylphosphate (Sigma, Dorset, UK) to paranitrophenol which produces a yellow colour that can be quantified. The reaction was carried out in 250µl of DEA buffer [1M Diethanolamine, 0.5mM $MgCl_2$: pH 9.8] with 5µl of homogenate or vesicle sample. The reaction was initiated with the addition of 25µl of p-nitrophenylphosphate substrate stock (3.75µg/µl) made fresh in DEA buffer. The absorbance was read at a wavelength of 410nm at 5 seconds after addition and again after 2 minutes 5 seconds. The change in absorbance gives the indication of alkaline phosphatase activity over 2 minutes. The activity value was then divided by the total protein concentration of the sample to give an approximation of purity. The purity values for homogenates and vesicles were used to determine the enrichment factor. Enrichment factor = vesicle purity/homogenate purity

#### 3.3.2.3 Assessment of Nanoparticle Size

A NanoSight LM10 (Malvern, Worcestershire, UK) was used to further assure spherical vesicles had been obtained. A heterogeneous population of vesicles was expected in regard to size due to the method used to vesiculate which involved forcing membranes to re-join using passage through a needle. One vesicle preparation from WKY and one from SHRSP were assessed. Vesicles were diluted 1:100 in IVB and approximately 500µl vesicle suspension was injected onto stage. After focusing the microscope, a 60 second video was recorded and analysed using Nanoparticle Tracking Analysis v2.3 software to track particle number and size.

### 3.3.3 $^{14}$C-MeAIB Transport Assay

This assay utilises a radiolabelled synthetic analogue of System A amino acids; $^{14}$C-methylaminoisobutyric acid ($^{14}$C-MeAIB). This substance can be transported into vesicles by system A (SysA) amino acid transporters and its accumulation within vesicles measured due to the isotope presence. Each sample of vesicles were diluted to 7mg/ml in IVB and brought to room temperature before use. The principle of this assay relies on the $Na^+$ dependent activity of the SysA transporter. Vesicles are incubated with 0.33mM $^{14}$C-MeAIB in an extracellular vesicle buffers (EVB) that contains $Na^+$ [145mM NaCl, 5mM Tris-base, 5mM HEPES; pH 7.4 ($Na^+$ EVB)] or [145mM KCl, 5mM Tris-base, 5mM HEPES; pH 7.4$^+$ [($K^+$ EVB)]. This allows $Na^+$ dependent transport to be estimated as well as indication of passive transport or leak of tracer into the vesicles. 20µl of vesicle sample was pipetted into round-bottomed plastic Ultraclear™ tubes (Beckman Coulter, High Wycombe, UK) and 20µl of appropriate EVB was pipetted directly into this suspension at time 0. Reactions were carried out at room temperature. Thorough mixing was achieved by pipetting and gentle vortexing. Reactions were stopped with the addition of 2ml cold (4°C) 'stop' solution [130mM NaCl, 10mM $Na_2HPO_4$, 4.2mM KCl, 1.2mM $MgSO_4$, 0.75mM $CaCl_2$; pH 7.4] at 15 seconds, 30 seconds, 45 seconds and 60 seconds. The entire tube content was dispensed onto 0.45µm pore cellulose filter paper (pre-soaked in 'stop' solution) and washed with 2x5ml 'stop' solution whilst being subject to vacuum filtration on a 12-cup vacuum filtration manifold (Model 1225, Millipore®, Hertfordshire, UK). The filter paper was then removed from manifold and placed in labelled scintillation vials. Vesicle uptakes were run in duplicate for each sample, each EVB and each time point. A 'no protein control' was included for each EVB where vesicles are replaced with 20µl of IVB only. Two positive controls for total isotope count were also included for each EVB, where 5µl EVB was added to a pre-soaked filter and placed directly into a scintillation vial. The filter membranes were dissolved and vesicles lysed with the addition of 2ml of 2-ethoxyethanol. Four scintillation vials which only contained 2ml of 2-ethoxyethanol were also included as a negative control (blanks). Finally, 10ml of scintillation fluid (Perkin Elmer, Buckinghamshire, UK) was added and the disintegrations per minute (DPM) of $^{14}$C alpha emission was read on a Packard Tri-carb 2100TR Liquid Scintillation Analyser.

The average DPM of the blanks was subtracted from each sample and positive control to correct for background radiation. Net DPM was calculated by further subtraction of the 'no protein control' from the samples. Uptake rate was corrected for protein content and expressed as pmol/µg. Finally, $Na^+$ dependent uptake was calculated.

### 3.3.4 Trophoblast Invasion and Spiral Artery Assessment

Serial sections of the placenta were prepared and subjected to immunohistochemical processing to highlight trophoblast (cytokeratin 7) presence and smooth muscle actin (outlined in Chapter 2).

Assessment of trophoblast invasion was restricted to the maternal mesometrial triangle tissue and this was separated into three zones (Figure 3-2). The number of positive pixels for the whole area and each individual zone was recorded. This was then presented as a proportion of positive staining in the whole tissue and a percentage of positive pixels restricted to each zone.

Three to four spiral arteries were identified in each mesometrial zone by a blinded observer. The same arteries were located on placentas stained for cytokeratin 7 and for SMA. Trophoblast association within the vessel (endovascular) and/or nearby the vessel; within the field of view, approximately 200-400µm from the vessel in all directions (interstitial) was noted as a yes (scored numerically as 1) or no (scored numerically as 0). The average for each zone was determined and expressed as a percentage of trophoblast association. The assessment of spiral artery remodelling was conducted using a scoring system for the presence/absence of SMA staining within vessels walls as well as the degree of rounding/separation of vascular smooth muscle cells (Table 3-1).

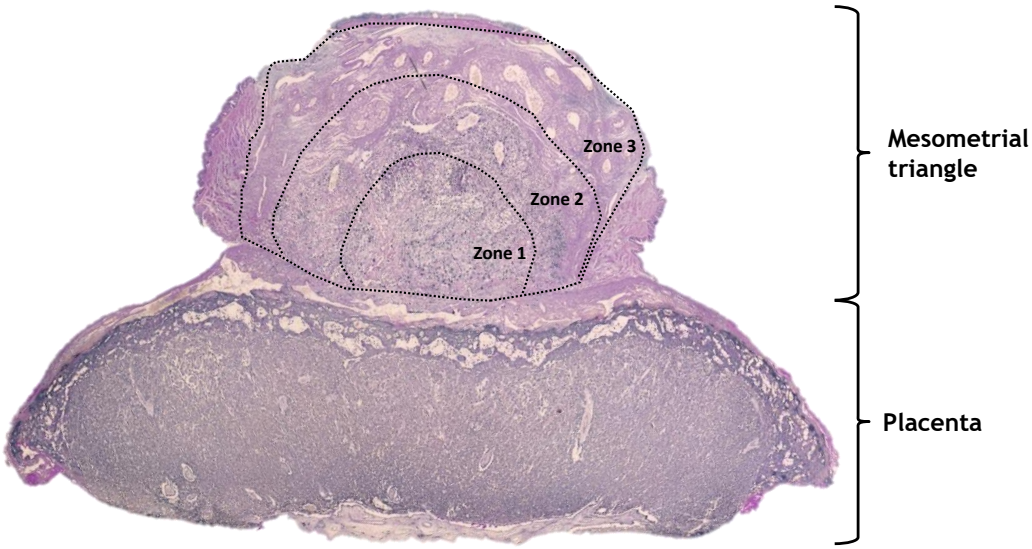


**Figure 3-2: A representative placental section highlighting trophoblast presence in the mesometrial triangle.**
Placental sections with the maternal mesometrial triangle attached were stained with cytokeratin 7. The dark purple staining indicates positive trophoblasts and these can be recorded in the placenta (which is composed mainly of trophoblasts) and the maternal tissue proximal to placental implantation (the mesometrial triangle). The zonal separation performed on analysis is indicated by the dashed lines and labels 1-3.

**Table 3-1: Spiral artery smooth muscle actin staining assessment scores**

| Score | Percentage of VSMC demonstrating rounding/separation |
|---|---|
| 1 | No visible SMA stain, complete loss of VSMC |
| 2 | >50% |
| 3 | 25%-50% |
| 4 | 10-25% |
| 5 | <10% |

The scoring method for assessing the amount of vascular smooth muscle cell (VSMC) dedifferentiation using the degree of rounding and separation observed adapted from the VSMC disruption assessment used by Lash *et al* (Lash et al., 2016).

### 3.3.5 Statistical Analysis

All data are presented as mean ±standard error (SEM) unless otherwise stated. Where appropriate normality was assessed using a Gaussian distribution. Where only two comparisons between SHRSP and WKY were required an unpaired student's t-test was conducted. In data presenting a rate of change over different pregnancy time points from the same animals a regression analysis was conducted for each strain between gestations and then compared using an unpaired student's t-test. Measurements with 3 or more groups and two influencing factors made from the same animal or placenta over the course of gestation/within different zones of the same tissue were subject to a repeated measure two-way ANOVA. Other data which compared 3 or more groups and had two influencing factors utilised an ordinary two-way ANOVA. Both were subject to a Sidak post-hoc test for additional comparison between set groups. Statistical analysis for the gene expression data compared the ΔCT values between WKY and SHRSP using an unpaired student's t-testing in each layer separately, then a repeated measures one-way ANOVA was used to examine changes across the layers for each strain separately. A p value$<0.05$ was determined as significant.

# 3.4 Results

## 3.4.1 Maternal Pregnancy Profile

Maternal body and tissue weights were recorded between 4 and 0 days pre-pregnancy (the non-pregnant (NP) weight) and at gestational day (GD) 6.5, 14.5, 18.5 and 20.5 time points. These weights are summarised in Table 3-2.

### 3.4.1.1 Weight Change throughout Gestation

Maternal weight gain was assessed by examining absolute weights and the rate of weight gain (Figure 3-3A). WKY had significantly larger weights than the SHRSP both pre-pregnancy and at each gestational time point. The overall rate of weight gain in WKY dams was also significantly greater than SHRSP (4.4±0.23 versus 3.0±0.28; $p<0.01$) (Figure 3-3A). The maternal weight gain was further investigated by removing the variable weight of the gravid uterus, thus producing information on pregnancy maternal induced weight gain, independent of number/size of fetal and placental units: the gravid-independent weight gain (Figure 3-3B). WKY had a significantly larger gravid-independent weight increase compared to SHRSP (26.5±2.02g versus 14.8±2.66; $p<0.01$) (Figure 3-3B).

### 3.4.1.2 Maternal tissue weights

Maternal hearts were dissected to obtain the mass of the left ventricle (LV) and both the left and right kidneys were weighed at sacrifice; these weights were then adjusted for tibia length. SHRSP normalised LV mass was found to be significantly greater than WKY at both NP (1.9±0.27 versus 1.6±0.18; $p<0.001$) and GD18.5 (1.8±0.17 versus 1.5±0.17; $p<0.05$) time points (Figure 3-4A). Pregnancy did not significantly affect the LV mass in either strain. The normalised kidney mass of NP SHRSP dams was significantly greater than that of NP WKY (4.3±0.31 versus 3.6±0.30; $p<0.001$). There was no difference between the two strains at GD18.5 (Figure 3-4B).

**Table 3-2: Maternal body and whole organ weights throughout gestation**

| | Gestation | Body (g) | Heart (g) | Liver (g) | Tibia (mm) |
|---|---|---|---|---|---|
| WKY | NP | 179.23 ± 4.7 (n=15) | 0.64 ± 0.01 (n=13) | 7.50 ± 0.42 (n=4) | 29.70 ± 0.78 (n=10) |
| | GD6.5 | 205.63 ± 3.1 *** (n=22) | 0.69 ± 0.02 (n=8) | 8.93 ± 0.32 * (n=5) | 31.83 ± 0.95 (n=6) |
| | GD14.5 | 220.37 ± 7.7 *** (n=3) | 0.73 ± 0.03 ** (n=3) | 11.93 ± 0.56 *** (n=3) | 32.00 ± 3.00 (n=3) |
| | GD18.5 | 249.74 ± 3.6 *** (n=16) | 0.72 ± 0.02 ** (n=8) | 11.24 ± 0.53 *** (n=3) | 32.75 ± 0.59 * (n=8) |
| | GD20.5 | 268.83 ± 8.1 *** (n=4) | 0.72 ± 0.05 (n=4) | 12.53 ± 0.67 *** (n=4) | 32.00 ± 0.41 (n=4) |
| SHRSP | NP | 169.23 ± 2.3 (n=15) | 0.69 ± 0.02 † (n=14) | 7.14 ± 0.13 (n=5) | 27.56 ± 0.91 (n=9) |
| | GD6.5 | 184.73 ± 2.4 ** ††† (n=20) | 0.73 ± 0.02 (n=8) | 8.30 ± 0.47 (n=3) | 31.63 ± 0.78 (n=8) |
| | GD14.5 | 210.43 ± 4.0 *** (n=4) | 0.80 ± 0.01 *** (n=5) | 9.45 ± 0.10 *** ††† (n=5) | 30.00 ± 1.03 (n=3) |
| | GD18.5 | 216.02 ± 4.9 *** ††† (n=14) | 0.79 ± 0.01 *** † (n=6) | 10.64 ± 0.36 *** (n=4) | 32.00 ± 1.30 ** (n=5) |
| | GD20.5 | 231.50 ± 6.2 *** †† (n=5) | 0.85 ± 0.01 *** † (n=5) | 10.45 ± 0.36 *** †† (n=5) | 31.25 ± 0.75 * (n=5) |

The maternal body weights, whole organ weights and tibia length were recorded pre-pregnancy and at different gestational time points. Significant differences were assessed using a two-way ANOVA with Sidak post-hoc comparison vs NP (*p<0.05, **p<0.01, ***p<0.001, ****p<0.0001) and vs WKY (†p<0.05, ††p<0.01, †††p<0.001, ††††p<0.0001). Data presented as mean ± SEM.

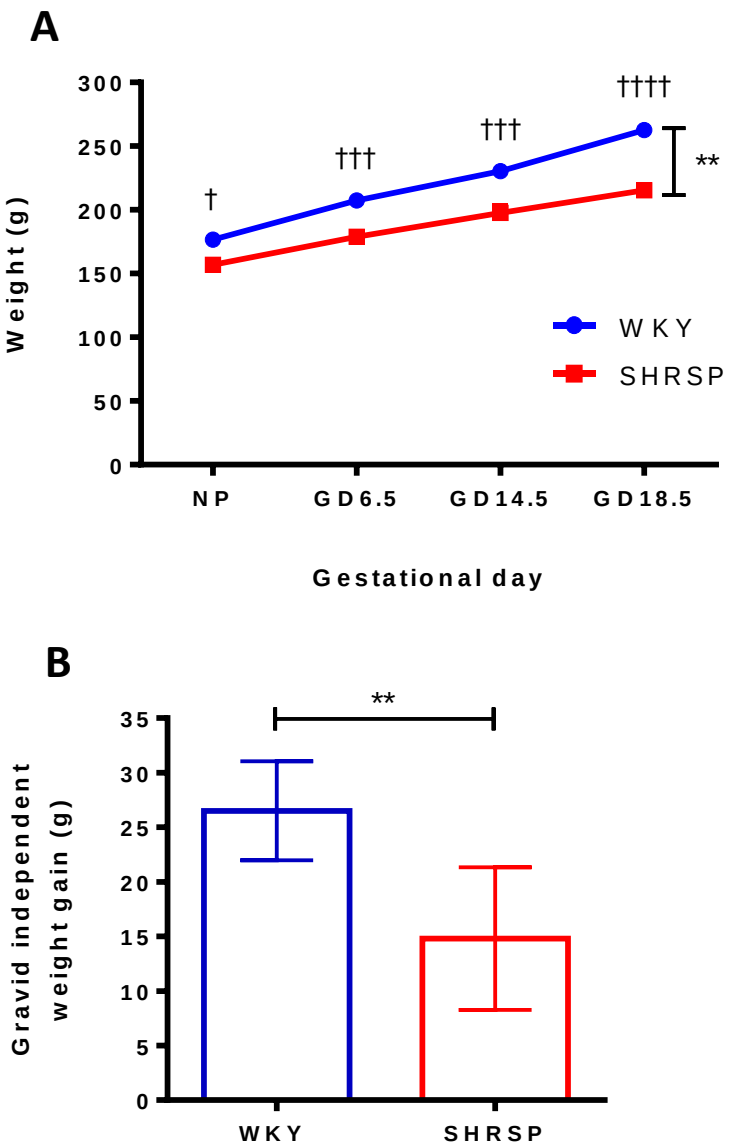


**Figure 3-3: Maternal weight change over gestation in WKY and SHRSP**
(A) The rate of total weight gain over gestation; NP was non-pregnant weights recorded between 4 and 0 days pre-pregnancy, the weights were then recorded on GD6.5, 14.5 and 18.5. Statistical significance between WKY and SHRSP was determined using unpaired students t-test (†p<0.05, †††p<0.001 and ††††p<0.0001), the overall weight gain rate was calculated using regression analysis for each dam and the gradients were then compared using unpaired students t-test (**p<0.01); n=5-6 dams. (B) The total amount of weight gained that was independent of the mass of the gravid uterus was calculated by subtracting the weight of the gravid uterine horn at sacrifice from the GD18.5 weight of the dam. The change from GD6.5 weights was then calculated to give a gravid independent weight increase over pregnancy. Statistical significance was determined using an unpaired students t-test (**p<0.01); n=5-6 dams.

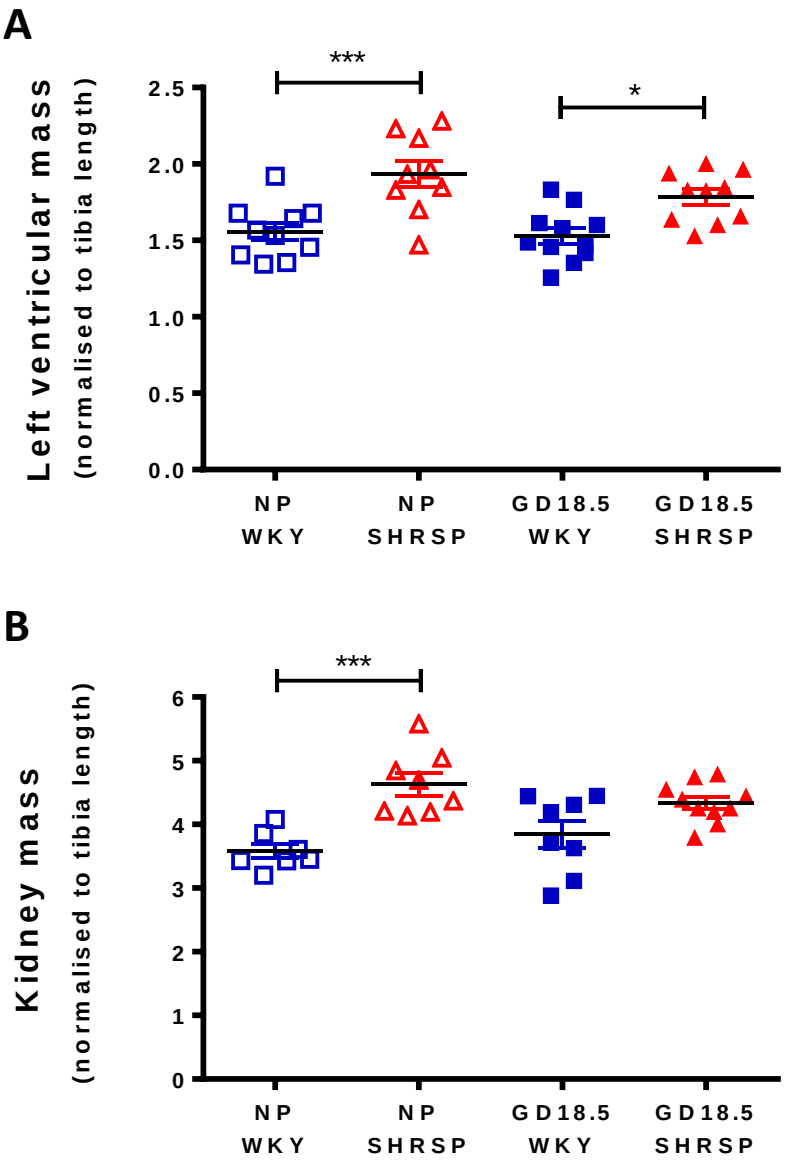


**Figure 3-4: Left ventricle and total kidney mass normalised to tibia length prior to and during pregnancy in WKY and SHRSP**
(A) Left ventricle mass (LVM) and (B) kidney mass was recorded at sacrifice in separate age-matched animals at a pre-pregnancy (NP) and at GD18.5 time point and normalised to tibia length. Statistical significance was determined using one-way ANOVA with Sidak post-test to examine differences between NP and GD18.5 in both strains as well as comparisons between WKY and SHRSP (*p<0.05, ***p<0.001); n=9-11.

#### 3.4.1.3 Cardiac Function

Echocardiography was used to assess cardiac function over gestation. Measurements of the anterior and posterior wall thickness during diastole and systole as well as the end diastolic and systolic diameter were used to calculate stroke volume (SV), cardiac output (CO), ejection fraction (EF) and fractional shortening (FS). SV was significantly increased in WKY between NP and GD18.5 (0.22±0.03ml versus 0.36±0.05; $p<0.01$). This was not observed in SHRSP. The SV of GD18.5 WKY was also significantly greater than that of GD18.5 SHRSP dams (0.36±0.05 versus 0.24±0.02; $p<0.05$) (Figure 3-5A). The CO response to pregnancy in WKY and SHRSP showed a significant increase from NP to GD18.5 (WKY: 80.5±5.44ml/min versus 125.3±12.28ml/min; $p<0.05$ and SHRSP: 51.7±4.09ml/min versus 87.4±6.33ml/min; $p<0.05$). The CO was also significantly increased in GD18.5 WKY dams compared to SHRSP ($p<0.05$) (Figure 3-5B). There were no significant differences observed in the FS or EF over the 18.5 days gestation, and no strain differences were found at any gestational stage (Figure 3-5C-D)

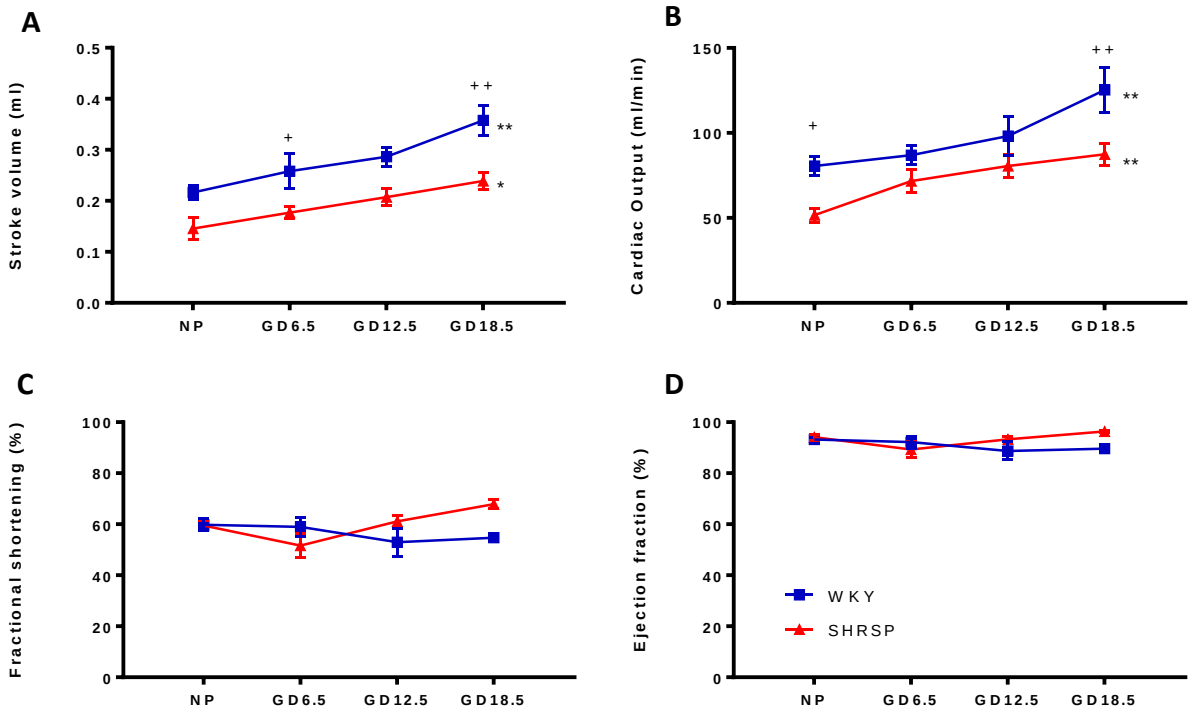


**Figure 3-5: Cardiac function calculated from echocardiographs recorded over gestation in WKY and SHRSP.**

The stroke volume (A), cardiac output (B), fractional shortening (C) and ejection fraction (D) of the heart were calculated from echocardiograph images taken one week prior to pregnancy (NP) and at each subsequent week of pregnancy (GD6.5, GD12.5 and GD18.5). Statistical significance was determined using a two-way ANOVA with Sidak post-hoc test to examine differences between strain at each gestation ($^{+}p<0.05$, $^{++}p<0.05$) and change over gestation from NP to GD18.5 (*p<0.05, **p<0.01); n=3-6.

#### 3.4.1.4 Urinary Analysis

Pregnancy did not significantly increase the water intake (Figure 3-6A) or urine output (Figure 3-6B) in either strain. Furthermore, there were no significant differences in the volume of water intake between WKY and SHRSP at any of the measured gestational time points (Figure 3-6A). Both strains appeared to have an increased urine output in the first two weeks of gestation. However, urine output was significantly lower in SHRSP compared to WKY during the last week of pregnancy (Figure 3-6B).

The albumin and creatinine concentrations were measured from 24-hour urine samples collected at time points one week prior to pregnancy (NP), during gestational week 1 (GD5.5-7.5) and during gestational week 2 (GD12.5-15.5). No significant differences were found in the albumin:creatinine ratios of WKY and SHRSP dams at any of the time points (Figure 3-6C).

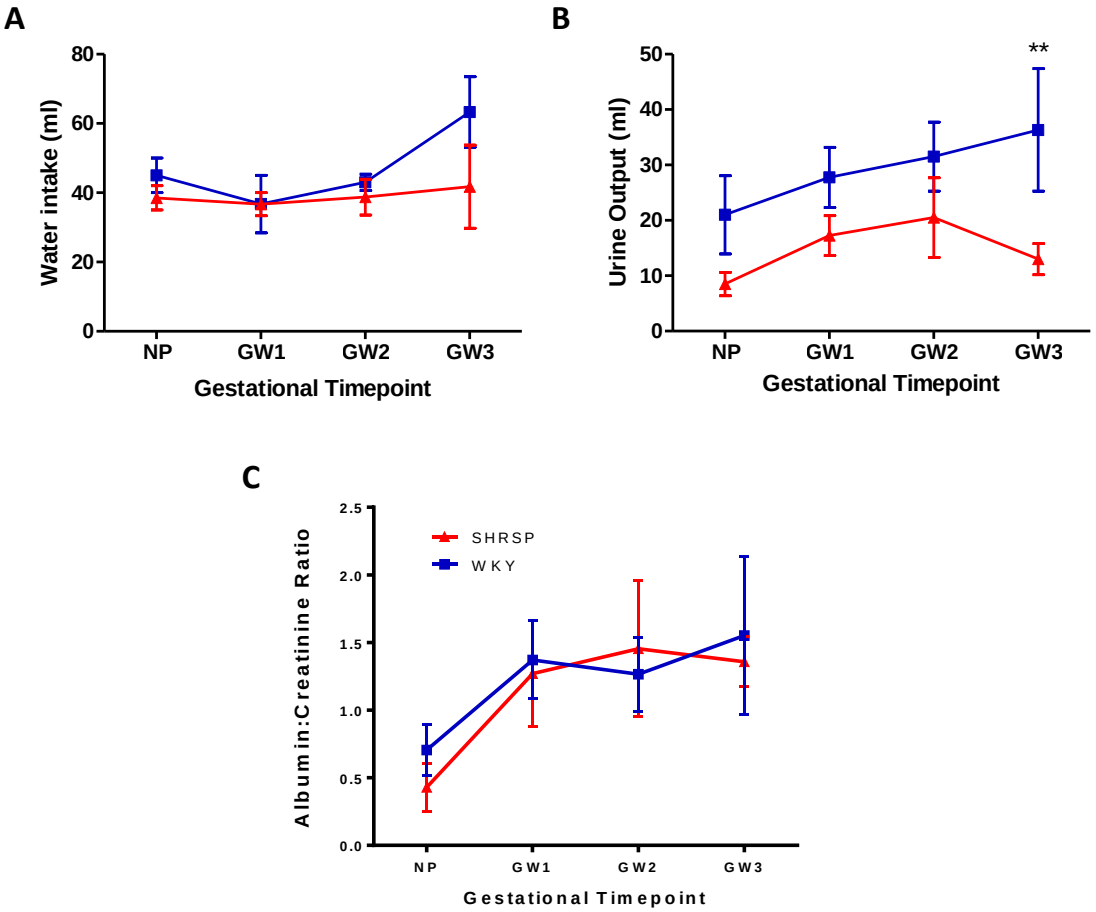


**Figure 3-6: Maternal urinary profile over gestation in WKY and SHRSP**
The water intake (A) and urine output (B) were recorded pre-pregnancy (NP) and during the 1st week (GW1: between GD5.5-7.5), the 2nd week (GW2: between GD12.5-15.5) and 3rd week (GW3 between GD16.5-18.5) of gestation. (C) The albumin and creatinine were measured from 24-hour urine samples collected pre-pregnancy (NP) and at gestational week 1 (GW1) and gestational week 2 (GW2). The albumin:creatinine ratio of these samples was then calculated. Data analysed using unpaired two-way ANOVA, with Bonferroni post-hoc tests to compare strains at the different time points; **p<0.01. Linear regression analysis was used for each strain to assess change over gestation using the gradient; n=3-4.

## 3.4.2 Offspring Outcome

### 3.4.2.1 Live litter size

The breeding database for SHRSP and WKY colonies maintained at the University of Glasgow was examined, allowing for the analysis of the number of pups born to each dam through brother x sister mating between 2009 to 2017. The average number of pups born to each primiparous dam was examined over this time period and each litter average presented in Figure 3-7A. The average number of pups born varied each year between 2009 and 2017, however there were no significant differences between WKY and SHRSP Figure 3-7B. The number of pups born to WKY mothers ranged from 2-14 and the range for SHRSP was 2-16 pups per litter. The only significant difference found was that fewer pups were born per litter to WKY dams in 2015 compared to 2017 ($6\pm1.3$ versus $11\pm0.7$; $p<0.05$).

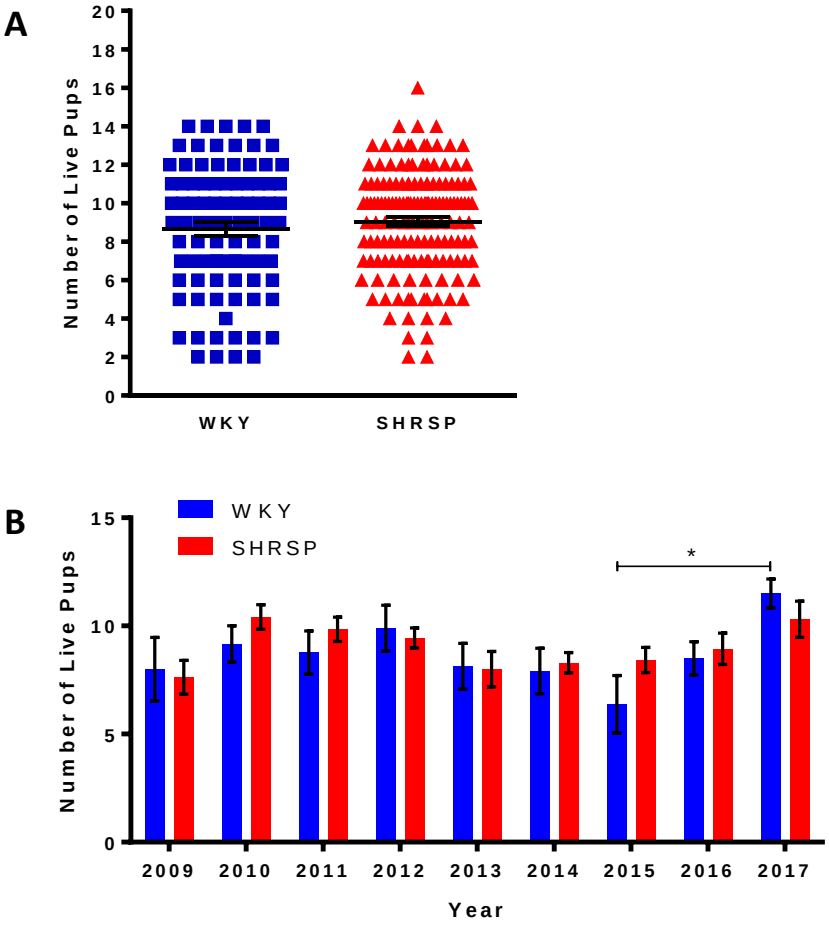


**Figure 3-7: The number of WKY and SHRSP pups per litter born between 2009 and 2017**
All live pups born to primiparous WKY and SHRSP mothers were recorded between 2009 and 2017. (A) The number of live pups born per litter in WKY and SHRSP; analysed using unpaired students t-test. (B) The number of average number of pups born per litter each year from 2009 to 2017 for WKY and SHRSP; analysed using two-way ANOVA to compare strain difference and change over time (*$p<0.05$); WKY n=89 litters, SHRSP n=154 litters

#### 3.4.2.2 GD18.5 Fetal Parameters

Representative images of the gravid WKY and SHRSP uterus are shown in Figure 3-8, along with images of individual fetoplacental units, the fetus and placenta.

The whole uterus was inspected and the number of fully formed fetuses was recorded, along with the number of any fetal resorptions. There were no significant differences in the frequency of resorptions found (Table 3-3).

There were no differences in the number of pups recorded per litter at GD18.5 (Figure 3-9). The average fetal weight for each litter was not significantly different between WKY and SHRSP (Figure 3-10A). In order to better assess fetal growth, a fetal weight distribution curve was generated by creating a histogram of all individual fetal weights and performing a non-linear fit of these histograms. This produced a curve for both WKY and SHRSP fetal weight proportions within their respective populations (Figure 3-10B). The $5^{th}$ centile was then calculated for the WKY fetal population, as fetal weights below this are regarded clinically as growth restricted in humans. This was found to be <0.86g, and 5.6% of SHRSP fetuses were under this weight. Further fetal measurements were conducted to assess for any growth restriction (Figure 3-11). There was no evidence of head sparing as the head:body weight ratio (determined by weighing fetal heads separately from the whole body) and head circumference were not significantly different between strain (Figure 3-11A-B). There was also no difference in the length of the fetus (Figure 3-11C). However, SHRSP fetal abdominal circumference was found to be significantly smaller than WKY (22.7±0.3mm versus 24.1±0.6mm; $p<0.05$) (Figure 3-11D).

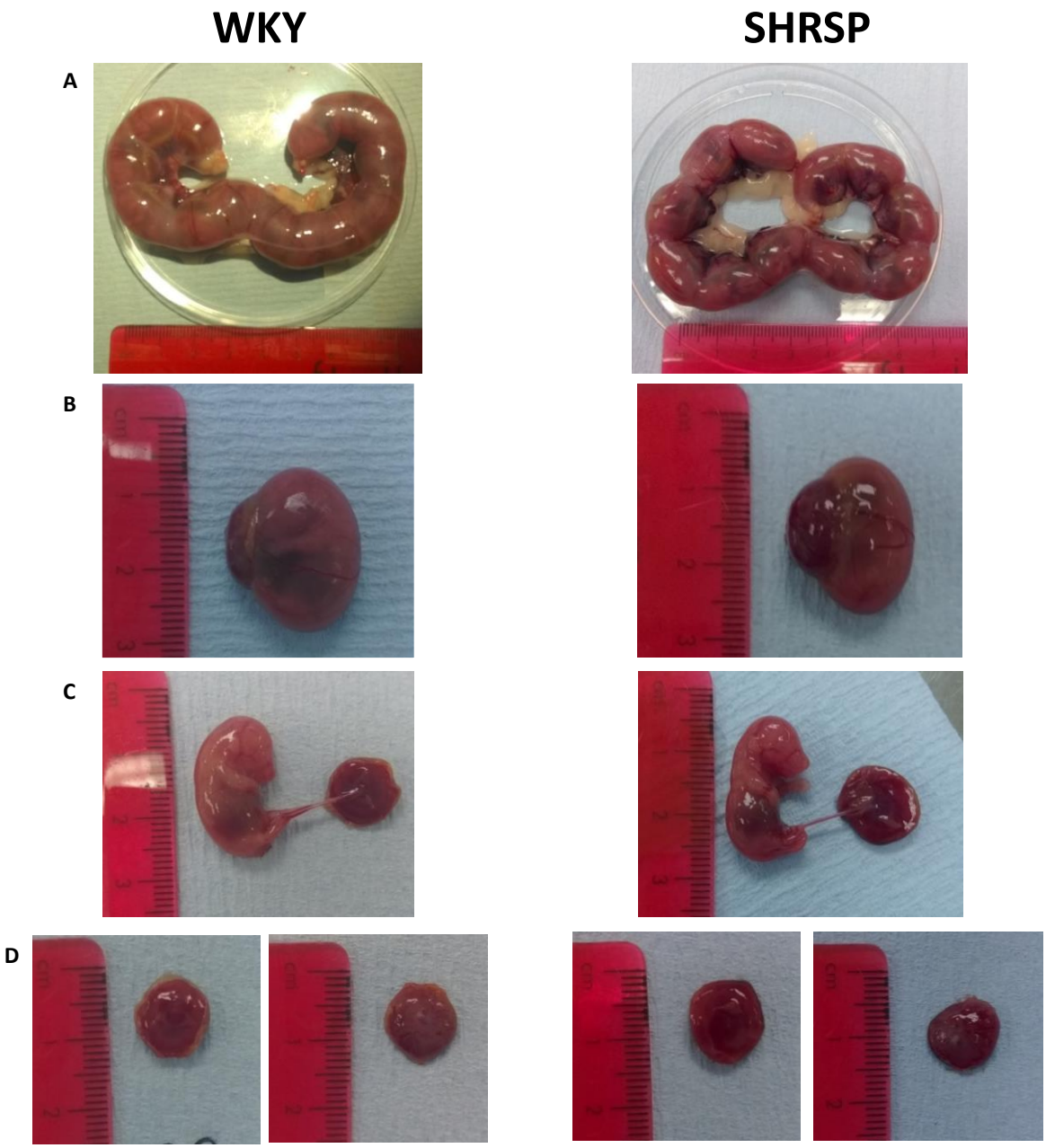


**Figure 3-8: Representative images of uteroplacental units of WKY and SHRSP at GD18.5**
(A) The whole gravid uterus for WKY and SHRSP, showing both horns of the fully pregnant rat uterus at GD18.5. (B) An individual fetoplacental unit still contained within the fetal membranes surrounded by amniotic fluid. (C) The fetus attached to its respective placenta via the umbilical cord. (D) The placenta dissected from membranes, fetus and umbilical cord left image is showing the chorionic plate surface (fetal side) and right image is showing the decidual layer (maternal side) for both WKY and SHRSP.

**Table 3-3: Resorption statistics for WKY and SHRSP pregnancies**

| Resorption information | WKY | SHRSP |
|---|---|---|
| Total number of pregnancies | 29 | 23 |
| Number exhibiting 1 or more resorptions | 15 | 8 |
| Ratio of resorptions to number of implant sites | 0.042 | 0.054 |
| % resorptions normalised to total litter size | 12.21 | 15.51 |

The total number of pregnancies and the number of these effected by resorptions are stated. The ratio of number of resorptions identified was not significantly different in WKY and SHRSP; similarly, there was no difference in the percentage of resorptions within a litter.

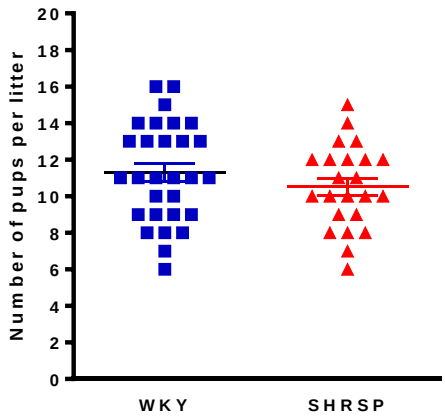


**Figure 3-9: Number of fetuses per litter at GD18.5 for WKY and SHRSP dams**
The number of pups per litter were counted at GD18.5 sacrifice. Statistical analysis was conducted using unpaired student's t-test; n=23-30 litters.

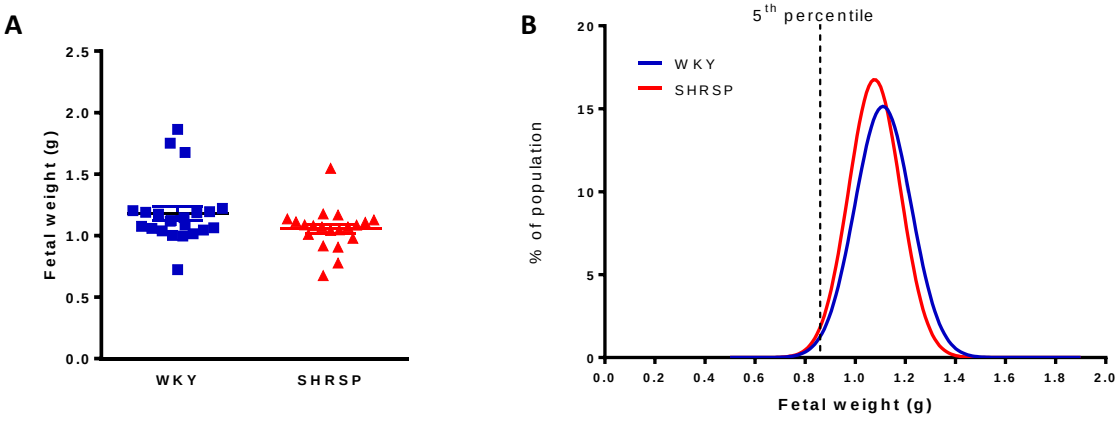


**Figure 3-10: GD18.5 fetal weights and size parameters for WKY and SHRSP.**
Each fetal weight was recorded individually at GD18.5. (A) A litter average for the fetal weight was plotted for WKY and SHRSP; n=20-23 litters, analysed using unpaired student's t-test. (B) Shows the fetal weight distributions, calculated from WKY and SHRSP individual fetal weights from all litters. The distribution curve indicates the range of weights of the population of WKY and SHRSP fetuses. The dotted line indicates the lowest 5$^{th}$ percentile for WKY fetal weights; WKY, n=228 (from 23 litters) and SHRSP n=205 (from 20 litters).

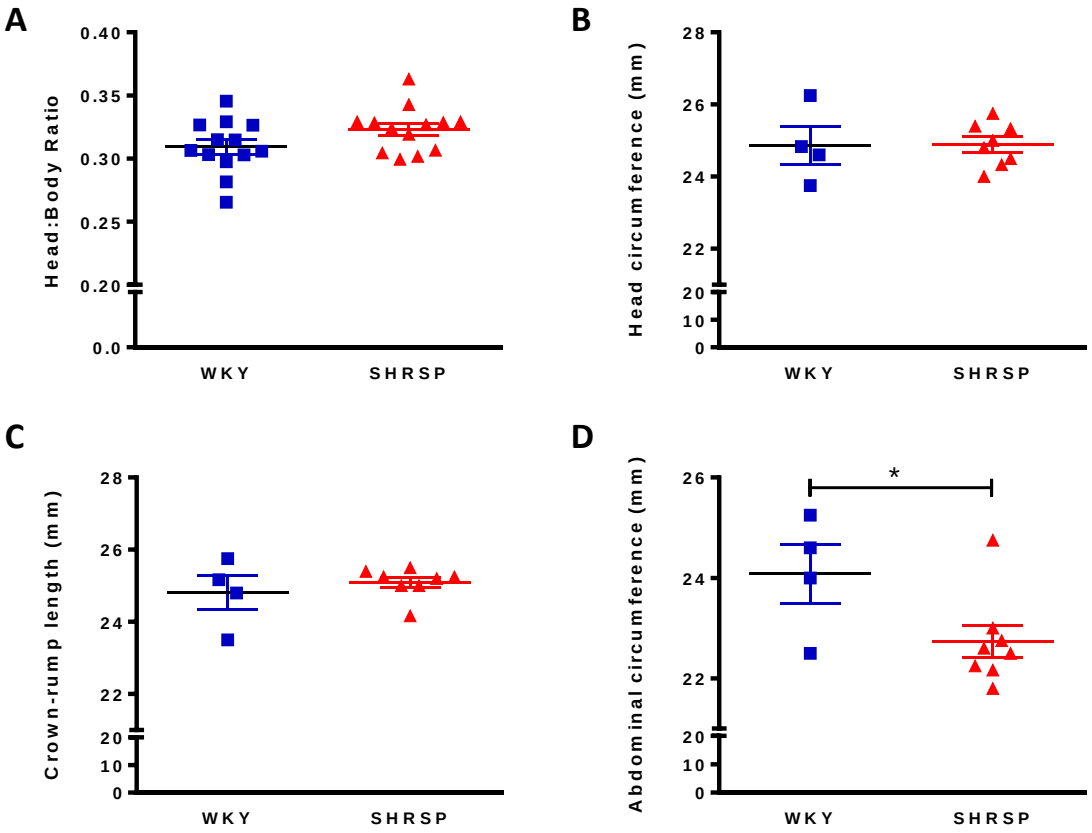


**Figure 3-11: Fetal size parameters measured at GD18.5 for WKY and SHRSP**
(A) Measurements of fetal size proportions were made by calculating the ratio of head weight to total body weight. Anthropometric measurements were performed using a cotton thread to measure (B) the head circumference; the circumference of the head above the ears and eyes, (C) the crown-rump length; the distance between the top of the head (intersection with the head circumference measure) and the base of the tail, following the curve of the fetal spine and (D) the abdominal circumference; the circumference around the fetal abdomen at the site of umbilical cord insertion. Statistical significance was determined using unpaired student's t-test (*$p<0.05$); n=13 for head:body weight ratio and n=4-8 for anthropometric measurements.

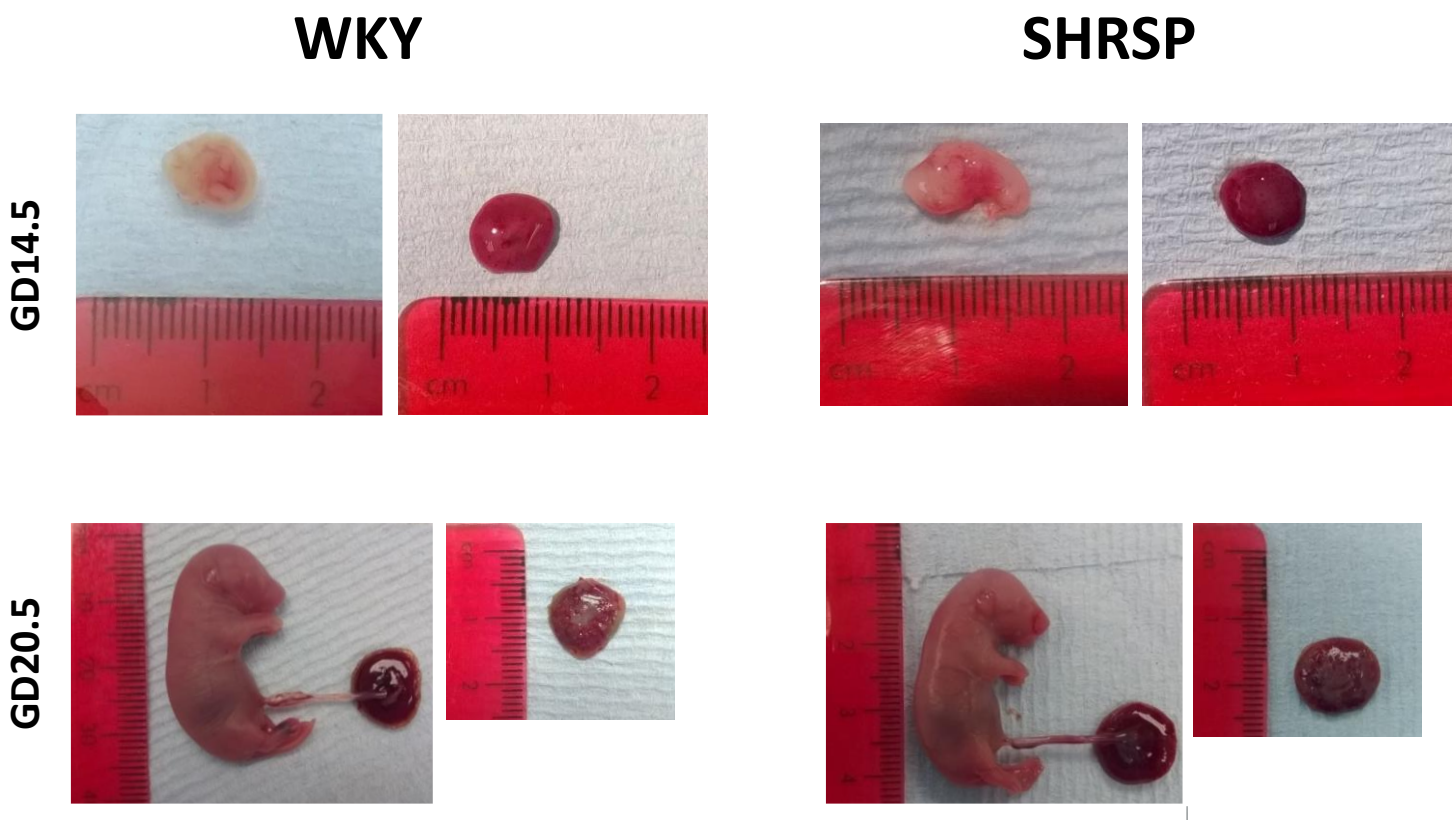


**Figure 3-12: Images of gestational day 14.5 and 20.5 fetus and placenta from WKY and SHRSP**
Representative images of GD14.5 and GD20.5 fetus and placenta are shown with fetal images on the left and placenta on the right. At GD14.5 the fetus is still in early stages of development and is smaller than the placenta. GD20.5 is approximately 2-3 days before birth for WKY and SHRSP dams, at this stage the fetal development is near completion and its size has increased exponentially.

#### 3.4.2.3 Fetal growth trajectory

Fetal weights were also investigated at GD14.5 and GD20.5. Figure 3-12 shows representative images of the fetus and placenta at these gestational stages. The rate of fetal growth between GD14.5 to GD18.5 significantly increased in both WKY and SHRSP (WKY: 0.097±0.003g versus 0.960±0.089g; $p<0.0001$ and SHRSP: 0.093±0.005g versus 0.973±0.044g; $p<0.0001$) and then again from GD18.5 to GD20.5 (WKY: 0.960±0.089g versus 2.75±0.07; $p<0.0001$ and SHRSP: 0.973±0.044g versus 2.62±0.04g; $p<0.0001$). The rate of growth significantly increased between GD18.5 and GD20.5 compared to GD14.5-GD18.5 in both WKY and SHRSP (WKY: 1.01±0.13 versus 0.16±0.04; $p<0.01$, and SHRSP: 0.83±0.02 versus 0.22±0.02; $p<0.001$) (Figure 3-13A). The late gestational stage of fetuses collected at GD20.5 allowed for gendering the litter and male and female weights were separated for analysis. There were no significant differences in fetal weights between WKY and SHRSP for both gender, and males and females were not significantly different from one another within each strain (Figure 3-13B).

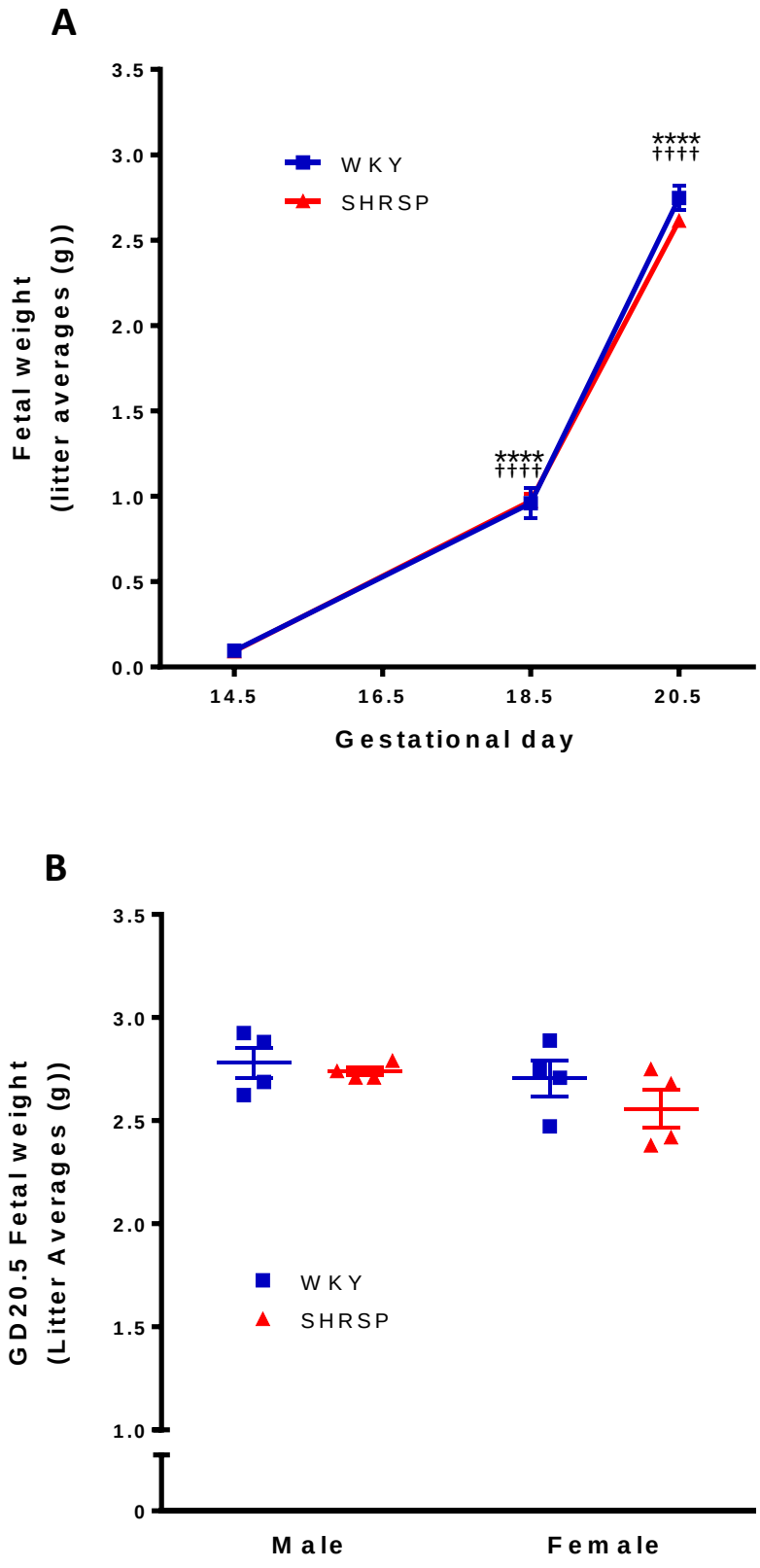


**Figure 3-13: Fetal growth trajectory and the gender separated weights at GD20.5**
(A) The fetal weights were recorded from separate pregnancies at GD14.5 (n=3-4 litters), GD18.5 (n=7-8 litters) and GD20.5 (n=4 litters). Statistical significance was determined by using a two-way ANOVA to examine differences between WKY and SHRSP at each time point as well as changes over gestation (****p<0.0001 vs GD14.5 WKY, ††††p<0.0001 vs SHRSP GD14.5). (B) Due to the advanced developmental stage of GD20.5 fetuses gender was able to be determined, thus each litter average was split into the male and female fetal weights. Analysed using one-way ANOVA.

## 3.4.3 Placental Outcome

Placentas were weighed and collected at GD14.5, 18.5 and 20.5 to examine placental characteristics of the SHRSP and WKY.

### 3.4.3.1 Placental growth trajectory, size and gross morphology

Placental weights at GD18.5 were not found to be significantly different between strains (Figure 3-14A). There was also no evidence of placental insufficiency relative to fetal size as the fetal:placental ratios were not significantly different between the two strains (Figure 3-14B).

Placental growth between GD14.5 and GD18.5 and GD20.5 was similar in WKY and SHRSP (Figure 3-15). Both strains demonstrated a significant increase in placental weight between GD14.5 and GD18.5 (WKY: 0.08±0.009g versus 0.23±0.004g; $p<0.0001$, and SHRSP: 0.07±0.009g versus 0.23±0.005g; $p<0.0001$) as well as a significant increase in weight between GD18.5 and GD20.5 (WKY: 0.23±0.004g versus 0.27±0.006g; $p<0.01$, and SHRSP: 0.23±0.005g versus 0.27±0.009g; $p<0.001$). The rate of increase was significantly greater between GD14.5 and 18.5 than between GD18.5 and GD20.5 in SHRSP (gradient of 0.04±0.002 versus 0.02±0.007; $p<0.05$).

Placentas were sectioned for histology and stained with PAS stain. This allowed for the visualisation of the placental layers (the junctional and labyrinth zones) as well as the maternal mesometrial triangle; which is the location of the decidua and myometrium (Figure 3-16A). The quantification of placental layer size was conducted by analysing the total pixel area of the junctional and the labyrinth zones. The proportional size of each layer was then determined along with the junctional:labyrinth ratio (Figure 3-16 B-C). WKY placentas were composed of 70±1.6% labyrinth zone to 30±1.5% junctional zone whereas the SHRSP had a slightly larger labyrinth proportion (77±1.4%) with a smaller junctional zone (23±1.4%). Both these layers were significantly different in proportions compared between strains ($p<0.01$) (Figure 3-16B). This is reflected in the significantly greater junctional:labyrinth ratios observed in WKY compared to SHRSP (0.44±0.03 versus 0.31±0.02; $p<0.01$) (Figure 3-16C).

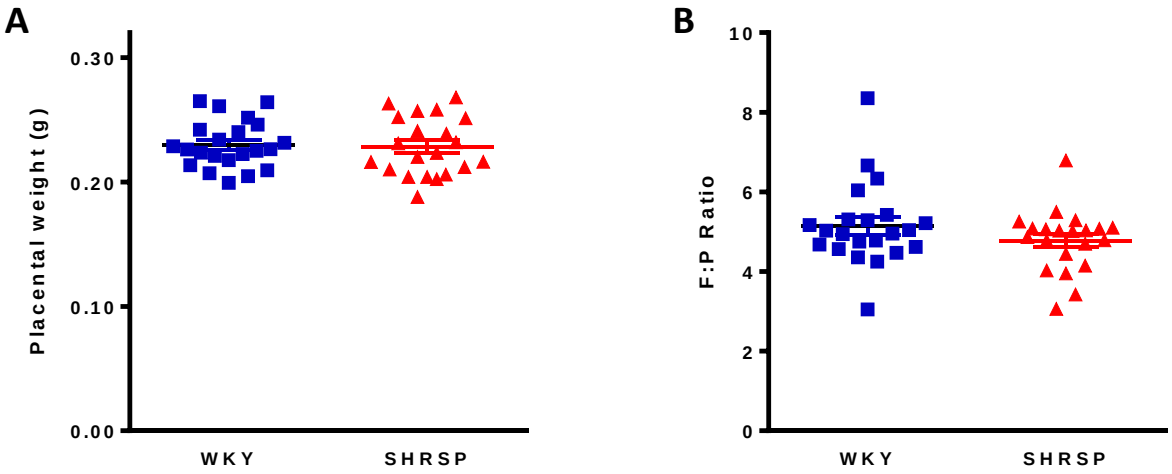


**Figure 3-14: Placental weights and the fetal:placental weight ratios at GD18.5**
(A) Placental weights recorded at GD18.5 for WKY and SHRSP, presented as litter averages. (B) The fetal weight to placental weight ratios expressed as averages for each litter to indicate any placental insufficiency. Assessed using unpaired student's t-test; n=21-23 litters.

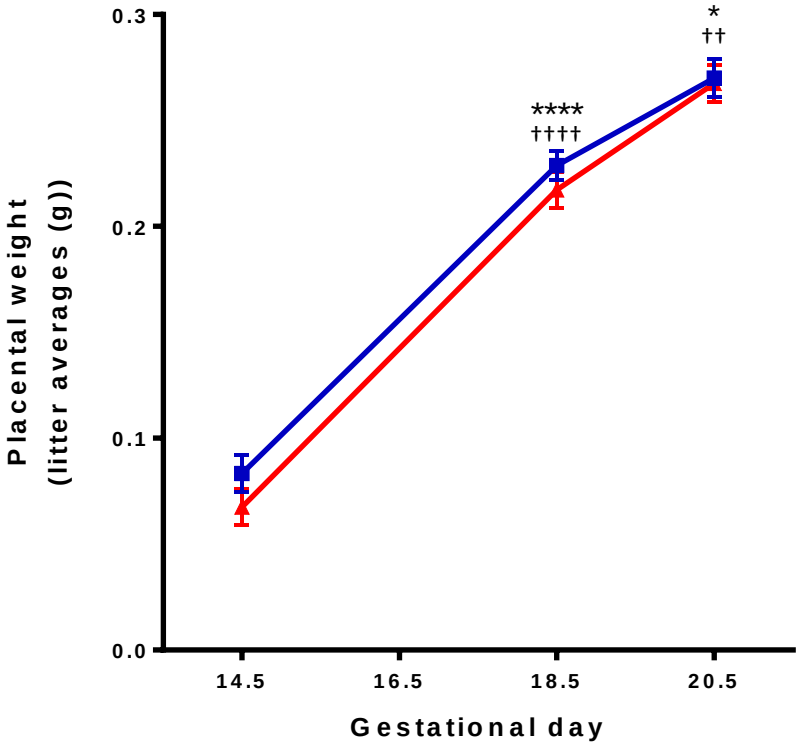


**Figure 3-15: Placental growth trajectory across gestation in WKY and SHRSP**
The placental weights were recorded from separate pregnancies at GD14.5 (n=3-4 litters), GD18.5 (n=7-8 litters) and GD20.5 (n=4 litters). Statistical significance was determined by using a two-way ANOVA to examine differences between WKY and SHRSP at each time point as well as changes over gestation (****p<0.0001 vs GD14.5 WKY, ††††p<0.0001 vs SHRSP GD14.5; *p<0.05 vs WKY GD18.5, ††p<0.01 vs SHRSP GD18.5).

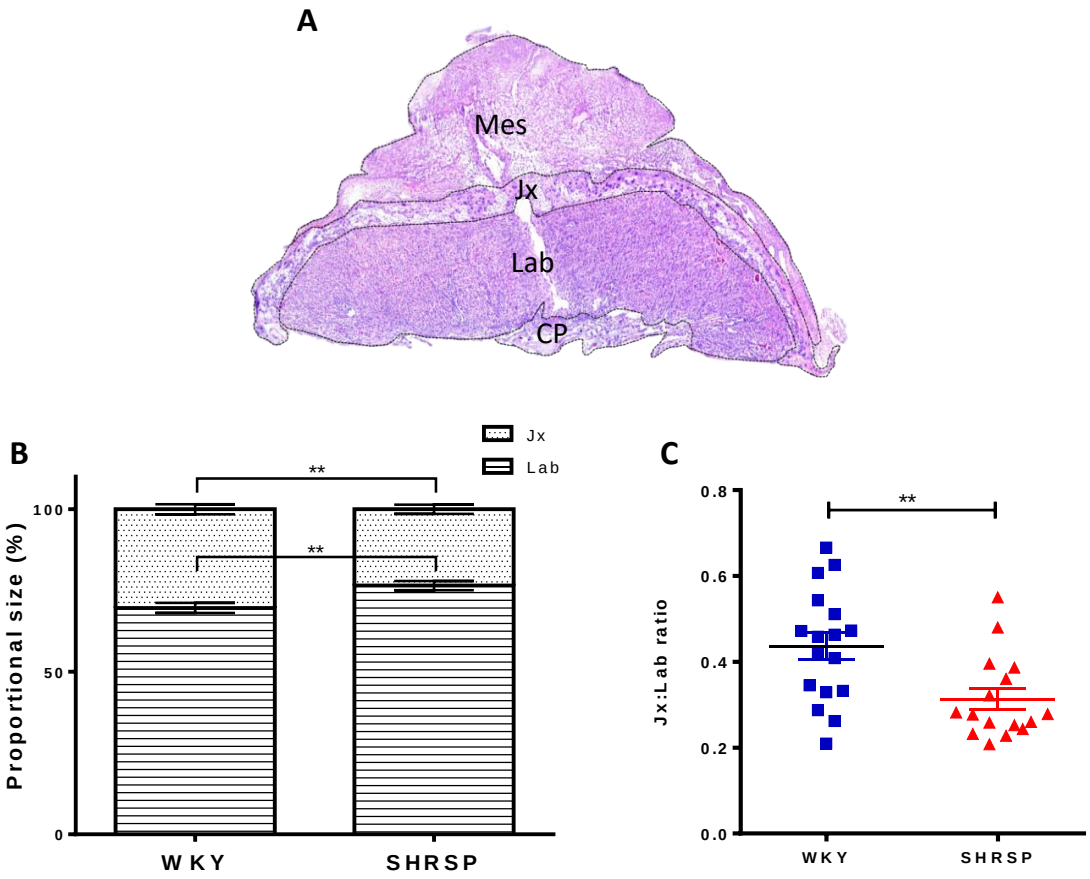


**Figure 3-16: Histological analysis of placental size using layer proportions**
(A) A representative image of the rodent placenta highlighting the different maternal, placental and fetal zones. Mes= maternal mesometrial triangle; Jx = placental junctional zone; Lab = placental labyrinth zone and CP= fetal chorionic plate. (B) The proportional size of the two placental zones (Jx and Lab) were determined using pixel number. Significant differences in layer proportion between WKY (n=9) and SHRSP (n=7) were determined using unpaired student's t-test (**p<0.01). (C) The proportional size was also expressed as a ratio between total pixel area of the junctional zone and total pixel area of the labyrinth zone (Jx:Lab ratio), statistical significance was determined using unpaired student's t-test (**p<0.05); n=16-17.

#### 3.4.3.2 Placental glycogen cell content

Placenta from WKY demonstrated significantly more PAS positive staining in the junctional zone of the placenta than SHRSP at GD14.5 (41.4±4.8% versus 16.6±2.5%; $p<0.01$) (Figure 3-17A). There were no significant differences observed in PAS staining between strains at GD20.5. WKY placentas demonstrated a significant loss of PAS positive staining between GD14.5 and GD20.5 (41.4±4.8% versus 15.74±3.2%; $p<0.001$), whereas the SHRSP showed no significant change over gestation. Representative images of WKY and SHRSP placenta from GD14.5 and 20.5 are demonstrated in Figure 3-17B-E.

#### 3.4.3.3 Placental collagen content

Placental collagen content was visualised using picrosirius red staining. This demonstrated significantly less collagen staining in the maternal mesometrial triangle of the SHRSP compared to WKY (46.0±5.2% versus 73.7±3.5%; $p<0.0001$) (Figure 3-18A-C). However this observation was changed in the labyrinth zones, with the percentage of positive staining found to be significantly increased in the SHRSP compared to WKY placenta (29.0±2.5% versus 8.8±1.0%; $p<0.0001$) (Figure 3-18A).

#### 3.4.3.4 Trophoblast invasion and Spiral Artery Remodelling

Trophoblast invasion into the mesometrial triangle was evaluated using immunohistochemistry, representative placental images of WKY and SHRSP are shown in Figure 3-19A-B. WKY were found to have a significantly higher proportion of cytokeratin 7 positive staining in the maternal mesometrial triangle than SHRSP (2.2±0.3% versus 0.68±0.1%; $p<0.01$) (Figure 3-19C). This invasion was then assessed according to depth of invasion through the three mesometrial zones. Whilst there were no significant differences between the percentage of positive staining between WKY and SHRSP in either zone, significantly less cytokeratin staining was observed in SHRSP zone 3 compared to zone 1(most proximal to the placenta) (10.9±2.1% versus 55.8±1.9%; $p<0.05$) (Figure 3-19D).

Spiral artery remodelling was assessed using a scoring system for dedifferentiation and loss of smooth muscle actin (SMA) staining around spiral

arteries in the 3 mesometrial zones (1= no SMA staining; 5 = >50% of the artery surrounded by SMA, with no rounding/separation of VSMC). There were no differences in the scores between WKY and SHRSP within any of the 3 zones (Figure 3-20A). Zone 1 had a significantly lower SMA score than zone 3 for WKY (1.7±0.1 versus 3.7±0.4; $p<0.01$); and a significantly lower score compared to zones 2 and 3 in SHRSP (1.5±0.2 versus 3.6±0.4; $p<0.01$ and 4.2±0.5; $p<0.001$). Representations of the SMA staining within each mesometrial zone is illustrated for WKY and SHRSP in Figure 3-20B. The presence of trophoblasts within (endovascular) and proximal to (interstitial) the spiral arteries was also assessed. These were assigned a presence (1) or absence (0) score and a percentage was calculated from all the arteries assessed in that zone of that mesometrial triangle. Both WKY and SHRSP had a significantly higher percentage of endovascular trophoblasts identified as present in spiral arteries in zone 1 compared to zone 2 (WKY; 80±13.3% versus 33.3±18.3%; $p<0.05$ and SHRSP; 91.7±8.3% versus 33.3±19.3%; $p<0.05$) (Figure 3-20C). There were no significant differences between the strains in either zone. There were no significant differences in interstitial trophoblast presence between the zones or between the strains (Figure 3-20D). The spiral arteries identified in zone 3 had no trophoblast association. Representative images of the trophoblast association with spiral arteries in each zone are presented in Figure 3-20E.

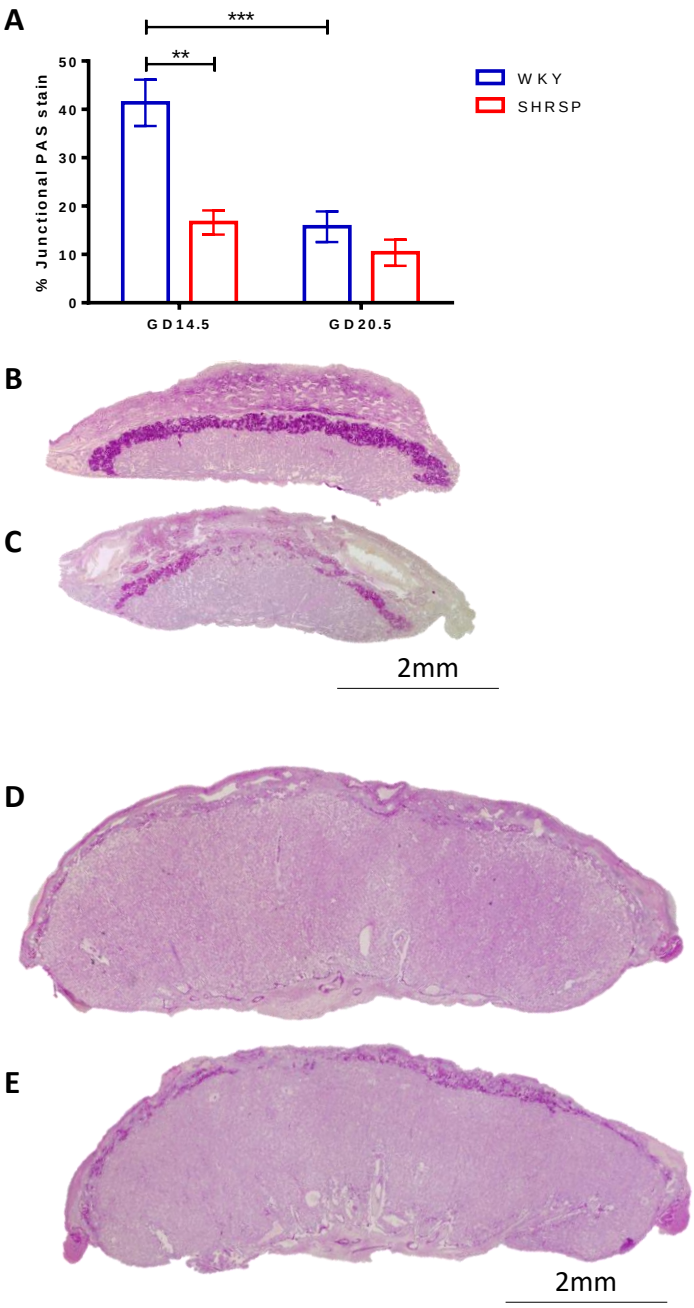


**Figure 3-17: PAS stained placenta from GD14.5 and GD20.5 from WKY and SHRSP**
(A) The percentage of positive PAS staining in the junctional zone of WKY and SHRSP placenta at GD14.5 (n=3-4) and GD20.5 (n=5-8) was quantified by a blinded observer using Image J. Statistical comparisons between WKY and SHRSP at each gestation and the difference between gestations of each strain was assessed using a two-way ANOVA with a Sidak post-hoc test (*p<0.05, **p<0.01, ***p<0.001). Representative images of the whole placenta at GD14.5 (B-WKY; C-SHRSP), and GD20.5 (D-WKY; E-SHRSP) stained using PAS, highlighting the positive magenta staining in the junctional zone.

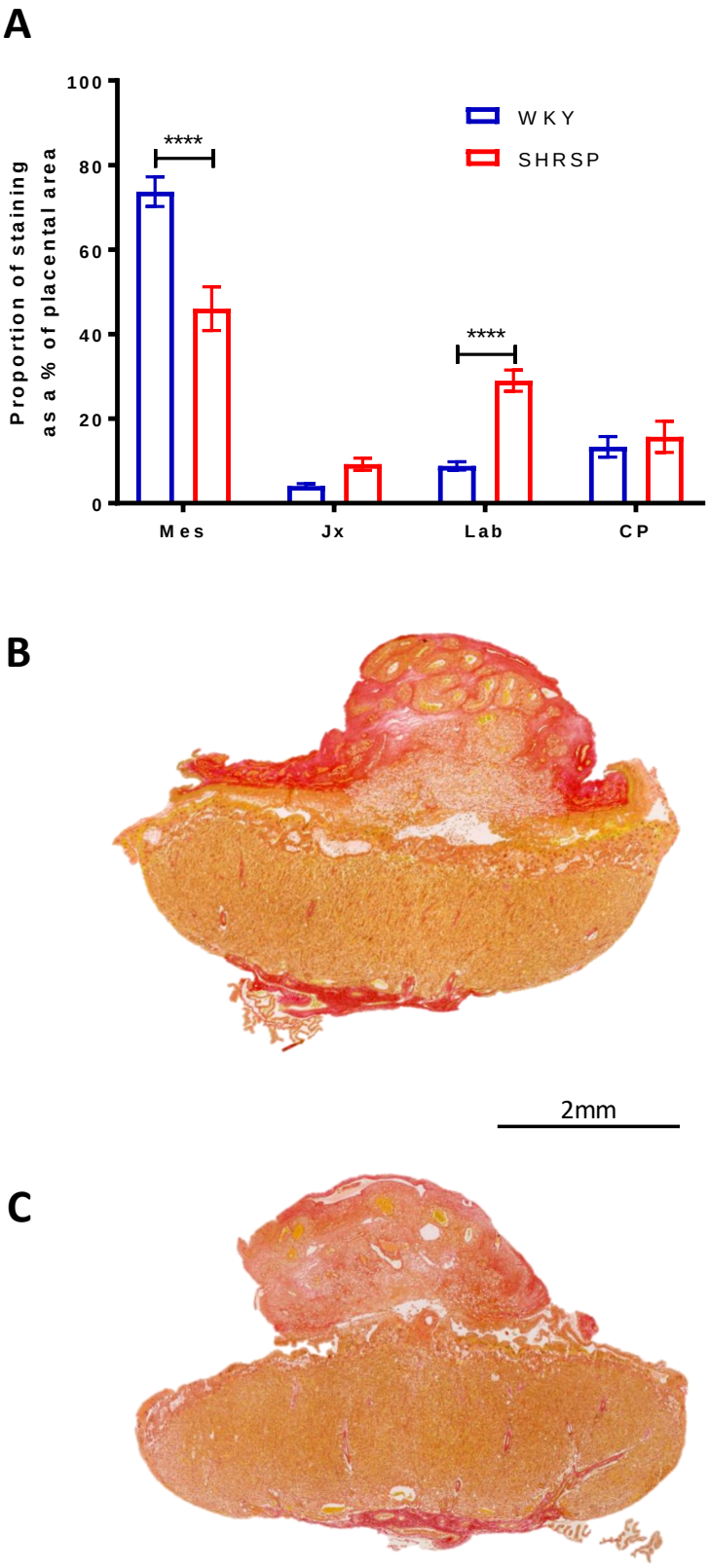


**Figure 3-18: Collagen staining of the GD18.5 placenta from WKY and SHRSP**
(A) The percentage of picrosirius red staining was quantified in the different maternal, placental and fetal zones (Mes= maternal mesometrial triangle; Jx = placental junctional zone; Lab = placental labyrinth zone and CP= fetal chorionic plate) and expressed as a percentage relative to the total size of that area revealed significant. Statistical comparisons between WKY (n=8) and SHRSP (n=7) in each zone was assessed using a two-way ANOVA with a Sidak post-hoc test (****p<0.0001). The collagen stained red, representative images of the whole placenta for (B) WKY and (C) SHRSP.

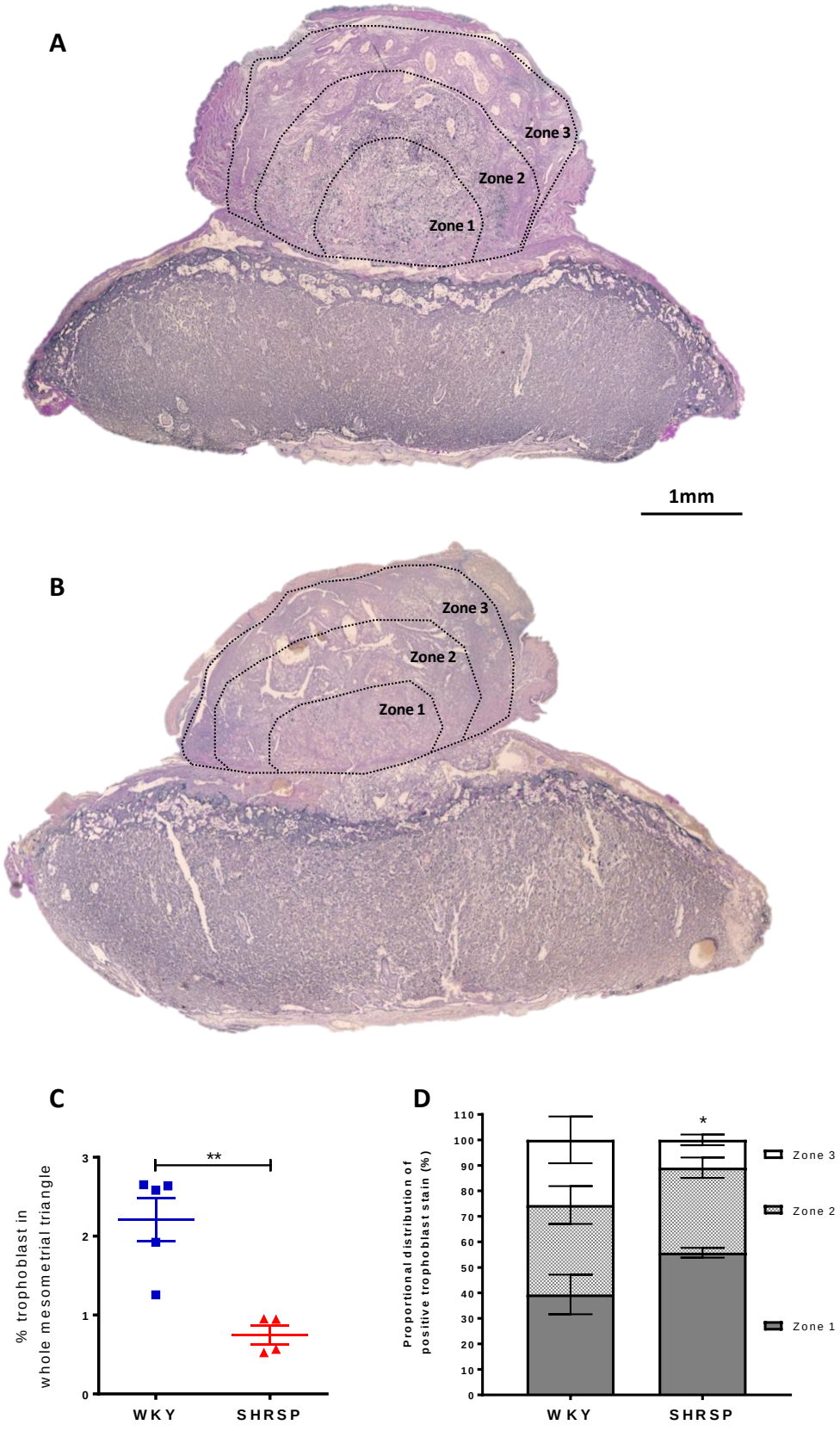


**Figure 3-19: Assessment of trophoblast invasion in WKY and SHRSP**
Representative images of trophoblast cytokeratin 7 staining in the mesometrial triangle of (A) WKY and (B) SHRSP. (C) The percentage of positive staining within the entire mesometrial triangle was quantified by a blinded observer using Image J software. Statistical significance was determined by using an unpaired student's t-test (**p<0.01). (D) Further quantification was obtained by expressing the total positive staining as a percentage in the different zones within the mesometrial triangle, with zone 1 being most proximal to the placenta and zone 3 most distal. Analysed using two-way ANOVA with Tukey post-hoc test; *p<0.05 Zone 1 vs Zone 3; n=4-5.

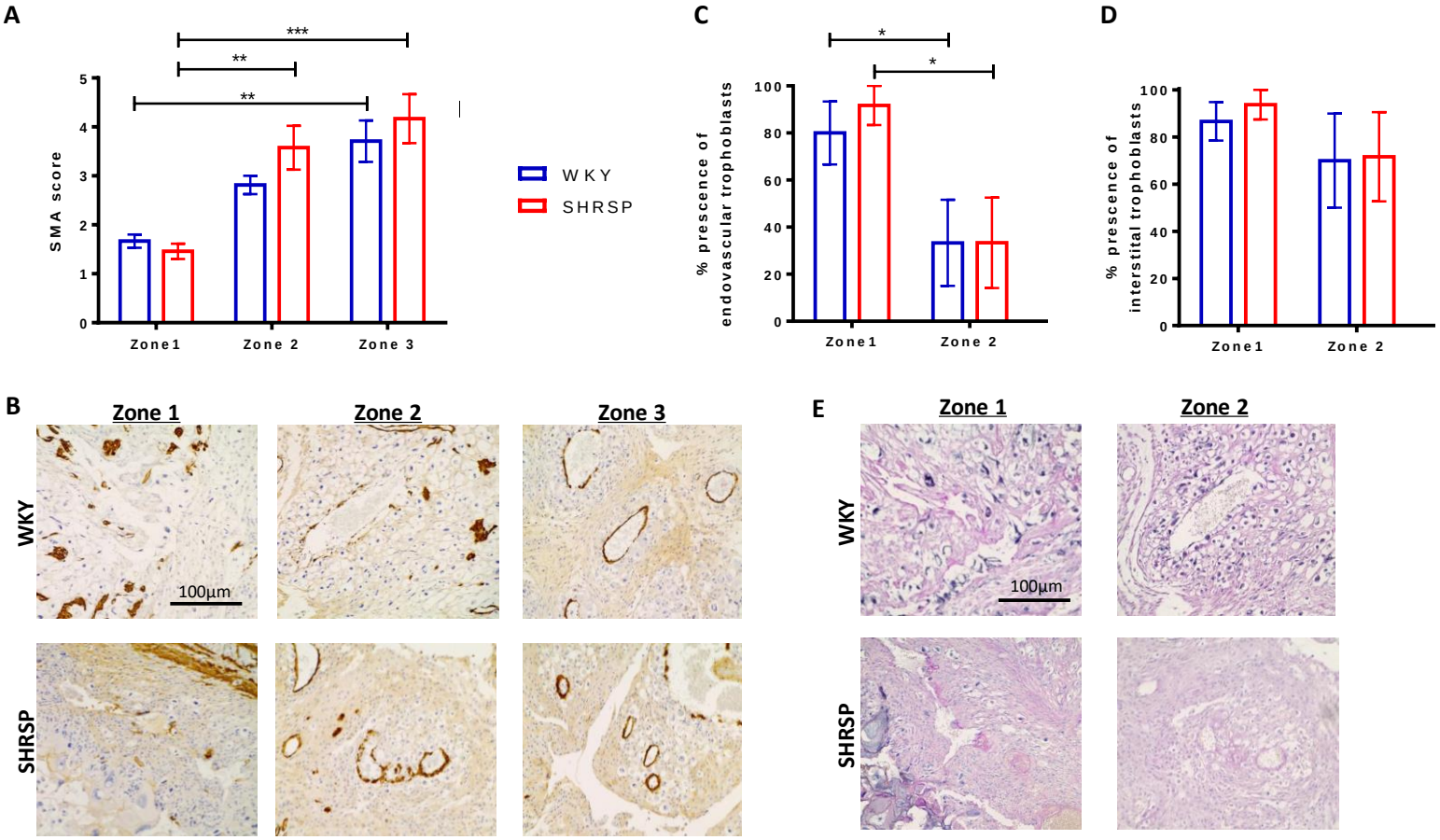


**Figure 3-20: Spiral artery remodelling assessment and scoring in WKY and SHRSP**
Between 3-4 spiral arteries were identified in each zone of the mesometrial triangle. (A) Vascular smooth muscle cell dedifferentiation was scored between 1 (no visible smooth muscle actin (SMA) staining and 5 (presence of SMA with <10% of rounding/separation of the VSMC in the vessel wall) by one observed blinded to strain and zone location. (B) Representative images of the spiral arteries of WKY and SHRSP in the 3 different zones. (C-D) The presence of endovascular and interstitial trophoblasts in and around the spiral arteries was recorded. The presence or absence was then calculated to reveal a percentage association of endovascular and interstitial trophoblasts within the spiral arteries in zone 1 and zone 2. Arteries in zone 3 had no endovascular or interstitial trophoblast association. (E) Representative images of endovascular and interstitial trophoblast association in zone 1 and 2 of the WKY and SHRSP mesometrial triangle. Statistical significance was determined using a two-way ANOVA with Tukey post-hoc test; n=15-20 arteries per zone, N=5 placentas.

#### 3.4.3.5 Placental Gene Expression

Placental RNA was extracted from the maternal, placental and fetal layers (mesometrial triangle, junctional and labyrinth zones and the chorionic plate; illustrated in Figure 3-16) in order to examine relative gene expression within the placenta.

Layer dissection accuracy was deemed appropriate due to the relative expression of desmin, prolactin and vascular endothelial growth factor receptor (*Vegfr*). Desmin expression, which is an intermediate filament protein expressed by decidualized cells, was significantly greater in the maternal mesometrial triangle and junctional zone compared to in the labyrinth and chorionic plate in both WKY and SHRSP (Figure 3-21A). Prolactin expression is located to trophoblast cells in the junctional zone and was found to have a significantly higher expression in the junctional zone compared to all other layers in both strains (Figure 3-21B). *Vegfr* expression localises to highly vascularised zones and expression was found to be significantly higher in the labyrinth and decidua zones compared to chorionic plate in both strains, with the junctional zone in WKY also having a significantly higher expression (Figure 3-21C).

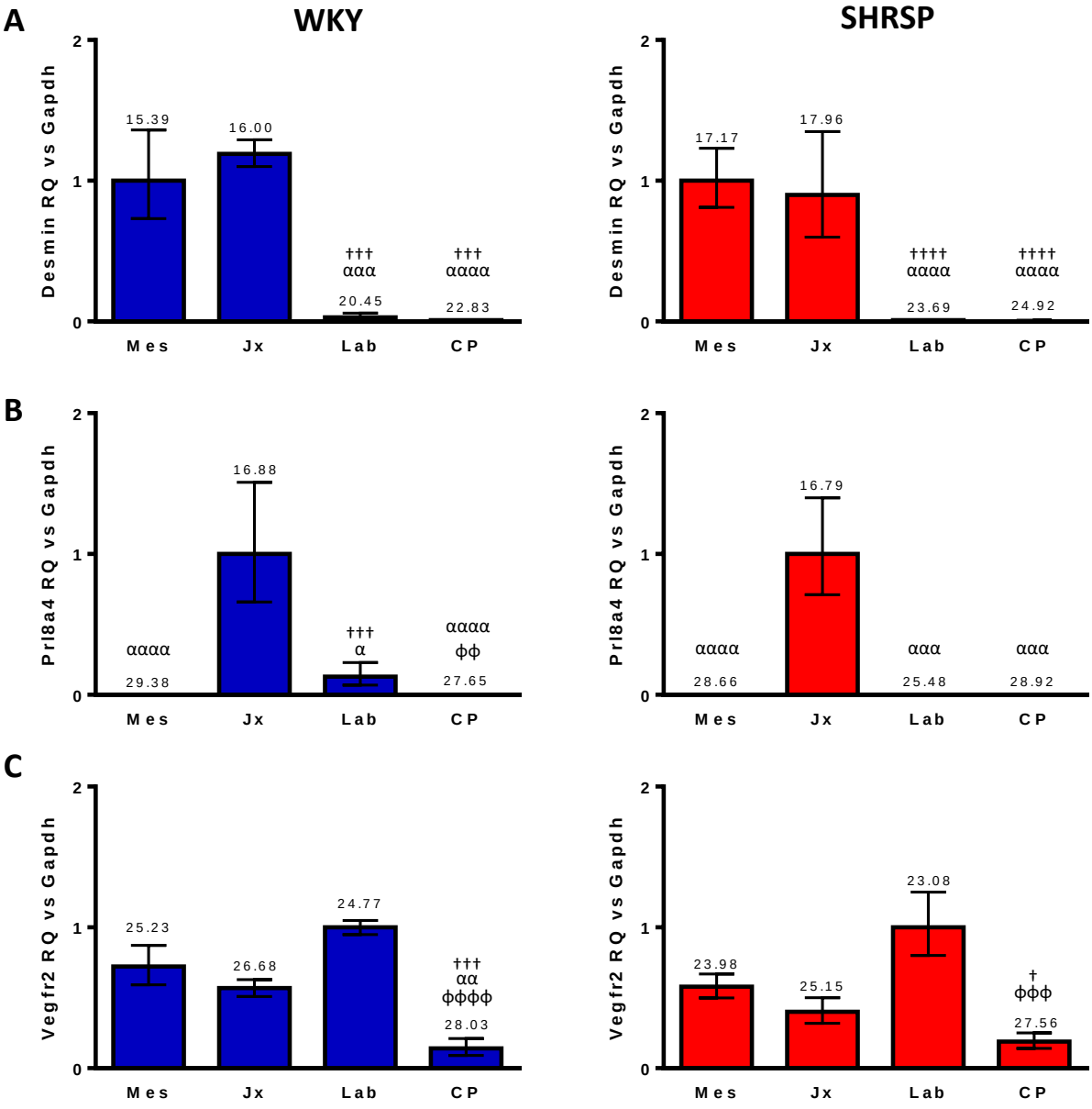


**Figure 3-21: Placental layer enrichment validated by specific gene expressions in the different placental zones.**

Gene expression within the Mes= maternal mesometrial triangle; Jx = placental junctional zone; Lab = placental labyrinth zone and CP= fetal chorionic plate were investigated to determine if accurate dissection of the placenta had taken place. Expression was normalised to *Gapdh* and is presented relative to the Mes. (A) Desmin expression highlights decidualized cells, (B) prolactin (Prl8a4) expression indicative of trophoblast giant cells and (C) vascular endothelial growth factor receptor (*Vegfr2*) expression indicating highly vascularised zones. Variation of expression was examined using the ΔCT values and tested for statistical significance using a one-way ANOVA with a Tukey post-hoc test; vs Mes: $^{\dagger}p<0.05$, $^{\dagger\dagger\dagger}p<0.001$, $^{\dagger\dagger\dagger\dagger}p<0.0001$; vs Jx: $^{\alpha}p<0.05$, $^{\alpha\alpha}p<0.01$, $^{\alpha\alpha\alpha}p<0.001$, $^{\alpha\alpha\alpha\alpha}p<0.0001$; vs Lab $^{\phi\phi}p<0.01$, $^{\phi\phi\phi}p<0.001$, $^{\phi\phi\phi\phi}p<0.0001$. n=5. Values above each bar indicate unadjusted cycle threshold values.

### 3.4.3.6 Gene expression of markers of oxidative stress and hypoxia

The gene expression profile across the maternal, placental and fetal layers was examined and then the layers were individually compared between WKY and SHRSP.

#### 3.4.3.6.1 Comparison of placental layers

*Sod1* expression in WKY was found to be significantly higher in the chorionic plate (CP) compared to the mesometrial triangle (2.1±0.16 ΔCT versus 3.0±0.21 ΔCT; $p<0.05$), there were no significant changes between the layers in SHRSP (Figure 3-22A). *Gpx1* expression was significantly higher in the mesometrial triangle compared to other layers in WKY (1.6±0.11 ΔCT versus 3.7±0.34 ΔCT (Jx); $p<0.0001$ and 3.9±0.15 ΔCT (Lab); $p<0.0001$ and 2.9±0.15 ΔCT (CP); $p<0.01$) and in SHRSP (1.7±0.07 ΔCT versus 3.5±0.25 ΔCT (Jx); $p<0.0001$ and 4.7±0.16 ΔCT (Lab); $p<0.0001$ and 2.6±0.26 ΔCT (CP); $p<0.05$). The expression in the fetal CP was also greater than the labyrinth zone in both strains ($p<0.05$) and significantly greater than the junctional zone in SHRSP only ($p<0.01$) (Figure 3-22B). In WKY the *Hif1a* expression was greater in the junctional zone compared to mesometrial triangle (6.6±0.11 ΔCT versus 7.3±0.15 ΔCT; $p<0.01$) and the labyrinth zone (6.6±0.11 ΔCT versus 7.1±0.07 ΔCT; $p<0.05$). In SHRSP this trend was altered as the mesometrial zone had the lowest expression compared to all other layers (7.5±0.10 ΔCT vs 6.4±0.12 ΔCT (Jx); $p<0.0001$, 6.6±0.07 ΔCT (Lab); $p<0.0001$ and 6.8±0.13 ΔCT (CP); $p<0.05$) (Figure 3-22C). *Vegf* expression in WKY was reduced in the junctional zone, compared to the mesometrial triangle and labyrinth zones (7.8±0.26 ΔCT versus 5.3±0.15 ΔCT (Mes); $p<0.0001$ and 5.8±0.11 ΔCT (Lab); $p<0.0001$. An increased labyrinth zone expression was also observed compared to fetal CP (5.8±0.11 ΔCT versus 7.2±0.10 ΔCT; $p<0.01$). In SHRSP placentas the expression trends were similar to WKY in that Vegf expression was significantly reduced in the junctional zone, compared to the mesometrial triangle and labyrinth zones (7.6±0.17 ΔCT versus 5.4±0.26 ΔCT (Mes); $p<0.0001$ and 6.2±0.12 ΔCT (Lab); $p<0.001$), however this strain also demonstrated reduced expression in the labyrinth and CP zones compared to the mesometrial triangle (5.4±0.26 ΔCT (Mes) versus 6.2±0.12 ΔCT (Lab); $p<0.05$ and versus 7.0±0.15 ΔCT (CP); $p<0.001$) (Figure 3-22D).

### 3.4.3.6.2 Comparison between strains

SHRSP had a significantly greater *Sod1* expression in the mesometrial triangle (2.1±0.13 ΔCT versus 3.0±0.21 ΔCT; p<0.01), junctional zone (1.62±0.12 ΔCT versus 2.8±0.17 ΔCT; p<0.01) and labyrinth zone (1.8±0.18 ΔCT versus 3.4±0.21 ΔCT; p<0.01) compared to WKY (Figure 3-22A). *Hif1a* expression was also increased in the SHRSP labyrinth layer compared to WKY (6.6±0.07 ΔCT versus 7.0±0.07 ΔCT; p<0.01) (Figure 3-22 C). *Gpx1* and *Vegf* expression were both significantly reduced in SHRSP labyrinth zones compared to WKY (*Gpx1*: 4.7±0.16 ΔCT versus 3.9±0.15 ΔCT; p<0.01 and *Vegf*: .6.2±0.14 ΔCT versus 5.8±0.11 ΔCT; p<0.05) (Figure 3-22B and D).

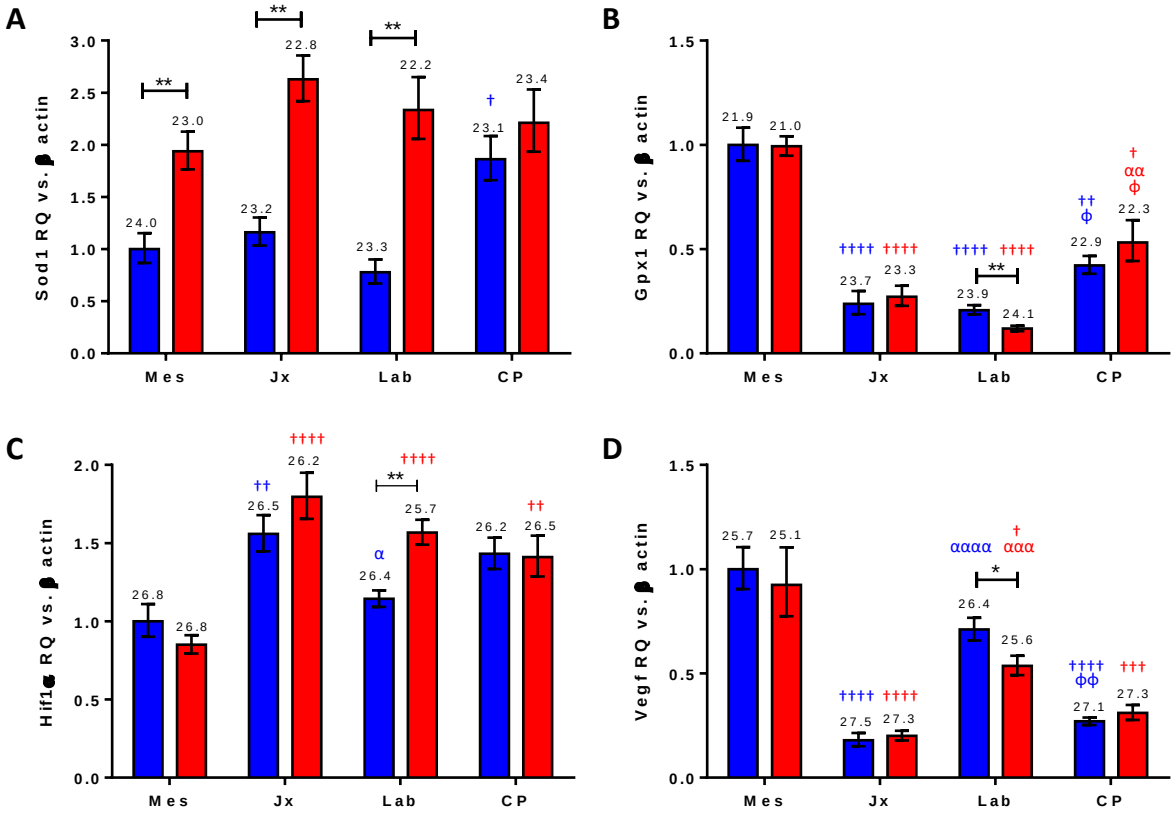


**Figure 3-22: Placental gene expression of markers of oxidative stress and hypoxia**
Expression of (A) superoxide dismutase 1 (*Sod1*), (B) glutathione peroxidase 1 (*Gpx1*), (C) Hypoxia-inducible factor 1α (*Hif1α*) and (D) vascular endothelial growth factor (*Vegf*) were normalised to β actin and presented relative to the mesometrial triangle portion of the WKY placenta. Statistical analysis was conducted on the ΔCT values for each layer (WKY n=4, SHRSP n=4) using an unpaired student's t-test to compare WKY and SHRSP within each individual layer (*p<0.05, **p<0.01) and a one-way ANOVA with Tukey's post-hoc test was then used to assess the change in expression across the layers within each strain, highlighted blue for WKY comparisons and red for SHRSP comparisons (vs Mes: †p<0.05, ††p<0.01 †††p<0.001, ††††p<0.0001; vs Jx: ᵅp<0.05, ᵅᵅp<0.01, ᵅᵅᵅp<0.001, ᵅᵅᵅᵅp<0.0001; vs Lab ᵠp<0.05, ᵠᵠp<0.01). Values above each bar indicate unadjusted cycle threshold values.

### 3.4.3.7 Gene expression of markers of extracellular matrix degradation

#### 3.4.3.7.1 Comparison of placental layers

*Mmp1* expression in WKY placenta demonstrated a significantly higher expression in the mesometrial triangle and junctional zone compared to the labyrinth zone (3.9±0.46 ΔCT (Mes) and 4.3±0.31 ΔCT (Jx) versus 8.7±0.43 ΔCT (Lab); $p<0.0001$ and $p<0.01$). This same trend was observed in SHRSP placental layers (2.3±0.32 ΔCT (Mes) and 2.8±0.45 ΔCT (Jx) versus 6.3±0.55 ΔCT (Lab); $p<0.01$ and $p<0.01$). This strain also demonstrated a significantly reduced CP expression compared to the mesometrial triangle and Jx zone (7.9±0.25 ΔCT (CP) versus 2.3±0.32 ΔCT (Mes); $p<0.01$, and 2.8±0.45 ΔCT (Jx); $p<0.01$) (Figure 3-23A). *Mmp8* expression was found to be significantly reduced in the CP layer compared to the junctional zone in WKY (Figure 3-23B). No other layer differences were determined in WKY or SHRSP, however the expression levels detected were low (cycle threshold values >32). *Mmp9* was most highly expressed in the Jx zone of the placenta in WKY compared to the mesometrial triangle and CP (8.2±0.30 ΔCT versus 10.2±0.20 ΔCT (Mes); $p<0.01$ or versus 12.6±0.62 ΔCT (CP); $p<0.05$). This pattern of expression was different in SHRSP, with the CP having a significantly lower expression than both the mesometrial triangle (12.5±0.31 ΔCT versus 7.8±0.28 ΔCT; $p<0.01$) and the Jx zone (versus 8.6±0.27 ΔCT; $p<0.01$) (Figure 3-23C). *Timp1* had an expression was higher in the mesometrial triangle compared to all other layers in WKY (6.4±0.16 ΔCT versus 9.8±0.26 ΔCT (Jx); $p<0.0001$ and 10.1±0.08 ΔCT (Lab); $p<0.0001$ and 9.6±0.68 ΔCT (CP); $p<0.0001$) and in SHRSP (6.2±0.13 ΔCT versus 8.8±0.32 ΔCT (Jx); $p<0.0001$ and 10.3±0.09 ΔCT (Lab); $p<0.0001$ and 9.2±0.27 ΔCT (CP); $p<0.0001$). SHRSP also demonstrated a significant increase in JX zone expression compared to Lab ($p<0.001$) and CP ($p<0.05$).

#### 3.4.3.7.2 Comparison between strains

*Mmp1* expression was found to be significantly higher in SHRSP compared to WKY in the mesometrial triangle (2.3±0.32 ΔCT versus 3.9±0.46 ΔCT; $p<0.05$), Jx zone (2.8±0.45 ΔCT versus 4.3±0.31 ΔCT; $p<0.05$) and Lab zone (6.3±0.55 ΔCT versus 8.7±0.43 ΔCT; $p<0.05$). *Mmp9* also demonstrated a significant increase in the SHRSP mesometrial triangle compared to WKY (7.8±0.28 ΔCT versus 8.2±0.30 ΔCT; $p<0.05$). Conversely *Mmp8* expression was decreased in this layer in SHRSP

compared to WKY (16.1±0.34 ΔCT versus 15.0±0.17 ΔCT; p<0.05). The expression of *Timp1*, a regulator of Mmps, was increased significantly in the Jx zone of SHRSP compared to WKY (8.8± 0.32 ΔCT versus 9.8±0.26 ΔCT: p<0.05), no differences were observed in the other zones.

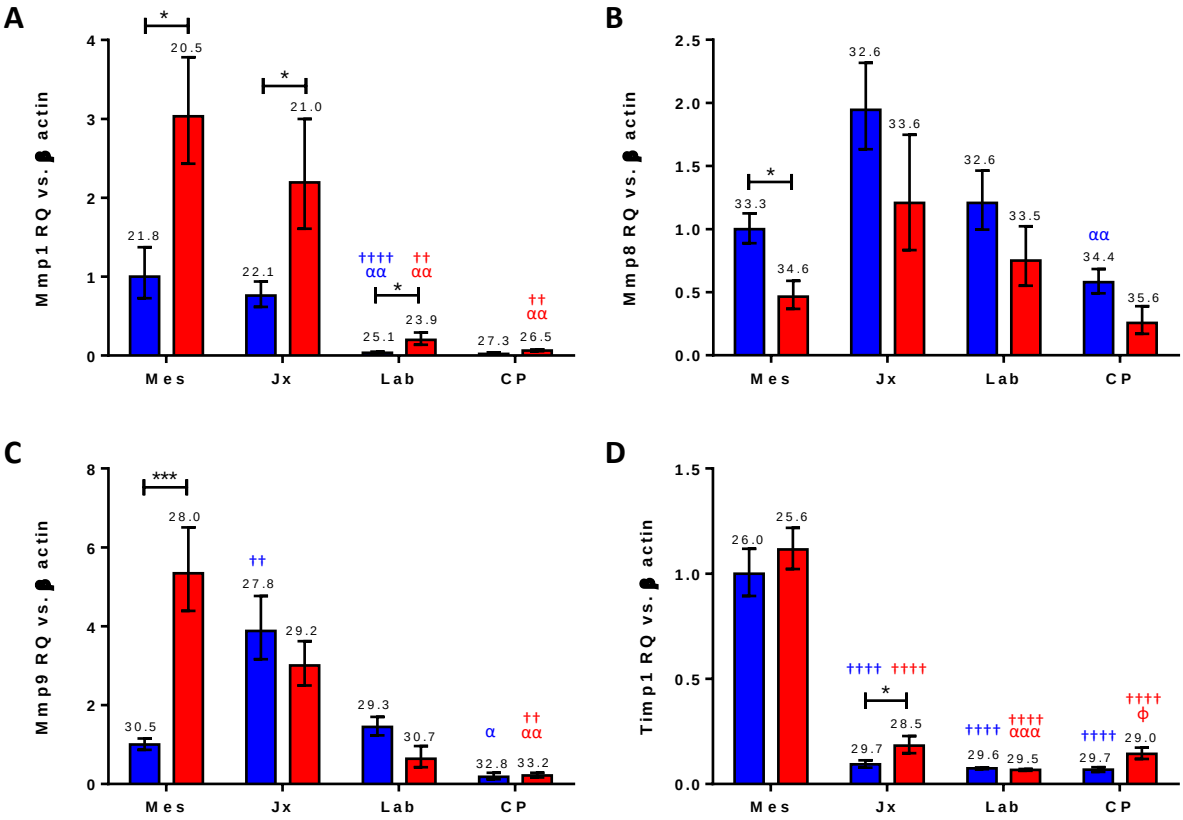


**Figure 3-23: Placental gene expression of markers of extracellular matrix degradation**
Expression of matrix metalloproteases 1 ((A) *Mmp1*), 8 ((B) *Mmp8*) and 9 ((C) *Mmp9*) as well as the tissue inhibitor of metalloproteinases 1 ((D) *Timp1*) were normalised to β actin and presented relative to the mesometrial triangle portion of the WKY placenta. Statistical analysis was conducted on the ΔCT values for each layer (WKY n=4, SHRSP n=4) using an unpaired student's t-test to compare WKY and SHRSP within each individual layer (*p<0.05, ***p<0.001) and a one-way ANOVA with Tukey's post-hoc test was then used to assess the change in expression across the layers within each strain, highlighted blue for WKY comparisons and red for SHRSP comparisons (vs Mes: ††p<0.01, ††††p<0.0001; vs Jx: $^{\alpha}$p<0.05, $^{\alpha\alpha}$p<0.01, $^{\alpha\alpha\alpha}$p<0.001; vs Lab $^{\varphi}$p<0.05). Values above each bar indicate unadjusted cycle threshold values.

#### 3.4.3.8 Gene expression of components of the placental renin-angiotensin system

Gene expression of several components of the renin angiotensin system were examined including the two main AngII receptors (AngII receptor type 1 (*Agtr1*) and type 2 (*Agtr2*)) and the angiotensin converting enzyme (*Ace2*).

##### 3.4.3.8.1 Comparison of placental layers

In WKY the expression of *Agtr1* was lowest in the junctional zone of the placenta compared to the mesometrial triangle (16.1±0.97 ΔCT versus 12.5±0.76 ΔCT; $p<0.05$) and the labyrinth zone (versus 11.8±0.77 ΔCT; $p<0.05$). In SHRSP the junctional zone also had the lowest expression compared to Mes (15.5±0.33 ΔCT versus 13.7±0.49 ΔCT; $p<0.01$), Lab (versus 11.7±0.29 ΔCT; $p<0.0001$) and CP (versus 12.6±0.45 ΔCT; $p<0.0001$) (Figure 3-24A). This strain also demonstrated a significant reduction in mesometrial *Agtr1* expression compared to Lab (13.7±0.49 ΔCT versus 11.7±0.29 ΔCT; $p<0.01$). *Agtr2* expression was significantly higher in the labyrinth zone compared to the mesometrial triangle in WKY (13.2±0.32 ΔCT versus 14.6±0.42 ΔCT; $p<0.05$) (Figure 3-24B). No significant changes in layer expression of *Agtr2* were found in SHRSP. The expression of *Ace2* was significantly higher in the labyrinth zone and CP compared to both Mes and Jx zones in WKY (9.1±0.26 ΔCT (Lab) and 10.8±0.37 ΔCT (CP) versus 17.3±0.71 ΔCT (Mes); $p<0.0001$ and $p<0.0001$ or versus 15.7±0.57 ΔCT (Jx); $p<0.0001$ and $p<0.0001$) and in SHRSP (10.1±0.21 ΔCT (Lab) and 10.8±0.08 ΔCT (CP) versus 17.4±0.51 ΔCT (Mes); $p<0.0001$ and $p<0.0001$ or versus 14.6±0.62 ΔCT (Jx); $p<0.0001$ and $p<0.0001$) (Figure 3-24C). SHRSP also had a significantly higher junctional zone expression compared to the mesometrial triangle ($p<0.001$). It is also of importance to note that the expression levels of *Ace2* in the mesometrial triangles were almost at undetectable levels (>35 cycle threshold).

##### 3.4.3.8.2 Comparison between strains

Expression differences between WKY and SHRSP were found for both AngII receptors and *Ace2* (Figure 3-24A-C). There was a significantly reduced *Agtr1* expression in the SHRSP mesometrial triangle compared to WKY (13.7±0.49 ΔCT versus 12.5±0.76 ΔCT; $p<0.05$) and an increased SHRSP expression in the junctional zone (15.5±0.33 ΔCT versus 16.1±0.97 ΔCT; $p<0.05$). The labyrinth

zone of SHRSP placenta was found to have a significantly lower expression of *Agtr2* (14.5±0.19 ΔCT versus 13.2±0.32 ΔCT; p<0.01) and Ace2 (10.1±0.21 ΔCT versus 9.1±0.26 ΔCT; p<0.05) compared to WKY.

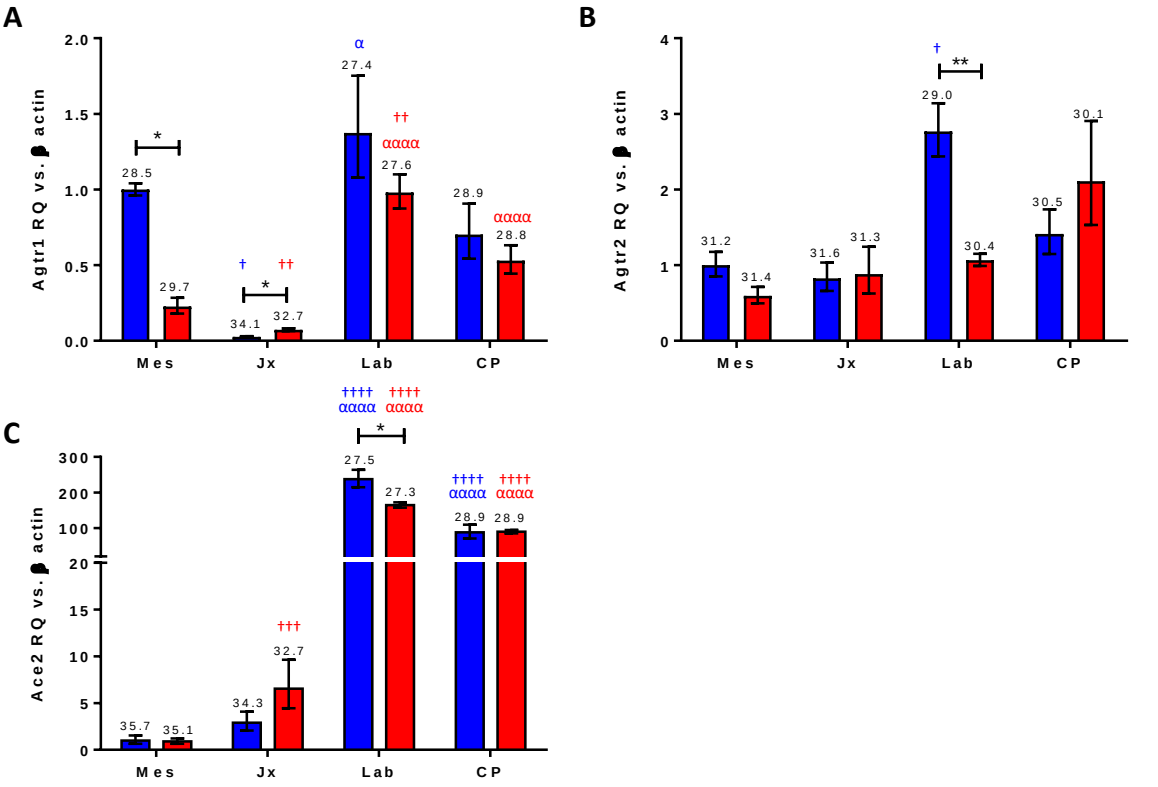


**Figure 3-24: Placental renin-angiotensin system gene expression in the WKY and SHRSP**
Expression of components of the renin-angiotensin system examined were (A) angiotensin receptor type 1 (*Agtr1a*), (B) angiotensin receptor type 2 (*Agtr2*) and (C) angiotensin converting enzyme (*Ace2*). Expression was normalised to β actin and presented relative to the mesometrial triangle portion of the WKY placenta. Statistical analysis was conducted on the ΔCT values for each layer (WKY n=4, SHRSP n=4) using an unpaired student's t-test to compare WKY and SHRSP within each individual layer (*p<0.05, **p<0.01) and a one-way ANOVA with Tukey's post-hoc test was then used to assess the change in expression across the layers within each strain, highlighted blue for WKY comparisons and red for SHRSP comparisons (vs Mes: $^{\dagger}$p<0.05, $^{\dagger\dagger}$p<0.01 $^{\dagger\dagger\dagger}$p<0.001, $^{\dagger\dagger\dagger\dagger}$p<0.0001; vs Jx: $^{\alpha}$p<0.05, $^{\alpha\alpha\alpha\alpha}$p<0.0001). Values above each bar indicate unadjusted cycle threshold values

### 3.4.3.9 Estimation of placental function using $C^{14}$-MeAIB transport assay

Maternal facing syncytiotrophoblast membrane vesicles were created from placental tissue to estimate the rate of transport of a synthetic System A analogue (MeAIB) *ex vivo*. Vesicle purity and correct membrane orientation was assessed using the alkaline phosphatase activity corrected for the protein concentration for the vesicle and its respective homogenate. An enrichment score was calculated based on the ratio of vesicle purity:homogenate purity. The protein concentrations of vesicles from WKY and SHRSP were not significantly different (Table 3-4). The vesicle alkaline phosphatase activity was higher than that of the homogenate in both WKY and SHRSP and therefore the enrichment scores were not significantly different between strains (Table 3-4). Vesicle quality and size was then assessed using nanoparticle tracking software on a NanoSight. Figure 3-25A-B shows representative traces of particle size estimation for WKY and SHRSP. Figure 3-25C illustrates the vesicle shapes and sizes from a still image representing the NanoSight recordings. This method of vesicle preparation cannot produce a heterogeneous particle size and the two strains did not have identical particle sizes when a small volume was measured using a NanoSight (approximately 500µl) (Table 3-5). However, the particle sizes did not differ greatly and the heterogeneous size would not affect the uptake experiments conducted as the vesicle preparation was mixed before use thus ensuring an even distribution of vesicles (Glazier et al., 1990).

The rate of transport of the radioisotope labelled$C^{14}$-MeAIB was determined in vesicles produced from WKY and SHRSP placenta over a period of 60 seconds. The movement of $C^{14}$-MeAIB into the vesicles was found to be via $Na^+$ dependent active transport, as the transport rate was higher in the presence of $Na^+$ than in the presence of $K^+$ at 30 seconds (22.7±0.77pmol/mg versus 8.5±4.28pmol/mg; $p<0.01$), 45 seconds (29.0±1.93pmol/mg versus 16.0±2.99pmol/mg; $p<0.01$) and 60 seconds (41.1±2.62pmol/mg versus 17.1±3.70pmol/mg; $p<0.0001$) in WKY. In SHRSP the transport was higher in the presence of $Na^+$ than $K^+$ at 30 seconds (17.3±1.69pmol/mg versus 5.0±1.94pmol/mg; $p<0.05$), 45 seconds (23.4±2.14pmol/mg versus 9.7±1.57pmol/mg; $p<0.01$) and 60 seconds (30.4±3.66pmol/mg versus 13.7±2.91pmol/mg; $p<0.0001$) (Figure 3-26A). The $Na^+$ dependent transport at 60 seconds was significantly greater that the transport at 15 seconds in both WKY (41.1±2.62pmol/mg versus

12.8±0.95pmol/mg; $p<0.01$) and SHRSP (30.4±3.66pmol/mg versus 9.4±2.22pmol/mg; $p<0.01$) vesicles (Figure 3-26B), however there were no significant differences in the overall rate of transport between strain (Figure 3-26C).

**Table 3-4: Vesicle quality and purity check**

| | WKY (n=4) | | SHRSP (n=6) | | WKY vs SHRSP | |
|---|---|---|---|---|---|---|
| | *Homogenate* | *Vesicles* | *Homogenate* | *Vesicle* | *Homogenate* | *Vesicle* |
| **Protein concentration (µg)** | 4.36 ±0.04 | 0.91 ±0.12 | 4.03 ±0.23 | 1.02 ±0.14 | NS | NS |
| **Alkaline phosphatase activity (product per µg protein min$^{-1}$)** | 0.03 ±0.003 | 0.17 ±0.016 | 0.03 ±0.003 | 0.25 ±0.009 | NS | P<0.01 |
| **Enrichment score** | | 6.48 ±0.44 | | 7.84 ±0.56 | | NS |

The protein concentration and alkaline phosphatase activity of homogenates and vesicles were used to calculate the enrichment score for each sample (n=4-6). Protein was calculated using a BCA protein assay and corrected for volume used to measure alkaline phosphatase activity. Statistical analysis conducted using unpaired student's t-test, sample size shown on table. Alkaline phosphatase activity of the vesicles and un-vesiculated homogenate was used to produce an enrichment score for the vesicles produced from WKY (n=4) and SHRSP (n=6) (more detail in section 3.3.2). An acceptable enrichment score that indicated good quality vesicles was between 6 and 10 (Glazier et al., 1990).

**Table 3-5: Placental syncytiotrophoblast membrane vesicle properties**

| | WKY | SHRSP |
|---|---|---|
| **Particle concentration** | 2.62x10$^{8}$ particles / ml | 2.17x10$^{8}$ particles / ml |
| **Particle size (nm)** | 72 ± 5.61 | 131 ± 24.96 |

An estimation of particle concentration and size was determined for one vesicle preparation from each strain using nanoparticle tracking on a NanoSight.

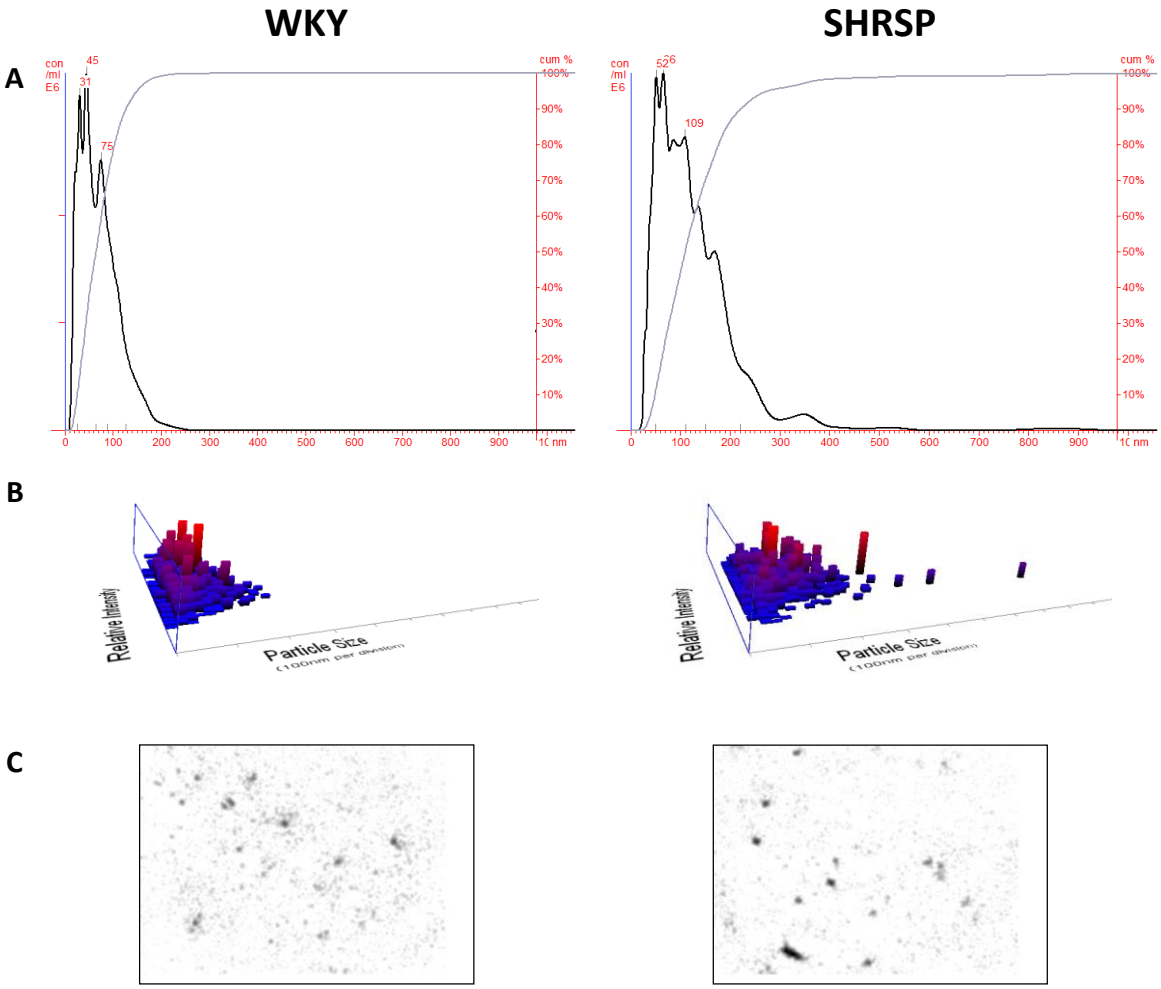


**Figure 3-25: Nanoparticle size information for WKY and SHRSP vesicles from NanoSight**
The NanoSight nanoparticle tracking software produced a distribution for particle size (A-B) (C) Representative images of the vesicles in solution show a mixed size population, black dots indicate one vesicle.

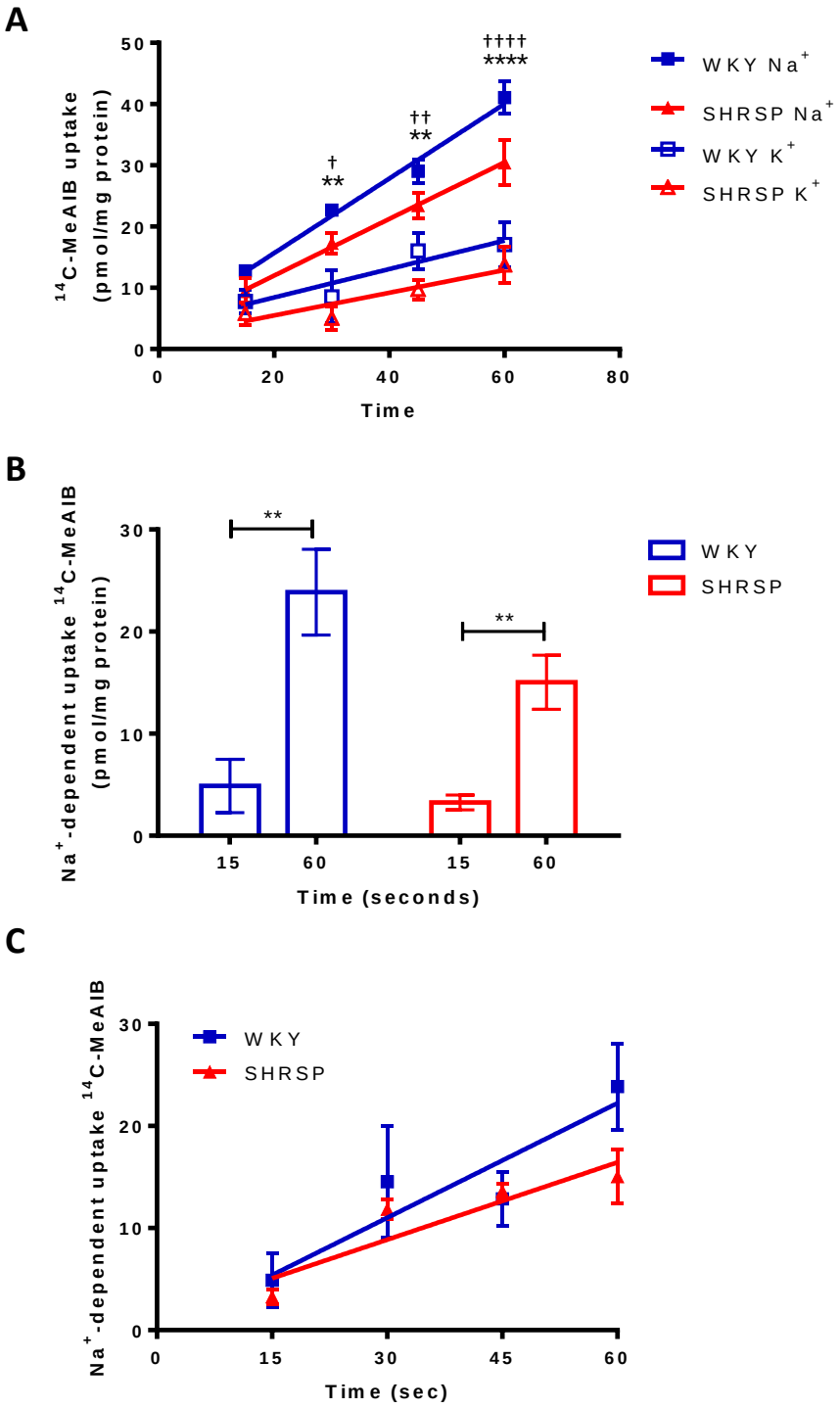


**Figure 3-26: Placental C$^{14}$MeAIB transport assay in WKY and SHRSP placental membrane vesicles**

(A) The absolute rates of transport in the presence of $Na^+$ and the absence of $Na^+$ (presence of $K^+$). Statistical significance was determined using a two-way ANOVA with Tukey's post-hoc test to examine the differences between $Na^+$ dependent and independent ($K^+$) transport at each time point; in WKY **p<0.01, ****p<0.0001; in SHRSP †p<0.05, †p<0.01, ††††p<0.0001. (B) The overall change in $Na^+$ dependent transport from 15 seconds to 60 seconds. Analysed using unpaired student's t-test; **p<0.01. (C) The $Na^+$ dependent rate adjusted for any $Na^+$ independent uptake. Analysed using regression analysis of line gradient, compared using an unpaired student's t-test; n=4.

## 3.5 Discussion

Hypertensive pregnancies not only impact fetal development and offspring health but have serious implications for the mother, both during the pregnancy and beyond. Having an appropriate animal model to assess maternal antihypertensive treatment options would be hugely beneficial. This chapter has provided information on the physiological response to pregnancy in WKY and SHRSP rats. The chronically hypertensive SHRSP produced apparently healthy offspring which can reach adulthood. However, these hypertensive dams did not have the same physiological response observed in normotensive WKY. Specifically, they demonstrated differences in pregnancy weight gain, cardiac profile and placental structure.

Profiling the maternal response to pregnancy is crucially important for assessing any pathology. The SHRSP demonstrated weight gain; however, this was at a slower rate than WKY. The weight gain was assessed as a change from non-pregnant as this corrected for the smaller starting weights of SHRSP. The subtraction of fetal and placental mass from maternal weight revealed that maternal specific weight gain was reduced in SHRSP compared to WKY. Healthy pregnancy is associated with an increased energy demand, and the nutritional flow to the fetus is sustained by the mothers fat stores, diet and changes to the metabolism (Thornburg et al., 2015). In previous studies male SHRSP have been found to have a reduced glucose uptake in skeletal and adipose tissues (James et al., 2001, Hajri et al., 2001), and therefore if the impaired weight gain during SHRSP pregnancy is a failure to increase adipose tissue energy stores this could impact the metabolic rate and impact the flow of nutrients to the fetus (Hajri et al., 2001, James et al., 2001). However, as focus was only given to weight gain this is just speculation, as a thorough evaluation of the muscle mass, metabolic rate and adiposity of the dams would be needed to determine if SHRSP impose a nutrient restriction of their offspring.

Major maternal cardiovascular adaptations to pregnancy are required to re-direct blood flow to the placenta to ensure the developing fetus receives appropriate nutrients (Wang, 2010). The physiological changes in the maternal cardiovascular system have been known for the past half century (Thornburg et al., 2015). These include a necessary increase in cardiac output by up to 50% for

singleton pregnancies (Hall et al., 2011). Both WKY and SHRSP exhibited an increased cardiac output, of up to 65%. However, the cardiac output of SHRSP was significantly smaller than WKY at the end of pregnancy. This could be accounted for due to a marginally lower pre-pregnancy cardiac output than WKY. Utilising echocardiography allows for the measurements of cardiac parameters throughout pregnancy in the same individual, unfortunately in this study, due to timing conflicts and imaging issues, not all the measurements for cardiac output, stroke volume, ejection fraction and fractional shortening were made for each animal at each gestational time point. The SHRSP further demonstrated potential cardiovascular impairment due to an increased LV mass both pre-pregnancy and at term. LV hypertrophy is associated with hypertension and is a risk factor for developing cardiovascular disease (Dominiczak et al., 1997, Koren et al., 1991). LV hypertrophy is well established in both male and female SHRSP rats and this adaptation to raised blood pressure becomes pathological in older animals (Dominiczak et al., 1997, Graham et al., 2004). However, during pregnancy the SHRSP demonstrated a normal ejection fraction and fractional shortening, which indicates that the hearts were functioning normally. The increased LV mass observed could be suggestive that SHRSP are not responding to the stress of pregnancy as efficiently as WKY and they are possibly at more risk of damage from the increased cardiovascular load. Women that develop hypertensive complications of pregnancy such as pre-eclampsia have also been found to exhibit some LV hypertrophic remodelling (Melchiorre et al., 2013).

Other phenotypes of pre-eclampsia were investigated in this characterisation of SHRSP pregnancy. Proteinuria, used as a marker of kidney damage in hypertension and pre-eclampsia, was not identified in either the normotensive or hypertensive rat strains during pregnancy. Studies in 20-week-old salt-challenged male SHRSP have shown the presence of proteinuria and abnormal renal morphology in an advanced hypertensive state, suggesting insults to the cardiovascular and renal systems can elicit pathological changes in the kidney (Koh-Tan et al., 2017). However, as no such alterations were observed in the pregnant SHRSP this suggests that the chronic hypertension plus pregnant state do not impact the kidney function. This study was limited in only investigating one protein (albumin) and not examining other excreted products, such as salts,

and furthermore was only collected for 24 hours. A more detailed urinary analysis and water intake/excretion profiles may have been possible by extending collection times to 48 hours. Even in the absence of evidence of proteinuria, sub-clinical damage cannot be ruled out without further investigations. For example glomerular filtration rate and histological examination of glomeruli structure would be most beneficial to provide more detailed information on the pregnant SHRSP kidney function (Lopes van Balen et al., 2018, Cunningham et al., 2016).

Fetal growth restriction (FGR) has long been associated with hypertensive pregnancies, especially those resulting from pre-existing maternal chronic hypertension (Srinivas et al., 2009, Lees and Ferrazzi, 2017). In this study, fetal growth was examined by means of absolute weights, weight centiles and fetal anthropological measurements. There was no evidence of growth restriction in SHRSP when using the proportional growth distribution curves. These curves are constructed to estimate whether the baby will be small for gestational age (<10$^{th}$ percentile) or classed as growth restricted (<5$^{th}$ percentile) (2013, Gordijn et al., 2016). Clinically, these have been shown to accurately highlight babies that are at risk of complications associated with FGR; whilst also accounting for the individual mother's size (Iliodromiti et al., 2017). SHRSP did not have more fetuses under the 5$^{th}$ centile than WKY. The fetal weights used to construct these distributions were obtained at GD18.5, which is approximately 4-5 days before parturition. This may be too early in fetal development in the rat to accurately determine FGR. However, fetal weights of groups examined at GD20.5 remained similar between the two strains. GD18.5 was used for the majority of studies as it is before the exponential fetal growth stage and thus minimises size variation due to minor time differences. The variation could arise from using copulation plugs to confirm pregnancy; when these plugs were found pregnancy was confirmed. However, checks were usually made at the start and end of each day therefore the number of hours before confirmation could fluctuate depending on actual time of mating. Other studies have used the presence of sperm from vaginal smears to confirm copulation, however these are still open to variation depending on when and how often the smears are conducted.

This study is the first to demonstrate no SHRSP fetal weight reductions compared to WKY. Only two other groups have examined and reported on the fetal weights of SHRSP versus WKY (Fuchi et al., 1995a, Barrientos et al., 2017). Barrientos *et al* determined growth restriction due to fetal weight and length reductions in SHRSP compared to WKY at GD18.5 and GD20.5 (Barrientos et al., 2017). What is interesting about their study is that the values for GD18.5 fetal weight for SHRSP and WKY (SHRSP: 0.55±0.001g, WKY: 0.70±0.01g) were much lower than the average fetal weight at this gestation found using the Glasgow strains (SHRSP: 1.06±0.04g WKY: 1.18±0.05g). The reason for these differences are not obvious, but could possibly be accounted for by the fact that SHRSP and WKY used in the Barrientos study were purchased from a commercially available source, whereas the Glasgow strains have been maintained as separate colonies since December 1991, therefore have been geographically isolated from other strains for nearly 27 years (Dominiczak et al., 1993). Fortunately, the time spent breeding these strains in house over this period has allowed for litter numbers from both to be recorded for over three decades. The changes over the past decade were evaluated and no difference found between the two strains. Many other studies in SHR and SHRSP report that the hypertensive strains have fewer pups per litter (Barrientos et al., 2017, Peracoli et al., 2001, Bassan et al., 2005), this was not the case in this study, and could be due to a much greater sample size being available, and therefore the SHRSP litters were evaluated over a much longer time period than previous studies, thus minimalizing variation often associated with short study timescales. The only significant difference observed between the fetuses from SHRSP and WKY dams in this study was that SHRSP demonstrated a reduced abdominal circumference. As these measurements of size are conducted physically with cotton thread it is open to some error. Measurements collected were only from a small number of litters due to the technique being employed late in the study, this reduces the power to determine whether significant differences truly exist.

An assessment of offspring outcome would further aid the fetal measures obtained in this study. Whilst no growth restriction was determined, the impact hypertension has on the offspring development after birth is still to be investigated in SHRSP rats. This is an important area as the development and origins of health and disease have long been known to be linked with the *in*

*utero* environment (Barker, 1991, Barker et al., 1993). Bassan *et al* found that SHR offspring, which are exposed to maternal hypertension *in utero*, have neurodevelopmental issues, specifically delayed neonatal reflexes (Bassan et al., 2005). Others have stated an association with pre-eclampsia and the development of stroke and hypertension and an increased risk of cardiovascular disease in humans (Davis et al., 2015).

A healthy and correctly functioning placenta is crucial to fetal survival and wellbeing. For this reason, the placental characteristics were examined in SHRSP and WKY. Appropriate placental growth was observed in both strains. Placental growth needs to occur rapidly prior to the rapid weight gain of the fetus as it is the organ that sustains the fetus. Placental weights can be used alongside the fetal weights to highlight any insufficiencies (Hayward et al., 2016). As no FGR was observed the ratio of fetal placental weights was not expected to change, and no differences were found. However, previous studies have suggested that SHRSP placenta have a reduced blood flow, reduced $Na^+/K^+$ ATPase activity and impaired trophoblast invasion (Small et al., 2016, Barrientos et al., 2017, Fuchi et al., 1995a). On examination of the morphology of SHRSP placenta differences were observed to that of WKY. The proportional sizes varied between WKY and SHRSP and there was a lower glycogen staining in the junctional zone. This placental zone is mainly composed of spongiotrophoblasts and trophoblastic glycogen cells (Malassiné et al., 2003). The full functions of the junctional zone are not fully understood; however, there is evidence to suggest it has an endocrine function and acts as a site of energy reserves for the placenta (Ain et al., 2003, Coan et al., 2006, Gebbe et al., 1972). The glycogen cell number is known to reduce as gestation progresses in rodents (Coan et al., 2006). However, SHRSP junctional zones exhibited a reduction in glycogen content at GD14.5 compared to WKY, which remained low at a later gestational stage. This suggests that the SHRSP placenta fails to develop glycogen stores, which in WKY, appear to be used up later in pregnancy when fetal growth is increasing rapidly. The lack of these stores in the SHRSP could implicate a placental dysfunction. As there were no placental or fetal size differences between strains it would suggest that the placenta of SHRSP could be maintaining appropriate nutrient delivery to the fetus yet cannot rely on placental energy stores as it has no

reserves, thus may be over-working to acquire both nutrients for itself and its fetus.

SHRSP trophoblast presence in the mesometrial triangle was found to be reduced in this study, which is in concurrence with Barrientos *et al* (Barrientos et al., 2017). However, as this is not a direct measure of invasion, further assessment was made using the zonal separation methods utilised by other groups (Barrientos et al., 2017, Geusens et al., 2008). This revealed that a greater proportion of SHRSP trophoblasts are located more proximal to the placenta (zone 1) than distal (zone 3), indicating a possible impairment of trophoblast invasion. Uterine spiral arteries branch from radial uterine arteries in the myometrium and extend into the decidualized uterus towards the placenta, remodelling of these terminal arteries is essential for normal pregnancy development (Pijnenborg et al., 2006). The spiral arteries transition to wide, low-resistance vessels accommodating an increase in placental specific blood flow (approximately 80% of the uterine perfusion is diverted to the placenta). Trophoblast involvement has long been established with this remodelling as the vessels lose their vascular smooth muscle definition and these cells are replaced with fibrinoid and trophoblast cells (Pijnenborg et al., 2006). In hypertensive complications of pregnancy, the remodelling occurs to a lesser extent, resulting from an impaired trophoblast invasion (Pijnenborg et al., 1991, Lyall et al., 2013). Investigations in this chapter revealed SHRSP spiral arteries in zones 2 and 3 of the mesometrial triangle had greater muscular definition than those that were fully remodelled in zone 1. This assessment may be improved by isolating trophoblasts and examining their invasive properties *in vitro* (Bevilacqua et al., 2014). However, as the majority of trophoblast invasion in rodents occurs between GD15 and peaks at GD18 (Ain et al., 2003), the time point chosen for this histological assessment was appropriate.

Further histological and gene expression assessment revealed that SHRSP placenta had less collagen staining and increased expression of *Mmp1* (collagenase) and *Mmp9* (gelatinase) in the maternal decidual tissue. This is paradoxical to other studies which have found hypertensive pregnancies have a reduced expression and activity of Mmps (Li et al., 2014, Dias-Junior et al., 2017). These studies focused mainly on *Mmp2* and *Mmp9* and their role in early

spiral artery vascular remodelling. Mmps are implicated in many stages of reproduction including the oestrus and menstrual cycles and pregnancy; specifically, trophoblast invasion, spiral artery remodelling and labour (Bischof et al., 1995, Geng et al., 2016, Harris et al., 2010). The ubiquitous functions and locations of many different Mmp could go some way to explaining the variations observed with different hypertensive models of pregnancy (Wang and Khalil, 2018). Furthermore, the SHRSP placentas in the present study were observed to have poorer structural stability when dissecting the layers compared to WKY. The structural integrity of the SHRSP and the structural collagen properties require further evaluation in order to establish any firm conclusions.

Hypoxia is crucial to early placental development and trophoblast differentiation which occurs in low oxygen tensions. Hif1α is a transcription factor, key in regulating gene expression in hypoxic conditions and its presence is necessary to sustain a pregnancy (Wakeland et al., 2017). A loss of Hif1α function has been shown to have embryonic lethality at mid-gestation and seriously impacts the vascularization of placenta and fetus (Ryan et al., 1998, Iyer et al., 1998). A hypoxic placental environment in the later stages of gestation can lead to oxidative stress and placental damage (Burton and Jauniaux, 2011). This has been associated with placental impairment leading to fetal development issues and encourages the development and progression of gestational hypertensive disorders (Aljunaidy et al., 2017, Myatt, 2006). An increased expression of Hif1α at these stages is suggestive of a poor placental situation as it indicates a hypoxic environment at a time when the placenta should be oxygen rich (Soares et al., 2017). SHRSP demonstrated an increased placental Hif1α expression at GD18.5. The expression of Sod1 was also found to increase in the placenta and mesometrial triangle of the SHRSP. Sod1 is an antioxidant enzyme that protects against oxidative stress by reducing the bioavailability of superoxide (Fukai and Ushio-Fukai, 2011). It has been located within human and rodent placentas and is crucial in oxidative stress balance (Jones et al., 2010, Jauniaux et al., 2000). The increase in hypoxia suggested by Hif1α could be interpreted as creating an environment that encourages reactive oxygen species production, and thus increasing damaging oxidative stresses. Yet the parallel increase in Sod1 expression implies that SHRSP placenta is attempting to maintain the balance of pro and anti-oxidants. However, this is a simplistic view as there are many more

factors that influence oxidative stress balance; such as other antioxidant enzymes. Glutathione peroxidase (*Gpx1*) is one of these enzymes (Conrad et al., 2007). Expression of *Gpx1* was investigated in the SHRSP placenta and found to have an opposite expression pattern to *Sod1*, with a decreased placental expression observed. This would skew the balance in favour of pro-oxidative species, leading to increased reactive oxygen species and possible placental damage. Further evaluation of oxidative stress state, by examining oxygen radicals, hydrogen peroxide and lipid peroxidation levels, would be beneficial to understanding placental function and damage.

Components of the renin-angiotensin system (RAS) were found to be dysregulated in the SHRSP placenta. The placenta has the largest extra-renal RAS, and its components and receptors have been located within rodent placenta throughout gestation (Vaswani et al., 2015, Paul et al., 2006, Williams et al., 2010). The RAS is crucial to maintaining the homeostasis of maternal cardiovascular and renal systems during pregnancy (Irani and Xia, 2011, Nielsen et al., 2000). AngII receptor type-2 ($AT_2R$) and angiotensin converting enzyme 2 (Ace2) both have protective roles in the vasculature. $AT_2R$ activation via AngII typically results in vasodilation, whilst Ace2 promotes the conversion of AngII to Ang1-7 which activates $AT_2R$ and Mas receptors which further promotes vasodilation (Irani and Xia, 2011, McKinney et al., 2014). The expressions of both $AT_2R$ (*Agtr2*) and *Ace2* were reduced in the highly vascularised placental labyrinth zone in SHRSP. This is the location for the exchange of maternal nutrients and oxygen and a reduction in these 'protective' components would suggest an impaired blood flow and therefore loss of function. This study also found that SHRSP had a reduced expression of AngII receptor type-1 ($AT_1R$) in the maternal mesometrial tissue. This receptor has a counter-regulatory mechanism to $AT_2R$ and is responsible for the vasoconstrictive response to AngII (McKinney et al., 2014). An increase in $AT_1R$ expression and activity has been described by some to be observed in pre-eclampsia (Herse et al., 2007). The reduction in expression in the hypertensive pregnancy of SHRSP is therefore contrary to that particular study, as a lower receptor expression would suggest lower AngII receptor mediated vasoconstriction (Takeda-Matsubara et al., 2004, Mishra et al., 2011). However, as the two main AngII receptors have contradictory responses when stimulated by AngII, the final response depends heavily on the

balance of expression of different receptors (McKinney et al., 2014). SHRSP also demonstrated an increase in $AT_1R$ expression in the junctional zone of the placenta. In human placental tissue $AT_1R$ has been located to the syncytiotrophoblasts and villous cytotrophoblast early in gestation and it has been found to be altered depending on the gestational stage in rodents (Tower et al., 2010, Vaswani et al., 2015). The rodent junctional zone in not highly vascularised and therefore suggests that the roles of the AngII receptors are varied and may have different functions in different placental compartments as gestation progresses. Cuffe *et al* found that placental $AT_1R$ expression increases in hypoxic pregnancies, which could partly explain the increase observed in this study (Cuffe et al., 2014). Furthermore, an imbalance of AngII receptors (a proportional increase in $AT_1R$ activation) has been found to reduce the placental transport of system A amino acids (Shibata et al., 2006). This study was limited in that only the gene expression of RAS components were investigated, and no assessment of receptor activation or function was conducted. This investigation would be key in dissecting the importance of the patterns of gene expression in the different placental layers.

Preliminary investigations into the functional transport capacity of the WKY and SHRSP placenta via system A (SysA) amino acid transporter were examined in this study at the GD18.5 time point. This is when the placenta are at their functional peak (Malassiné et al., 2003). There was evidence that the SysA transporter is present on the maternal facing membranes of syncytiotrophoblasts in SHRSP and WKY placenta and that this transporter is functional. This is the first study to show this in SHRSP and WKY. The vesicle uptake experiments were limited due to small numbers of biological replicates, this occurred due to the need for protocol optimisation prior to carrying out the full experiment. This data was suggestive of SHRSP exhibiting a lower transport capacity; however, the small sample size and variability in $Na^+$ dependent transport rate between animals would require further investigation to determine whether significance exists between strains. SysA transport was assessed due to being intimately involved in the development of FGR and placental transport in hypertensive pregnancies has been found to be reduced (Glazier et al., 1996, Glazier et al., 1997, Mahendran et al., 1993). SHRSP placenta have previously been found to have a reduced $Na^+/K^+$ ATPase activity which was thought to contribute to the

growth retardation observed in this strain (Fuchi et al., 1995a). More precise measures of placental transport can be conducted *in vivo*. These include the unidirectional maternofetal transfer of a radiolabelled amino acid across the placenta by introducing this amino acid to maternal systemic circulation and measuring its abundance in the fetus (Lean et al., 2017). Performing these studies would give a better overview of placental transport systems and delivery of nutrients to the fetus in SHRSP and WKY.

Impairments within the maternal cardiovascular system and the placenta are increasingly recognised as important partners in the development of pre-eclampsia. It is therefore becoming crucial to recognise the maternal influence of these gestational hypertensive disorders. The development of a model which has a significant maternal influence will be vital to the further study of gestational hypertension. Non-pregnant SHRSP rats are excellent, well established cardiovascular risk models and this study has provided some evidence that the normotensive and hypertensive strains respond to pregnancy differently. The chronically hypertensive SHRSP showed minor impairments in maternal cardiovascular adaptations to pregnancy as well as placental abnormalities; however, this occurred with no alterations of litter size or major impact on fetal growth. Chapter 6 describes how the SHRSP model responds to a cardiovascular challenge by means of AngII administration during pregnancy and how this increased cardiovascular load can mimic superimposed pre-eclampsia.

# Chapter 4 Vascular changes in SHRSP pregnancy

## 4.1 Introduction

The haemodynamic and cardiovascular changes, described in Chapter 1, are pregnancy-specific adaptations that ensure the re-direction of blood flow to the placenta. Uterine blood flow is approximately 10 times greater by the end of the first trimester in healthy human singleton pregnancies and continues to increase throughout gestation, reaching levels of between 500-800ml/min (Hale et al., 2009, Wang, 2010, Browne et al., 2015, Osol and Mandala, 2009). This is vital to the wellbeing of the pregnancy. The increase in cardiac output (CO), described in section 1.1.1, increases the capacity for blood flow and a decrease in total peripheral vascular resistance occurs in tandem to the CO changes to ensure there is no increase in blood pressure in healthy normotensive pregnancies (Robson et al., 1989). This reduced systemic vascular resistance ensures that there is no opposition to uterine blood flow and the uterine index is increased, suggesting a larger proportion of CO is directed to the placenta during pregnancy, which is crucial for achieving appropriate fetal growth (Hale et al., 2009, Mahendru et al., 2017). The reduction in systemic vascular resistance has been found to occur as early as 6 weeks gestation, which suggests that alterations to blood flow are not solely due to local changes driven by the placenta but are influenced by systemic hormonal changes (Chapman et al., 1998). Prior to 10-12 weeks gestation relatively little endocrine control is derived from the placenta and adaptations to accommodate pregnancy are under maternal control (Gellersen et al., 2007, Tal et al., 2000). The main uterine artery in rodents has been shown to increase in diameter and begin the remodelling process in pseudopregnancy, giving evidence towards a maternal control of early uterine artery remodelling (van der Heijden et al., 2005b, Osol and Mandala, 2009, Paller et al., 1989).

A central component to the development of gestational hypertensive disorders, such as pre-eclampsia, is a reduction in uteroplacental perfusion (Bosio et al., 1999, Goulopoulou, 2017). However, the vascular pathology in these conditions is still not fully understood. Placental under perfusion may result from systemic and uteroplacental vascular dysfunction, and a dysfunctional placenta can result in increased production of antiangiogenic and inflammatory factors which are released into systemic circulation propagating endothelial dysfunction and vascular impairment (summarised in Figure 4-1) (Ali and Khalil, 2015,

Goulopoulou, 2017). It is still not fully understood which is the cause and which the consequence.

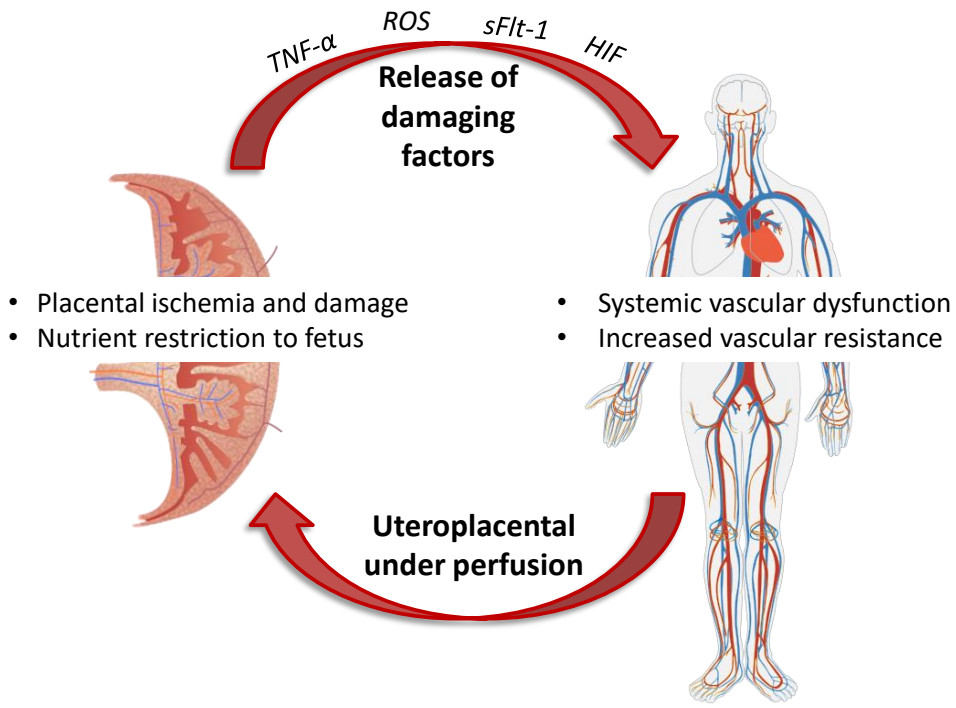


**Figure 4-1: Illustration of the influences increased vascular resistance and placental under perfusion have on each other**
The cause/consequence relationship of the under perfused placenta exacerbating the systemic vascular dysfunction and encouraging a hypertensive response, adapted from review by Goulopoulou *et al* (Goulopoulou, 2017).

Whilst examining the uterine artery response is vitally important to reveal local controls and dysregulations, the systemic responses should not be overlooked. Systemic vascular dysfunction plays a significant role in the development of hypertensive disorders of pregnancy (Rang et al., 2008, Ramirez et al., 2011). Total peripheral resistance has been found to increase in pre-eclampsia and early studies by Gant *et al* highlighted systemic vascular dysfunction associated with hypertensive disorders of pregnancy and their increased vasoconstrictive response to AngII (Bosio et al., 1999, Visser and Wallenburg, 1991, Gant et al., 1973). The myogenic control of resistance arteries is vitally important in maintaining blood pressure (Kublickiene et al., 1998, Ramirez et al., 2011). The medial layer of these small arteries (composed mainly of vascular smooth muscle cells (VSMC) and elastin fibres) contracts or relaxes in response to increases or decreases in blood flow/volume in order to maintain blood pressure (Touyz, 2014). During normal pregnancy the response of the VSMC are altered as the blood volume increases with no increased contractile response and therefore no change in blood pressure (Kublickiene et al., 1997). In fact, the arteries become more vasodilatory and less responsive to vasoconstrictive substances (Kublickiene et al., 1997). However, the reverse has been observed in situations of reduced uterine perfusion in the rat (Ramirez et al., 2011), and in human hypertensive pregnancy (Kublickiene et al., 1997, Kublickiene et al., 1998).

The previous chapter highlighted the importance of maternal influences of gestational hypertension and provided evidence that the cardiovascular adaptations to pregnancy in chronically hypertensive SHRSP rat are impaired; which is also observed in gestational hypertensive disorders (Robson et al., 1989, Stott et al., 2017, Visser and Wallenburg, 1991). The changes in uteroplacental blood flow of SHRSP pregnancy were examined by Small *et al* using uterine artery Doppler at gestational day (GD6.5, 12.5 and 18.5) (Small et al., 2016). This study found SHRSP pregnancy to be associated with restricted blood flow within the uterine artery and abnormal vascular function at GD18.5 compared to WKY. This finding was due to SHRSP retaining their pre-pregnant uterine artery vascular function and no blood flow changes where apparent across gestation (Small et al., 2016). This study also concluded that virgin SHRSP uterine arteries have a more vasoconstrictive phenotype than WKY (Small et al., 2016). This raises the question of whether SHRSP uterine arteries are impaired pre-

pregnancy and thus ignore cues to reduce their resistance and encourage an increased blood flow during pregnancy, as is observed in the normotensive WKY. Few investigations have examined systemic vasculature and no studies have examined early vascular changes during pregnancy in SHRSP. This chapter was designed to study the responses of systemic vasculature to pregnancy in SHRSP and WKY and to characterise in depth the maternal control of early uterine artery remodelling.

## 4.2 Hypothesis and Aims

### 4.2.1 Hypothesis

The absence of a pregnancy-dependent increase in uteroplacental blood flow in SHRSP is due to a lack of response of systemic and uterine vascular systems to pregnancy.

### 4.2.2 Aims

- Evaluate the functional and mechanical properties of mesenteric arteries over the course of gestation in SHRSP and WKY

- Assess early (GD6.5) uterine specific vascular remodelling associated with the first 6 days of gestation in SHRSP and WKY

- Determine the influence that maternal plasma from early (GD6.5) and late (GD18.5) gestation has on non-pregnant uterine artery function

- Examine properties of uterine artery vascular smooth muscle cells from virgin and GD6.5 SHRSP and WKY

## 4.3 Materials and Methods

Details of mesenteric and uterine artery dissection are outlined in the general materials and methods section 2.4.3. Functional studies were conducted using wire myography, detailed in section 2.5.1, and passive mechanical wall properties were assessed using pressure myography, detailed in section 2.5.2.

### 4.3.1 Uterine Artery Plasma Incubation

To examine the maternal endocrine control on uterine artery function, non-pregnant arteries were incubated with maternal plasmas of different strain/pregnancy stage prior to performing wire myography. Uterine arteries from 13-14 week old virgin WKY and SHRSP rats were equally sectioned (Figure 4-2). Each artery section was exposed to a different plasma condition (Non-pregnant (NP) WKY, NP SHRSP and either GD6.5 WKY, GD6.5 SHRSP or GD18.5 WKY, GD18.5 SHRSP) by placing the artery into PSS containing 3% v/v plasma at 4°C for ~18 hours. Plasma was isolated from blood taken via cardiac puncture in non-pregnant and GD6.5 or GD18.5 pregnant WKY and SHRSP dams as outlined in sections 2.4.1. Wire myography was performed as detailed in section 2.5.1, for each plasma condition in duplicate. Preliminary dose response experiments revealed that these uterine arteries reached 80% of maximal contraction with $1x10^{-5}$M noradrenaline; therefore this was the preconstriction dose used.

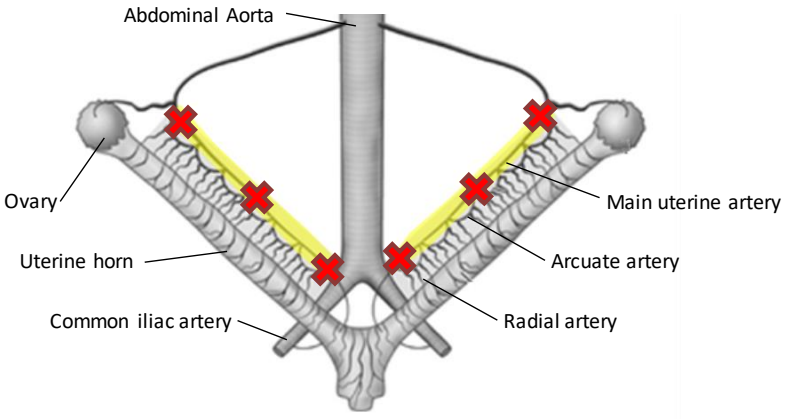


**Figure 4-2: Non-pregnant uterus highlighting uterine artery dissection**
The main uterine artery was dissected from surrounding tissue and the vein. The yellow highlighted regions were used for functional assessment and were sectioned at the sites marked with red crosses. This produced four sections of the uterine artery from one animal. Each section was placed in different plasma conditions. Image adapted from (Osol and Moore, 2014) with permission.

## 4.3.2 Vascular smooth muscle cell

Vascular smooth muscle cells (VSMC) were isolated and cultured as described in section 2.6.

### 4.3.2.1 Migration Scratch Assay

VSMC were used between passage (P)3 and P5 (after P5 cell growth slowed, viability was reduced to <50% and the time taken to reach confluency in a T75 was greater than 1 week). For each cell type (NP WKY, GD6.5 WKY, NP SHRSP and GD6.5 SHRSP) 6 wells were plated in complete DMEM for one scratch assay experiment at a cell density of $1x10^5$ cells per well. Once a confluent monolayer of cells was established (between 24 and 36 hours after plating) the media was removed and wells washed briefly with sterile 1x PBS. The cells were then incubated with DMEM containing 0.5% FBS for 48 hours at 37°C. This ensured all cells were at the same stage of the cell cycle and reduced the proliferation ability of VSMCs. At time zero (T0) the cell monolayers were scratched using a P200 pipette tip, guided by a ruler. The media in all wells was replaced with DMEM containing 10% FBS and gently swirled to smooth scratch edges. All media was then removed. Wells rinsed with 1x PBS as previously stated and DMEM containing either 0.5% FBS (acting as a negative control) or 10% FBS (to stimulate cell migration) was added. Each condition was conducted in triplicate. Three images from each well were taken of the scratch at 10x magnification using an EVOS microscope, set for phase observation 4/10PH, at T0, T1 (6 hours), T2 (12 hours) and T3 (24 hours). Plates were returned to a 37°C incubator with 5% oxygen in between time points. Markings on the base of the wells ensured scratch was central and images were taken in the same locations.

Images were analysed by measuring the width of the scratch by drawing 15-20 straight lines from one edge to the other (Figure 4-3) using Image J software. An average for each image at each time point was calculated. The T1, T2 and T3 averages were subtracted from their T0 average and expressed as a percentage. Further to this the 0.5% FBS controls were subtracted from the 10% FBS to give a FBS dependent migration value for each time point.

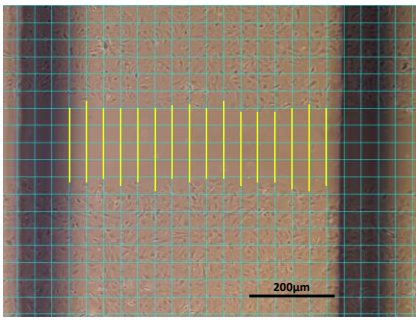


**Figure 4-3: Representative image of scratch assay analysis**
Each image was overlaid with a grid to ensure measurements across wound were linear. 15-20 measurements were made between marked lines for each image to give representation of width across the well.

### 4.3.3 Statistical Analysis

The area under the curve (AUC) and the half maximal response ($EC_{50}$) was calculated for all untreated mesenteric and uterine artery myography dose response curves and these were then compared using one-way ANOVA with Sidak post-hoc test. Maximal KPSS responses were compared using one-way ANOVA and Sidak post-hoc test. Uterine arteries incubated with 3% plasma were analysed in the same manner, with the AUC and $EC_{50}$ values calculated, however a repeated-measures one-way ANOVA with Sidak post-hoc testing was used for the comparisons due to each vessel having 4 segments with different plasma incubations. The pressure myography curves could not be analysed in the same way as the dose response curve, so a two-way repeated measures ANOVA was used to assess the changes at each pressure between the groups using a Sidak post-hoc test. Finally the percentage migration at 24 hours was compared across strain, pregnancy and FBS condition using a two-way ANOVA. Further analysis of the rate of migration was assessed using linear regressions compared using one-way ANOVA with Sidak post-hoc test.

# 4.4 Results

## 4.4.1 Systemic Vascular Function and Mechanical Properties

### 4.4.1.1 Mesenteric Artery Function across Gestation

*Ex vivo* mesenteric artery function was determined in virgin WKY and SHRSP and at early (GD6.5) and late pregnancy (GD18.5) time points. Segment lengths used were not significantly different between strains or gestational age (summarised in Table 4-1), therefore reducing variation between active effective pressure calculations. No significant relaxation or constriction responses were observed between NP and GD6.5 in either strain (Figure 4-4A-G). There were also no significant functional changes between strains at NP or GD6.5 time points (Figure 4-4A-G). Mesenteric arteries from WKY dams did exhibit a significantly increased vasodilation response to carbachol in late pregnancy (GD18.5) (220±25.8 AUC versus 388±34.7 AUC; $p<0.01$) (Figure 4-4A-B). An overall trend towards increased sodium nitroprusside mediated dilation was observed in WKY GD18.5 arteries compared to NP, with the GD18.5 arteries demonstrating a reduced half maximal response, nearing significance, compared to NP (1.55±0.6 $x10^{-7}$ M versus 3.01±1.1 $x10^{-5}$ M; $p<0.05$) (Figure 4-4C-D). The GD18.5 WKY mesenteric arteries also exhibited a significantly increased vasodilatory response to carbachol compared to GD18.5 SHRSP (220±25.8 AUC versus 389±26.8 AUC; $p<0.01$) (Figure 4-4A). No significant differences were observed between NP and GD18.5 SHRSP mesenteric arteries relaxation responses (Figure 4-4A-D). Neither strain nor pregnancy affected the contractile response of mesenteric arteries; there were no significant differences in the contractile responses to noradrenaline or maximal contractions to KPSS (Figure 4-4E-G).

**Table 4-1: Length (mm) of segments of mesenteric artery used for wire myography**

| | Non Pregnant | GD6.5 | GD18.5 |
|---|---|---|---|
| **WKY** | 1.95±0.04 | 1.96±0.03 | 1.87±0.04 |
| **SHRSP** | 1.90±0.02 | 1.90±0.06 | 1.90±0.02 |

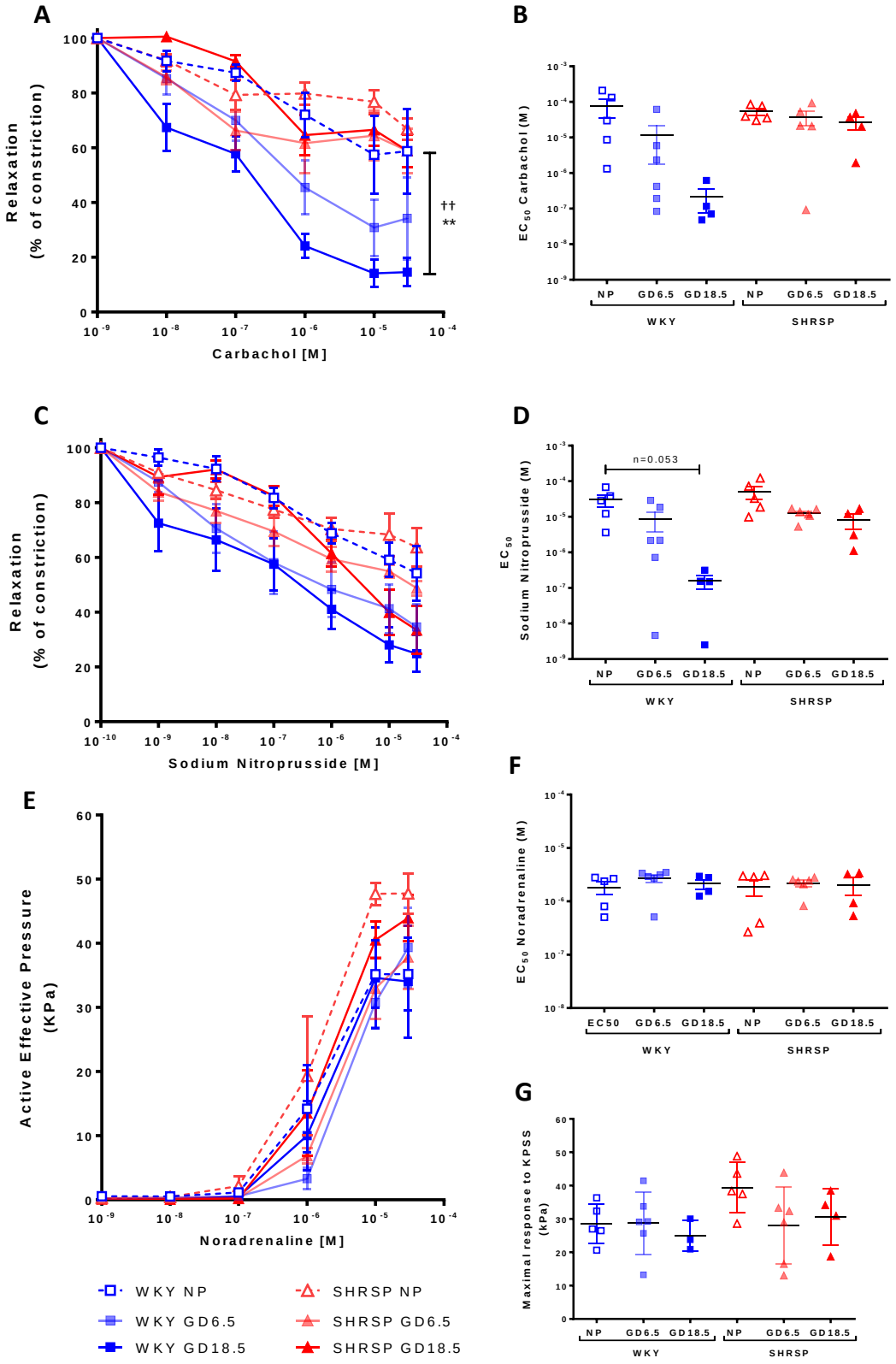


**Figure 4-4: Mesenteric Artery Function Throughout Gestation**
The functional responses of mesenteric arteries from non-pregnant (NP) (n=5), GD6.5 (n=6) and GD18.5 (n=3-4) pregnant WKY and SHRSP assessed using wire myography. The relaxation response to carbachol (A-B) and sodium nitroprusside (C-D) are presented as a percentage of constriction to $2x10^{-5}$M noradrenaline and the half maximal responses ($EC_{50}$). The contractile response to noradrenaline expressed as an (E) active effective pressure and (F) the half maximal responses ($EC_{50}$) for each curve. Statistical significance determined by comparing area under the curve and $EC_{50}$ values using one-way ANOVA with Sidak post-hoc test. (G) The maximal response to KCl (in KPSS); analysed using one-way ANOVA with Sidak post-hoc test. Data presented as mean±SEM.

#### 4.4.1.2 Mesenteric Artery Passive Wall Properties across Gestation

The internal and external diameter of mesenteric arteries were measured using pressure myography and the cross-sectional area, wall thickness, wall stress and the stress/strain relationship were calculated. Pregnancy had no significant influence on the overall change in WKY or SHRSP mesenteric artery diameter; however SHRSP GD18.5 arteries demonstrated a significant increase in internal diameter at 110mmHg compared to NP arteries (305±15.2μm versus 241±17.8μm; $p<0.05$) (Figure 4-5A-B). The mesenteric arteries from both strains showed a significant reduction in cross-sectional area in GD18.5 arteries compared to NP arteries at pressures greater than 40mmHg (e.g. WKY: 49861±6672$\mu m^2$ versus 68092±9946$\mu m^2$; $p<0.05$ at 110mmHg. SHRSP: 29589±5148$\mu m^2$ versus 53714±2532$\mu m^2$; $p<0.05$ at 110mmHg) (Figure 4-5C). Mesenteric arteries from SHRSP GD18.5 dams had a significantly reduced wall thickness compared to NP SHRSP for the entire pressure curve (28.1±4.4μm versus 57.7±3.8μm; $p<0.001$ at 110mmHg) (Figure 4-5D). There were no significant differences between NP and GD6.5 mesenteric arteries of either strain in any of the measured/calculated structural parameters (Figure 4-5A-F). Both WKY and SHRSP GD18.5 mesenteric arteries demonstrated an increased wall stress, with SHRSP GD18.5 arteries being significantly greater than NP at pressures above 60mmHg (0.98±0.14x$10^6$ dynes/$cm^2$ versus 0.32±0.04x$10^6$ dynes/$cm^2$; $p<0.0001$ at 110mmHg) and WKY GD18.5 arteries demonstrating a significantly increased wall stress, compared to NP WKY arteries at pressures above 100mmHg (0.80±0.19x$10^6$ dynes/$cm^2$ versus 0.47±0.09x$10^6$ dynes/$cm^2$; $p<0.01$ at 110mmHg) (Figure 4-5E). The mesenteric vascular stiffness (as measured by the stress/strain relationship) was not changed over pregnancy (Figure 4-5F).

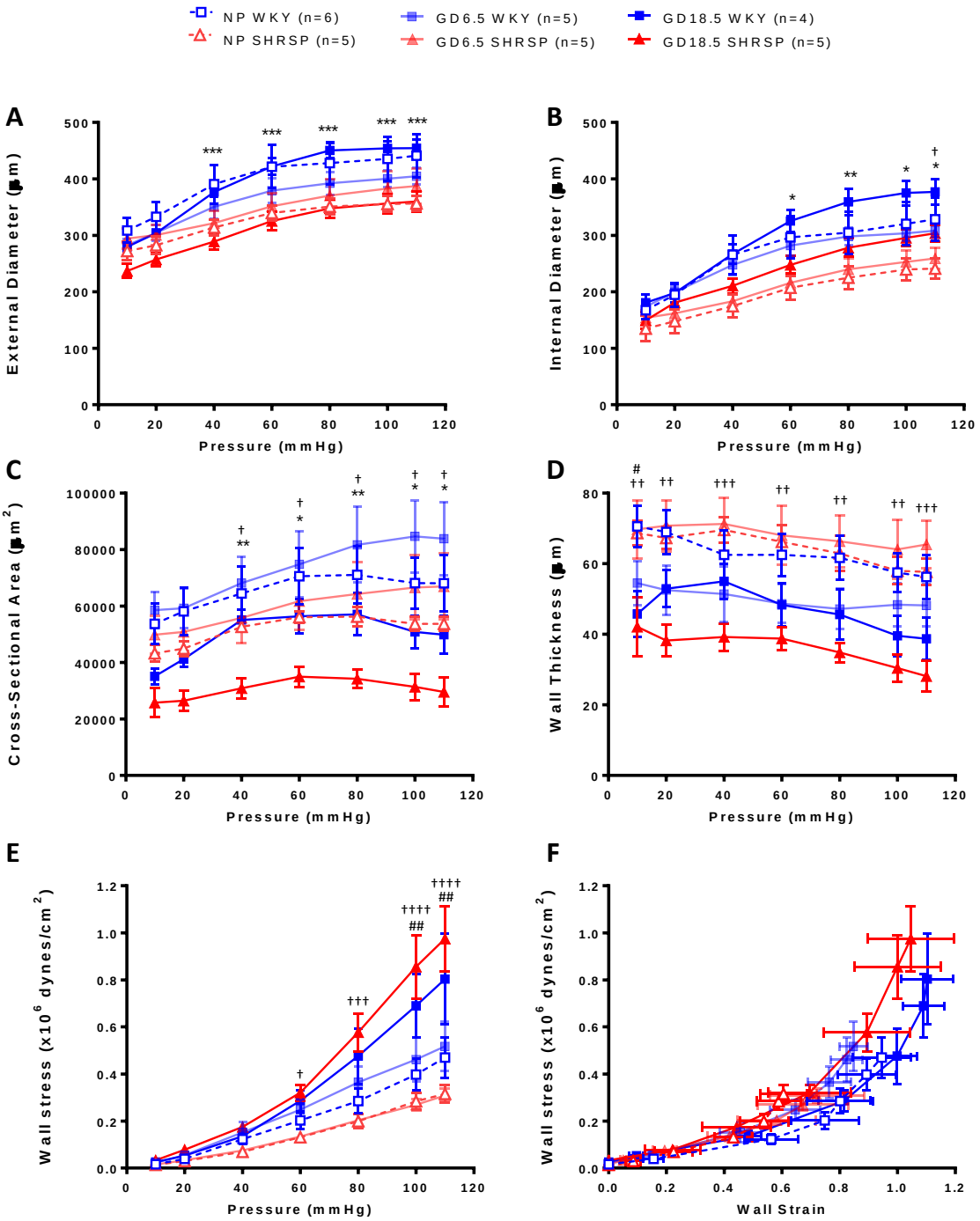


**Figure 4-5: Mesenteric Artery Mechanical Wall Properties throughout Gestation**
Non-pregnant (NP) and pregnant GD6.5 and GD18.5 mesenteric artery external (A) and internal (B) diameter were measured over a range of physiological pressures using pressure myography. The vessel cross-sectional area (C), wall thickness (D) and wall stress (E) were calculated. The relationship between wall stress and strain was also plotted (F). Data presented as mean ±SEM (n=4-6); statistical significance was determined using a repeated measures two-way ANOVA with Sidak post-hoc test comparing change from NP in both strains; $^{\#}p<0.05$, $^{\#\#}p<0.01$ NP vs GD18 WKY, $^{\dagger}p<0.05$, $^{\dagger\dagger}p<0.01$, $^{\dagger\dagger\dagger}p<0.001$, $^{\dagger\dagger\dagger\dagger}p<0.0001$ NP vs GD18.5 SHRSP; and change between strains; $^{*}p<0.05$, $^{**}p<0.01$, $^{***}p<0.001$ GD18 WKY vs GD18 SHRSP.

## 4.4.2 Uterine Specific Vascular Structure and Function

### 4.4.2.1 Uterine Artery Function at Gestational Day 6.5

Uterine artery function in SHRSP and WKY was examined at GD6.5, an early gestational time point in rats. No significant differences were found in any of the uterine artery responses to carbachol (Figure 4-6A-B), SNP (Figure 4-6C-D) or noradrenaline (Figure 4-6E-F). There was also no significant changes observed in the maximal constriction responses in either comparisons across pregnancy or between WKY and SHRSP (Figure 4-6G).

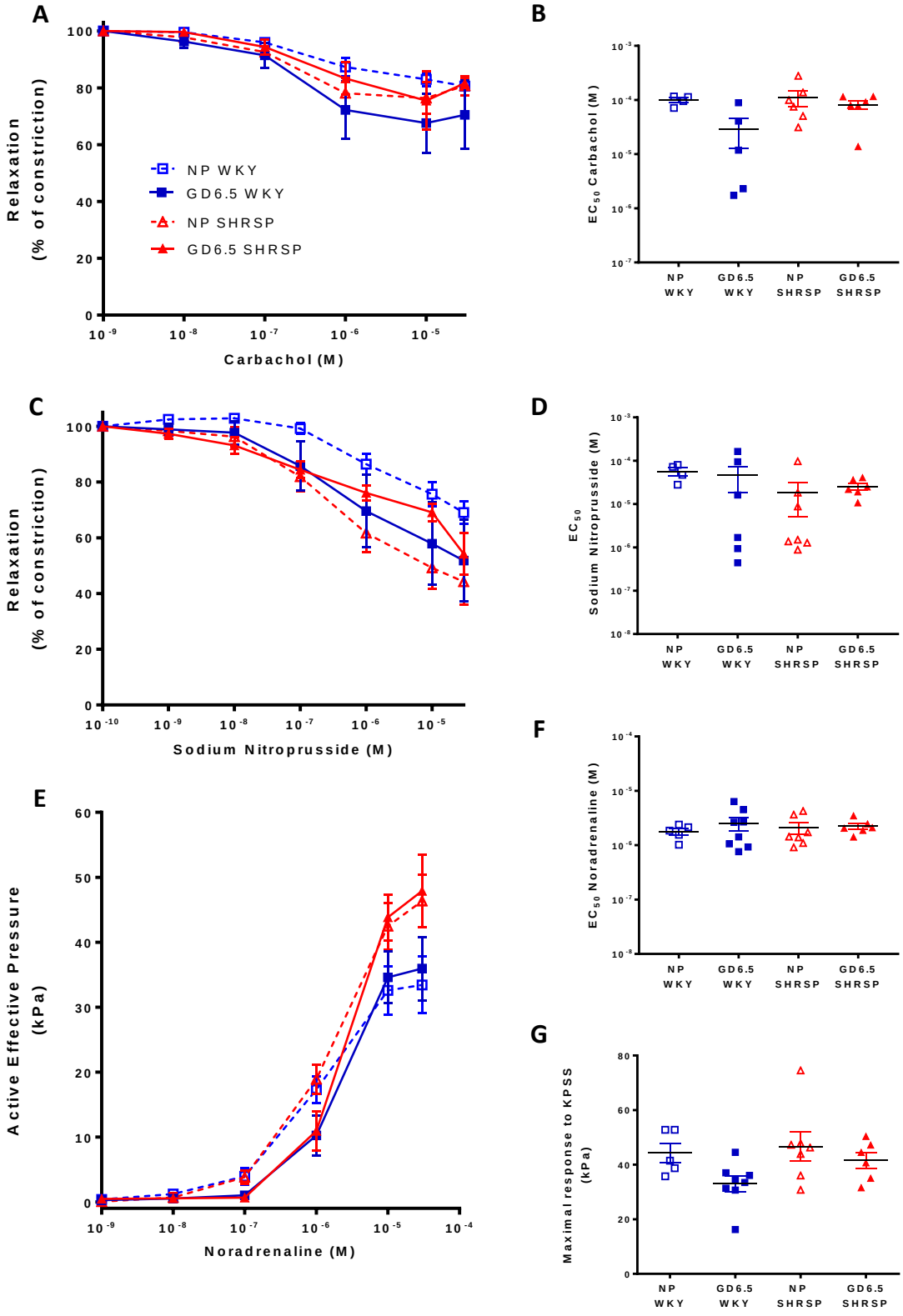


**Figure 4-6: The Impact of Early Pregnancy (GD6.5) on Uterine Artery Function**
Functional response of non-pregnant (NP) and GD6.5 uterine arteries from WKY and SHRSP dams. The relaxation response to carbachol (A-B) and sodium nitroprusside (C-D) are presented as a percentage of constriction to $2x10^{-5}$M noradrenaline and the half maximal responses ($EC_{50}$). The contractile response to noradrenaline (E-F) expressed as an active effective pressure and the half maximal responses ($EC_{50}$) for each curve. Statistical significance determined by comparing area under the curve and $EC_{50}$ values using one-way ANOVA with Sidak post-hoc test; NP n=4-7, GD6.5 n=6-7 (G) The maximal response to KCl (in KPSS); analysed using one-way ANOVA with Sidak post-hoc test.

#### 4.4.2.2 Uterine Artery Passive Wall Properties at Gestational Day 6.5

NP WKY uterine arteries had a significantly larger internal and external diameter than NP SHRSP at pressures greater than 40mmHg (e.g. internal: 390±10.4μm versus 324±16.7μm at 110mmHg; $p<0.01$ and external: 464±8.7μm versus 416±10.7μm at 110mmHg; $p<0.01$) (Figure 4-7A-B). There was no significant difference in the diameter changes between NP and GD6.5 uterine arteries. Only the SHRSP arteries demonstrated a significant pregnancy-dependent difference in cross-sectional area, and only at 80mmHg (NP: $5.15\pm0.4x10^4$ $\mu m^2$ versus GD6.5: $7.09\pm0.8x10^4$ $\mu m^2$; $p<0.05$) (Figure 4-7C). Wall thickness was increased in the WKY GD6.5 arteries only at 10mmHg (62.3±4.9μm versus 44.1±4.2μm at 110mmHg; $p<0.01$), no other significant differences were observed. GD6.5 uterine arteries from WKY dams demonstrated a significantly reduced wall stress at 110mmHg compared to NP ($0.61\pm0.11x10^6$ dynes/$cm^2$ versus $0.86\pm0.09x10^6$ dynes/$cm^2$; $p<0.01$). Furthermore, WKY vessels were found to have a significantly increased wall stress at 110mmHg compared to SHRSP NP ($0.86\pm0.09x10^6$ dynes/$cm^2$ versus $0.58\pm0.10x10^6$ dynes/$cm^2$; $p<0.05$) and GD6.5 ($0.61\pm0.11x10^6$ dynes/$cm^2$ versus $0.40\pm0.05x10^6$ dynes/$cm^2$; $p<0.05$) vessels. (Figure 4-7E). Distensibility of the NP arteries was similar in both strains and was not altered by pregnancy in WKY. (Figure 4-7F)

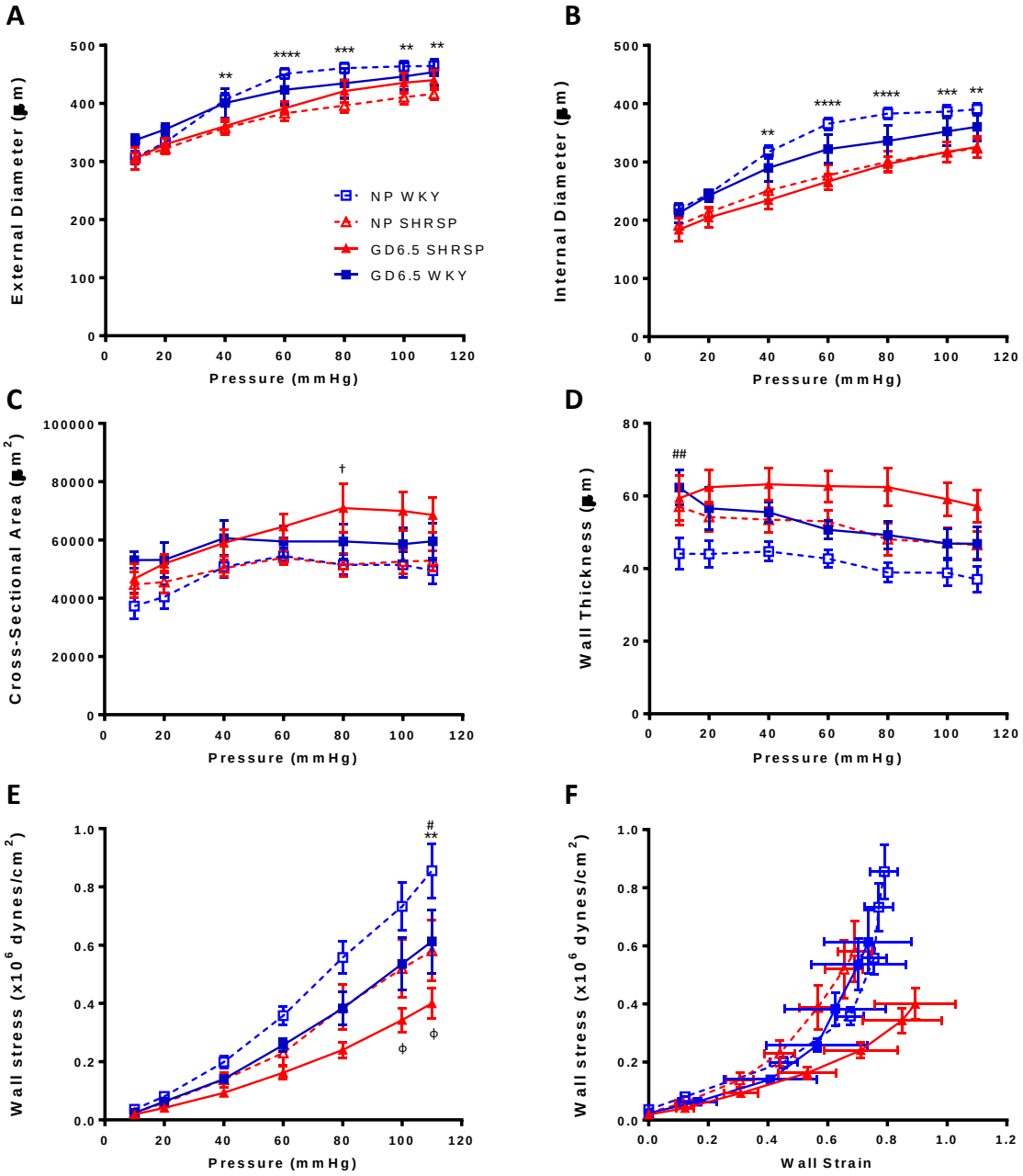


**Figure 4-7: The Impact of Early Pregnancy (GD6.5) on Uterine Artery Passive Mechanical Wall Properties**

Pressure myography was used to measure the external (A) and internal (B) diameter of WKY and SHRSP uterine arteries from non-pregnant (NP) (n=10-11) and GD6.5 pregnant (n=6) dams. Cross-sectional area (C), wall thickness (D) and wall stress (E) were calculated along with plotting the wall stress/strain relationship (F). (A-E) Data are presented as means ±SEM. Statistical significance was determined using a repeated measures two-way ANOVA with Sidak post-hoc test comparing change between NP and GD6.5 in both strains; $^{\#}p<0.05$, $^{\#\#}p<0.01$ WKY and $^{\dagger}p<0.05$ SHRSP; and change between strains; *p<0.05, **p<0.01, ***p<0.001 NP WKY vs NP SHRSP and $^{\varphi}p<0.05$ GD6.5 WKY vs GD6.5 SHRSP.

### 4.4.2.3 Early Pregnancy (GD6.5) Plasma Impact on WKY Uterine Artery Function

Uterine arteries from non-pregnant WKY were exposed to 3% NP plasma or 3% GD6.5 plasma from either WKY or SHRSP for ~18 hours at 4°C. The function of these vessels was assessed using wire myography. No significant differences were found in the vessels in response to vasodilators (carbachol and SNP (Figure 4-8A-B) or the vasoconstrictor noradrenaline (Figure 4-8C). Incubation with WKY GD6.5 plasma significantly reduced the maximal constriction response to KPSS compared to NP WKY plasma (27±5.3KPa versus 44±6.5KPa; $p<0.05$) (Figure 4-8D). No significant differences were observed with GD6.5 SHRSP plasma.

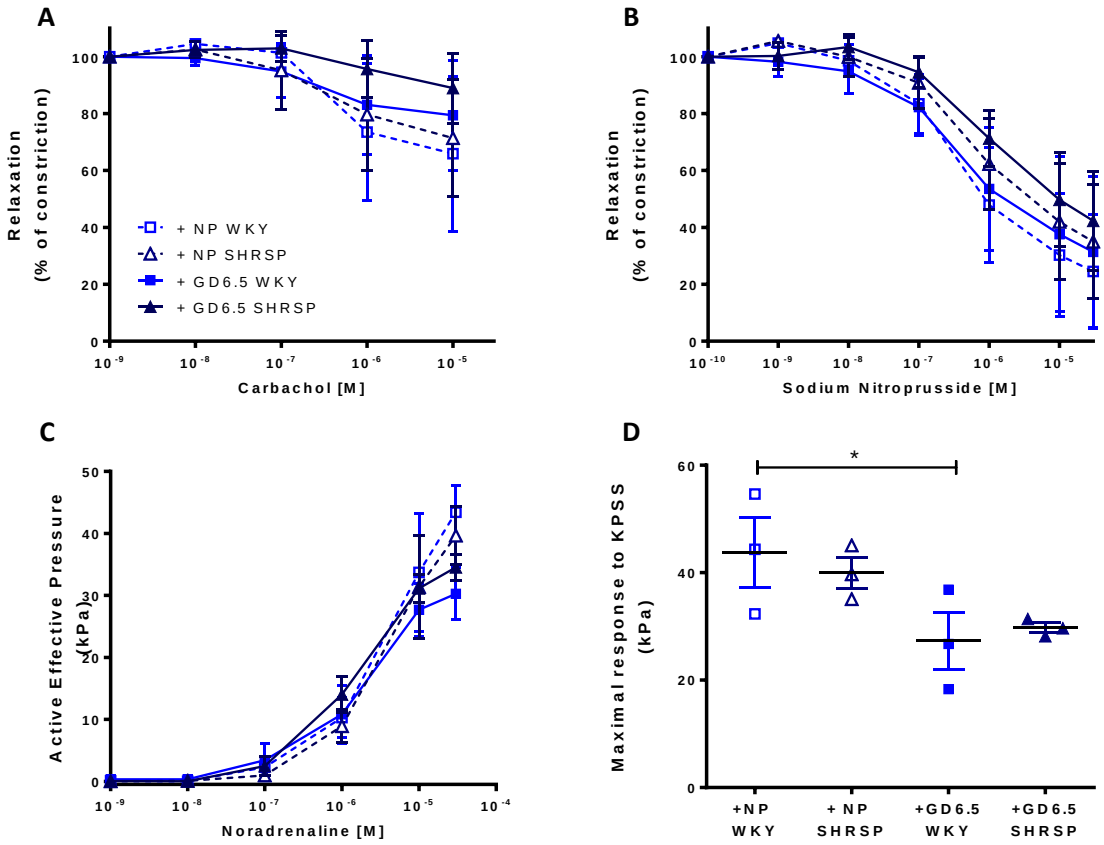


**Figure 4-8: Functional responses of WKY uterine arteries incubated with GD6.5 plasma**
Wire myography was used to assess function of non-pregnant uterine artery from virgin WKYs after incubation with 3% plasma from NP and GD6.5 WKY and SHRSP dams. The relaxation response to (A) carbachol and (B) sodium nitroprusside as a percentage of constriction to $1x10^{-5}$M noradrenaline. (C) The contractile response to noradrenaline. Data analysed by comparing the area under the curve and $EC_{50}$ values for each curve using a repeated measure one-way ANOVA with Sidak post-hoc test. (D) The maximal response to KPSS; analysed using repeated measure one-way ANOVA with Sidak post-hoc test; *$p<0.05$; n=3.

### 4.4.2.4 Early Pregnancy (GD6.5) Plasma Impact on SHRSP Uterine Artery Function

Uterine arteries from non-pregnant SHRSP were exposed to 3% NP plasma or 3% GD6.5 plasma from either WKY or SHRSP for ~18 hours at 4°C. The function of these vessels was assessed using wire myography. No significant differences were found in the vessels in response to vasodilators (carbachol and SNP) (Figure 4-9A-B) or the vasoconstrictor noradrenaline (Figure 4-9C). Incubation with plasma also had no significant effects on maximal constriction response to KPSS (Figure 4-9D).

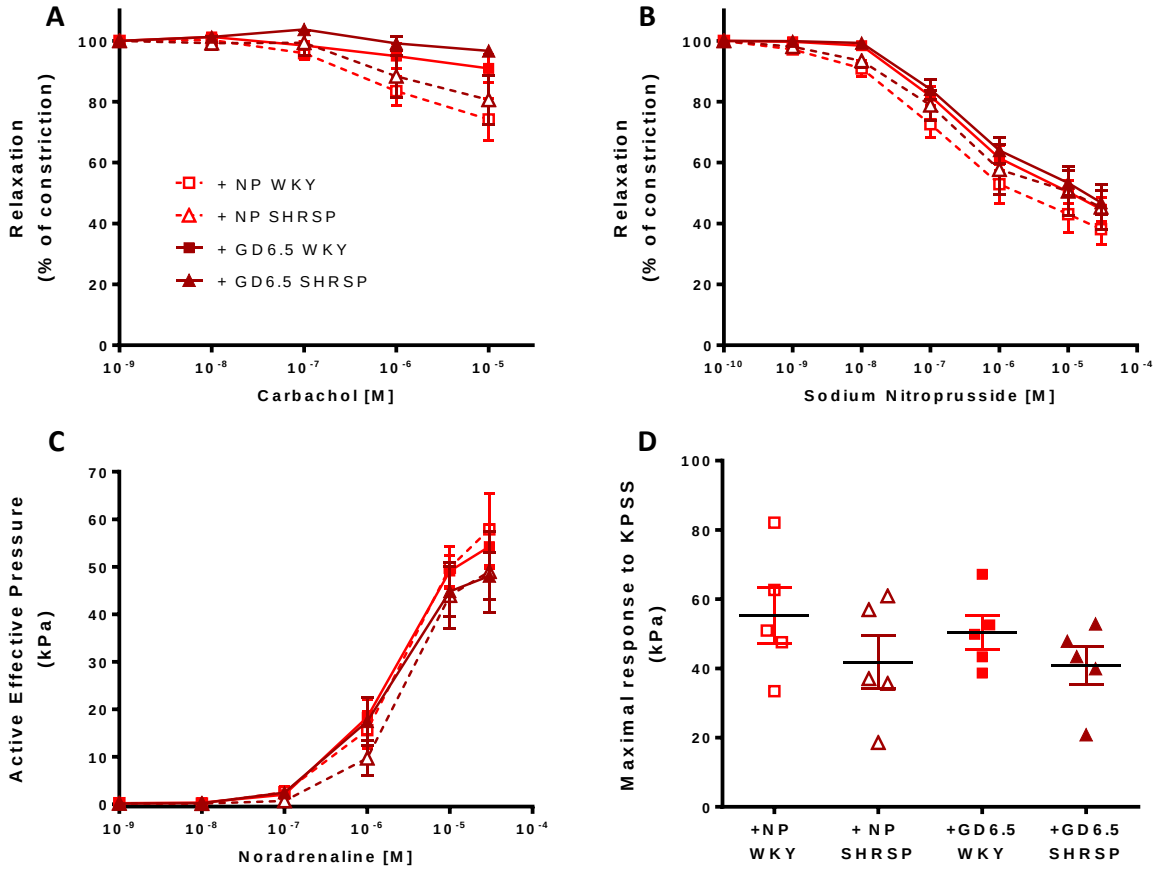


**Figure 4-9: Functional responses of SHRSP uterine arteries incubated with GD6.5 plasma**
Non-pregnant SHRSP uterine artery function was assessed using wire myography after incubation with non-pregnant (NP) or GD6.5 plasma from WKY and SHRSP. (A) The endothelium independent vasodilation to carbachol expressed as a percentage of $10^{-5}$M noradrenaline constriction. (B) The endothelium independent relaxation response to sodium nitroprusside expressed as a percentage of $10^{-5}$M noradrenaline constriction. (C) The contractile response to noradrenaline. Data analysed by comparing the area under the curve and $EC_{50}$ values for each curve using a repeated measure one-way ANOVA with Sidak post-hoc test. (D) The maximal response to KPSS; analysed using repeated measure one-way ANOVA with Sidak post-hoc test; *p<0.05; n=5.

### 4.4.2.5 Late Pregnancy (GD18.5) Plasma Impact on WKY Uterine Artery Function

The function of non-pregnant WKY uterine arteries was assessed after incubation with 3% NP plasma or 3% GD18.5 plasma from either WKY or SHRSP for ~18 hours at 4°C. Plasma incubation did not significantly change the response to carbachol (Figure 4-10A) or SNP (Figure 4-10B). Incubation with NP or GD18.5 plasma had no significant impact on the response to noradrenaline or on maximal constriction response to KPSS (Figure 4-10C-D).

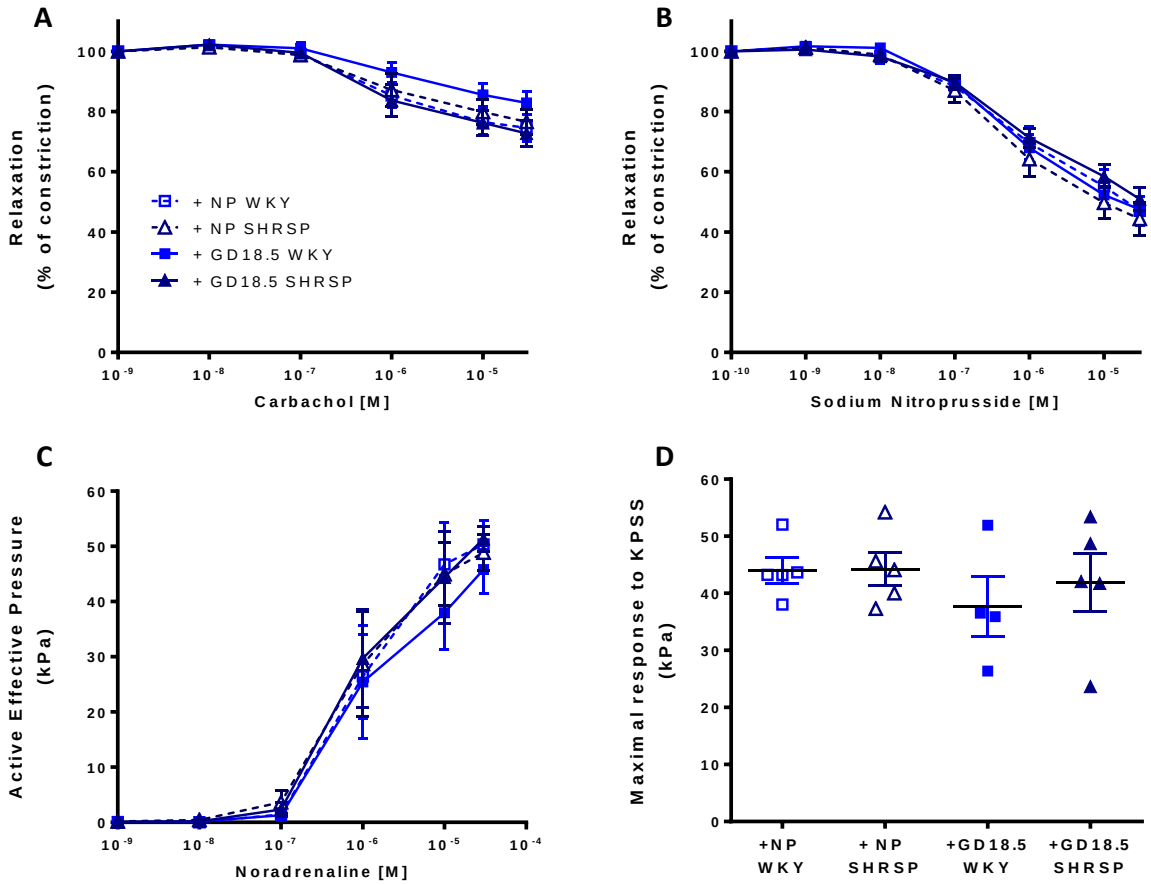


**Figure 4-10: Functional responses of WKY uterine arteries incubated with GD18.5 plasma**
Non-pregnant WKY uterine arteries were incubated with non-pregnant (NP) and GD18.5 pregnant plasma from WKY and SHRSP dams. Functional response to carbachol (A) and sodium nitroprusside (B) determined endothelium dependent and independent vasodilation as a percentage of constriction to $10^{-5}$M noradrenaline. (C) The contractile response determined by a dose response to noradrenaline. Data analysed by comparing the area under the curve and $EC_{50}$ values for each curve using a repeated measure one-way ANOVA with Sidak post-hoc test. (D) The maximal response to KPSS; analysed using repeated measure one-way ANOVA with Sidak post-hoc test; *p<0.05; n=4-5

#### 4.4.2.6 Late Pregnancy (GD18.5) Plasma Impact on SHRSP Uterine Artery Function

Non-pregnant SHRSP uterine arteries incubated with NP and GD18.5 plasma demonstrated no significant functional changes in vasodilation (Figure 4-11A-B) or constriction (Figure 4-11C-D) responses.

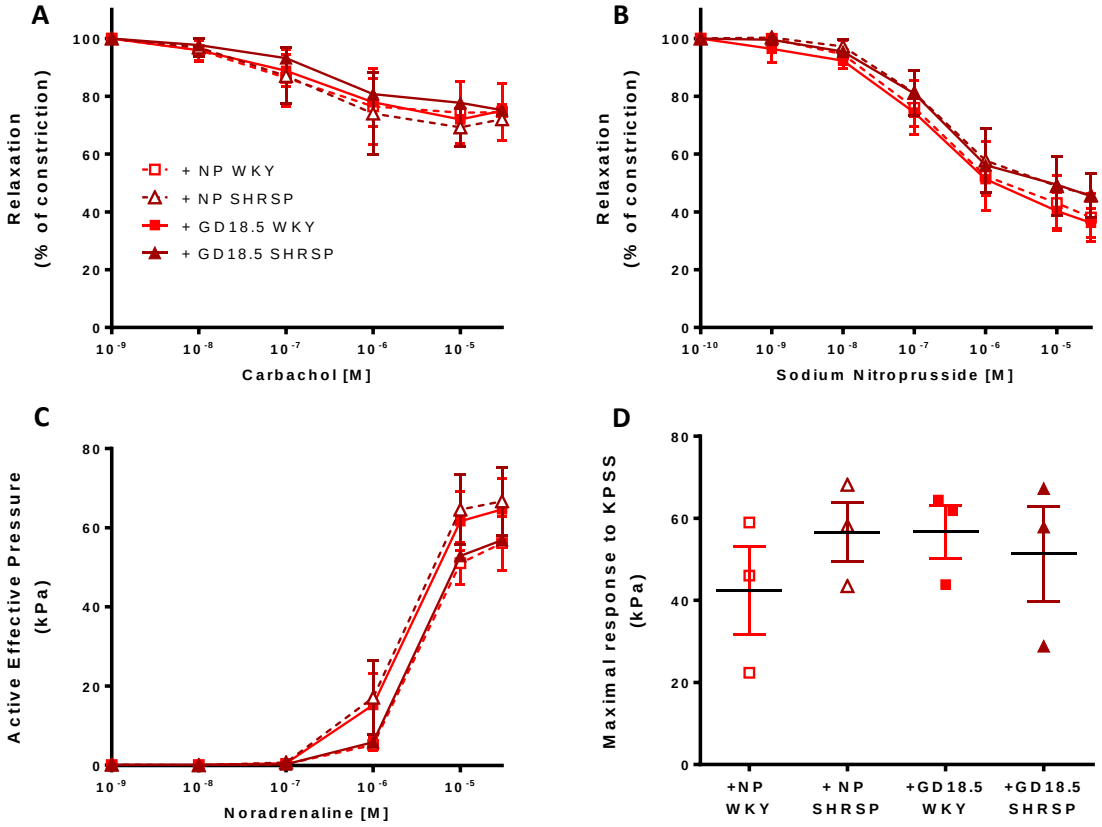


**Figure 4-11: Functional responses of SHRSP uterine arteries incubated with GD18.5 plasma** Non-pregnant SHRSP uterine arteries were incubated with non-pregnant (NP) and GD18.5 pregnant plasma from WKY and SHRSP dams. Functional response to carbachol (A) and sodium nitroprusside (B) determined endothelium dependent and independent vasodilation as a percentage of constriction to $10^{-5}$M noradrenaline. (C) The contractile response determined by a dose response to noradrenaline. Data analysed by comparing the area under the curve and $EC_{50}$ values for each curve using a repeated measure one-way ANOVA with Sidak post-hoc test. (D) The maximal response to KPSS; analysed using repeated measure one-way ANOVA with Sidak post-hoc test; *p<0.05; n=3.

### 4.4.3 Uterine Artery Vascular Smooth Muscle Cell Migration

Vascular smooth muscle cells (VSMC) were isolated from uterine arteries at non-pregnant and GD6.5 time points. VSMC migration rates were estimated using a wound closure assay (Figure 4-12A). No significant differences in migration capability were found in VSMCs exposed to 0.5% FBS (Figure 4-12B). GD6.5 VSMCs stimulated with 10% FBS showed significantly more migration compared to their 0.5% FBS control for both WKY and SHRSP (WKY: 44.6±11.5 versus 17.2±5.3; $p<0.05$, SHRSP: 58.7±14.1 versus 24.1±3.1; $p<0.05$) (Figure 4-12B). GD6.5 SHRSP VSMCs exposed to 10% FBS also demonstrated an increased migration compared to NP SHRSP cells (58.7±14.1 versus 19.7±3.9; $p<0.05$) (Figure 4-12B). FBS-dependent migration was not significantly different between strain at any time point (Figure 4-12C).

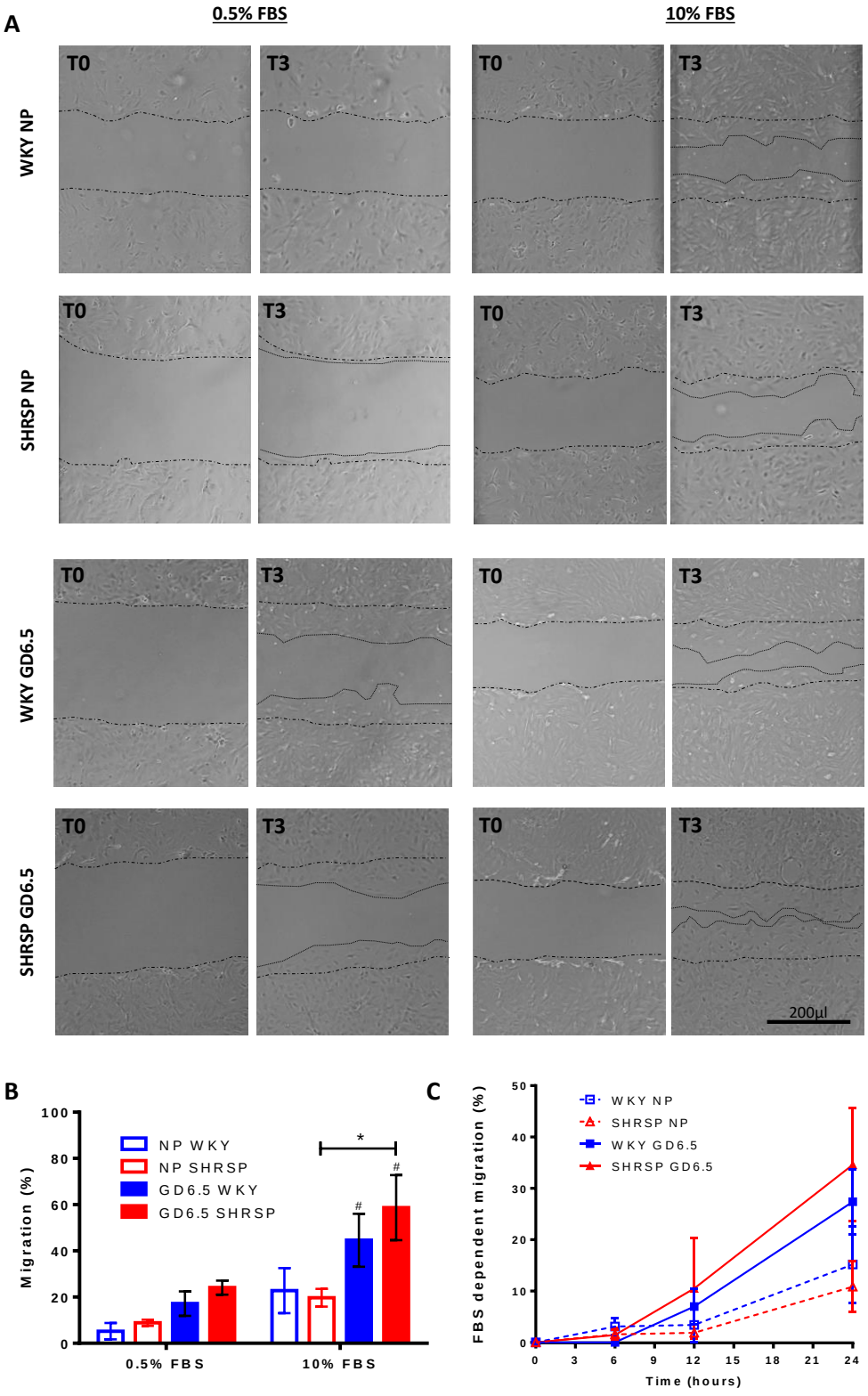


**Figure 4-12: Migration of uterine artery vascular smooth muscle cells from WKY and SHRSP** VSMCs were isolated from uterine arteries from non-pregnant (NP) and GD6.5 pregnant WKY and SHRSP dams. Migration was measured over 24 hours in the presence (10%) and absence of FBS (0.5%) after 48 hour serum starvation. (A) Representative images of NP and GD6.5 WKY and SHRSP uterine artery VSMC wound closure at 0 hours (T0) and after 24 hours (T3) in 0.5% and 10% FBS. Original scratch outlined at T0 and superimposed on T3, with dotted lines highlighting the migration of cells into the wound. (B) Migration at 24 hours was measured and expressed as a percentage; statistically analysed using repeated-measure two-way ANOVA with Sidak post-hoc test; *p<0.05 versus NP; #p<0.05 versus 0.5% FBS. (C) The change in migration between 0.5% FBS and 10% FBS (FBS dependent) over the three time points (6 hour, 12 hour and 24 hour); rate of change analysed using linear regression compared using repeated measures two-way ANOVA with Sidak post-hoc test. Data expressed as mean ±SEM; n=3.

## 4.5 Discussion

This chapter provides evidence that the systemic mesenteric resistance arteries of WKY rats become more responsive to vasorelaxation as pregnancy progresses and that SHRSP vessels have a functional impairment in this regard. The increased relaxation response in WKY rats is in parallel with the observations of GD18.5 uterine arteries from these strains (Small et al., 2016). The SHRSP mesenteric arteries demonstrated significantly reduced wall thickness and smaller cross-sectional area in response to pregnancy. Whilst WKY mesenteric arteries were found to have a significantly reduced cross-sectional area, with only minimal change to the wall thickness. These GD18.5 WKY arteries also exhibited a larger diameter compared to SHRSP. GD18.5 arteries in both strains demonstrated higher wall strain than their non-pregnant counterparts, indicative of an increased ability to stretch in response to the greatest strain. These findings suggest that pregnancy influences WKY and SHRSP mesenteric artery mechanical properties in a similar manner. Artery diameter changes are crucial in increasing or decreasing vascular resistance (Touyz, 2014). Pre-eclamptic women have an increased systemic vascular resistance compared to normotensive pregnancies (Bosio et al., 1999, Stott et al., 2017). This may be an artefact of hypertensive women retaining their pre-pregnancy vascular function. The significantly reduced wall thickness of the mesenteric artery observed in pregnant SHRSP dams suggests a hypotrophic remodelling. Previous studies have found that resistance arteries in male spontaneously hypertensive rat models typically demonstrate eutrophic remodelling in response to hypertension, resulting in reduced lumen diameter in the absence of wall thickness changes (Arribas et al., 1997, Intengan et al., 1999). This was observed in the non-pregnant SHRSP compared to non-pregnant WKY in this chapter, suggesting hypertensive remodelling is the same in females as in males. However, it is unclear why pregnancy in the SHRSP appears to reduce wall thickness and medial cross-sectional area of the mesenteric arteries. Whilst hypertension is generally associated with a narrowing of resistance vessels and increased peripheral vascular resistance, the opposite is the case for healthy pregnancy (Touyz, 2014, Mandala and Osol, 2012). Neither of these conditions are usually associated with the outward hypotrophic remodelling observed in SHRSP. This remodelling type has been observed in arteries from SHR rats where hypertension has been

ameliorated with the use of calcium channel blocker Felodipine (Ledingham and Laverty, 2001). The findings from this chapter reveal that mesenteric arteries from WKY dams undergo a pregnancy-dependent increase in responsiveness to vasodilation, thus providing a mechanism for the reduced vascular resistance associated with pregnancy. This functional response was not observed in SHRSP mesenteric arteries. Whilst both WKY and SHRSP demonstrated some narrowing of the mesenteric artery, it was more pronounced in the SHRSP. This may suggest that the significant reduction in wall thickness in mesenteric arteries from SHRSP could be an attempt by the vessels to reduce vascular resistance in order to accommodate the increased blood flow during gestation. A more in-depth investigation of the mesenteric structural and mechanical properties would need to be conducted in order to fully answer this.

Pregnancy-dependent systemic vascular structural and functional changes have not been fully evaluated in humans, due to tissue inaccessibility and the associated risks. One study is utilising mathematical modelling of the cardiovascular adaptations to pregnancy and can be manipulated to highlight changes in hypertensive disorders (Corsini et al., 2017). However, this still requires reference and for this reason, appropriate animal models are invaluable. Investigating total peripheral vascular resistance *in vivo* was not conducted in SHRSP or WKY pregnancy and would be a beneficial addition to this study.

Alongside the assessment of mesenteric artery changes over pregnancy, the uterine arteries were investigated early in gestation, specifically before any major placental influenced remodelling. Previously GD18.5 uterine arteries from normotensive WKY have been found to respond to pregnancy by becoming less constrictive with more pronounced vasodilatory responses. However this has not been observed in the SHRSP (Small et al., 2016). Early gestational changes of the rat uterine artery investigated in this chapter are more likely to be controlled by hormonal influences as the placenta is not fully established until GD12-15, with trophoblast invasion peaking around GD18.5 (Caluwaerts et al., 2005, Soares et al., 2012). Early pregnancy (GD6.5) uterine arteries demonstrated no significant differences in the functional response to vasodilation or vasoconstriction when compared to non-pregnant uterine arteries in either SHRSP or WKY.

Trends towards hypertrophic remodelling were observed in WKY GD6.5 uterine artery structure, with a trend towards an increased wall thickness and reduced internal diameter. This is contradictory to the changes observed at GD18.5 (Small et al., 2016). Previous studies in rats have found the lumen diameter has a 60% increase by late pregnancy compared to non-pregnant (Osol and Mandala, 2009, Osol and Cipolla, 1993, Small et al., 2016). The early wall thickness changes observed in this study may be associated with VSMC axial hypertrophy or hyperplasia (Osol and Mandala, 2009, Cipolla and Osol, 1994). Uterine vascular remodelling occurs throughout the menstrual cycle, as well as during pregnancy, suggesting some degree of hormonal control (Brosens et al., 2009). Progesterone and oestrogen, the classical reproductive hormones, have the ability to alter vascular function and influence angiogenesis (Chandran et al., 2016, Orshal and Khalil, 2004). Oestrogen peaks prior to ovulation during the menstrual cycle of non-pregnant women (Orshal and Khalil, 2004). It has been found to exert non-genomic changes to vascular smooth muscle to encourage vasodilation (Orshal and Khalil, 2004). During pregnancy progesterone is produced first by the corpus luteum and then production is taken over by the established placenta (Davis and Rueda, 2002). Progesterone has a different role to oestrogen in regards to vascular function. It has been found to inhibit VSMCs contractility and impact cellular proliferation, which could lead to the initiation of vascular remodelling in the uterine arteries (Barbagallo et al., 2001, Tal et al., 2000, Lee et al., 1997). Yet, as these two hormones are not the only endocrine factors influencing this gestational stage, further assessment of hormonal changes in the first week of SHRSP and WKY gestation would need to be conducted. It would be interesting to investigate the remodelling and mechanical wall properties in pseudopregnancy in SHRSP and WKY, as this could delineate maternal control of vascular remodelling in the absence of any fetal and placental influences.

Non-pregnant uterine arteries where incubated with maternal plasma to examine whether circulating factors from pregnancy could directly influence vascular function *ex vivo*. Non-pregnant WKY arteries exposed to WKY GD6.5 plasma had a significantly lower contractile response to high-potassium depolarization than their non-pregnant plasma counterpart. The plasma components involved in the regulation of vascular smooth muscle contractility also have the ability to influence other vasodilatory and contractile components

of the systemic circulation, such as circulating hormones and endothelium derived vasodilatory substances (Jackson, 2000). As already stated, early pregnancy is associated with multiple alterations in hormone production compared to the non-pregnant state, which could alter the ability of VSMC to constrict on depolarisation (Tal et al., 2000). However, due to the variability in maximum contractile response and complex interplay of different local and systemic factors, this would require a more thorough mechanistic evaluation to determine any physiological relevance. Neither GD6.5 nor GD18.5 plasma had any significant impact on the endothelium dependent (carbachol- acetylcholine mimic) or independent (SNP- nitric oxide (NO) donor) vasodilatory responses of the non-pregnant uterine arteries from either strain. NO has a crucial yet contradictory relationship in mediating vascular changes in pregnancy and hypertensive pregnancies (outlined in review by Saldek *et al* (Sladek et al., 1997)). NO biosynthesis increases in the circulatory system during normotensive pregnancy to maintain a reduced vascular resistance in the gravid state (Xu et al., 1996, Conrad et al., 1993). Many studies have shown an inhibition or lack of nitric oxide synthase enzymes produce symptoms of gestational hypertensive disorders, highlighting its essential role in maintaining appropriate vascular tone during healthy pregnancy (Kulandavelu et al., 2006, van der Heijden et al., 2005a, Kulandavelu et al., 2013, Molnár et al., 1994, Baylis et al., 1992, Barron et al., 2010). Interestingly no significant changes were observed in any vasodilatory or vasoconstrictive functions in WKY and SHRSP non-pregnant arteries incubated with GD18.5 plasma from either strain. The non-pregnant SHRSP arteries had no functional responses to pregnant plasma at any gestational stage; which could be interpreted as SHRSP maternal plasma lacking factors that propagate a pre-eclamptic like phenotype (Goulopoulou, 2017). However, as these incubation studies were performed on non-pregnant UA which are already less responsive than during pregnancy, it may not be possible to discern these defects. Further limitations of this study, was that plasma concentration was diluted in physiological saline to 3%. This was chosen due to previous studies examining the effect of high and low density lipoproteins on WKY and SHRSP vessel function, however for the purpose of examining all circulatory factors in this study that concentration may have been too low and should have been raised to a more physiological level. Furthermore, it may have been wiser to perfuse these artery explants rather than incubate with plasma

factors, to ensure a more physiological environment with the plasma in contact with the inside endothelium lining of the arteries.

Pregnancy-dependent vascular remodelling has been associated with a change in VSMCs from quiescent to more migratory and proliferative (Cipolla and Osol, 1994). Moreover, the major circumferential remodelling changes of the uterine artery during pregnancy have been attributed to changes in VSMC mass and length (Cipolla and Osol, 1994, Mandala and Osol, 2012). In the present study, both WKY and SHRSP demonstrated increased migration in VSMCs isolated from pregnant uterine arteries, with early pregnant SHRSP VSMCs demonstrating significantly more migration than non-pregnant. In both WKY and SHRSP, the migration of GD6.5 uterine artery VSMCs was significantly increased upon FBS-stimulation compared to the same VSMCs in the absence of 0.5% FBS, this was not observed in the VCMCs from non-pregnant uterine arteries. This is suggestive that the VSMC of GD6.5 uterine arteries have a more migratory/proliferative phenotype than those from a non-pregnant state. These altered cellular properties of the uterine arteries in WKY and SHRSP dams suggest that these vessels are preparing for remodelling events, even at early gestational stages. However, as the proliferation of these cells was not directly evaluated in this study, a more thorough investigation into the characteristics of VSMCs from uterine arteries at early and late pregnancy time points would be beneficial. Similarly, to give a more all-encompassing evaluation of the cellular composition of these arteries other cell types could be isolated. For example the functional responses observed in GD18.5 arteries are endothelium dependent (Small et al., 2016). Thus, relaxation responses could be influenced by endothelial cell derived factors which could be investigated *in vitro* using primary uterine artery endothelial cells.

The main limitation that must be considered for the studies presented in this chapter is the small sample size used (often n=3) which will greatly impact any statistically significant interpretations. In particular, the measurements of vascular function and passive mechanical properties were measured using myography which has the possibility to introduce large variation to a study, which could have been overcome with a greater number of biological replicates. However, this chapter has provided evidence that remodelling occurs in the

systemic vasculature during pregnancy, and that SHRSP dams have impaired systemic vascular responses. This may impact the re-direction of blood flow to the uteroplacental unit that is required for a favourable pregnancy outcome. Also revealed in this chapter, was that during early gestation uterine arteries from WKY and SHRSP dams demonstrate no functional or structural differences. This is in contrast to the changes observed in WKY late pregnancy where uterine arteries show remodelling associated with increased responsiveness to vasodilators and reduced sensitivity to contractile agents, whereas the SHRSP uterine arteries show similarity between early and late pregnancy, both lacking functional or structural changes (Small et al., 2016). This highlights the need to further investigate the underlying molecular factors which contribute to the eventual failure to remodel in the uterine arteries of SHRSP dams. Molecular investigations into the transcriptome profile of the uterine arteries was conducted by RNA-Seq analysis, the results of which are described in Chapter 5.

# Chapter 5 Transcriptome profiling of early pregnancy uterine arteries

## 5.1 Introduction

Transcriptome profiling of maternal, placental and fetal tissues during pregnancy can provide dynamic information on the uterine environment. Advancement in high throughput sequencing technologies, such as microarrays and RNA sequencing (RNA-Seq), can reveal details about the changes to the transcriptome of specific tissues at different time points and in various pregnancy pathophysiologies (Wang et al., 2009). Transcriptomic studies have already revealed a vast number of genes to be implicated in the development of pregnancy complications such as pre-eclampsia, fetal growth restriction and gestational diabetes (Enquobahrie et al., 2008, Kaartokallio et al., 2015). These genes have been found to be involved in crucial biological pathways that play key roles in pregnancy development, such as inflammation, oxidative stress and the maternal immune regulation (Walker et al., 2015, Burton and Jauniaux, 2011, Brewer et al., 2013). Pregnancy is a relatively short physiological change, occurring over a 40 week period in humans, which requires rapid and dynamic changes in gene expression and RNA processing (Robertson et al., 1975). Any deviations from the norm will have profound impact on maternal adaptations, placental function and fetal outcome. Due to this, a genomic approach is too static. Studying changes at the transcript level is more appropriate as it reveals a snapshot of the genes being actively transcribed at different time points (Kim et al., 2012).

Only 596 studies have studied transcriptomic changes in pregnancy using microarray or RNA sequencing (RNA-Seq) technologies; based on ArrayExpress search conducted April 2018 (Filtered for 'RNA Assay' experiment type; search terms: *("pregnancy"[MeSH Terms] OR "pregnancy"[All Fields]) OR ("gravidity"[MeSH Terms] OR "gravidity"[All Fields] OR "pregnant"[All Fields])*. Most of these studies employed microarray technologies (536), with only 60 utilising RNA-Seq. Many studies have focused on changes in placental tissue or cells (Enquobahrie et al., 2008, Kaartokallio et al., 2015, Sood et al., 2006, Kim et al., 2012, Shankar et al., 2012). Whilst this can give an indication of any dysregulation of gene expression in pregnancy complications, it doesn't inform on maternal gene responses to pregnancy or lack thereof. Only 20 of the 60 RNA-Seq specific studies focused on the maternal gene expression during pregnancy. With the focus of these studies examining trophoblast interactions with decidual

cells or with human aortic vascular smooth muscle cells *in vitro* (Bird et al., 1998, Cale et al., 1997, Fukushima et al., 2008, Gifford et al., 2003, Gong et al., 2014, Harris et al., 2010, Hess et al., 2007, Houser et al., 2011, Jokhi et al., 1994, Nelson et al., 2016, Wallace et al., 2013, Wang et al., 2012, Weston et al., 2002, Weston et al., 2003). Some have examined the total transcriptome profile of complete myometrial/decidual tissue biopsies, giving some indication of maternal changes (Autio-Harmainen et al., 1992, Chen et al., 2000, Gibb and Sun, 1996, Herse et al., 2012, Kitaya et al., 2007, Peng et al., 2015, Penna et al., 2010, Rider et al., 2000, Wu et al., 2000, Founds et al., 2013, Lian et al., 2010). However, no studies have specifically investigated the gene expression profile of isolated whole vessels in the maternal uterine vasculature during pregnancy.

During pregnancy, the maternal uteroplacental vasculature undergoes essential remodelling (Pijnenborg et al., 2006). This adaptation relies on mechanisms that are not fully understood and even less is known about the gene expression changes required for successful remodelling. RNA-Seq has major advantages over other gene expression assays as it can fully examine the RNA profile including non-coding RNA (for example miRNA, lncRNA and snRNA) from relatively small amounts of starting material, it is not limited to a specified catalogue of RNA (therefore avoids biases of examining only expected changes) and has a much more dynamic range of quantifying gene expression (from detecting small fold changes up to >8000 fold changes) (Wang et al., 2009). This approach can reveal key transcriptional regulations that the underlying molecular development of both physiological and pathophysiological processes.

Impaired uteroplacental remodelling and the associated reduced uteroplacental haemodynamics have a well-established influence on the development of pre-eclampsia and fetal growth restriction in humans (Brosens et al., 1972, Robertson et al., 1975). Impaired trophoblast invasion has been suggested to be the main contributor to impaired vascular remodelling (Geusens et al., 2010, Lyall et al., 2013), however little is understood about the maternal vasculatures response to these cells, and even less is known about how the maternal uteroplacental circulation is regulated prior to the invasion of trophoblasts (Jauniaux et al., 2000). The lack of investigation into maternal uterine artery

gene expression profiles during pregnancy could be due to the inaccessibility of maternal tissue during pregnancy. Many samples are collected at delivery, yet at this time point is too late to observe active remodelling changes (Robson et al., 2002, Lash et al., 2016). Maternal tissue can also be obtained from early pregnancy terminations however these samples are difficult to obtain due to ethical considerations and the sample size is often very small (Robson et al., 2012, Pitman et al., 2013). It is for these reasons that animal models must be utilised in the study of early vascular remodelling in pregnancy.

The genome of both the SHRSP and WKY strains, bred in-house at the University of Glasgow, have been sequenced and therefore RNA-Seq references for alignment are available. The SHRSP rat has a deficiency in uterine artery remodelling, demonstrated by an impaired uteroplacental blood flow at GD18.5 (Barrientos et al., 2017, Small et al., 2016). To examine the maternal vascular response to pregnancy, vessels must be examined prior to any fetal influence from the trophoblast invasion. Implantation in the rat occurs between gestational day (GD) 5.5 and 6.5, with trophoblast invasion beginning at mid-gestation (between GD14.5 and GD15.5), reaching a peak at approximately GD18.5 (Vercruysse et al., 2006, Phillips and Poyser, 1981, Ain et al., 2003). The SHRSP did not show any structural or functional alterations by GD6.5 of pregnancy (Chapter 4) and produced similar numbers of offspring (of similar weight) as the WKY rats (Chapter 3), yet SHRSP has previously demonstrated an impaired uteroplacental blood flow at GD18.5 (Small et al., 2016). Therefore, it is of paramount importance to uncover any pregnancy dependent transcriptomic alterations to ascertain physiological responses; as well as investigating the maternal vascular responses to pregnancy in a model of chronic hypertension.

## 5.2 Hypothesis and Aims

### 5.2.1 Hypothesis

Differences in the transcriptome of SHRSP and WKY rats are responsible for altered uterine artery gene expression in the SHRSP which affects its ability to remodel in response to pregnancy.

### 5.2.2 Aims

- To determine early (GD6.5) pregnancy dependent expression changes of protein-coding genes at the transcript level of uterine arteries from SHRSP and WKY.

- Predict the influences any gene changes have on vessel function between non-pregnant and pregnant uterine arteries.

- Validate differentially expressed genes in key pathways.

- Identify lncRNA expression changes in the uterine artery between strains and across early pregnancy.

## 5.3 Materials and Methods

Uterine arteries from virgin 13-week-old and GD6.5 pregnant age-matched WKY and SHRSP were dissected as in the general materials and methods (section 2.4.3). These arteries were stored at -80°C until tissue was homogenised and RNA was extracted and the quality checked using the Agilent Bioanalyzer as described in the general materials and methods (section 2.2.1).

### 5.3.1 RNA Sequencing

RNA sequencing (RNA-Seq) was conducted by Glasgow Polyomics. A minimum of 400ng total RNA was processed using the Illumina TruSeq Stranded Total RNA with Ribo-Zero Gold kit, following the manufacturer's guidelines. The gene and transcript expression profiling were conducted using the NextSeq500® Illumina sequencing system, with paired-end sequencing at a depth of 50 million reads per sample. Adapter and quality trimming of the reads was preformed using CutAdapt and Sickle software packages. FastQC was used to ensure sequence quality was suitable throughout processing. Reads were then mapped using the Ensembl Rnor_6 reference genome and tested for differential expression using DESeq2 software package (Bioconductor 3.6). Base mean of gene and transcript expressions across all groups were determined. Comparisons were made between the strains and pregnant state for transcript level analysis, illustrated in Figure 5-1and Figure 5-2.

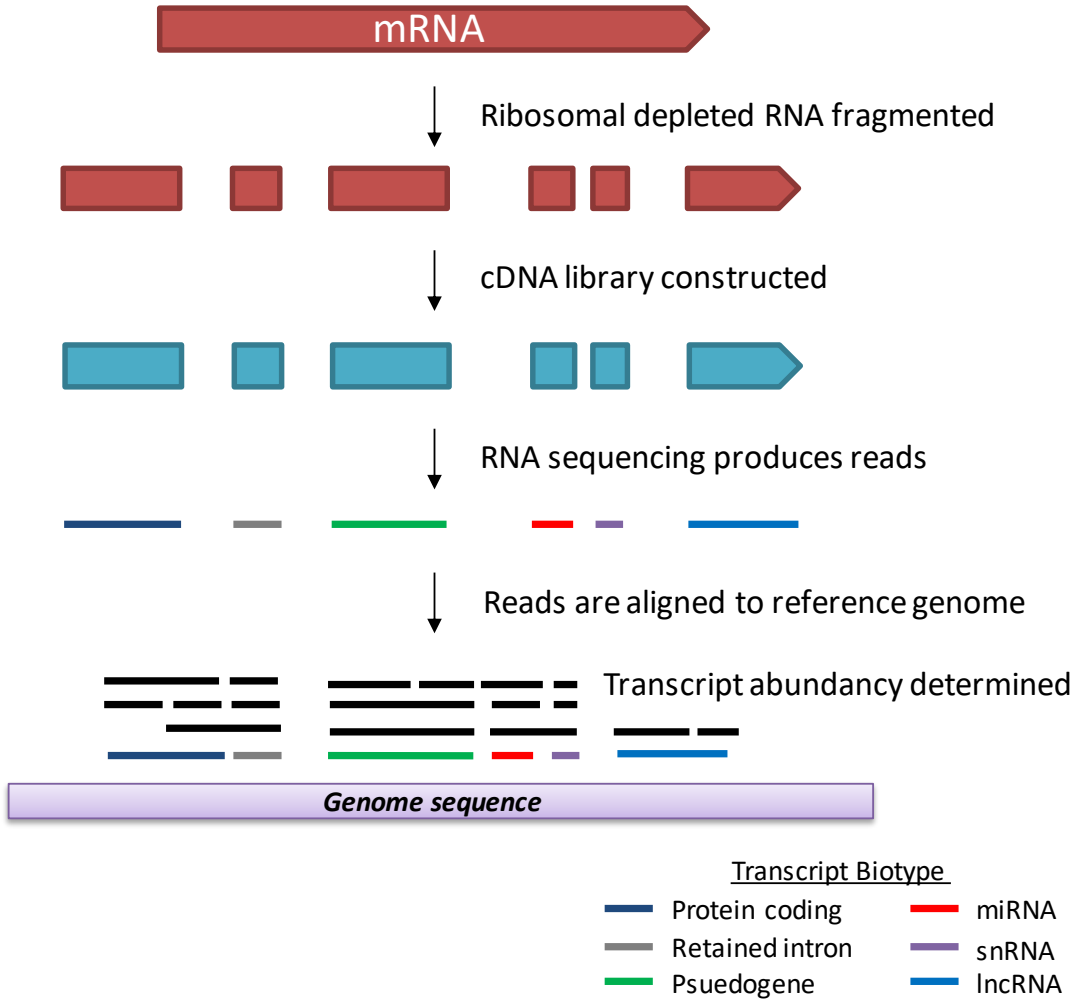


**Figure 5-1: Schematic illustration of the RNA sequencing process**
Total RNA is extracted from tissue and undergoes ribosomal depletion and the preparation of a cDNA library using paired end sequencing. The library is then sequenced and mapping programs are used to align the reads with a reference genome. This can determine transcript biotype and chromosomal location. The reads are then quantified to give the number of fragments per kilobase of transcript per million mapped reads (FPKM). These values can determine fold change when compared between two samples. miRNA = microRNA, snRNA = small nuclear RNA, lncRNA = long non-coding RNA.

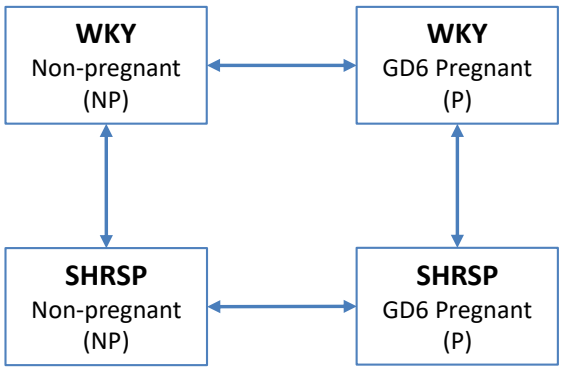


**Figure 5-2: Multiple comparison groups for DESeq2 analysis of reads**
RNA samples from uterine arteries were compared between strain both at the non-pregnant (NP) and gestational day (GD)6.5 pregnant (P) stage, as well as between NP and P for WKY and SHRSP. Arrows indicate comparisons, n=3 for each group.

### 5.3.2 Data Handling and Analysis

Lists of differentially expressed transcripts were examined by biotype and the false discovery rate (which determines the significance of expression changes) was restricted to (padj)<0.05. This revealed less than 1000 changes so no further restrictions were applied for analysis. Differential transcript expression was examined using a comparison between WKY NPvsP and SHRSP NPvsP and a comparison between NP WKYvsSHRSP and P WKYvsSHRSP (Figure 5-2). This examined the different number of significantly differentially expressed transcripts between the comparison groups and those that overlapped. Expression increased or decreased relative to the second group; for example, if comparison was A vs B expression differences are expressed relative to B, i.e. a negative fold change would be a decrease in A relative to B.

Heatmaps were created for quality control assessment of the expression datasets. The 50 most significant differentially expressed genes in each comparison group were chosen, giving a total of 148 genes due to some overlap between groups. The individual intensities for each uterine artery sample of these genes were then entered into Heatmapper web software, and a heatmap created (Babicki et al., 2016). Centroid linkage hierarchical clustering was performed for the transcripts and samples to assess the similarity between different samples of the same group. Similar expression intensities are expected between uterine arteries from the same pregnancy/strain group as these should have similar RNA profiles. Any differences would suggest variation in sample preparation.

Ingenuity® Pathway Analysis (IPA: Qiagen) was used to functionally correlate transcript expression profiles and produce biological relevance pathway changes to protein coding gene expression. The differentially expressed transcripts were filtered with padj<0.05 and to confirm quantifiable expression the fragments per kilobase of transcript per million mapped reads (FPKM) criteria was >1.0. An expression analysis was conducted for each dataset to highlight key disease and function pathway involvement. This was further investigated using a core comparison analysis of the datasets to identify differences in canonical pathways and assign activation z-scores for each comparison group. The z-score is a predictor of activation state of transcriptional regulators, inferred from

observed gene expression. Its numerical value is determined as a statistical measure of the similarity/differences between expected relationships (from literature) and the observed gene expression (input from RNA-Seq study). A negative z-score suggests inhibition of that pathway or function, whereas a positive value suggests activation.

### 5.3.3 Validation of key genes using Taqman q-RT PCR

Taqman® q-RT PCR was performed as previously described in the general materials and methods (section 2.2.3.2) using the primers illustrated in Table 2-2.

### 5.3.4 Investigations of detected lncRNA

All significantly differentially expressed lncRNAs were identified using Ensembl. This also provided location information for each lncRNA. There is evidence to suggest that lncRNAs can influence expression of adjacent genes, therefore the proximity of these RNAs to protein coding genes was assessed (Wang and Chang, 2011). The number of protein coding genes that were within 5 million base pairs of the lncRNA was noted (Ballantyne et al., 2016), with any that were also found to be significantly differentially expressed examined in more detail, with location and forward/reverse strand direction recorded.

One lncRNA from each comparison group was chosen for further validation, along with others of interest signified by their proximity to differentially expressed protein coding genes, in total 6 lncRNA were further examined. Standard PCR was used to amplify the transcripts from cDNA, produced from RT-PCR described in the general materials and methods (section 2.2.2). Primers were designed to span exon-exon boundaries where possible (Table 5-1). PCR was conducted in a 96-well plate where the final concentrations per well were: 1x ThermoPol® reaction buffer (New England Biolabs, Hitchen, UK), 0.5mM of each dNTP, 0.5mM of forward primer, 0.5mM of reverse primer and 0.625 U/µl Taq polymerase. A total volume of 20µl in each well was achieved using RNase free sterile water. 1µl of cDNA template (prepared as in general materials and methods section 2.2.2) was added. The PCR was run on a 96-well Dyad DiscipleTM thermal cycler (MJ Research, Massachusetts, USA) with the following temperature cycles: an initial denaturation step of 94°C for 5 minutes then a cycle of denaturing at

94°C for 30 seconds, annealing at 58°C for 30 seconds and extension at 68°C for 1.5 minutes; for 35 cycles, with a final elongation step of 5 minutes at 68°C. Loading buffer (New England Biolabs, Hitchen, UK) was added to the PCR product (1:6 dilution) and the products were run on a 1.5% agarose gel containing 0.66% ethidium bromide. A 100bp DNA ladder (Promega, Southampton, UK) was run alongside the samples. Gels were run for 40 minutes at 90V and imaged on Gel Doc™ XR+ System and presence/absence of bands of correct size were noted. The expression of any lncRNA that produced positive bands of the correct fragment size was examined using SYBR Green qRT-PCR, as described in general materials and methods section 2.2.3.1, using the primers in Table 5-1.

**Table 5-1: Primer sequences for six differentially expressed lncRNA**

| lncRNA | Forward Primer 3' -> 5' | Reverse Primer 3' -> 5' | Fragment size |
|---|---|---|---|
| AABR07051787.1 | TGTCTATGAGCTGCCGGTC | GGATCTCAAGCACTTGCTTG | 222bp |
| AABR07069473.1 | CGAAGGCGGCTTGGATTTAG | ATGTCTTGCTCTGGAGGAGC | 370bp |
| AABR07055801.1 | CGGCTGTGAAGCTAGCAGT | TCTCCCTGGGTAAGTCCTG | 106bp |
| AABR07069816.1 | ATCCTCTGTGATGTCACCAG | TGTTGATTACCACAGGGCCA | 255bp |
| AABR07008309.1 | CTGGAAGAAGCAGAGAGTAG | AAGATGTCCCTTCTGAACGG | 140bp |
| Rn50_X_0663.2* | AATGCCGTGGACTGCACAATG | ATGTGCTCCGAAGGTCAGACA | 197bp |

* lncRNA Rn50_X_0663.2 had only one exon, so primers do not span exon-exon boundary.

## 5.3.5 Intracellular Calcium Release in Uterine Artery VSMCs

Vascular smooth muscle cells (VSMC) were isolated and cultured as described in general materials and methods section 2.6. Cells were used between passage 4 and 6 and were not used later than this due to a change in growth. After reaching confluency in a T75 flask the cells were removed from the flask and counted as previously described (section 2.6.3). Cells were seeded onto a 12 well plate at a density of $1x10^6$ cells per well in complete DMEM media. Each cell type was seeded into 3 wells to provide technical replicates. The cells were then allowed to reach 80% confluency (between 28 and 72 hours). Cells were then starved of serum, by replacing complete media with DMEM containing 0.5% FBS for 72 hours) to ensure the cells all began at the same growth cycle stage and that there was no FBS in the media during the experiment as this can alter the calcium release observed.

The calcium release was measured using the fluorescent calcium indicator, Cal-520® AM (ab171868, Abcam, Cambridge, UK). This calcium sensitive dye works by being pre-loaded into cells and its lipophilic blocking groups are cleaved once inside the cell, causing it to remain intracellularly. When calcium is release the Cal-520 fluorescence greatly increases and produces detectable signals that can be recorded. Cells were briefly rinsed with 0.5% (v/v) FBS DMEM medium containing HEPES [100IU/ml penicillin, 100µg/ml streptomycin, 2mM L-glutamine, 5.5mM D-glucose, 1mM sodium pyruvate, 25mM HEPES] (22320 Gibco, ThermoFisher Scientific, Paisley, UK) and 400µl of HEPES-DMEM media containing 2µM Cal-520 AM was added to the cells. The cells were protected from light to prevent bleaching and incubated at 37°C for 75 minutes. After incubation Cal-520/HEPES media was removed and cells were washed once with 1ml of $Ca^{2+}$ free HEPES solution [20mM HEPES, 130mM NaCl, 5mM KCl, 1mM $MgCl_2$, 10mM glucose, 0.1mM EDTA; pH7.4] and then 800µl of $Ca^{2+}$ free HEPES solution was added and the cells were incubated at room temperature for 30 minutes, protected from light.

Visualisation of the calcium release was conducted using live cell microscopy (Ziess Axio Observer Z1, Carl Zeiss Ltd, Cambridge, UK). The cells were placed on a heated mount at 37°C and a field of vision was found with focusing adjustments conducted using bright field microscopy settings. Once the cells were located the microscope was switched to detection of fluorescent wavelengths of Ex/Em 490/525nm. Baseline fluorescence was recorded for 2 minutes before 100µl 1mM angiotensin II was added to the first well and timed for 2 minutes. At the 4-minute mark 100µl 1mM ionomycin was added and the resulting fluorescent change recorded for 2 minutes. This process was repeated for all technical replicates and cell types.

The mean intensity for the field of vision was recorded every 1.2 seconds using Zen software. The average baseline value (between 0 and 2 minutes) was subtracted from all subsequent intensity measurements and this was used to construct a trace of intracellular $Ca^{2+}$ release caused by AngII and ionomycin. The difference between baseline and peak AngII stimulated and baseline and peak ionomycin stimulated $Ca^{2+}$ release was calculated.

## 5.4 Results

### 5.4.1 RNA Quality Control Prior to RNA Sequencing

Prior to conducting the RNA Sequencing the total RNA purity and integrity was assessed using an Agilent Bioanalyzer. The gel-like image produced by the Bioanalyzer shows distinct bands for 18S and 28S. This suggests the RNA is of an acceptable quality as degradation would have resulted in fragmentation, producing many more bands. An electropherogram profile of the RNA in each sample was also produced. An example is shown in Figure 5-3 that shows distinct peaks in fluorescence at approximately 2000 to 4000 nucleotides in size, which is indicative of 18S and 28S RNA respectively. The fluorescent peaks of these RNAs were used to determine the RNA integrity number for each sample, presented in Table 5-2. Eight of the 11 samples tested had a RIN higher than 7 and all were above the accepted RIN of 5, which is indicative of some degradation but is trivial when using ribosomal depletion library preparation for RNA sequencing. All samples demonstrated peaks between 50 and 200nts which suggests small RNA fragments have been retained during extraction, these could include miRNA however these would have been lost during library preparation for RNA sequencing as this RNA-Seq was not designed to include detection of these RNAs.

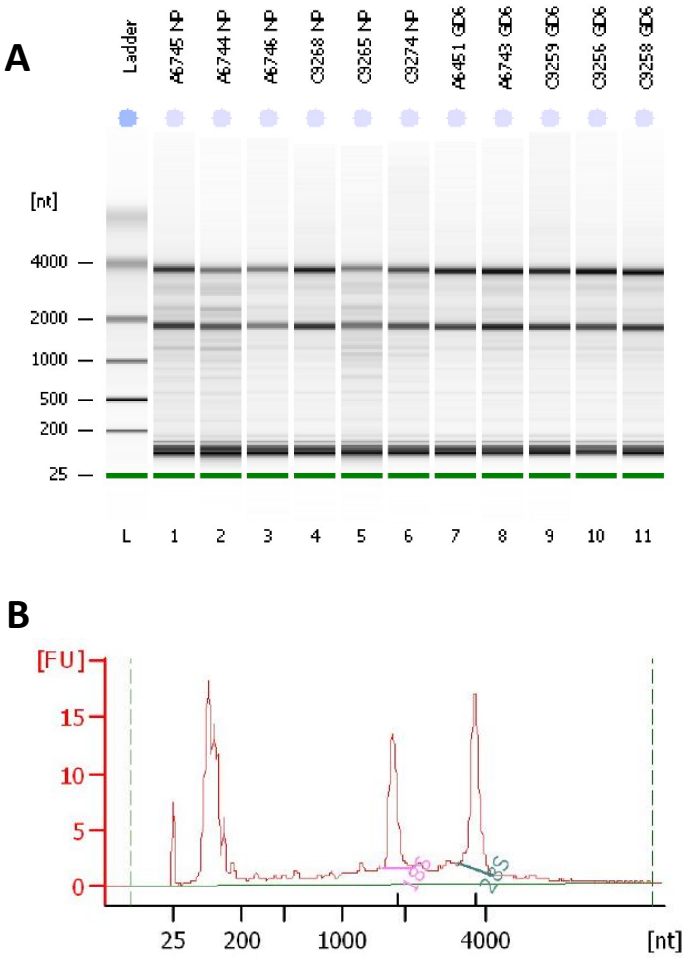


**Figure 5-3: Example of Agilent Bioanalyzer 2100 results.**
A RNA picochip assay of non-pregnant (NP) and GD6.5 pregnant WKY (A numbers) and SHRSP (C numbers) uterine arteries allowed assessment of RNA quality and integrity. (A) The analysis produced a gel-like image which highlights 28S at ~4000 nucleotides (nts) and 18S at ~2000nts, some degraded and small RNA is indicated by the band at ~100nts. (B) The electropherogram for sample A6743 GD6 shows that the 28S and 18S RNA have a distinct large fluorescent peak in the appropriate locations. Another peak apparent between 50-200nts is indicative of smaller RNA fragments (such as long non-coding) and is also evident of partial degradation. The peak at 25nt represents the DNA marker.

**Table 5-2: Agilent Bioanalyzer determined RNA Integrity Number (RIN) for each sample**

| | WKY | | | | | | SHRSP | | | | | |
|---|---|---|---|---|---|---|---|---|---|---|---|---|
| | Non-pregnant | | | Pregnant (GD6) | | | Non-pregnant | | | Pregnant (GD6) | | |
| *ID* | *A45* | *A44* | *A46* | *A51* | *A43* | *A50* | *C65* | *C74* | *C68* | *C56* | *C58* | *C59* |
| RIN | 6.8 | 5.8 | 6.5 | 7.9 | 7.7 | --- | 7.8 | 5.5 | 7.1 | 7.9 | 7.8 | 7.5 |

Sample A50 did not undergo Agilent Bioanalysis as the pico-chip RNA assay had a limit of 11 samples (plus one ladder control). Animal ID's are presented for reference; A = WKY and C = SHRSP.

### 5.4.2 RNA Quality Control Post-RNA Sequencing

A principal component analysis plot was constructed to visualise the variation between individual samples and groups in the experiment. All gene expression interpretations were made from these comparison groups (n=3). Figure 5-4 shows that the transcript reads for each sample are clearly segregated across pregnancy (PC1=30% variance) and across strain (PC2=18% variance). As the variation across pregnancy is the largest, this suggests that pregnancy has more of an impact on transcript expression in the uterine arteries than differences between strains.

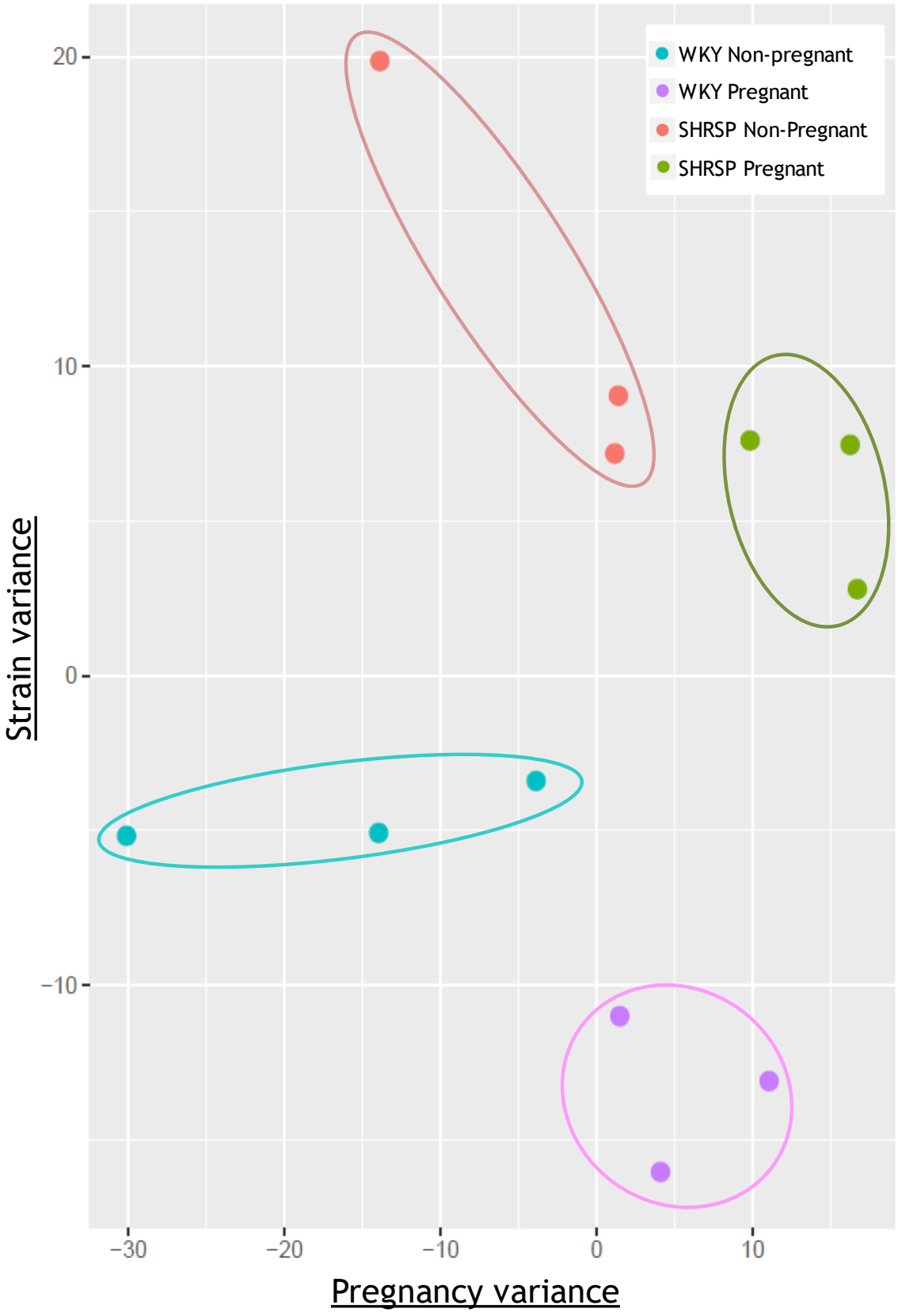


**Figure 5-4: Principal component analysis of each individual uterine artery transcript expression**
This plot shows that the transcript expressions of each sample cluster between strain and pregnancy. Principal component 1 was attributed to pregnancy and demonstrated the largest variance (30%). Principal component 2 was the strain variance between WKY and SHRSP, accounting for 18% variance.

### 5.4.3 Summary of Differentially Expressed Transcripts

Mean Average (MA) plots were constructed to show global distribution of expressed transcripts (Figure 5-5). It distributes each transcript based on the log-fold change (y-axis) and the normalised mean expression (x-axis). Each transcript is represented on the plot, with red dots indicating significantly differentially expressed transcripts that have a padj<0.05. The MA plots for each of the four comparison groups indicates that each have a sizeable portion of significant differentially expressed genes.

The number of significantly differentially expressed (DE) transcripts for each comparison group is stated in Table 5-3. This highlights the comparison of non-pregnant vs. pregnant vessels in WKY and SHRSP. There were found to be a greater number of DE transcripts in the SHRSP group compared to WKY, with the majority being upregulated in the pregnant uterine artery. Common DE transcripts were viewed by comparing the transcript ID's from the original WKY and SHRSP comparisons of non-pregnant vs pregnant using online software Venny (http://bioinfogp.cnb.csic.es/tools/venny) (Figure 5-6). This showed that there were 32 common upregulated transcripts and 115 common downregulated transcripts in response to pregnancy in both strains.

Table 5-3 also shows the number of DE transcripts between WKY and SHRSP uterine arteries in the non-pregnant and pregnant state, as well as a comparison of these two groups. This shows common DE transcripts which suggests the transcriptional expression of these transcripts are unaffected by pregnant state.

A heatmap was constructed using the individual means of the 50 most significant DE transcripts (padj<0.05) from each of the comparison groups (148 DE transcripts in total) to determine the reliability of the differential expression between samples (Figure 5-7). These transcripts were chosen to give a representation of transcriptional changes in each individual sample. Hierarchical clustering was applied, which grouped the individual samples according to pregnancy then according to strain. This suggests that there are robust transcriptional differences between non-pregnant and GD6.5 pregnant uterine artery and that these are of a reliable uniformity within each sample group.

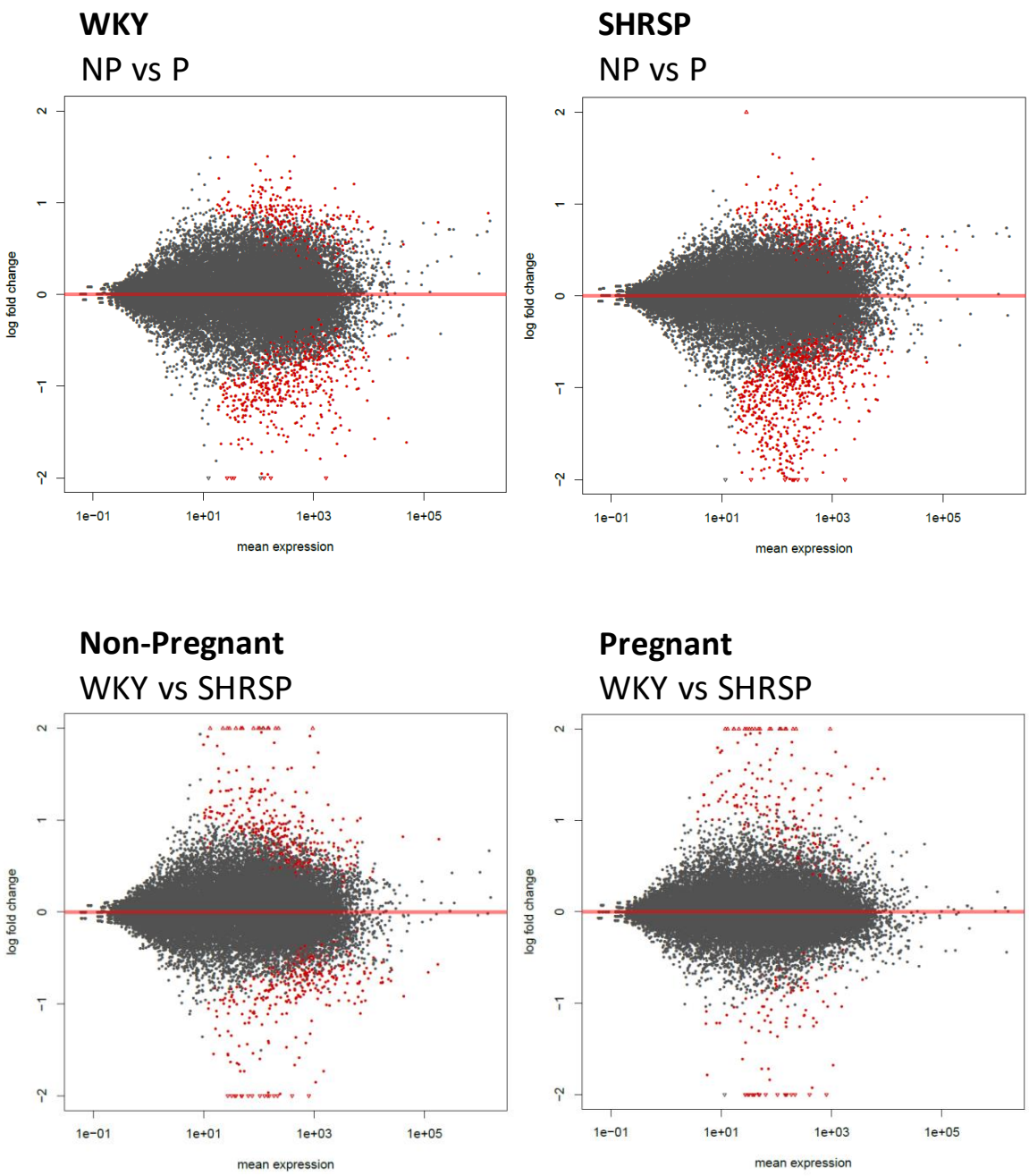


**Figure 5-5: Mean-Average (MA) plots for each comparison group.**
An MA plot was constructed for each comparison group in order to visualise the transcriptomic expression differences. Each transcript is represented by one dot and the plots illustrate the distribution of the fold change verses mean expression intensity. (A-B) Changes induced by pregnancy. (C-D) Changes induced by strain. Significant (<0.05 padj) differentially expressed genes are indicated by red dots.

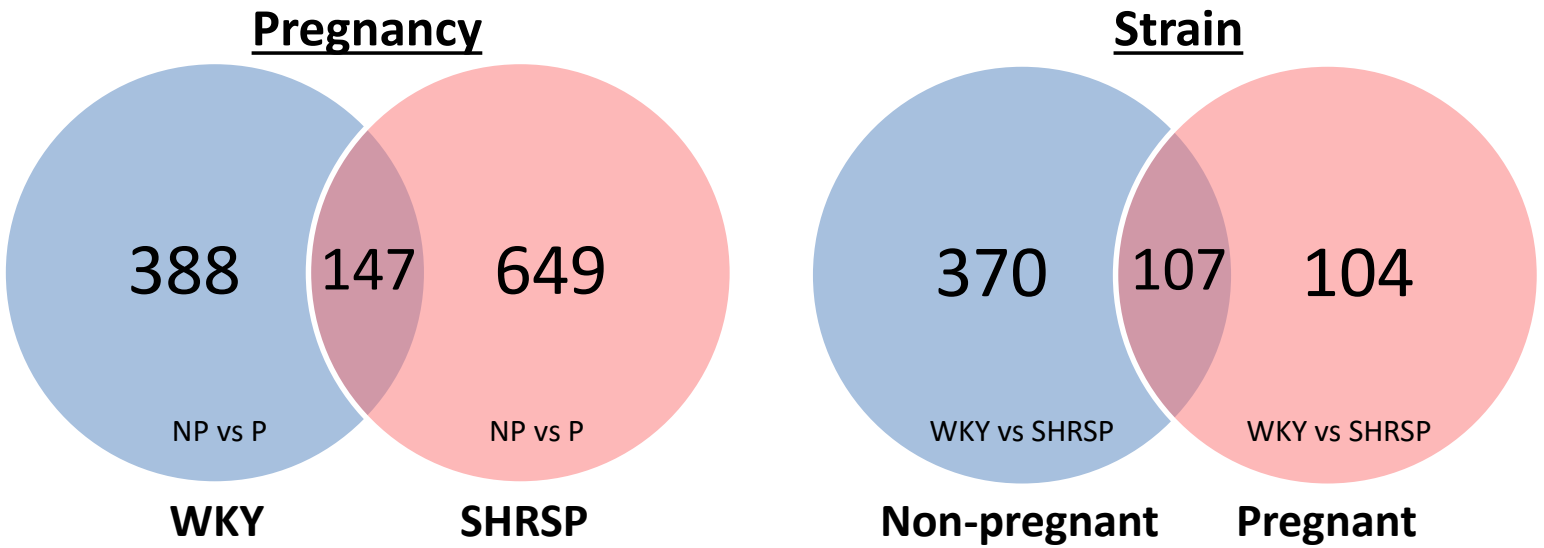


**Figure 5-6: Venn diagrams illustrating the number of differentially expressed gene transcripts that are common or distinctive to pregnancy and strain.** The significantly DE transcripts from each of the 4 comparison groups (WKY NP vs P; SHRSP NP vs P; Non-pregnant WKY vs SHRSP and Pregnant WKY vs SHRSP) were compared to reveal similarities and differences in significant transcript expression number over pregnancy and strain. The numbers used in the Venn diagrams were determined using http://bioinfogp.cnb.csic.es/tools/venny/

**Table 5-3: Number of significantly upregulated and downregulated gene transcripts in each group and the number that are common between WKY and SHRSP or between non-pregnant and pregnant**

| | Non-Pregnant vs Pregnant | | | WKY vs SHRSP | | |
|---|---|---|---|---|---|---|
| | WKY | SHRSP | *Common* | Non-Pregnant | Pregnant | *Common* |
| **Upregulated** | 177 | 166 | *32* | 245 | 135 | *55* |
| **Downregulated** | 358 | 630 | *115* | 232 | 76 | *52* |
| **Total** | 535 | 796 | *147* | 477 | 211 | *107* |

The DE transcripts between the original four comparison groups were limited to padj<0.05 to give the total number of significantly DE genes and the number of common genes determined from Figure 5-6. This was further split into the number of upregulated (higher in 1st group; i.e. in non-pregnant or WKY) and downregulated (lower in 1st group) genes in each group.

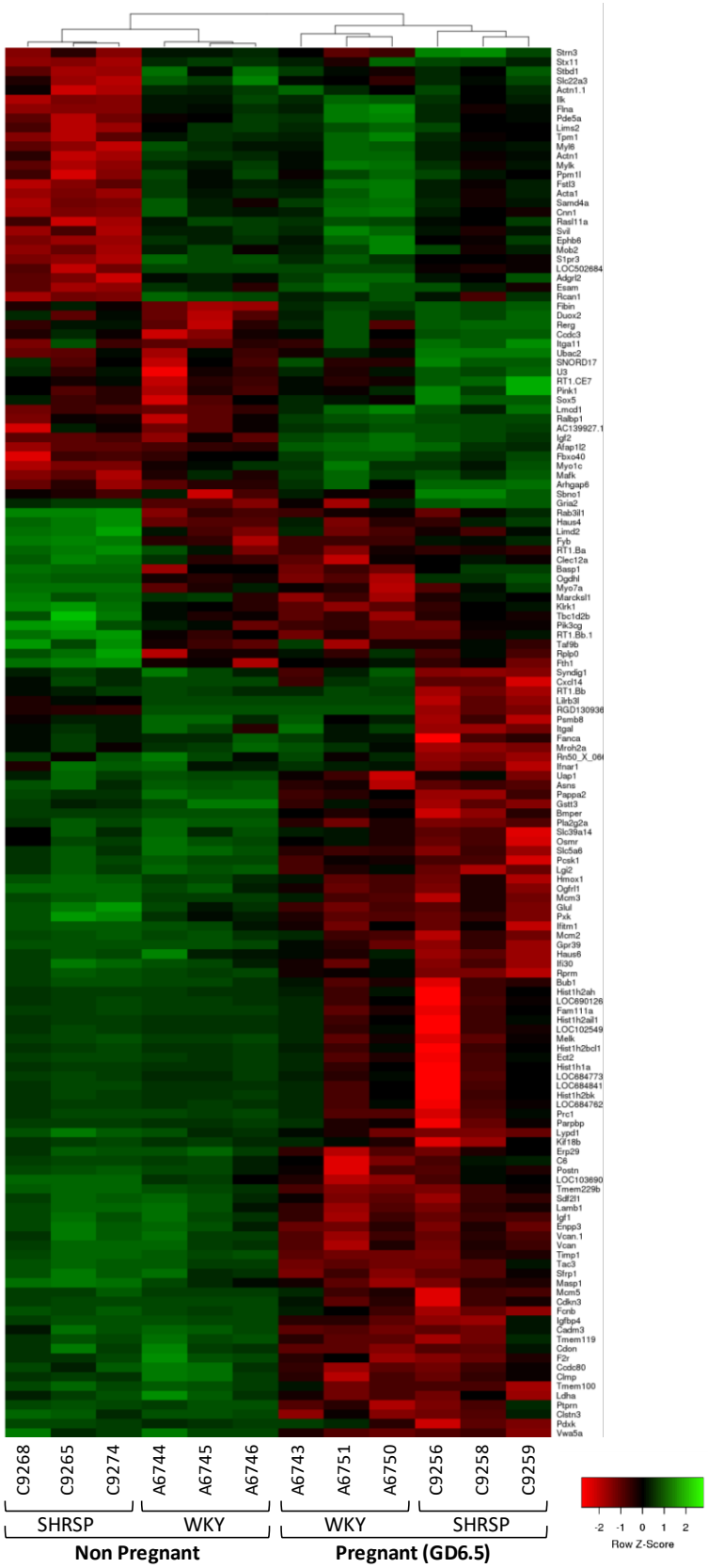


**Figure 5-7: Heatmap of the individual intensity of the most significant differentially gene transcripts**

The heatmap demonstrates the individual intensities of the top 50 most significant DE genes (padj<0.05) from each comparison group. Hierarchical centroid linkage clustering was applied for each individual uterine artery (labelled with animal ID at base). Row z-score indicates the intensity change of samples for that particular gene transcript. The dendrogram at the top shows gene expression clusters within strains and groups non-pregnant and pregnant separately within that cluster. Heatmap was generated using http://www.heatmapper.ca/

### 5.4.4 Pregnancy Associated Genes

Due to the vast data sets generated in the RNA-Seq experiment, the remainder of this chapter focuses on the comparison between non-pregnant and pregnant uterine artery transcript expression differences of WKY and SHRSP separately. These comparisons had the largest number of DE transcripts in both strains and would allow for the investigation of changes across pregnancy. The 147 DE genes that were revealed to be pregnancy dependent in section 5.4.3 were uploaded to IPA® to investigate their predicted involvement in biological functions. Figure 5-8 shows the most likely biological functions predicted to be influenced by this subset of DE genes. The most significant are cellular movement and cell growth & proliferation.

IPA® assigned activation z-scores to each comparison group for different canonical pathways based on the pattern of gene expression changes across pregnancy. These were then compared using a core comparison analysis. Figure 5-9 shows the heatmap of the comparison between WKY and SHRSP. A more negative z-score suggests that the genes in that pathway are downregulated in respect to the non-pregnant state.

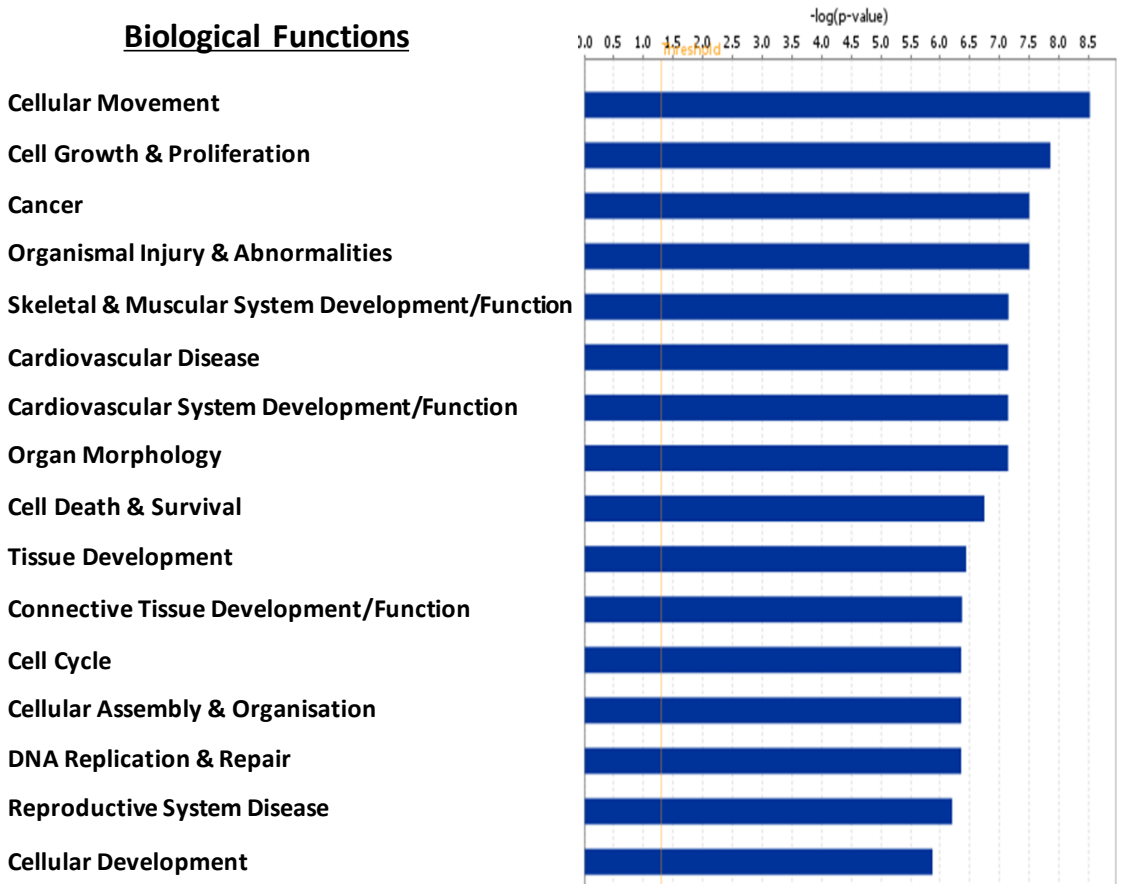


**Figure 5-8: Important biological functions altered due to pregnancy determined by IPA®**
The 147 DE genes found to be common to pregnancy in WKY and SHRSP were predicted to have the most significant influences on these biological functions. The bars represent the likely hood of these genes influencing this function (-log(p-value); the longer bars represent lower p-values and therefore more statistically likely.

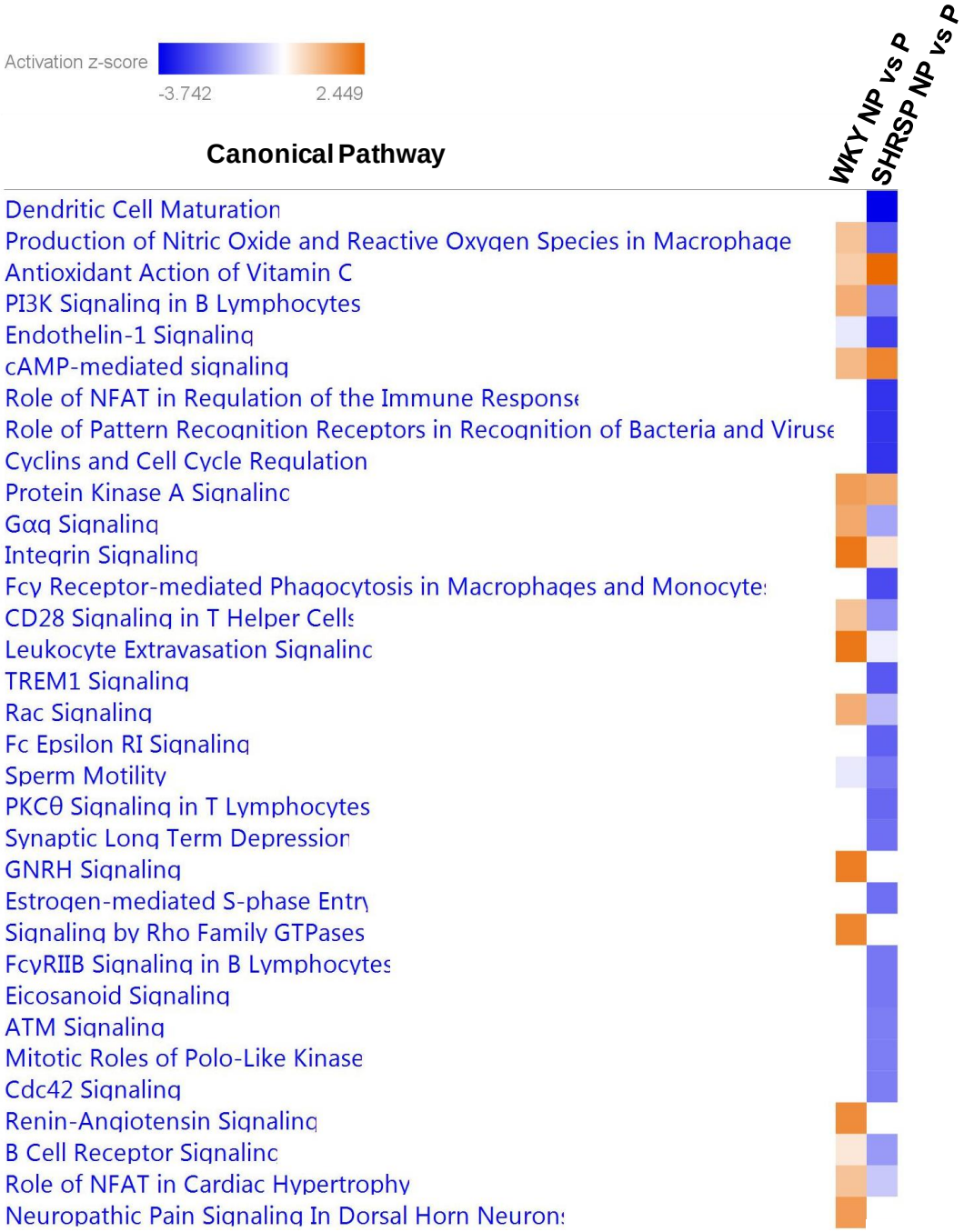


**Figure 5-9: Canonical pathway prediction for WKY and SHRSP non-pregnant vs pregnant**
The canonical pathway activation was predicted by the gene expression profiles in IPA. An activation z-score was assigned (blue = increase relative to non-pregnant; orange = decrease relative to non-pregnant) to each pathway and group and the list is presented with the biggest differences between the two comparison groups. NP = non-pregnant; P = pregnant.

### 5.4.5 Differences in Strain Response to Pregnancy

The following sections focus on some differences identified between WKY and SHRSP uterine artery's response to pregnancy. This was led by differences observed in the canonical pathway z-scores and core comparisons as well as by known factors that would influence vessel function, such as calcium signalling and mitochondrial function.

### 5.4.6 Production of Reactive Oxygen Species by NADPH Oxidase

The z-score for the production of reactive oxygen species (ROS) via NADPH Oxidase was -2.13 for the NPvP SHRSP group and 1 for NPvsP WKY. This interpretation suggests that the SHRSP uterine arteries ROS expression is increased during pregnancy and the WKY remains unchanged. The genes responsible for subunits of NADPH oxidase 2 were found to have a reduced expression in non-pregnant uterine arteries compared to pregnant in the SHRSP group only (Figure 5-10). This suggests that the SHRSP uterine arteries may have an increased *Nox2* expression in the first 6 days of pregnancy, which is not the case in WKY. Table 5-4 demonstrates the fold change values and significance (padj) of key gene changes involved.

The expressions of *Cyba* (p22-phox) and *Cybb* (Gp91) in the uterine arteries of non-pregnant and GD6.5 pregnant rats were validated firstly by using qRT-PCR. There was a significant increase in the expression of *Cyba* in GD6.5 pregnant uterine arteries compared to non-pregnant in SHRSP, whereas there was no difference in expression in WKY vessels (Figure 5-11A). There was no significant difference in *Cybb* gene expression in WKY or SHRSP, however the SHRSP showed a trend towards an increased expression with a 3-fold increase (Figure 5-11B). The expression of these two genes was also compared from uterine arteries of GD18.5 pregnant dams. These showed no significant difference between strains (Figure 5-11C-D). These vessels were not compared to the non-pregnant vessels from the same strain as the *B2m* housekeeper expression was found to reduce by GD18.5.

Functional validation of changes in *Nox2* expression was conducted using IHC. Staining for Nox2 revealed no differences in the protein levels of Nox2 in uterine arteries from NP, GD6.5 and GD18.5 WKY and SHRSP (Figure 5-12).

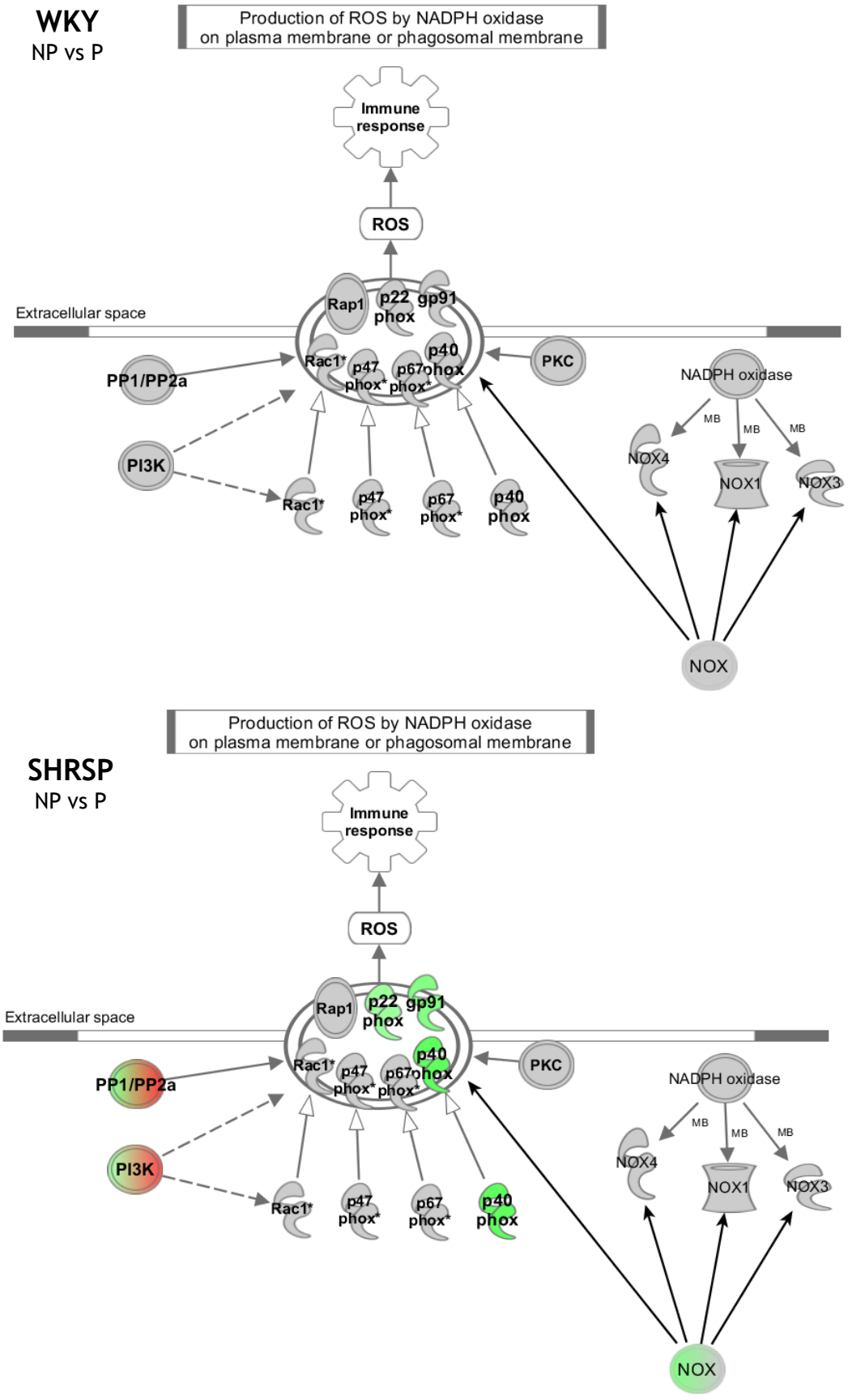


**Figure 5-10: The network of genes involved with the production of ROS via NADPH oxidase**
The pathway of ROS production was highlighted by IPA and further investigation revealed gene expression changes in the NADPH oxidase subunits in SHRSP only. WKY expression levels remained the same in pregnancy as in non-pregnant (grey), where-as 3 subunits had an increased expression (green) and two had conflicting expression (green/red) in pregnant compared to non-pregnant vessels.

**Table 5-4: Genes involved in ROS production via NADPH Oxidase**

| | Gene Symbol | | WKY NP vs P | | SHRSP NP vs P | |
|---|---|---|---|---|---|---|
| Gene Name | Rat | Human | padj | FC | padj | FC |
| **NADPH oxidase 2** | | | | | | |
| Cytochrome b-245 α chain | *Cyba* | *p22-phox* | 0.7491 | -1.10 | ***0.0105*** | ***-1.62*** |
| Cytochrome b-245 ß chain | *Cybb* | *Gp91* | 0.3246 | -1.39 | ***0.0154*** | ***-1.85*** |
| Neutrophil cytosolic factor 2 | *Ncf2*P* | *p67-phox* | 0.7745 | -1.17 | 0.0562 | -2.03 |
| Neutrophil cytosolic factor 4 | *Ncf4* | *p40-phox* | 0.1582 | -1.53 | ***0.0003*** | ***-2.21*** |
| **Phosphatidylinositol 3 kinase complex** | | | | | | |
| Fibroblast growth factor receptor 3 | *Fgfr3** | *FGFR3* | 0.3786 | 1.31 | ***0.0426*** | ***1.64*** |
| Phosphatidylinositol-bisphosphate 3-kinase catalytic subunit γ | *Pik3cg* | *PIK3CG* | 0.6709 | -1.10 | ***0.0036*** | ***-1.52*** |
| **Protein phosphatase 1/2A complex** | | | | | | |
| Protein phosphatase, $Mg^{2+}/Mn^{2+}$ dependent 1L | *Ppm1l* | *PPM1L* | 0.9566 | 1.02 | ***0.0467*** | ***1.36*** |
| Protein phosphatase 1 regulatory inhibitor subunit 14B | *Ppp1r14b* | *PPP1R14B* | 0.1956 | -1.31 | ***0.0001*** | ***-1.76*** |
| Protein phosphatase 1 regulatory subunit 3C | *Ppp1r3c* | *PPP1R3C* | 0.1623 | 1.50 | ***0.0213*** | ***1.73*** |

The NADPH oxidase subunit genes and the associated complexes had a significantly altered expression in SHRSP (padj <0.05; shown in bold). The same genes did not reach significance in WKY. * indicates 2 or more transcript variants for that gene. Ncf2 $^{P}$ is a non-coding processed transcript in rat.

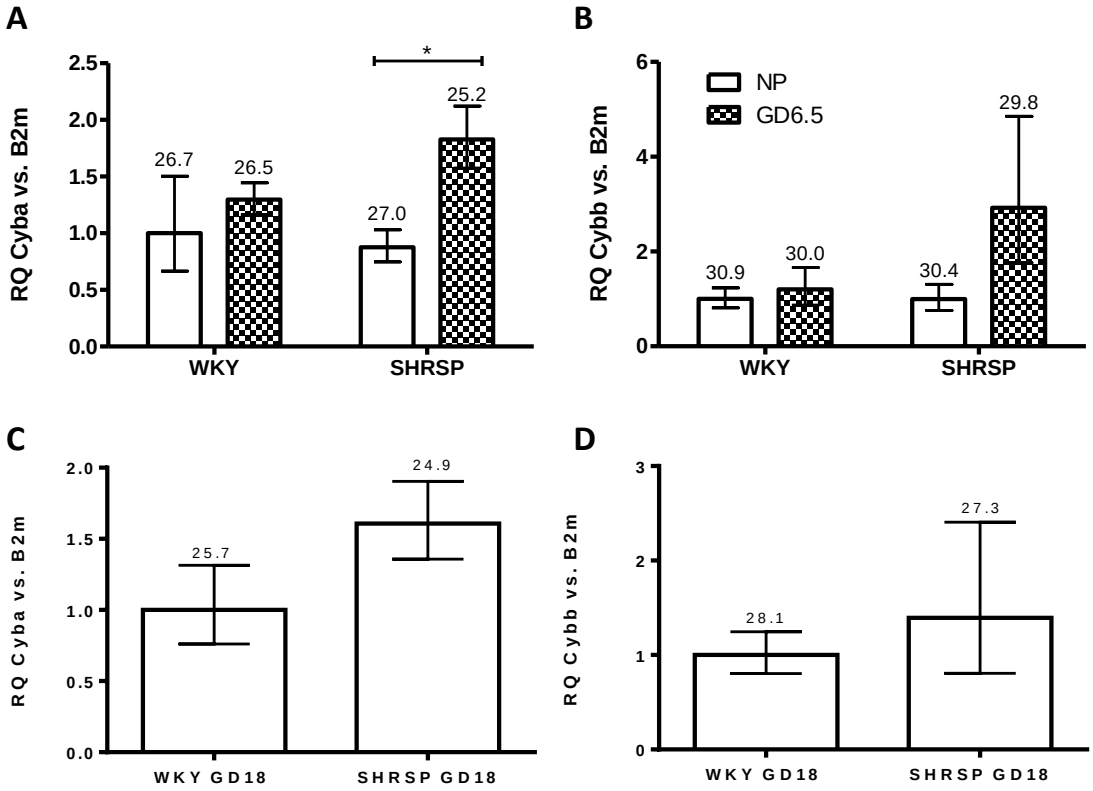


**Figure 5-11: Validation of *Cyba* and *Cybb* expression in uterine arteries using qRT-PCT**
(A) *Cyba* expression was found to be increased in GD6.5 SHRSP uterine arteries compared to non-pregnant (n=4-5). (B) No significant changes in *Cybb* expression where observed in either strain (n=4-5). Comparisons at GD18.5 found no differences between WKY and SHRSP for (C) *Cyba* or (D) *Cybb* (n=3-4). Numbers above bars represent average cycle threshold (CT) values. Data expressed as relative quantity (RQ) to *B2m* housekeeper, and relative to WKY NP or WKY GD18.5. Analysed using one-way ANOVA (A-B) or student's t-test (C-D); *p<0.05.

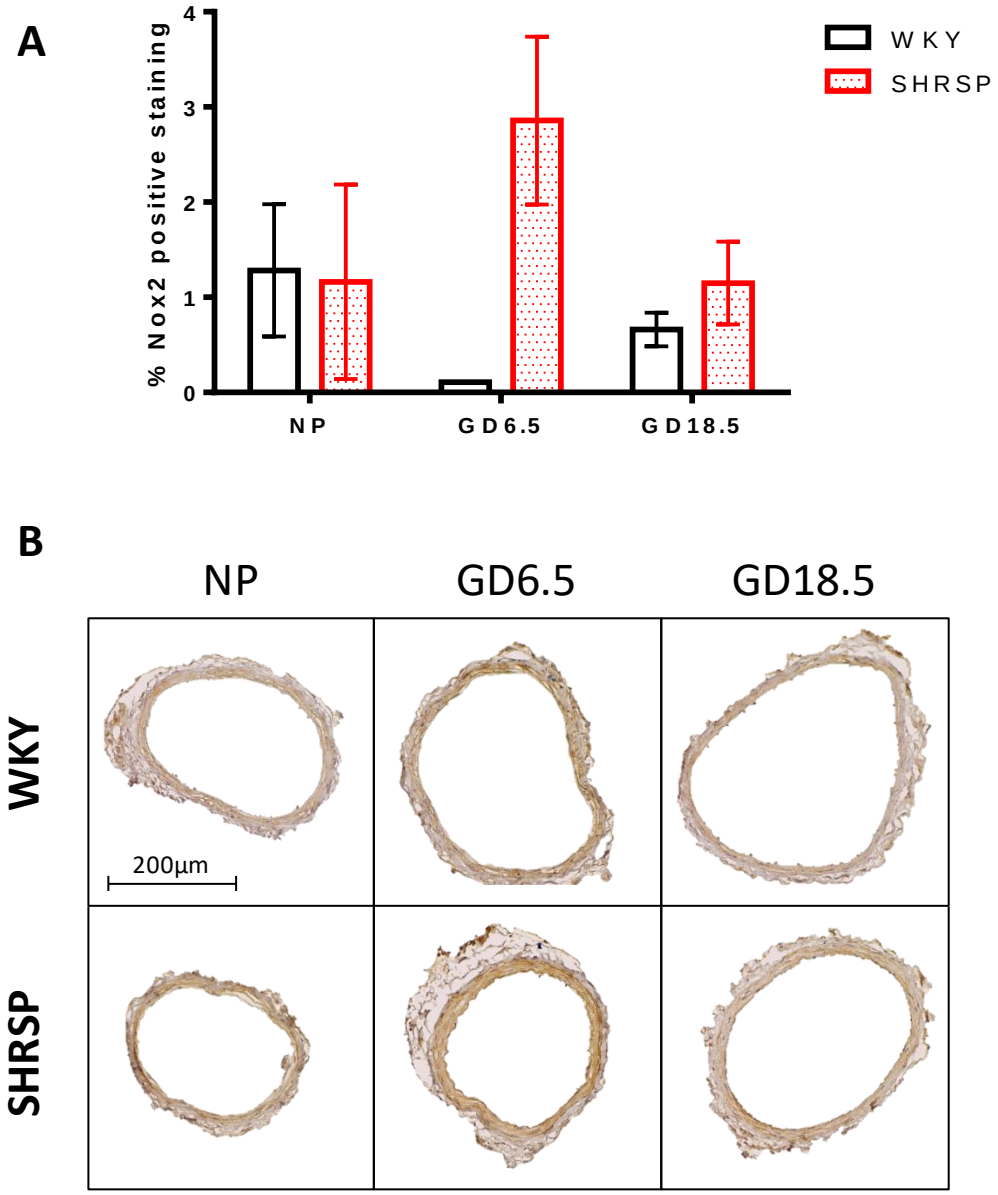


**Figure 5-12: Quantification of Nox2 and Immunohistochemical location in uterine arteries** Uterine arteries fixed at 120mmHg were stained for Nox2. (A) Staining was quantified as a percentage of the total vessel area. No statistical analysis could be established due to low n numbers. WKY: non-pregnant (NP) n= 2, GD6.5 n=1, GD18.5 n=4; SHRSP: NP n=2, GD6.5 n=4, GD18.5 n=2. (B) Representative images of the Nox2 staining.

### 5.4.7 Calcium Signalling Differences

Pathway analysis on IPA revealed pregnancy dependent changes in the α adrenergic signalling pathway was not the same between WKY and SHRSP (Figure 5-9), with WKY having an expression pattern that suggested reduction in $Ca^{2+}$ signalling in the pregnant vessels (Figure 5-13). The expressions of inositol-trisphosphate receptor (*Ip3r*), phospholipase C (*Plc*) and $Ca^{2+}$/calmodulin dependent protein kinase (*Camk2*) gene transcripts in non-pregnant vessels from WKY were significantly greater than that of the pregnant vessels of the same strain, and calmodulin 1 (*Calm1*) was observed to have an increased expression during pregnancy (Table 5-5). The same pattern of differential expression is not observed in SHRSP vessels. In this strain, there are no significant differences in *Ip3r* or *Calm1*, which suggest the release and sequestering of $Ca^{2+}$ is not altered during pregnancy by this mechanism. However, there are reductions in the expression of *Camk2* and myosin light chain kinase (*Mylk*) in pregnant SHRSP uterine arteries.

Taqman® qRT-PCR was conducted to validate the expression of *Calm1*, *Ip3r* and *Mylk*, to determine consistency with the RNA-Seq analysis. The RNA-Seq analysis identified that *Calm1* expression increased in WKY GD6.5 compared to NP uterine arteries, with no changes in the SHRSP comparison group. However, qRT-PCR revealed no significant differences between the GD6.5 and NP WKY vessels, and uterine arteries from GD6.5 SHRSP compared to NP SHRSP were found to have a significantly increased *Calm1* expression (Figure 5-14). The expression of inositol trisphosphate receptor type 1 (*Itpr1*), was significantly greater in SHRSP compared to WKY at GD6.5 (Figure 5-14), however there was no apparent change in expression over the course of pregnancy in either strain, which somewhat contradicts the RNA-Seq results. *Mylk* expression, was found to be reduced in SHRSP GD6.5 uterine arteries compared to NP in the RNA-Seq dataset, but was not significantly different between any of the groups when using qRT-PCR (Figure 5-14). The qRT-PCR results suggest that *Ip3r* may be more highly expressed in SHRSP compared to WKY, which would increase $Ca^{2+}$ release in the hypertensive strain potentially leading to detrimental effects due to the potential for increased VSMC contraction.

Further investigation of the intracellular $Ca^{2+}$ signalling was conducted by visualising intracellular $Ca^{2+}$ release using fluorescent Cal-520. The pre-loaded cells fluoresced when exposed to agonists of calcium release. Figure 5-15 shows the fluorescent intensity of VSMC from WKY non-pregnant and GD6.5 pregnant uterine arteries. The first peak was the angiotensin II stimulated $Ca^{2+}$ release. This shows that the non-pregnant VSMCs responded more to AngII than the pregnant cells. Both cell types responded with similar intensities to ionomycin. When the maximal delta peak for AngII intensity was calculated for each replicate, there was found to be a significantly higher response in the non-pregnant cells compared to the pregnant, this significant difference was not observed in response to ionomycin. These results are technical replicates from one cell isolation for non-pregnant and pregnant WKY VSMCs. Due to technical issues with preparation of VSMC from SHRSP uterine arteries it was not possible to complete the $Ca^{2+}$release experiments for this strain.

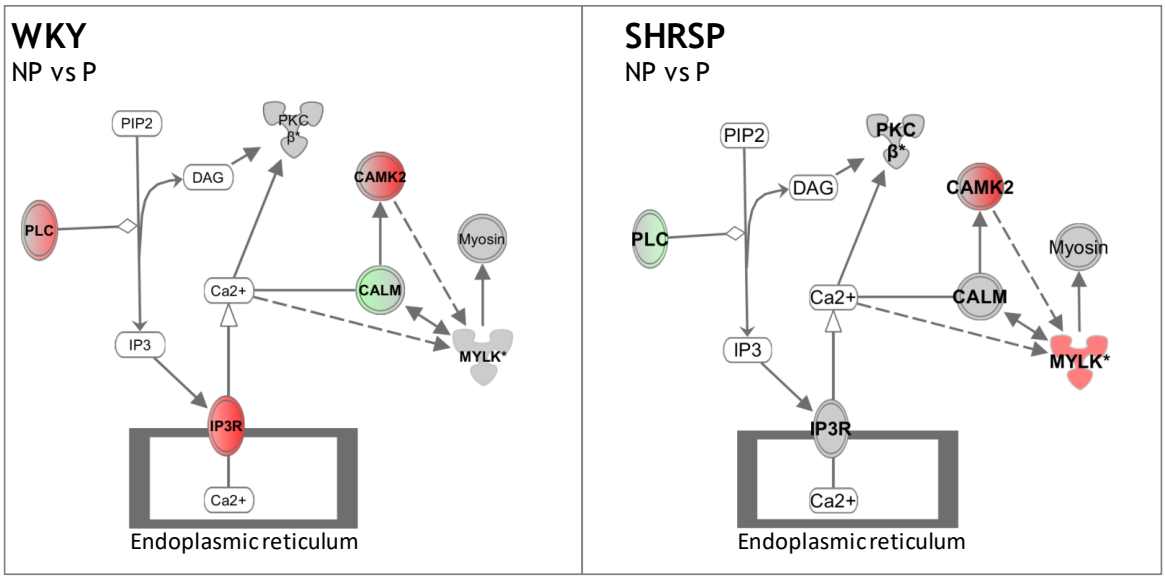


**Figure 5-13: Components of intracellular calcium release in vascular smooth muscle cells** Gene interaction network created from IPA shows that there is differential expression of genes involved in $Ca^{2+}$ release during pregnancy in both strains; however different gene changes are occurring in the two strains. Red = reduced expression and green = increased expression in the pregnant (P) uterine artery relative to non-pregnant (NP)

**Table 5-5: The significantly differentially expressed genes involved in calcium release and regulation**

| Genes involved in $Ca^{2+}$ release in **WKY** | Gene Symbol | Ensembl Transcript ID | NP vs P | |
|---|---|---|---|---|
| | | | padj | FC |
| Calmodulin 1 | *Calm1* | ENSRNOT00000022603 | 0.013873 | -1.46 |
| Calcium/calmodulin dependent protein kinase II delta | *Camk2d**+ | ENSRNOT00000016026 | 0.016504 | 1.93 |
| | | ENSRNOT00000015564 | 0.020787 | 1.81 |
| Inositol 1,4,5-trisphosphate receptor type 1 | *Itpr1** | ENSRNOT00000082723 | 0.007585 | 2.54 |
| Inositol 1,4,5-trisphosphate receptor type 2 | *Itpr2* | ENSRNOT00000040645 | 0.034061 | 1.32 |
| Phospholipase C gamma 2 | *Plcg2* | ENSRNOT00000090165 | 0.001353 | 1.50 |

| Genes involved in $Ca^{2+}$ release in **SHRSP** | Gene Symbol | Ensembl Transcript ID | NP vs P | |
|---|---|---|---|---|
| | | | padj | FC |
| Calcium/calmodulin dependent protein kinase II delta | *Camk2d** | ENSRNOT00000016026 | 0.009844 | 1.93 |
| Myosin light chain 6 | *Myl6** | ENSRNOT00000082518 | 0.000923 | 1.48 |
| Myosin light chain kinase | *Mylk** | ENSRNOT00000067060 | 0.041940 | 1.44 |
| Phospholipase C like 2 | *Plcl2* | ENSRNOT00000018146 | 0.049080 | -1.32 |

The false discovery rate (padj) and fold change (FC) of significant (padj <0.05) DE gene transcripts in WKY and SHRSP intracellular calcium release. * indicates 2 or more transcript variants for that gene. + 2 or more transcripts of the gene were found to be significantly differentially expressed.

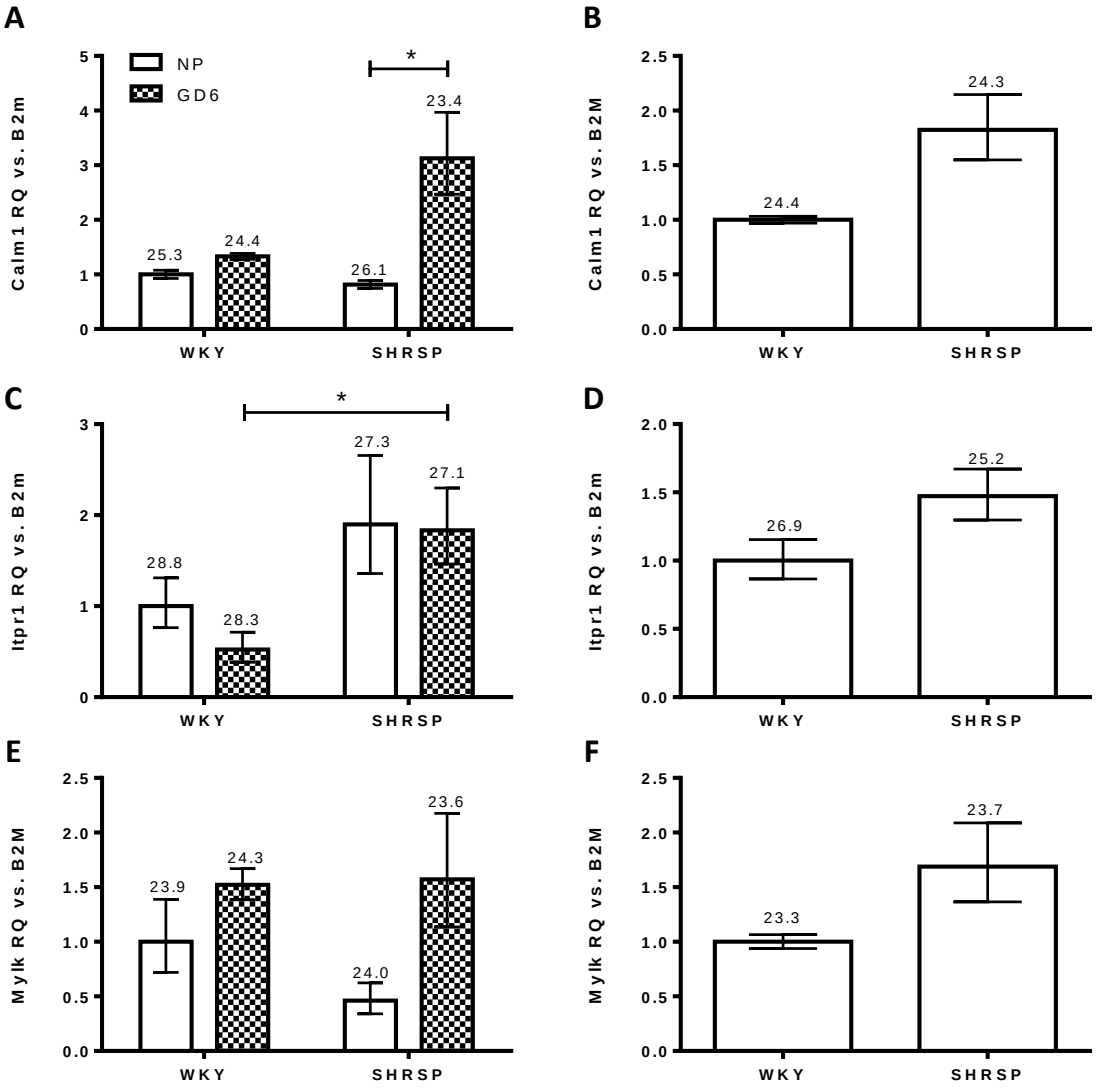


**Figure 5-14: Expression of genes involved in calcium signalling cascade measured using qRT-PCR**

(A-B) *Calm1*, (C-D) *Itpr1* and (E-F) *Mylk* expression was analysed using qRT-PCR in non-pregnant (NP) (n=3), GD6.5 (n=4) and GD18.5 (n=3) pregnant uterine arteries. (A) Expression of *Calm1* was increased in SHRSP pregnancy, but not significantly in WKY pregnancy or between strains. (B) There were also no differences between strains at GD18.5. (C) Expression of *Itpr1* was not significantly changed over pregnancy in both strains yet was significantly higher in GD6.5 SHRSP vs GD6.5 WKY. (D) There was no significant change in expression at GD18.5. (E-F) *Mylk* expression was not found to be significantly changed in either a strain or pregnancy manner. Numbers above bars represent average cycle threshold (CT) values. Data normalised to *B2m* housekeeper, and expressed as relative quantity (RQ) to WKY NP or WKY GD18.5. Analysed one-way ANOVA with Bonferroni post-hoc test when comparing NP vs GD6 in WKY and SHRSP, or with student's t-test when analysing GD18; *p<0.05.

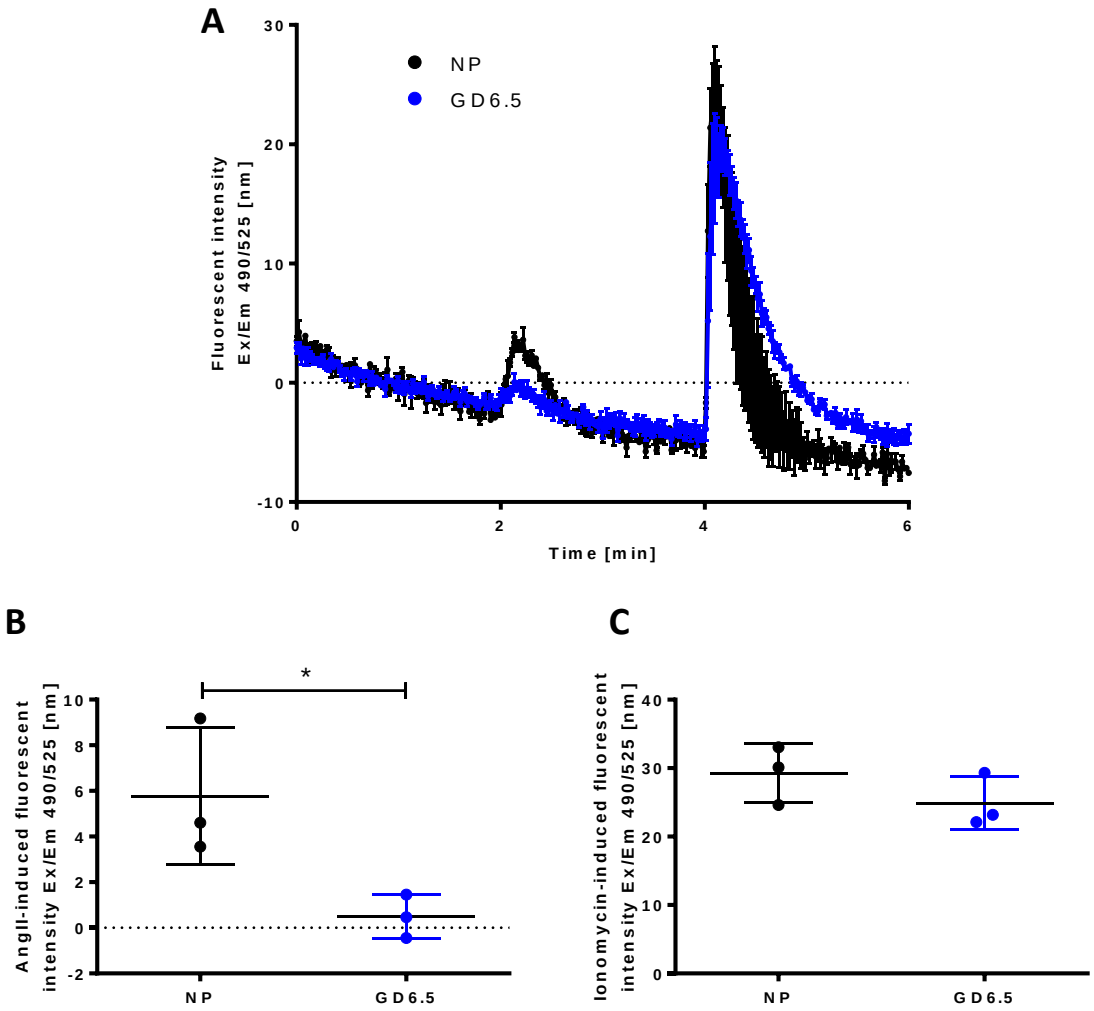


**Figure 5-15: Calcium release measured by Cal-520 fluorescent intensity in WKY uterine artery vascular smooth muscle cells**

(A) Calcium release was measured over 6 minutes. A fluorescence baseline was established between 0-2 minutes and subtracted from the trace. AngII addition occurred at 2 minutes and a re-establishment of baseline was reached before ionomycin was added at 4 minutes. The dip observed in baseline throughout the experiment was due to bleaching of the fluorophore. (B) Non-pregnant (NP) VSMCs produce greater fluorescent intensity in response to AngII than GD6.5 pregnant VSMCs. (C) No differences were observed in the responses to ionomycin between NP and GD6.5 VSMCs. Analysed using student's t-test; *p<0.05; n=3.

### 5.4.8 Inflammatory Response to Pregnancy

WKY and SHRSP displayed differential gene expression profiles that suggested an increased inflammatory response to pregnancy in the uterine arteries in the first 6 days of gestation. However, the genes influencing this change were varied between strains (Figure 5-16 and Figure 5-17). A total of 40 genes contribute to the predicted increased inflammatory response in WKY, these are illustrated in Figure 5-16 and Table 5-6. There were more than double the number of contributing genes in the SHRSP uterine arteries; a total of 88 genes contributed to the increased inflammatory response, shown in Figure 5-17 and Table 5-7. SHRSP and WKY had 19 contributing genes that overlapped (Table 5-8) showing the same directionality and similar fold changes. One gene of particular interest was phospholipase A2 (*Pla2g2a*) as it had the highest fold change of all the inflammatory-associated genes in both WKY and SHRSP. The expression of this gene was validated using qRT-PCR (Figure 5-18A), which confirmed that expression increased significantly in the pregnant vessels from both WKY and SHRSP. Additionally, there was a significant increase in *Pla2g2a* expression in uterine arteries from non-pregnant SHRSP compared to non-pregnant WKY. Another gene involved in the inflammatory response to pregnancy in both strains was ficolin A, this gene was not found to be present in non-pregnant vessels from both strains (CT value for WKY averaged 38.0, undetermined in SHRSP) but was present in GD6.5 vessels (Figure 5-18B). The RNA-Seq analysis identified a fold change of -1.87 for WKY and -1.82 for SHRSP, suggesting an increase in expression, however due to the low expression in NP uterine arteries (determined by a high CT or undetectable PCR product using qRT-PCR), it may be possible that ficolin expression is switched on in the uterine artery during pregnancy.

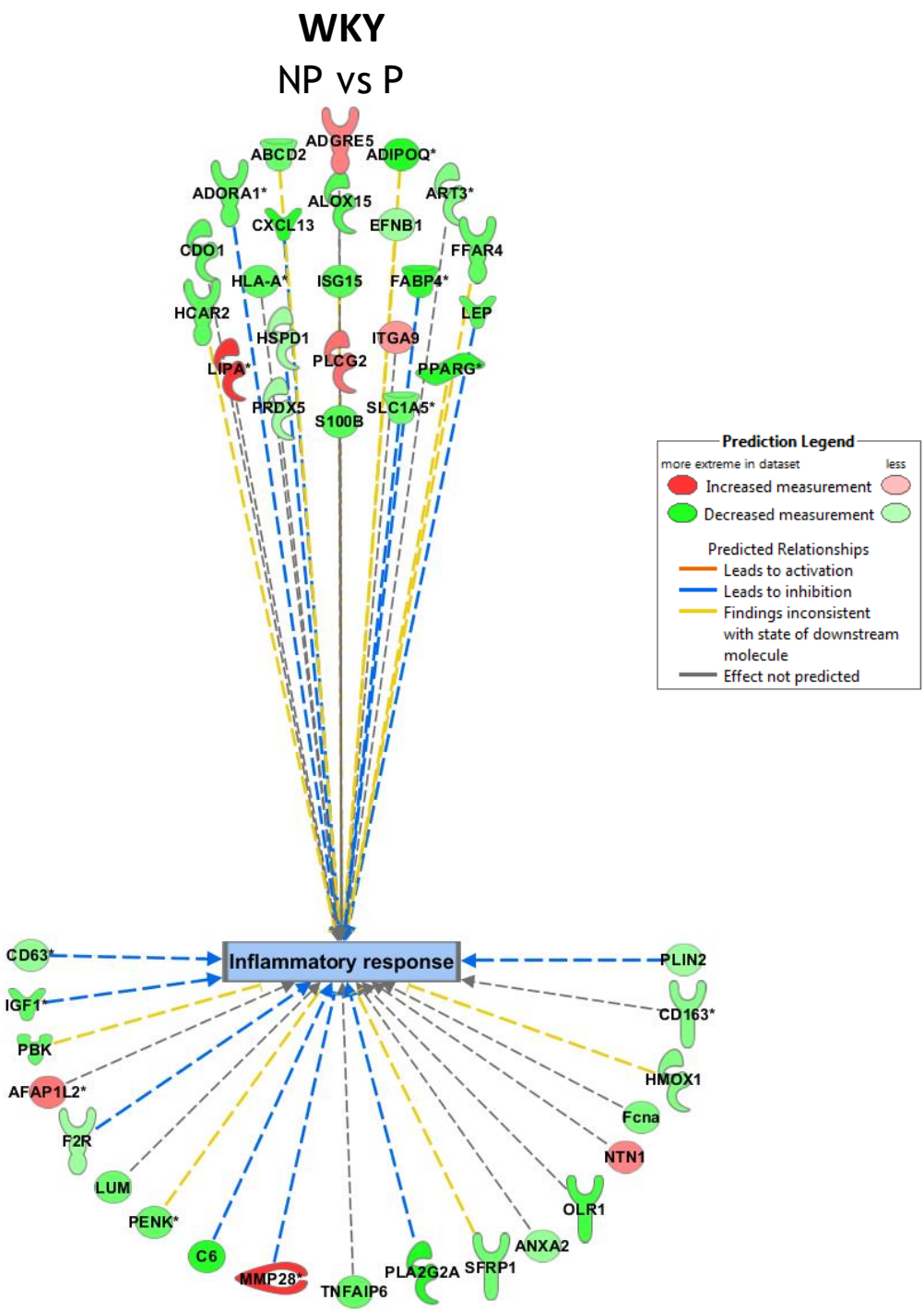


**Figure 5-16: Genes predicted to influence inflammatory response during pregnancy in WKY uterine arteries**

The WKY uterine artery gene expression profile had a predicted enhancement of the inflammatory response in GD6.5 pregnant (P) uterine arteries compared to non-pregnant (NP). A total of 40 genes contributed to this prediction. The 19 genes common to WKY and SHRSP pathways are shown as lower semi-circle. These genes had the same differential expression direction (i.e. increased or decreased in both WKY and SHRSP). An increased measurement (red) indicates that gene was more highly expressed in the non-pregnant (NP) uterine artery, and thus reduced over pregnancy and vice versa for a decreased measurement (green).

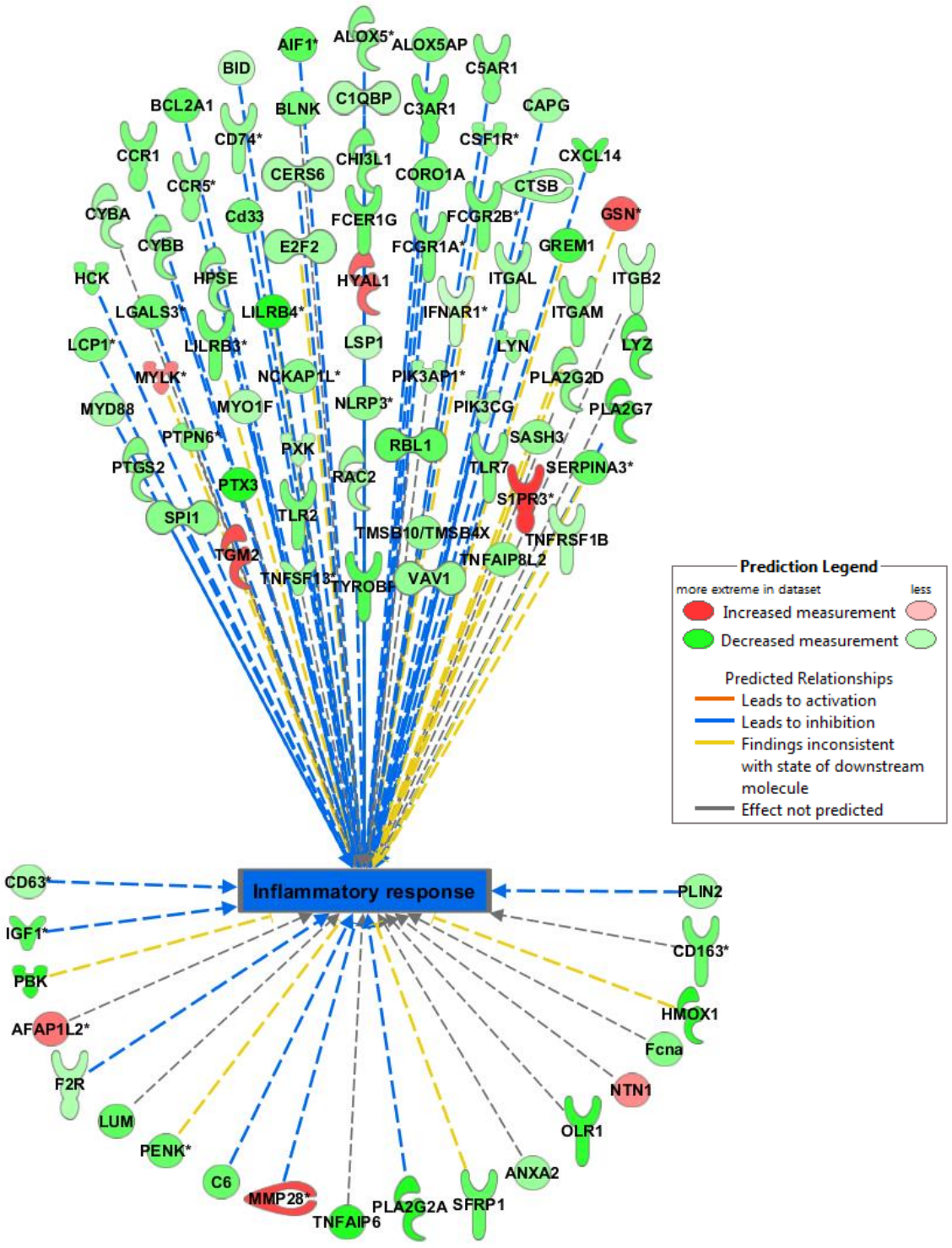


**Figure 5-17: Genes predicted to influence inflammatory response during pregnancy in SHRSP uterine arteries**

The SHRSP uterine artery gene expression profile had a predicted enhancement of the inflammatory response in GD6.5 pregnant (P) uterine arteries compared to non-pregnant (NP). A total of 88 genes contributed to this prediction. The 19 genes common to WKY and SHRSP pathways are shown as lower semi-circle. These genes had the same differential expression direction (i.e. increased or decreased in both WKY and SHRSP). An increased measurement (red) indicates that gene was more highly expressed in the non-pregnant (NP) uterine artery, and thus reduced over pregnancy and vice versa for a decreased measurement (green)

**Table 5-6: Differential expression of inflammatory genes specific to WKY pregnancy**

| WKY Specific Inflammatory genes | Gene Symbol | Ensembl Transcript ID (ENSRNO) | WKY NP vs P | |
|---|---|---|---|---|
| | | | padj | FC |
| Adhesion G protein-coupled receptor E5 | *Adgre5* | T00000006152 | 0.003724 | 1.43 |
| Peroxiredoxin 5 | *Prdx5* | T00000028687 | 0.041195 | -1.57 |
| C-X-C motif chemokine ligand 13 | *Cxcl13* | T00000039383 | 0.000200 | -3.22 |
| Solute carrier family 1 member 5 | *Slc1a5** | T00000021455 | 0.002071 | -2.06 |
| Peroxisome proliferator-activated receptor gamma | *Pparg** | T00000012137 | 0.001617 | -2.86 |
| Heat shock protein family D member 1 | *Hspd1* | T00000066589 | 0.033457 | -1.58 |
| Integrin subunit alpha 9 | *Itga9* | T00000015113 | 0.030174 | 1.34 |
| RT1 class Ia, locus A1 | *Rt1-a1** | T00000078972 | 0.020952 | -2.24 |
| Arachidonate 15-lipoxygenase | *Alox15* | T00000026038 | 0.011840 | -2.36 |
| Hydroxycarboxylic acid receptor 2 | *Hcar2* | T00000032249 | 0.034305 | -2.20 |
| Lipase A, lysosomal acid type | *Lipa** | T00000025845 | 0.007890 | 1.96 |
| ISG15 ubiquitin-like modifier | *Isg15* | T00000039263 | 0.012420 | -2.31 |
| Adenosine A1 receptor | *Adora1** | T00000004602 | 0.030174 | -2.23 |
| Fatty acid binding protein 4 | *Fabp4** | T00000014701 | 0.001000 | -2.79 |
| Adiponectin, C1Q and collagen domain containing | *Adipoq**[a] | T00000002492 | 0.000586 | -3.10 |
| | | T00000089988 | 0.016504 | -1.73 |
| Free fatty acid receptor 4 | *Ffar4* | T00000034563 | 0.036322 | -2.18 |
| Ephrin B1 | *Efnb1* | T00000009635 | 0.045673 | -1.61 |
| ADP-ribosyltransferase 3 | *Art3** | T00000052035 | 0.038451 | -1.85 |
| Phospholipase C, gamma 2 | *Plcg2* | T00000090165 | 0.001353 | 1.50 |
| ATP binding cassette subfamily D member 2 | *Abcd2* | T00000021064 | 0.026721 | -2.08 |
| S100 calcium binding protein B | *S100b* | T00000001743 | 0.004339 | -2.28 |

The fold change (FC) and significance of this change (padj) of all 21 significant (padj <0.05) DE gene transcripts that are specific to WKY uterine arteries during the first 6 days of pregnancy. * indicates 2 or more transcript variants for that gene; [a] All transcripts of that gene were found to have a significantly altered expression.

**Table 5-7: SHRSP differentially expressed genes influencing the inflammatory response to pregnancy**

| SHRSP Specific Inflammatory genes | Gene Symbol | Ensembl Transcript ID ENSRNOT00 | SHRSP NP vs P | |
|---|---|---|---|---|
| | | | padj | FC |
| Spi-1 proto-oncogene | *Spi1* | 000016306 | 0.000051 | -1.77 |
| Pentraxin 3 | *Ptx3* | 000016541 | 0.000059 | -3.13 |
| Leukocyte immunoglobulin like receptor B4 | *Lilrb4** | 000077186 | 0.000067 | -3.02 |
| Transglutaminase 2 | *Tgm2* | 000018328 | 0.000139 | 1.64 |
| HCK proto-oncogene, Src family tyrosine kinase | *Hck* | 000012432 | 0.000155 | -2.01 |
| Integrin subunit alpha D | *Itgad* | 000026748 | 0.000178 | -1.89 |
| Sphingosine-1-phosphate receptor 3 | *S1pr3** | 000019473 | 0.000190 | 1.76 |
| Lysozyme 2 | *Lyz2* | 000007747 | 0.000309 | -2.38 |
| Phospholipase A2 group VII | *Pla2g7* | 000038222 | 0.000441 | -2.67 |
| RB transcriptional corepressor like 1 | *Rbl1* | 000064824 | 0.000863 | -2.20 |
| Tyro protein tyrosine kinase binding protein | *Tyrobp* | 000028284 | 0.000920 | -2.34 |
| Rac family small GTPase 2 | *Rac2* | 000009994 | 0.001000 | -1.64 |
| Leukocyte immunoglobulin like receptor B3 | *Lilrb3* | 000077327 | 0.001503 | -2.08 |
| Complement C3a receptor 1 | *C3ar1* | 000012216 | 0.001602 | -2.20 |
| Fc fragment of IgE receptor Ig | *Fcer1g* | 000029179 | 0.001955 | -2.12 |
| BCL2-related protein A1 | *Bcl2a1* | 000039850 | 0.001965 | -2.22 |
| Coronin 1A | *Coro1a* | 000026496 | 0.002225 | -1.98 |
| Myeloid differentiation primary response 88 | *Myd88* | 000018341 | 0.002251 | -1.51 |
| CD74 molecule | *Cd74** | 000025344 | 0.002819 | -1.69 |
| Arachidonate 5-lipoxygenase | *Alox5** | 000017633 | 0.002857 | -1.86 |
| Galectin 3 | *Lgals3** | 000014216 | 0.003148 | -1.99 |
| Gremlin 1 | *Grem1* | 000037895 | 0.003525 | -2.52 |
| NCK associated protein 1 like | *Nckap1l** | 000088956 | 0.003525 | -1.77 |
| Phosphatidylinositol-4,5-bisphosphate 3-kinase γ | *Pik3cg* | 000012487 | 0.003553 | -1.52 |
| Complement C5a receptor 1 | *C5ar1* | 000073034 | 0.004601 | -1.86 |
| Allograft inflammatory factor 1 | *Aif1** | 000001135 | 0.004957 | -2.26 |
| Colony stimulating factor 1 receptor | *Csf1r*[*+] | 000079360 | 0.005573 | -1.82 |
| | | 000049357 | 0.039505 | -1.61 |
| LYN proto-oncogene, Src family tyrosine kinase | *Lyn* | 000011130 | 0.005573 | -1.71 |
| Thymosin, beta 10-like | *Ptmb10* | 000022846 | 0.005725 | -1.70 |
| Capping actin protein, gelsolin like | *Capg* | 000018562 | 0.006066 | -1.57 |
| Lymphocyte cytosolic protein 1 | *Lcp1** | 000014502 | 0.007300 | -1.91 |
| C-X-C motif chemokine ligand 14 | *Cxcl14* | 000016009 | 0.008176 | -2.41 |
| TNF alpha induced protein 8 like 2 | *Tnfaip8l2* | 000028642 | 0.010489 | -1.77 |
| Cytochrome b-245 alpha chain | *Cyba* | 000017564 | 0.010523 | -1.62 |
| Complement C1q binding protein | *C1qbp* | 000037517 | 0.010964 | -1.47 |
| Vav guanine nucleotide exchange factor 1 | *Vav1* | 000073294 | 0.012376 | -1.68 |
| phospholipase A2 | *Pla2g2d* | 000022579 | 0.013372 | -1.84 |
| SAM and SH3 domain containing 3 | *Sash3* | 000006035 | 0.013372 | -1.70 |
| Fc fragment of IgG receptor IIb | *Fcgr2b** | 000035400 | 0.013517 | -1.98 |
| Cytochrome b-245 beta chain | *Cybb* | 000038994 | 0.015395 | -1.85 |
| Interferon alpha and beta receptor subunit 1 | *Ifnar1** | 000029985 | 0.015877 | -1.32 |
| CD33 molecule | *Cd33* | 000047473 | 0.017657 | -1.97 |
| Serine protease inhibitor | *LOC299282** | 000014073 | 0.019724 | -2.21 |

| | | | | |
|---|---|---|---|---|
| Cathepsin B | *Ctsb* | 000014177 | 0.019965 | -1.66 |
| Phosphoinositide-3-kinase adaptor protein 1 | *Pik3ap1** | 000017938 | 0.020698 | -1.61 |
| BH3 interacting domain death agonist | *Bid* | 000016776 | 0.021381 | -1.41 |
| Integrin subunit beta 2 | *Itgb2* | 000001639 | 0.021507 | -1.47 |
| Chitinase 3 like 1 | *Chi3l1* | 000078599 | 0.022693 | -1.97 |
| Myosin IF | *Myo1f* | 000011513 | 0.022829 | -1.50 |
| Fc fragment of IgG receptor Ia | *Fcgr1a** | 000028780 | 0.024666 | -1.92 |
| TNF receptor superfamily member 1B | *Tnfrsf1b* | 000022478 | 0.025100 | -1.49 |
| B-cell linker | *Blnk* | 000019014 | 0.026700 | -1.88 |
| Ceramide synthase 6 | *Cers6* | 000058763 | 0.033069 | -1.52 |
| NLR family, pyrin domain containing 3 | *Nlrp3** | 000004280 | 0.033258 | -1.71 |
| Toll-like receptor 7 | *Tlr7* | 000005620 | 0.033979 | -1.90 |
| Protein tyrosine phosphatase, non-receptor type 6 | *Ptpn6** | 000082739 | 0.034012 | -1.87 |
| Chemokine (C-C motif) receptor 5 | *Ccr5** | 000082774 | 0.034842 | -1.76 |
| Lymphocyte-specific protein 1 | *Lsp1* | 000054864 | 0.035562 | -1.37 |
| Heparanase | *Hpse* | 000002983 | 0.039026 | -1.83 |
| Toll-like receptor 2 | *Tlr2* | 000013025 | 0.039978 | -1.97 |
| Arachidonate 5-lipoxygenase activating protein | *Alox5ap* | 000001207 | 0.040572 | -1.91 |
| Gelsolin | *Gsn** | 000025857 | 0.040572 | 1.56 |
| Integrin subunit alpha L | *Itgal* | 000024404 | 0.041281 | -1.58 |
| Myosin light chain kinase | *Mylk** | 000067060 | 0.041940 | 1.44 |
| TNF superfamily member 13 | *Tnfsf13** | 000056903 | 0.042795 | -1.69 |
| E2F transcription factor 2 | *E2f2* | 000072618 | 0.043386 | -1.61 |
| Hyaluronoglucosaminidase 1 | *Hyal1* | 000021408 | 0.044235 | 1.54 |
| C-C motif chemokine receptor 1 | *Ccr1* | 000008772 | 0.045020 | -1.92 |
| Prostaglandin-endoperoxide synthase 2 | *Ptgs2* | 000003567 | 0.046684 | -1.87 |

The fold change (FC) and false discovery rate (padj) of all 69 significant (padj <0.05) DE gene transcripts that are specific to SHRSP uterine arteries during the first 6 days of pregnancy. *indicates 2 or more transcript variants for that gene. [+] 2 or more transcripts of that gene were found to be significantly differentially expressed in one or both comparison group

**Table 5-8: Common inflammatory response genes that were differentially expressed in response to pregnancy**

| Common Inflammatory genes | Gene Symbol | Ensembl Transcript ID (ENSRNO) | WKY NP vs P | | SHRSP NP vs P | |
|---|---|---|---|---|---|---|
| | | | padj | FC | padj | FC |
| Phospholipase A2 | *Pla2g2a* | T00000022827 | $1.28x10^{-20}$ | -7.17 | $7.11x10^{-11}$ | -4.29 |
| Heme oxygenase 1 | *Hmox1* | T00000019192 | 0.021005 | -1.85 | $1.36x10^{-8}$ | -3.22 |
| Actin Filament Associated Protein 1 Like 2 | *Afap1l2** | T00000073346 | $2.74x10^{-07}$ | 1.47 | $8.43x10^{-8}$ | 1.47 |
| Insulin-like growth factor 1 | *Igf1*+* | T00000085680 | 0.021526 | -2.22 | *0.413053* | *-1.45* |
| | | T00000038780 | $1.43x10^{-04}$ | -2.18 | $7.52x10^{-6}$ | -2.32 |
| Secreted frizzled-related protein 1 | *Sfrp1* | T00000024128 | $6.20x10^{-04}$ | -2.01 | $1.96x10^{-5}$ | -2.19 |
| PDZ binding kinase | *Pbk* | T00000064306 | 0.039028 | -2.17 | $3.14x10^{-4}$ | -3.02 |
| TNF alpha induced protein 6 | *Tnfaip6* | T00000070792 | 0.044179 | -2.12 | $3.16x10^{-4}$ | -2.98 |
| Oxidized low density lipoprotein (lectin-like) receptor 1 | *Olr1* | T00000086390 | 0.008740 | -2.51 | 0.000995 | -2.79 |
| Lumican | *Lum* | T00000006109 | 0.018769 | -2.04 | 0.003533 | -2.20 |
| CD163 molecule | *Cd163*+* | T00000084588 | 0.009832 | -1.80 | $5.51x10^{-4}$ | -1.98 |
| | | T00000068407 | *0.325710* | *-1.44* | 0.008154 | -2.08 |
| Perilipin 2 | *Plin2* | T00000009749 | 0.031875 | -1.60 | 0.018484 | -1.61 |
| Proenkephalin | *Penk** | T00000011892 | 0.031493 | -2.10 | 0.019099 | -2.12 |
| Ficolin A | *Fcna* | T00000023022 | 0.020869 | -1.87 | 0.021104 | -1.82 |
| Coagulation factor II (thrombin) receptor | *F2r* | T00000074626 | 0.006113 | -1.60 | 0.022944 | -1.47 |
| Netrin 1 | *Ntn1* | T00000005255 | 0.024627 | 1.41 | 0.023718 | 1.39 |
| Complement C6 | *C6* | T00000033112 | $5.97x10^{-4}$ | -2.90 | 0.026000 | -2.09 |
| Annexin A2 | *Anxa2* | T00000038677 | 0.035889 | -1.65 | 0.030282 | -1.64 |
| Matrix metalloproteinase-28 | *Mmp28* | T00000083214 | 0.023786 | 1.77 | 0.034051 | 1.68 |
| Cd63 molecule | *Cd63** | T00000010180 | 0.009568 | -1.67 | 0.043524 | -1.51 |

The fold change (FC) and false discovery rate (padj) of 21 significant (padj <0.05) DE gene transcripts that are common to both WKY and SHRSP uterine arteries during the first 6 days of pregnancy. *indicates 2 or more transcript variants for that gene, +indicates 2 transcripts of that gene were found to be significantly differentially expressed in one comparison group; non-significant changes written in italics.

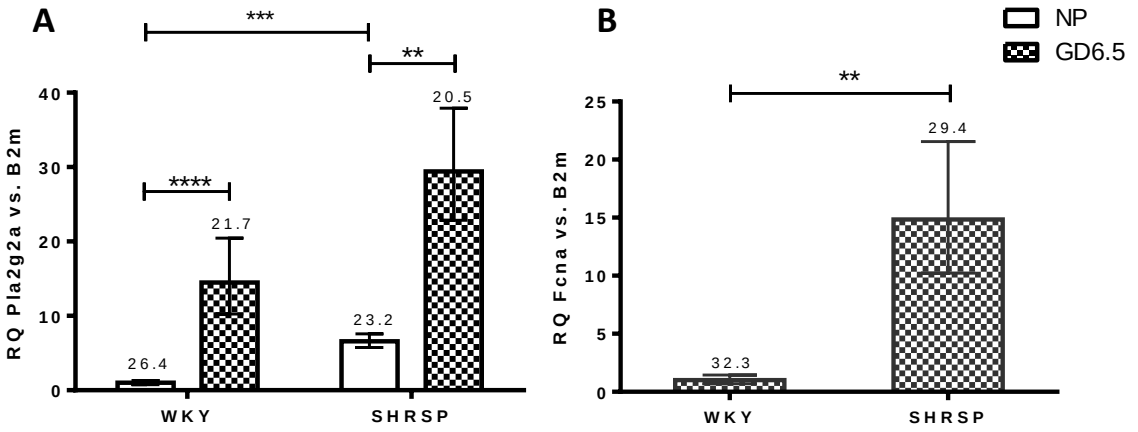


**Figure 5-18: Gene expression quantification of phospholipase A2 and ficolin A in WKY and SHRSP**

(A) Phospholipase A2 (*Pla2g2a*) expression was found to increase in GD6.5 uterine arteries relative to non-pregnant (NP) in both WKY and SHRSP. The relative quantity was also greater in NP SHRSP compared to NP WKY. Analysed using one-ANOVA of the dCT values; **p<0.01, ***p<0.001, ****p<0.0001; n=5-6. (B) Ficolin A (*Fcna*) expression was only detected in GD6.5 uterine arteries and was significantly higher in SHRSP (n=5) relative to WKY (n=4). Analysed using student's t-test of the dCT values; **p<0.01. Numbers above bars indicate the average cycle threshold (CT) values. Data normalised to *B2m* expression and presented as a relative quantity (RQ) to WKY NP (A) or WKY GD6.5 (B).

### 5.4.9 Mitochondrial Function Differences

Pregnancy induced mitochondrial changes were predicted by IPA® to occur only in the WKY group due to the differential expression of the genes stated in Table 5-9. SHRSP did not show any significant differences between non-pregnant and pregnant arteries (Figure 5-19). The genes listed in Table 5-9 are predicted to increase mitochondrial function in WKY GD6.5 pregnant vessels (Figure 5-19)

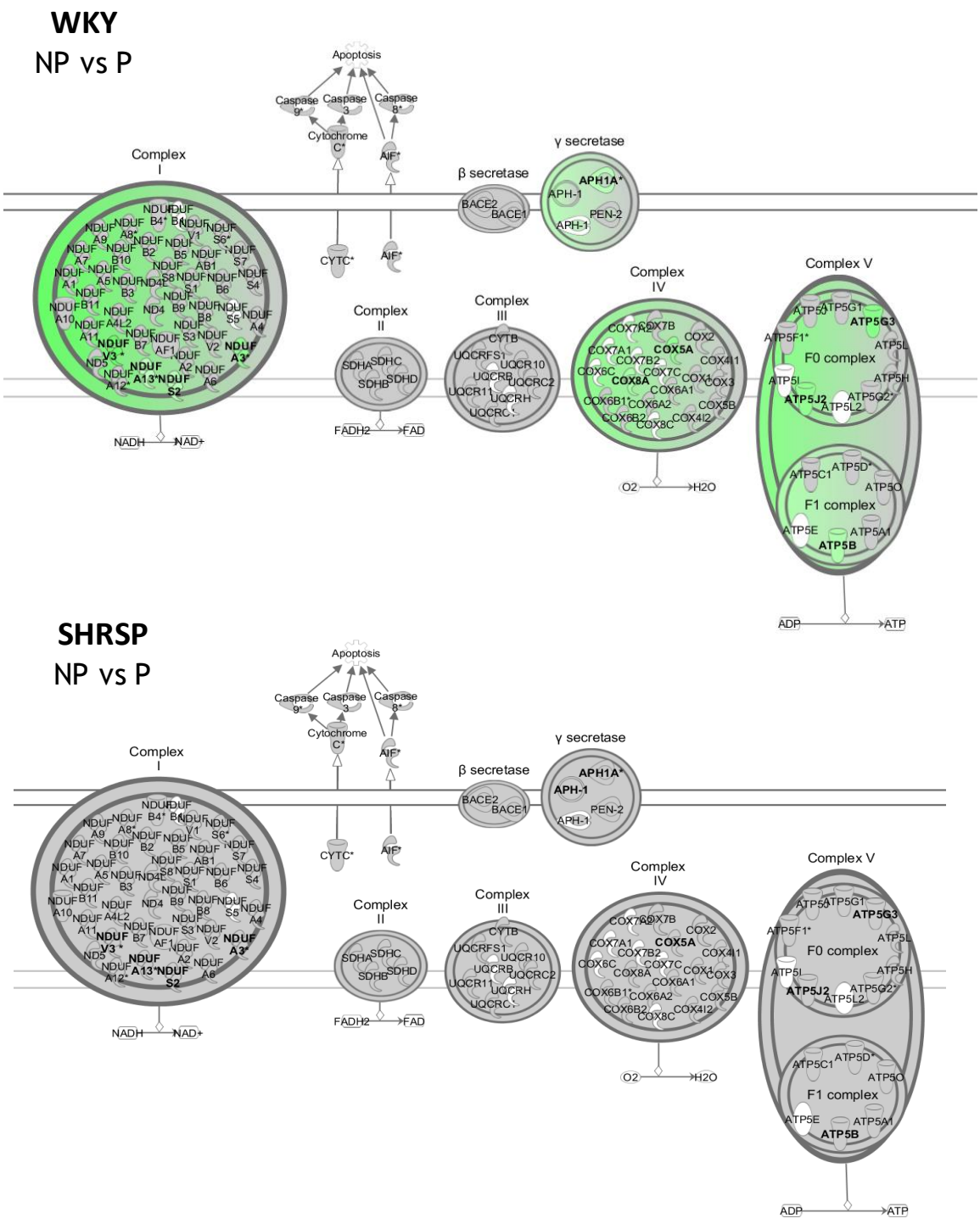


**Figure 5-19: Differential expression of mitochondrial genes in response to pregnancy in WKY and SHRSP**

IPA identified changes in mitochondrial function due to the differential expression of genes in complex I, IV and V and in γ secretase in WKY. These genes had an increased expression in GD6.5 pregnant (P) compared to non-pregnant (NP) and are highlighted in green and bold. No gene changes were found in SHRSP.

**Table 5-9: The differentially expressed genes involved in mitochondrial function changes due to pregnancy**

| Gene name | Gene Symbol | Ensembl Transcript ID | WKY NP vs P | | SHRSP NP vs P | |
|---|---|---|---|---|---|---|
| | | | padj | FC | padj | FC |
| **γ secretase** | | | | | | |
| Aph-1 homolog A, γ-secretase subunit | *Aph1a** | ENSRNOT00000056289 | ***0.034281*** | ***-1.42*** | 0.148424 | -1.30 |
| **Complex I** | | | | | | |
| Nadh:ubiquinone oxidoreductase subunit A3 | *Ndufa3* | ENSRNOT00000091288 | ***0.033190*** | ***-1.75*** | 0.521554 | -1.26 |
| Nadh:ubiquinone oxidoreductase subunit V3 | *Ndufv3** | ENSRNOT00000086272 | ***0.007563*** | ***-2.13*** | 0.750155 | -1.15 |
| Nadh:ubiquinone oxidoreductase core subunit S2 | *Ndufs2* | ENSRNOT00000058423 | ***0.049292*** | ***-1.42*** | 0.863587 | -1.05 |
| Nadh:ubiquinone oxidoreductase subunit A13 | *Ndufa13* | ENSRNOT00000027980 | ***0.024985*** | ***-1.38*** | 0.557827 | -1.12 |
| **Complex IV** | | | | | | |
| Cytochrome c oxidase subunit 5A | *Cox5a* | ENSRNOT00000025525 | ***0.030155*** | ***-1.74*** | 0.434517 | -1.30 |
| Cytochrome c oxidase subunit 8A | *Cox8a* | ENSRNOT00000028754 | ***0.028464*** | ***-1.54*** | 0.836964 | -1.07 |
| **Complex V** | | | | | | |
| ***F0 complex*** | | | | | | |
| ATP synthase, $H^+$ transporting, mitochondrial f0 complex subunit C3 (subunit 9) | *Atp5g3* | ENSRNOT00000058234 | ***0.023756*** | ***-1.80*** | 0.581195 | -1.23 |
| ATP synthase, $H^+$ transporting, mitochondrial f0 complex subunit F2 | *Atp5j2* | ENSRNOT00000033537 | ***0.006157*** | ***-1.70*** | 0.654905 | -1.14 |
| ***F1 complex*** | | | | | | |
| ATP synthase, $H^+$ transporting, mitochondrial F1 complex, ß polypeptide | *Atp5b* | ENSRNOT00000003965 | ***0.012193*** | ***-1.50*** | 0.849460 | -1.05 |

The fold change (FC) and false discovery rate (padj) of mitochondrial genes that were significantly differentially expressed in WKY non-pregnant (NP) vs pregnant (P) and the FC and padj or the same genes from SHRSP NP vs P. Significance is defined as padj <0.05. *genes which have multiple transcripts.

### 5.4.10 Long non-coding RNAs

A major advantage to using RNA-Seq to investigate the transcriptome profile of uterine arteries is that it can detect non-coding transcripts such as long-non-coding RNA (lncRNA). Of the 1966 lncRNAs that were detected in this study, 19 were found to be significantly differentially expressed in one or more of the comparison groups (Table 5-10). These 19 lncRNAs were assessed for proximity to significantly DE protein coding genes, 13 were found to be within 5 million base pairs of significantly DE protein coding genes (Table 5-11). At least one lncRNA was chosen from each comparison group, with a fold change >-2 or <2, to be validated by end-point PCR (Table 5-12). LncRNA 1, 2, 3 and 6 all produce a positive product (visualised on an agarose gel, indicated by band at the appropriate location for the size of the product (Figure 5-20)), indicating that these lncRNAs are transcribed and spliced. These four lncRNA were quantified using SYBR Green qRT-PCR. lncRNA 1 and 2 produced more than one melt-curve peak indicating there is more than one product and therefore could not be accurately quantified (Figure 5-21). However, lncRNA 3 and 6 both produced one product (Figure 5-22). The expression of lncRNA 3 was found to be reduced in vessels from GD6.5 SHRSP compared to non-pregnant which confirmed findings from the RNA-Seq analysis; however, there was no significant difference between the two strains (Figure 5-23). LncRNA 6 showed no significant changes in expression in either of the four comparison groups (Figure 5-23). These lncRNAs were investigated further at a later stage of pregnancy (GD18.5) and lncRNA 3 was found to have a significantly higher expression in WKY compared to SHRSP; no significant changes were observed in lncRNA 6 (Figure 5-24).

**Table 5-10: Significantly differentially expressed lncRNA in the four comparison groups**

| Comparison Group | lncRNA | Ensembl ID | padj | Fold change |
|---|---|---|---|---|
| WKY NP vs P | *AABR07069816.1* | ENSRNOT00000086487 | 0.020451 | -2.23 |
| | *AABR07069840.1* | ENSRNOT00000090495 | 0.028785 | -1.91 |
| SHRSP NP vs P | *AABR07008309.1* | ENSRNOT00000083729 | 0.003342 | -2.10 |
| | *AABR07072528.2* | ENSRNOT00000090119 | 0.013971 | 1.38 |
| | *Rn50_X_0663.2* | ENSRNOT00000076358 | 0.014578 | -2.05 |
| | *AABR07006038.2* | ENSRNOT00000088263 | 0.018484 | 1.31 |
| | *AABR07035065.1* | ENSRNOT00000086043 | 0.024834 | 1.59 |
| | *AABR07019088.1* | ENSRNOT00000084024 | 0.028182 | 1.20 |
| NP WKY vs SHRSP | ***AABR07051787.1*** | **ENSRNOT00000084727** | **$1.05x10^{-16}$** | **-3.91** |
| | ***AABR07001634.1*** | **ENSRNOT00000078019** | **$2.77\ x10^{-11}$** | **-2.68** |
| | ***AABR07030366.1*** | **ENSRNOT00000088573** | **0.000107** | **2.50** |
| | *Rn50_X_0663.3* | ENSRNOT00000041963 | 0.000689 | -2.92 |
| | *AABR07030091.1* | ENSRNOT00000088428 | 0.009267 | -2.14 |
| | *LOC100909586* | ENSRNOT00000086712 | 0.026629 | -1.74 |
| | *AABR07048342.1* | ENSRNOT00000083131 | 0.031622 | -1.94 |
| | *AABR07069473.1* | ENSRNOT00000087743 | 0.032714 | -2.20 |
| | *AABR07043772.1* | ENSRNOT00000077876 | 0.040692 | -1.57 |
| | *AABR07041724.2* | ENSRNOT00000080023 | 0.044570 | -1.66 |
| P WKY vs SHRSP | ***AABR07051787.1*** | **ENSRNOT00000084727** | **1.47E-20** | **-4.08** |
| | ***AABR07001634.1*** | **ENSRNOT00000078019** | **2.47E-09** | **-2.38** |
| | ***AABR07030366.1*** | **ENSRNOT00000088573** | **0.000846** | **2.26** |
| | *AABR07055801.1* | ENSRNOT00000079790 | 0.037022 | 2.10 |

Significantly DE lncRNAs were observed in all comparison groups. Significance was defined as padj <0.05. LncRNA presented in bold highlights duplicates that were differentially expressed in more than one comparison group. LncRNA in bold indicated significant differential expression in more than one group. NP = non-pregnant, P = pregnant.

**Table 5-11: LncRNAs proximal to significantly differentially expressed protein coding genes**

| Group | lncRNA | Direction | Fold change | padj | # proximal pc genes | # significant DE pc genes | PC gene names | Transcript ID | Direction | Fold change | padj |
|---|---|---|---|---|---|---|---|---|---|---|---|
| WKY NP vs P | *AABR07069816.1* | R | -2.23 | 0.020451 | 117 | 2 | *Vwa5a* | ENSRNOT00000015986 | F | -2.19 | 0.001353 |
| | | | | | | | *Hepacam* | ENSRNOT00000012248 | F | 1.90 | 0.029884 |
| | *AABR07069840.1* | R | -1.91 | 0.028785 | 129 | 2 | *Vwa5a* | ENSRNOT00000015986 | F | -2.19 | 0.001353 |
| | | | | | | | *Hepacam* | ENSRNOT00000012248 | F | 1.90 | 0.029884 |
| SHRSP NP vs P | ***AABR07008309.1*** | **F** | **-2.10** | **0.003342** | 41 | 1 | ***C6*** | **ENSRNOT00000033112** | **F** | **-2.09** | **0.026000** |
| | ***AABR07006038.2*** | **R** | **1.31** | **0.018484** | 191 | 7 | *Ifitm1* | ENSRNOT00000005645 | F | -3.20 | $5.88 \times 10^{-7}$ |
| | | | | | | | *Igf2* | ENSRNOT00000073850 | R | 1.92 | $8.62 \times 10^{-6}$ |
| | | | | | | | *Ap2a2* | ENSRNOT00000064254 | F | -1.48 | 0.002450 |
| | | | | | | | ***Mir675*** | **ENSRNOT00000062103** | **R** | **-2.19** | **0.009040** |
| | | | | | | | ***Mob2*** | **ENSRNOT00000027195** | **R** | **1.53** | **0.030760** |
| | | | | | | | *Lsp1* | ENSRNOT00000054864 | F | -1.37 | 0.035560 |
| | | | | | | | ***Igf2*** | **ENSRNOT00000080246** | **R** | **2.05** | **0.043060** |
| | ***AABR07035065.1*** | **F** | **1.59** | **0.024834** | 67 | 4 | *Map2k7* | ENSRNOT00000084460 | R | 1.84 | 0.001090 |
| | | | | | | | ***Rfc3*** | **ENSRNOT00000001444** | **F** | **-2.06** | **0.007220** |
| | | | | | | | *Rxfp2* | ENSRNOT00000001197 | R | 1.64 | 0.015660 |
| | | | | | | | ***Stxbp2*** | **ENSRNOT00000001322** | **F** | **-1.64** | **0.035880** |
| NP WKY vs SHRSP | *Rn50_X_0663.3* | R | -2.92 | 0.000689 | 104 | 3 | *Mrpl4* | ENSRNOT00000049706 | F | 1.81 | $6.49 \times 10^{-5}$ |
| | | | | | | | *Cnn1* | ENSRNOT00000029577 | F | -1.71 | 0.001027 |
| | | | | | | | *Ldlr* | ENSRNOT00000013496 | F | -1.82 | 0.002510 |
| | ***AABR07069473.1*** | **F** | **-2.20** | **0.032714** | 92 | 2 | ***Aldoc*** | **ENSRNOT00000015535** | **F** | **-2.00** | **0.000299** |
| | | | | | | | ***Vtn*** | **ENSRNOT00000039954** | **F** | **-2.14** | **0.002527** |
| | ***AABR07030091.1*** | **R** | **-2.14** | **0.009267** | 101 | 2 | *Samd14* | ENSRNOT00000005519 | F | 2.96 | 0.000596 |
| | | | | | | | ***Abcc3*** | **ENSRNOT00000079711** | **R** | **1.96** | **0.021220** |
| | ***LOC100909586*** | **F** | **-1.74** | **0.026629** | 57 | 3 | *Vcl* | ENSRNOT00000015179 | R | -1.58 | 0.001553 |
| | | | | | | | *Plau* | ENSRNOT00000014273 | R | -1.68 | 0.024306 |
| | | | | | | | ***Kcnk5*** | **ENSRNOT00000075153** | **F** | **1.63** | **0.041872** |
| | *AABR07041724.2* | R | -1.66 | 0.04457 | 115 | 2 | *Plekhg4* | ENSRNOT00000022439 | F | 2.50 | 0.007947 |

| | | | | | | | | | | | |
|---|---|---|---|---|---|---|---|---|---|---|---|
| | | | | | | | *Ces2g* | ENSRNOT00000048385 | F | -1.63 | 0.017913 |
| | *AABR07043772.1* | F | -1.57 | 0.040692 | 48 | 1 | *Eda2r* | ENSRNOT00000017429 | R | 2.12 | 0.041872 |
| | ***AABR07030366.1*** | **R** | **2.50** | **0.000107** | 35 | 1 | *AABR07041724.1* | ENSRNOT00000085536 | R | -4.36 | $2.19 \times 10^{-13}$ |
| P WKY vs SHRSP | *AABR07051787.1* | R | -4.08 | $1.47 \times 10^{-20}$ | 79 | 1 | *Crb2* | ENSRNOT00000037257 | F | 2.36 | 0.029324 |
| | ***AABR07030366.1*** | **R** | **2.26** | **0.000846** | 101 | 1 | *Samd14* | ENSRNOT00000005519 | F | 2.44 | 0.018565 |

The proximity of lncRNA to significant DE protein coding (PC) genes used the cut-off of within 5 million base pairs in either direction from the lncRNA. Genes in bold signify that the protein coding gene is on the same strand as the lncRNA.

**Table 5-12: Selected lncRNA for PCR validation**

| Comparison Group | lncRNA | lncRNA No. | padj | Fold change |
|---|---|---|---|---|
| **NP WKY vs NP SHRSP** | *AABR07051787.1* | 1 | $1.05x10^{-16}$ | -3.91 |
| | *AABR07069473.1* | 2 | 0.032714 | -2.20 |
| **P WKY vs P SHRSP** | *AABR07051787.1* | 1 | 1.47E-20 | -4.08 |
| | *AABR07055801.1* | 3 | 0.037022 | 2.10 |
| **WKY NP vs P** | *AABR07069816.1* | 4 | 0.020451 | -2.23 |
| **SHRSP NP vs P** | *AABR07008309.1* | 5 | 0.003342 | -2.10 |
| | *Rn50_X_0663.2* | 6 | 0.014578 | -2.05 |

The lncRNAs with the greatest fold change were chosen to be validated along with one that was identified to be proximal to significant DE protein coding genes (lncRNA2). Primers were then designed spanning exon-exon boundaries (apart from the primers for lncRNA 6 which only had one exon).

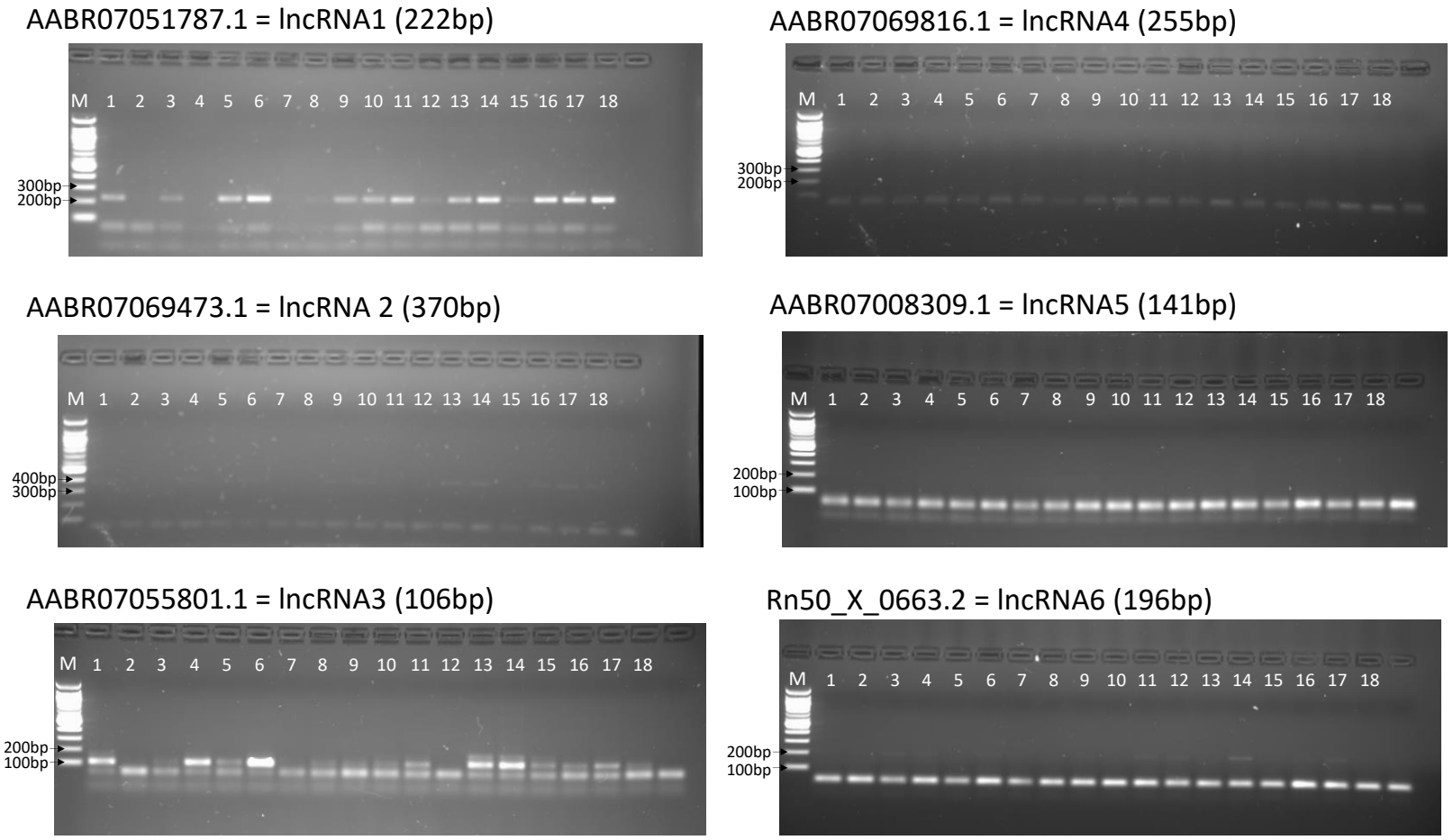


**Figure 5-20: LncRNA PCR products visualised on agarose gels.**
All 6 lncRNA were amplified using PCR and the products visualised on 1.5% agarose gel. Products of approximately the correct size were observed for at least one sample from lncRNA1, 2, 3 and 6. Fragment size is indicated in base pairs (bp) for all lncRNA. Lanes 1-3 = NP WKY, lanes 4-6 = NP SHRSP, lanes 7-9 = GD6.5 WKY, lanes 10-12 = GD6.5 SHRSP, lanes 13-15 = GD18.5 WKY and lanes 16-18 = GD18.5 for all lncRNA except lncRNA1; where lanes 1-2 and 4 = NP WKY, lanes 3 and 5-6 = NP SHRSP. The final lane was used as a non-template control, any product visualised here was assumed to be primer dimer formation.

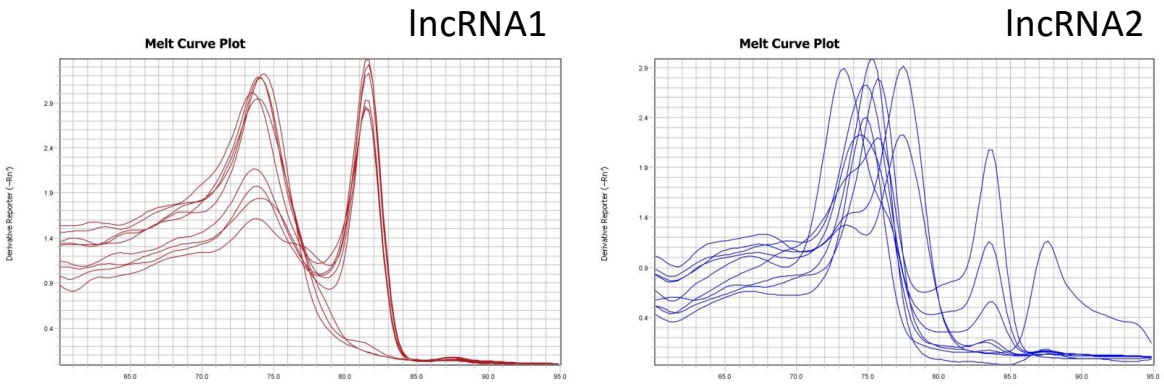


**Figure 5-21: Melt curves of SYBR Green qRT-PCR products for lncRNA1 and lncRNA2**
The expression differences of lncRNA1 and 2 could not be quantified using SYBR Green qRT-PCR as the melt curves demonstrated more than one product was being amplified.

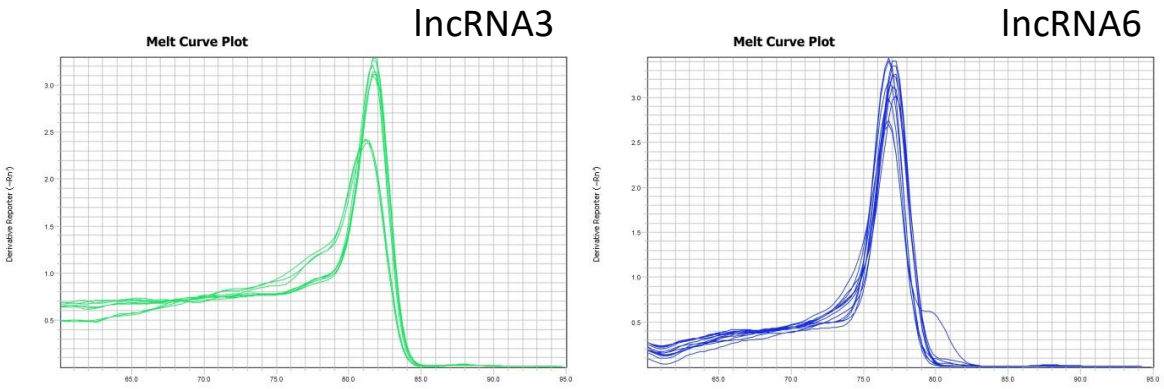


**Figure 5-22: Melt curves of SYBR Green qRT-PCR product for lncRNA3 and lncRNA 6.**
Melt curves produced from the SYBR Green qRT-PCR of lncRNA 3 and 6 demonstrated that only one product was amplified.

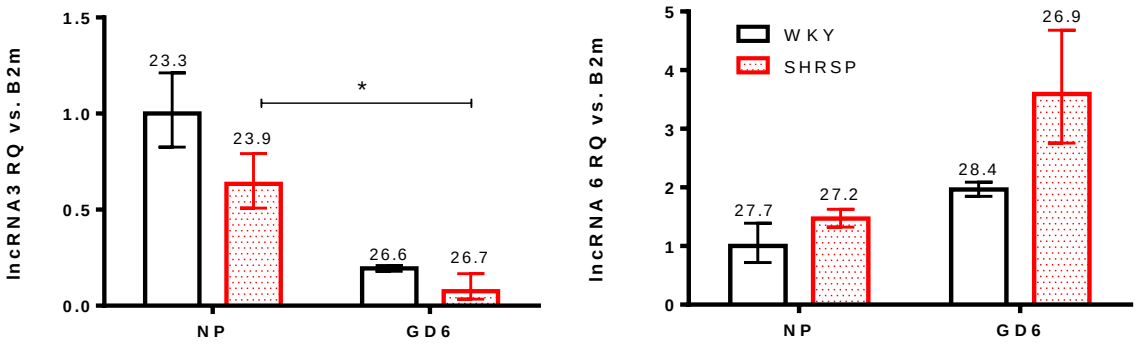


**Figure 5-23: Quantification of lncRNA3 and lncRNA6 in non-pregnant and pregnant WKY and SHRSP**
The relative quantities (RQ) of lncRNA3 and 6 were determined comparing to non-pregnant (NP) WKY. This revealed that lncRNA3 expression was significantly decreased in only one comparison group (SHRSP GD6.5 vs NP). No significant changes in expression were found between any of the comparison groups for lncRNA6. Numbers above bars represent average cycle threshold (CT) values. Data normalised to *B2m* housekeeper and expressed as relative quantity (RQ) to WKY NP. Analysed using one-way ANOVA with Tukey post-hoc test for the four comparison groups previously stated; *p<0.05; n=3-4.

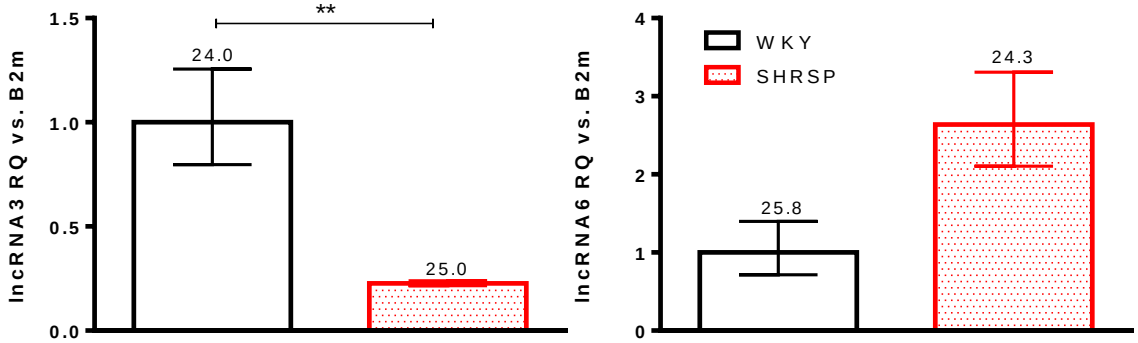


**Figure 5-24: Quantification of lncRNA3 and lncRNA6 at GD18.5 in WKY and SHRSP**
The expression levels of the lncRNA was assessed at GD18.5. LncRNA3 was significantly reduced in SHRSP compared to WKY. There were no significant differences between WKY and SHRSP lncRNA6 expression. Numbers above bars represent average cycle threshold (CT) values. Data normalised to *B2m* housekeeper and expressed as relative quantity (RQ) to WKY. Analysed using student's t-test **p<0.01, n=3.

## 5.5 Discussion

This chapter focused on the changes of the transcriptome profile of uterine arteries in WKY and SHRSP from NP to GD6.5. This provided information on maternal gene expression responses to the 1st week of pregnancy, prior to any observed functional vascular changes. This novel study joins only a few studies that have focused on maternal gene expression during pregnancy. It is the first to have a specific focus of examining the maternal uterine vasculature response to early pregnancy.

The findings from the RNA sequencing study and qRT-PCR validation are at the mRNA transcriptional level, with preliminary follow-up of some of these findings using protein expression (e.g. Nox2) and functional validation (e.g. measurement of calcium signalling). The results provide an insight into the strain differences of WKY and SHRSP, as well as evidence that the transcriptome profile changes in response to pregnancy. The findings of common gene changes to both SHRSP and WKY suggest a necessary vascular response to pregnancy that is conserved in both strains. The biological functions associated with these common gene changes are functions associated with vascular remodelling in pregnancy, as well as other pathological vascular remodelling processes such as hypertension and atherosclerosis (Tajsic and Morrell, 2011, Gomez and Owens, 2012, Ballantyne et al., 2016, Cipolla and Osol, 1994, van der Heijden et al., 2005b). Yet, the pregnancy dependent gene expression changes apparent in WKY and SHRSP uterine arteries do differ, suggesting the two strains have different adaptations to early pregnancy but both successfully produce similar numbers of offspring (see Chapter 3). Interestingly, the number of differential gene changes observed are greater in the SHRSP NPvsP group than in the WKY NPvsP group. This is a feature that has been observed in the SHRSP transcriptome previously, in different tissue. Bailey *et al* demonstrated that the largest number of gene changes in the brain occurred in salt-loaded SHRSP compared to non-salt loaded SHRSP as opposed to the salt-loading changes in WKY (Bailey et al., 2018). This suggests altered gene expressions in response to stressors (such as salt or pregnancy) could be exaggerated in the hypertensive SHRSP rats.

From the analysis of predicted function using the differentially expressed gene profiles in IPA®, four major differences were identified between WKY and SHRSP

response to pregnancy. These included changes to NADPH oxidase expression, $Ca^{2+}$ signalling, inflammation and mitochondrial function. These highlighted pathways are crucial to vascular function and have been implicated in hypertensive disorders of pregnancy as well as in cardiovascular disease (Konior et al., 2014, Sitras et al., 2015, McLachlan et al., 2014, Rubattu et al., 2014). A study of the placental proteome found that the major signalling pathways affected in pre-eclamptic placenta were inflammation and mitochondrial organisation (Jin et al., 2017). These pathways are also influenced by each other with mitochondria and NADPH oxidase both contributing to the production of ROS and this in turn can influence $Ca^{2+}$ signalling and inflammation (Gorlach et al., 2015, Jonckheere et al., 2012). These are important physiological processes required for normal vascular function; however common to the dysregulation of these processes is an imbalance in reactive oxygen species production and metabolism, which can lead to increased oxidative stress and vascular damage.

NADPH oxidase (Nox) is a major source of reactive oxygen species (ROS) and the hyper activation of these enzymes are known to play key roles in vascular endothelial dysfunction and remodelling in the development of hypertension (Montezano and Touyz, 2014). The production of ROS is key to the correct function of many intracellular signalling pathways, including initiating calcium signalling, influencing mitochondrial function and mediating inflammatory responses (Rubattu et al., 2014, Lee and Griendling, 2008, Montezano and Touyz, 2014). There are many isoforms of Nox that have different roles in vascular physiology. The differential gene expressions in this study suggested dysregulation of Nox2 in SHRSP pregnancy, due to the differential expression of the catalytic gp91 subunit (*Cybb*) and regulatory subunit p40phox (*Ncf4*) (Konior et al., 2014, Rivera et al., 2010). Nox2 is expressed in many tissues and in cell types including VSMCs, adventitial fibroblasts, perivascular adipocytes, endothelial cells and macrophages (Konior et al., 2014, Montezano and Touyz, 2014, Datla and Griendling, 2010). It is unclear in this instance which cell type has differential Nox2 gene expression in SHRSP as these can all be found within the vasculature and localisation was not confirmed in the immunohistochemical analysis. An increased ROS production was predicted for the SHRSP vessels due to the increased expression of Nox2 subunits. A dysregulation of Nox2 in the vasculature (including the aorta, coronary artery, saphenous vein and resistance

arteries) has been linked to endothelial dysfunction, inflammation and fibrosis in hypertension (Montezano and Touyz, 2014, Wang et al., 2001, Guzik et al., 2004, Guzik et al., 2006, Touyz et al., 2005). Animal models have shown that Nox2 plays a pathological role in induced hypertension models (Rivera et al., 2010). Wang, *et al,* showed that $Nox2^{-/-}$ mice did not demonstrate increased ROS production or vascular hypertrophy when exposed to AngII induced hypertension (Wang et al., 2001). Due to Nox2's association with hypertension its expression has been previously examined in the SHRSP, as this is a well-established model of human essential hypertension (Davidson et al., 1995, Yamori et al., 1981). Akasaki *et al* found *Cybb* and *Cyba* to be unchanged between WKY and SHRSP (Akasaki et al., 2006). This study also provided no evidence that *Cybb* and *Cyba* expression differs between WKY and SHRSP, only *Cyba* increases in the uterine artery of SHRSP over the first week of pregnancy, a pattern that is not observed in WKY.

Pregnancy dependent changes to gene expression within mitochondria, in complex I, IV and V of the electron transport chain were observed only in WKY. Mitochondria provide energy in the form of ATP to all functioning cells and ROS by-products are produced from the electron transport chain (Han et al., 2001). The maternal energy demand increases during pregnancy due the increase in demands on the cardiovascular, respiratory and renal systems (Pitkin, 1999). One of the sites within the mitochondria that demonstrated an increased gene expression in this study was Complex V. This is also known as ATP synthase and is the final stage of the electron transport chain responsible for ATP synthesis (Jonckheere et al., 2012). This suggests the WKY have an increased energy production in the uterine arteries during the first week of pregnancy, which was not observed in SHRSP. The dysregulation of mitochondrial functions has been associated with cardiovascular disease and hypertension (Ballinger, 2005, Gutierrez et al., 2006, Kokoszka et al., 2001). Changes in mitochondria have also been documented in many pregnancy pathologies, such as pre-eclampsia, fetal growth restriction and gestational diabetes (Furui et al., 1994, Zhou et al., 2017, Mayeur et al., 2013, Holland et al., 2017). However, the changes that have been reported vary on whether the mitochondria content increases or decreases (Holland et al., 2017). Pre-eclampsia has been associated with reduced mitochondrial expression and activity, and thus a shortage of ATP (Zhou et al.,

2017). A reduction of movement of electrons through the electron transport chain can result in an increase ROS production, which is often observed in pre-eclampsia (Furui et al., 1994).

It is interesting that Nox2 and mitochondria both contribute to ROS production and yet in SHRSP pregnancy there is an increased Nox2 expression and no change in mitochondrial components, where as in WKY there is no change in Nox2 expression yet a predicted increase in mitochondrial function. This could suggest that different processes could be altering ROS status during pregnancy in the two different strains. The predicted pregnancy dependent increase in mitochondrial function observed in WKY uterine arteries was due to increases in gene expression in more than one complex; therefore it is a reasonable assumption that the mitochondria are not over producing superoxide (which are known to be produced and can leak from complex I) as the increases in expression of genes in other complexes will keep the flow of electrons moving through the transport chain, thus keeping ROS production at a physiological level (Turrens, 2003). The natural increase in ROS which are associated with increased mitochondrial activity, is likely to be counteracted by increased antioxidant activity. The SHRSP do not show any alterations in mitochondrial gene expression in response to early pregnancy. SHRSP rats have previously been associated with mitochondrial dysfunction (Tokoro et al., 1996), therefore it is possible that the lack of observed pregnancy dependent gene changes is indication of this dysfunction. As mentioned in previous chapters, pregnancy places an increased stress on the maternal cardiovascular system, therefore it could be speculated that pregnancy places an extra demand for energy on the blood vessels, particularly the uteroplacental circulation. The increased expression of several subunits of the mitochondrial electron transport chain observed in WKY may be a pregnancy-induced adaptation to meet the demands for increased energy provision. However, these adaptations were not observed in SHRSP uterine arteries, which may indicate that mitochondria in the blood vessels of SHRSP dams are unable to respond to the increased energy demands placed upon them by pregnancy.

Both WKY and SHRSP were found to have gene expression changes that suggested an increased inflammatory response to pregnancy in the uterine artery. This was

expected as inflammation plays key roles in implantation, pregnancy and labour (Stephen et al., 2015, Bowen et al., 2002, Hauguel-de Mouzon and Guerre-Millo, 2006). However, there was an increased number of differentially expressed genes predicted to influence inflammation in SHRSP, and conditions such as pre-eclampsia and other gestational hypertensive disorders have been associated with an increased inflammatory response (Redman et al., 1999, Trifonova et al., 2014). Some of the SHRSP specific inflammatory genes that were dysregulated were also found in the other specified pathways, such as *Cyba* and *Cybb* from Nox2 and *Mylk* from the calcium signalling pathway. This may suggest that the altered gene expression profile in pregnant SHRSP uterine arteries have a broad effect on many different pathways. This study was able to reveal this interplay due to assessing the transcriptome as opposed to the genome. Therefore, the total gene network and interactions of the differentially expressed genes was visualised as opposed to just acknowledging their presence/absence.

Alterations to genes involved in intracellular calcium release were observed in both WKY and SHRSP pregnancy. This could impact on the molecular communications within the uteroplacental vasculature as $Ca^{2+}$ is a major signalling molecule (Gorlach et al., 2015). The observed genes that had altered transcript expression were different in each strain, with *Ip3R* and *Calm1* showing differential expression only in WKY pregnancy and *Mylk* expression changes observed only in the SHRSP. The WKY gene changes suggest that early pregnancy in these dams is associated with a reduced release of $Ca^{2+}$ in the uterine arteries. An increase in $Ca^{2+}$-calmodulin binding would in turn reduce the availability of intracellular $Ca^{2+}$ and thus diminish constriction responses of vascular smooth muscle. Vascular contraction relies heavily on the interactions of myosin light chain kinase (Mylk) and calmodulin (Calm) as Mylk is Ca2+/calmodulin-dependent (Webb, 2003). Interestingly these two genes show strain specific expression, with pregnant WKY demonstrating an increase in vascular *Calm1* expression with no change in *Mylk*, and SHRSP demonstrating a pregnancy dependent decrease in *Mylk*, with no change in *Calm1*. It is unclear how these expression changes could alter cellular function as their functions are normally interdependent (Webb, 2003). It could be speculated that the 'normal' WKY response to reduce contractility in pregnant vessels does not occur in SHRSP, thus other gene expression changes account for the small reduction in

vasomotor tone observed at GD18.5 (Small et al., 2016). WKY appeared to have a pregnancy-dependent reduction in $Ca^{2+}$ release via the reduction in *Ip3R* expression. However, this expression could not be validated using qRT-PCR, which identified significantly lower expression of *Ip3R* transcript Itpr1 in GD6.5 WKY compared to SHRSP but only a trend towards reduced expression between GD6.5 to NP WKY uterine arteries. The Taqman® probe used in this expression validation was designed to recognise a conserved area in all transcripts between the exon-exon boundaries of the last exons, so this should not have influenced a difference in expression quantification methods. However, due to multiple transcripts influencing expression levels there may have been more variation in the qRT-PCR as this focuses on one transcript of a protein coding gene, where RNA-Seq provides expression data on all transcripts.

Functional calcium signalling was investigated in the VSMC of WKY uterine arteries. Calcium release was found to be reduced in VSMC isolated from pregnant WKY compared to their non-pregnant counterparts, which is consistent with the predictions from the RNA-Seq experiment. However, these cellular function studies were preliminary and would benefit greatly from conducting experiments with greater numbers as well as a comparison to SHRSP VSMC. (Holland et al., 2017) (Haché et al., 2011) It is well recognized that the main contributors of ROS (mitochondria and NADPH oxidase) can influence calcium signalling (Gorlach et al., 2015). This would be an interesting area to study further in the uterine arteries from non-pregnant and pregnant WKY and SHRSP, to determine whether the SHRSP environment at GD6.5 is more detrimental than that of WKY.

Focus was given to the non-pregnant vs pregnant comparison groups in this study since this allowed us to gain insight into the overall characterisation of the early stages of pregnancy dependent uterine artery remodelling. However, the RNA-Seq also produced data regarding strain differences. It revealed that the number of significantly differentially expressed genes was much greater in the non-pregnant strain comparison than the pregnant comparison. It is unclear why this was the case. The relatively short pregnancy of a rat (between 21-23 days) creates an issue with specific timings of tissue collection, which could introduce variation in the pregnant groups thus increasing confidence intervals and

reducing significant detection. An attempt to minimize this variation was made by sacrificing dams at the same time of day and immediately dissecting and freezing the arteries. However, pregnancy confirmation by the presence of a copulation plug meant that there could have been a delay of up to 12 hours after mating for pregnancy to be confirmed. This could introduce variation in the length of an already short gestation, and therefore variation in the transcriptome. Fortunately, this variation would be present and detected in both RNA-Seq and qRT-PCR experiments, unfortunately; due to low RNA quantity, the same samples could not be used for both gene expression assessments. Another factor that could influence the transcriptomic profile of the uterine arteries is the oestrous cycle stage of the rat pre-pregnancy. Details of oestrus cycle stage were not ascertained in this study. These issues could have also influenced the qRT-PCR validation experiments also leading to a lack of significance due to variation within the same group. The conclusions stated would be more robust if further characterisation of the protein expression was conducted and functional studies examining mitochondrial and Nox2 function and calcium release were further investigated in the primary VSMCs.

Previous pregnancy focused transcriptome studies have mainly utilised microarray technology (Enquobahrie et al., 2008, Akehurst et al., 2015, De Felice et al., 2015, Zhao et al., 2014, Lian et al., 2010, Lian et al., 2013, Sitras et al., 2015, Highet et al., 2016). Microarrays produce information about expression of a set of pre-determined genes. This allows for information on specific gene expressions but does not cover the entire genome (Cox et al., 2015, Chandran et al., 2016). RNA sequencing is more beneficial in this respect as it allows for the profiling of tissue and time point specific expression of actively transcribed RNAs. This technique therefore provides information not only on typical protein coding genes, but also on the expression of lncRNAs. There is an emerging role for lncRNAs in regulating and influencing gene expression, which may be dependent on their location and proximity to protein coding genes (Wang and Chang, 2011). In this study the RNA-Seq aligned 1966 lncRNAs with the rat genome. This shows the RNA-Seq accurately detected approximately 60% of the known lncRNAs in rat, however this animal strain has less known lncRNAs (3,288) compared to both mouse and human (9,443 and 14,720 respectively; see Table 1-3 in section 1.3.2 for more comparison details)

This study revealed 19 lncRNAs were significantly differentially expressed between the study groups, with 13 being proximal to a significantly differentially expressed protein coding gene. These genes had a range of functions and it would be beneficial to examine these protein coding genes and their transcriptional regulation in more detail in future. The expression of lncRNA AABR07055801.1 was validated using qRT-PCR, providing more robust evidence of a true expression change. Understanding the role of these lncRNAs will require further study, which is hindered in rat models due to lack of lncRNA investigation and discoveries when compared to the mouse. However, the genome of both WKY and SHRSP has been sequenced and parallels can be drawn between the two animal models as well as new lncRNA discoveries, which would eventually lead to the ability to fully classify them and determine their influence on gene expression and/or biological function.

The RNA-Seq performed in this chapter allowed a vast dataset of gene expression information to be generated. This could be utilised to identify major pathways involved in vascular remodelling. The RNA-Seq analysis provided information on hundreds of significantly differentially expressed transcribed RNAs; only a small subset were investigated during this study. This has been a major drawback, as only a collection of changes observed in RNA-Seq studies are published. Therefore, there is wide variation of the publicised genes that have been found to be dysregulated in gestational hypertensive disorders. This issue has begun to be overcome by full data sets being inputted into repositories (such as the ArrayExpress Archive hosted by the European Bioinformatics Institute), which could lead to a more in-depth examination of RNA-Seq profiles in future.

The major limitation to deciphering any underlying molecular changes to uterine artery functions in this study was that the validation was limited to just three main findings, and furthermore due to time constraints only small sample sizes were available. Future studies should also be considered to fully evaluate functional changes in the key pathways noted in this chapter. For example, Nox2 gene expression changes were found in both the RNA-Seq and qPCR validation as well as the Nox2 changes being evident at the protein level, however this did not provide any information of NADPH production or Nox2 activity which would be beneficial to know in the future.

This study provided evidence that the transcriptome of uterine arteries of WKY and SHRSP respond differently to pregnancy resulting in different gene signatures. Pregnancy was found to be the dominant driver of gene expression changes, with more changes detected between non-pregnant and pregnant uterine arteries, with differences between strains more difficult to detect. It is still unknown whether the SHRSP responses are altering gene expression to adapt to a hypertensive phenotype or whether the gene expression differences are indicating an early dysfunction of the uterine artery's ability to remodel in response to pregnancy. By GD18.5 the SHRSP inability of the uterine artery to adapt to pregnancy correctly is obvious; yet the subtle gene expression changes detected at this early pregnancy time point (GD6.5) make this an intriguing model to study maternal-driven vascular remodelling in hypertensive pregnancy.

# Chapter 6 SHRSP as a Model of Superimposed Pre-Eclampsia

## 6.1 Introduction

Between 25-30% of the population of premenopausal women are estimated to suffer from chronic hypertension (August et al., 2015). These women have a significant increased risk of developing pre-eclampsia during pregnancy. Pre-eclampsia superimposed on chronic hypertension is estimated to effect 15-25% of pregnancies worldwide (August et al., 2015). It is a condition that is increasing in prevalence in the Western world (Savitz et al., 2014, Kearney et al., 2005); possibly due to an increase in childbearing women possessing maternal risk factors for hypertension before pregnancy, such as obesity and advanced maternal age. Superimposed pre-eclampsia is diagnosed by the observations of any of the features used to diagnose pre-eclampsia, detailed in section 1.2, where the pregnant women has already had a hypertension diagnosis pre-pregnancy (or before the 20$^{th}$ week of gestation) (Preeclampsia-Foundation, 2010). The detection of superimposed pre-eclampsia is crucial as it impacts high-risk women (i.e. those with pre-existing hypertension) and can worsen rapidly. Further complications can arise as many premenopausal women are not routinely screened for hypertension, therefore high blood pressure may not be identified pre-conception. Furthermore, pre-pregnancy hypertension can be masked in the first and second trimester by the physiological pregnancy-associated decrease in blood pressure (Hermida and Ayala, 2002). Women with pre-existing hypertension have a significant increased risk of morbidity and mortality, mostly due to the complications associated with a significant further increase in blood pressure (Bramham et al., 2014). This can have a hugely negative impact on the developing fetus and can impact the child's development later in life (Bramham et al., 2014).

The renin-angiotensin system (RAS) plays a crucial role in cardiovascular haemostasis during pregnancy (Chapman et al., 1998). There is a stimulation of RAS components during pregnancy which is contributes significantly to the increased blood volume and cardiac output associated with healthy pregnancy (Figure 6-1) (Langer et al., 1998). The placenta is the largest extra-renal contributor to the RAS and has a major influence over the local RAS regulation and the production of angiotensin II (AngII) (Ihara et al., 1987, Li et al., 2000, Herse et al., 2007). Whilst the production of AngII increases in healthy pregnancy, it is paradoxically associated with a reduced sensitivity to its pressor

response (Gant et al., 1973). Contrary to this, in gestational hypertensive disorders, a dysregulation of the RAS has been observed without alterations in AngII production (Langer et al., 1998). This has been found to lead to AngII vascular hypersensitivity via the $AT_1$ receptor illustrated in Figure 6-2.

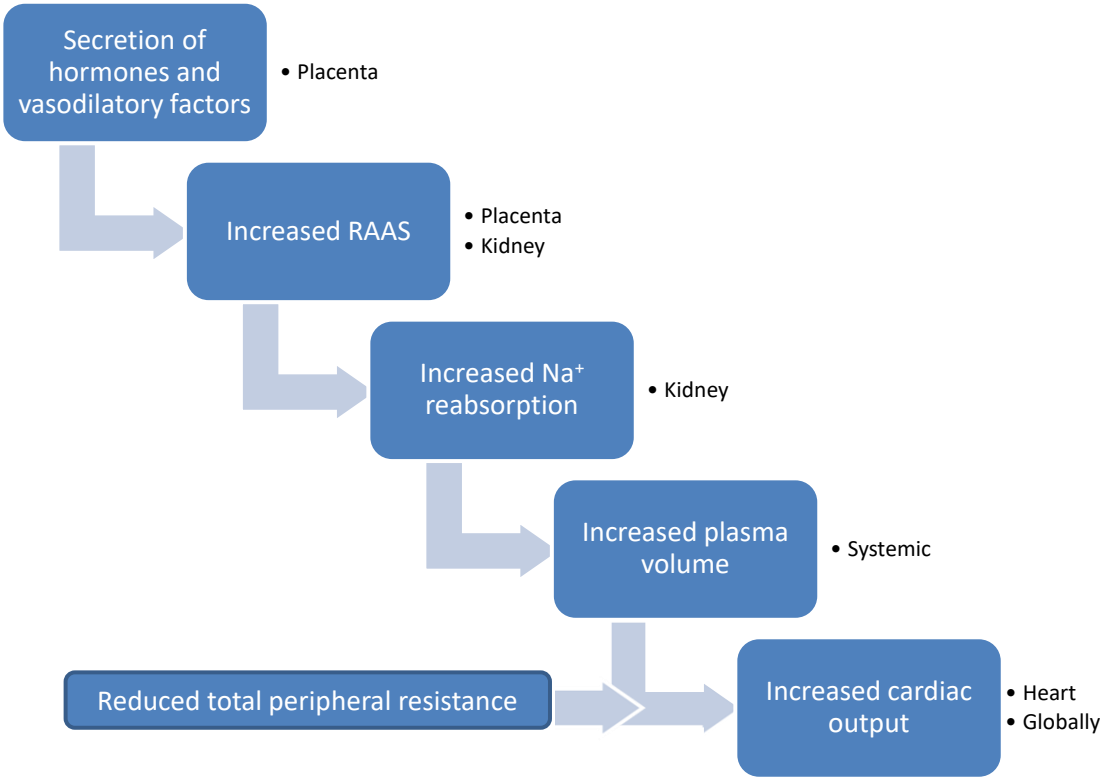


**Figure 6-1: The cascade of physiological changes associated with pregnancy**
Outlined are the major physiological changes that occur to increase cardiac output in pregnant women. The blue boxes are the changes whilst the text beside is the organ responsible/affected.

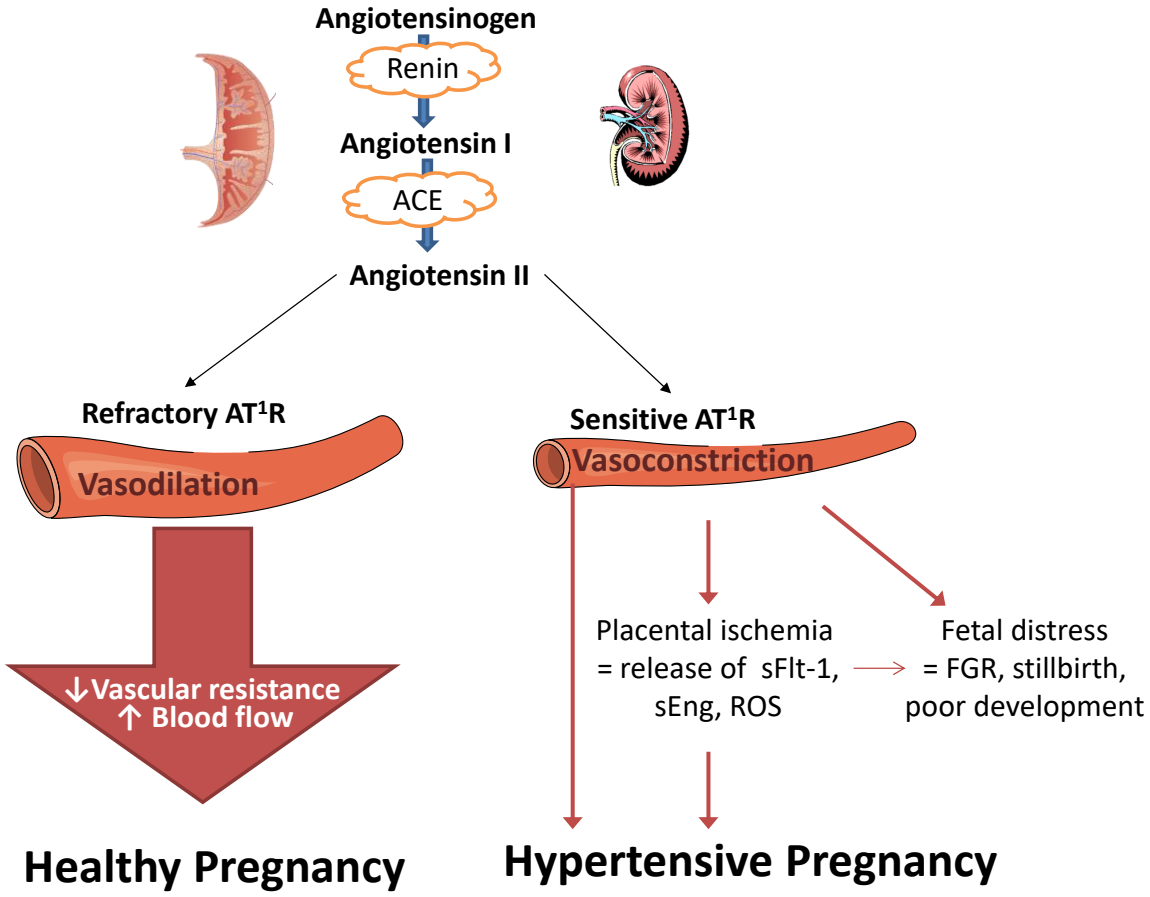


**Figure 6-2: The role of the RAS in healthy and hypertensive pregnancy**
Increases in the RAS are common to both healthy and hypertensive pregnancy. This diagram illustrates the main AngII mediated effects or lack thereof on the vasculature of pregnant women and the outcomes of improper vasodilation due to the AngII receptor type 1 ($AT^1R$) change in sensitivity.

Irrespective of its prevalence and impact on the health and wellbeing of both mother and child; chronic hypertension during pregnancy is relatively under-studied in comparison to other gestational hypertensive disorders, such as pre-eclampsia. A search of the NCBI PubMed database revealed that in 2017 of 1347 papers published on gestational hypertensive disorders 71% focused on pre-eclampsia whereas only 1.6% focused specifically in superimposed pre-eclampsia (search conducted in January 2018; full details of search terms in Appendix 8.2). Having an appropriate animal model on which to study the underlying disease mechanisms would help inform future investigations in women and provide a platform for clinical trials of novel therapeutics.

AngII infusion in rodents has been used by several groups to mimic hypertensive disorders during pregnancy (Arguelles et al., 2017, Xue et al., 2017, Shirasuna et al., 2015, Bohlender et al., 2000, Takimoto et al., 1996, Hering et al., 2010, Verlohren et al., 2010). The chief focus has been on hypertension development in later life in offspring exposed to AngII *in utero* with few AngII infusion models investigating maternal adaptations. Shirasuna et al have demonstrated that an infusion of AngII in pregnant wild type and inflammasome deficient mice causes an increase in blood pressure and reduction in fetal weight that is associated with increased placental inflammation (Shirasuna et al., 2015). Infusion of AngII in pregnant Sprague-Dawley rats had similar maternal effects and found that further to the pro-inflammatory cytokines in the brain of the offspring, as adults they had an increased pressor response to AngII (Brewer et al., 2013, Xue et al., 2017). Circulating and local placental AngII have been investigated using a refined transgenic cross rodent model which increases placental-specific AngII production (Hering et al., 2010, Geusens et al., 2008, Verlohren et al., 2008, Bohlender et al., 2000, Takimoto et al., 1996). The consensus from these studies revealed that dams exhibited a sudden yet sustained increase in blood pressure from mid-gestation which returned to pre-pregnancy levels after delivery. This was found alongside an increase in proteinuria, evidence of kidney damage and a reduction in fetal weight, all commonly associated with pre-eclampsia in humans.

As mentioned in previous chapters, the pregnant stroke-prone spontaneously hypertensive (SHRSP) rat is hypertensive prior to and throughout gestation (Small

et al., 2016). The elevated blood pressure associated with this model is accompanied with reduced uteroplacental blood flow and impaired uterine artery function during pregnancy (Small et al., 2016). This impaired vascular response to pregnancy is a key phenotype of human pre-eclampsia and was found to occur independently of the chronic hypertension in SHRSP rats. Despite these complications, the SHRSP are able to produce viable offspring at birth and they lack the more severe characteristics of pre-eclampsia. For this reason, this study was designed to impose a greater challenge to the cardiovascular system of pregnant SHRSP, using infusion of AngII, to generate a novel model of superimposed pre-eclampsia.

## 6.2 Hypothesis and Aims

### 6.2.1 Hypothesis

Angiotensin II infusion will increase the hypertensive insult on the maternal cardiovascular system of the pregnant SHRSP and imitate superimposed pre-eclampsia phenotypes.

### 6.2.2 Aims

- To develop an animal model useful for the study of gestational hypertensive conditions that arise on a background of chronic hypertension

- To investigate how AngII infusion impacts the maternal cardiovascular and renal system during pregnancy in SHRSP rats

- To assess if AngII infusion impacts pregnancy dependent vascular adaptations

- To examine any impact AngII infusion during pregnancy has on fetal development and placental structure

## 6.3 Materials and Methods

Animals were housed and mated as described in general materials and methods section 2.3). Urines were collected using 24-hour collections in metabolic cages at time points; one-week pre-pregnancy, at GD6.5 and at GD14.5. Echocardiography and uterine Dopplers were recorded at these time points, along with venous blood collected from the tail vein. Maternal blood pressure was recorded at the time points specified above via tail cuff plethysmography or monitored throughout gestation and parturition using radiotelemetry. Maternal tissue and fetoplacental units were obtained at gestational GD18.5, a time point at the end of pregnancy yet prior to the dip in blood pressure observed in SHRSP dams (Small et al., 2016). Functional and passive mechanical properties of the uterine and mesenteric arteries was assessed using myography. Placentas were dissected and fixed or frozen for histological or gene expression analysis. Full details of these methods can be found in the general materials and methods (sections 2.2, 2.3, 2.4 and 2.5).

### 6.3.1 Angiotensin II Treatment via Osmotic Minipump

AngII doses were delivered via osmotic minipumps implanted in pregnant rats. The dose was determined with guidance from Dr Ralf Dechend and Dr Florian Herse, according to AngII treatment regimes used previously in pregnant rat studies (Hering et al., 2010). Prior to AngII infusion dams were weighed at GD9.5 and randomly assigned to either vehicle, 500ng/kg/min AngII or 1000ng/kg/min AngII treatment groups.

ALZET® 2002 osmotic minipumps (Charles River, Kent, UK) were used to obtain a constant infusion of AngII over the last 8-12 days of pregnancy from GD10.5. These minipumps had a constant 0.5µl/hour flow rate for 14 days, after this period flow rate was unreliable. Preparation of AngII solutions and the minipumps were carried out under sterile conditions and sterile latex, powder-free gloves were worn at all times when handling the minipump. A stock 50µg/µl AngII solution was prepared using sterile $H_2O$. The ALZET® 2002 osmotic minipumps have a reservoir volume of 200µl therefore, in order to achieve complete filling of the minipump, AngII stock was then diluted in sterile $H_2O$ to a volume of 300µl. This dilution was calculated as required based on the GD9.5 weight of the dam and which treatment group she belonged, as well as the flow

rate of the osmotic minipump. The minipump and flow moderator were removed from packaging and placed in a sterile pre-weighed 5ml Sterilin™ container (VWR, Leicestershire, UK). The weight of the empty minipump was recorded. A filling tube (sterile blunt tipped needle appropriate for 200µl reservoir volume) (Charles River, Kent, UK) was attached to a 1ml syringe containing 300µl of appropriately diluted AngII solution. The minipump was carefully filled by inserting the filling tube into the reservoir and expelling the solution slowly in an upright position. It was of crucial importance that no air bubbles were forced into the minipump reservoir by rapid filling or trapped air in the syringe as this can interfere with the flow rate. Once filled, the flow moderator was gently inserted into the reservoir and any excess solution wiped away. The minipumps were then returned to the same 5ml Sterilin™ container and re-weighed. The difference between this weight and the original empty weight (mg) gave an indication of the volume of solution loaded into the pump (µl); this was always greater than 90% of the stated mean fill volume stated on the manufacturers product insert. Filled minipumps were then primed overnight by placing in 0.9% sterile saline solution at room temperature. This ensured that upon implantation the minipump begins delivery of AngII at the correct rate immediately.

#### 6.3.1.1 Minipump Implantation Surgery

Surgery was conducted under sterile conditions with the operating table covered with sterile surgical drapes and surgical gowns and gloves were worn at all times. All instruments were autoclaved prior to use. Dams at GD10.5 were anaesthetised as in section 2.3.2 and maintained at 3% isoflurane in 1.5L/min oxygen. The procedure was carried out in the prone position, with the animal slightly turned on its left side. The right flank of the dam was shaved and swabbed with povidone-iodine solution (Betadine®). A superficial incision (approximately 3cm in length) was made in the skin parallel to the shoulder blade using surgical scissors. The left side of the incision was held with toothed forceps and gently lifted. The skin was parted from the muscular layer underneath by gently opening and part-closing the scissors within the incision to produce a subcutaneous pocket. The pocket was held open and the minipump was removed from the saline solution using toothed forceps. The minipump was inserted subcutaneously, with the flow moderator distal to the incision site. The incision was then sutured using VICRYL® Ethicon sutures (NU-CARE,

Bedfordshire, UK). Rats were given 5mg/kg Rymadil analgesic subcutaneously and placed in clean cages. The well-being of the dams was checked daily.

### 6.3.2 Neonatal Sacrifice

Dams placed in the radiotelemetry group were allowed to progress to parturition. The number of neonates born was recorded as soon as the litter was observed (between 1-14 hours after birth) and this was allocated as the day of birth. Litter number was recorded and the neonates were weighed together on day 1 and day 2. The weights were divided by litter number to give a neonatal weight average for each dam. Neonates were sacrificed using decapitation on day 2 due to the minipumps implanted in dams at GD10.5 (section6.3.1) only having a reliable constant infusion for 14 days. Approximately 1-2ml of blood was collected in EDTA BD Vacutainer® tubes with 50µl of 25mM 1,10-phenanthroline monohydrate (a metalloprotease inhibitor to prevent AngII degradation) and placed on ice to prevent clotting (Düsterdieck and McElwee, 1971). Blood remained at 4°C for no longer than 30 minutes before being centrifuged at 1200xg for 20 minutes at 4°C to obtain plasma. The plasma was collected and stored at -80°C. The neonatal heads and bodies were weighed and recorded. Hearts and kidneys were then dissected and snap frozen in liquid nitrogen for RNA extraction and subsequent gene expression analysis (detailed in sections 2.2.1, 2.2.2, and 2.2.3)

### 6.3.3 Enzyme Immunoassay Detection of Plasma AngII

The concentration of AngII in plasma samples collected in section 6.3.2 was determined using an SPI-bio enzyme immunoassay (EIA) kit assay specific for AngII detection (Bertin Bioreagent, Yvelines, France). Samples where defrosted and kept on ice. The angiotensin peptides were extracted from the sample by passing 1ml of plasma through a washed and prepared phenyl column and eluting absorbed peptides with methanol. The methanol was evaporated and the peptides resuspended in 500µl of EIA buffer and centrifuged at 3000xg for 10 minutes at 4°C. Standards, reagents and buffers were prepared as instructed by manufacturer's instructions and all samples and reagents brought to room temperature. Standard concentrations ranged from 125pg/ml to 0.98pg/ml. Samples, standards and an AngII quality control were diluted 1:1 with EIA buffer

and added to the 96-well EIA plate in duplicate. The plate was covered and incubated at room temperature for one hour with gentle agitation on a Rotatest orbital plate shaker (LUCKHAM R100, at low speed). Equal amounts of glutaraldehyde and borane trimethylamine (50µl) were added to each reaction; excluding the blank wells, which would act as a negative control. These reagents covalently linked the peptides to the immobilised anti-AngII antibody and denatured them in order to release the epitope. The plate was washed with the supplied wash buffer 5 times and any excess buffer was removed by blotting the plate on absorbent paper. This released epitope was detected using 100µl AngII tracer that was conjugated to acetylcholinesterase. The plate was covered and incubated overnight at 4°C. The plate was washed as previously described, this wash process was repeated twice, and 200µl of Ellman's reagent, containing the enzymatic substrate, was added to each well. The plate was covered and incubated at room temperature in the dark for 1 hour. The production of the chromogen (5-thio-2-nitrobenzoic acid) appeared yellow and the plate was read on a SpectraMax M2 microplate reader (Molecular Devices, Berkshire, UK) at 410nm. Blanks were subtracted from all samples and standards and a standard curve constructed to extrapolate the unknown sample concentrations.

### 6.3.4 Scoring of Placental Glycogen Staining

Placental sections were stained with periodic acid Schiff, as in the general materials and methods section 2.2.6.2, and imaged, as in section 2.2.8. Placental glycogen cell content was determined by the percentage of positive magenta staining in the junctional zone, this section was outlined and staining intensity measured as a percentage of positive pixels (section 2.2.8). Placenta were also scored for junctional zone disorganisation with 1 denoting organised and structured cell layers comprising of glycogen cells trophoblast giant cells and spongiotrophoblasts, and 5 being the highest score for observing disorganisation, associated with almost complete loss of structured, ordered cell layers with major gaps between cell types.

# 6.4 Results

## 6.4.1 Maternal Pregnancy Profile

### 6.4.1.1 Survival Rate

AngII infusion was conducted in pregnant WKY and SHRSP rats. WKY rats were included as normotensive controls; however they were removed from further study after a pilot study revealed very low survival rate. Figure 6-3 illustrates the proportion of dams that survived (grey) or that were removed from the study early due to deterioration of health (red); study length was to GD18.5. WKY had 100% survival in the vehicle treated group, but only a 25% survival when treated with 500ng/kg/min AngII and none survived the 1000ng/kg/min AngII treatment. The deterioration of health in the latter group was much more rapid (between 2 and 4 days after infusion began) than that of the SHRSP dams, thus the WKY rats were removed from further study. Dams were removed from the study due to a weight loss of >20% of their pre-pregnancy weight and a loss in the condition of the animal. Better survival rates were observed in SHRSP dams. The entire group of vehicle treated dams survived for the duration of the study; with a 12.5% removal from study for 500ng/kg/min AngII treatment and a 33.3% removal from study for 1000ng/kg/min AngII treatment.

Table 6-1 details the numbers of pregnancies that resulted in a successful pregnancy carried until study completion (GD18.5), animals that showed deterioration and where removed from study but were still carrying a pregnancy and also those animals that had lost the pregnancy post-AngII infusion.

**Table 6-1: Pregnancy success and failure rates**

| | WKY | | | SHRSP | | |
|---|---|---|---|---|---|---|
| | Vehicle | AngII 500ng | AngII 1000ng | Vehicle | AngII 500ng | AngII 1000ng |
| *Number of pregnant dams* | 6 | 4 | 2 | 8 | 8 | 15 |
| *Fetal survival to GD18.5* | 6 | 1 | 0 | 8 | 7 | 10 |
| *Pregnant at time of removal from study* | - | 1 | 0 | - | 1 | 3 |
| *Total litter resorption at time of removal* | - | - | 2 | - | - | 2 |

The total number of pregnant rats used and whether they carried a pregnancy to term (GD18.5) or were removed from the study prior to this time point due to deterioration of maternal health. Also indicated is whether the pregnancy was still apparent (by the presence of well-developed fetuses) or whether pregnancy had been lost (evident by the appearance of a total resorption of all fetoplacental units) at the time of maternal death.

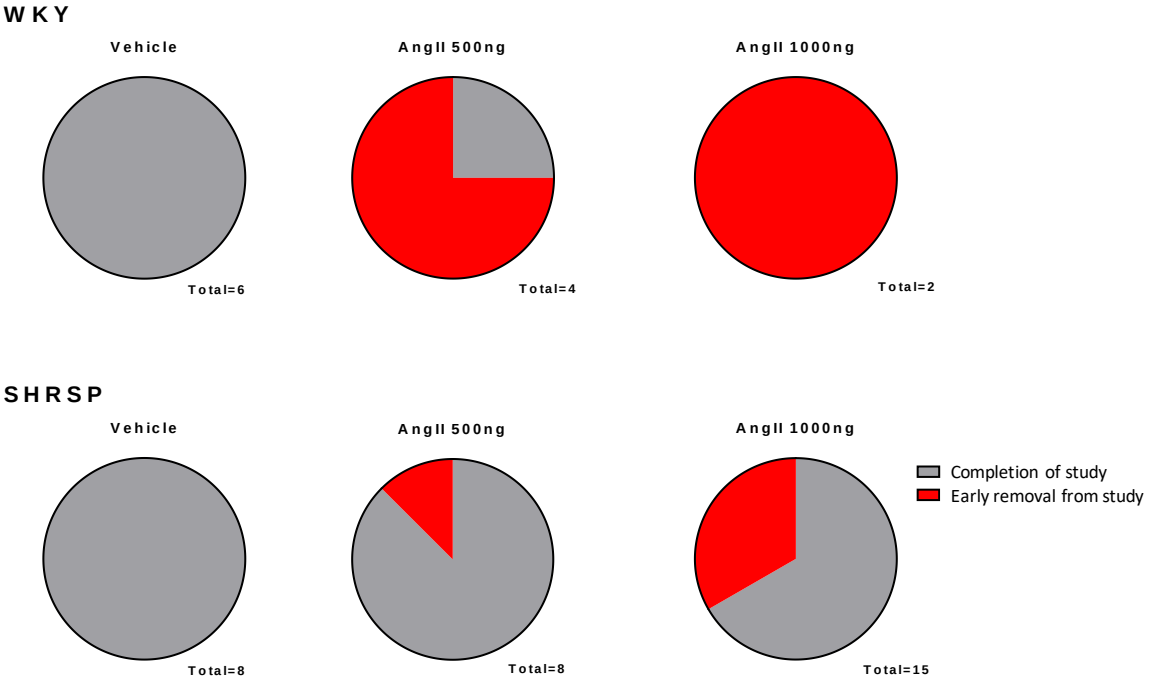


**Figure 6-3: Survival rates as a proportion of total number of dams used in study group**
The proportional survival of dams that completed the study successfully (grey shade) and dams that were removed due to deterioration of health (red), with the total of pregnant rats used stated to the right of each group. Completion of the study was determined by carrying the pregnancy to GD18.5.

#### 6.4.1.2 AngII Influence on Maternal Weight Change

Pregnancy is associated with an increase in weight, due to increases in maternal adipose tissue, blood volume and the developing fetuses. The vehicle treated SHRSP exhibited a net maternal weight gain over the course of pregnancy, independent of the weight of the gravid uterus (147±5.3g GD0.5 versus 186±2.9g GD18.5; $p<0.001$), whilst the dams in the 500ng/kg/min AngII treatment group did not demonstrate a significant change in maternal weight (147±9.3g GD0.5 versus 170.0±9.7g GD18.5) and the 1000ng/kg/min AngII treatment group had a net decrease in gravid independent weight over the course of pregnancy (154±3.2g GD0.5 versus 133.7.3±g GD18.5; $p<0.05$) (Figure 6-4A). By GD18.5 the gravid maternal weights of dams treated with 1000ng/kg/min AngII were significantly less than the 500ng/kg/min AngII treatment group and the vehicle group (160.0±10.3g versus 199.8±14.5g and 213.0±4.8g respectively; $p<0.01$ and $p<0.0001$) (Figure 6-4B). These weight changes were not due to a reduction in the number of fetuses per litter as the weight change was corrected for the number of fetuses (Figure 6-4C). The weight change per fetus was significantly less in the 1000ng/kg/min treatment group compared to all other groups (1000ng/kg/min: 0.4±2.5g versus 500ng/kg/min: 5±1.0g; $p<0.01$ and vehicle: 7±1.4g; $p<0.001$), with a negative weight change indicating 3 of the dams in this group fell below their pre-pregnancy weight (Figure 6-4C).

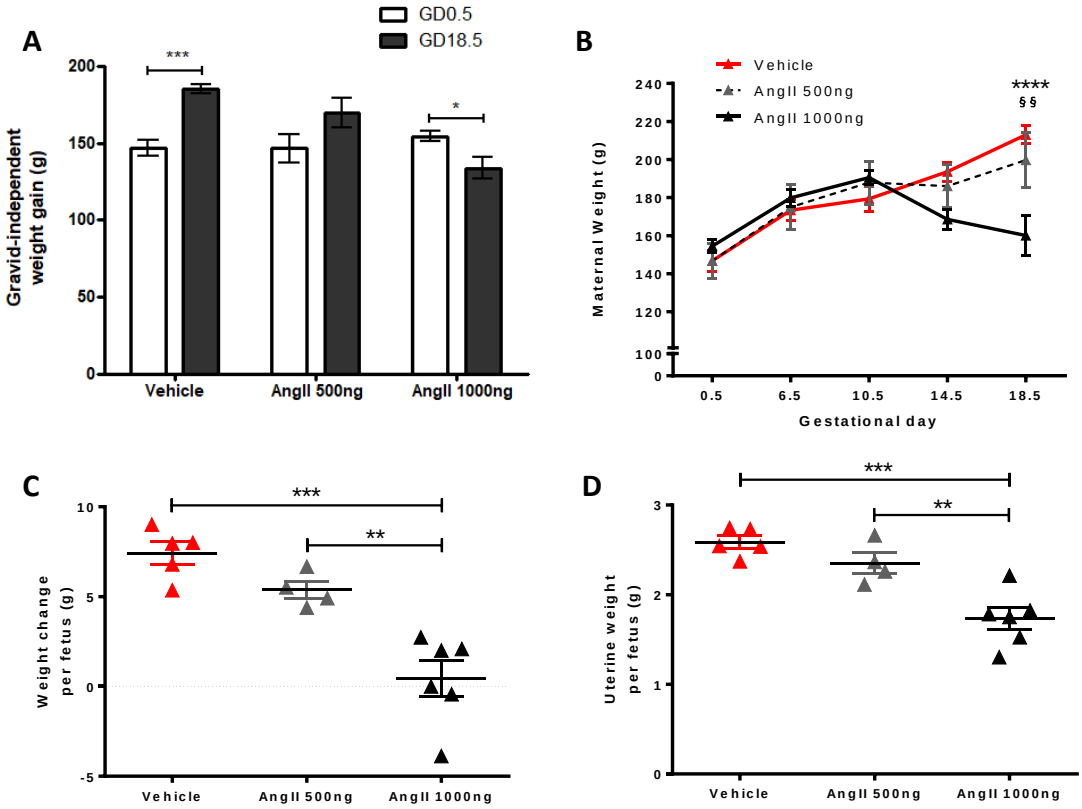


**Figure 6-4: Maternal weight change from the beginning of pregnancy to term**
Maternal weights were recorded throughout pregnancy. **(**A) The pregnancy independent maternal weight change was significantly increased from GD0.5 (when pregnancy was confirmed) to GD18.5 in the vehicle group (***p<0.001; n=5) but was unchanged in dams treated with 500ng/kg/min AngII (n=4) and reduced in 1000ng/kg/min AngII treated dams (*p<0.05; n=6); analysed using one-way ANOVA with Tukey post-hoc test. (B) The weight change across pregnancy including the fetoplacental unit weights shows all pregnant dams gained weight before minipump implantation (GD10.5) and the 1000ng/kg/min AngII treated dams lose this pregnancy weight with AngII infusion and by GD18.5 have a significantly lower weight than vehicle and 500ng/kg/min AngII treated dams (****p<0.0001 vs vehicle; §§p<0.01 vs 500ng/kg/min AngII, n=4-6; analysed using two-way ANOVA with Bonferroni post-hoc test). (C) The total weight gain expressed per fetus reduced any influence litter size had on maternal weight change. This showed 1000ng/kg/min AngII treated dams did not put on as much weight as the vehicle or 500ng/kg/min AngII treated dams; with some AngII 1000ng dams losing weight by GD18.5 (***p<0.001 vs vehicle and **p<0.01 vs 500ng/kg/min AngII treated dams). (D) The total uterine weight (including the fetoplacental units) at GD18.5 corrected for the number of fetuses per littler was significantly lower in the 1000ng/kg/min AngII treated group compared to both other groups (***p<0.001 vs vehicle and **p<0.01 vs 500ng/kg/min AngII treated dams). All data are expressed as mean ±SEM; analysed using one-way ANOVA with Tukey post-hoc test

#### 6.4.1.3 Blood Pressure Profile of AngII Infused SHRSP Dams

Blood pressure monitoring of AngII infused SHRSP dams was conducted using tail cuff plethysmography; detailed in the general materials and methods section 2.3.4, as a pilot study to determine appropriate AngII doses. All the SHRSP dams were borderline hypertensive prior to pregnancy compared to non-pregnant WKY rats as a reference strain (Vehicle: 141±8.5mmHg, 500ng/kg/min: 143±13.4mmHg and 1000ng/kg/min: 147±3.3mmHg). Figure 6-5A details the blood pressure of the SHRSP dams in each treatment group over the course of pregnancy; pre and post AngII infusion (which was implanted via minipump at GD10.5). The vehicle treated SHRSP rats remained borderline hypertensive, with no significant changes over the course of pregnancy (GD6.5: 139±5.7mmHg, GD14.5: 132±1.6mmHg and GD18.5: 141±13.7mmHg). There was a significant increase in the blood pressure of dams treated with 500ng/kg/min AngII GD14.5 (4 days post AngII infusion) compared to both pre-pregnancy and pre-AngII infusion (GD6.5) blood pressure measures (NP: 143±13.4mmHg, GD6.5; 150.1±7.3mmHg versus GD14.5: 180±0.4mmHg; $p<0.05$). However, by the later stages of pregnancy (GD18.5) the blood pressure was no longer significantly higher than pre-pregnancy or pre-AngII measurements (171±8.0mmHg). The dams in the 1000ng/kg/min AngII treatment group had a significant increase in blood pressure compared to pre-pregnancy (NP: 147±3.3mmHg versus GD14.5: 172±7.7mmHg; $p<0.05$, and GD18.5: 195±7.2mmHg; $p<0.001$). This treatment group also showed a significant increase in blood pressure from GD6.5, prior to AngII minipump implantation in both post-AngII infusion measurements (GD6.5: 146±6.5mmHg; $p<0.001$ and $p<0.05$ respectively). A significant increase between GD14.5 and GD18.5 was also determined in the 1000ng/kg/min treatment group ($p<0.05$). The change in blood pressure is represented in Figure 6-5B. Both SHRSP AngII treatment groups had a significant increase in blood pressure from a non-pregnant baseline compared to the vehicle treated group at GD14.5 (500ng/kg/min AngII: 23±8.0mmHg, 1000ng/kg/min AngII: 24±8.2mmHg versus vehicle: -5±8.5mmHg change; $p<0.05$ and $p<0.01$ respectively). Only dams in the 1000ng/kg/min AngII treatment group demonstrated a significantly raised blood pressure at GD18.5 (47±6.9mmHg versus 0.6±6.9mmHg change; $p<0.001$).

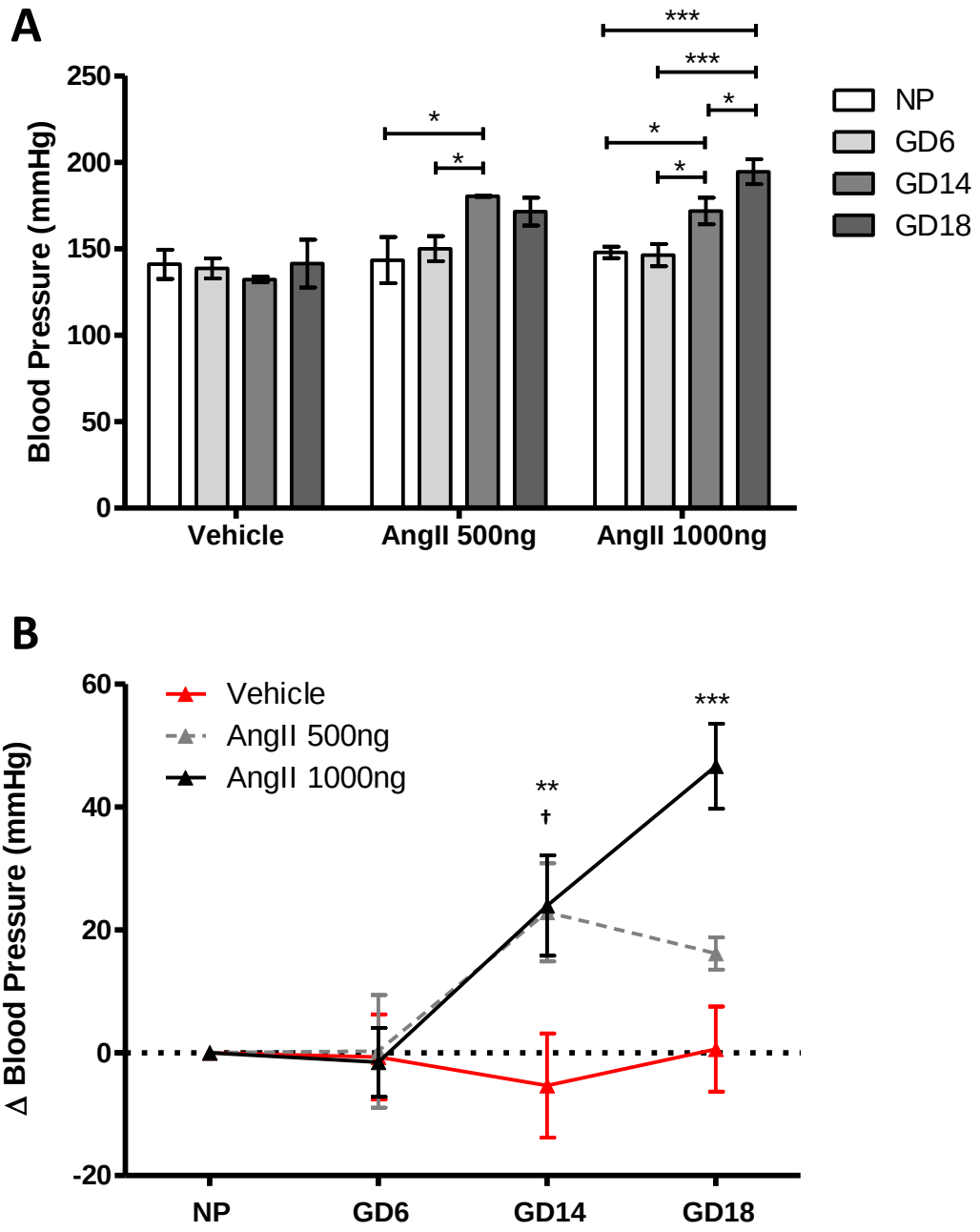


**Figure 6-5: The influence of AngII treatment on maternal blood pressure pre-pregnancy and at three specific pregnant time points.**
Blood pressure was measured at a non-pregnant (NP) time point and at pregnant, pre-AngII infusion (GD6.5) and pregnant, post AngII infusion (GD14.5 and GD18.5) time points by tail cuff plethysmography. (A) The absolute values of systolic blood pressure at the different time points. There was no significant change between non-pregnant and pregnant blood pressures in the vehicle. The blood pressure of 500ng/kg/min AngII and 1000ng/kg/min AngII treated dams showed a significant increases from NP and GD6.5 (pre-AngII infusion). 1000ng/kg/min AngII treatment also showed a significant increase at GD18.5 compared to all other time points. Data expressed as mean ±SEM; time points compared within each separate group; analysed using repeated measure one-way ANOVA with Tukey post-hoc test; *p<0.05, ***p<0.001 n=4-6. (B) The blood pressure across pregnancy expressed as a change from NP. Both AngII treatment groups had significantly higher blood pressure than vehicle at GD14.5 (AngII 500ng: †p<0.05 and AngII 1000ng: **p<0.01), only 1000ng/kg/min AngII demonstrated significant change from vehicle at GD18.5 (***p<0.001); analysed using two-way ANOVA with Bonferroni post-hoc test; n=4-6.

#### 6.4.1.4 Direct Haemodynamic Measurements of AngII Infused SHRSP Dams

Radiotelemetry is the gold standard in blood pressure monitoring in conscious animals and was used to fully assess haemodynamic changes, including systolic and diastolic blood pressures, activity and heart rate. These direct measurements were obtained for one week prior to pregnancy (during this time the animal was mated) and throughout gestation and parturition. Data for untreated WKY rats was obtained from previous radiotelemetry experiments conducted in 2013; however data was analysed at the same time as the SHRSP rats in this study. All SHRSP groups had a significantly higher average blood pressure in the 5 days before pregnancy than the untreated WKY group (SHRSP: 156±0.6mmHg, 153±0.6mmHg, 157±0.5mmHg versus WKY: 118±0.6mmHg; systolic pressure; $p<0.01$). There were no significant differences in any of the measured haemodynamic parameters between the pregnant vehicle SHRSP group and either pregnant AngII treatment group prior to AngII infusion, between GD0.5 and GD10 (Figure 6-6 and Figure 6-7). After AngII infusion only the 1000ng/kg/min AngII infusion caused a significant increase in systolic blood pressure compared to vehicle after GD10.5 (192±2.1mmHg versus 144±2.3mmHg; $p<0.05$) (Figure 6-6A), whereas diastolic pressure was significantly increased in both the 500ng/kg/min AngII and the 1000ng/kg/min AngII treatment groups (157±2.3mmHg and 158±2.2mmHg versus 105±1.7mmHg; $p<0.01$ respectively) compared to vehicle after GD10.5 (Figure 6-6B). Mean heart rate was not significantly affected by AngII treatment (Figure 6-7A); however a sudden decrease was observed in the 1000ng/kg/min AngII treatment group immediately after minipump implantation and this group also demonstrated a change in the typical diurnal rhythm, with a loss of amplitude after AngII infusion. The activity, as measured by count of movement, was measured every 5 minutes throughout the experiment. Dams treated with AngII were found to be more sedentary than the vehicle SHRSP group. The 1000ng/kg/min AngII treatment group was significantly less active than the vehicle group during the nocturnal (awake) periods after AngII infusion at GD10.5 (2.4±0.3 counts/min versus 3.1±0.2 counts/min; $p<0.05$) (Figure 6-7B).

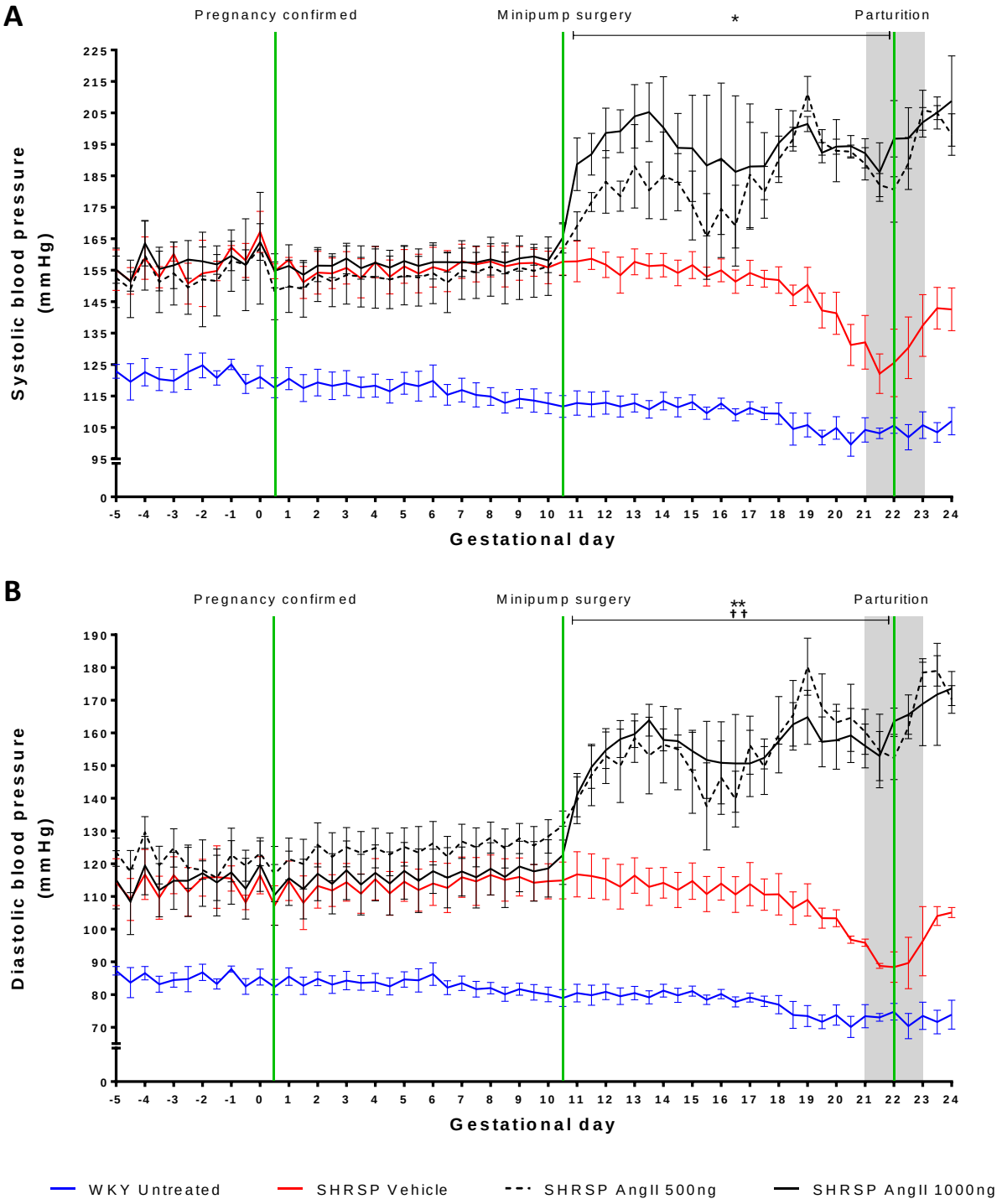


**Figure 6-6: Radiotelemetry measurement of systolic and diastolic blood pressure of pregnant AngII treated dams**

Radiotelemetry measured conscious blood pressure for 5 days prior to pregnancy and then throughout gestation and parturition. Parturition in SHRSP and WKY falls between the greyed area (GD21-23) and was not exactly the same day for each animal. Pregnant WKY untreated rats are presented as a reference for normotensive values. (A) Systolic and (B) diastolic blood pressures of the SHRSP rats are greater than WKY and all SHRSP groups were equal prior to pregnancy and prior to AngII infusion (minipump surgery). Systolic and diastolic blood pressure was significantly increased in 1000ng/kg/min AngII treated dams (*$p<0.05$; **$p<0.01$), and only diastolic blood pressure was significantly increased in the 500ng/kg/min AngII treatment group (††$p<0.01$) compared to vehicle SHRSP. Data expressed as day and night mean values ±SEM; analysed using one-way ANOVA comparison of AUC of separate segments (pre-AngII and post-AngII infusion) with Tukey post-hoc test; n=3 for all SHRSP groups, n=4 for untreated WKY.

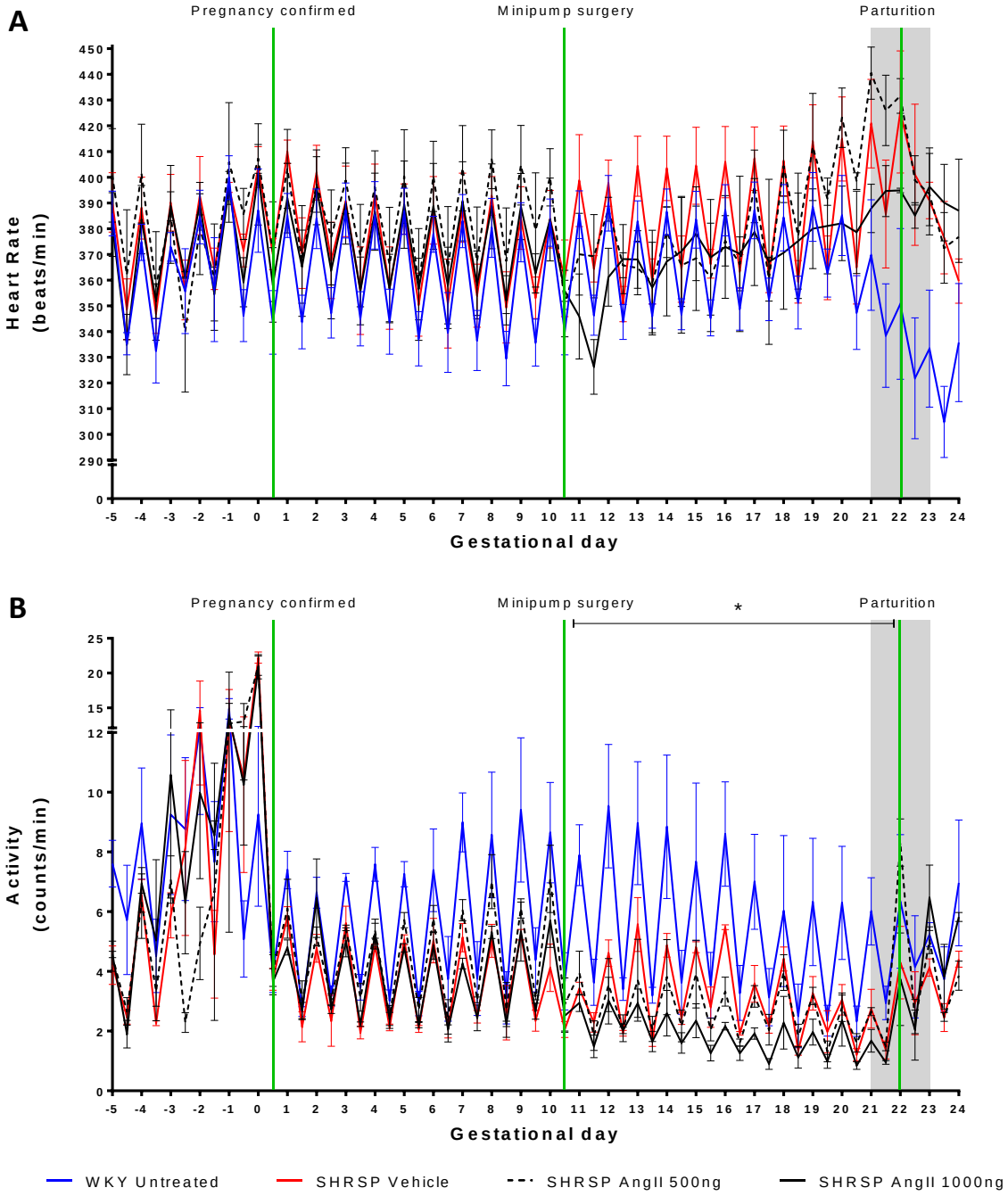


**Figure 6-7: Radiotelemetry measurement of heart rate and activity during pregnancy**
Conscious heart rate and activity counts were measured for 5 days prior to pregnancy and then throughout gestation and parturition. Pregnant WKY untreated rats are presented as a reference for normotensive values. (A) The heart rate pre-AngII infusion (minipump implantation) is similar in all SHRSP groups and the untreated WKY. Post AngII infusion there is no significant difference in the AUC of the AngII treatment groups compared to vehicle, however the 1000ng/kg/min AngII treated dams demonstrate a drop in heart rate immediately after minipump implantation and decreased amplitude of the nocturnal values, reducing the diurnal rhythm. (B) The activity pre-pregnancy increased during mating periods (GD-4 to GD0) and was similar between all SHRSP groups during pregnancy pre-AngII infusion. SHRSP treated with 1000ng/kg/min AngII had a significantly lower activity after minipump implantation than the vehicle SHRSP group (*$p<0.05$). Data expressed as day and night mean values ±SEM; analysed using one-way ANOVA comparison of AUC of separate segments (pre-AngII and post-AngII infusion) with Tukey post-hoc test; n=3 for all SHRSP groups, n=4 for untreated WKY.

#### 6.4.1.5 Cardiac Profile

Echocardiography on anaesthetised dams showed that that stroke volume (SV) (Figure 6-8A) and cardiac output (CO) (Figure 6-8B) increase with gestation in vehicle treated dams (SV: 140±16µl NP versus 214±17µl GD18.5 ($p<0.01$); CO: 54±6ml/min NP versus 81±5ml/min; $p<0.05$). The dams in the 500ng/kg/min AngII treatment group did not show this response to pregnancy and furthermore the dams in the 1000ng/kg/min AngII treatment group had a significantly reduced SV (90±15µl versus 155±12µl; $p<0.05$) and CO (36±6ml/min versus 59±5ml/min; $p<0.05$) compared to non-pregnant measurements. This treatment group also showed significant reductions post-AngII infusion (at GD14.5 and GD18.5) compared to pregnant pre-AngII infusion (GD6.5) in SV (123±11µl and 90±15µl versus 192±17µl; $p<0.05$ and $p<0.001$ respectively) and CO (47±4ml/min and 36±6ml/min versus 73±6ml/min; $p<0.05$ and $p<0.001$ respectively). There were no differences in calculated fractional shortening (Figure 6-8C) or ejection fraction (Figure 6-8D) between the treatment groups and there were no changes over the course of pregnancy. The left ventricular mass calculated using echocardiography was normalised to tibia length and no changes were observed over pregnancy (Figure 6-8E). At sacrifice (GD18.5) the left ventricles were dissected and weighed; these weights were normalised to tibia length and are in line with the echocardiography data (Figure 6-8F).

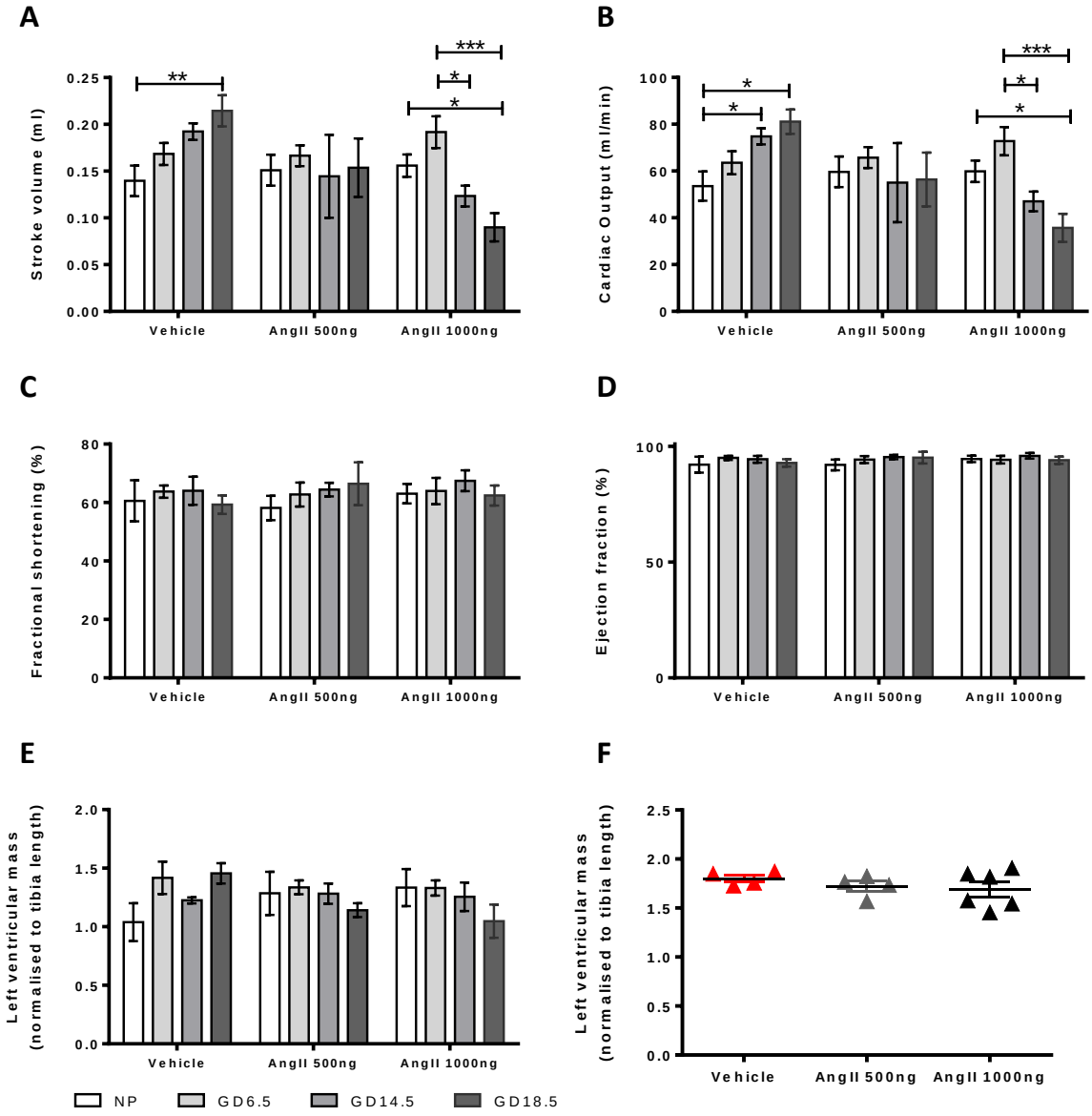


**Figure 6-8: Echocardiography estimations of cardiac function and left ventricle mass**
Echocardiography was conducted at NP (pre-pregnancy) (n=4) and GD 6.5 (n=4-6), 14.5 (n=3-6) and 18.5 (n=3-6) pregnancy time points. (A) Stroke volume increased from NP to GD18.5 in vehicle treated SHRSP, this change was not apparent in the 500ng/kg/min AngII treated group and was reversed, with stroke volume decreasing across pregnancy in the 1000ng/kg/min AngII treatment group. (B) Cardiac output calculated from stroke volume and conscious heart rate data. The vehicle group was found to have an increased cardiac output at GD18.5, whereas there was no change in the 500ng/kg/min AngII group and AngII treatment at 1000ng/kg/min caused a significant decrease compared to NP and pre-AngII infusion (GD6.5). No change was determined for (C) fractional shortening or (D) ejection fraction. (E) The left ventricular mass was calculated from the echocardiography measures and normalised to tibia length. There were no significant differences across pregnancy regardless of AngII infusion. This was supported by weights of the left ventricle taken at GD18.5 sacrifice (n= 4-6) (F). Data presented as mean ±SEM; *p<0.05; n=4-6, **p<0.01 vs NP; *p<0.05, ***p<0.001 vs GD6.5; analysed using one-way ANOVA for comparisons across pregnancy within each treatment group; or for comparison across treatment groups for left ventricular mass at sacrifice.

#### 6.4.1.6 Urinary Analysis

24 hour water intake and urine excretion was measured at a pre-pregnancy time point (NP) and pre-AngII infusion (GD6.5) and post-AngII infusion (GD14.5) using metabolic cages. There were no differences in water intake (Figure 6-9A) or urine excretion (Figure 6-9B) between either treatment groups at the pre-pregnancy or pre-AngII infusion time points. There were significant increases in water intake (56.8±6ml versus 30.8±2ml; $p<0.01$) and urine excretion (48.2±7ml versus 16.8±3ml; $p<0.0001$) at GD14.5 in the 1000ng/kg/min AngII treatment group compared to vehicle. The 1000ng/kg/min AngII treatment group was the only treatment group that had a significant change from pre-pregnancy to GD14.5 for both water intake (26.0±3ml versus 56.8±6ml; $p<0.001$) and urine excretion (9.9±0.8 versus 48.2±7ml; $p<0.0001$). This group also had a significantly increased urine excretion compared to the 500ng/kg/min treatment group (48.2±7ml versus 17.4±2ml; $p<0.0001$). The proportional urine excretion (corrected for volume intake) (Figure 6-9C) was also significantly greater in the 1000ng/kg/min AngII treatment group compared to vehicle (73.6±3% versus 53.7±7%; $p<0.05$) and to the 500ng/kg/min AngII group (73.6±3% versus 41.6±4%; $p<0.001$). The 1000ng/kg/min AngII treatment group was found to have a significantly increased albumin:creatinine ratio (Figure 6-9D) at GD14.5 compared to vehicle (3.0±0.26 versus 0.5±0.19; $p<0.0001$). This group also had a significantly higher albumin:creatinine ratio (ACR) when compared to the 500ng/kg/min AngII treatment group (3.0±0.26 versus 1.3±0.20; $p<0.0001$) and was the only treatment group to demonstrate an increase in ACR by GD14.5 compared to pre-pregnancy (GD0) levels (3.0±0.26 versus 0.6±0.06; $p<0.0001$)

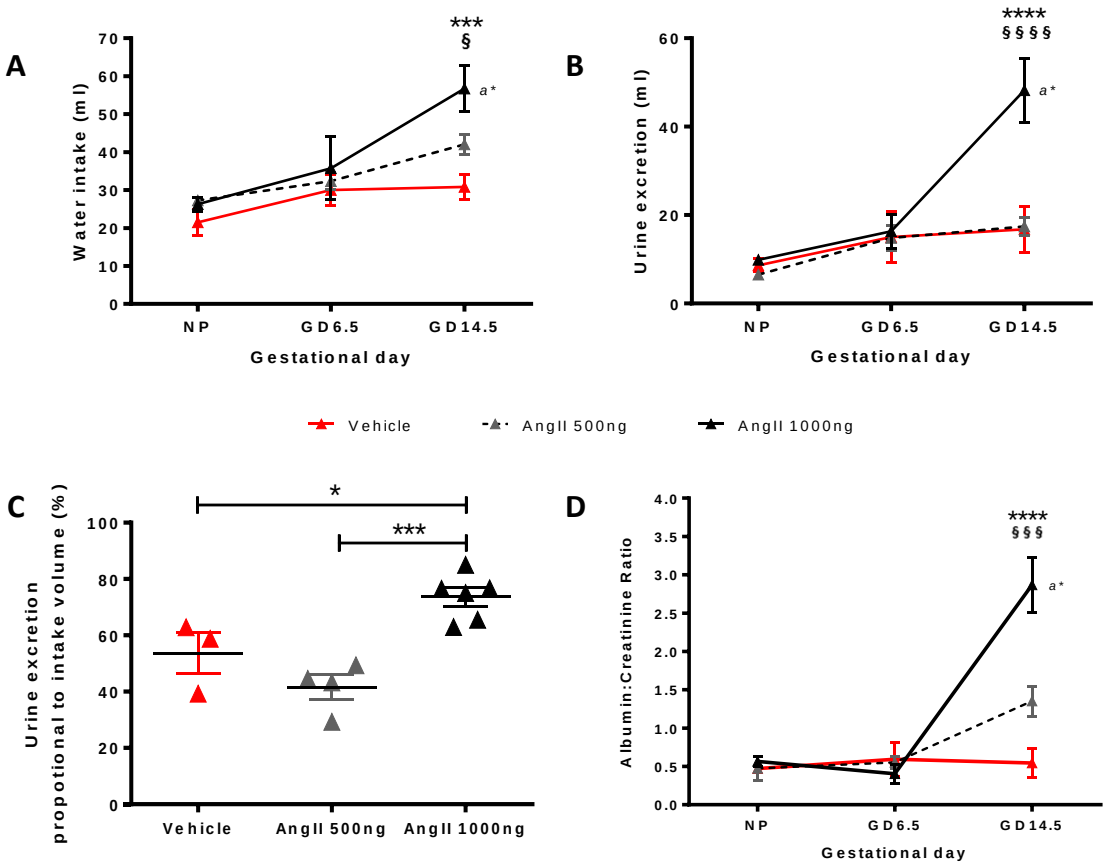


**Figure 6-9: The effect of AngII infusion on water intake and urine excretion during pregnancy**

Metabolic cages were used to collect 24-hour measurements of water intake and urine excretion at a week prior to pregnancy (NP)), pregnant pre-AngII (GD6.5-7.5) and pregnant post-AngII (GD14.5-15.5) time points. (A) Water intake did not change across pregnancy in the vehicle or AngII 500ng/kg/min treatment group. 1000ng/kg/min AngII treatment caused as significant increase in volume drank. (B) The urine excretion volume increased after AngII infusion only in the 1000ng/kg/min AngII treatment group. (C) The proportional excretion of urine to total volume intake at GD14.5 was significantly higher in 1000ng/kg/min AngII treated dams (*p<0.05, ***p<0.001; analysed by one-way ANOVA). (D) The concentration of albumin and creatinine was measured from urine samples at each time point and expressed as a ratio of albumin to creatinine. The 1000ng/kg/min AngII treated dams were the only group to have a significant increase in the albumin:creatinine ratio. Data expressed as mean ±SEM (n=3-6); comparisons across gestation and treatment were analysed using a two-way ANOVA with Bonferroni post-hoc tests; ***p<0.001, ****p<0.0001 AngII 1000ng vs vehicle; §p<0.05, §§§p<0.001 §§§§p<0.0001 AngII 1000ng vs AngII 500ng; *a**p<0.0001 NP vs GD14.5.

#### 6.4.1.7 Kidney Morphology

Kidney morphology was assessed using periodic acid Schiff (PAS) and picrosirius red staining (Figure 6-10). The PAS stain was used to critically examine the cortex, with specific focus on the glomerular regions. Representative images of the cortex show areas of possible glomeruli swelling in the kidneys exposed to AngII infusion (Figure 6-10A). The vehicle treated SHRSP shows a typical glomeruli structure with clear cell definition within in the glomeruli capillaries and visible space between the visceral and parietal layers of the Bowman's capsule. There is evidence of Bowman's capsule defects in the kidneys of both AngII treatment groups, with a reduction in the space observed between the visceral and parietal layers.

AngII treatment did not significantly alter picrosirius red staining in GD18.5 maternal kidneys (Figure 6-10B-C). The assessment of positive staining was restricted to the cortex and medulla regions and expressed as a percentage of the total kidney area. All groups examined had a significantly greater proportion of staining in the medulla than the cortex (Vehicle: 1.9±0.30% versus 0.5±0.18%; $p<0.01$, 500ng/kg/min AngII: 1.8±0.35% versus 0.4±0.06%; $p<0.01$, 1000ng/kg/min AngII: 1.8±0.30% versus 0.5±0.02%; $p<0.01$).

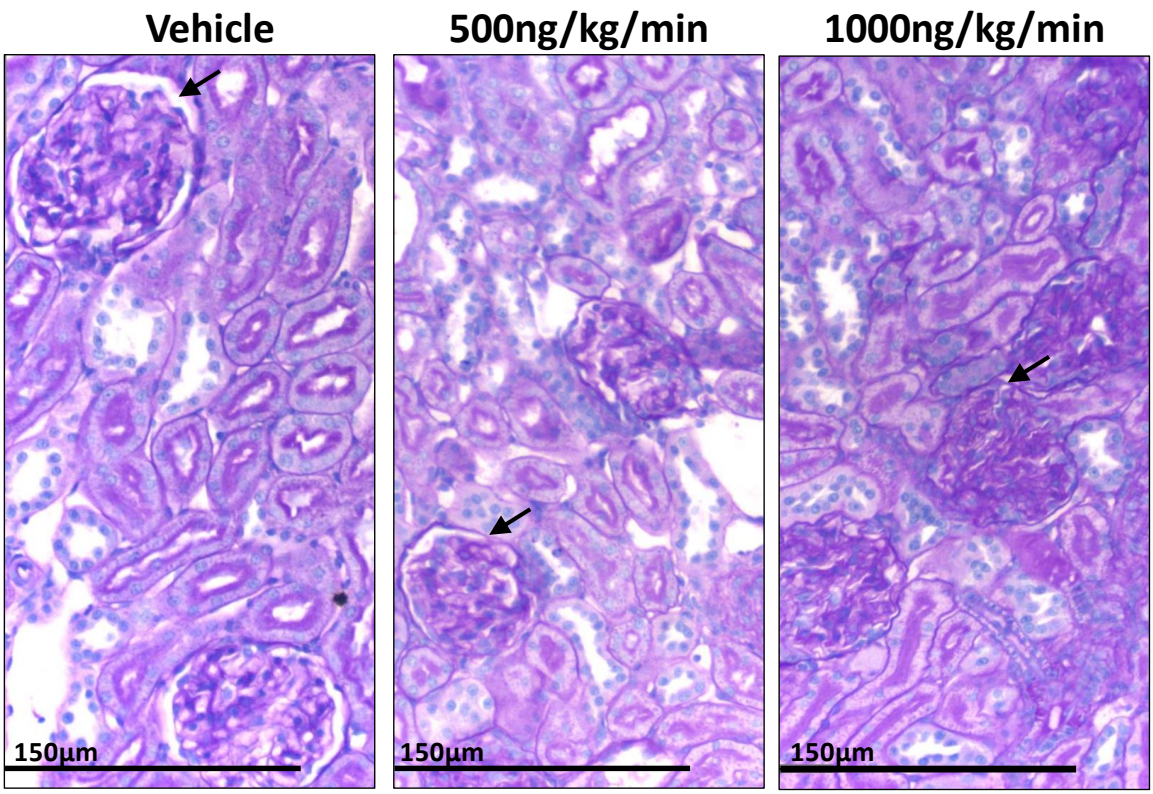


**Figure 6-10: Histological examination of GD18.5 kidneys from vehicle and AngII treated dams.**
Periodic acid Schiff stain allowed for the morphological examination of maternal kidneys. Observationally, the area between parietal and visceral layers surrounding the glomeruli, the Bowman's space, was reduced in the kidneys from AngII treated dams (indicated by arrows), n=4 kidneys examined for each treatment group.

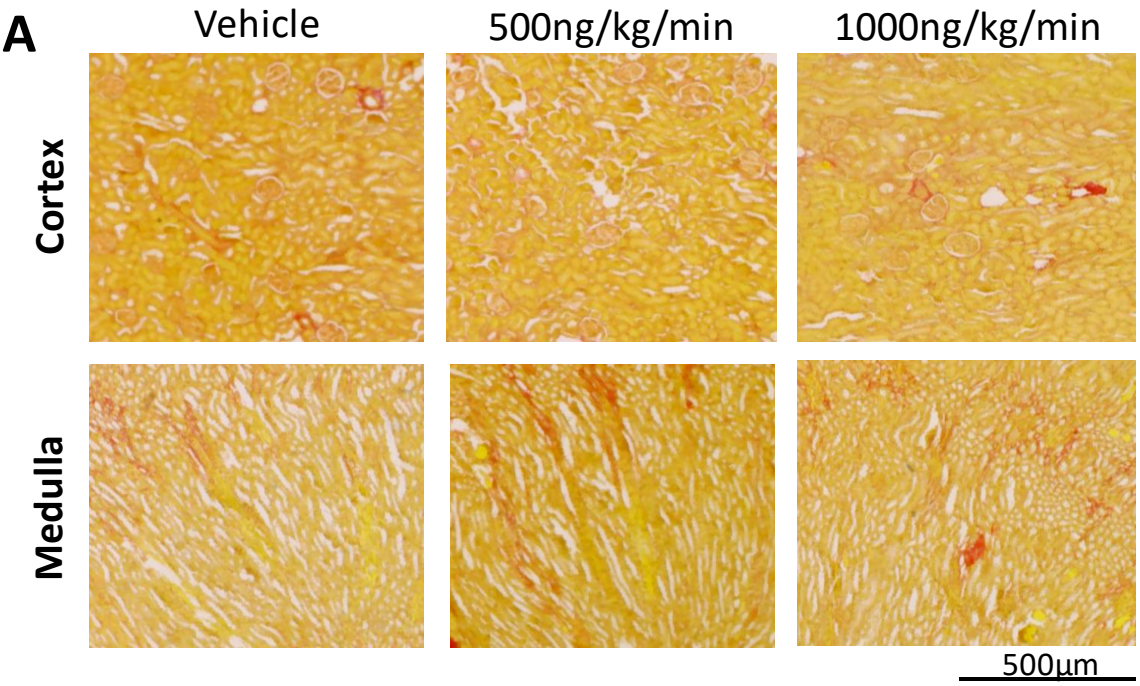


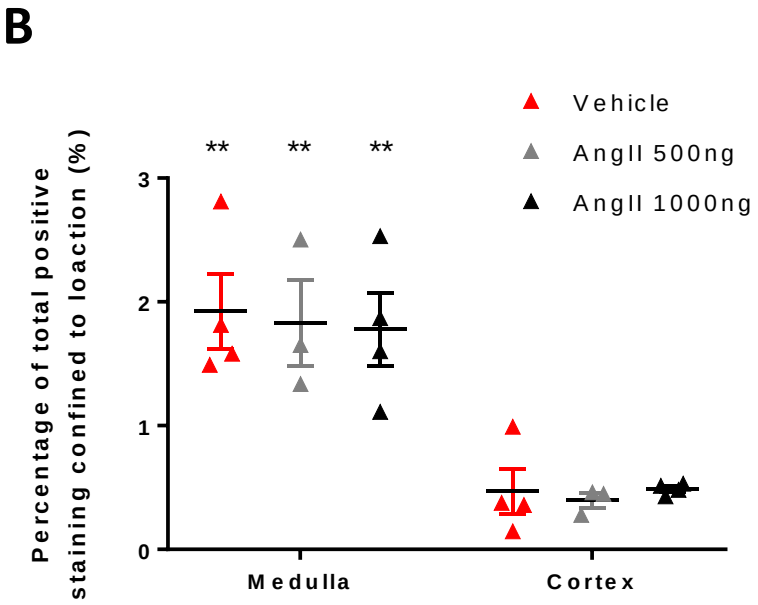


**Figure 6-11: Examination of collagen content in GD18.5 kidneys from vehicle and AngII treated dams.**
(A) Picrosirius red stain was conducted to identify differences in collagen deposition within the kidney, representative images of the medulla and cortex from kidneys from each treatment group are shown. (B) The percentage of medulla and cortical staining as a proportion of the whole kidney was determined by a blinded observer using Image J to identify positively stained pixels. Statistical analysis was conducted using a repeated measure two-way ANOVA with Tukey post-hoc test; **p<0.01 medulla vs cortex within same treatment group; n=4.

#### 6.4.1.8 *In Vivo* Uterine Artery Blood Flow

Uterine artery blood flow was imaged *in vivo* using Doppler ultrasound; this was then assessed by measuring the systolic/diastolic (S/D) peak ratio and the resistance index (RI). There was no evidence of significant differences in the S/D ratio (Figure 6-12A) or RI (Figure 6-12B) between the three treatment groups at each gestational age. All groups showed a trend towards a decrease in S/D ratio and RI at GD18 compared to pre-pregnancy, however this did not reach significance. A representation of the uterine artery Doppler trace at pre-pregnancy and GD18.5 are shown in Figure 6-12C.

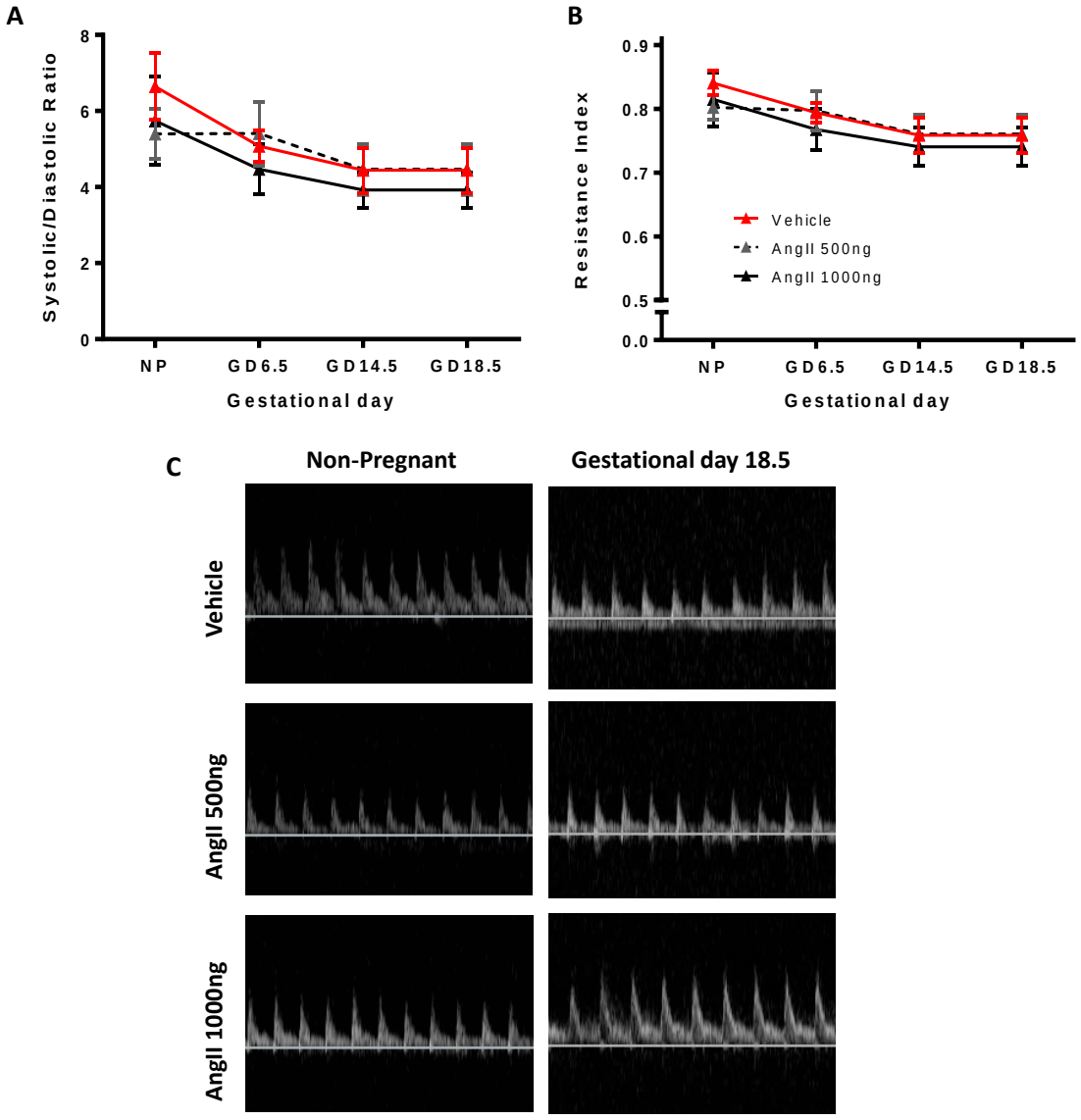


**Figure 6-12: Doppler ultrasound examination of uterine artery blood flow**
Uterine artery blood flow was assessed using waveform measurements from Doppler ultrasound taken a week prior to pregnancy (Non-pregnant – NP) and at GD6.5, 14.5 and 18.5. **(**A) The peak systolic and end diastolic volumes were measured and expressed as a ratio. (B) Resistance index was calculated from the peak systolic and end diastolic volumes. Neither of these parameters changed with gestation or with AngII treatment. (C) Representative images of waveform traces of the three SHRSP treatment groups pre-pregnancy and at the end of gestation show no significant differences. Data expressed as mean ±SEM; n=3-6; analysed using two-way ANOVA with Bonferroni post-hoc test.

#### 6.4.1.9 *Ex Vivo* Uterine Artery Function

The uterine artery functional responses to a vasoconstrictor (noradrenaline) and vasodilators (the synthetic analogue of acetylcholine: carbachol, and nitric oxide donor: sodium nitroprusside) were assessed using wire myography at GD18.5. Uterine arteries from either AngII treatment groups did not demonstrate any significant differences in contractile responses to noradrenaline from vehicle treated arteries (Figure 6-13A). AngII treatment also did not significantly alter vasodilation responses to carbachol (Figure 6-13B) or sodium nitroprusside (Figure 6-13C). Uterine arteries from vehicle, 500ng/kg/min AngII and 1000ng/kg/min AngII treatment groups all had similar contractile responses to exogenously applied AngII ($1x10^{-8}$M) (Figure 6-13D).

#### 6.4.1.10 *Ex Vivo* Uterine Artery Passive Mechanical Properties

External and internal diameter was measured over a range of physiological pressures using arteries at GD18.5 mounted on a pressure myograph, and structural parameters were calculated. The uterine arteries from 1000ng/kg/min AngII treated dams had a significantly reduced external (Figure 6-14A) and internal (Figure 6-14B) diameter compared to vehicle (421±20μm versus 531±20μm; $p<0.05$ at 110mmHg and 338±23μm versus 431±31μm; $p<0.01$ at 110mmHg, respectively). These arteries also demonstrated a significantly reduced cross-sectional area compared to vehicle treated ($4.9x10^4$±1963$\mu m^2$ versus $8.3x10^4$±2793$\mu m^2$; $p<0.05$ at 110mmHg) (Figure 6-14C). The uterine arteries from dams in the 500ng/kg/min treatment group also demonstrated a significant decrease in internal diameter compared to vehicle, but only at pressures greater than 40mmHg (363±26μm versus 531±20μm; $p<0.05$ at 110mmHg) (Figure 6-14B). These arteries demonstrated a reduced cross-sectional area only at a pressure of 40mmHg, compared to vehicle ($6.3x10^4$±7573$\mu m^2$ versus $8.7x10^4$±5405$\mu m^2$; $p<0.05$) (Figure 6-14C). Neither AngII treatment group demonstrated a significant change in uterine artery wall thickness (Figure 6-14D). Wall stress increased as pressure within the artery increased, however there was no alteration in wall stress response between the two treatment groups (Figure 6-14E). AngII treatment did not significantly alter the vessels stress/strain relationship (Figure 6-14F).

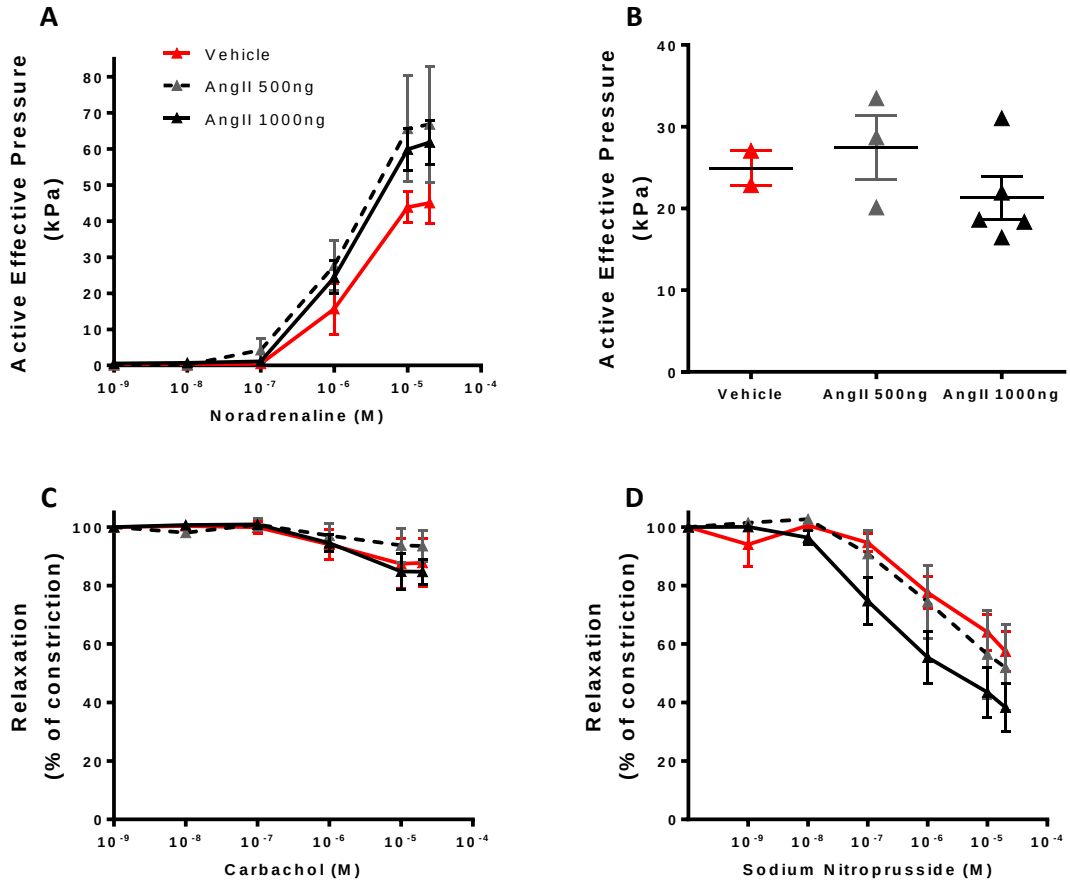


**Figure 6-13: Wire myography assessment of GD18.5 uterine artery function from AngII treated dams**

Functional responses of GD18.5 uterine arteries were assessed *ex vivo* using wire myography. (A) Contractile response to increasing concentrations of noradrenaline was not affected by *in vivo* AngII infusion. (B) All uterine arteries responded similarly to a maximum concentration of $1x10^{-8}$ M AngII and there was no significant difference between the AngII treatment group (500ng/kg/min vs 1000ng/kg/min; analysed using unpaired students t-test). (C-D) There were no significant differences between vehicle and AngII treatment groups when vasodilation was assessed using carbachol and sodium nitroprusside. Data expressed as mean ±SEM; n=3-6; dose response curves used to calculated AUC or $EC_{50}$ values of each curve and comparisons made using one-way ANOVA with Sidak post-hoc test.

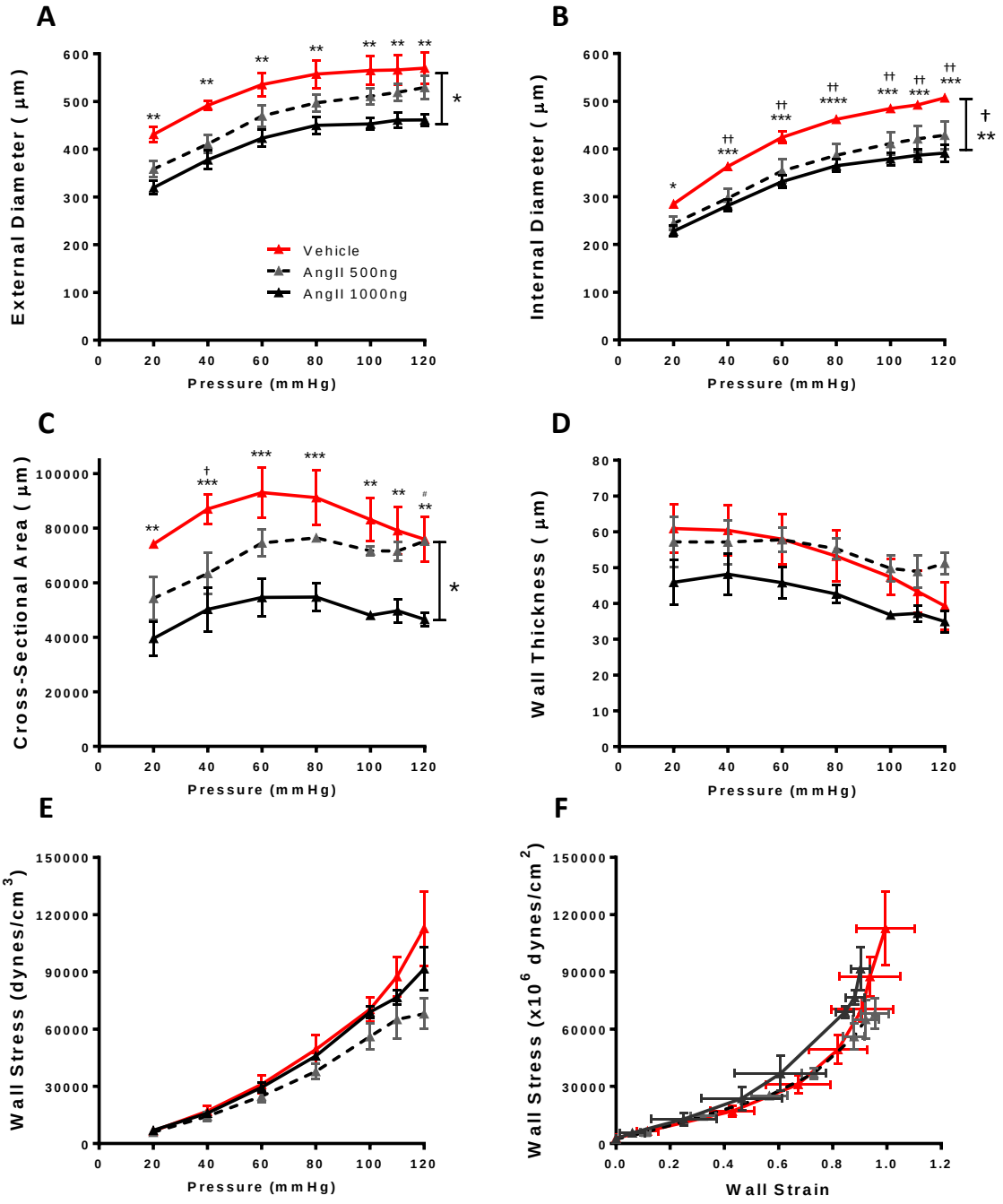


**Figure 6-14: Structural parameters of GD18.5 uterine arteries obtained from pressure myography**

Pressure myography was used to directly measure the external and internal vessel diameter over a range of physiological pressures (10-120mmHg), these were then used to calculate a range of structural parameters. (A) The external diameter was significantly reduced in uterine arteries from 1000ng/kg/min AngII treated dams. (B) The internal diameter of the arteries from 1000ng/kg/min and 500ng/kg/min AngII treated dams were significantly reduced compared to vehicle. (C) The cross-sectional area of 1000ng/kg/min AngII treated uterine arteries was significantly smaller, yet there was no significant change in the (D) wall thickness, (E) wall stress or (F) the stress/strain relationships of the uterine arteries. Data presented as mean ±SEM (n=3-4); statistical significance was determined using AUC compared using one-way ANOVA with Sidak post-test to compare overall pressure response trends (*p<0.05, **p<0.01 Vehicle vs 1000ng/kg/min; †p<0.05 Vehicle vs 500ng/kg/min). A repeated measures two-way ANOVA with Sidak post-hoc test was also conducted to compare changes between treatment groups at each pressure; *p<0.05, **p<0.01, ***p<0.001 Vehicle vs 1000ng/kg/min AngII; ††p<0.01 Vehicle vs 500ng/kg/min; #p<0.05 500ng/kg/min vs 1000ng/kg/min.

#### 6.4.1.11 Systemic vascular characteristics

Mesenteric arteries were analysed using wire and pressure myography in the same manner as uterine arteries. Functional analysis using wire myography did not reveal any significant changes in vascular responses to noradrenaline (Figure 6-15A). However, the half maximal response of the arteries from vehicle treated dams demonstrated a significant reduction compared to arteries 500ng/kg/min AngII treated dams ($1.50\pm0.78x10^{-6}$M versus $4.37\pm0.79x10^{-6}$M; $p<0.05$) (Figure 6-15B). No significant changes in responses to carbachol (Figure 6-15B), or SNP (Figure 6-15C) were observed, and the half maximal responses were unchanged. There was no significant differences determined between the vehicle and 500ng/kg/min AngII treatment group for any of the passive mechanical properties determined from pressure myography (Figure 6-16A-F). Statistical significance could not be determined in any measured or calculated structural parameter for arteries from 1000ng/kg/min AngII treated dams due to low numbers (Figure 6-16).

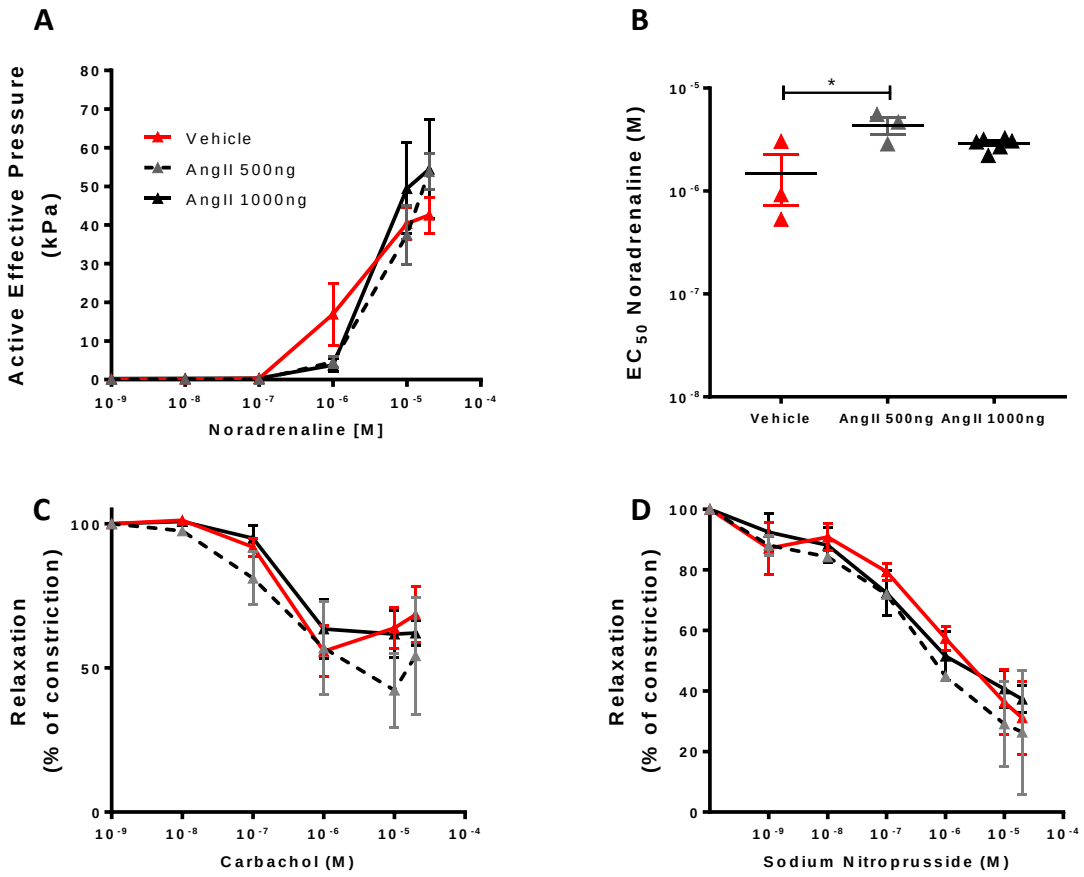


**Figure 6-15: Functional responses of the mesenteric arteries of GD18.5 dams**
Wire myography assessed the functional responses of GD18.5 third order mesenteric arteries. The contractile response to noradrenaline expressed as (A) an active effective pressure and (B) the half maximal responses ($EC_{50}$) for each curve. (C-D) The vasodilation responses to carbachol and sodium nitroprusside expressed as a percentage of $2x10^{-5}$M noradrenaline constriction. Data expressed as mean ±SEM (n=3-5); statistical significance determined using comparisons of AUC or $EC_{50}$ values of each curve using one-way ANOVA with Sidak post-hoc test; *p<0.05.

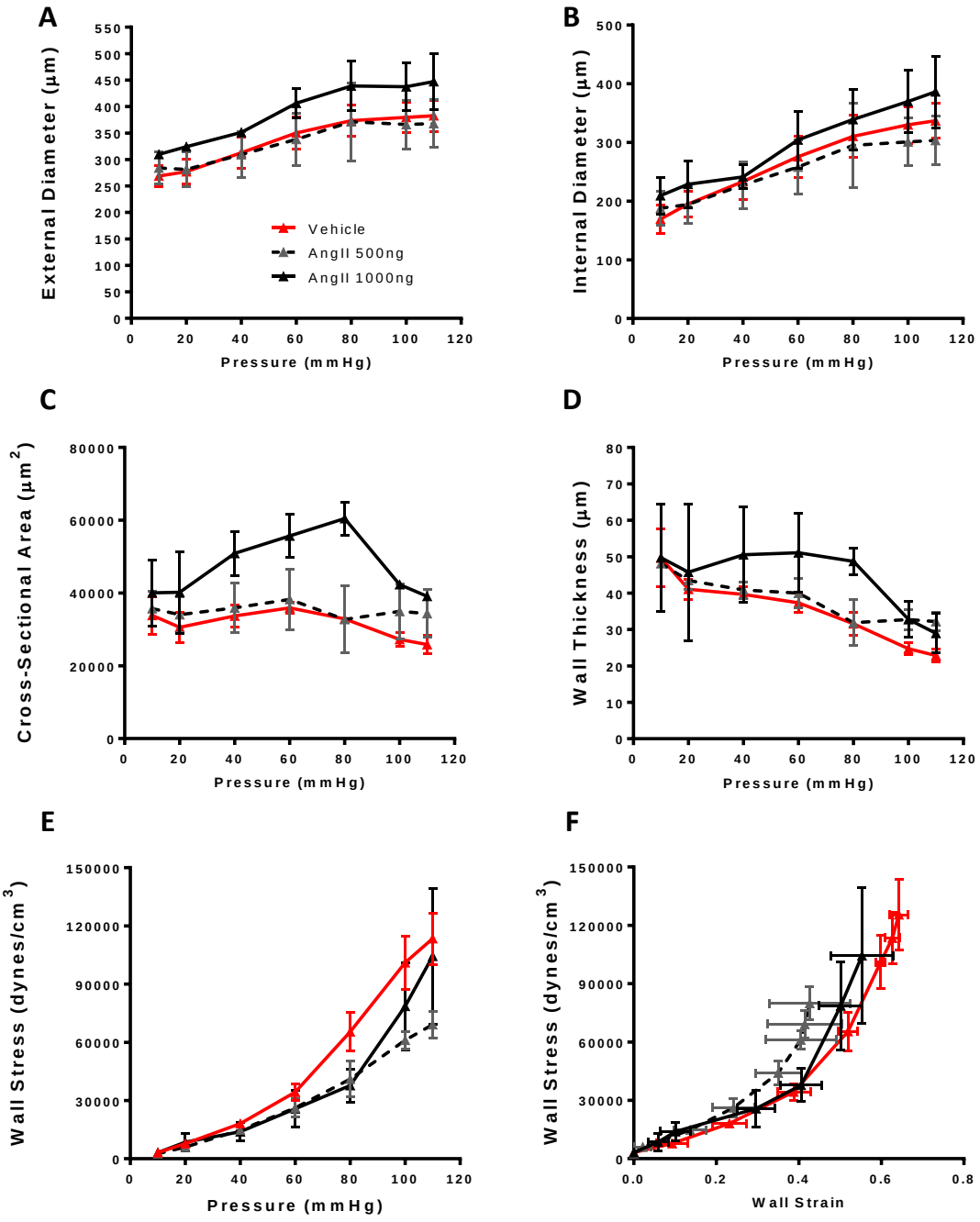


**Figure 6-16: Mesenteric artery structural parameters from pressure myography**
Pressure myography was used to directly measure the external and internal vessel diameter over a range of physiological pressures (10-120mmHg), these were then used to calculate a range of structural parameters. No changes were observed in (A) external diameter, (B) internal diameter, (C) cross-sectional area, (D) wall thickness, (E) wall stress or (F) the stress/strain relationships of the mesenteric arteries. Data expressed as mean ±SEM (n=2-4); comparisons only made between vehicle (n=4) and 500ng/kg/min AngII (n=3) treatment groups. Statistical significance was determined using AUC compared using one-way ANOVA with Sidak post-test to compare overall pressure response trends.

## 6.4.2 Offspring Outcome

### 6.4.2.1 Fetal weight and size distribution

AngII treatment had no significant effects on the number of pups in each litter at the fetal (GD18.5) or neonatal stage (Figure 6-17). Fetal weights and anthropometric measurements were taken at GD18.5. The fetuses exposed to 1000ng/kg/min AngII treatment had a significantly reduced weight compared to both vehicle and the 500ng/kg/min AngII treatment groups (0.71±0.04g versus 1.08±0.03g; $p<0.0001$) (Figure 6-18A). Representative images of the fetal size at GD18.5 are shown in Figure 6-18B. This reduction in size was symetrical and there was no evidence of head sparing as similar significant reductions in abdominal circumference (18±0.8mm versus 23±0.2mm; $p<0.001$), crown-rump length (21±0.7mm versus 25±0.1mm; $p<0.001$) and head circumference (21±0.8 versus 25±0.2mm; $p<0.01$) were observed and there were no changes to the head:body ratio between the vehicle and AngII treatment groups (Figure 6-18C-F). Fetuses from the 1000ng/kg/min treatment group also showed a significant reduction in weight (0.71±0.04g versus 0.99±0.04g; $p<0.0001$) and abdominal circumference (18±0.8mm versus 22±0.3mm; $p<0.01$), crown-rump length (21±0.7mm versus 24±0.6mm; $p<0.05$) and head circumference (21±0.8 versus 24±0.4mm; $p<0.05$) compared to the 500ng/kg/min AngII treatment group (Figure 6-18A-E). To give a more clinical representation of the fetal growth the weight data was expressed as a weight distribution curve (Figure 6-19). The $5^{th}$ centile for vehicle treated fetal weights was calculated to be weights that fell under 0.94g. Using this centile threshold it was concluded that 47.8% of fetuses from 500ng/kg/min treated dams and 95.7% from 1000ng/kg/min treated dams were below this threshold, and would be classed as growth restricted clinically.

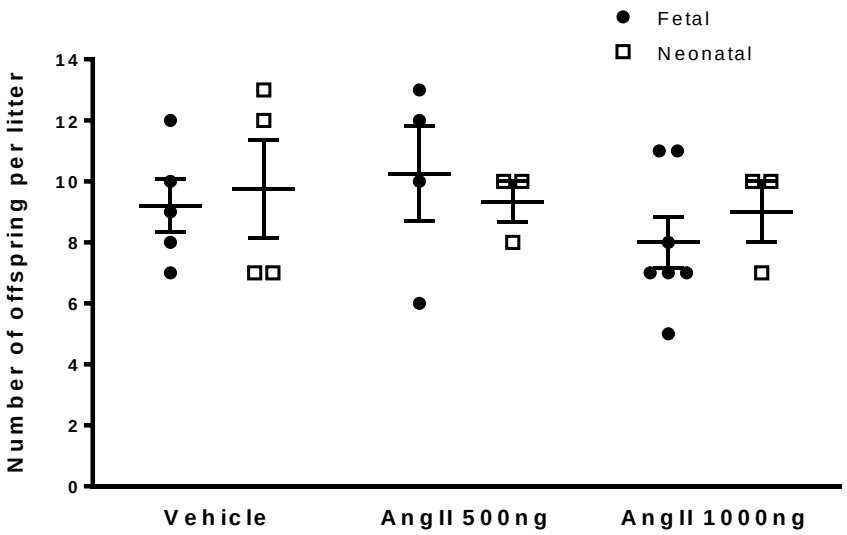


**Figure 6-17: Number of offspring per litter at GD18.5 fetal stage and at birth**
The number of offspring per litter was recorded at GD18.5 (fetal) and on the date of birth (neonatal). AngII treatment did not significantly alter the number of offspring at either developmental stage. There was no difference between fetal and neonatal litter sizes in any of the treatment groups. Data presented as individual litter averages ±SEM (n=3-7); analysed using two-way ANOVA with Bonferroni post-hoc test.

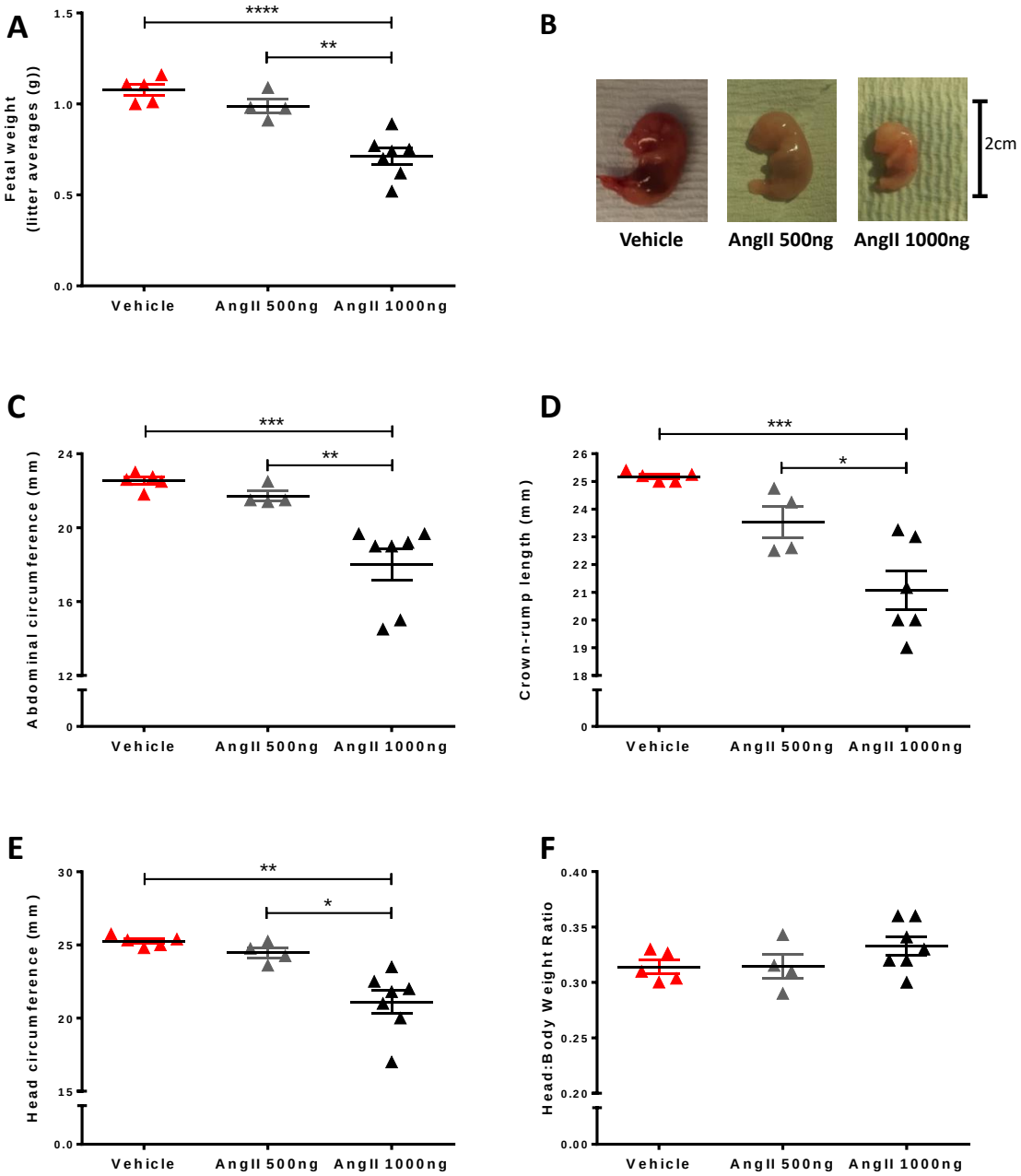


**Figure 6-18: Weights and anthropometric measurements of GD18.5 fetuses**
At GD18.5 the fetuses were removed from the uterine horn, all amniotic fluid and membranes were removed and they were separated from their placenta. (A) Fetal weight was significantly reduced with 1000ng/kg/min AngII treatment. (B) Representative images of fetal size show that fetuses from 1000ng/kg/min AngII treated dams are smaller. The anthropometric measurements of (C) abdominal circumference, (D) crown:rump length and (E) head circumference are all significantly reduced with 1000ng/kg/min AngII treatment. (F) There was no difference in the head body weight ratios. Data presented as individual litter averages with mean ±SEM; n=4-7; analysed using one-way ANOVA with Tukey post-hoc test; *p<0.05, **p<0.01, ***p<0.001, ****p<0.0001.

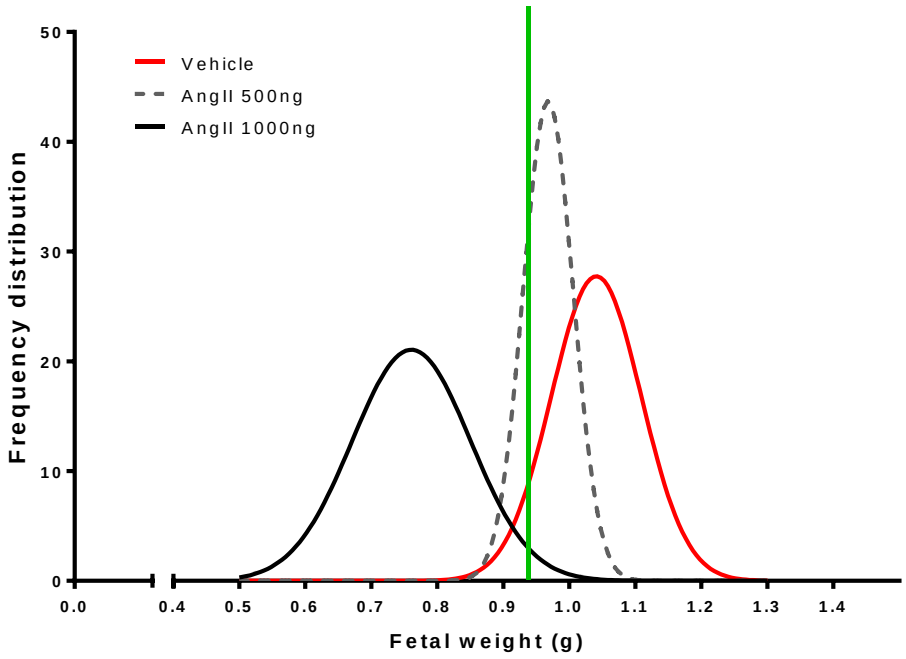


**Figure 6-19: Frequency distribution of all GD18.5 fetal weights**
The proportion of total fetal weights at GD18.5 that fall below the 5$^{th}$ centile (green line) was determined by constructing a non-linear fit of frequency distributions of fetal weights for each treatment group. The 5$^{th}$ centile was determined from vehicle SHRSP (n=37 fetuses, from 5 pregnancies) fetal weights (i.e. the lowest 5% of fetal weights). 47.8% of fetuses from 500ng/kg/min treated dams (n=42 fetuses from 4 pregnancies) and 95.7% from 1000ng/kg/min treated dams (n=54 fetuses from 8 pregnancies) were below this threshold limit.

#### 6.4.2.2 Live Birth Differences and Neonatal Size

A group of dams on each treatment were allowed to progress to parturition in order to investigate the neonatal outcome. The number of live births per litter was recorded at on day of birth and on neonatal day 2 (Table 6-2). There was no change in the number of neonates per litter in the vehicle group or the 500ng/kg/min AngII treatment group. The 1000ng/kg/min AngII treatment group was the only group to have a neonate death in the first two days.

Neonate weights were recorded on day 1 and day 2 after birth. The neonates from vehicle treatment and 500ng/kg/min AngII treatment groups both showed a significant weight gain in this time period (Vehicle: 5.1±0.2g to 5.4±0.2g; $p<0.001$, AngII 500ng/kg/min: 4.4±0.3g to 4.6±0.3g; $p<0.01$) (Figure 6-20A). No significance was found between day 1 and day 2 in the neonates from the 1000ng/kg/min AngII treatment group; however data was only collected for 2 litters' therefore statistical analysis could not be conducted (Figure 6-20A). There were no significant differences in neonatal weight gain between the vehicle and 500ng/kg/min AngII treatment groups (Figure 6-20B). No evidence of asymmetrical growth restriction was observed in the 500ng/kg/min AngII (Figure 6-20C).

There were no significant differences in the weights of males versus females at neonatal day 2 in any of the treatment groups. There were also no significant differences in the weight reductions of each gender in response to either AngII treatment (Figure 6-20D).

**Table 6-2: Number of live neonates per litter on the date of birth and two days later**

| | Vehicle (n=4 dams) | AngII 500ng (n=3 dams) | AngII 1000ng (n=3 dams) |
|---|---|---|---|
| *Day of birth* | 9.75±1.6 | 9.33±0.7 | 9.00±1.0 |
| *Neonatal day 2* | 9.75±1.6 | 9.33±0.7 | 8.00±1.2 |

The number of offspring born was recorded as soon as the litter was found (and this day was noted as the date of birth) and then again two days later on neonatal day 2. The vehicle and 500ng/kg/min AngII treatment groups had the same number of offspring on neonatal day two as they had had on the date of birth. The 1000ng/kg/min AngII treatment group was the only group to show offspring death over this two day period; however this was not significantly different. Data presented as litter average ±SEM; analysis between date of birth and neonatal day 2 differences by paired student's t-test.

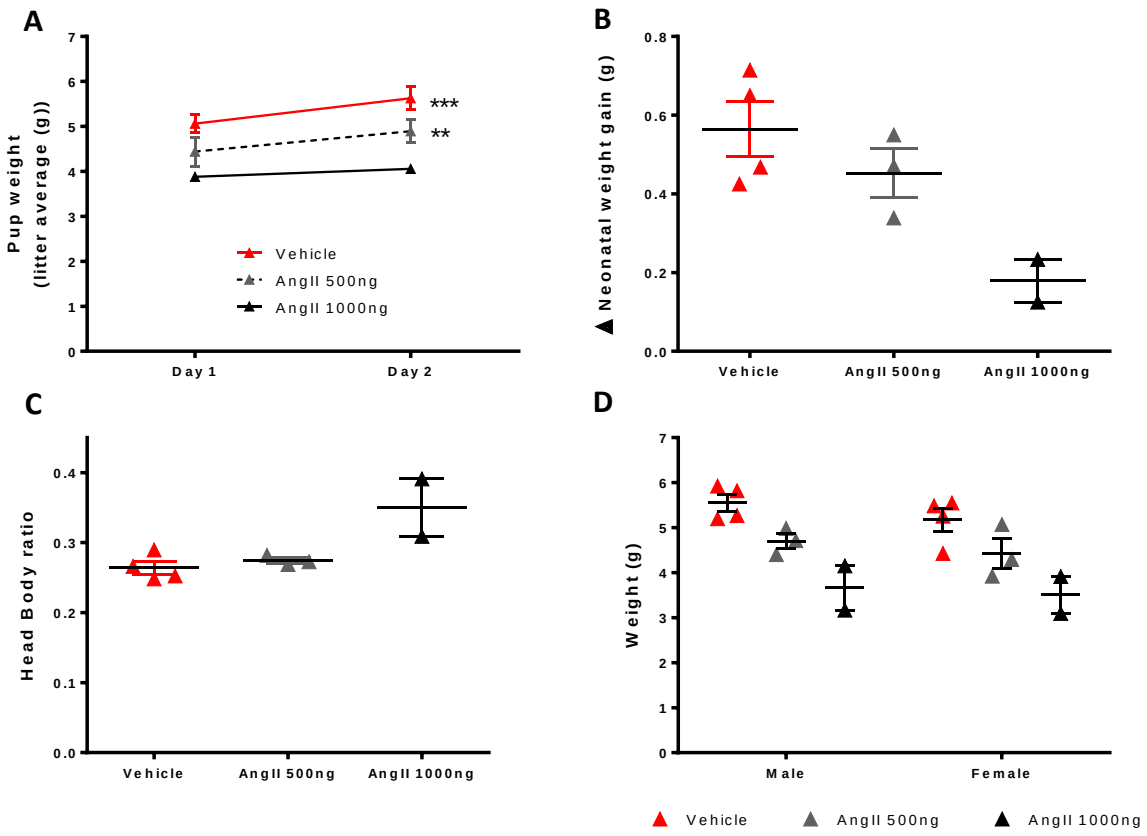


**Figure 6-20: Live neonatal weights recorded in the two days following birth**
Weights of the total litter were recorded on neonatal day one and two, these values were corrected for the number of pups on that day. (A) The rate of growth over 24 hours (between day 1 and day 2) was found to be similar between vehicle (gradient of 0.56±0.07) and 500ng/kg/min AngII treatment group (gradient of 0.45±0.06). (B) The increase in weight from day 1 to day 2 was calculated as the Δ weight gain. No significant differences were determined between treatment groups. (C) The head weights were recorded at sacrifice on day 2 and expressed as a ratio to total body weight. There were no significant differences observed with AngII treatment. (D) At sacrifice on day 2 the neonates were gendered and there was found to be no gender disparity in weight changes. Data is presented as mean litter average ±SEM. All statistical analysis was conducted on vehicle (n=4) and 500ng/kg/min AngII treatment (n=3) groups only as data set for 1000ng/kg/min AngII treatment was not large enough to determine significance (n=2). The differences in gradients and the comparisons between genders within each treatment group was conducted using an unpaired student's t-test. Other statistical tests were one-way ANOVA with Tukey post hoc test.

#### 6.4.2.3 Neonatal changes in AngII and RAS gene expression

The concentration of AngII in neonatal plasma was assessed via an ELISA for AngII. In untreated WKY and vehicle treated SHRSP the concentration of AngII was below detectable levels (Figure 6-21). The plasma collected from neonates from AngII treated dams had detectable concentrations; 500ng/kg/min AngII treatment group demonstrated concentrations of 11.2±5pg/ml (n=2) and the 1000ng/kg/min AngII treatment group had a concentration of 48.2pg/ml (n=1).

The gene expression of RAS components downstream of AngII were investigated in the neonatal kidney using qRT-PCR (Figure 6-22). AngII treatment did not change the gene expression levels of either AngII receptor (*Agtr1a* or *Agtr2*) in the neonatal kidneys, compared to vehicle. There was a significantly increased expression of angiotensin converting enzyme 2 (*Ace2*) in the kidneys of neonates that had been exposed to 1000ng/kg/min AngII treatment compared to vehicle (11.4±0.15 ΔCT versus 10.9±0.07 ΔCT; $p<0.05$), this did not reach significance in neonates from the 500ng/kg/min treatment group; however this may be due to the low statistical power as this group had only 3 biological replicates (Figure 6-22).

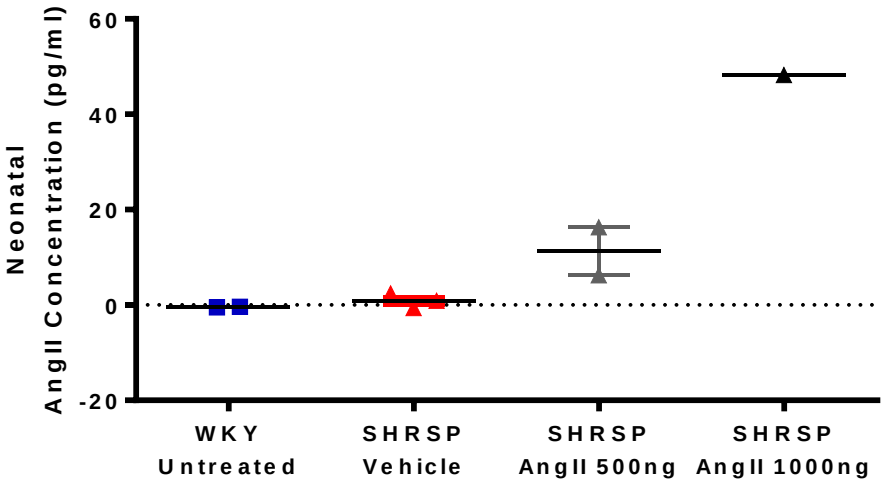


**Figure 6-21: Neonatal plasma AngII concentration on neonatal day two**
The AngII concentrations in neonatal day 2 plasma were determined using an ELISA. There were no detectable levels in plasma from untreated WKY (n=3) or vehicle SHRSP (n=3) neonates. There were detectable levels in all samples from AngII treated pregnancies. The increase observed in 500ng/kg/min AngII treatment group (n=2) was increased further in the 1000ng/kg/min AngII treatment group (n=1). Plasma samples collected as pooled litter samples and data presented as mean ±SEM.

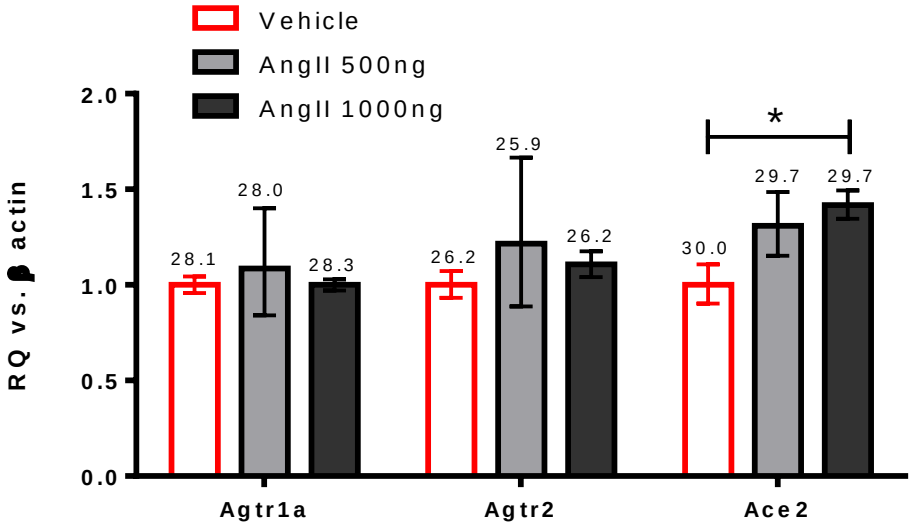


**Figure 6-22: Gene expression of AngII receptor type 1 (*Agtr1a*) and type 2 (*Agtr2*) and angiotensin converting enzyme 2 (*Ace2*) in the neonatal kidney.**
Gene expressions of components of the RAS were analysed using qRT-PCR and are presented as relative quantities (RQ) compared to vehicle. All gene expression was normalised to *β actin* expression. AngII treatment during pregnancy did not significantly change the expression of either receptor (Agtr1a and Agtr2). Ace2 expression was significantly higher in the kidneys from neonates exposed to 1000ng/kg/min AngII treatment *in utero*. Data presented as $2^{-\Delta\Delta CT}$ relative to vehicle ±SEM relative to the ΔCT. Statistical analysis was conducted using ΔCT values compared using one-way ANOVA with Tukey post-hoc test; n=3-8; *p<0.05.

## 6.4.3 Placental Characteristics

### 6.4.3.1 Placental Morphology

Placental weights followed the same pattern of change as fetal weights (section 6.4.2.1) which identified 1000ng/kg/min AngII treatment caused a significant reduction in placental weights compared to vehicle (0.16±0.007g versus 0.24±0.008g; $p<0.0001$) and compared to the 500ng/kg/min AngII treatment group (0.16±0.007g versus 0.21±0.002g; $p<0.01$) (Figure 6-23A). No significant difference was observed between vehicle and the 500ng/kg/min AngII treatment group. Fetal: placental ratios were determined and found that there was no significant change between the two AngII and vehicle treatment groups (Figure 6-23B)

The placental gross morphology was assessed using PAS staining to identify the junctional and labyrinth placental layers. Representative images of the full placental cross-sectional area are shown in Figure 6-25. There were no differences in the proportional size of the two zones between the three treatment groups, with the junctional zone being between 18-21% of total placental size (Figure 6-24). The junctional zone appeared to lose its defined structure with AngII treatment (Figure 6-26A). The PAS staining intensity in the junctional zone was significantly reduced in the 1000ng/kg/min AngII treatment group compared to the vehicle group (4±1.6% versus 13±1.5%; $p<0.05$) (Figure 6-26B). The cellular organisation of the junctional zone was visually assessed by a blinded observer and given a score corresponding to its structural organisation (with 1 being organised typical structure, with ordered distribution of cell types and five being the highest score with evidence of no structural order and many large vacuous regions with sparse and disorganised distribution of cell types). Placentas from 1000ng/kg/min AngII treatment groups scored significantly higher than the vehicle treated group (3.8±0.40 versus 2.1±0.31; $p<0.05$) (Figure 6-26C). No statistically significant differences were observed in the placenta from the 500ng/kg/min AngII treatment group.

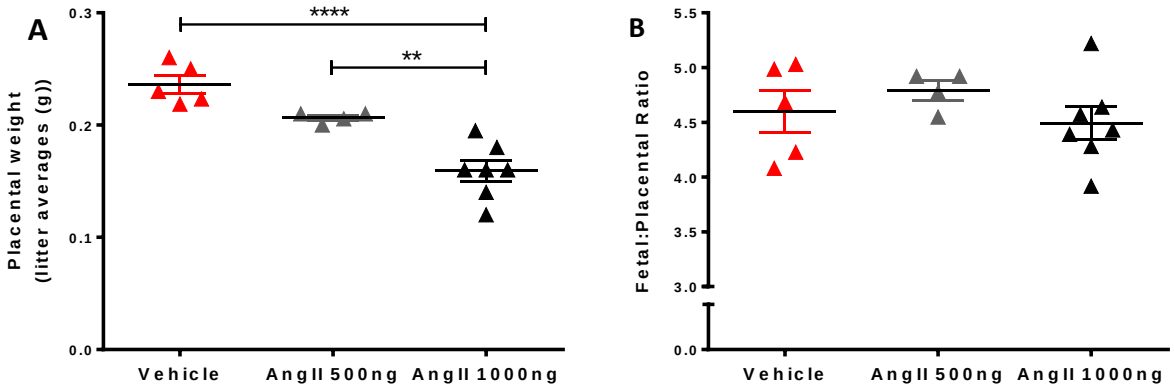


**Figure 6-23: Placental weights and fetal:placental weight ratio determined at GD18.5**
The placentas were separated from the fetus after being removed from the uterus. Excess fluid was removed by blotting with absorbent swabs. (A) Weights were recorded for each placenta and were averaged to give a litter mean. There was a significant reduction in placental weight in to 1000ng/kg/min AngII treatment group compared to vehicle and 500ng/kg/min AngII groups. (B) The ratio of fetal weigh to placental weight was calculated and showed that fetal and placental weight reductions followed the same pattern as there was no significant difference in the weight ratios. Data presented as litter average with mean ±SEM; n=4-6; statistical significance determined using one-way ANOVA with Sidak post-hoc test; **p<0.01, ***p<0.001.

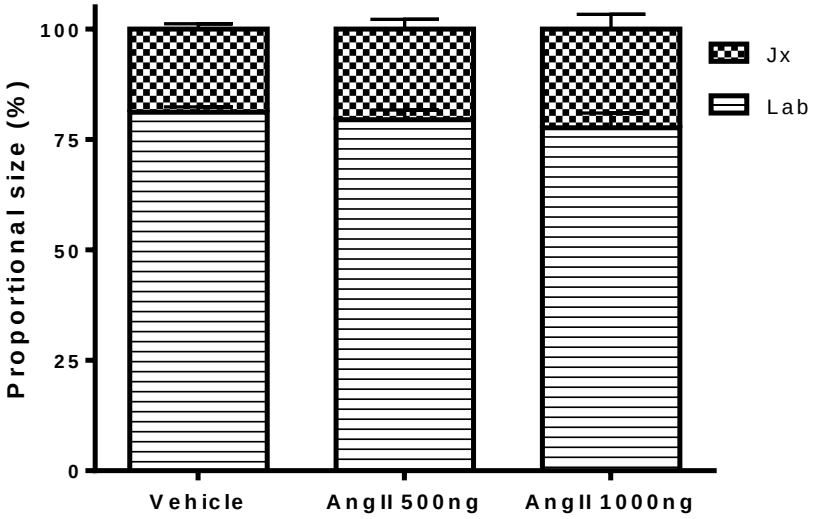


**Figure 6-24: Placental layer size expressed as a proportion of the total placenta**
Placental sections stained with periodic acid shciff stain were used to determine total placental size and the size of the junctional zone and labyrinth zones. The percentage of placenta that the junctional (Jx) and labyrinth (Lab) zones occupy is not altered with AngII treatment. Data presented as stacked mean ±SEM; n=3-5. Analysed using repeated measure two-way ANOVA, with SIdak post-hoc test comparing change between treatment group for each zone.

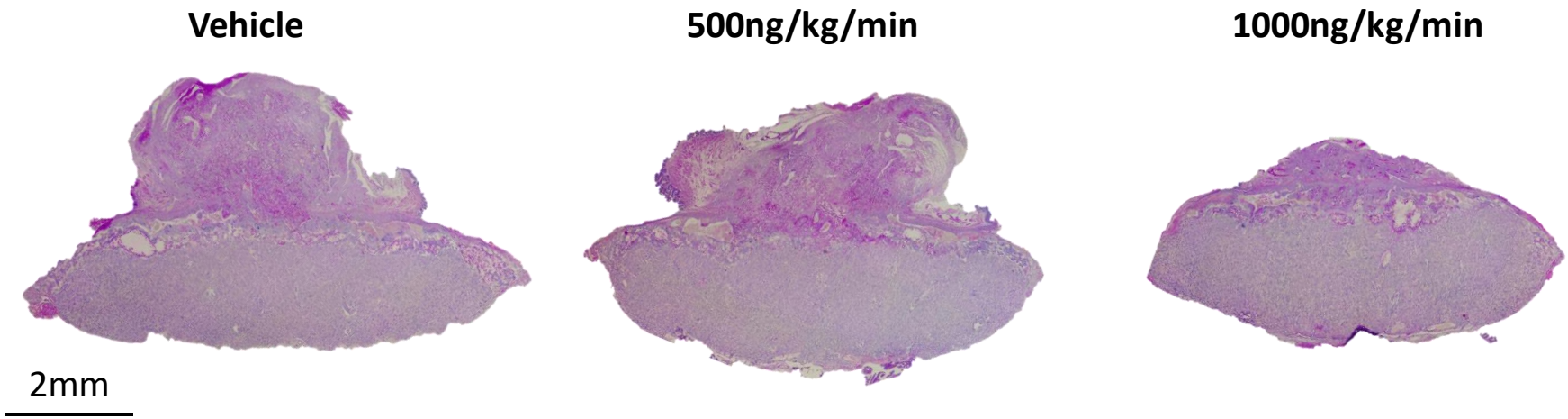


**Figure 6-25: Representative cross-sections of the GD18.5 placenta**
Composite images of GD18.5 placenta, showing the structure and layer definition of vehicle, 500ng/kg/min AngII treated and 1000ng/kg/min AngII treated placenta.

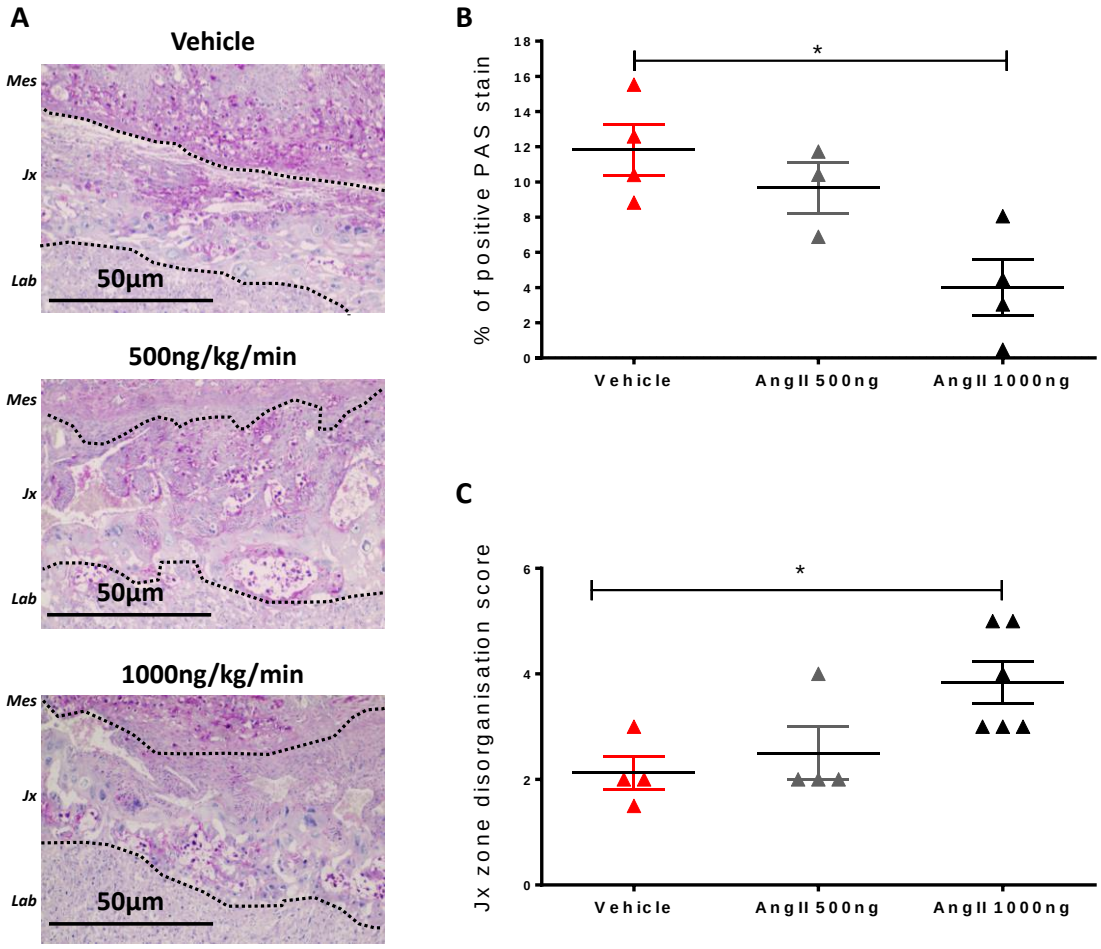


**Figure 6-26: Periodic acid Schiff assessment of the junctional zone of the placenta**
The morphology of the placenta was assessed visually using PAS staining at the midpoint (n=3-4). The junctional zone was identified by expected location and cellular morphology. (A) Representative images of the junctional zone at 10x magnification showing differences in staining intensity and structural organisation. (B) The percentage of pink positive staining within the outlined junctional zone was significantly reduced in 1000ng/kg/min AngII treatment groups. (C) The junctional zone was scored for disorganisation of the expected structure by a blinded operator with 1 = organised typical structure, with ordered distribution of cell types; 5 = no order and many large vacuous regions with sparse and disorganised distribution of cell types. The placenta from 1000ng/kg/min AngII treatment groups had a significantly greater disorganisation score. Mes = mesometrial triangle; Jx = junctional zone; Lab = labyrinth zone. Statistical analysis conducted using one-way ANOVA with Sidak post-hoc test; *p<0.05

### 6.4.3.2 Placental gene expression

The expression of genes involved in the RAS (Figure 6-27), oxidative stress (Figure 6-28), extracellular matrix degradation, hypoxia (Figure 6-29) and inflammation (Figure 6-30) were compared over the maternal component of the placenta (the mesometrial triangle (Mes)) and the two distinct placental layers (the junctional (Jx) and labyrinth (Lab) zones). The $AT^1$ (*Agtr1a*) and $AT^2$ (*Agtr2*) receptors had a 4.4 and 4.6 fold increase in expression, respectively, in the mesometrial triangle of the 1000ng/kg/min AngII treatment group compared to vehicle (*Agtr1a*: 11.7±0.3 ΔCT versus 13.8±0.6 ΔCT; $p<0.05$ and *Agtr2*: 13.8±0.7 ΔCT versus 15.4±0.5 ΔCT; $p<0.05$) (Figure 6-27 A-B). The $AT^2$ receptor also demonstrated a 14 fold increase in the junctional zone of placenta from 1000ng/kg/min AngII treated SHRSP compared to vehicle (12.1±0.9 ΔCT versus 14.8±0.9 ΔCT; $p<0.05$) (Figure 6-27B). The labyrinth zone had the highest levels of *Ace2* gene expression in all treatment groups and the 1000ng/kg/min AngII treatment significantly decreased the expression compared to vehicle and the 500ng/kg/min treatment group (10.7±0.2 ΔCT versus 9.9±0.1 ΔCT; $p<0.05$ and 10.1±0.1 ΔCT; $p<0.01$, respectively) (Figure 6-27C). The expression of *Ace* was undetectable in these experiments (CT values >38).

The expression of markers of oxidative stress (*Sod1*) and hypoxia (*Vegf1* and *Hif1a*) were not influenced by AngII treatment at either dose (Figure 6-28A-C). However, there was variation in the pattern of expression observed between layers, with vehicle treated dams having significantly greater *Sod1* expression in the placental junctional zone compared to the other locations examined. This variation between layers was not observed in the two AngII treatment groups.

Matrix-metalloprotease 2 and 9 gene expressions were found to be reduced in the mesometrial triangle of the 1000ng/kg/min AngII treatment group (Figure 6-29A-B). *Mmp2* (2.7±0.1 ΔCT versus 2.1±0.2 ΔCT; $p<0.05$) and *Mmp9* (14.1±0.2 ΔCT versus 12.6±0.3 ΔCT; $p<0.01$) both had a reduced expression in the 1000ng/kg/min AngII treatment group compared to vehicle, with *Mmp9* also having a significantly reduced expression in the 1000ng/kg/min group compared to the 500ng/kg/min AngII treatment group (4.1±0.2 ΔCT versus 13.2±0.2 ΔCT; $p<0.05$). There was no AngII-treatment dependent expression differences in *Mmp8* or the tissue inhibitor of Mmps (*Timp1*) (Figure 6-29C-D).

The expression of the C-C chemokine ligand 2 (*Ccl2*); a chemokine responsible for recruitment of monocytes and T-cells at sites of inflammation, and its receptor, the C-C chemokine receptor 11 (*Ccrl1*) were not significantly altered by AngII treatment in any of the maternal or placental locations (Figure 6-30A-B).

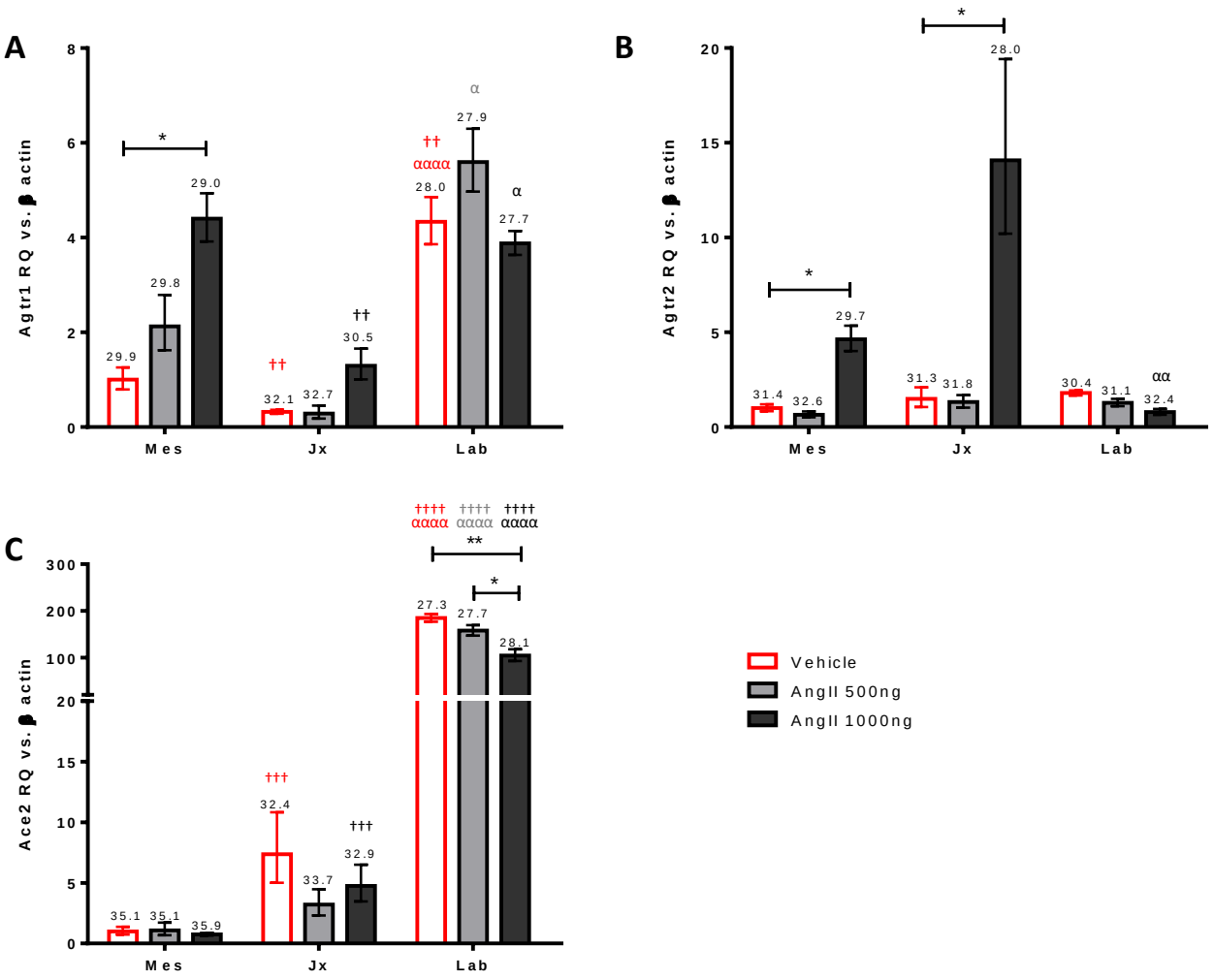


**Figure 6-27: RAS component gene expression across the maternal and placental layers**
Gene expressions of components of the RAS were analysed using qRT-PCR and are presented as relative quantities (RQ). All gene expression was normalised to *β actin* expression. (A) AngII receptor type 1 (*Agtr1a*) and (B) type 2 (*Agtr2*) expression was increased in the maternal mesometrial triangle layer (Mes) in placenta from 1000ng/kg/min AngII treated dams. *Agtr2* gene expression was also significantly increased in the junctional layer (Jx). (C) The expression of *Ace2* was greatest in the labyrinth zone (Lab) and this expression was decreased in the 1000ng/kg/min AngII treatment group. Data presented as $2^{-\Delta\Delta CT}$ relative to vehicle mesometrial triangle (Mes) ±SEM relative to the ΔCT. Statistical analysis was conducted using ΔCT values compared using one-way ANOVA with Tukeys post-hoc test for comparisons over treatment group (*p<0.05, **p<0.01), and separately compared expression change over the different layers for each treatment group (vs Mes: †p<0.05, ††p<0.01; vs Jx: ᵅp<0.05, ᵅᵅp<0.01, ᵅᵅᵅp<0.001) (n=4-5). Values above each bar indicate unadjusted cycle threshold values.

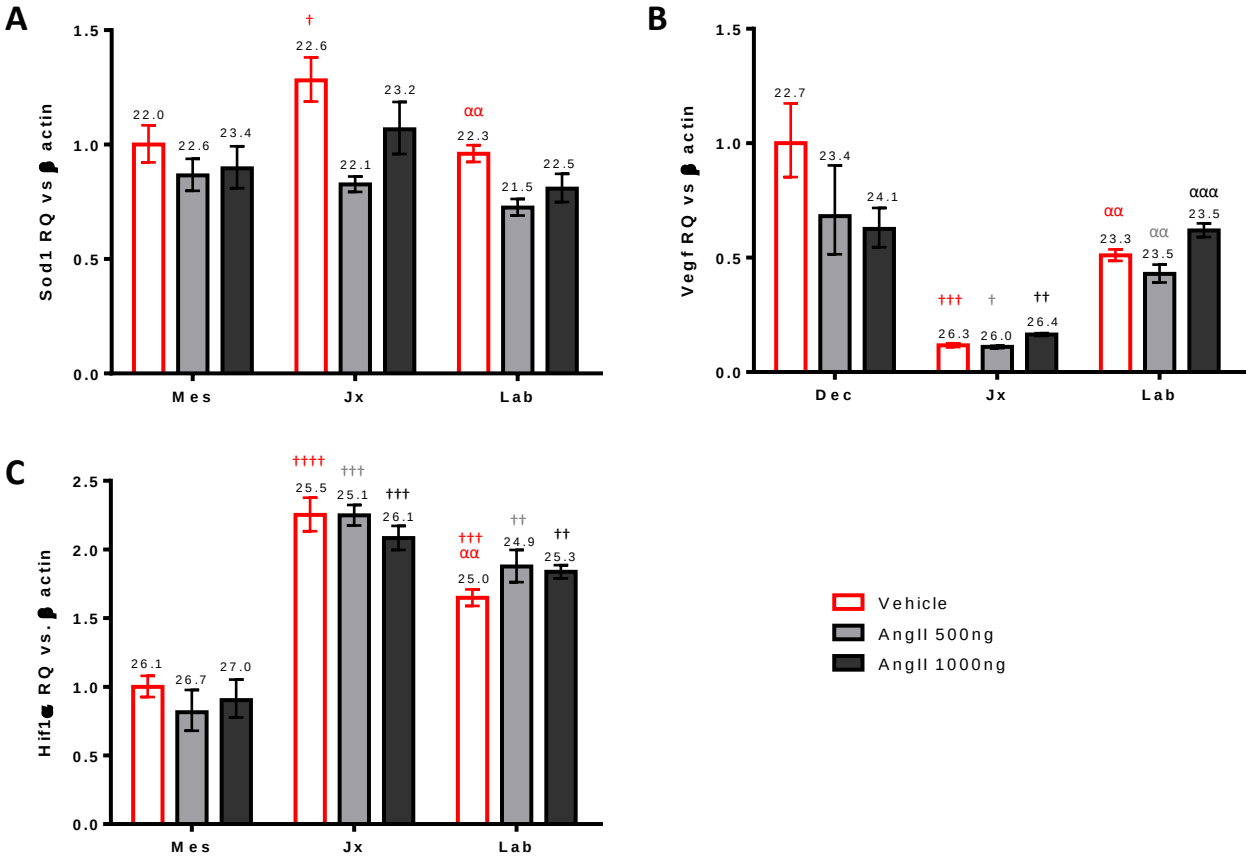


**Figure 6-28: Gene expression of markers of oxidative stress and hypoxia across the maternal and placental layers**

Gene expressions of (A) superoxide dismutase 1 (*Sod1*), (B) vascular endothelial growth factor receptor (*Vegf1*) and (C) hypoxia-inducible factor α (*Hif1α*) were analysed using qRT-PCR and are presented as relative quantities (RQ). All gene expression was normalised to *β actin* expression. There were no significant differences in the expression due to AngII treatment within each layer (Mes = mesometrial triangle; Jx = junctional zone; Lab = labyrinth zone). Data presented as $2^{-\Delta\Delta CT}$ relative to vehicle Mes ±SEM relative to the ΔCT. Statistical analysis was conducted using ΔCT values compared using one-way ANOVA with Tukeys post-hoc test for comparisons over treatment group and separately compared expression change over the different layers for each treatment group (vs Mes: †p<0.05, ††p<0.01; †††p<0.001; ††††p<0.0001 vs Jx: ᵅᵅp<0.01, ᵅᵅᵅp<0.001) (n=4-5). Values above each bar indicate unadjusted cycle threshold values.

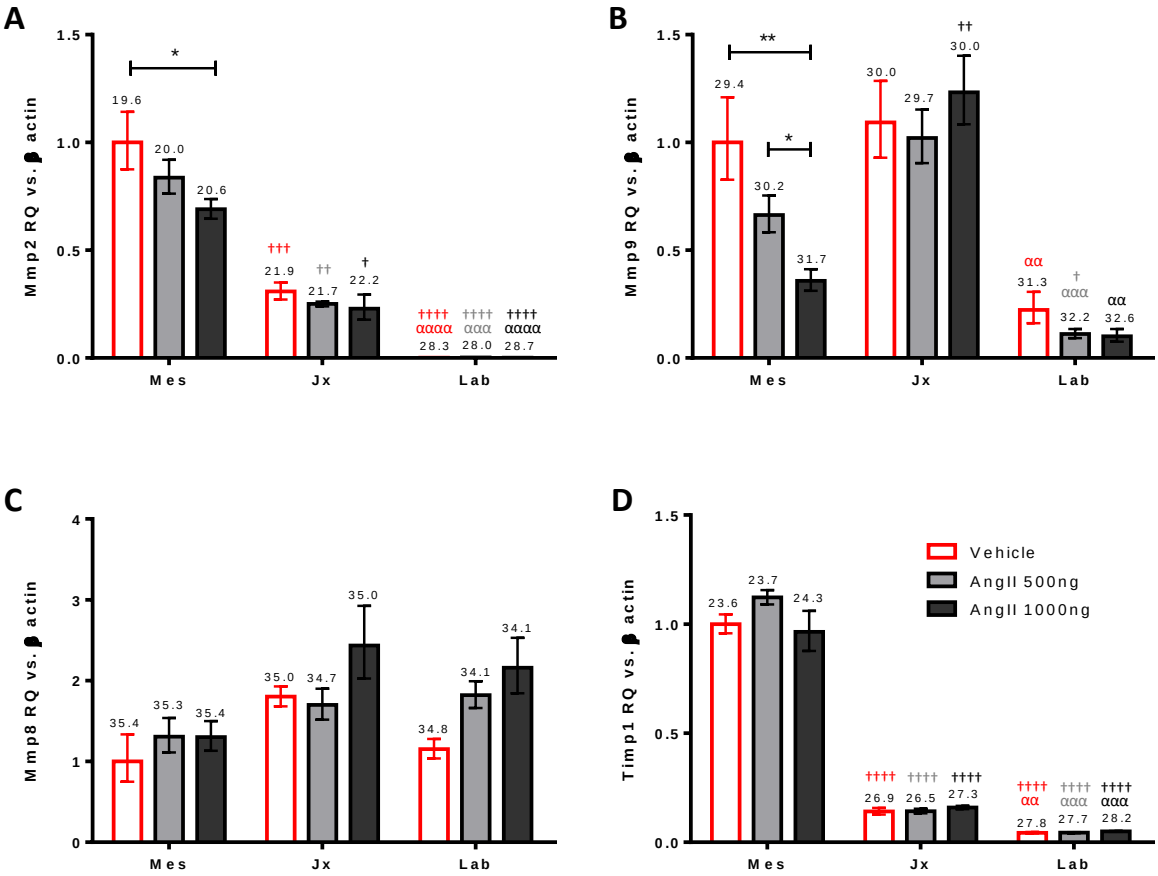


**Figure 6-29: Gene expression of factors influencing extracellular matrix composition and degradation**

Gene expressions of (A-C) matrix metalloprotease (*Mmp*) 2, 9 and 8 and (D) tissue inhibitor of metalloproteinase 1 (*Timp1*) were analysed using qRT-PCR and are presented as relative quantities (RQ). All gene expression was normalised to *β actin* expression. *Mmp2* and *Mmp9* were significantly less expressed in the mesometrial triangle (Mes) of placenta from 1000ng/kg/min AngII treated dams. There were no significant differences in response to AngII treatment in the placental layers (junctional (Jx) and labyrinth (Lab) zones). There were also no significant differences in expression of *Mmp8* or *Timp1* in any of the investigated locations. Data presented as $2^{-\Delta\Delta CT}$ relative to vehicle mesometrial triangle (Mes) ±SEM relative to the ΔCT. Statistical analysis was conducted using ΔCT values compared using one-way ANOVA with Tukeys post-hoc test for comparisons over treatment group (*p<0.05, **p<0.01), and separately compared expression change over the different layers for each treatment group (vs Mes: †p<0.05, ††p<0.01; †††p<0.001; ††††p<0.0001 vs Jx: ᵅᵅp<0.01, ᵅᵅᵅp<0.001; ᵅᵅᵅᵅp<0.0001) (n=4-5). Values above each bar indicate unadjusted cycle threshold values.

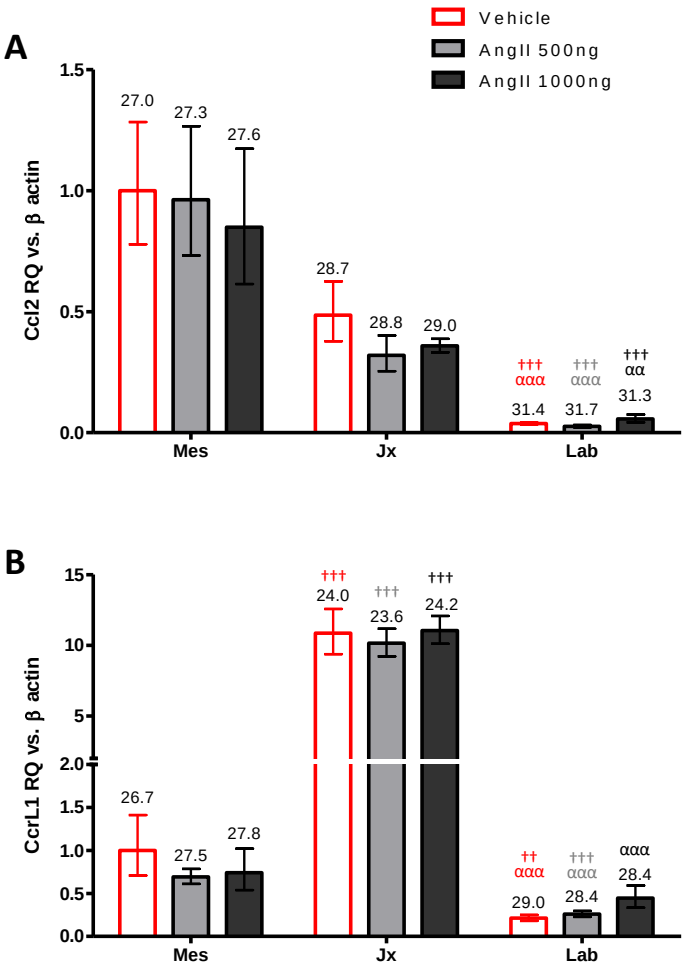


**Figure 6-30: Gene expression of factors influencing placental inflammatory response**
Gene expressions of (A) C-C chemokine ligand 2 (*Ccl2*) and (B) C-C chemokine receptor type 11 (*CcrL1*) were analysed using qRT-PCR and are presented as relative quantities (RQ). All gene expression was normalised to *β actin* expression. There were also no significant differences in expression of either gene in any of the investigated maternal (mesometrial triangle: Mes) or placental (junctional zone: Jx and labyrinth zone: Lab) layers. Data presented as $2^{-\Delta\Delta CT}$ relative to vehicle mesometrial triangle (Mes) ±SEM relative to the ΔCT. Statistical analysis was conducted using ΔCT values compared using one-way ANOVA with Tukeys post-hoc test for comparisons over treatment group, and separately compared expression change over the different layers for each treatment group (vs Mes: ††p<0.01; †††p<0.001 vs Jx: ᵅᵅp<0.01, ᵅᵅᵅp<0.001) (n=4-5). Values above each bar indicate unadjusted cycle threshold values.

## 6.5 Discussion

This chapter has provided evidence that AngII infusion in the pregnant SHRSP can mimic phenotypes of superimposed pre-eclampsia. The data presented indicate that SHRSP treated with the 1000ng/kg/min dose of AngII had an impairment of their haemodynamic and cardiovascular responses to pregnancy. Phenotypes of severe pre-eclampsia; such as a further elevation of blood pressure, decreased cardiac output, proteinuria, fetal growth restriction (FGR) and placental abnormalities were all documented in this study.

The SHRSP rat has pre-existing chronic hypertension which made it an ideal candidate for studying superimposed pre-eclampsia. The current study intended to use normotensive rats (WKY) as a control strain for AngII infusion during pregnancy in the SHRSP strain. However, this was unsuccessful due to the low survival of the WKY dams. The more rapid deterioration observed in maternal health in AngII treated WKY rats was unexpected and may suggest that SHRSP rats having compensatory mechanisms that allow these dams to cope with a high blood pressure during pregnancy. Chronically hypertensive SHRSP males have been found to have higher plasma AngII levels than WKY in later adult life (25 weeks) (Kim et al., 1991). This suggests that SHRSP are exposed to 'high' AngII concentrations during adult life and thus may be primed to deal with this insult on the cardiovascular system (Kim et al., 1991). The same may be true for females, although this has not been previously investigated.

Vehicle treated SHRSP dams demonstrated maternal weight gain and increased cardiac output during pregnancy, despite pre-existing hypertension. In human pregnancy maternal weight is found to increase by approximately 12.5kg, on average (Thornburg et al., 2015). This increase can be attributed to an approximate 10% increase in protein, 30% increase in fat and 60% increase in water, with the gravid uterus only accounting for 10% of this weight increase (Thornburg et al., 2015). The increases in cardiac output are essential to maintain adequate organ perfusion in the mother whilst increasing uteroplacental blood flow in order to sustain the developing fetus and placenta. The AngII treated dams did not show this increase in weight or cardiac output, and in fact showed a 'gradient' of pathophysiology in which there was no change in the CO with the lower AngII dose and negative impact on CO in the higher

AngII treatment group as this demonstrated a reduction over pregnancy. The weight loss associated with the higher (1000ng/kg/min) AngII treatment group could be in part attributed to the increased urine excretion observed, however further measurements of body composition would need to be conducted to conclude this. Reductions in weight gain have been associated with poor fetal outcome and impaired CO is often observed in severe pre-eclampsia in humans (Visser and Wallenburg, 1991, Stott et al., 2017).

Tail cuff plethysmography and radiotelemetry both confirmed AngII administration was responsible for an increase in systolic and diastolic blood pressure, as anticipated. However, the radiotelemetry revealed a disruption of the diurnal heart rate rhythm. The dip observed immediately post-AngII infusion in the 1000ng/kg/min treatment group could be accounted for by an activation of the baroreflex. The sudden increase in blood pressure activates the stretch sensitive baroreceptors which signal to reduce heart rate in order to reduce blood pressure. This may also account for the loss of amplitude observed in this group as the constant active firing of the receptors can lead to desensitization and thus loss of diurnal control. Interestingly, many cardiac events occur early morning suggesting circadian rhythm plays an important role in the homeostasis of the cardiovascular system and likewise the onset of labour is more common at these times. The blood pressure profiles of the vehicle and AngII treated SHRSP should be judged with caution, this is due to the limited sample size. Only three dams from each group were analysed. This was due to equipment and time constraints, but also due to uncertainty over pregnancy outcome, i.e. some dams did not give birth and it was unclear whether they had not been pregnant to begin with or had lost the pregnancy. These animals were removed as to not add variation of the impact of AngII on no-pregnant SHRSP blood pressure.

Treatment with AngII impacted the kidney function of SHRSP evident by the increased urine production with increased proteinuria. ACR in the 1000ng/kg/min AngII treated group was higher despite increased urine production. This increase in urine production is in contrast to the physiological role of AngII in the kidney to stimulate water reabsorption. Further kidney abnormalities were noted in the reduction of the Bowman's space in kidneys from dams treated with AngII. This morphological assessment provides some

evidence that AngII infusion impacts on the structure of the renal corpuscle. However, assessment of glomeruli function and filtration rates would be provide a more in depth renal evaluation of this model.

Pre-eclampsia is associated with endothelial dysfunction and an increased vascular resistance (Steegers et al., 2010). Small *et al* have previously shown that pregnant uterine arteries from SHRSP have an impaired blood flow, and impaired responses to vasoconstrictors and vasodilators (Small et al., 2016). The AngII treatment did not significantly alter the uterine artery blood flow *in vivo* or impact significantly on the *ex vivo* functional properties. This could be due to uterine arteries from SHRSP having a 'maximum impairment' regardless of treatment; therefore, it is possible that the blood flow and function of the uterine arteries are as inefficient as they can be whilst still maintaining a pregnancy. The uterine artery sensitivity to exogenous AngII was unchanged between treatment groups. Other studies using the transgenic human angiotensinogen-renin cross have found that exposing uterine arteries from the transgenic dams to AngII *ex vivo* does increase contractile responses, suggesting these animals have increased sensitivity to AngII (Hering et al., 2010, Verlohren et al., 2008). It is possible that the lack of responses observed in our SHRSP model could be due to a low exposure time during pregnancy (a total of 8 days AngII infusion) compared to similar studies, or that the systemic increase in AngII has different effects than the more localised AngII exposure in the transgenic model; around the uteroplacental area (Hering et al., 2010, Xue et al., 2017). Alternatively, SHRSP rats have a different genetic profile to the Sprague Dawley rats used as the transgenic background which alters the proportion of AngII receptors available. However further pharmacological manipulations would need to be conducted to confirm this.

There was evidence of reduced uterine artery diameter with reduced cross-sectional area suggesting the period of AngII infusion in pregnancy is having an impact on uterine artery structure and may be indicative of a lack of appropriate pregnancy associated remodelling (Small et al., 2016). Healthy pregnancy is associated with outward hypertrophic remodelling of uterine vasculature (Osol and Mandala, 2009). This creates an increased vessel diameter with wider lumen due to dedifferentiation of vascular smooth muscle cells and allows the

increased blood flow to the placenta (Lash et al., 2010b). Changes observed in these AngII treated dams were more akin to inward eutrophic remodelling, a reduction in diameter with no change in wall thickness, which is associated with small arteries and hypertension. However, it is possible that the vessels are not undergoing any remodelling, and are simply remaining at in a pre-pregnancy state. In order for this to be fully investigated uterine arteries from untreated dams at GD10.5 would need to be studied to determine the remodelling that had already taken place before AngII infusion began. Pre-eclampsia in humans has been associated with a lack of the outward hypertrophic remodelling observed in normal pregnancy (Mandala and Osol, 2012).

The mesenteric arteries were used as a representation of the systemic vasculature. Pressure myography showed that 500ng/kg/min AngII treatment had no significant effect on vessel structure over a range of physiological pressures. Unfortunately, a major limitation to this study was that only two sets of mesenteric arteries were successfully assessed using pressure myography and thus no robust conclusion can be drawn from the highest AngII treated group.

As well as investigating the effects AngII-induced hypertension during pregnancy has on maternal health, this study assessed the effect elevated AngII had on placental and fetal development. The main finding was that the offspring from AngII treated dams had a reduced size both at the fetal stage and neonatal. Fetal growth restriction (FGR) is the failure of the fetus to reach its genetically predetermined growth potential and commonly occurs alongside pre-eclampsia (Bamfo and Odibo, 2011). FGR and pre-eclampsia have similar risk factors and in some instances the pre-eclampsia can be the cause of FGR and in others the FGR may be occur independently (Odegard et al., 2000). FGR is associated with a separate set of risks to the fetus, such as an increased risk of stillbirth (Gardosi et al., 2013). Clinically if a fetus is determined to be below the lowest 5$^{th}$ percentile of the population of fetal weights it is deemed growth restricted (Gardosi et al., 2013). The majority of fetuses from the 1000ng/kg/min AngII treatment group had a weight that fell under the 5$^{th}$ centile for normal SHRSP fetal weights at GD18.5. Smaller neonatal weights were also observed and the growth rate in the first two days was reduced in the offspring exposed to the high dose AngII treatment *in utero*. However, due to the low sample size for

neonates (with measurements for only two 1000ng/kg/min AngII treated litters being available) the interpretations of neonatal growth are very preliminary. Furthermore, the offspring development after parturition was only limitedly examined in this study. The *in utero* environment plays a vital role in fetal development and has been linked to the developmental origins of health and cardiovascular disease (The Barker Hypothesis) (Barker et al., 1993). Dysregulation of the RAS *in utero* has been associated with pathophysiological responses in the offspring in later life and has been linked to the development of hypertension (Arguelles et al., 2017, Xue et al., 2017, Sibai, 2002). Xue *et al* demonstrated offspring exposed to low pressor AngII *in utero* developed a hyper-sensitivity to AngII-induced hypertension as adults (Xue et al., 2017). These offspring had a higher chance of developing cardiovascular disease due to differences in developmental programming *in utero* compared to untreated counterparts (Xue et al., 2017). The cause for the growth restriction in the SHRSP-AngII infusion model used in this study is unclear as there were no further deficiencies in uteroplacental blood flow of AngII treated SHRSP rats. This suggests that there was no restriction of nutrient availability to the placenta and thus the fetus via impaired blood flow. However, we did not investigate the impact of AngII on the spiral arteries of these dams. It is these vessels which undergo the most remodelling and there is general agreement that a failure of remodelling is linked to the development of pre-eclampsia and FGR. Another factor that could impair fetal growth is placental function and its transport capacity, however this was not assessed in this study. In human placenta an activation of the $AT^1R$ via AngII has been found to reduce the placental transport of system-A amino acids (Shibata et al., 2006).

Placental abnormalities were evident when examining the morphology of the placenta as there was a reduction in positive PAS staining in the junctional zone, which also appeared disorganised compared to vehicle. PAS staining can identify glycogen, glycoproteins and glycolipids (Akison et al., 2017). The stain can be used to highlight the glycogen cells of the junctional zone in the placenta. These cells are known to disappear before parturition and the functions of the glycogen stores are not fully understood (Akison et al., 2017, Furukawa et al., 2014). The depletion of these stores associated with the AngII treatment may be indicative of the placenta struggling to maintain an appropriate function and

possibly utilising the glycogen reserves as it is not receiving appropriate nutrients from the mother. This is concurrent with growing evidence that placental glycogen depletion is associated with complications of pregnancy and fetal distress (Akison et al., 2017). However, the glycogen stores in human and rodent placenta differ as humans do not have the sub-populations of giant trophoblast cells (Furukawa et al., 2014). Any interpretation of placental function would require a more rigorous study of function and metabolism before any substantial conclusions were drawn.

The placenta is the main extra renal source of AngII, and has been found to process all the components for a working RAS (Nielsen et al., 2000). Vaswani *et al* found there is a gestational dependent increase in the expression of RAS components in rodent placenta (Vaswani et al., 2013, Vaswani et al., 2015). This study suggests that the placental RAS is dynamic throughout pregnancy and can be altered by changes in AngII. Placental gene expression investigated in this chapter revealed that AngII infusion influenced the expression of the angiotensin receptors ($AT^1R$ and $AT^2R$) and *Ace2* in different layers of the placenta. The AngII receptors have been located within the placenta in humans and rats, amongst many other placental mammals (Nielsen et al., 2000). The $AT^1R$ has been found in rodent placenta and its expression has been found to be altered by AngII concentrations in humans (Kalenga et al., Kalenga et al., 1996). The $AT^2R$ subtype has been found to be the more prominent type found in non-pregnant rat uterus and human myometrium (Nielsen et al., 2000, de Gasparo et al.). Both receptor subtypes were identified in SHRSP placenta in this study and were found to be upregulated in the maternal tissue (the mesometrial triangle) when concentrations of AngII treatment were highest. This layer is highly vascularised and an increased expression of $AT^1R$ could suggest an increased sensitivity to AngII and thus an enhanced constriction response and restriction of blood flow to the placenta. Pre-eclampsia has been associated with an increased activation of the $AT^1R$ via the angiotensin II type I receptor agonistic autoantibody ($AT^1$-AA) (Wallukat et al., 1999, Herse and LaMarca, 2013). The presence of this autoantibody has not been investigated in SHRSP pregnancy. There was also, however, an increase in $AT^2R$ expression in this maternal layer. $AT^2R$ expression was also found to increase more than 10-fold in the junctional zone in the presence of elevated AngII. A strength of these studies was the placenta

dissections performed, which gives a better representation of the gene expressions in the placenta and the different functions of the cells within it. Previously, studies have identified AngII receptors in the placenta, however they have not been localised to a particular layer. Analysing gene expression in this manner this will help evaluate the roles these receptors play in physiological and pathophysiological pregnancies. A key enzyme involved in removing AngII is Ace2. This enzyme removes AngII by cleaving the peptide to form Ang1-7, which is proposed to have a vascular protective effect. This study provided evidence that increases in AngII cause a decrease in *Ace2* expression in the labyrinth zone. This could be exacerbating any possible damage AngII is causing in the placenta as it is not being broken down and thus prolonging negative effects. Ace2 is mainly found in vascular endothelial cells, and the placental labyrinth is highly vascularised with many fetal vessels surrounding maternal blood sinuses. It is unclear from this study where *Ace2* expression is changed within this zone. The effects of AngII on the placental RAS gene expression will have occurred in a relatively short period of time (8 days) however AngII was administered once the rodent placental cell lineages are established, during the formation of the chorioallantoic placenta. This suggests that AngII infusion may be causing placental dysfunction rather than causing a failure of placental development since viable fetuses were able to develop.

Matrix metalloprotease 2 and 9 are gelatinases that degrade various extracellular matrix components. They are largely expressed in maternal decidua and play an important role in early vascular remodelling and are then also involved in parturition (Naruse et al., 2009, Dias-Junior et al., 2017, Raffetto and Khalil, 2008, Geng et al., 2016). These Mmps were found to be decreased in the maternal layer of SHRSP rats exposed to high AngII concentrations. A reduction of uterine *Mmp2* and *9* has been associated with increased placental ischaemia in the reduced uterine perfusion model of pre-eclampsia in rats, which further suggests AngII is having a detrimental effect on the placenta (Dias-Junior et al., 2017).

The placenta analysis was limited in that the main findings were related to gene expression changes. Many of these expression changes could have impacted on placental function, such as transport, which unfortunately was not examined in

this study. Due to this model utilising AngII, a thorough characterisation of the functional placental RAS would have been greatly beneficial.

To summarise, AngII infusion during pregnancy in SHRSP rats impacts on the maternal cardiovascular and renal systems as well as causing a growth restriction in the offspring, that is possibly mediated by placental dysfunction. The impact in adult SHRSP offspring that were exposed to this increased AngII *in utero* was not determined in this study but would be a useful tool in investigating the effects a hypertensive pregnancy can have on development. Furthermore, the impact on the maternal systems in the SHRSP have mimicked those changes observed with severe hypertensive disorders and could be utilised to investigate whether maternal health is negatively altered post-pregnancy and if there is a generation of an increased cardiovascular risk because of this elevated hypertensive insult during pregnancy. This model has the ability to be adapted to expose the already hypertensive mother to different degrees of cardiovascular stress. This will be useful in determining underlying mechanisms of gestational hypertension and in the assessment of novel therapeutic strategies in future and, when used in parallel with other animal models, has the potential to aid our understanding of pre-eclamptic conditions.

# Chapter 7 General Discussion

The prevalence of hypertension in modern society is rapidly increasing the frequency of pregnancies with hypertensive complications (Roberts et al., 2011). The impact this has on the mother is not only relevant during pregnancy but also for decades after (Bokslag et al., 2017). Furthermore, the associated risks to the fetus have been well established, thus making the need to fully understand these disorders all the more pressing (Staley et al., 2015). The maternal cardiovascular system is now more accepted as a major influencer of pregnancy-related hypertensive disorder development than it once was (Kalafat and Thilaganathan, 2017). Therefore, there is a more prominent need for investigation of pregnancy related hypertension stemming from a maternal pathology. In order for this to be achieved it is crucial that appropriate animal models are developed to uncover the underlying mechanisms of the disorders in order to determine treatments.

The SHRSP rat is known to have pre-existing hypertension that is maintained through pregnancy (Small et al., 2016). This is associated with an impaired maternal vascular response, evident by reduced uteroplacental blood flow and impaired uterine artery function (Small et al., 2016). The work outlined in this thesis focuses on pregnancy in SHRSP rats in order to provide information on an impaired vascular response to pregnancy, and allow for the evaluation of placental and fetal development in a hypertensive environment. Prior to this work, the need for a more thorough characterisation of SHRSP pregnancy was identified. Pregnancy in this strain has been investigated by relatively few groups (Small et al., 2016, Barrientos et al., 2017, Yamada et al., 1981, Fuchi et al., 1995a), and there have been omissions in regards to the pregnancy-driven cardiovascular adaptations of the SHRSP dam. The work of this thesis compiles a thorough characterisation of the SHRSP maternal adaptations to pregnancy, alongside assessment of fetal and placental outcomes. The investigations in SHRSP dams were conducted in parallel with investigations of pregnancy adaptations in the normotensive reference strain, WKY. Profiling the physiological maternal response to pregnancy was crucial for the correct assessment of any pathological change observed in SHRSP pregnancy. The cardiovascular parameters measured using echocardiography in this study, have to our knowledge, never been used to investigate pregnancy in WKY or SHRSP before. The cardiovascular adaptations to pregnancy, outlined in Chapter 1.1.1,

revealed WKY dams mirrored the pregnancy-associated changes observed in healthy humans (Robson et al., 1989). Interestingly, the increase in cardiac output observed in WKY pregnancy was also observed in SHRSP dams. Pathologies identified by other studies, such as proteinuria, were not observed in this cohort of pregnant SHRSP (Small et al., 2016, Barrientos et al., 2017). Proteinuria is often associated with more severe hypertensive disorders of pregnancy and the findings of this work suggested SHRSP dams have a milder gestational hypertensive phenotype. This suggestion was supplemented by the findings of similar fetal size and number per litter between WKY and SHRSP, which is in contrast to other studies which have demonstrated significant fetal growth restriction and implantation issues in the SHRSP (Fuchi et al., 1995a, Small et al., 2016, Barrientos et al., 2017). The yearly variation in litter sizes revealed in this thesis, from the large numbers of recorded matings over the last decade, suggest caution should be applied when interpreting results from a single study cohort of animals. A more definitive consensus on the litter size and fetal weights will be achieved eventually through conducting more studies and thus further reporting on SHRSP pregnancies. Yet, SHRSP pregnancy, investigated in this thesis, was not without impairment. Left ventricular hypertrophy, inferred from the increased left ventricular mass, was still evident in SHRSP dams during pregnancy. Cardiac hypertrophic remodelling has been associated with pre-eclampsia in humans (Melchiorre et al., 2013), and would suggest the maternal cardiovascular response to pregnancy in SHRSP dams was not as efficient as that of the normotensive WKY.

Previously, Small *et al*, have shown that SHRSP dams have a reduced uterine artery blood flow during pregnancy and that the uterine artery is less responsive to vasodilation than the WKY (Small et al., 2016). Healthy pregnancy is associated with reduced vascular resistance and an increased blood flow to the uterus (Ferrazzi et al., 2018, Osol and Moore, 2014), yet in the SHRSP the uterine artery blood flow was reduced and delivery to the uteroplacental unit was restricted. Fuchi *et al* also found evidence that the central spiral artery that supplies the placenta had a reduced lumen in SHRSP dams (Fuchi et al., 1995b). Further investigations of pregnancy-dependent maternal vascular changes in the SHRSP were conducted in this thesis, firstly, by examining the mesenteric artery changes through gestation, outlined in Chapter 4. These resistance arteries are

often used as proxy for interpreting what is occurring systemically in other hypertensive pathologies (Kopf et al., 2018, Klein et al., 2018, Wynne et al., 2018). There was evidence of pregnancy-dependent increases in vasodilatory response in the WKY which were absent in the SHRSP dams. Both strains demonstrated an overall gestational-dependent reduction in cross-sectional area, however, the SHRSP exhibited a smaller cross-sectional area compared to the WKY at term; this was associated with wall thinning of the mesenteric arteries. Hypertension is generally associated with a narrowing of the vasculature, whilst pregnancy achieves the opposite aiming to reduce total peripheral resistance (Poppas et al., 1997). There was evidence of an increased lumen size in both strains, yet SHRSP showed significant wall thinning that was not observed in WKY. This implies that systemic vascular adaptation to pregnancy is different between strains, yet it is possible that these different mechanisms occur to allow the same outcome; which is a vascular system that can cope with the increased blood volume associated with pregnancy. Measurements of blood volume and total peripheral resistance would provide further evidence to support or refute these conclusions.

One of the main aims of this thesis was to determine the underlying mechanisms of uterine artery impairment previously observed in late gestation. Work was conducted to establish whether the uterine artery impairment was apparent between non-pregnant WKY and SHRSP and in the early stages of pregnancy (GD6.5). This early gestational time point is post-implantation but prior to the establishment and invasion of placental cells, and so allowed for the investigation of maternally driven remodelling effectors (Soares et al., 2012). There were no differences in the functional response or passive mechanical properties of uterine arteries between non-pregnant and early pregnant state in either strain. This observation was intriguing as it provided further evidence that the eventual impairment was not pre-existing and therefore could not be attributed to maternal hypertension alone. In an attempt to reveal the influences of maternal pregnancy-dependent plasma factors on uterine artery function, non-pregnant uterine artery explants were incubated with plasma from non-pregnant and early/late pregnant dams. The results of which concluded that circulating factors in early gestation may have a more prominent role in altering vascular function. However, as no functional differences were observed between

strains at this early gestational time point the logical step was to then investigate transcriptional alterations between uterine arteries from non-pregnant rats and dams in these early stages of pregnancy.

The work in Chapter 5 was the first to utilise RNA-Seq to profile the transcriptional changes of the uterine arteries during pregnancy. The number of expression changes revealed were vast, and only a fraction of the potential implications were expanded upon in subsequent data analysis and experiments. A number of similar uterine artery gene expression changes were identified between WKY and SHRSP in response to pregnancy, which suggests that some adaptations to pregnancy are essential and conserved between the two strains. However, the profile of uterine artery gene expression between non-pregnant and pregnant states also demonstrated numerous differences. When taken with the fact that there were no observed functional differences this is all the more interesting, as it suggests that at a molecular level the two strains are already responding to pregnancy differently even after only a relatively short period of gestation. Some of the pathways that were identified belonged to an overarching theme of increased energy production/demand and increased inflammatory and oxidative stress production. SHRSP uterine arteries demonstrated an increased expression of Nox2 subunits and a changed expression pattern of genes influencing inflammatory response that suggests a more inflammatory environment in these pregnant SHRSP vessels than in WKY. An increased Nox2 expression has been identified to propagate oxidative damage within the vascular system in hypertension (Harvey et al., 2017). It is not clear from the work in this thesis why SHRSP pregnancy elicits this gene expression change, but the hypothesis derived from these findings is that the uterine arteries of SHRSP are primed for to respond differently to pregnancy-associated remodelling stimuli. Previous studies in older, male SHRSP rats have demonstrated that the damage to the vascular system is associated with increased ROS production and inflammation compared to WKY (Harvey et al., 2017, Akasaki et al., 2006, Nakamura et al., 2008). Whilst no differences between the gene expression of non-pregnant strains was revealed in this work, both pregnancy and age can increase stress within the cardiovascular system and may be doing so via similar mechanisms (Hibbard et al., 2015, Weisfeldt, 1998). Further analysis of functional and gene expression changes of the uterine artery as gestation

progresses could be conducted to determine when the impairment occurs. In order to fully determine the mechanisms of SHRSP uterine artery remodelling (or lack thereof) it would also be beneficial to look at the individual cell types composing the uterine artery. Nox2, for example, is mainly located in endothelial cells, whereas the majority of differentially expressed genes identified as involved in $Ca^{2+}$ regulation reside in the VSMC (Selemidis et al., 2008, Webb, 2003). Work towards examining the different cell types was initiated in this thesis as VSMC were isolated and WKY $Ca^{2+}$ signalling investigated *in vitro*. With advancements in RNA-Seq capabilities there is the potential to examine the gene expression profiles of specific cell populations. The sensitivity of RNA-Seq means that low volumes of starting material can now be used which could utilise the isolation of the different cell populations or laser capture of specific regions (Nelson et al., 2016).

The changes specific to the uterine vascular transcriptome have not previously been investigated during pregnancy in any species or model, furthermore no other vascular beds have been examined across gestation. RNA-Seq technologies are incredibly beneficial in determining alterations in gene expressions that occur over short periods of time and in providing insight into transcriptional regulation, and thus are well suited to the relatively short timescale of change over the gestational period (Wang et al., 2009). Many pregnancy-related studies have focused on the transcriptome profile of the placenta, which is understandable as this vital pregnancy-specific organ is central to the success and maintenance of pregnancies (Kaartokallio et al., 2015, Cox et al., 2015, Nelson et al., 2016, Wakeland et al., 2017). However, the acceptance of the theory that hypertensive disorders of pregnancy are solely placental syndromes is waning, with the maternal cardiovascular system being at the forefront of alternate concepts of disorder development (Kalafat and Thilaganathan, 2017). It has been suggested that it is the maladaptation's of the cardiovascular system that result in the symptoms, and thus, the vascular system gene expression regulation and alterations that occur in response to pregnancy should be of key importance. Of course, in human pregnancy it is only possible to sample microvasculature, such as resistance arteries from subcutaneous fat biopsies or spiral arteries from decidual/myometrial biopsies taken from the placental bed (Corcoran et al., 2012, Cockell and Poston, 1997), and this sampling is often

conducted only at term; therefore, the gene expression changes cannot compare early gestational changes. These issues can be overcome by the use of appropriate animal models, which allow for the precise investigation into physiological and pathophysiological pregnancy-dependent changes.

Another strength of RNA-Seq technologies is that it allows the informative assessment on non-coding RNAs. In this thesis the focus was placed upon protein coding genes, with only limited investigation of the lncRNAs conducted. LncRNAs can modify many cellular processes, most crucially for the context of this work are the roles involved with control of RNA expression (Wang and Chang, 2011, Wang et al., 2017). There are many proposed actions of this epigenetic regulation, from direct promotion/silencing of genes to modifications of the methylation status (Wang and Chang, 2011, Wang et al., 2017), and a range of diverse and complex mechanisms of action that are specific for individual lncRNAs and locations (Wang et al., 2017). In human studies, lncRNAs identified in the placenta have been implicated in the development of pre-eclampsia (He et al., 2013, Li et al., 2018). The study of lncRNAs is still a rapidly expanding field, with the majority of work conducted in humans and mice. This can be seen as a drawback in conducting gene expression research in rats, however the SHRSP rat is a widely used genetic model of hypertension and has had its genome sequenced, so has potential to keep pace with other species.

A large proportion of the work in this thesis has focused on the determination of maternally driven pathologies associated with hypertensive pregnancy in the SHRSP. Yet both maternal and placental factors have been shown to play a crucial role in the development of hypertensive disorders of pregnancy, and the placental involvement should not be ignored. Placental abnormalities have been observed in SHRSP pregnancies prior to this study, with this thesis providing further evidence towards placental impairment (Fuchi et al., 1995a, Small et al., 2016, Barrientos et al., 2017). Placental glycogen content was lower in SHRSP than WKY at mid-gestation and late gestation. Placental glycogen cells found in the junctional zone of the rodent placenta are known for their accumulation of glycogen (Coan et al., 2006). Their precise functions have not yet been identified, however, one possible function is that they are an energy supply for the placenta (Gebbe et al., 1972). This is supported by the findings of depleted

glycogen in late gestation, when the exponential growth of the fetus places a greater demand on maternal resources thus using the placental glycogen reserves to meet those demands (Coan et al., 2006). This makes the reduced glycogen content of SHRSP placenta observed in this thesis of key interest in evaluating any pathophysiology associated with SHRSP pregnancy. The SHRSP did not establish normal levels of placental glycogen reserves and therefore may have a limited energy supply in later gestational periods. The SHRSP placenta has been found to have reduced $Na^+/K^+$ ATPase activity, which would suggest a reduced transport of amino acids via $Na^+$ dependent transporters (Fuchi et al., 1995a). An attempt to clarify the transport capacity of SHRSP placenta was made in this study and the methodology optimised to assess transport of neutral amino acids across the maternal-placental barrier in WKY and SHRSP. The approach was successfully used to measure the rate of the $Na^+$ coupled system A transporter. This preliminary data could be built upon to not only characterise the transport of these neutral amino acids, but also other amino acids and substances such as glucose and calcium transport. Issues with SHRSP placentation development were further highlighted by the proportionally reduced depth of trophoblast invasion into the maternal mesometrial triangle and the reduced gene expression of key Mmps involved in regulating this invasion. Further analysis revealed evidence of shallower spiral artery remodelling in SHRSP placenta and placental gene expression profiles which were suggestive of increased oxidative stress and hypoxia as well as changes in the placental RAS components.

This work has shown that abnormalities of SHRSP pregnancy stem from both maternal and placental driven factors. It may be beneficial to directly assess the proportional control that these factors have on SHRSP pregnancy development by utilising embryo transfer studies in future work. This would allow the maternal and placental influences to be studied independently, with SHRSP placenta invading into WKY uterine tissues and secreting placentally derived factors into a normotensive circulatory system. This would have the potential to answer the question of whether the uterine arteries of SHRSP dams are failing to respond to pregnancy-dependent signals stimulated by the placenta, whether there is a lack of signalling from the SHRSP placenta, or perhaps a combination of the two.

A final and important focus of this thesis was in establishing a novel model of superimposed pre-eclampsia. Utilising the commonly used method of infusing AngII to induce hypertension, this work was the first to increase systemic AngII in hypertensive pregnant rats. Many of the phenotypes of severe human pre-eclampsia were found in the AngII-SHRSP model, such as reduced cardiac output, kidney damage and associated FGR (Tranquilli et al., 2014). The rationale for developing this model was that the maternal cardiovascular system is placed under considerable stress during pregnancy and in cases such as pre-eclampsia the maternal cardiovascular system fails to adapt normally to an increased load. Increasing the blood pressure via artificial increases of circulating AngII created an environment of heightened maternal cardiovascular stress (Kalafat and Thilaganathan, 2017). Interestingly, this study found that the normotensive WKY were highly sensitive to the increases in systemic AngII, more so than the SHRSP as indicated by their rapid deterioration of health. It has yet to be determined why this is the case and the mechanisms behind this paradox. A possible theory as to why WKY dams rapidly deteriorate when exposed to high levels of AngII is that they do not spontaneously develop hypertension as the SHRSP do. As SHRSP age their blood pressure increases to severely hypertensive levels (>200mmHg). Therefore, even though the animals used in this study were relatively young and had not reached their maximum blood pressure, they may possess compensatory mechanisms that allow them to withstand high blood pressure levels in early life. As a normotensive model, WKY rats may not have mechanisms in place to cope with a sudden increase in blood pressure. The different mechanical properties and functional responses of the mesenteric and uterine arteries to pregnancy in WKY and SHRSP rats, along with the different transcriptome of the two models at the non-pregnant stage, highlights that the two strains have different vascular mechanisms in place to deal with cardiovascular stress. The WKY responds to the physiological stress of pregnancy appropriately, whereas the SHRSP does not. However, under pathological conditions, such as with AngII infusion, the WKY is unable to cope. This finding could possibly have implications in the mechanistic studies of hypertension as well as in understanding of pregnancy disorders. However, other normotensive rodents have been subject to the same high level AngII infusion during pregnancy and survived (Hering et al., 2010), thus more in depth analysis of female WKY hypertensive responses are required.

Some of the findings in this thesis are in contrast to previous studies which conclude that SHRSP do not show evidence of FGR, yet when this strain was subject to increased cardiovascular stress, using AngII infusion, the fetal growth was negatively impacted. Reduced fetal size is often associated with a reduced uteroplacental blood flow (Burton et al., 2009, Intapad et al., 2014). This can be observed in (and is a possible cause of) pre-eclampsia, yet can also cause FGR in the absence of any hypertensive phenotypes (Bamfo and Odibo, 2011). The growth restriction associated with increased systemic AngII was maintained into the neonatal period for offspring from AngII treated damns, which indicates a developmental handicap of these animals exposed to AngII *in utero*. Indeed, this is an area that has been studied in SHRSP with regards to cardiovascular disease development and poor *in utero* environment (Otani et al., 2012, Otani et al., 2004). In this study, preliminary investigations were conducted to examine the impact of the increased maternal cardiovascular stress on the offspring's physiology. Weights and growth trajectories, AngII plasma concentration and gene expression of RAS components in the kidneys identified that offspring which developed in a detrimental (high AngII) environment were smaller, had elevated AngII in their own systemic circulation and had an increased *Ace2* expression. Dysregulation of RAS *in utero* has been found to sensitise the offspring to the development of hypertension as adults (Xue et al., 2017). It is well established that the development of offspring from hypertensive pregnancies are impacted directly from a restricted *in utero* environment, but an emerging field is transgenerational epigenetic modifications that can be passed to subsequent generations (Ho, 2014). This is a mechanism that regulates gene expression independent of genetic information (Skinner, 2011). Modifications occur globally in the fetus and female offspring that develop during exposure to a hypertensive insult *in utero* can transfer these epigenetic modifications to their own offspring (Skinner, 2011). This complex mechanism and the role it plays in development of cardiovascular disease still requires further investigation, yet it highlights the importance of the need to better diagnose, treat and eventually prevent pregnancies impacted by hypertension. The cause of the growth restriction was not fully determined in this project. However, the impaired uteroplacental blood flow in untreated SHRSP was not worsened by AngII infusion. This is noteworthy as it suggests other mechanisms must be influencing fetal growth. The structural organisation of the placenta, specifically the junctional zone, was

negatively affected by AngII infusion. This zone is the main endocrine compartment of the rodent placenta and may have wider implications on the observed FGR (Coan et al., 2006, Ain et al., 2003). AngII has been found be involved in the regulation of trophoblast invasion and can reduce the activity of $Na^+/K^+$ ATPase and SysA transport in the placenta (Shibata et al., 2006). These findings do not answer the question of why AngII infusion creates a model of fetal growth restriction, but it does suggest that restricted placental blood flow is not the only factor.

Treatment options for all hypertensive disorders of pregnancy are lacking (Fisk and Atun, 2008). However, hypertensive complications in an already hypertensive mother are less well studied than other hypertensive conditions. Manipulations of the pre-existing hypertension in SHRSP pregnancy will be a useful tool in understanding the pathologies and will also provide a robust animal model for investigating therapies. A main strength of the infusion model utilised in this thesis is that it can be adapted to study variations of severity. We showed a gradient of pathologies, with the 1000ng/kg/min 'high' AngII treatment group showing large, statistically significant changes from vehicle and with the 500ng/kg/min 'low' AngII group showing similar directionality of changes but often to a lesser extent. Furthermore, the RAS involvement appears to be interlinked with SHRSP impairments. AngII plays more roles in physiology and pathophysiology than simply stimulating vasoconstriction. It has also been shown to stimulate vascular production of reactive oxygen species via NADPH oxidases, including Nox2 (Nguyen Dinh Cat et al., 2013). Considering the findings that SHRSP have increased *Nox2* mRNA expression in uterine arteries during pregnancy, revealed in Chapter 5, the AngII-SHRSP model is even more compelling. Other manipulations of the RAS have been considered to be involved in the development of hypertensive disorders of pregnancy, such as propagated activation of AngII receptor type 1 via the angiotensin II type I receptor agonistic autoantibody ($AT^1$-AA). Circulatory AngII is not found at increased level in pre-eclamptic women, yet there is evidence of elevated $AT^1$-AA (Herse and LaMarca, 2013, Wallukat et al., 1999). This works via the same AngII receptor responsible for the vascular damage and altered placental function, and is associated with reduced uteroplacental perfusion. Investigating its presence in SHRSP physiology and subsequent manipulations would greatly increase the understanding of RAS

dysregulation in pregnancy associated hypertensive disorders and expand the usefulness of SHRSP as a model of superimposed pre-eclampsia.

This thesis has provided information on the systemic and uterine specific vascular responses to pregnancy, the underlying transcriptional differences that could potentially be driving the varied responses and the impact that severe cardiovascular impairment can have on fetal and placental development in hypertensive pregnancies. Whilst much is still unknown about hypertensive disorders during pregnancy, there is greater evidence to support that similarly presenting disorders stem from different causes. With that in mind, focusing on the maternal dysfunction is a promising area that will require an intimate knowledge of physiological and pathophysiological response. The work in this thesis has provided the means to create an easily reproducible rodent model to investigate underlying mechanisms in the development of pre-eclamptic like conditions.

# Chapter 8 Appendix

# 8.1 Sacrifice Sheet

## 8.1.1 GD18.5 Fetal and Placental Data

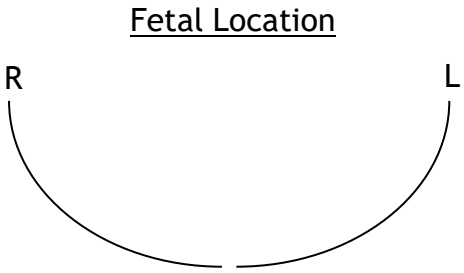


Date:
Strain:
Maternal ID:
Maternal weight:
**GD .....**

| | | |
|---|---|---|
| **Heart** | W | LV |
| **Kidney** | L | R |
| **Liver** | | |
| **Tibia** | | |
| **Uterus** | | |

| **Fetal #** | **Fetal weight** | **Placental weight** | **Fetal Measures** | | | | |
|---|---|---|---|---|---|---|---|
| | | | **Head** | **C:R** | **HC** | **AC** | **NOTES** |
| | | | | | | | |
| | | | | | | | |
| | | | | | | | |
| | | | | | | | |
| | | | | | | | |
| | | | | | | | |
| | | | | | | | |
| | | | | | | | |
| | | | | | | | |
| | | | | | | | |
| | | | | | | | |
| | | | | | | | |
| | | | | | | | |
| | | | | | | | |
| | | | | | | | |
| | | | | | | | |

## 8.1.2 GD6.5 Maternal Data

### Six day harvest protocol

Date:
Strain:
Maternal ID:

**Weights**

Maternal: ……
Heart: ……
Kidney: ……
Liver: ……
Tibia: ……
Whole Uterus: ……

Embedded Location

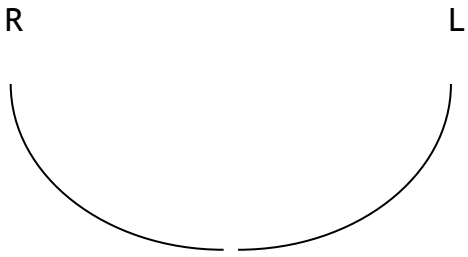


**Collection check list (tick)**

| | Fix | S/F | Myography |
|---|---|---|---|
| Mesenteric artery | | | |
| Uterine artery | | | |
| Uterus units | | | |
| Kidney | | | |
| Adrenal | | | |

## 8.2 PubMed Search Terms

Search terms ("hypertension, pregnancy-induced"[MeSH Terms] OR ("hypertension"[All Fields] AND "pregnancy-induced"[All Fields]) OR "pregnancy-induced hypertension"[All Fields] OR ("gestational"[All Fields] AND "hypertension"[All Fields]) OR "gestational hypertension"[All Fields]) where limited to the year published 2017. This revealed 1347 studies in the database. The search was then filtered to add the following terms: AND ("pre-eclampsia"[MeSH Terms] OR "pre-eclampsia"[All Fields] OR "preeclampsia"[All Fields]), this revealed 962 publications that included pre-eclampsia. This search also contained those with specific focus on superimposed preeclampsia so the further search amendment was added: AND "superimposed"[All Fields] OR "superimpose"[All Fields]. This revealed 22 publications in 2017. Therefore the total number of publications was deemed to be 1347, the number containing preeclampsia studies without superimposed preeclampsia were recorded as 930 and with 22 including superimposed. No reviews were excluded from the search.

# List of References


ACOG 2013. Hypertension in pregnancy. Report of the American College of Obstetricians and Gynecologists' Task Force on Hypertension in Pregnancy. *Obstet Gynecol.,* 122**,** 1122-31.

AIN, R., CANHAM, L. N. & SOARES, M. J. 2003. Gestation stage-dependent intrauterine trophoblast cell invasion in the rat and mouse: novel endocrine phenotype and regulation. *Dev Biol,* 260**,** 176-90.

AKASAKI, T., OHYA, Y., KURODA, J., ETO, K., ABE, I., SUMIMOTO, H. & IIDA, M. 2006. Increased expression of gp91phox homologues of NAD(P)H oxidase in the aortic media during chronic hypertension: involvement of the renin-angiotensin system. *Hypertens Res,* 29**,** 813-20.

AKEHURST, C., SMALL, H. Y., SHARAFETDINOVA, L., FORREST, R., BEATTIE, W., BROWN, C. E., ROBINSON, S. W., MCCLURE, J. D., WORK, L. M., CARTY, D. M., MCBRIDE, M. W., FREEMAN, D. J. & DELLES, C. 2015. Differential expression of microRNA-206 and its target genes in preeclampsia. *J Hypertens,* 33**,** 2068-74.

AKISON, L. K., NITERT, M. D., CLIFTON, V. L., MORITZ, K. M. & SIMMONS, D. G. 2017. Review: Alterations in placental glycogen deposition in complicated pregnancies: Current preclinical and clinical evidence. *Placenta,* 54**,** 52-58.

ALEXANDER, B. T., KASSAB, S. E., MILLER, M. T., ABRAM, S. R., RECKELHOFF, J. F., BENNETT, W. A. & GRANGER, J. P. 2001. Reduced uterine perfusion pressure during pregnancy in the rat is associated with increases in arterial pressure and changes in renal nitric oxide. *Hypertension,* 37**,** 1191-5.

ALI, S. M. & KHALIL, R. A. 2015. Genetic, immune and vasoactive factors in the vascular dysfunction associated with hypertension in pregnancy. *Expert Opin Ther Targets,* 19**,** 1495-515.

ALJUNAIDY, M. M., MORTON, J. S., COOKE, C. M. & DAVIDGE, S. T. 2017. Prenatal hypoxia and placental oxidative stress: linkages to developmental origins of cardiovascular disease. *Am J Physiol Regul Integr Comp Physiol,* 313**,** R395-R399.

ANTHONY, M. & BERG, M. J. 2002. Biologic and molecular mechanisms for sex differences in pharmacokinetics, pharmacodynamics, and pharmacogenetics: Part II. *J Womens Health Gend Based Med,* 11**,** 617-29.

ANTZA, C., CIFKOVA, R. & KOTSIS, V. 2017. Hypertensive complications of pregnancy: a clinical overview. *Metabolism,* 20**,** 30323-2.

ARGUELLES, J., PERILLAN, C., BELTZ, T. G., XUE, B., BADAUE-PASSOS, D., VEGA, J. A. & JOHNSON, A. K. 2017. The effects of experimental gestational hypertension on maternal blood pressure and fluid intake and pre-weanling hypothalamic neuronal activity. *Appetite,* 116**,** 65-74.

ARRIBAS, S. M., HILLIER, C., GONZÁLEZ, C., MCGRORY, S., DOMINICZAK, A. F. & MCGRATH, J. C. 1997. Cellular aspects of vascular remodeling in hypertension revealed by confocal microscopy. *Hypertension,* 30**,** 1455-64.

ATANUR, S. S., DIAZ, A. G., MARATOU, K., SARKIS, A., ROTIVAL, M., GAME, L., TSCHANNEN, M. R., KAISAKI, P. J., OTTO, G. W., MA, M. C., KEANE, T. M., HUMMEL, O., SAAR, K., CHEN, W., GURYEV, V., GOPALAKRISHNAN, K., GARRETT, M. R., JOE, B., CITTERIO, L., BIANCHI, G., MCBRIDE, M., DOMINICZAK, A., ADAMS, D. J., SERIKAWA, T., FLICEK, P., CUPPEN, E., HUBNER, N., PETRETTO, E., GAUGUIER, D., KWITEK, A., JACOB, H. & AITMAN, T. J. 2013. Genome sequencing reveals loci under artificial selection that underlie disease phenotypes in the laboratory rat. *Cell,* 154**,** 691-703.

ATHERTON, J. C., BU'LOCK, D. & PIRIE, S. C. 1982. The effect of pseudopregnancy on glomerular filtration rate and salt and water reabsorption in the rat. *J Physiol,* 324**,** 11-20.

AUGUST, P., JEYABALAN, A. & ROBERTS, J. M. 2015. Chapter 18 - Chronic Hypertension and Pregnancy. *Chesley's Hypertensive Disorders in Pregnancy (Fourth Edition).* San Diego: Academic Press.

AUTIO-HARMAINEN, H., HURSKAINEN, T., NISKASAARI, K., HOYHTYA, M. & TRYGGVASON, K. 1992. Simultaneous expression of 70 kilodalton type IV collagenase and type IV collagen alpha 1 (IV) chain genes by cells of early human placenta and gestational endometrium. *Lab Invest.,* 67**,** 191-200.

BABICKI, S., ARNDT, D., MARCU, A., LIANG, Y., GRANT, J. R., MACIEJEWSKI, A. & WISHART, D. S. 2016. Heatmapper: web-enabled heat mapping for all. *Nucleic Acids Res,* 44**,** W147-53.

BAILEY, E. L., MCBRIDE, M. W., MCCLURE, J. D., BEATTIE, W., GRAHAM, D., DOMINICZAK, A. F., SMITH, C. & WARDLAW, J. M. 2018. Effects of dietary salt on gene and protein expression in brain tissue of a model of sporadic small vessel disease. *Clin Sci (Lond)*.

BAIRD, J. N. 1981. Eclampsia in a lowland gorilla. *Am J Obstet Gynecol,* 141**,** 345-6.

BALLANTYNE, M. D., PINEL, K., DAKIN, R., VESEY, A. T., DIVER, L., MACKENZIE, R., GARCIA, R., WELSH, P., SATTAR, N., HAMILTON, G., JOSHI, N., DWECK, M. R., MIANO, J. M., MCBRIDE, M. W., NEWBY, D. E., MCDONALD, R. A. & BAKER, A. H. 2016. Smooth Muscle Enriched Long Noncoding RNA (SMILR) Regulates Cell Proliferation. *Circulation,* 133**,** 2050-65.

BALLINGER, S. W. 2005. Mitochondrial dysfunction in cardiovascular disease. *Free Radic Biol Med,* 38**,** 1278-95.

BAMFO, J. E. & ODIBO, A. O. 2011. Diagnosis and management of fetal growth restriction. *J Pregnancy,* 2011**,** 640715.

BARBAGALLO, M., DOMINGUEZ, L. J., LICATA, G., SHAN, J., BING, L., KARPINSKI, E., PANG, P. K. & RESNICK, L. M. 2001. Vascular Effects of Progesterone : Role of Cellular Calcium Regulation. *Hypertension,* 37**,** 142-147.

BARKER, D. J. 1991. The intrauterine environment and adult cardiovascular disease. *Ciba Found Symp,* 156**,** 3-10; discussion 10-6.

BARKER, D. J., GLUCKMAN, P. D., GODFREY, K. M., HARDING, J. E., OWENS, J. A. & ROBINSON, J. S. 1993. Fetal nutrition and cardiovascular disease in adult life. *Lancet,* 341**,** 938-41.

BARRIENTOS, G., PUSSETTO, M., ROSE, M., STAFF, A. C., BLOIS, S. M. & TOBLLI, J. E. 2017. Defective trophoblast invasion underlies fetal growth restriction and pre-eclampsia-like symptoms in the stroke-prone spontaneously hypertensive rat. *Mol Hum Reprod*.

BARRON, C., MANDALA, M. & OSOL, G. 2010. Effects of pregnancy, hypertension and nitric oxide inhibition on rat uterine artery myogenic reactivity. *J Vasc Res,* 47**,** 463-71.

BASSAN, H., BASSAN, M., PINHASOV, A., KARIV, N., GILADI, E., GOZES, I. & HAREL, S. 2005. The pregnant spontaneously hypertensive rat as a model of asymmetric intrauterine growth retardation and neurodevelopmental delay. *Hypertens Pregnancy,* 24**,** 201-11.

BATEMAN, B. T., BANSIL, P., HERNANDEZ-DIAZ, S., MHYRE, J. M., CALLAGHAN, W. M. & KUKLINA, E. V. 2012. Prevalence, trends, and outcomes of chronic hypertension: a nationwide sample of delivery admissions. *Am J Obstet Gynecol,* 206**,** 134.e1-8.

BAYLIS, C., MITRUKA, B. & DENG, A. 1992. Chronic blockade of nitric oxide synthesis in the rat produces systemic hypertension and glomerular damage. *J Clin Invest,* 90**,** 278-81.

BERECEK, K. H., SCHWERTSCHLAG, U. & GROSS, F. 1980. Alterations in renal vascular resistance and reactivity in spontaneous hypertension of rats. *Am J Physiol,* 238**,** H287-93.

BEVILACQUA, E., LORENZON, A. R., BANDEIRA, C. L., HOSHIDA, M. S., GARBELINI, M. C. D. L. & GONÇALVES, C. R. 2014. Ectoplacental Cone Isolation, Culture and Assessment. *In:* CROY, A., YAMADA, A. T., DEMAYO, F. J. & ADAMSON, S. L. (eds.) *The Guide to Investigation of Mouse Pregnancy.* Boston: Academic Press.

BIRD, I. M., MILLICAN, D. S. & MAGNESS, R. R. 1998. Specific pregnancy-induced angiotensin II type-1 receptor expression in ovine uterine artery does not involve formation of alternate splice variants or alternate promoter usage. *Biol Reprod.,* 59**,** 219-24.

BISCHOF, P., MARTELLI, M., CAMPANA, A., ITOH, Y., OGATA, Y. & NAGASE, H. 1995. Importance of matrix metalloproteinases in human trophoblast invasion. *Early Pregnancy,* 1**,** 263-9.

BOBEK, G., SURMON, L., MIRABITO, K. M., MAKRIS, A. & HENNESSY, A. 2015. Placental Regulation of Inflammation and Hypoxia after TNF-α Infusion in Mice. *Am J Reprod Immunol,* 74**,** 407-18.

BOHLENDER, J., GANTEN, D. & LUFT, F. C. 2000. Rats transgenic for human renin and human angiotensinogen as a model for gestational hypertension. *J Am Soc Nephrol,* 11**,** 2056-61.

BOKSLAG, A., TEUNISSEN, P. W., FRANSSEN, C., VAN KESTEREN, F., KAMP, O., GANZEVOORT, W., PAULUS, W. J. & DE GROOT, C. J. 2017. Effect of early-onset preeclampsia on cardiovascular risk in the fifth decade of life. *Am J Obstet Gynecol,* 216**,** 523.e1–523.e7.

BOSIO, P. M., MCKENNA, P. J., CONROY, R. & O'HERLIHY, C. 1999. Maternal central hemodynamics in hypertensive disorders of pregnancy. *Obstet Gynecol,* 94**,** 978-84.

BOWEN, J. M., CHAMLEY, L., KEELAN, J. A. & MITCHELL, M. D. 2002. Cytokines of the placenta and extra-placental membranes: roles and regulation during human pregnancy and parturition. *Placenta,* 23**,** 257-73.

BRAMHAM, K., PARNELL, B., NELSON-PIERCY, C., SEED, P. T., POSTON, L. & CHAPPELL, L. C. 2014. Chronic hypertension and pregnancy outcomes: systematic review and meta-analysis. *BMJ,* 348**,** g2301.

BRENNAN, L., MORTON, J. S., QUON, A. & DAVIDGE, S. T. 2016. Postpartum Vascular Dysfunction in the Reduced Uteroplacental Perfusion Model of Preeclampsia. *PLoS One,* 11**,** e0162487.

BRENNAN, L. J., MORTON, J. S. & DAVIDGE, S. T. 2014. Vascular dysfunction in preeclampsia. *Microcirculation,* 21**,** 4-14.

BREWER, J., LIU, R., LU, Y., SCOTT, J., WALLACE, K., WALLUKAT, G., MOSELEY, J., HERSE, F., DECHEND, R., MARTIN, J. N. & LAMARCA, B. 2013. Endothelin-1, oxidative stress, and endogenous angiotensin II: mechanisms of angiotensin II type I receptor autoantibody-enhanced renal and blood pressure response during pregnancy. *Hypertension,* 62**,** 886-92.

BROSENS, I. A., ROBERTSON, W. B. & DIXON, H. G. 1972. The role of the spiral arteries in the pathogenesis of preeclampsia. *Obstet Gynecol Annu,* 1**,** 177-91.

BROSENS, J. J., PARKER, M. G., MCINDOE, A., PIJNENBORG, R. & BROSENS, I. A. 2009. A role for menstruation in preconditioning the uterus for successful pregnancy. *Am J Obstet Gynecol,* 200**,** 615.e1-6.

BROWNE, V. A., JULIAN, C. G., TOLEDO-JALDIN, L., CIOFFI-RAGAN, D., VARGAS, E. & MOORE, L. G. 2015. Uterine artery blood flow, fetal hypoxia and fetal growth. *Philosophical Transactions of the Royal Society B: Biological Sciences,* 370**,** 20140068.

BURTON, G. J. & JAUNIAUX, E. 2011. Oxidative stress. *Best Pract Res Clin Obstet Gynaecol,* 25**,** 287-99.

BURTON, G. J., WATSON, A. L., HEMPSTOCK, J., SKEPPER, J. N. & JAUNIAUX, E. 2002. Uterine glands provide histiotrophic nutrition for the human fetus during the first trimester of pregnancy. *J Clin Endocrinol Metab,* 87**,** 2954-9.

BURTON, G. J., WOODS, A. W., JAUNIAUX, E. & KINGDOM, J. C. 2009. Rheological and physiological consequences of conversion of the maternal spiral arteries for uteroplacental blood flow during human pregnancy. *Placenta,* 30**,** 473-82.

CALE, J. M., MILLICAN, D. S., ITOH, H., MAGNESS, R. R. & BIRD, I. M. 1997. Pregnancy induces an increase in the expression of glyceraldehyde-3-phosphate dehydrogenase in uterine artery endothelial cells. *J Soc Gynecol Investig.,* 4**,** 284-92.

CALUWAERTS, S., VERCRUYSSE, L., LUYTEN, C. & PIJNENBORG, R. 2005. Endovascular trophoblast invasion and associated structural changes in uterine spiral arteries of the pregnant rat. *Placenta.* England.

CHAKRABORTY, D., RUMI, M. A., KONNO, T. & SOARES, M. J. 2011. Natural killer cells direct hemochorial placentation by regulating hypoxia-inducible factor dependent trophoblast lineage decisions. *Proc Natl Acad Sci U S A,* 108**,** 16295-300.

CHANDRAN, S., CAIRNS, M. T., O'BRIEN, M., O'CONNELL, E., MASHAYEKHI, K. & SMITH, T. J. 2016. Effects of combined progesterone and 17β-estradiol treatment on the transcriptome of cultured human myometrial smooth muscle cells. *Physiol Genomics,* 48**,** 50-61.

CHAPMAN, A. B., ABRAHAM, W. T., ZAMUDIO, S., COFFIN, C., MEROUANI, A., YOUNG, D., JOHNSON, A., OSORIO, F., GOLDBERG, C., MOORE, L. G., DAHMS, T. & SCHRIER, R. W. 1998. Temporal relationships between hormonal and hemodynamic changes in early human pregnancy. *Kidney Int,* 54**,** 2056-63.

CHEN, C., SPENCER, T. E. & BAZER, F. W. 2000. Fibroblast growth factor-10: a stromal mediator of epithelial function in the ovine uterus. *Biol Reprod.,* 63**,** 959-66.

CHESLEY, L. C. & TEPPER, I. H. 1967. Effects of progesterone and estrogen on the sensitivity to angiotensin II. *J Clin Endocrinol Metab,* 27**,** 576-81.

CHIU, A. T., HERBLIN, W. F., MCCALL, D. E., ARDECKY, R. J., CARINI, D. J., DUNCIA, J. V., PEASE, L. J., WONG, P. C., WEXLER, R. R. & JOHNSON, A. L. 1989. Identification of angiotensin II receptor subtypes. *Biochem Biophys Res Commun,* 165**,** 196-203.

CHRISTIANSON, R. E. 1976. Studies on blood pressure during pregnancy: I. Influence of parity and age. *American Journal of Obstetrics and Gynecology,* 125**,** 509-513.

CHU, Z. M. & BEILIN, L. J. 1993. Nitric oxide-mediated changes in vascular reactivity in pregnancy in spontaneously hypertensive rats. *Br J Pharmacol,* 110**,** 1184-8.

CIPOLLA, M. & OSOL, G. 1994. Hypertrophic and hyperplastic effects of pregnancy on the rat uterine arterial wall. *Am J Obstet Gynecol,* 171**,** 805-11.

CLAPP, J. F. & CAPELESS, E. 1997. Cardiovascular Function Before, During, and After the First and Subsequent Pregnancies. *The American Journal of Cardiology,* 80**,** 1469-1473.

CLARK, J. S., JEFFS, B., DAVIDSON, A. O., LEE, W. K., ANDERSON, N. H., BIHOREAU, M. T., BROSNAN, M. J., DEVLIN, A. M., KELMAN, A. W., LINDPAINTNER, K. & DOMINICZAK, A. F. 1996. Quantitative trait loci in genetically hypertensive rats. Possible sex specificity. *Hypertension,* 28**,** 898-906.

CNATTINGIUS, S., REILLY, M., PAWITAN, Y. & LICHTENSTEIN, P. 2004. Maternal and fetal genetic factors account for most of familial aggregation of preeclampsia: a population-based Swedish cohort study. *Am J Med Genet A,* 130A**,** 365-71.

COAN, P. M., CONROY, N., BURTON, G. J. & FERGUSON-SMITH, A. C. 2006. Origin and characteristics of glycogen cells in the developing murine placenta. *Developmental Dynamics,* 235**,** 3280-3294.

COCKELL, A. P. & POSTON, L. 1997. Flow-mediated vasodilatation is enhanced in normal pregnancy but reduced in preeclampsia. *Hypertension,* 30**,** 247-51.

COHEN, M., WUILLEMIN, C., IRION, O. & BISCHOF, P. 2010. Role of decidua in trophoblastic invasion. *Neuro Endocrinol Lett,* 31**,** 193-7.

CONRAD, K. P. 1984. Renal hemodynamics during pregnancy in chronically catheterized, conscious rats. *Kidney Int,* 26**,** 24-9.

CONRAD, K. P., JOFFE, G. M., KRUSZYNA, H., KRUSZYNA, R., ROCHELLE, L. G., SMITH, R. P., CHAVEZ, J. E. & MOSHER, M. D. 1993. Identification of increased nitric oxide biosynthesis during pregnancy in rats. *FASEB J,* 7**,** 566-71.

CONRAD, K. P., STILLMAN, I. E. & LINDHEIMER, M. D. 2015. Chapter 16 - The Kidney in Normal Pregnancy and Preeclampsia. *Chesley's Hypertensive Disorders in Pregnancy (Fourth Edition).* San Diego: Academic Press.

CONRAD, M., SCHNEIDER, M., SEILER, A. & BORNKAMM, G. W. 2007. Physiological role of phospholipid hydroperoxide glutathione peroxidase in mammals. *Biol Chem,* 388**,** 1019-25.

COOKE, C. L. & DAVIDGE, S. T. 2003. Pregnancy-induced alterations of vascular function in mouse mesenteric and uterine arteries. *Biol Reprod,* 68**,** 1072-7.

CORCORAN, J. J., CHARNOCK, J. C., MARTIN, J., TAGGART, M. J. & WESTWOOD, M. 2012. Differential effect of insulin like growth factor-I on constriction of human uterine and placental arteries. *J Clin Endocrinol Metab,* 97**,** E2098-104.

CORSINI, C., CERVI, E., MIGLIAVACCA, F., SCHIEVANO, S., HSIA, T. Y. & PENNATI, G. 2017. Mathematical modelling of the maternal cardiovascular system in the three stages of pregnancy. *Med Eng Phys,* 47**,** 55-63.

COX, B., LEAVEY, K., NOSI, U., WONG, F. & KINGDOM, J. 2015. Placental transcriptome in development and pathology: expression, function, and methods of analysis. *Am J Obstet Gynecol,* 213**,** S138-51.

CREWS, J. K., HERRINGTON, J. N., GRANGER, J. P. & KHALIL, R. A. 2000. Decreased endothelium-dependent vascular relaxation during reduction of uterine perfusion pressure in pregnant rat. *Hypertension,* 35**,** 367-72.

CRISPI, F., MIRANDA, J. & GRATACÓS, E. 2018. Long-term cardiovascular consequences of fetal growth restriction: biology, clinical implications, and opportunities for prevention of adult disease. *Am J Obstet Gynecol,* 218**,** S869-S879.

CUFFE, J. S., WALTON, S. L., STEANE, S. E., SINGH, R. R., SIMMONS, D. G. & MORITZ, K. M. 2014. The effects of gestational age and maternal hypoxia on the placental renin angiotensin system in the mouse. *Placenta,* 35**,** 953-61.

CUNNINGHAM, M. W., WILLIAMS, J. M., AMARAL, L., USRY, N., WALLUKAT, G., DECHEND, R. & LAMARCA, B. 2016. Agonistic Autoantibodies to the Angiotensin II Type 1 Receptor Enhance Angiotensin II-Induced Renal Vascular Sensitivity and Reduce Renal Function During Pregnancy. *Hypertension,* 68**,** 1308-1313.

DATLA, S. R. & GRIENDLING, K. K. 2010. Reactive oxygen species, NADPH oxidases, and hypertension. *Hypertension,* 56**,** 325-30.

DAVIDGE, S. T. & MCLAUGHLIN, M. K. 1992. Endogenous modulation of the blunted adrenergic response in resistance-sized mesenteric arteries from the pregnant rat. *Am J Obstet Gynecol,* 167**,** 1691-8.

DAVIDSON, A. O., SCHORK, N., JAQUES, B. C., KELMAN, A. W., SUTCLIFFE, R. G., REID, J. L. & DOMINICZAK, A. F. 1995. Blood pressure in genetically hypertensive rats. Influence of the Y chromosome. *Hypertension,* 26**,** 452-9.

DAVIS, E. F., LEWANDOWSKI, A. J., AYE, C., WILLIAMSON, W., BOARDMAN, H., HUANG, R. C., MORI, T. A., NEWNHAM, J., BEILIN, L. J. & LEESON, P. 2015. Clinical cardiovascular risk during young adulthood in offspring of hypertensive pregnancies: insights from a 20-year prospective follow-up birth cohort. *BMJ Open,* 5**,** e008136.

DAVIS, J. S. & RUEDA, B. R. 2002. The corpus luteum: an ovarian structure with maternal instincts and suicidal tendencies. *Front Biosci,* 7**,** d1949-78.

DAVISON, J. M. & DUNLOP, W. 1980. Renal hemodynamics and tubular function normal human pregnancy. *Kidney Int,* 18**,** 152-61.

DAVISSON, R. L., HOFFMANN, D. S., BUTZ, G. M., ALDAPE, G., SCHLAGER, G., MERRILL, D. C., SETHI, S., WEISS, R. M. & BATES, J. N. 2002. Discovery of a spontaneous genetic mouse model of preeclampsia. *Hypertension,* 39**,** 337-42.

DE FELICE, B., MANFELLOTTO, F., PALUMBO, A., TROISI, J., ZULLO, F., DI CARLO, C., DI SPIEZIO SARDO, A., DE STEFANO, N., FERBO, U. & GUIDA, M. 2015. Genome-wide microRNA expression profiling in placentas from pregnant women exposed to BPA. *BMC Med Genomics,* 8**,** 56.

DE GASPARO, M., WHITEBREAD S FAU - MELE, M., MELE M FAU - MOTANI, A. S., MOTANI AS FAU - WHITCOMBE, P. J., WHITCOMBE PJ FAU - RAMJOUE, H. P., RAMJOUE HP FAU - KAMBER, B. & KAMBER, B. Biochemical characterization of two angiotensin II receptor subtypes in the rat.

DECHEND, R., VIEDT, C., MÜLLER, D. N., UGELE, B., BRANDES, R. P., WALLUKAT, G., PARK, J. K., JANKE, J., BARTA, P., THEUER, J., FIEBELER, A., HOMUTH, V., DIETZ, R., HALLER, H., KREUZER, J. & LUFT, F. C. 2003. AT1 receptor agonistic antibodies from preeclamptic patients stimulate NADPH oxidase. *Circulation,* 107**,** 1632-9.

DELLES, C., MCBRIDE, M. W., PADMANABHAN, S. & DOMINICZAK, A. F. 2008. The genetics of cardiovascular disease. *Trends Endocrinol Metab,* 19**,** 309-16.

DENNEY, J. M., BIRD, C., GENDRON-FITZPATRICK, A., SAMPENE, E., BIRD, I. M. & SHAH, D. M. 2017. Renin-angiotensin system transgenic mouse model recapitulates pathophysiology similar to human preeclampsia with renal injury that may be mediated through VEGF. *Am J Physiol Renal Physiol,* 312**,** F445-F455.

DESFORGES, M., MYNETT, K. J., JONES, R. L., GREENWOOD, S. L., WESTWOOD, M., SIBLEY, C. P. & GLAZIER, J. D. 2009. The SNAT4 isoform of the system A amino acid transporter is functional in human placental microvillous plasma membrane. *J Physiol,* 587**,** 61-72.

DESFORGES, M. & SIBLEY, C. P. 2010. Placental nutrient supply and fetal growth. *Int J Dev Biol,* 54**,** 377-90.

DI CASTRO, S., SCARPINO, S., MARCHITTI, S., BIANCHI, F., STANZIONE, R., COTUGNO, M., SIRONI, L., GELOSA, P., DURANTI, E., RUCO, L., VOLPE, M. & RUBATTU, S. 2013.

Differential modulation of uncoupling protein 2 in kidneys of stroke-prone spontaneously hypertensive rats under high-salt/low-potassium diet. *Hypertension,* 61**,** 534-41.

DIAS-JUNIOR, C. A., CHEN, J., CUI, N., CHIANG, C. L., ZHU, M., REN, Z., POSSOMATO-VIEIRA, J. S. & KHALIL, R. A. 2017. Angiogenic imbalance and diminished matrix metalloproteinase-2 and -9 underlie regional decreases in uteroplacental vascularization and feto-placental growth in hypertensive pregnancy. *Biochemical Pharmacology,* 146**,** 101-116.

DILWORTH, M. R., KUSINSKI, L. C., COWLEY, E., WARD, B. S., HUSAIN, S. M., CONSTÂNCIA, M., SIBLEY, C. P. & GLAZIER, J. D. 2010. Placental-specific Igf2 knockout mice exhibit hypocalcemia and adaptive changes in placental calcium transport. *Proc Natl Acad Sci U S A,* 107**,** 3894-9.

DILWORTH, M. R. & SIBLEY, C. P. 2013. Review: Transport across the placenta of mice and women. *Placenta,* 34 Suppl**,** S34-9.

DOMINICZAK, A. F., DEVLIN, A. M., BROSNAN, M. J., ANDERSON, N. H., GRAHAM, D., CLARK, J. S., MCPHADEN, A., HAMILTON, C. A. & REID, J. L. 1997. Left ventricular hypertrophy and arterial blood pressure in experimental models of hypertension. *Adv Exp Med Biol,* 432**,** 23-33.

DOMINICZAK, A. F., MCLAREN, Y., KUSEL, J. R., BALL, D. L., GOODFRIEND, T. L., BOHR, D. F. & REID, J. L. 1993. Lateral diffusion and fatty acid composition in vascular smooth muscle membrane from stroke-prone spontaneously hypertensive rats. *Am J Hypertens,* 6**,** 1003-8.

DULEY, L. 2009. The global impact of pre-eclampsia and eclampsia. *Semin Perinatol,* 33**,** 130-7.

DUNLOP, W. 1981. Serial changes in renal haemodynamics during normal human pregnancy. *Br J Obstet Gynaecol,* 88**,** 1-9.

DÜSTERDIECK, G. & MCELWEE, G. 1971. Estimation of angiotensin II concentration in human plasma by radioimmunoassay. Some applications to physiological and clinical states. *Eur J Clin Invest,* 2**,** 32-8.

DUVEKOT, J. J., CHERIEX, E. C., PIETERS, F. A., MENHEERE, P. P. & PEETERS, L. H. 1993. Early pregnancy changes in hemodynamics and volume homeostasis are consecutive adjustments triggered by a primary fall in systemic vascular tone. *Am J Obstet Gynecol,* 169**,** 1382-92.

ENQUOBAHRIE, D. A., MELLER, M., RICE, K., PSATY, B. M., SISCOVICK, D. S. & WILLIAMS, M. A. 2008. Differential placental gene expression in preeclampsia. *Am J Obstet Gynecol,* 199**,** 566.e1-11.

EVANS, A. L., BROWN, W., KENYON, C. J., MAXTED, K. J. & SMITH, D. C. 1994. Improved system for measuring systolic blood pressure in the conscious rat. *Med Biol Eng Comput,* 32**,** 101-2.

FERRAZZI, E., STAMPALIJA, T., MONASTA, L., DI MARTINO, D., VONCK, S. & GYSELAERS, W. 2018. Maternal hemodynamics: a method to classify hypertensive disorders of pregnancy. *Am J Obstet Gynecol,* 218**,** 124.e1-124.e11.

FISK, N. M. & ATUN, R. 2008. Market failure and the poverty of new drugs in maternal health. *PLoS Med,* 5**,** e22.

FLEISCHER, A., SCHULMAN, H., FARMAKIDES, G., BRACERO, L., GRUNFELD, L., ROCHELSON, B. & KOENIGSBERG, M. 1986. Uterine artery Doppler velocimetry in pregnant women with hypertension. *Am J Obstet Gynecol,* 154**,** 806-13.

FOUNDS, S. A., FALLERT-JUNECKO, B., REINHART, T. A. & PARKS, W. T. 2013. LAIR2-expressing extravillous trophoblasts associate with maternal spiral arterioles undergoing physiologic conversion. *Placenta.,* 34**,** 248-55. doi: 10.1016/j.placenta.2012.09.017. Epub 2013 Jan 16.

FRANK, H.-G. 2017. Placental Development. *In:* ABMAN, S. H., ROWITCH, D. H., BENITZ, W. E. & FOX, W. W. (eds.) *Fetal and Neonatal Physiology (Fifth Edition).* Philadelphia, PA: Elsevier.

FRASER, A., TILLING, K., MACDONALD-WALLIS, C., SATTAR, N., BRION, M. J., BENFIELD, L., NESS, A., DEANFIELD, J., HINGORANI, A., NELSON, S. M., SMITH, G. D. & LAWLOR, D. A. 2010. Association of maternal weight gain in pregnancy with offspring obesity and metabolic and vascular traits in childhood. *Circulation,* 121**,** 2557-64.

FRIEDLAENDER, C. 1870. *Physiologisch-anatomische Untersuchungen über den Uterus*, Simmel & Company.

FUCHI, I., HIGASHINO, H., NODA, K., SUZUKI, A. & MATSUBARA, Y. 1995a. Placental Na+, K+ activated ATP-ase activity in SHRSP in connection with pregnancy induced hypertension and intra-uterine growth retardation. *Clin Exp Pharmacol Physiol Suppl,* 22**,** S283-5.

FUCHI, I., NODA, K. & MATSUBARA, Y. 1995b. Studies on pregnancy hypertension and IUGR-SFD: effects of drugs on the blood vessels in the placenta of pregnant SHRSP. *Clin Exp Pharmacol Physiol Suppl,* 22**,** S286-7.

FUKAI, T. & USHIO-FUKAI, M. 2011. Superoxide dismutases: role in redox signaling, vascular function, and diseases. *Antioxid Redox Signal,* 15**,** 1583-606.

FUKUSHIMA, K., MURATA, M., HACHISUGA, M., TSUKIMORI, K., SEKI, H., TAKEDA, S., KATO, K. & WAKE, N. 2008. Gene expression profiles by microarray analysis during matrigel-induced tube formation in a human extravillous trophoblast cell line: comparison with endothelial cells. *Placenta.,* 29**,** 898-904. doi: 10.1016/j.placenta.2008.07.015.

FURUI, T., KURAUCHI, O., TANAKA, M., MIZUTANI, S., OZAWA, T. & TOMODA, Y. 1994. Decrease in cytochrome c oxidase and cytochrome oxidase subunit I messenger RNA levels in preeclamptic pregnancies. *Obstet Gynecol,* 84**,** 283-8.

FURUKAWA, S., KURODA, Y. & SUGIYAMA, A. 2014. A comparison of the histological structure of the placenta in experimental animals. *J Toxicol Pathol,* 27**,** 11-8.

GAILLARD, R., STEEGERS, E. A., DUIJTS, L., FELIX, J. F., HOFMAN, A., FRANCO, O. H. & JADDOE, V. W. 2014. Childhood cardiometabolic outcomes of maternal obesity during pregnancy: the Generation R Study. *Hypertension,* 63**,** 683-91.

GANT, N. F., DALEY, G. L., CHAND, S., WHALLEY, P. J. & MACDONALD, P. C. 1973. A study of angiotensin II pressor response throughout primigravid pregnancy. *J Clin Invest,* 52**,** 2682-9.

GARDOSI, J., MADURASINGHE, V., WILLIAMS, M., MALIK, A. & FRANCIS, A. 2013. Maternal and fetal risk factors for stillbirth: population based study. *Bmj,* 346**,** f108.

GEBBE, S. G., DEMERS, L. M., GREEP, R. O. & VILLEE, C. A. 1972. The effects of hypoxia on placental glycogen metabolism. *Am J Obstet Gynecol,* 114**,** 540-5.

GELLERSEN, B., BROSENS, I. A. & BROSENS, J. J. 2007. Decidualization of the human endometrium: mechanisms, functions, and clinical perspectives. *Semin Reprod Med,* 25**,** 445-53.

GENG, J., HUANG, C. & JIANG, S. 2016. Roles and regulation of the matrix metalloproteinase system in parturition. *Mol Reprod Dev,* 83**,** 276-86.

GEORGE, E. M., GARRETT, M. R. & GRANGER, J. P. 2014. Placental ischemia induces changes in gene expression in chorionic tissue. *Mamm Genome,* 25**,** 253-61.

GERBER, R. T., ANWAR, M. A. & POSTON, L. 1998. Enhanced acetylcholine induced relaxation in small mesenteric arteries from pregnant rats: an important role for endothelium-derived hyperpolarizing factor (EDHF). *Br J Pharmacol,* 125**,** 455-60.

GEUSENS, N., HERING, L., VERLOHREN, S., LUYTEN, C., DRIJKONINGEN, K., TAUBE, M., VERCRUYSSE, L., HANSSENS, M., DECHEND, R. & PIJNENBORG, R. 2010. Changes in endovascular trophoblast invasion and spiral artery remodelling at term in a transgenic preeclamptic rat model. *Placenta,* 31**,** 320-6.

GEUSENS, N., VERLOHREN, S., LUYTEN, C., TAUBE, M., HERING, L., VERCRUYSSE, L., HANSSENS, M., DUDENHAUSEN, J. W., DECHEND, R. & PIJNENBORG, R. 2008. Endovascular trophoblast invasion, spiral artery remodelling and uteroplacental haemodynamics in a transgenic rat model of pre-eclampsia. *Placenta,* 29**,** 614-23.

GIARDINA, J. B., COCKRELL, K. L., GRANGER, J. P. & KHALIL, R. A. 2002. Low-Salt Diet Enhances Vascular Reactivity and Ca(2+) Entry in Pregnant Rats With Normal and Reduced Uterine Perfusion Pressure. *Hypertension,* 39**,** 368.

GIBB, W. & SUN, M. 1996. Localization of prostaglandin H synthase type 2 protein and mRNA in term human fetal membranes and decidua. *J Endocrinol.,* 150**,** 497-503.

GIFFORD, S. M., CALE, J. M., TSOI, S., MAGNESS, R. R. & BIRD, I. M. 2003. Pregnancy-specific changes in uterine artery endothelial cell signaling in vivo are both programmed and retained in primary culture. *Endocrinology.,* 144**,** 3639-50. doi: 10.1210/en.2002-0006.

GLAZIER, J. D., CETIN, I., PERUGINO, G., RONZONI, S., GREY, A. M., MAHENDRAN, D., MARCONI, A. M., PARDI, G. & SIBLEY, C. P. 1997. Association between the activity of the system A amino acid transporter in the microvillous plasma membrane of the human placenta and severity of fetal compromise in intrauterine growth restriction. *Pediatr Res,* 42**,** 514-9.

GLAZIER, J. D., JONES, C. J. & SIBLEY, C. P. 1990. Preparation of plasma membrane vesicles from the rat placenta at term and measurement of Na+ uptake. *Placenta,* 11**,** 451-463.

GLAZIER, J. D., SIBLEY, C. P. & CARTER, A. M. 1996. Effect of fetal growth restriction on system A amino acid transporter activity in the maternal facing plasma membrane of rat syncytiotrophoblast. *Pediatr Res,* 40**,** 325-9.

GLUCKMAN, P. D., HANSON, M. A., COOPER, C. & THORNBURG, K. L. 2008. Effect of in utero and early-life conditions on adult health and disease. *N Engl J Med,* 359**,** 61-73.

GOMEZ, D. & OWENS, G. K. 2012. Smooth muscle cell phenotypic switching in atherosclerosis. *Cardiovasc Res,* 95**,** 156-64.

GOMPF, H., LUFT, F. C. & MORANO, I. 2002. Nitric oxide synthase upregulation and the predelivery blood pressure decrease in spontaneously hypertensive rats. *J Hypertens,* 20**,** 255-61.

GONG, X., LIU, Y., CHEN, Z., XU, C., LU, Q. & JIN, Z. 2014. Insights into the paracrine effects of uterine natural killer cells. *Mol Med Rep.,* 10**,** 2851-60. doi: 10.3892/mmr.2014.2626. Epub 2014 Oct 13.

GORDIJN, S. J., BEUNE, I. M., THILAGANATHAN, B., PAPAGEORGHIOU, A., BASCHAT, A. A., BAKER, P. N., SILVER, R. M., WYNIA, K. & GANZEVOORT, W. 2016. Consensus definition of fetal growth restriction: a Delphi procedure. *Ultrasound Obstet Gynecol,* 48**,** 333-9.

GORLACH, A., BERTRAM, K., HUDECOVA, S. & KRIZANOVA, O. 2015. Calcium and ROS: A mutual interplay. *Redox Biol.,* 6:260-71.**,** 10.1016/j.redox.2015.08.010. Epub 2015 Aug 11.

GOULOPOULOU, S. 2017. Maternal Vascular Physiology in Preeclampsia. *Hypertension,* 70**,** 1066-1073.

GRAHAM, D., HAMILTON, C., BEATTIE, E., SPIERS, A. & DOMINICZAK, A. F. 2004. Comparison of the effects of omapatrilat and irbesartan/hydrochlorothiazide on endothelial function and cardiac hypertrophy in the stroke-prone spontaneously hypertensive rat: sex differences. *J Hypertens,* 22**,** 329-37.

GRANGER, J. P., LAMARCA, B. B., COCKRELL, K., SEDEEK, M., BALZI, C., CHANDLER, D. & BENNETT, W. 2006. Reduced uterine perfusion pressure (RUPP) model for studying cardiovascular-renal dysfunction in response to placental ischemia. *Methods Mol Med,* 122**,** 383-92.

GRIGSBY, P. L. 2016. Animal Models to Study Placental Development and Function throughout Normal and Dysfunctional Human Pregnancy. *Semin Reprod Med,* 34**,** 11-6.

GROSSER, O. 1927. *Frühentwicklung, Eihautbildung und Placentation des Menschen und der Säugetiere*, JF Bergmann.

GUEDES, M. & CANAVARRO, M. C. 2014. Characteristics of primiparous women of advanced age and their partners: a homogenous or heterogenous group? *Birth,* 41**,** 46-55.

GUTIERREZ, J., BALLINGER, S. W., DARLEY-USMAR, V. M. & LANDAR, A. 2006. Free radicals, mitochondria, and oxidized lipids: the emerging role in signal transduction in vascular cells. *Circ Res,* 99**,** 924-32.

GUTTMACHER, A. E., MADDOX, Y. T. & SPONG, C. Y. 2014. The Human Placenta Project: placental structure, development, and function in real time. *Placenta,* 35**,** 303-4.

GUZIK, T. J., SADOWSKI, J., GUZIK, B., JOPEK, A., KAPELAK, B., PRZYBYLOWSKI, P., WIERZBICKI, K., KORBUT, R., HARRISON, D. G. & CHANNON, K. M. 2006. Coronary artery superoxide production and nox isoform expression in human coronary artery disease. *Arterioscler Thromb Vasc Biol,* 26**,** 333-9.

GUZIK, T. J., SADOWSKI, J., KAPELAK, B., JOPEK, A., RUDZINSKI, P., PILLAI, R., KORBUT, R. & CHANNON, K. M. 2004. Systemic regulation of vascular NAD(P)H oxidase activity and nox isoform expression in human arteries and veins. *Arterioscler Thromb Vasc Biol,* 24**,** 1614-20.

HACHÉ, S., TAKSER, L., LEBELLEGO, F., WEILER, H., LEDUC, L., FOREST, J. C., GIGUÈRE, Y., MASSE, A., BARBEAU, B. & LAFOND, J. 2011. Alteration of calcium homeostasis in

primary preeclamptic syncytiotrophoblasts: effect on calcium exchange in placenta. *J Cell Mol Med,* 15**,** 654-67.

HACK, M., FLANNERY, D. J., SCHLUCHTER, M., CARTAR, L., BORAWSKI, E. & KLEIN, N. 2002. Outcomes in young adulthood for very-low-birth-weight infants. *N Engl J Med,* 346**,** 149-57.

HAJRI, T., IBRAHIMI, A., COBURN, C. T., KNAPP, F. F., KURTZ, T., PRAVENEC, M. & ABUMRAD, N. A. 2001. Defective fatty acid uptake in the spontaneously hypertensive rat is a primary determinant of altered glucose metabolism, hyperinsulinemia, and myocardial hypertrophy. *J Biol Chem,* 276**,** 23661-6.

HALE, S. A., SCHONBERG, A., BADGER, G. J. & BERNSTEIN, I. M. 2009. Relationship between prepregnancy and early pregnancy uterine blood flow and resistance index. *Reprod Sci,* 16**,** 1091-6.

HALL, M. E., GEORGE, E. M. & GRANGER, J. P. 2011. The heart during pregnancy. *Rev Esp Cardiol,* 64**,** 1045-50.

HAN, D., WILLIAMS, E. & CADENAS, E. 2001. Mitochondrial respiratory chain-dependent generation of superoxide anion and its release into the intermembrane space. *Biochem J,* 353**,** 411-6.

HARRIS, L. K., SMITH, S. D., KEOGH, R. J., JONES, R. L., BAKER, P. N., KNOFLER, M., CARTWRIGHT, J. E., WHITLEY, G. S. & APLIN, J. D. 2010. Trophoblast- and vascular smooth muscle cell-derived MMP-12 mediates elastolysis during uterine spiral artery remodeling. *Am J Pathol.,* 177**,** 2103-15. doi: 10.2353/ajpath.2010.100182. Epub 2010 Aug 27.

HARVEY, A. P., MONTEZANO, A. C., HOOD, K. Y., LOPES, R. A., RIOS, F., CERAVOLO, G., GRAHAM, D. & TOUYZ, R. M. 2017. Vascular dysfunction and fibrosis in stroke-prone spontaneously hypertensive rats: The aldosterone-mineralocorticoid receptor-Nox1 axis. *Life Sci,* 179**,** 110-119.

HAUGUEL-DE MOUZON, S. & GUERRE-MILLO, M. 2006. The placenta cytokine network and inflammatory signals. *Placenta,* 27**,** 794-8.

HAYWARD, C. E., LEAN, S., SIBLEY, C. P., JONES, R. L., WAREING, M., GREENWOOD, S. L. & DILWORTH, M. R. 2016. Placental Adaptation: What Can We Learn from Birthweight:Placental Weight Ratio? *Front Physiol,* 7**,** 28.

HE, X., HE, Y., XI, B., ZHENG, J., ZENG, X., CAI, Q., OUYANG, Y., WANG, C., ZHOU, X., HUANG, H., DENG, W., XIN, S., HUANG, Q. & LIU, H. 2013. LncRNAs expression in preeclampsia placenta reveals the potential role of LncRNAs contributing to preeclampsia pathogenesis. *PLoS One,* 8**,** e81437.

HEFLER, L. A., TEMPFER, C. B., MORENO, R. M., O'BRIEN, W. E. & GREGG, A. R. 2001. Endothelial-derived nitric oxide and angiotensinogen: blood pressure and metabolism during mouse pregnancy. *Am J Physiol Regul Integr Comp Physiol,* 280**,** R174-82.

HERING, L., HERSE, F., GEUSENS, N., VERLOHREN, S., WENZEL, K., STAFF, A. C., BROSNIHAN, K. B., HUPPERTZ, B., LUFT, F. C., MULLER, D. N., PIJNENBORG, R., CARTWRIGHT, J. E. & DECHEND, R. 2010. Effects of circulating and local uteroplacental angiotensin II in rat pregnancy. *Hypertension,* 56**,** 311-8.

HERMIDA, R. C. & AYALA, D. E. 2002. Prognostic Value of Office and Ambulatory Blood Pressure Measurements in Pregnancy. *Hypertension,* 40**,** 298.

HERSE, F., DECHEND, R., HARSEM, N. K., WALLUKAT, G., JANKE, J., QADRI, F., HERING, L., MULLER, D. N., LUFT, F. C. & STAFF, A. C. 2007. Dysregulation of the circulating and tissue-based renin-angiotensin system in preeclampsia. *Hypertension,* 49**,** 604-11.

HERSE, F. & LAMARCA, B. 2013. Angiotensin II type 1 receptor autoantibody (AT1-AA)-mediated pregnancy hypertension. *Am J Reprod Immunol,* 69**,** 413-8.

HERSE, F., LAMARCA, B., HUBEL, C. A., KAARTOKALLIO, T., LOKKI, A. I., EKHOLM, E., LAIVUORI, H., GAUSTER, M., HUPPERTZ, B., SUGULLE, M., RYAN, M. J., NOVOTNY, S., BREWER, J., PARK, J. K., KACIK, M., HOYER, J., VERLOHREN, S., WALLUKAT, G., ROTHE, M., LUFT, F. C., MULLER, D. N., SCHUNCK, W. H., STAFF, A. C. & DECHEND, R. 2012. Cytochrome P450 subfamily 2J polypeptide 2 expression and circulating epoxyeicosatrienoic metabolites in preeclampsia. *Circulation.,* 126**,** 2990-9. doi: 10.1161/CIRCULATIONAHA.112.127340. Epub 2012 Nov 15.

HESLEHURST, N., ELLS, L. J., SIMPSON, H., BATTERHAM, A., WILKINSON, J. & SUMMERBELL, C. D. 2007. Trends in maternal obesity incidence rates, demographic predictors, and health inequalities in 36,821 women over a 15-year period. *BJOG,* 114**,** 187-94.

HESS, A. P., HAMILTON, A. E., TALBI, S., DOSIOU, C., NYEGAARD, M., NAYAK, N., GENBECEV-KRTOLICA, O., MAVROGIANIS, P., FERRER, K., KRUESSEL, J., FAZLEABAS, A. T., FISHER, S. J. & GIUDICE, L. C. 2007. Decidual stromal cell response to paracrine signals from the trophoblast: amplification of immune and angiogenic modulators. *Biol Reprod.,* 76**,** 102-17. doi: 10.1095/biolreprod.106.054791. Epub 2006 Oct 4.

HEYWARD, C. Y., SONES, J. L., LOB, H. E., YUEN, L. C., ABBOTT, K. E., HUANG, W., BEGUN, Z. R., BUTLER, S. D., AUGUST, A., LEIFER, C. A. & DAVISSON, R. L. 2017. The decidua of preeclamptic-like BPH/5 mice exhibits an exaggerated inflammatory response during early pregnancy. *J Reprod Immunol,* 120**,** 27-33.

HIBBARD, J. U., SHROFF, S. G. & CUNNINGHAM, F. G. 2015. Chapter 14 - Cardiovascular Alterations in Normal and Preeclamptic Pregnancy. *Chesley's Hypertensive Disorders in Pregnancy (Fourth Edition).* San Diego: Academic Press.

HIGHET, A. R., BUCKBERRY, S., MAYNE, B. T., KHODA, S. M., BIANCO-MIOTTO, T. & ROBERTS, C. T. 2016. First trimester trophoblasts forming endothelial-like tubes in vitro emulate a 'blood vessel development' gene expression profile. *Gene Expr Patterns.,* 21**,** 103-10. doi: 10.1016/j.gep.2016.05.001. Epub 2016 May 21.

HILBERT, P., LINDPAINTNER, K., BECKMANN, J. S., SERIKAWA, T., SOUBRIER, F., DUBAY, C., CARTWRIGHT, P., DE GOUYON, B., JULIER, C. & TAKAHASI, S. 1991. Chromosomal mapping of two genetic loci associated with blood-pressure regulation in hereditary hypertensive rats. *Nature,* 353**,** 521-9.

HIMMELMANN, A., SVENSSON, A. & HANSSON, L. 1994. Relation of maternal blood pressure during pregnancy to birth weight and blood pressure in children. The Hypertension in Pregnancy Offspring Study. *J Intern Med,* 235**,** 347-52.

HO, D. H. 2014. Transgenerational epigenetics: the role of maternal effects in cardiovascular development. *Integr Comp Biol,* 54**,** 43-51.

HOLLAND, O., DEKKER NITERT, M., GALLO, L. A., VEJZOVIC, M., FISHER, J. J. & PERKINS, A. V. 2017. Review: Placental mitochondrial function and structure in gestational disorders. *Placenta,* 54**,** 2-9.

HOLTAN, S. G., CREEDON, D. J., HALUSKA, P. & MARKOVIC, S. N. 2009. Cancer and pregnancy: parallels in growth, invasion, and immune modulation and implications for cancer therapeutic agents. *Mayo Clin Proc,* 84**,** 985-1000.

HORIUCHI, M., AKISHITA, M. & DZAU, V. J. 1999. Recent progress in angiotensin II type 2 receptor research in the cardiovascular system. *Hypertension,* 33**,** 613-21.

HOUSER, B. L., TILBURGS, T., HILL, J., NICOTRA, M. L. & STROMINGER, J. L. 2011. Two unique human decidual macrophage populations. *J Immunol.,* 186**,** 2633-42. doi: 10.4049/jimmunol.1003153. Epub 2011 Jan 21.

HUNG, T. H., SKEPPER, J. N. & BURTON, G. J. 2001. In vitro ischemia-reperfusion injury in term human placenta as a model for oxidative stress in pathological pregnancies. *Am J Pathol,* 159**,** 1031-43.

HUNTER, S. & ROBSON, S. C. 1992. Adaptation of the maternal heart in pregnancy. *Br Heart J,* 68**,** 540-3.

HUPPERTZ, B. 2008. The anatomy of the normal placenta. *J Clin Pathol,* 61**,** 1296-302.

IACOVIDOU, N., VARSAMI, M. & SYGGELLOU, A. 2010. Neonatal outcome of preterm delivery. *Ann N Y Acad Sci,* 1205**,** 130-4.

IHARA, Y., TAII, S. & MORI, T. 1987. Expression of renin and angiotensinogen genes in the human placental tissues. *Endocrinol Jpn,* 34**,** 887-96.

ILIODROMITI, S., MACKAY, D. F., SMITH, G. C., PELL, J. P., SATTAR, N., LAWLOR, D. A. & NELSON, S. M. 2017. Customised and Noncustomised Birth Weight Centiles and Prediction of Stillbirth and Infant Mortality and Morbidity: A Cohort Study of 979,912 Term Singleton Pregnancies in Scotland. *PLoS Med,* 14**,** e1002228.

IMMONEN, I., SIIMES, A., STENMAN, U. H., KÄRKKÄINEN, J. & FYHRQUIST, F. 1983. Plasma renin substrate and oestrogens in normal pregnancy. *Scand J Clin Lab Invest,* 43**,** 61-5.

INTAPAD, S., WARRINGTON, J. P., SPRADLEY, F. T., PALEI, A. C., DRUMMOND, H. A., RYAN, M. J., GRANGER, J. P. & ALEXANDER, B. T. 2014. Reduced uterine perfusion pressure induces hypertension in the pregnant mouse. *Am J Physiol Regul Integr Comp Physiol.,* 307**,** R1353-7. doi: 10.1152/ajpregu.00268.2014. Epub 2014 Oct 8.

INTENGAN, H. D., THIBAULT, G., LI, J. S. & SCHIFFRIN, E. L. 1999. Resistance artery mechanics, structure, and extracellular components in spontaneously hypertensive rats : effects of angiotensin receptor antagonism and converting enzyme inhibition. *Circulation,* 100**,** 2267-75.

IRANI, R. A. & XIA, Y. 2011. Renin angiotensin signaling in normal pregnancy and preeclampsia. *Semin Nephrol,* 31**,** 47-58.

ITSKOVITZ, J., SEALEY, J. E., GLORIOSO, N. & ROSENWAKS, Z. 1987. Plasma prorenin response to human chorionic gonadotropin in ovarian-hyperstimulated women: correlation with the number of ovarian follicles and steroid hormone concentrations. *Proc Natl Acad Sci U S A,* 84**,** 7285-9.

IYER, N. V., KOTCH, L. E., AGANI, F., LEUNG, S. W., LAUGHNER, E., WENGER, R. H., GASSMANN, M., GEARHART, J. D., LAWLER, A. M., YU, A. Y. & SEMENZA, G. L. 1998. Cellular and developmental control of O2 homeostasis by hypoxia-inducible factor 1 alpha. *Genes Dev.,* 12**,** 149-62.

JACKSON, W. F. 2000. Ion channels and vascular tone. *Hypertension,* 35**,** 173-8.

JACOB, H. J., LINDPAINTNER, K., LINCOLN, S. E., KUSUMI, K., BUNKER, R. K., MAO, Y. P., GANTEN, D., DZAU, V. J. & LANDER, E. S. 1991. Genetic mapping of a gene causing hypertension in the stroke-prone spontaneously hypertensive rat. *Cell,* 67**,** 213-24.

JAMES, D. J., CAIRNS, F., SALT, I. P., MURPHY, G. J., DOMINICZAK, A. F., CONNELL, J. M. C. & GOULD, G. W. 2001. Skeletal Muscle of Stroke-Prone Spontaneously Hypertensive Rats Exhibits Reduced Insulin-Stimulated Glucose Transport and Elevated Levels of Caveolin and Flotillin. *Diabetes,* 50**,** 2148.

JANSSON, T. 2001. Amino acid transporters in the human placenta. *Pediatr Res,* 49**,** 141-7.

JAUNIAUX, E., WATSON, A. L., HEMPSTOCK, J., BAO, Y. P., SKEPPER, J. N. & BURTON, G. J. 2000. Onset of maternal arterial blood flow and placental oxidative stress. A possible factor in human early pregnancy failure. *Am J Pathol,* 157**,** 2111-22.

JESMIN, S., HATTORI, Y., TOGASHI, H., UENO, K., YOSHIOKA, M. & SAKUMA, I. 2005. Age-related changes in cardiac expression of VEGF and its angiogenic receptor KDR in stroke-prone spontaneously hypertensive rats. *Mol Cell Biochem,* 272**,** 63-73.

JIN, X., XU, Z., CAO, J., SHAO, P., ZHOU, M., QIN, Z., LIU, Y., YU, F., ZHOU, X., JI, W., CAI, W., MA, Y., WANG, C., SHAN, N., YANG, N., CHEN, X. & LI, Y. 2017. Proteomics analysis of human placenta reveals glutathione metabolism dysfunction as the underlying pathogenesis for preeclampsia. *Biochim Biophys Acta.,* 1865**,** 1207-1214. doi: 10.1016/j.bbapap.2017.07.003. Epub 2017 Jul 10.

JOHANSSON, M., JANSSON, T. & POWELL, T. L. 2000. Na(+)-K(+)-ATPase is distributed to microvillous and basal membrane of the syncytiotrophoblast in human placenta. *Am J Physiol Regul Integr Comp Physiol,* 279**,** R287-94.

JOKHI, P. P., KING, A., SHARKEY, A. M., SMITH, S. K. & LOKE, Y. W. 1994. Screening for cytokine messenger ribonucleic acids in purified human decidual lymphocyte populations by the reverse-transcriptase polymerase chain reaction. *J Immunol.,* 153**,** 4427-35.

JONCKHEERE, A. I., SMEITINK, J. A. & RODENBURG, R. J. 2012. Mitochondrial ATP synthase: architecture, function and pathology. *J Inherit Metab Dis,* 35**,** 211-25.

JONES, C. J. & FOX, H. 1991. Ultrastructure of the normal human placenta. *Electron Microsc Rev,* 4**,** 129-78.

JONES, M. L., MARK, P. J., LEWIS, J. L., MORI, T. A., KEELAN, J. A. & WADDELL, B. J. 2010. Antioxidant defenses in the rat placenta in late gestation: increased labyrinthine expression of superoxide dismutases, glutathione peroxidase 3, and uncoupling protein 2. *Biol Reprod,* 83**,** 254-60.

KAARTOKALLIO, T., CERVERA, A., KYLLÖNEN, A., LAIVUORI, K. & GROUP, F. C. I. 2015. Gene expression profiling of pre-eclamptic placentae by RNA sequencing. *Sci Rep,* 5**,** 14107.

KAISERMAN-ABRAMOF, I. R. & PADYKULA, H. A. 1989. Angiogenesis in the postovulatory primate endometrium: the coiled arteriolar system. *Anat Rec,* 224**,** 479-89.

KALAFAT, E. & THILAGANATHAN, B. 2017. Cardiovascular origins of preeclampsia. *Curr Opin Obstet Gynecol,* 29**,** 383-389.

KALENGA, M. K., DE GASPARO, M., THOMAS, K. & DE HERTOGH, R. 1996. Angiotensin II and its different receptor subtypes in placenta and fetal membranes. *Placenta,* 17**,** 103-110.

KALENGA, M. K., DE HERTOGH R FAU - WHITEBREAD, S., WHITEBREAD S FAU - VANKRIEKEN, L., VANKRIEKEN L FAU - THOMAS, K., THOMAS K FAU - DE GASPARO, M. & DE GASPARO, M. [Distribution of the concentrations of angiotensin II (A II), A II receptors, hPL, prolactin, and steroids in human fetal membranes].

KANAGALINGAM, M. G., FOROUHI, N. G., GREER, I. A. & SATTAR, N. 2005. Changes in booking body mass index over a decade: retrospective analysis from a Glasgow Maternity Hospital. *BJOG,* 112**,** 1431-3.

KANASAKI, K., PALMSTEN, K., SUGIMOTO, H., AHMAD, S., HAMANO, Y., XIE, L., PARRY, S., AUGUSTIN, H. G., GATTONE, V. H., FOLKMAN, J., STRAUSS, J. F. & KALLURI, R. 2008. Deficiency in catechol-O-methyltransferase and 2-methoxyoestradiol is associated with pre-eclampsia. *Nature.,* 453**,** 1117-21. doi: 10.1038/nature06951. Epub 2008 May 11.

KAWADA, N., IMAI, E., KARBER, A., WELCH, W. J. & WILCOX, C. S. 2002. A mouse model of angiotensin II slow pressor response: role of oxidative stress. *J Am Soc Nephrol,* 13**,** 2860-8.

KEARNEY, P. M., WHELTON, M., REYNOLDS, K., MUNTNER, P., WHELTON, P. K. & HE, J. 2005. Global burden of hypertension: analysis of worldwide data. *The Lancet,* 365**,** 217-223.

KENNY, L. C., BLACK, M. A., POSTON, L., TAYLOR, R., MYERS, J. E., BAKER, P. N., MCCOWAN, L. M., SIMPSON, N. A., DEKKER, G. A., ROBERTS, C. T., RODEMS, K., NOLAND, B., RAYMUNDO, M., WALKER, J. J. & NORTH, R. A. 2014. Early pregnancy prediction of preeclampsia in nulliparous women, combining clinical risk and biomarkers: the Screening for Pregnancy Endpoints (SCOPE) international cohort study. *Hypertension,* 64**,** 644-52.

KERR, S., BROSNAN, M. J., MCINTYRE, M., REID, J. L., DOMINICZAK, A. F. & HAMILTON, C. A. 1999. Superoxide anion production is increased in a model of genetic hypertension: role of the endothelium. *Hypertension,* 33**,** 1353-8.

KHONG, T. Y., ADEMA, E. D. & ERWICH, J. J. 2003. On an anatomical basis for the increase in birth weight in second and subsequent born children. *Placenta,* 24**,** 348-53.

KIM, J., ZHAO, K., JIANG, P., LU, Z. X., WANG, J., MURRAY, J. C. & XING, Y. 2012. Transcriptome landscape of the human placenta. *BMC Genomics,* 13**,** 115.

KIM, S., HOSOI, M., SHIMAMOTO, K., TAKADA, T. & YAMAMOTO, K. 1991. Increased production of angiotensin II in the adrenal gland of stroke-prone spontaneously hypertensive rats with malignant hypertension. *Biochemical and Biophysical Research Communications,* 178**,** 151-157.

KING, A. & LOKE, Y. W. 1997. Placental vascular remodelling. *Lancet,* 350**,** 220-1.

KITAYA, K., YASUO, T., YAMAGUCHI, T., FUSHIKI, S. & HONJO, H. 2007. Genes regulated by interferon-gamma in human uterine microvascular endothelial cells. *Int J Mol Med.,* 20**,** 689-97.

KLEIN, A., JOSEPH, P. D., CHRISTENSEN, V. G., JENSEN, L. J. & JACOBSEN, J. C. B. 2018. Lack of Tone in Mouse Small Mesenteric Arteries Leads to Outward Remodeling, which can be Prevented by Prolonged Agonist-Induced Vasoconstriction. *Am J Physiol Heart Circ Physiol*.

KLEINROUWELER, C. E., VAN UITERT, M., MOERLAND, P. D., RIS-STALPERS, C., VAN DER POST, J. A. & AFINK, G. B. 2013. Differentially expressed genes in the pre-eclamptic placenta: a systematic review and meta-analysis. *PLoS One,* 8**,** e68991.

KLIMAN, H. J. 2000. Uteroplacental Blood Flow : The Story of Decidualization, Menstruation, and Trophoblast Invasion. *The American Journal of Pathology,* 157**,** 1759-1768.

KNOCK, G. A., SULLIVAN, M. H., MCCARTHY, A., ELDER, M. G., POLAK, J. M. & WHARTON, J. 1994. Angiotensin II (AT1) vascular binding sites in human placentae from normal-term, preeclamptic and growth retarded pregnancies. *J Pharmacol Exp Ther,* 271**,** 1007-15.

KOH-TAN, H. H., DASHTI, M., WANG, T., BEATTIE, W., MCCLURE, J., YOUNG, B., DOMINICZAK, A. F., MCBRIDE, M. W. & GRAHAM, D. 2017. Dissecting the genetic components of a quantitative trait locus for blood pressure and renal pathology on rat chromosome 3. *J Hypertens,* 35**,** 319-329.

KOKOSZKA, J. E., COSKUN, P., ESPOSITO, L. A. & WALLACE, D. C. 2001. Increased mitochondrial oxidative stress in the Sod2 (+/-) mouse results in the age-related decline of mitochondrial function culminating in increased apoptosis. *Proc Natl Acad Sci U S A,* 98**,** 2278-83.

KONIOR, A., SCHRAMM, A., CZESNIKIEWICZ-GUZIK, M. & GUZIK, T. J. 2014. NADPH oxidases in vascular pathology. *Antioxid Redox Signal,* 20**,** 2794-814.

KOPF, P. G., PHELPS, L. E., SCHUPBACH, C. D., JOHNSON, A. K. & PEULER, J. D. 2018. Differential effects of long-term slow-pressor and subpressor angiotensin II on contractile and relaxant reactivity of resistance versus conductance arteries. *Physiol Rep,* 6.

KOREN, M. J., DEVEREUX, R. B., CASALE, P. N., SAVAGE, D. D. & LARAGH, J. H. 1991. Relation of left ventricular mass and geometry to morbidity and mortality in uncomplicated essential hypertension. *Ann Intern Med,* 114**,** 345-52.

KUBLICKIENE, K.-R., GRUNEWALD, C., LINDBLOM, B. & NISELL, H. 1998. Myogenic and Endothelial Properties of Myometrial Resistance Arteries from Women with Preeclampsia. *Hypertension in Pregnancy,* 17**,** 271-281.

KUBLICKIENE, K. R., KUBLICKAS, M., LINDBLOM, B., LUNELL, N. O. & NISELL, H. 1997. A comparison of myogenic and endothelial properties of myometrial and omental resistance vessels in late pregnancy. *Am J Obstet Gynecol,* 176**,** 560-6.

KUBLICKIENE, K. R., LINDBLOM, B., KRÜGER, K. & NISELL, H. 2000. Preeclampsia: evidence for impaired shear stress-mediated nitric oxide release in uterine circulation. *Am J Obstet Gynecol,* 183**,** 160-6.

KULANDAVELU, S., QU, D. & ADAMSON, S. L. 2006. Cardiovascular function in mice during normal pregnancy and in the absence of endothelial NO synthase. *Hypertension,* 47**,** 1175-82.

KULANDAVELU, S., WHITELEY, K. J., BAINBRIDGE, S. A., QU, D. & ADAMSON, S. L. 2013. Endothelial NO synthase augments fetoplacental blood flow, placental vascularization, and fetal growth in mice. *Hypertension,* 61**,** 259-66.

KUSINSKI, L. C., JONES, C. J., BAKER, P. N., SIBLEY, C. P. & GLAZIER, J. D. 2010. Isolation of plasma membrane vesicles from mouse placenta at term and measurement of system A and system beta amino acid transporter activity. *Placenta,* 31**,** 53-9.

KUSINSKI, L. C., STANLEY, J. L., DILWORTH, M. R., HIRT, C. J., ANDERSSON, I. J., RENSHALL, L. J., BAKER, B. C., BAKER, P. N., SIBLEY, C. P., WAREING, M. & GLAZIER, J. D. 2012. eNOS knockout mouse as a model of fetal growth restriction with an impaired uterine artery function and placental transport phenotype. *Am J Physiol Regul Integr Comp Physiol,* 303**,** R86-93.

LANGER, B., GRIMA, M., COQUARD, C., BADER, A. M., SCHLAEDER, G. & IMBS, J. L. 1998. Plasma active renin, angiotensin I, and angiotensin II during pregnancy and in preeclampsia. *Obstet Gynecol,* 91**,** 196-202.

LASH, G. E., OTUN, H. A., INNES, B. A., PERCIVAL, K., SEARLE, R. F., ROBSON, S. C. & BULMER, J. N. 2010a. Regulation of extravillous trophoblast invasion by uterine natural killer cells is dependent on gestational age. *Hum Reprod,* 25**,** 1137-45.

LASH, G. E., PITMAN, H., MORGAN, H. L., INNES, B. A., AGWU, C. N. & BULMER, J. N. 2016. Decidual macrophages: key regulators of vascular remodeling in human pregnancy. *J Leukoc Biol,* 100**,** 315-25.

LASH, G. E., ROBSON, S. C. & BULMER, J. N. 2010b. Review: Functional role of uterine natural killer (uNK) cells in human early pregnancy decidua. *Placenta,* 31 Suppl**,** S87-92.

LAWLER, J., OSMAN, M., SHELTON, J. A. & YEH, J. 2007. Population-based analysis of hypertensive disorders in pregnancy. *Hypertens Pregnancy,* 26**,** 67-76.

LEAN, S. C., HEAZELL, A. E. P., DILWORTH, M. R., MILLS, T. A. & JONES, R. L. 2017. Placental Dysfunction Underlies Increased Risk of Fetal Growth Restriction and Stillbirth in Advanced Maternal Age Women. *Sci Rep,* 7**,** 9677.

LECARPENTIER, E., TSATSARIS, V., GOFFINET, F., CABROL, D., SIBAI, B. & HADDAD, B. 2013. Risk factors of superimposed preeclampsia in women with essential chronic hypertension treated before pregnancy. *PLoS One,* 8**,** e62140.

LEDINGHAM, J. M. & LAVERTY, R. 2001. Effects of nitric oxide synthase inhibition and low-salt diet on blood pressure and mesenteric resistance artery remodelling in genetically hypertensive rats. *Clin Exp Pharmacol Physiol,* 28**,** 761-3.

LEE, M. Y. & GRIENDLING, K. K. 2008. Redox signaling, vascular function, and hypertension. *Antioxid Redox Signal.,* 10**,** 1045-59. doi: 10.1089/ars.2007.1986.

LEE, W. S., HARDER, J. A., YOSHIZUMI, M., LEE, M. E. & HABER, E. 1997. Progesterone inhibits arterial smooth muscle cell proliferation. *Nat Med,* 3**,** 1005-8.

LEES, C. & FERRAZZI, E. 2017. Relevance of Haemodynamics in Treating Pre-eclampsia. *Curr Hypertens Rep,* 19**,** 76.

LEUNG, P. S., TSAI, S. J., WALLUKAT, G., LEUNG, T. N. & LAU, T. K. 2001. The upregulation of angiotensin II receptor AT(1) in human preeclamptic placenta. *Mol Cell Endocrinol,* 184**,** 95-102.

LEWIS, R. M., BATCHELOR, D. C., BASSETT, N. S., JOHNSTON, B. M., NAPIER, J. & SKINNER, S. J. 1997. Perinatal growth disturbance in the spontaneously hypertensive rat. *Pediatr Res,* 42**,** 758-64.

LI, C., ANSARI, R., YU, Z. & SHAH, D. 2000. Definitive molecular evidence of renin-angiotensin system in human uterine decidual cells. *Hypertension,* 36**,** 159-64.

LI, J. L., LI, R., GAO, Y., GUO, W. C., SHI, P. X. & LI, M. 2018. LncRNA CCAT1 promotes the progression of preeclampsia by regulating CDK4. *Eur Rev Med Pharmacol Sci,* 22**,** 1216-1223.

LI, W., MATA, K. M., MAZZUCA, M. Q. & KHALIL, R. A. 2014. Altered matrix metalloproteinase-2 and -9 expression/activity links placental ischemia and anti-angiogenic sFlt-1 to uteroplacental and vascular remodeling and collagen deposition in hypertensive pregnancy. *Biochem Pharmacol,* 89**,** 370-85.

LIAN, I. A., LANGAAS, M., MOSES, E. & JOHANSSON, Å. 2013. Differential gene expression at the maternal-fetal interface in preeclampsia is influenced by gestational age. *PLoS One,* 8**,** e69848.

LIAN, I. A., TOFT, J. H., OLSEN, G. D., LANGAAS, M., BJORGE, L., EIDE, I. P., BORDAHL, P. E. & AUSTGULEN, R. 2010. Matrix metalloproteinase 1 in pre-eclampsia and fetal growth restriction: reduced gene expression in decidual tissue and protein expression in extravillous trophoblasts. *Placenta.* England.

LINDHARD, J. 1915. Über das Minutenvolum des Herzens bei Ruhe und bei Muskelarbeit. *Pflüger's Archiv für die gesamte Physiologie des Menschen und der Tiere,* 161**,** 233-383.

LIU, L. Y., YANG, T., JI, J., WEN, Q., MORGAN, A. A., JIN, B., CHEN, G., LYELL, D. J., STEVENSON, D. K., LING, X. B. & BUTTE, A. J. 2013. Integrating multiple 'omics' analyses identifies serological protein biomarkers for preeclampsia. *BMC Med,* 11**,** 236.

LOPES, R. A., NEVES, K. B., TOSTES, R. C., MONTEZANO, A. C. & TOUYZ, R. M. 2015. Downregulation of Nuclear Factor Erythroid 2-Related Factor and Associated Antioxidant Genes Contributes to Redox-Sensitive Vascular Dysfunction in Hypertension. *Hypertension,* 66**,** 1240-50.

LOPES VAN BALEN, V. A., SPAAN, J. J., CORNELIS, T., HEIDEMA, W. M., SCHOLTEN, R. R. & SPAANDERMAN, M. E. A. 2018. Endothelial and kidney function in women with a history of preeclampsia and healthy parous controls: A case control study. *Microvasc Res,* 116**,** 71-76.

LORENZ, R. P., PICCHIO, L. P., WEISZ, J. & LLOYD, T. 1984. The relationship between reproductive performance and blood pressure in the spontaneously hypertensive rat. *Am J Obstet Gynecol,* 150**,** 519-23.

LYALL, F., ROBSON, S. C. & BULMER, J. N. 2013. Spiral artery remodeling and trophoblast invasion in preeclampsia and fetal growth restriction: relationship to clinical outcome. *Hypertension,* 62**,** 1046-54.

MAAS, J. W., GROOTHUIS, P. G., DUNSELMAN, G. A., DE GOEIJ, A. F., STRUYKER BOUDIER, H. A. & EVERS, J. L. 2001. Endometrial angiogenesis throughout the human menstrual cycle. *Hum Reprod,* 16**,** 1557-61.

MADAZLI, R., BENIAN, A., AYDIN, S., UZUN, H. & TOLUN, N. 2002. The plasma and placental levels of malondialdehyde, glutathione and superoxide dismutase in pre-eclampsia. *J Obstet Gynaecol,* 22**,** 477-80.

MAHENDRAN, D., DONNAI, P., GLAZIER, J. D., D'SOUZA, S. W., BOYD, R. D. & SIBLEY, C. P. 1993. Amino acid (system A) transporter activity in microvillous membrane vesicles from the placentas of appropriate and small for gestational age babies. *Pediatr Res,* 34**,** 661-5.

MAHENDRU, A. A., FOO, F. L., MCENIERY, C. M., EVERETT, T. R., WILKINSON, I. B. & LEES, C. C. 2017. Change in maternal cardiac output from preconception to mid-pregnancy is associated with birth weight in healthy pregnancies. *Ultrasound Obstet Gynecol,* 49**,** 78-84.

MALASSINÉ, A., FRENDO, J. L. & EVAIN-BRION, D. 2003. A comparison of placental development and endocrine functions between the human and mouse model. *Hum Reprod Update,* 9**,** 531-9.

MANDALA, M. & OSOL, G. 2012. Physiological remodelling of the maternal uterine circulation during pregnancy. *Basic Clin Pharmacol Toxicol,* 110**,** 12-8.

MARSHALL, F. H. A. 1910. *The physiology of reproduction*, London, New York and Toronto: Longmans, Green & Co.

MARY, S., SMALL, H. Y., SIWY, J., MULLEN, W., GIRI, A. & DELLES, C. 2017. Polymerization-Incompetent Uromodulin in the Pregnant Stroke-Prone Spontaneously Hypertensive Rat. *Hypertension,* 69**,** 910-918.

MASSANI, Z. M., SANGUINETTI, R., GALLEGOS, R. & RAIMONDI, D. 1967. Angiotensin blood levels in normal and toxemic pregnancies. *Am J Obstet Gynecol,* 99**,** 313-7.

MATSUSAKA, T., NIIMURA, F., SHIMIZU, A., PASTAN, I., SAITO, A., KOBORI, H., NISHIYAMA, A. & ICHIKAWA, I. 2012. Liver angiotensinogen is the primary source of renal angiotensin II. *J Am Soc Nephrol,* 23**,** 1181-9.

MAYEUR, S., LANCEL, S., THEYS, N., LUKASZEWSKI, M. A., DUBAN-DEWEER, S., BASTIDE, B., HACHANI, J., CECCHELLI, R., BRETON, C., GABORY, A., STORME, L., REUSENS, B., JUNIEN, C., VIEAU, D. & LESAGE, J. 2013. Maternal calorie restriction modulates placental mitochondrial biogenesis and bioenergetic efficiency: putative involvement in fetoplacental growth defects in rats. *Am J Physiol Endocrinol Metab,* 304**,** E14-22.

MCCARTHY, F. P., KINGDOM, J. C., KENNY, L. C. & WALSH, S. K. 2011. Animal models of preeclampsia; uses and limitations. *Placenta,* 32**,** 413-9.

MCCARTY, R. & KOPIN, I. J. 1978. Pregnancy: its effects on blood pressure, heart rate and sympatho-adrenal activity in spontaneously hypertensive rats. *Proc Soc Exp Biol Med,* 158**,** 242-4.

MCKINNEY, C. A., FATTAH, C., LOUGHREY, C. M., MILLIGAN, G. & NICKLIN, S. A. 2014. Angiotensin-(1-7) and angiotensin-(1-9): function in cardiac and vascular remodelling. *Clin Sci (Lond),* 126**,** 815-27.

MCLACHLAN, J., BEATTIE, E., MURPHY, M. P., KOH-TAN, C. H., OLSON, E., BEATTIE, W., DOMINICZAK, A. F., NICKLIN, S. A. & GRAHAM, D. 2014. Combined therapeutic benefit of mitochondria-targeted antioxidant, MitoQ10, and angiotensin receptor blocker, losartan, on cardiovascular function. *J Hypertens,* 32**,** 555-64.

MELCHIORRE, K., SUTHERLAND, G., SHARMA, R., NANNI, M. & THILAGANATHAN, B. 2013. Mid-gestational maternal cardiovascular profile in preterm and term pre-eclampsia: a prospective study. *BJOG,* 120**,** 496-504.

MESSERLI, F. H., WILLIAMS, B. & RITZ, E. 2007. Essential hypertension. *Lancet,* 370**,** 591-603.

MIKKELSEN, E., LAURIDSEN, H., NIELSEN, P. M., QI, H., NØRLINGER, T., ANDERSEN, M. D., ULDBJERG, N., LAUSTSEN, C., SANDAGER, P. & PEDERSEN, M. 2017. The chinchilla as a novel animal model of pregnancy. *R Soc Open Sci,* 4**,** 161098.

MISHRA, N., NUGENT, W. H., MAHAVADI, S. & WALSH, S. W. 2011. Mechanisms of enhanced vascular reactivity in preeclampsia. *Hypertension,* 58**,** 867-73.

MOFFETT-KING, A. 2002. Natural killer cells and pregnancy. *Nat Rev Immunol,* 2**,** 656-63.

MOLNÁR, M., SÜTÖ, T., TÓTH, T. & HERTELENDY, F. 1994. Prolonged blockade of nitric oxide synthesis in gravid rats produces sustained hypertension, proteinuria, thrombocytopenia, and intrauterine growth retardation. *Am J Obstet Gynecol,* 170**,** 1458-66.

MONTEZANO, A. C. & TOUYZ, R. M. 2014. Reactive oxygen species, vascular Noxs, and hypertension: focus on translational and clinical research. *Antioxid Redox Signal,* 20**,** 164-82.

MORGAN, T., CRAVEN, C. & WARD, K. 1998. Human spiral artery renin-angiotensin system. *Hypertension,* 32**,** 683-7.

MURPHY, S. R., LAMARCA, B., COCKRELL, K., ARANY, M. & GRANGER, J. P. 2012. L-arginine supplementation abolishes the blood pressure and endothelin response to chronic increases in plasma sFlt-1 in pregnant rats. *Am J Physiol Regul Integr Comp Physiol.,* 302**,** R259-63. doi: 10.1152/ajpregu.00319.2011. Epub 2011 Nov 9.

MYATT, L. 2006. Placental adaptive responses and fetal programming. *J Physiol,* 572**,** 25-30.

MYATT, L. & CUI, X. 2004. Oxidative stress in the placenta. *Histochem Cell Biol,* 122**,** 369-82.

MYERS, J. E., TUYTTEN, R., THOMAS, G., LAROY, W., KAS, K., VANPOUCKE, G., ROBERTS, C. T., KENNY, L. C., SIMPSON, N. A., BAKER, P. N. & NORTH, R. A. 2013. Integrated proteomics pipeline yields novel biomarkers for predicting preeclampsia. *Hypertension,* 61**,** 1281-8.

N.I.C.E 2010. National Institute for Health and Care Excellence. Hypertension in pregnancy: diagnosis and management. *NICE guidelines CG107*.

NAKAMURA, T., YAMAMOTO, E., KATAOKA, K., YAMASHITA, T., TOKUTOMI, Y., DONG, Y. F., MATSUBA, S., OGAWA, H. & KIM-MITSUYAMA, S. 2008. Beneficial effects of pioglitazone on hypertensive cardiovascular injury are enhanced by combination with candesartan. *Hypertension,* 51**,** 296-301.

NARUSE, K., LASH, G. E., INNES, B. A., OTUN, H. A., SEARLE, R. F., ROBSON, S. C. & BULMER, J. N. 2009. Localization of matrix metalloproteinase (MMP)-2, MMP-9 and tissue inhibitors for MMPs (TIMPs) in uterine natural killer cells in early human pregnancy. *Hum Reprod,* 24**,** 553-61.

NAVARATNAM, K., ALFIREVIC, Z., BAKER, P. N., GLUUD, C., GRUTTNER, B., KUBLICKIENE, K., ZEEMAN, G. & KENNY, L. C. 2013. A multi-centre phase IIa clinical study of predictive testing for preeclampsia: improved pregnancy outcomes via early detection (IMPROvED). *BMC Pregnancy Childbirth.,* 13:226.**,** 10.1186/1471-2393-13-226.

NELSON, A. C., MOULD, A. W., BIKOFF, E. K. & ROBERTSON, E. J. 2016. Single-cell RNA-seq reveals cell type-specific transcriptional signatures at the maternal-foetal interface during pregnancy. *Nat Commun,* 7**,** 11414.

NGUYEN DINH CAT, A., MONTEZANO, A. C., BURGER, D. & TOUYZ, R. M. 2013. Angiotensin II, NADPH oxidase, and redox signaling in the vasculature. *Antioxid Redox Signal,* 19**,** 1110-20.

NIELSEN, A. H., SCHAUSER, K. H. & POULSEN, K. 2000. Current topic: the uteroplacental renin-angiotensin system. *Placenta,* 21**,** 468-77.

NORAMBUENA, J., PIJNENBORG, R. & BROSENS, I. 1984. Decidual changes in the endometrium and morphological adaptation of the associated supplying arteries in the normal and diabetic pseudopregnant rat. *Placenta,* 5**,** 249-60.

ODEGARD, R. A., VATTEN, L. J., NILSEN, S. T., SALVESEN, K. A. & AUSTGULEN, R. 2000. Preeclampsia and fetal growth. *Obstet Gynecol.,* 96**,** 950-5.

ODUTAYO, A. & HLADUNEWICH, M. 2012. Obstetric nephrology: renal hemodynamic and metabolic physiology in normal pregnancy. *Clin J Am Soc Nephrol,* 7**,** 2073-80.

OKAMOTO, K. & AOKI, K. 1963. Development of a strain of spontaneously hypertensive rats. *Jpn Circ J,* 27**,** 282-93.

ORSHAL, J. M. & KHALIL, R. A. 2004. Gender, sex hormones, and vascular tone. *Am J Physiol Regul Integr Comp Physiol,* 286**,** R233-49.

OSOL, G. & CIPOLLA, M. 1993. Pregnancy-induced changes in the three-dimensional mechanical properties of pressurized rat uteroplacental (radial) arteries. *Am J Obstet Gynecol,* 168**,** 268-74.

OSOL, G. & MANDALA, M. 2009. Maternal uterine vascular remodeling during pregnancy. *Physiology (Bethesda),* 24**,** 58-71.

OSOL, G. & MOORE, L. G. 2014. Maternal uterine vascular remodeling during pregnancy. *Microcirculation,* 21**,** 38-47.

OTANI, L., SHIRASAKA, N., YOSHIZUMI, H. & MURAKAMI, T. 2004. The effects of maternal mild protein restriction on stroke incidence and blood pressure in stroke-prone spontaneously hypertensive rats (SHRSP). *Biosci Biotechnol Biochem,* 68**,** 488-94.

OTANI, L., SUGIMOTO, N., KAJI, M., MURAI, M., CHANG, S. J., KATO, H. & MURAKAMI, T. 2012. Role of the renin-angiotensin-aldosterone system in the enhancement of salt sensitivity caused by prenatal protein restriction in stroke-prone spontaneously hypertensive rats. *J Nutr Biochem,* 23**,** 892-9.

PALLER, M. S. 1984. Mechanism of decreased pressor responsiveness to ANG II, NE, and vasopressin in pregnant rats. *Am J Physiol,* 247**,** H100-8.

PALLER, M. S., GREGORINI, G. & FERRIS, T. F. 1989. Pressor responsiveness in pseudopregnant and pregnant rats: role of maternal factors. *Am J Physiol,* 257**,** R866-71.

PARHAM, P. 2004. NK Cells and Trophoblasts: Partners in Pregnancy. *The Journal of Experimental Medicine,* 200**,** 951-955.

PAUL, M., POYAN MEHR, A. & KREUTZ, R. 2006. Physiology of local renin-angiotensin systems. *Physiol Rev,* 86**,** 747-803.

PENG, J., MONSIVAIS, D., YOU, R., ZHONG, H., PANGAS, S. A. & MATZUK, M. M. 2015. Uterine activin receptor-like kinase 5 is crucial for blastocyst implantation and placental development. *Proc Natl Acad Sci U S A.,* 112**,** E5098-107. doi: 10.1073/pnas.1514498112. Epub 2015 Aug 24.

PENNA, I. A., HONGLING, D., KALLEN, A. N. & TAYLOR, H. S. 2010. Endothelin type A receptor (ETA) expression is regulated by HOXA10 in human endometrial stromal cells. *Reprod Sci.,* 17**,** 471-6. doi: 10.1177/1933719110361961.

PERACOLI, J. C., RUDGE, M. V., SARTORI, M. S. & DA SILVA FRANCO, R. J. 2001. Effects of hypertension on maternal adaptations to pregnancy: experimental study on spontaneously hypertensive rats. *Sao Paulo Med J,* 119**,** 54-8.

PHILLIPS, C. A. & POYSER, N. L. 1981. Studies on the involvement of prostaglandins in implantation in the rat. *J Reprod Fertil,* 62**,** 73-81.

PIJNENBORG, R., ANTHONY, J., DAVEY, D. A., REES, A., TILTMAN, A., VERCRUYSSE, L. & VAN ASSCHE, A. 1991. Placental bed spiral arteries in the hypertensive disorders of pregnancy. *Br J Obstet Gynaecol,* 98**,** 648-55.

PIJNENBORG, R., VERCRUYSSE, L. & HANSSENS, M. 2006. The uterine spiral arteries in human pregnancy: facts and controversies. *Placenta,* 27**,** 939-58.

PITKIN, R. M. 1999. Energy in pregnancy. *Am J Clin Nutr,* 69**,** 583.

PITMAN, H., INNES, B. A., ROBSON, S. C., BULMER, J. N. & LASH, G. E. 2013. Altered expression of interleukin-6, interleukin-8 and their receptors in decidua of women with sporadic miscarriage. *Hum Reprod,* 28**,** 2075-86.

PODJARNY, E., LOSONCZY, G. & BAYLIS, C. 2004. Animal models of preeclampsia. *Semin Nephrol,* 24**,** 596-606.

POON, L. C., AKOLEKAR, R., LACHMANN, R., BETA, J. & NICOLAIDES, K. H. 2010. Hypertensive disorders in pregnancy: screening by biophysical and biochemical markers at 11-13 weeks. *Ultrasound Obstet Gynecol,* 35**,** 662-70.

POPPAS, A., SHROFF, S. G., KORCARZ, C. E., HIBBARD, J. U., BERGER, D. S., LINDHEIMER, M. D. & LANG, R. M. 1997. Serial Assessment of the Cardiovascular System in Normal Pregnancy. *Circulation,* 95**,** 2407.

PREECLAMPSIA-FOUNDATION. 2010. *About Preeclampsia* [Online]. Preeclampsia Foundation Official Site. [Accessed 11th May 2018].

PRITCHARD, J. A. 1965. Changes in The Blood Volume During Pregnancy and Delivery. *Anesthesiology,* 26**,** 393-9.

RAFFETTO, J. D. & KHALIL, R. A. 2008. Matrix metalloproteinases and their inhibitors in vascular remodeling and vascular disease. *Biochem Pharmacol.* England.

RAMIREZ, R. J., DEBRAH, J. & NOVAK, J. 2011. Increased myogenic responses of resistance-sized mesenteric arteries after reduced uterine perfusion pressure in pregnant rats. *Hypertens Pregnancy,* 30**,** 45-57.

RANG, S., VAN MONTFRANS, G. A. & WOLF, H. 2008. Serial hemodynamic measurement in normal pregnancy, preeclampsia, and intrauterine growth restriction. *Am J Obstet Gynecol,* 198**,** 519.e1-9.

REDMAN, C. W., SACKS, G. P. & SARGENT, I. L. 1999. Preeclampsia: an excessive maternal inflammatory response to pregnancy. *Am J Obstet Gynecol,* 180**,** 499-506.

RICHTER, H. G., HANSELL, J. A., RAUT, S. & GIUSSANI, D. A. 2009. Melatonin improves placental efficiency and birth weight and increases the placental expression of antioxidant enzymes in undernourished pregnancy. *J Pineal Res.,* 46**,** 357-64. doi: 10.1111/j.1600-079X.2009.00671.x. Epub 2009 Mar 25.

RIDER, V., JONES, S. R., FOSTER, R. T. & IMAKAWA, K. 2000. Changes in the temporal and spatial expression of H beta 58 during formation and maturation of the chorioallantoic placenta in the Rat. *Biol Reprod.,* 63**,** 1735-46.

RIVERA, J., SOBEY, C. G., WALDUCK, A. K. & DRUMMOND, G. R. 2010. Nox isoforms in vascular pathophysiology: insights from transgenic and knockout mouse models. *Redox Rep,* 15**,** 50-63.

ROBERTS, C. L., FORD, J. B., ALGERT, C. S., ANTONSEN, S., CHALMERS, J., CNATTINGIUS, S., GOKHALE, M., KOTELCHUCK, M., MELVE, K. K., LANGRIDGE, A., MORRIS, C., MORRIS, J. M., NASSAR, N., NORMAN, J. E., NORRIE, J., SØRENSEN, H. T., WALKER, R. & WEIR, C. J. 2011. Population-based trends in pregnancy hypertension and pre-eclampsia: an international comparative study. *BMJ Open,* 1**,** e000101.

ROBERTSON, W. B., BROSENS, I. & DIXON, G. 1975. Uteroplacental vascular pathology. *Eur J Obstet Gynecol Reprod Biol,* 5**,** 47-65.

ROBSON, A., HARRIS, L. K., INNES, B. A., LASH, G. E., ALJUNAIDY, M. M., APLIN, J. D., BAKER, P. N., ROBSON, S. C. & BULMER, J. N. 2012. Uterine natural killer cells initiate spiral artery remodeling in human pregnancy. *FASEB J,* 26**,** 4876-85.

ROBSON, S. C., HUNTER, S., BOYS, R. J. & DUNLOP, W. 1989. Serial study of factors influencing changes in cardiac output during human pregnancy. *Am J Physiol,* 256**,** H1060-5.

ROBSON, S. C., SIMPSON, H., BALL, E., LYALL, F. & BULMER, J. N. 2002. Punch biopsy of the human placental bed. *Am J Obstet Gynecol,* 187**,** 1349-55.

ROGER, V. L., GO, A. S., LLOYD-JONES, D. M., BENJAMIN, E. J., BERRY, J. D., BORDEN, W. B., BRAVATA, D. M., DAI, S., FORD, E. S., FOX, C. S., FULLERTON, H. J., GILLESPIE, C., HAILPERN, S. M., HEIT, J. A., HOWARD, V. J., KISSELA, B. M., KITTNER, S. J., LACKLAND, D. T., LICHTMAN, J. H., LISABETH, L. D., MAKUC, D. M., MARCUS, G. M., MARELLI, A., MATCHAR, D. B., MOY, C. S., MOZAFFARIAN, D., MUSSOLINO, M. E., NICHOL, G., PAYNTER, N. P., SOLIMAN, E. Z., SORLIE, P. D., SOTOODEHNIA, N., TURAN, T. N., VIRANI, S. S., WONG, N. D., WOO, D., TURNER, M. B. & SUBCOMMITTEE, A. H. A. S. C. A. S. S. 2012. Heart disease and stroke statistics--2012 update: a report from the American Heart Association. *Circulation,* 125**,** e2-e220.

ROSEBOOM, T., DE ROOIJ, S. & PAINTER, R. 2006. The Dutch famine and its long-term consequences for adult health. *Early Hum Dev,* 82**,** 485-91.

ROSSANT, J. & CROSS, J. C. 2001. Placental development: lessons from mouse mutants. *Nat Rev Genet,* 2**,** 538-48.

ROVINSKY, J. J. & JAFFIN, H. 1965. Cardiovascular hemodynamics in pregnancy. *American Journal of Obstetrics & Gynecology,* 93**,** 1-15.

RUBATTU, S., PAGLIARO, B., PIERELLI, G., SANTOLAMAZZA, C., CASTRO, S. D., MENNUNI, S. & VOLPE, M. 2014. Pathogenesis of target organ damage in hypertension: role of mitochondrial oxidative stress. *Int J Mol Sci,* 16**,** 823-39.

RYAN, H. E., LO, J. & JOHNSON, R. S. 1998. HIF-1 alpha is required for solid tumor formation and embryonic vascularization. *EMBO J.,* 17**,** 3005-15. doi: 10.1093/emboj/17.11.3005.

SANGHAVI, M. & RUTHERFORD, J. D. 2014. Cardiovascular physiology of pregnancy. *Circulation,* 130**,** 1003-8.

SATTAR, N. & GREER, I. A. 2002. Pregnancy complications and maternal cardiovascular risk: opportunities for intervention and screening? *Bmj,* 325**,** 157-60.

SAVITZ, D. A., DANILACK, V. A., ENGEL, S. M., ELSTON, B. & LIPKIND, H. S. 2014. Descriptive Epidemiology of Chronic Hypertension, Gestational Hypertension, and Preeclampsia in New York State, 1995–2004. *Maternal and child health journal,* 18**,** 829-838.

SAXENA, A. R., KARUMANCHI, S. A., BROWN, N. J., ROYLE, C. M., MCELRATH, T. F. & SEELY, E. W. 2010. Increased sensitivity to angiotensin II is present postpartum in women with a history of hypertensive pregnancy. *Hypertension,* 55**,** 1239-45.

SAY, L., CHOU, D., GEMMILL, A., TUNÇALP, Ö., MOLLER, A. B., DANIELS, J., GÜLMEZOGLU, A. M., TEMMERMAN, M. & ALKEMA, L. 2014. Global causes of maternal death: a WHO systematic analysis. *Lancet Glob Health,* 2**,** e323-33.

SCOTT, J. N. 1986. Placental Parameters in the Spontaneously Hypertensive Rat and Control Strain Wlstar-Kyoto Rat. *Clinical and Experimental Hypertension. Part B: Hypertension in Pregnancy,* 5**,** 19-28.

SCOTT, J. N., GOECKE, J. C. & REAM, L. J. 1985. Placentas from spontaneously hypertensive rats and control strain Wistar-Kyoto rats. *Lab Anim Sci,* 35**,** 146-9.

SELEMIDIS, S., SOBEY, C. G., WINGLER, K., SCHMIDT, H. H. & DRUMMOND, G. R. 2008. NADPH oxidases in the vasculature: molecular features, roles in disease and pharmacological inhibition. *Pharmacol Ther,* 120**,** 254-91.

SHAH, D. M. 2005. Role of the renin-angiotensin system in the pathogenesis of preeclampsia. *Am J Physiol Renal Physiol,* 288**,** F614-25.

SHANKAR, K., ZHONG, Y., KANG, P., BLACKBURN, M. L., SOARES, M. J., BADGER, T. M. & GOMEZ-ACEVEDO, H. 2012. RNA-seq analysis of the functional compartments within the rat placentation site. *Endocrinology,* 153**,** 1999-2011.

SHESELY, E. G., GILBERT, C., GRANDERSON, G., CARRETERO, C. D., CARRETERO, O. A. & BEIERWALTES, W. H. 2001. Nitric oxide synthase gene knockout mice do not become hypertensive during pregnancy. *Am J Obstet Gynecol,* 185**,** 1198-203.

SHIBATA, E., POWERS, R. W., RAJAKUMAR, A., VON VERSEN-HÖYNCK, F., GALLAHER, M. J., LYKINS, D. L., ROBERTS, J. M. & HUBEL, C. A. 2006. Angiotensin II decreases system A amino acid transporter activity in human placental villous fragments through AT1 receptor activation. *Am J Physiol Endocrinol Metab,* 291**,** E1009-16.

SHIRASUNA, K., KARASAWA, T., USUI, F., KOBAYASHI, M., KOMADA, T., KIMURA, H., KAWASHIMA, A., OHKUCHI, A., TANIGUCHI, S. & TAKAHASHI, M. 2015. NLRP3 Deficiency Improves Angiotensin II-Induced Hypertension But Not Fetal Growth Restriction During Pregnancy. *Endocrinology,* 156**,** 4281-92.

SIBAI, B. M. 2002. Chronic hypertension in pregnancy. *Obstet Gynecol,* 100**,** 369-77.

SIBAI, B. M., LINDHEIMER, M., HAUTH, J., CARITIS, S., VANDORSTEN, P., KLEBANOFF, M., MACPHERSON, C., LANDON, M., MIODOVNIK, M., PAUL, R., MEIS, P. & DOMBROWSKI, M. 1998. Risk factors for preeclampsia, abruptio placentae, and adverse neonatal outcomes among women with chronic hypertension. National Institute of Child Health and Human Development Network of Maternal-Fetal Medicine Units. *N Engl J Med,* 339**,** 667-71.

SIDERI, M., DE VIRGILIIS, G., RAINOLDI, R. & REMOTTI, G. 1984. The Ultrastructural Basis of the Nutritional Transfer: Evidence of Different Patterns in the Plasma Membranes of the Multilayered Placental Barrier. *In:* MILLER, R. K. & THIEDE, H. A. (eds.) *Fetal Nutrition, Metabolism, and Immunology: The Role of the Placenta.* Boston, MA: Springer US.

SIMMONS, L. A., GILLIN, A. G. & JEREMY, R. W. 2002. Structural and functional changes in left ventricle during normotensive and preeclamptic pregnancy. *Am J Physiol Heart Circ Physiol,* 283**,** H1627-33.

SINCLAIR, K. D., LEA, R. G., REES, W. D. & YOUNG, L. E. 2007. The developmental origins of health and disease: current theories and epigenetic mechanisms. *Soc Reprod Fertil Suppl,* 64**,** 425-43.

SITRAS, V., FENTON, C. & ACHARYA, G. 2015. Gene expression profile in cardiovascular disease and preeclampsia: a meta-analysis of the transcriptome based on raw data from human studies deposited in Gene Expression Omnibus. *Placenta,* 36**,** 170-8.

SKEGGS, L. T., KAHN, J. R. & SHUMWAY, N. P. 1956. The preparation and function of the hypertensin-converting enzyme. *J Exp Med,* 103**,** 295-9.

SKINNER, M. K. 2011. Role of epigenetics in developmental biology and transgenerational inheritance. *Birth Defects Res C Embryo Today,* 93**,** 51-5.

SLADEK, S. M., MAGNESS, R. R. & CONRAD, K. P. 1997. Nitric oxide and pregnancy. *Am J Physiol,* 272**,** R441-63.

SMALL, H. Y., MORGAN, H., BEATTIE, E., GRIFFIN, S., INDAHL, M., DELLES, C. & GRAHAM, D. 2016. Abnormal uterine artery remodelling in the stroke-prone spontaneously hypertensive rat. *Placenta,* 37**,** 34-44.

SOARES, M. J., CHAKRABORTY, D., KARIM RUMI, M. A., KONNO, T. & RENAUD, S. J. 2012. Rat placentation: an experimental model for investigating the hemochorial maternal-fetal interface. *Placenta,* 33**,** 233-43.

SOARES, M. J., IQBAL, K. & KOZAI, K. 2017. Hypoxia and Placental Development. *Birth Defects Res,* 109**,** 1309-1329.

SOMA-PILLAY, P., LOUW, M. C., ADEYEMO, A. O., MAKIN, J. & PATTINSON, R. C. 2017. Cardiac diastolic function after recovery from pre-eclampsia. *Cardiovasc J Afr,* 28**,** 1-6.

SOOBRYAN, N., MURUGESAN, S., PHOSWA, W., GATHIRAM, P., MOODLEY, J. & MACKRAJ, I. 2017. The effects of sildenafil citrate on uterine angiogenic status and serum inflammatory markers in an L-NAME rat model of pre-eclampsia. *Eur J Pharmacol,* 795**,** 101-107.

SOOD, R., ZEHNDER, J. L., DRUZIN, M. L. & BROWN, P. O. 2006. Gene expression patterns in human placenta. *Proc Natl Acad Sci U S A,* 103**,** 5478-83.

SPARKS, M. A., CROWLEY, S. D., GURLEY, S. B., MIROTSOU, M. & COFFMAN, T. M. 2014. Classical Renin-Angiotensin system in kidney physiology. *Compr Physiol,* 4**,** 1201-28.

SPETH, R. C. & KIM, K. H. 1990. Discrimination of two angiotensin II receptor subtypes with a selective agonist analogue of angiotensin II, p-aminophenylalanine6 angiotensin II. *Biochem Biophys Res Commun,* 169**,** 997-1006.

SRINIVAS, S. K., EDLOW, A. G., NEFF, P. M., SAMMEL, M. D., ANDRELA, C. M. & ELOVITZ, M. A. 2009. Rethinking IUGR in preeclampsia: dependent or independent of maternal hypertension? *J Perinatol,* 29**,** 680-4.

STALEY, J. R., BRADLEY, J., SILVERWOOD, R. J., HOWE, L. D., TILLING, K., LAWLOR, D. A. & MACDONALD-WALLIS, C. 2015. Associations of blood pressure in pregnancy with offspring blood pressure trajectories during childhood and adolescence: findings from a prospective study. *J Am Heart Assoc,* 4.

STANLEY, J. L., ANDERSSON, I. J., POUDEL, R., RUEDA-CLAUSEN, C. F., SIBLEY, C. P., DAVIDGE, S. T. & BAKER, P. N. 2012. Sildenafil citrate rescues fetal growth in the catechol-O-methyl transferase knockout mouse model. *Hypertension,* 59**,** 1021-8.

STAUN-RAM, E., GOLDMAN, S., GABARIN, D. & SHALEV, E. 2004. Expression and importance of matrix metalloproteinase 2 and 9 (MMP-2 and -9) in human trophoblast invasion. *Reprod Biol Endocrinol,* 2**,** 59.

STEEGERS, E. A., VON DADELSZEN, P., DUVEKOT, J. J. & PIJNENBORG, R. 2010. Pre-eclampsia. *Lancet,* 376**,** 631-44.

STEEL, S. A., PEARCE, J. M. & CHAMBERLAIN, G. 1988. Doppler ultrasound of the uteroplacental circulation as a screening test for severe pre-eclampsia with intra-uterine growth retardation. *Eur J Obstet Gynecol Reprod Biol,* 28**,** 279-87.

STEPHEN, G. L., LUI, S., HAMILTON, S. A., TOWER, C. L., HARRIS, L. K., STEVENS, A. & JONES, R. L. 2015. Transcriptomic profiling of human choriodecidua during term labor: inflammation as a key driver of labor. *Am J Reprod Immunol.,* 73**,** 36-55. doi: 10.1111/aji.12328. Epub 2014 Oct 4.

STOTT, D., NZELU, O., NICOLAIDES, K. H. & KAMETAS, N. A. 2017. Maternal haemodynamics in normal pregnancies and in pregnancies affected by pre-eclampsia. *Ultrasound Obstet Gynecol*.

STOUT, C. & LEMMON, W. B. 1969. Glomerular capillary endothelial swelling in a pregnant chimpanzee. *Am J Obstet Gynecol,* 105**,** 212-5.

TAJSIC, T. & MORRELL, N. W. 2011. Smooth muscle cell hypertrophy, proliferation, migration and apoptosis in pulmonary hypertension. *Compr Physiol,* 1**,** 295-317.

TAKEDA-MATSUBARA, Y., IWAI, M., CUI, T. X., SHIUCHI, T., LIU, H. W., OKUMURA, M., ITO, M. & HORIUCHI, M. 2004. Roles of angiotensin type 1 and 2 receptors in pregnancy-associated blood pressure change. *Am J Hypertens,* 17**,** 684-9.

TAKEDA, Y., YONEDA, T., DEMURA, M., FURUKAWA, K., MIYAMORI, I. & MABUCHI, H. 2001. Effects of high sodium intake on cardiovascular aldosterone synthesis in stroke-prone spontaneously hypertensive rats. *J Hypertens,* 19**,** 635-9.

TAKEMORI, K., ISHIDA, H. & ITO, H. 2005. Continuous inhibition of the renin-angiotensin system and protection from hypertensive end-organ damage by brief treatment with angiotensin II type 1 receptor blocker in stroke-prone spontaneously hypertensive rats. *Life Sci,* 77**,** 2233-45.

TAKIMOTO, E., ISHIDA, J., SUGIYAMA, F., HORIGUCHI, H., MURAKAMI, K. & FUKAMIZU, A. 1996. Hypertension induced in pregnant mice by placental renin and maternal angiotensinogen. *Science,* 274**,** 995-8.

TAL, R., TAYLOR, H. S., BURNEY, R. O., MOONEY, S. B. & GIUDICE, L. C. 2000. Endocrinology of Pregnancy. *In:* DE GROOT LJ, C. G., DUNGAN K, ET AL (ed.) *Endotext.* South Dartmouth (MA).

TAN, K., ZHANG, Z., MIAO, K., YU, Y., SUI, L., TIAN, J. & AN, L. 2016. Dynamic integrated analysis of DNA methylation and gene expression profiles in in vivo and in vitro fertilized mouse post-implantation extraembryonic and placental tissues. *Mol Hum Reprod*.

TAYYAR, A., GUERRA, L., WRIGHT, A., WRIGHT, D. & NICOLAIDES, K. H. 2015. Uterine artery pulsatility index in the three trimesters of pregnancy: effects of maternal characteristics and medical history. *Ultrasound Obstet Gynecol,* 45**,** 689-97.

THORNBURG, K. L., BAGBY, S. P. & GIRAUD, G. D. 2015. Chapter 43 - Maternal Adaptations to Pregnancy. *Knobil and Neill's Physiology of Reproduction (Fourth Edition).* San Diego: Academic Press.

THORNBURG, K. L., JACOBSON, S.-L., GIRAUD, G. D. & MORTON, M. J. 2000. Hemodynamic changes in pregnancy. *Seminars in Perinatology,* 24**,** 11-14.

THORNTON, J. G. & ONWUDE, J. L. 1992. Convulsions in pregnancy in related gorillas. *Am J Obstet Gynecol,* 167**,** 240-1.

TOBIAN, L., TOMBOULIAN, A. & JANECEK, J. 1959. The effect of high perfusion pressures on the granulation of juxtaglomerular cells in an isolated kidney. *J Clin Invest,* 38**,** 605-10.

TOKORO, T., ITO, H. & SUZUKI, T. 1996. Alterations in mitochondrial DNA and enzyme activities in hypertrophied myocardium of stroke-prone SHRS. *Clin Exp Hypertens,* 18**,** 595-606.

TOUYZ, R. M. 2014. Blood Pressure Regulation and Pathology. *In:* WILLIS, M., HOMEISTER, J. W. & STONE, J. R. (eds.) *Cellular and Molecular Pathobiology of Cardiovascular Disease.* San Diego: Academic Press.

TOUYZ, R. M., YAO, G., QUINN, M. T., PAGANO, P. J. & SCHIFFRIN, E. L. 2005. p47phox associates with the cytoskeleton through cortactin in human vascular smooth muscle cells: role in NAD(P)H oxidase regulation by angiotensin II. *Arterioscler Thromb Vasc Biol,* 25**,** 512-8.

TOWER, C. L., LUI, S., CHARLESWORTH, N. R., SMITH, S. D., APLIN, J. D. & JONES, R. L. 2010. Differential expression of angiotensin II type 1 and type 2 receptors at the maternal-fetal interface: potential roles in early placental development. *Reproduction,* 140**,** 931-42.

TRANQUILLI, A. L., DEKKER, G., MAGEE, L., ROBERTS, J., SIBAI, B. M., STEYN, W., ZEEMAN, G. G. & BROWN, M. A. 2014. The classification, diagnosis and management of the hypertensive disorders of pregnancy: A revised statement from the ISSHP. *Pregnancy Hypertens,* 4**,** 97-104.

TRIFONOVA, E. A., GABIDULINA, T. V., ERSHOV, N. I., SEREBROVA, V. N., VOROZHISHCHEVA, A. Y. & STEPANOV, V. A. 2014. Analysis of the placental tissue transcriptome of normal and preeclampsia complicated pregnancies. *Acta Naturae,* 6**,** 71-83.

TURRENS, J. F. 2003. Mitochondrial formation of reactive oxygen species. *J Physiol.,* 552**,** 335-44. doi: 10.1113/jphysiol.2003.049478.

UEDA, H., SAITO, N., SUGANUMA, Y. & MATSUO, H. 1979. The blood pressure, life span, body weight in both sexes of SHRSP during 55 weeks under specific pathogen free system [proceedings]. *Jpn Heart J,* 20**,** 752.

VALENSISE, H., VASAPOLLO, B., GAGLIARDI, G. & NOVELLI, G. P. 2008. Early and late preeclampsia: two different maternal hemodynamic states in the latent phase of the disease. *Hypertension,* 52**,** 873-80.

VAN DER HEIJDEN, O. W., ESSERS, Y. P., FAZZI, G., PEETERS, L. L., DE MEY, J. G. & VAN EYS, G. J. 2005a. Uterine artery remodeling and reproductive performance are impaired in endothelial nitric oxide synthase-deficient mice. *Biol Reprod,* 72**,** 1161-8.

VAN DER HEIJDEN, O. W., ESSERS, Y. P., SPAANDERMAN, M. E., DE MEY, J. G., VAN EYS, G. J. & PEETERS, L. L. 2005b. Uterine artery remodeling in pseudopregnancy is comparable to that in early pregnancy. *Biol Reprod,* 73**,** 1289-93.

VASAPOLLO, B., NOVELLI, G. P. & VALENSISE, H. 2008. Total vascular resistance and left ventricular morphology as screening tools for complications in pregnancy. *Hypertension,* 51**,** 1020-6.

VASWANI, K., CHAN, H. W., VERMA, P., DEKKER NITERT, M., PEIRIS, H. N., WOOD-BRADLEY, R. J., ARMITAGE, J. A., RICE, G. E. & MITCHELL, M. D. 2015. The rat placental renin-angiotensin system - a gestational gene expression study. *Reprod Biol Endocrinol,* 13**,** 89.

VASWANI, K., HUM, M. W., CHAN, H. W., RYAN, J., WOOD-BRADLEY, R. J., NITERT, M. D., MITCHELL, M. D., ARMITAGE, J. A. & RICE, G. E. 2013. The effect of gestational age on angiogenic gene expression in the rat placenta. *PLoS One,* 8**,** e83762.

VERCRUYSSE, L., CALUWAERTS, S., LUYTEN, C. & PIJNENBORG, R. 2006. Interstitial trophoblast invasion in the decidua and mesometrial triangle during the last third of pregnancy in the rat. *Placenta,* 27**,** 22-33.

VERLOHREN, S., GEUSENS, N., MORTON, J., VERHAEGEN, I., HERING, L., HERSE, F., DUDENHAUSEN, J. W., MULLER, D. N., LUFT, F. C., CARTWRIGHT, J. E., DAVIDGE, S. T., PIJNENBORG, R. & DECHEND, R. 2010. Inhibition of trophoblast-induced spiral artery remodeling reduces placental perfusion in rat pregnancy. *Hypertension,* 56**,** 304-10.

VERLOHREN, S., NIEHOFF, M., HERING, L., GEUSENS, N., HERSE, F., TINTU, A. N., PLAGEMANN, A., LENOBLE, F., PIJNENBORG, R., MULLER, D. N., LUFT, F. C., DUDENHAUSEN, J. W., GOLLASCH, M. & DECHEND, R. 2008. Uterine vascular function in a transgenic preeclampsia rat model. *Hypertension,* 51**,** 547-53.

VISSER, W. & WALLENBURG, H. C. 1991. Central hemodynamic observations in untreated preeclamptic patients. *Hypertension,* 17**,** 1072-7.

WADASINGHE, S. U., METCALF, L., METCALF, P. & PERRY, D. 2016. Maternal Physiologic Renal Pelvis Dilatation in Pregnancy: Sonographic Reference Data. *J Ultrasound Med,* 35**,** 2659-2664.

WAKELAND, A. K., SONCIN, F., MORETTO-ZITA, M., CHANG, C. W., HORII, M., PIZZO, D., NELSON, K. K., LAURENT, L. C. & PARAST, M. M. 2017. Hypoxia Directs Human Extravillous Trophoblast Differentiation in a Hypoxia-Inducible Factor-Dependent Manner. *Am J Pathol,* 187**,** 767-780.

WALKER, C. G., MEIER, S., HUSSEIN, H., MCDOUGALL, S., BURKE, C. R., ROCHE, J. R. & MITCHELL, M. D. 2015. Modulation of the immune system during postpartum uterine inflammation. *Physiol Genomics,* 47**,** 89-101.

WALLACE, A. E., CARTWRIGHT, J. E., BEGUM, R., LAING, K., THILAGANATHAN, B. & WHITLEY, G. S. 2013. Trophoblast-induced changes in C-x-C motif chemokine 10 expression contribute to vascular smooth muscle cell dedifferentiation during spiral artery remodeling. *Arterioscler Thromb Vasc Biol.,* 33**,** e93-e101. doi: 10.1161/ATVBAHA.112.300354. Epub 2013 Jan 3.

WALLUKAT, G., HOMUTH, V., FISCHER, T., LINDSCHAU, C., HORSTKAMP, B., JÜPNER, A., BAUR, E., NISSEN, E., VETTER, K., NEICHEL, D., DUDENHAUSEN, J. W., HALLER, H. & LUFT, F. C. 1999. Patients with preeclampsia develop agonistic autoantibodies against the angiotensin AT1 receptor. *J Clin Invest,* 103**,** 945-52.

WALSH, S. K., ENGLISH, F. A., JOHNS, E. J. & KENNY, L. C. 2009. Plasma-mediated vascular dysfunction in the reduced uterine perfusion pressure model of preeclampsia: a microvascular characterization. *Hypertension.,* 54**,** 345-51. doi: 10.1161/HYPERTENSIONAHA.109.132191. Epub 2009 Jun 29.

WANG, C., WANG, L., DING, Y., LU, X., ZHANG, G., YANG, J., ZHENG, H., WANG, H., JIANG, Y. & XU, L. 2017. LncRNA Structural Characteristics in Epigenetic Regulation. *Int J Mol Sci,* 18.

WANG, H. D., XU, S., JOHNS, D. G., DU, Y., QUINN, M. T., CAYATTE, A. J. & COHEN, R. A. 2001. Role of NADPH oxidase in the vascular hypertrophic and oxidative stress response to angiotensin II in mice. *Circ Res,* 88**,** 947-53.

WANG, K. C. & CHANG, H. Y. 2011. Molecular mechanisms of long noncoding RNAs. *Mol Cell,* 43**,** 904-14.

WANG, X. & KHALIL, R. A. 2018. Matrix Metalloproteinases, Vascular Remodeling, and Vascular Disease. *Adv Pharmacol,* 81**,** 241-330.

WANG, Y. 2010. Placental Blood Circulation. *Vascular biology of the placenta.* 1 ed.: Morgan & Claypool Life Sciences.

WANG, Y., FAN, H., ZHAO, G., LIU, D., DU, L., WANG, Z., HU, Y. & HOU, Y. 2012. miR-16 inhibits the proliferation and angiogenesis-regulating potential of mesenchymal stem cells in severe pre-eclampsia. *FEBS J.,* 279**,** 4510-24. doi: 10.1111/febs.12037. Epub 2012 Nov 22.

WANG, Z., GERSTEIN, M. & SNYDER, M. 2009. RNA-Seq: a revolutionary tool for transcriptomics. *Nat Rev Genet,* 10**,** 57-63.

WATKINS, A. J., SIROVICA, S., STOKES, B., ISAACS, M., ADDISON, O. & MARTIN, R. A. 2017. Paternal low protein diet programs preimplantation embryo gene expression, fetal growth and skeletal development in mice. *Biochim Biophys Acta,* 1863**,** 1371-1381.

WEBB, R. C. 2003. Smooth muscle contraction and relaxation. *Adv Physiol Educ,* 27**,** 201-6.

WEISFELDT, M. 1998. Aging, changes in the cardiovascular system, and responses to stress. *Am J Hypertens,* 11**,** 41S-45S.

WESTON, G. C., CANN, L. & ROGERS, P. A. 2003. Myometrial microvascular endothelial cells express oxytocin receptor. *BJOG.,* 110**,** 149-56.

WESTON, G. C., HAVIV, I. & ROGERS, P. A. 2002. Microarray analysis of VEGF-responsive genes in myometrial endothelial cells. *Mol Hum Reprod.,* 8**,** 855-63.

WHELTON, P. K., CAREY, R. M., ARONOW, W. S., CASEY, D. E., COLLINS, K. J., DENNISON HIMMELFARB, C., DEPALMA, S. M., GIDDING, S., JAMERSON, K. A., JONES, D. W., MACLAUGHLIN, E. J., MUNTNER, P., OVBIAGELE, B., SMITH, S. C., SPENCER, C. C., STAFFORD, R. S., TALER, S. J., THOMAS, R. J., WILLIAMS, K. A., WILLIAMSON, J. D. & WRIGHT, J. T. 2017. ACC/AHA/AAPA/ABC/ACPM/AGS/APhA/ASH/ASPC/NMA/PCNA Guideline for the Prevention, Detection, Evaluation, and Management of High Blood Pressure in Adults. *Hypertension***,** https://doi.org/10.1161/HYP.0000000000000065.

WHITEBREAD, S., MELE, M., KAMBER, B. & DE GASPARO, M. 1989. Preliminary biochemical characterization of two angiotensin II receptor subtypes. *Biochem Biophys Res Commun,* 163**,** 284-91.

WHITLEY, G. S. & CARTWRIGHT, J. E. 2010. Cellular and molecular regulation of spiral artery remodelling: lessons from the cardiovascular field. *Placenta,* 31**,** 465-74.

WILLIAMS, P. J., MISTRY, H. D., INNES, B. A., BULMER, J. N. & BROUGHTON PIPKIN, F. 2010. Expression of AT1R, AT2R and AT4R and their roles in extravillous trophoblast invasion in the human. *Placenta.* Netherlands: 2010 Elsevier Ltd.

WINSHIP, A. & DIMITRIADIS, E. 2018. Interleukin 11 is upregulated in preeclampsia and leads to inflammation and preeclampsia features in mice. *J Reprod Immunol,* 125**,** 32-38.

WOODING, P. & BURTON, G. 2008. Haemochorial Placentation: Mouse, Rabbit, Man, Apes, Monkeys. *Comparative Placentation: Structures, Functions and Evolution.* Berlin, Heidelberg: Springer Berlin Heidelberg.

WU, W. X., MA, X. H., SMITH, G. C. & NATHANIELSZ, P. W. 2000. Differential distribution of ERalpha and ERbeta mRNA in intrauterine tissues of the pregnant rhesus monkey. *Am J Physiol Cell Physiol.,* 278**,** C190-8. doi: 10.1152/ajpcell.2000.278.1.C190.

WYNNE, B., LABAZI, H., LIMA, V., CARNEIRO, F., WEBB, R. C., TOSTES, R. C. & GIACHINI, F. R. 2018. Mesenteric arteries from spontaneously hypertensive stroke-prone rats exhibit an increase in NO-dependent vasorelaxation. *Can J Physiol Pharmacol*.

XU, D. L., MARTIN, P. Y., ST JOHN, J., TSAI, P., SUMMER, S. N., OHARA, M., KIM, J. K. & SCHRIER, R. W. 1996. Upregulation of endothelial and neuronal constitutive nitric oxide synthase in pregnant rats. *Am J Physiol,* 271**,** R1739-45.

XUE, B., YIN, H., GUO, F., BELTZ, T. G., THUNHORST, R. L. & JOHNSON, A. K. 2017. Maternal Gestational Hypertension-Induced Sensitization of Angiotensin II Hypertension Is Reversed by Renal Denervation or Angiotensin-Converting Enzyme Inhibition in Rat Offspring. *Hypertension,* 69**,** 669-677.

YAMADA, N., KIDO, K., TAMAI, T., MUKAI, M. & HAYASHI, S. 1981. Hypertensive effects on pregnancy in spontaneously hypertensive rats (SHR) and stroke-prone SHR (SHRSP). *Int J Biol Res Pregnancy,* 2**,** 80-4.

YAMORI, Y. & HORIE, R. 1977. Developmental course of hypertension and regional cerebral blood flow in stroke-prone spontaneously hypertensive rats. *Stroke,* 8**,** 456-61.

YAMORI, Y., IGAWA, T., KANBE, T., KIHARA, M., NARA, Y. & HORIE, R. 1981. Mechanisms of structural vascular changes in genetic hypertension: analyses on cultured vascular smooth muscle cells from spontaneously hypertensive rats. *Clin Sci (Lond),* 61 Suppl 7**,** 121s-123s.

YAMORI, Y. & OKAMOTO, K. 1974. Spontaneous hypertension in the rat. A model for human "essential" hypertension. *Verh Dtsch Ges Inn Med,* 80**,** 168-70.

ZHAO, G., ZHOU, X., CHEN, S., MIAO, H., FAN, H., WANG, Z., HU, Y. & HOU, Y. 2014. Differential expression of microRNAs in decidua-derived mesenchymal stem cells from patients with pre-eclampsia. *J Biomed Sci,* 21**,** 81.

ZHOU, C. C., AHMAD, S., MI, T., XIA, L., ABBASI, S., HEWETT, P. W., SUN, C., AHMED, A., KELLEMS, R. E. & XIA, Y. 2007. Angiotensin II induces soluble fms-Like tyrosine kinase-1 release via calcineurin signaling pathway in pregnancy. *Circ Res,* 100**,** 88-95.

ZHOU, C. C., ZHANG, Y., IRANI, R. A., ZHANG, H., MI, T., POPEK, E. J., HICKS, M. J., RAMIN, S. M., KELLEMS, R. E. & XIA, Y. 2008. Angiotensin receptor agonistic autoantibodies induce pre-eclampsia in pregnant mice. *Nat Med,* 14**,** 855-62.

ZHOU, X., HAN, T. L., CHEN, H., BAKER, P. N., QI, H. & ZHANG, H. 2017. Impaired mitochondrial fusion, autophagy, biogenesis and dysregulated lipid metabolism is associated with preeclampsia. *Exp Cell Res,* 359**,** 195-204.